

UNITED 87  
FILE 1

McConnell

USGS-OFR-87-408

USGS-OFR-87-408

**UNITED STATES DEPARTMENT OF THE INTERIOR  
GEOLOGICAL SURVEY**

**EVALUATION OF THE SEISMICITY OF THE SOUTHERN GREAT BASIN  
AND ITS RELATIONSHIP TO THE TECTONIC FRAMEWORK OF THE REGION**

by

**A. M. Rogers, S. C. Harmsen, and M. E. Meremonte**

**Open-File Report 87-408**

**Prepared in cooperation with the  
Nevada Operations Office  
U.S. Department of Energy  
(Interagency Agreement DE-AI08-78ET44802)**

This report is preliminary and has not been reviewed for conformity with U.S. Geological Survey editorial standards and stratigraphic nomenclature. Company names are for descriptive purposes only and do not constitute endorsement by the U.S. Geological Survey.

**Denver, Colorado  
1987**

Copies of this Open-File Report  
may be purchased from

Open-File Services Section  
Branch of Distribution  
U.S. Geological Survey  
Box 25425, Federal Center  
Denver, Colorado 80225

**PREPAYMENT IS REQUIRED**

Price information will be published  
in the monthly listing  
"New Publications of the Geological Survey"

**FOR ADDITIONAL ORDERING INFORMATION**

**CALL: Commercial: (303) 236-1603**  
**FTS: 776-1603**

**USGS-OFR-87-408**

**USGS-OFR-87-408**

**UNITED STATES  
DEPARTMENT OF THE INTERIOR  
GEOLOGICAL SURVEY**

**Denver, Colorado**

**EVALUATION OF THE SEISMICITY OF THE SOUTHERN GREAT BASIN  
AND ITS RELATIONSHIP TO THE TECTONIC FRAMEWORK OF THE REGION**

**by**

**A. M. Rogers, S. C. Harmsen, and M. E. Meremonte**

# CONTENTS

	Page
Abstract . . . . .	1
Introduction . . . . .	3
Acknowledgements . . . . .	7
Hypocenter determination details . . . . .	8
Magnitude estimation details . . . . .	9
Focal mechanism details . . . . .	14
The association of earthquakes and faults . . . . .	18
Seismicity overview . . . . .	18
Earthquakes in the vicinity of Jackass Flats . . . . .	33
Earthquakes in the vicinity of Mercury Valley . . . . .	33
Jackass Flats-Rock Valley-Mercury Valley areas . . . . .	33
Funeral Mountains Seismicity . . . . .	36
Earthquake activity near Lathrop Wells . . . . .	37
Striped Hills-Rock Valley Earthquakes . . . . .	37
Seismicity at Dome Mountain 1983 . . . . .	40
Earthquakes at Thirsty Canyon and vicinity . . . . .	40
Seismicity at Sarcobatus Flat 1981 through 1983 . . . . .	43
Earthquakes near Scottys Junction . . . . .	44
Seismicity in the vicinity of Slate Ridge and Mt. Dunfee . . . . .	44
Earthquakes near Yucca Flat . . . . .	48
Earthquakes in Indian Spring Valley . . . . .	48
Earthquakes in the Pahrnagat Region . . . . .	52
Earthquakes in North Pahroc Range . . . . .	52
Earthquakes and structure: summary . . . . .	52
Depth of focus distribution 1982-1983 . . . . .	55
1982-1983 relocations using velocity gradient models . . . . .	55
Geographic variation in the depth distributions . . . . .	60
Focal mechanisms and the regional stress field . . . . .	60
Earthquake density in the southern Great Basin . . . . .	70
Discussion of seismicity and tectonics . . . . .	77
SGB Microearthquakes and their relevance to the occurrence of larger earthquakes . . . . .	80
Seismicity and local structure at Yucca Mountain . . . . .	81
Regional structure, Great Basin tectonic models, and the characteristics of contemporary seismicity . . . . .	82
Summary . . . . .	90
References cited . . . . .	93
Appendix A. System frequency response curves and calibrations . . . . .	101
Appendix B. Station codes, locations, instrumentation and polarity reversals . . . . .	107



Appendix C. Input parameters to HYPO71 . . . . .	113
Appendix D. Catalog of August 1978 through December 1983 hypocenters keyed to maps of SGB quadrangle names . . . . .	115
Appendix E. 1982-1983 focal mechanisms with table summarizing mechanisms computed 1979-1983 . . . . .	166
Appendix F. Stereographic plots of southern Great Basin earthquake hypocenters at selected locations . . . . .	187

## ILLUSTRATIONS

	Page
Plate 1.- Seismicity and focal mechanisms for the period August 1, 1978, through December 31, 1983 in the southern Great Basin . . . . .	In pocket
Figure 1.- Map of generalized seismic zones and tectonic features in the southern Great Basin. . . . .	4
Figure 2.- Southern Great Basin seismograph stations . . . . .	5
Figure 3.- Ratio of free surface displacement amplitude for the converted $SV - P$ ray to the $SV$ ray for vertical and horizontal components versus ray angle of incidence. . . . .	10
Figure 4.- Scattergram of the predicted $M_D$ plotted as a function of observed $M_L^{SGB}$ . . . . .	13
Figure 5.- (a), Scattergram of $M_{ca}$ versus $M_L$ for 250 digitally recorded SGB earthquakes (b), Comparison of $M_{ca}$ station corrections with $M_L^{SGB}$ station corrections. . . . .	15
Figure 6.- The theoretical $S$ to $P$ amplitude ratios due to interface- and free surface effects for rays leaving the second and third layers of SGB velocity model. . . . .	17
Figure 7.- Regional seismicity, August 1, 1978 through December 31, 1983. Boxes indicate the areas shown in figures 10 through 16. . . . .	20
Figure 8.- Regional seismicity for the calendar years 1982 and 1983. Boxes indicate the areas shown in figures 10 through 16. . . . .	21
Figure 9.- Historical southern Great Basin seismicity spanning the time period 1868 through August, 1978. . . . .	22
Figure 10.- Seismicity and focal mechanisms in the southern NTS region, for the time period August 1, 1978, through December 31, 1983. . . . .	23
Figure 11.- Faults, seismicity and location of drillhole G1 at Yucca Mountain . . . . .	24
Figure 12.- Seismicity and focal mechanisms in the northern NTS region for the period August 1, 1978, through December 31, 1983. . . . .	25
Figure 13.- Seismicity and focal mechanisms west of NTS for the time period August 1, 1978, through December 31, 1983. . . . .	26
Figure 14.- Seismicity east of NTS for the time period August 1, 1978, through December 31, 1983. . . . .	27

Figure 15.— Seismicity in the Pahrnagat shear zone for the time period August 1, 1978, through December 31, 1983. . . . .	28
Figure 16.— Seismicity and focal mechanism in the vicinity of the Pahroc Valley and North Pahroc Range for the period August 1, 1978, through December 31, 1983. . . . .	29
Figure 17.— Map of regional seismicity for the period August 1, 1978 through December 31, 1983, with boxes outlining areas contained in following depth section figures. . . . .	30
Figure 18.— (a), Depth sections for 1979-1983 seismicity of eastern Jackass Flats and Lookout Peak. (b), Depth sections for the earthquakes in the southern part of Jackass Flats. . . . .	34
Figure 19.— (a), Depth sections for 1979-1983 seismicity north of Mercury Valley. (b), Depth sections for 1979-1983 seismicity in Mercury Valley near the earthquake of 831211 with faults . . . . .	35
Figure 20.— Depth section of the 1980-1983 Funeral Mountains seismicity. . . . .	38
Figure 21.— Depth sections for 1979-1983 earthquake activity in the vicinity of the Lathrop Wells. . . . .	39
Figure 22.— Depth sections for 1979-1983 activity in the vicinity of the Striped Hills. . . . .	39
Figure 23.— Epicenters and depth sections for earthquakes in the vicinity of Dome Mountain. . . . .	41
Figure 24.— Depth sections for 1979-1983 earthquakes in the vicinity of Thirsty Canyon . . . . .	42
Figure 25.— Depth sections for activity during the period 1979-1983 in Sarcobatus Flat series c. . . . .	45
Figure 26. Depth sections and a focal mechanism for activity in Sarcobatus Flat series b. . . . .	46
Figure 27.— (a), Depth section in Sarcobatus Flat series a. (b), Depth sections for Sarcobatus Flat series d . . . . .	47
Figure 28.— Depth sections for earthquakes in the Slate Ridge region, 25 km west of Scottys Junction. . . . .	49
Figure 29.— Depth sections for earthquakes in the vicinity of Yucca Flat. . . . .	50
Figure 30.— (a), Depth sections for earthquakes in the Indian Spring Valley and Spotted Range, just east of NTS. (b), Depth sections for earthquakes in the vicinity of the town of Indian Springs and Highway 95. . . . .	51
Figure 31.— (a) Pahrnagat Shear Zone depth sections (b) Same data, different projection planes. . . . .	53
Figure 32.— Depth sections for the North Pahroc Range. . . . .	54
Figure 33.— Distribution of focal depths for well-located SGB earthquakes for the calendar years 1982 and 1983. . . . .	56
Figure 34.— $P$ -wave velocity, $v_p$ , versus depth for 3 SGB velocity models . . . . .	57

Figure 35.- Distribution of average standard depth-of-focus error versus estimated depth of focus, for the data plotted in Figure 33. . . . .	58
Figure 36.- Probability of an earthquake occurring at a depth $z$ using velocity model M0 and the same data as in Figure 33. . . . .	59
Figure 37.- Distribution of focal depths below mean station elevation obtained using velocity model M1 and HYPOELLIPSE. . . . .	61
Figure 38.- Distribution of focal depths below mean station elevation obtained using velocity model M2 and HYPOELLIPSE. . . . .	62
Figure 39.- Distribution of focal depths for (a) the eastern SGB (b) the central SGB, and (c) the western SGB with inset map showing the three regions. . . . .	63
Figure 40.- (a), Intersection of pressure dihedral and tension dihedral for 29 southern Great Basin earthquake focal mechanisms. (b), Same as 40 (a) using only the 14 earthquakes having depth of focus, $z \leq 6$ km. (c), Same as 40 (a) using only the 15 earthquakes having $z > 6$ km. . . . .	65
Figure 41.- Inferred directions of principal stress components, $\sigma_1, \sigma_2$ , and $\sigma_3$ , shown in Table 3. . . . .	66
Figure 42.- Thirty southern Great Basin earthquake focal mechanisms plotted in depth section over the meridional range of the SGB network. . . . .	68
Figure 43.- Four models showing how vertical and horizontal stresses may be distributed with depth. . . . .	69
Figure 44.- Distribution of number of earthquakes per unit area as a function of distance from Yucca Mountain. . . . .	71
Figure 45.- Distribution of $\log_{10}(E)$ , where $E$ represents the cumulative earthquake energy release, as a function of epicentral distance from Yucca Mountain. . . . .	74
Figure 46.- Contours of earthquake energy release in the southern Great Basin of Nevada and California for the period August 1, 1978 through December 31, 1983. . . . .	75
Figure 47.- Countours of earthquake energy release in the southern Great Basin of Nevada and California for the period 1865 through July, 1978. . . . .	76
Figure 48.- Contours of earthquake energy release for the period August 1, 1978 through December 31, 1983 in depth section for earthquakes projected onto an east-west plane (a) and a north-south (b) plane. . . . .	78
Figure 49.- (a) Depth-of-focus distribution of August, 1978 through December, 1983, earthquakes projected onto an east-west plane. (b) Depth-of-focus distribution of the same earthquakes projected onto a north-south plane. . . . .	80
Figure 50.- Depth distribution of earthquake energy for the period August, 1978 through December, 1983. . . . .	84
Figure 51.- Schematic diagrams showing: (a), dextral slip along north-trending faults in the southern Great Basin and sinistral slip along north-trending faults at the eastern margin of the Great Basin; (b), dextral slip on north-trending faults and normal slip on north-northeast trending faults; (c), how north-south	

shortening and east-west extension in the southern Great Basin is accomodated by wrench faulting on northwest- and northeast- trending conjugate faults; and (d), a block-rotation model resulting from differential rates of strain in the northern Great Basin and Mojave block . . . . .	86
---	----

#### Appendix A Illustrations

Figure A1. Frequency (amplitude) response of L4C into digital computer . . .	105
Figure A2. Frequency (amplitude) response of S13Y into helicorder . . . . .	106

#### Appendix D Illustrations

Figure D1. Quadrangle names in northeast quarter of southern Great Basin. .	116
Figure D2. Quadrangle names in southeast quarter of southern Great Basin. .	117
Figure D3. Quadrangle names in northwest quarter of southern Great Basin. .	118
Figure D4. Quadrangle names in southwest quarter of southern Great Basin, with location of a Bare Mountain chemical explosion . . . . .	119
Figure D5. Seismograms from three Yucca Mountain stations recording a Bare Mountain chemical explosion of 1982-08-24 . . . . .	119

#### Appendix E Illustrations

Figure E1. Jackass Flats focal mechanism . . . . .	168
Figure E2. Mercury Valley (Camp Desert Rock quadrangle) focal mechanism . .	169
Figure E3. Composite focal mechanism from several shallow Funeral Mountains (Big Dune quadrangle) earthquakes. . . . .	170
Figure E4. Composite focal mechanism from several Funeral Mountains earthquakes. . . . .	171
Figure E5. Composite focal mechanism from several Funeral Mountains earthquakes. . . . .	172
Figure E6. Lathrop Wells focal mechanism . . . . .	173
Figure E7. Striped Hills focal mechanism . . . . .	174
Figure E8. Dome Mountain (south flank of Timber Mountain) focal mechanism	175
Figure E9. Focal mechanism for earthquake 830217 in the Thirsty Canyon area.	176
Figure E10. Focal mechanism for earthquake 830224 in the Thirsty Canyon area.	177
Figure E11. Sarcobatus Flat (Springdale quadrangle) composite focal mechanism	178
Figure E12. Sarcobatus Flat focal mechanism . . . . .	179
Figure E13. Sarcobatus Flat focal mechanism. . . . .	180
Figure E14. Sarcobatus Flat composite focal mechanism. . . . .	181
Figure E15. Scottys Junction focal mechanism. . . . .	182
Figure E16. Another Scottys Junction focal mechanism. . . . .	183
Figure E17. Mt. Dunfee (Gold Point quadrangle) focal mechanism. . . . .	184
Figure E18. Indian Spring Valley focal mechanism . . . . .	185

Figure E19. North Pahroc Range (Hiko NE quadrangle) focal mechanism . . .	186
---	-----

#### Appendix F Illustrations

Figure F1. (a) Stereo projections of hypocenters in the northern Jackass Flats and adjacent regions; this region is the same as in Figure 18a. (b) Stereo pair for southern Jackass Flats earthquakes, same region as in Figure 18b. . . . .	188
Figure F2. Stereo pair for the Mercury Valley earthquakes, same region as in Figure 19. . . . .	189
Figure F3. Stereo pair for the Funeral Mountain earthquakes, same region as in Figure 20. . . . .	189
Figure F4. Stereo pair for the Lathrop Wells earthquakes, same region as in Figure 21. . . . .	190
Figure F5. Stereo pair for the Striped Hills earthquakes, same region as in Figure 22. . . . .	190
Figure F6. Stereo pair for the Dome Mountain earthquakes, same region as in Figure 23. . . . .	191
Figure F7. Stereo pair for the Thirsty Canyon-Black Mountain earthquakes, same region as in Figure 24. . . . .	192
Figure F8. Stereo pair for the series b and c earthquakes at Sarcobatus Flat, same region as in Figures 25 and 26. . . . .	192
Figure F9. Stereo pair for the series a and d earthquakes at Sarcobatus Flat, same region as in Figure 27. . . . .	193
Figure F10. Stereo pair for the Slate Ridge earthquakes, same region as in Figure 28. . . . .	193
Figure F11. Stereo pair for the Yucca Flat earthquakes, same region as in Figure 29. . . . .	194
Figure F12. Stereo pair for the Indian Spring Valley earthquakes, same region as in Figure 30. . . . .	194
Figure F13. Stereo pair for the Pahrnagat Range earthquakes, same region as in Figure 31. . . . .	195
Figure F14. Stereo pair for the North Pahroc Range earthquakes, same region as in Figure 32. . . . .	195
Figure F15. (a) Stereo pair for the southern Nevada Test Site. (b) Depth sections for the <i>western</i> part of Figure F15a. . . . .	196

#### Tables

Table 1.- HYPO71 earthquake location quality for 1982-1983 earthquakes . . .	8
Table 2.- Summary table relating seismicity and mapped faults . . . . .	31
Table 3.- Principal stress directions resulting from minimizing variation in $\frac{\sigma_1 - \sigma_2}{\sigma_1 - \sigma_3}$ for SGB focal mechanisms . . . . .	66

Table 4.- Seismogenic areas in the vicinity of Yucca Mountain and the NTS . . .	72
Table A1.- Values of constants appropriate for SGB seismometers . . . . .	102
Table C1.- Southern Great Basin velocity model . . . . .	118
Table C2.- HYPO71 test variables as discussed in Lee and Lahr (1975) . . .	118
Table E1.- Table summarizing focal mechanisms computed for SGB earthquakes 1979-1983 . . . . .	167

# **Evaluation of the Seismicity of the Southern Great Basin and Its Relationship to the Tectonic Framework of the Region**

by

**A. M. Rogers, S. C. Harmsen, and M. E. Meremonte**

## **ABSTRACT**

Seismograph network recordings of local and regional earthquakes are being collected in the southern Great Basin to aid in the evaluation of the seismic hazard at a potential high-level radioactive waste repository site at Yucca Mountain in the southwestern Nevada Test Site. Data for 1522 earthquakes for the calendar years 1982 and 1983 are reported herein. In the period August, 1978 through December, 1983, 2800 earthquakes were located within and adjacent to the southern Great Basin seismograph network. Earthquake hypocenters, selected focal mechanisms, and other inferred seismicity characteristics are presented and discussed in relation to the local and regional geologic framework.

The principal features of hypocenters in the SGB are as follows. (1) Earthquakes are distributed in an east-west-trending band between  $36^{\circ}$  to  $38^{\circ}$  N. (2) Earthquakes display primarily strike-slip and normal-slip deformation styles over a depth range from near-surface to 10-15 km with an apparent preference for dextral slip on north-trending faults; a notable uniformity in the regional stress orientation is inferred, with the least principal stress oriented west-northwest. Approximately equal intermediate and greatest principal stress magnitudes are inferred throughout the seismogenic crust, and horizontal stress orientations are rotated clockwise in relation to the stress orientation existing in the surrounding regions. (3) It is commonly difficult to associate earthquake clusters with specific faults, particularly range front faults, although epicenter alignments and earthquake nodal planes are frequently subparallel to nearby structural grain. Two other characteristics of the seismicity have been noted, although further testing will be required to provide additional assurance that these features are not artifacts of data processing. (4) In some areas hypocenters appear to align within steeply-plunging cylindrical volumes of rock that may span depths from near-surface to 10-15 km; other hypocentral groups exhibit tabular shapes that are oriented north to northeast. (5) A seismicity minimum is observed between the depths of 3.5 to 4.0 km.

Although in many cases we are unable to relate specific earthquake activity to specific faults, we do observe correlations between earthquake epicenter lineations, focal mechanism nodal planes, and mapped Quaternary and pre-Quaternary structural grain. From these observations we conclude that faults in the region that strike from approximately north to east-northeast should be considered favorably oriented for activity in the current stress regime. Three styles of faulting are observed for focal mechanisms depending on fault orientation. These styles are dextral, sinistral, and normal faulting on north-, east-northeast- and northeast-trending faults, respectively. Dextral faulting appears to be the predominant deformation mode. Oblique faulting is observed on intermediate fault orientations having appropriate dip angles. From the proximate co-existence of this range of focal mechanisms, we conclude that the regional stress field is consistently axially symmetric both geographically and with depth. That is, the intermediate and greatest principal stresses have about equal magnitude throughout the brittle crust. This conclusion is not in accord with stresses measured by hydrofrac experiments at Yucca Mountain. The regional stress field orientation, as inferred from new and previously published focal mechanisms, is characterized by a gently west-northwest-plunging minimum compressive stress and a gently north-northeast-plunging maximum compressive stress. Although this stress field is conducive to slip on north to east-northeast-trending faults, no faults on Yucca Mountain having these orientations experienced detectable

earthquakes during the 1982-1983 period. During the 1982-1983 time span, the nearest activity to the proposed repository was at Dome Mountain, about 15 km north of Yucca Mountain. However, from 1978, when regional monitoring began in this area, until 1983 one earthquake has occurred at Yucca Mountain.

Earthquake energy release per unit area is 3 orders of magnitude lower in the vicinity of Yucca Mountain compared to the regional levels. The Yucca Mountain zone of quiescence extends to the west and is connected with a zone of low-level energy release paralleling the Furnace Creek-Death Valley fault zones. At least two interpretations of this observation are possible. First, Yucca Mountain and the zone to the west could be regions of low stress due either to some form of tectonic uncoupling or previous prehistoric seismic energy release. Second, this area could be analogous to a seismic gap, where stresses are high and faults are presently locked. The lack of seismicity in the Yucca Mountain block (i.e., the upper 4 km), the disparity between the inferred regional stresses and the hydrofrac measured stresses at Yucca Mountain, and the geologic data suggesting that Yucca Mountain is underlain by detachment faults are consistent with the conclusion that Yucca Mountain is uncoupled from the regional stress field; however, other interpretations are possible. This conclusion does not preclude the possibility of significant earthquake activity on faults underlying a detachment surface. Furthermore, earthquake activity is not precluded at some magnitude level on the proposed detachment or suggested listric faults that trend through Yucca Mountain and bottom in the detachment.

Research on the attenuation of ground motion in this region indicates that  $Q$  in the southern Great Basin is high relative to California, having values in the range of 700 to 900 over the frequency band 1 to 10 Hz. Peak amplitude attenuation functions derived from our data indicate that local magnitudes reported by California observatories for earthquakes in this region may be overestimated by as much as 0.8 magnitude units in some cases. Both of these factors affect the assessment of the earthquake hazard in this region.



## Introduction

This report is the third in a series of addenda, updates, and revisions to earlier reports by Rogers and others (1981, 1983). Earlier reports presented earthquake data collected using the southern Great Basin (SGB) seismograph network, preliminary interpretations of the data and background information. Rogers and others (1983) also raised several issues regarding the seismicity and tectonics of the region. In this report, we add data collected during the calendar years 1982-83, reassess the data, and discuss some of the important consequential problems. The format of this report differs from the earlier ones in that it does not include the phase readings, durations, and first motions for each station (Rogers and others, 1983, Appendix D). Because these data are occasionally revised and because their publication requires considerable space, we believe they are best released in microfiche format at the conclusion of the study. This report does include an earthquake hypocenter list for the 1978-1983 reporting period, presenting the latest revised earthquake locations and magnitudes.

The principal intent of this report is to make data obtained by the network generally available, to indicate the progress of ongoing research, and to present preliminary interpretations of these data. Appendices A, B, C, D and E set forth the basic data related to earthquake parameters for the 1982 and 1983 calendar years. Earthquake origin times, epicenters, focal depths, magnitudes and information pertaining to the location quality for the period August, 1978 through December, 1983 are tabulated in Appendix D. A large body of data on teleseisms and regional earthquakes has also been archived by the network, but these data are not discussed herein. Locations in Appendix D and focal mechanisms in Appendix E are keyed to the geographical quadrangles (usually 7.5 by 7.5 minutes) shown in Figures D1-D4. The main body of this report presents and discusses these data, sometimes including past as well as more recent data in order to preserve continuity and perspective.

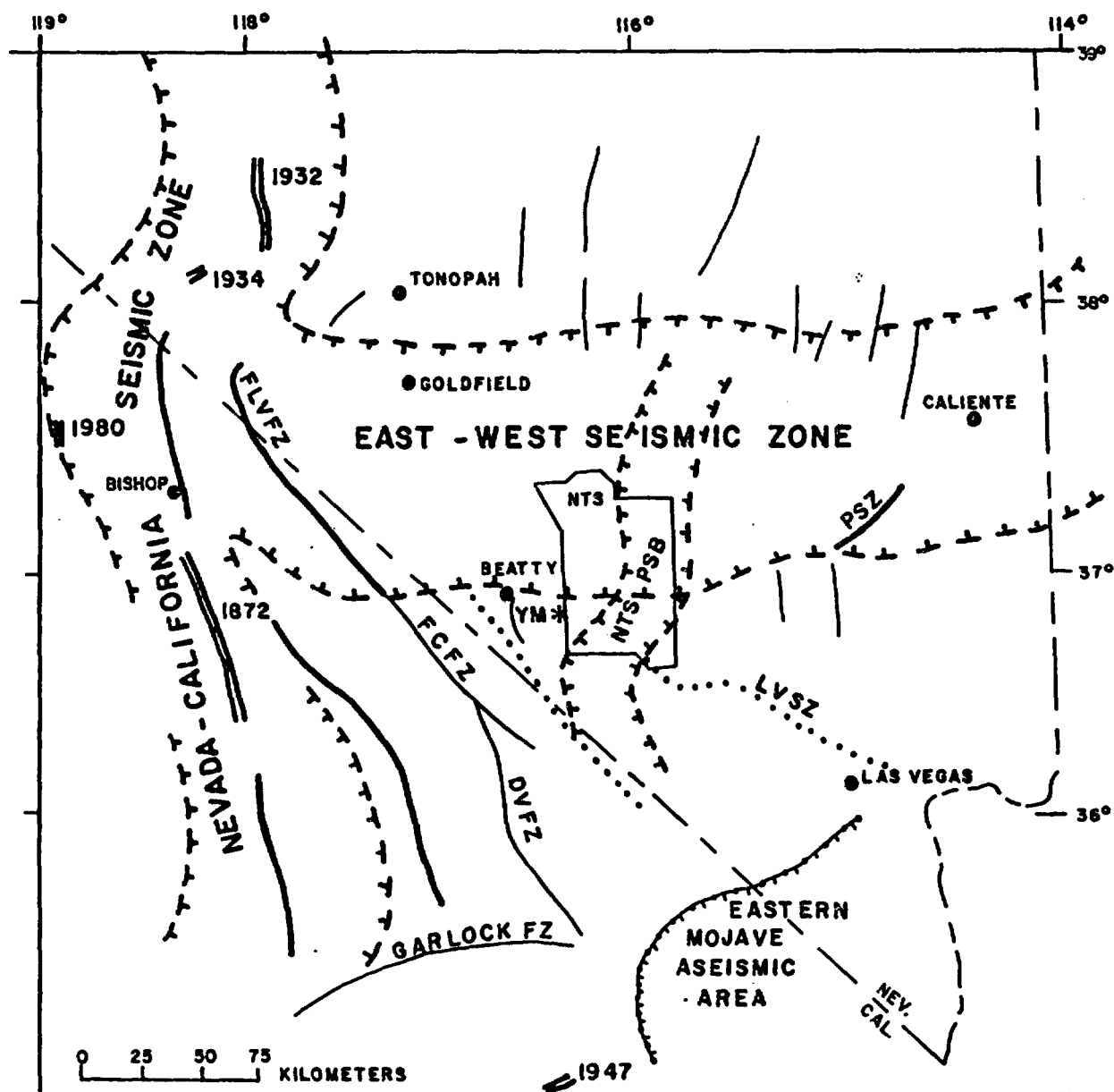
In 1979 a 47-station vertical-component seismic network was installed within a 160 km radius of Yucca Mountain to locate and study earthquakes. The network covers the tectonic features of greatest significance relative to seismic hazard assessment at NTS (Figure 1), including

- (1) Fish Lake Valley-Death Valley-Furnace Creek fault zones,
- (2) the apparent east-west belt of seismicity from 37° to 38° north latitude, and
- (3) the NTS "paleoseismic zone."

These and other features have been discussed in Rogers and others (1983); Carr (1984) reviewed the tectonics of the NTS region.

The locations of the current southern Great Basin network stations are shown in Figure 2. In May 1981, a six-station supplemental mini-net was deployed on Yucca Mountain to lower the detection threshold and to improve location accuracy for earthquakes at the proposed site. During the final half of 1984, horizontal component instruments were deployed at stations PRN, GMR, EPN, GMN, YMT4, LSM, and JON (the solid inverted triangles, Figure 2). These serve multiple purposes, including enhanced shear-wave arrival time detection, magnitude estimation for larger earthquakes, and earthquake-radiation-pattern determination.

The analog data from this seismograph network are continuously digitized ("sampled") by a PDP 11/34 computer, and the sampled data are then processed using time-domain digital processors designed to detect earthquakes and other seismic phenomena. When "events" are detected, the network digital data are stored on magnetic tape and later analyzed on a DEC PDP 11/70 computer. A discussion of the telemetry and electronics is given in Appendix A, where the frequency response curves for all systems in use are derived. The combined hardware-software package, including high-resolution graphics display terminals, results in accurate estimation of phase arrival



EXPLANATION	
1872	
==	Historic rupture, year
-T-T-	Seismically active with Quaternary faults
- - -	Seismically inactive with Quaternary faults
....	Seismically inactive without Quaternary faults
-T-T-	Eastern Mojave aseismic area
*YM	Yucca Mountain
NTS	Nevada Test Site
FLVZ	Fish Lake Valley fault zone
FCFZ	Furnace Creek fault zone
DVFZ	Death Valley fault zone
LVSZ	Las Vegas Valley Shear zone
PSZ	Pahranagat Shear zone
NTSPSB	Nevada Test Site Paleoseismic Belt

Figure 1.-Map of generalized seismic zones and tectonic features in the southern Great Basin.



times, thus reducing one source of potential error in the hypocenter location process. The uniformly high station gains, combined with the processing tools now in use, give the network the capability of recording earthquakes having local magnitudes as low as  $M_L = 0.0$ , with region-wide sensitivity at  $M_L = 1.0$ . When the computer fails, due to computer malfunction such as tape write errors, Develocorder films serve as a backup by recording activity continuously. The 11/34 computer is occasionally taken off-line for system development work and for complete backups. The down-time during the 1982-1983 reporting period was about 5% to 6%, and the films were scanned for these time periods; thus, the catalog in this report should be essentially complete. Known mining blasts and nuclear tests have been removed from the catalog, but a few possible blasts near Bare Mountain have been retained and tagged in Appendix D.

## ACKNOWLEDGMENTS

Field equipment maintenance and calibration was provided by Don Morgan of the Stanwick Corporation, under the direction of Dee Overturf and Tom Bice of the USGS, who were also responsible for equipment service and calibration at the recording facility in Golden, Colorado.

An automatic focal mechanism determination program that uses both first motion *P* polarities and *S*-to-*P* wavelet amplitude ratios was provided by Arthur Snoke of Virginia Polytechnic Institute and State University (Snoke and others, 1984). All of the mechanisms presented in this report were determined from potential solutions generated by this computer program.

We gratefully acknowledge the thorough reviews and discussions that have been provided to the authors by R. E. Anderson, K. F. Fox, W. J. Carr, D. M. Perkins, H. S. Swolfs, W. J. Spence, and G. C. P. King.

## HYPOCENTER DETERMINATION DETAILS

The same crustal velocity model, program parameters, and hypocenter quality definitions that were reported in Rogers and others (1983) are used for the locations presented in this report (Appendix D). Earthquake hypocenters are computed using HYPO71 (Lee and Lahr, 1975). The coefficients for the local duration magnitude formula are different than in previous reports as discussed in the magnitude section below. The breakdown of 1982-1983 locations by quality is as follows:

Q	Number	Percent
A	25	1.6
B	442	29.0
C	792	52.0
D	263	17.4

Table 1. HYPO71 earthquake location quality for 1982-1983 earthquakes.

Shear wave (*SV*) arrivals were used to constrain locations for most of the events in this report. One potential problem in using *S*-phase arrivals is that they may be misidentified on vertical-component seismograms because of *SV*-to-*P* conversion at near-surface high-impedance contacts. This early arriving *SV*-to-*P* phase (*SP*) can in some cases be misidentified as the *SV*-arrival (*SS*). Using the standard SGB velocity model, denoted here as M0, we examine the ratio of the free surface *SP*-to-*SS* displacement amplitudes on both vertical and horizontal components (Figure 3) (Young and Braile, 1976). This plot shows that the vertical component (solid curve) of the converted *SP*-phase has amplitude about 57% that of the *SS* or less, except near the critical angle of the reflected *SP*-phase, where the refracted *SP* has free surface amplitude about 75% that of the *SS*-phase. In practice the *SS*-phase is readily identified on the vertical component records in most cases. Identification of the *SS*-phase on horizontal records is even more favorable, as might be expected; in the worst case (i.e., all *S*-energy in *SV* and none in *SH*), the free surface *SP*-amplitude only becomes significant relative to *SS* for a narrow range of angles of incidence between 45° and 55° (Figure 3, dashed curve). Horizontal component seismographs in the network, installed during the last half of 1984, have rarely recorded *SP*- conversions this large, indicating that *SH* is also contributing substantial energy to the seismograms. The difference in arrival times of *SP* and *SS* due to a weathered layer having two km thickness, and a shear wave incident at 52° at its base, using model M0, is 0.82 seconds. An examination of many vertical and corresponding horizontal SGB seismograms reveals the presence of the *SP*-phase having about 50% to 60% the *SS*-amplitude, but we have never observed an *SP*-phase having more than about 60% the *SS*-amplitude, where the *SS*-arrival was authenticated on horizontal seismograms. Since horizontal records have become available, vertical *S*-arrival times are now routinely checked against horizontal *S*-times at the same station or at a nearby station for consistency.

The assessment of the importance of misidentified *S* arrivals on hypocenter estimation is probably best conducted on an earthquake by earthquake basis. Generalizations are difficult because the influence of the *S* readings is dependent on station azimuth and distance, travel time residual, amount of data redundancy (most solutions are vastly overdetermined), adequacy of *P* and *S* velocity models, weights assigned by the analyst to the *S* arrivals, and other factors. A HYPO71 "A"-quality solution having 20 or more phase readings will be nearly unaffected if as many as 50% of the *S* arrivals are in fact *SP* converted phases given that the *P* phases are correctly scaled: arrival time residual weighing will automatically diminish the influence of those misidentified *S* arrivals to zero. A HYPO71 "C"-quality solution having 8 phase readings and 50% misidentified *S* phases may or may not show a non-trivial depth of focus bias, i.e., the likelihood is greater in this

case that the misidentified *S* readings will influence the final solution. We conducted numerical experiments by creating a phase arrival set that was in some ways typical of a very small earthquake on the edge of the SGB network: 6 *P*- and 2 *S*-arrivals were used, the *P* arrivals were assigned uniformly distributed random errors in the range  $\pm 0.05$  seconds, one or both of the *S* arrivals were assumed to be misidentified, and were thus 0.4 to 0.8 seconds early, the azimuthal gap was  $180^\circ$ , and the nearest station was slightly more than one focal depth from the epicenter. Using only the *P* data, the solution depth converged to within 2% of the true depth of focus (8.09 km). Adding two *S*-readings, one correct and the other 0.6 seconds early, did not significantly degrade the solution (4% error in estimated depth) when both were given equal weights (HYPO71 2) by the analyst; finally, by removing the *S* arrival that had the large negative (-0.57 second) residual, the analyst recovered the true solution (to within 1%). For shallow-focus earthquakes (1 to 3 km below sea-level), the presence of a mixture of *SP* and true *S* arrivals along with 6 accurate *P* arrivals was not deleterious to the depth estimates. The basic conclusion of these and many other experiments is that about 6 or more accurate *P* arrivals are usually sufficient to determine the true hypocentral parameters, even with mediocre azimuthal coverage ( $180^\circ$ ), *at least when the velocity model closely corresponds to the local velocity structure*, and the addition of a mix of well- and mis-identified *S* readings tends at worst not to degrade the solution and often decreases the parameter error estimates, if down-weighting of phases having large residuals has been applied. From these considerations, we believe that adding horizontal-component seismometers at various locations throughout the SGB in mid 1984, and subsequently scaling *S* phases more accurately, has reduced the average standard error estimates associated with hypocenter parameter estimates, but has not had much effect on the parameter estimates themselves.

### MAGNITUDE ESTIMATION DETAILS

The first step in the estimation of local magnitude in a given region is the determination of a region-dependent attenuation correction. In the past seismologists have generally assumed that the correction applied by Richter (1958) could be applied in any region in order to maintain consistency. This attenuation correction is called the "log  $A_0$ " curve. Recent studies by Bakun and Joyner (1984) and Rogers and others (1987) have found that the log  $A_0$  curve is regionally dependent and is related to the average crustal  $Q$ .  $Q$  values near 700-900 for 1 to 10 Hz *S* waves have been determined for the southern Great Basin (Rogers and others, 1987), and, in comparison, a  $Q$  determination for central California of  $Q = 135f$ ,  $f$  in Hz, was found by Bakun and Joyner (1984) using a similar technique. (The ground motion frequency is specified by  $f$ ). Operation of Wood-Anderson seismographs in the region is another requirement for the determination of local magnitude. Herrmann and Kijko (1983) and Rogers and others (1987) have demonstrated that a magnitude value closely approximating Richter magnitude can be calculated using the peak amplitudes from earthquakes recorded using the U. S. Geological Survey telemetered network. This magnitude value should be properly called  $M_{bLg}$ , because calculation of the magnitude uses a formula that resembles the original  $M_{bLg}$  distance correction and because the peak amplitude used is the maximum value recorded in the shear-wave train on a vertical-component instrument. The computation of this magnitude is as follows (Rogers and others, 1987):

$$M_{bLg} = \log_{10}(PWA) - \log_{10}(A_0)$$

$$-\log_{10}(A_0) = 0.833 \log_{10}(r) + 0.00164r + 0.88,$$

where  $r$  = hypocentral distance in km and PWA is a pseudo-Wood-Anderson peak amplitude multiplied by factors to correct the vertical component to an estimated peak horizontal motion

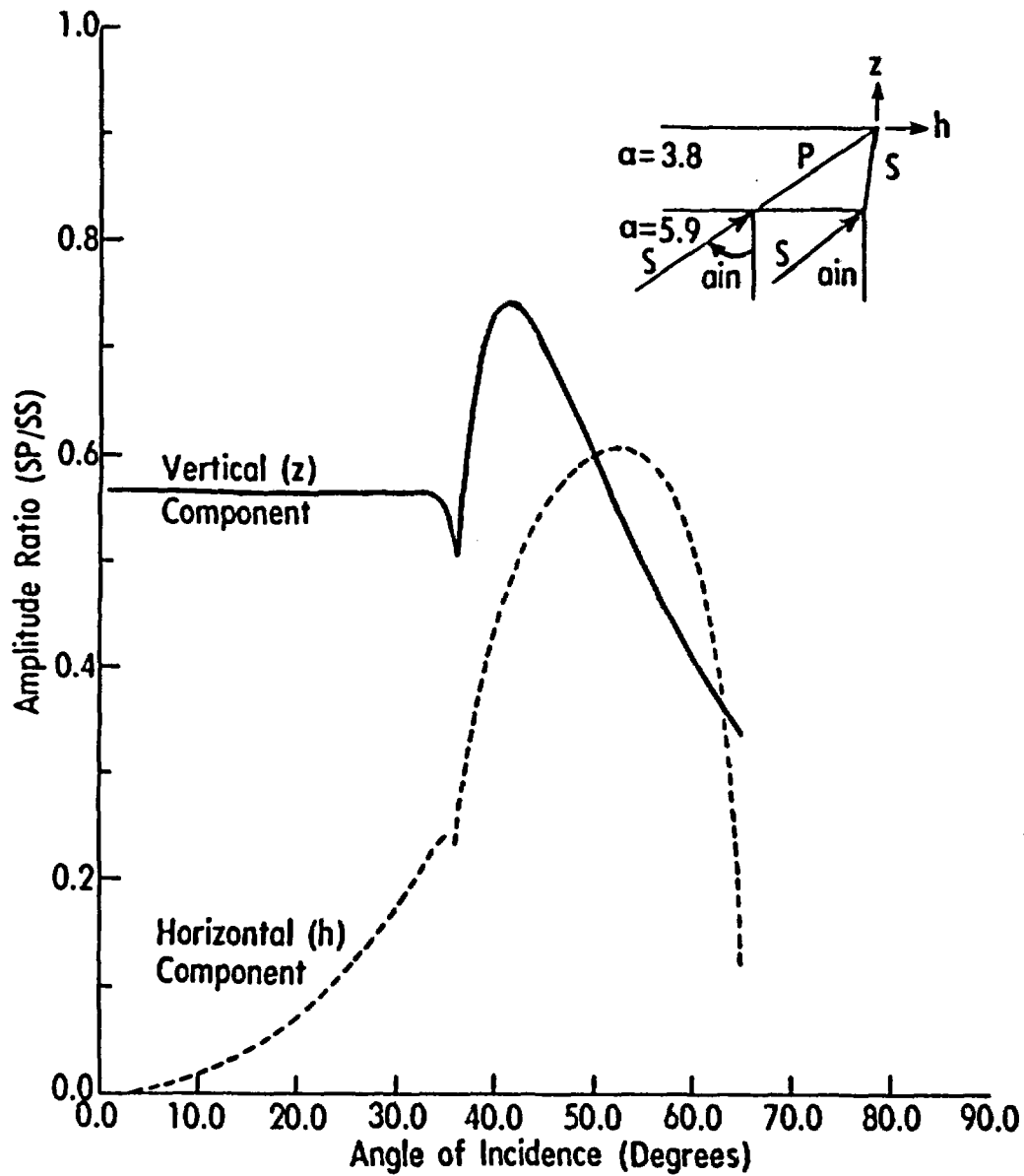


Figure 3.— Ratio of free surface displacement amplitude of the  $SVP$  to the  $SVSV$  ray for the vertical (solid) and horizontal (dashed) components plotted as a function of angle of incidence of a plane  $SV$  wave at the base of the weathered layer. The inset indicates the ray geometry.  $\alpha$  is the  $P$  wave velocity (km/sec). Beyond  $63^\circ$ , the refracted  $P$  ceases to exist for the velocity model used here.



and a factor to correct a PWA amplitude for a residual instrument response effect (see Rogers and others, 1987 for details). The value of these factors are 1.75 and 1.41, respectively. When one or more peak amplitude readings are available for an earthquake,  $M_{bLg}$  is computed and reported in Appendix D.

The estimation of local magnitude,  $M_L$  or  $M_{bLg}$ , from coda duration and source-station distance has been found to be a practical alternative to magnitude estimation based on wavelet amplitude (Lee and others, 1972). This method first requires development of an empirical relationship between  $M_L$  and coda duration. The task is to find the best coefficients  $a, b, c$ , and possibly  $d$  in the expression

$$\begin{aligned} M_d &= a \log_{10}(r) + br + c + dh + STA_k \\ &= M_L + \text{residual} \end{aligned}$$

where

- $M_d$  = duration magnitude estimate,
- $M_L$  = a local magnitude estimate, preferably a true Wood-Anderson magnitude  
or in this case a network  $M_{bLg}$ ,
- $r$  = total coda duration in seconds,
- $r$  = source-station distance in km (epicentral or hypocentral),
- $h$  = earthquake depth of focus in km,
- $STA_k = k^{th}$  station magnitude correction,

and the ranges of independent variables over which these coefficients may be used. It has been recognized (Aki and Chouet, 1975) that regional variations in tectonics and attenuation affect the rate of decay of coda, and that total measured coda duration is a function of the passband of the instruments in use (e.g., Bakun and Lindh, 1977); therefore, we expect that any  $M_d$  formula should be unique to each local network, indeed, to each instrument type within a network. In the southern Great Basin, all instruments have similar responses, and differences are absorbed into station corrections.

In the following we assume that an accurate estimate of  $M_L$  for each event has been obtained by independent means. For the SGB network,  $M_L$  is an  $M_{bLg}$  value. We estimate coda  $r$  on a Tektronix graphics display screen or on Develocorder films. Epicentral or hypocentral distance,  $r$ , is routinely obtained from a standard local earthquake location program. The statistical parameters  $a, b, c$ , and  $STA_k$ ,  $k = 1, \dots, nsta$ , are estimated from regression on the model above, using the constraint that  $\left(\sum_{k=1}^{nsta} STA_k\right) = 0.0$ . In this study, we set  $d = 0.0$  and use hypocentral distances rather than epicentral distances. The linear nature of the regression curve above requires that the duration magnitude - local magnitude relationship be linear in the range in which the magnitude data are used. A non-linear relationship is observed between coda duration and  $M_L$  for events with less than ten second durations; thus, events having average coda length less than ten seconds are excluded from the regression analysis. Also, low magnitude ( $M_L < 0.5$ ) events are excluded from the regression analyses because  $M_L$  should always be available for these events (i.e., even the nearest stations to these earthquakes should not saturate so peak amplitudes may be scaled). In the regression which follows,  $M_{bLg}$  may be thought of as the observed response variable, and  $M_d$  as the predicted response. The regressions performed here minimized the quantity

$$\sum_{i,j} (\overline{M_{bLg}(i)} - M_d(i,j))^2,$$

where  $\overline{M_{bLg}(i)}$  = average  $M_{bLg}$

scaled at five or more stations, for the  $i^{\text{th}}$  earthquake, and where  $j$  indicates the  $j^{\text{th}}$  station having a coda duration reading for that earthquake.

The results of this regression are

$$M_d = 1.67(\pm 0.028) \log_{10} r + 0.00227(\pm 0.00011)r - 1.28 + STA_k(\pm ERRSTA_k)$$

where  $r$  = hypocentral distance (km). The regression is based on 133 earthquakes, 1903 duration readings, and 56 stations used. The resulting model standard deviation estimate = 0.2094, and the parameter standard error estimates are given in parentheses. The constant  $c = -1.28$  has no error estimate because  $c$  was obtained by a *a posteriori* application of the station constraint to the results of a regression analysis in which station terms were unconstrained and in which  $c$  was not explicitly included. The plot of  $M_d$  (predicted) vs.  $M_L$  (observed) (Figure 4), shows a linear fit for  $0.5 \leq M_L \leq 2.5$ . This duration magnitude formula was used for the duration magnitudes we report.

The plot of  $M_d$  vs.  $M_L$  suggests that the duration magnitude tends to underestimate  $M_L$  for  $M_L > 2.5$  suggesting a non-linear relationship between  $M_L$  and  $\log(r)$  for  $M_L$  values above 2.5. This relationship is difficult to evaluate because the entire seismograph network frequently records clipped peak amplitudes for events having  $M_L > 2.7$ . In networks that monitor seismicity having a larger range of magnitudes, with some lower gain stations available for scaling peak amplitudes, a pronounced non-linearity in the  $\log(r)$  vs  $M_L$  relationship has been observed and is equivalent to non-linearity between  $M_L$  and  $M_d$  over large ranges of  $M_L$  (for example, Bakun and Lindh, 1977). The nonlinearity may be modelled by using a  $(\log(r))^2$  dependence instead of a  $\log(r)$  dependence in the regression, or alternatively, by fitting the  $M_d$  vs  $M_L$  relationship by two or more line segments. Although we have examined the applicability of both of these methods to our data set, the limited number of data points in the appropriate magnitude range prevent us from using them with confidence. Thus, at present we will use the expression above. (In 1986, amplifier gains at LSM horizontal component seismometers were lowered to 38 db, and gains at YMT4 horizontal component seismometers were lowered to 60 db, thereby increasing the network's effective dynamic range. LSM now records amplitudes on-scale for a 100 km distant  $M_L = 4.0$  earthquake. Preliminary evidence from a few larger SGB earthquakes scaled at LSM indicates that the  $M_d$  formula above may underestimate  $M_L$  by about 0.5 units for a  $M_L = 3.5$  earthquake. These details will be discussed in a future report.)

Finally, a third method of estimating magnitude has been discussed by Johnson (1979). This method is based on a measurement of the coda amplitude and the time after the P-wave arrival time that this amplitude occurs. This technique permits magnitude estimates even if the peak amplitudes on the record are offscale and/or the entire coda length has not been "saved" by the digital system. In order to apply this method we first compute an unnormalized magnitude value at station  $j$  using Johnson's equations and constants:

$$\overline{M_{cj}} = \overline{R(r)} - A_0(j) + q \log_{10}(r),$$

where

$r$  = time after the P-wave onset,

$R(r)$  =  $\log_{10}$  of the mean coda amplitude in a 5-second time window centered around  $r$ ,

$A_0(j)$  = a constant dependent on the gain at station  $j$ ,  
and on site effects,

and  $q = 1.8$  = a constant defining the shape of the coda.

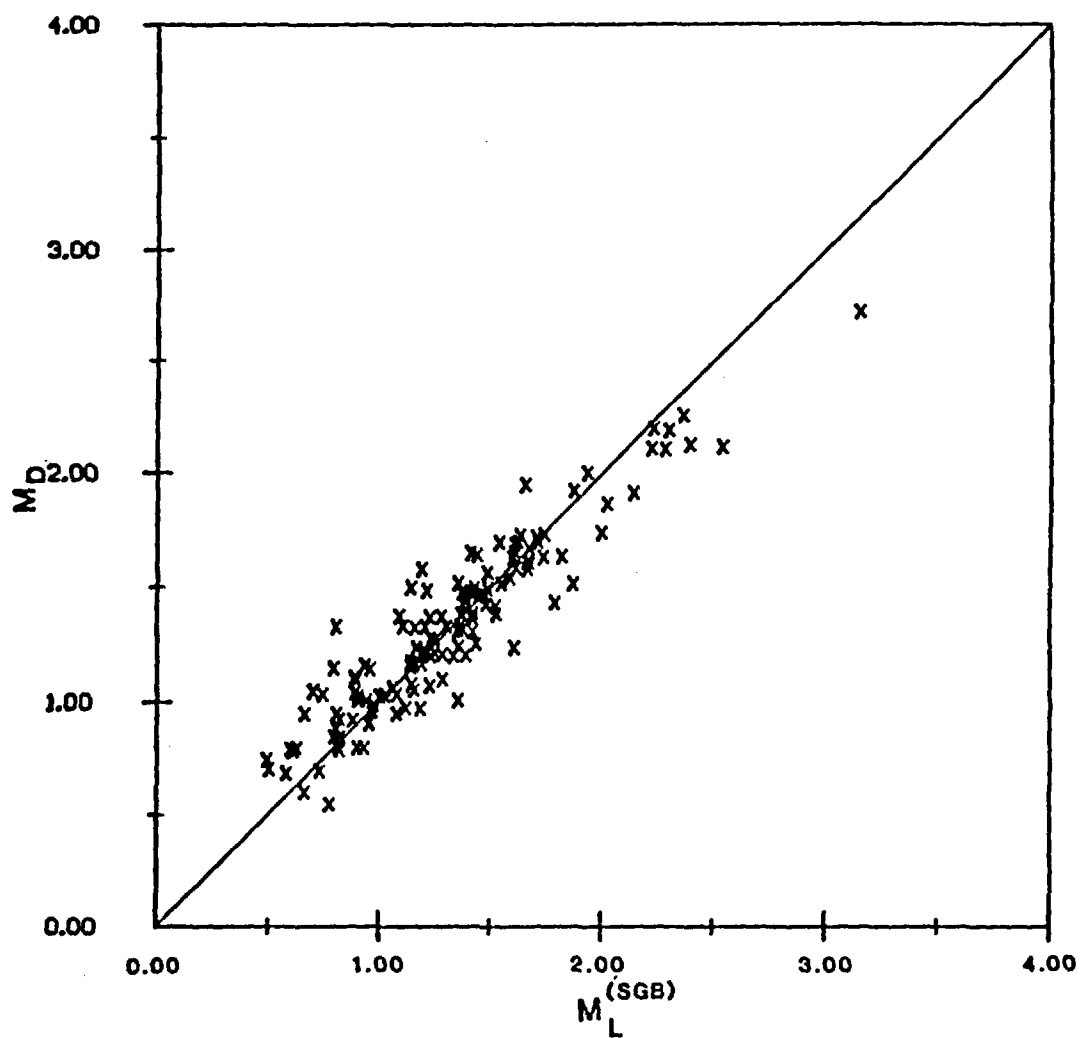


Figure 4.- Scattergram of the predicted  $M_D$  plotted as a function of observed  $M_L^{SGB}$  resulting from the regression of duration magnitude coefficients on  $M_L^{SGB}$  for 133 digitally recorded SGB earthquakes.

In principle  $q$  should be determined from the data for each region; however, in this case we determined that a reasonably stable magnitude value could be determined using the value of  $q$  determined by Johnson (1979). Generally, each station coda permits several  $M_{cj}$  estimates, one in each non clipped time window, which are then averaged. We compute  $A_0(j)$  as the average station residual for a large catalog of event  $M_{cj}$  estimates. The initial  $M_{cj}$  value is calibrated against the local magnitude,  $M_{bLg}$ , by regression of  $M'_{cj} = \overline{M_{cj}} + A_0(j)$  against  $M_{bLg}$  for a large number of earthquakes. Double averaging is here intended to indicate that several raw  $M_{cj}$  estimates at each station are obtained (one per unclipped 5 second time window), and then several stations are averaged to obtain the uncalibrated magnitude,  $M'_{cj}$ . For our data set, the coda-amplitude magnitude,  $M_{ca}$ , that closely approximates  $M_{bLg}$  is calculated from

$$M_{ca} = 0.85 M'_{cj} - 1.77.$$

Figure 5 shows the correlation between resulting coda-amplitude magnitude,  $M_{ca}$ , and  $M_{bLg}$ , designated in the figure as  $M_L^{SGB}$ . The errors, discussed above, in linearly extrapolating the  $M_L$  formula beyond the observed  $M_{bLg}$  range are also present for the  $M_{ca}$  magnitude formula when it is used to estimate magnitudes higher than about  $M = 2.5$ . Thus, the  $M_{ca}$  formula will also require revision in the future.

For reference, we also show, in Figure 5, the relation between the  $A_0$  station corrections used to compute  $M_{cj}$  and the  $M_L^{SGB}$  station corrections. The strong correlation between the two station terms for a given instrument type and gain indicates the importance of site effects on station estimates of both magnitude types,  $M_{ca}$  and  $M_L^{SGB}$ .

A more detailed discussion of magnitudes and how our new scale relates to other network magnitude estimates is presented by Rogers and others (1987). In terms of earthquake hazard estimation, a significant result of this study is a reduction in magnitude values by as much as 0.5 to 1.0 magnitude units for a given earthquake when compared to previous estimates based on magnitude scales developed for California earthquakes. As a result of this study, magnitudes for all earthquakes recorded by this network for the period from August 1978 through December 1983 have been recomputed (Appendix D). Rogers and others (1987) also noted that magnitudes for historical earthquakes in this region reported by California observatories may be overestimated by as much as 0.8 magnitude units. The overestimation is the result of applying an inappropriate log  $A_0$  curve, and is thus dependent on epicentral distance but independent of earthquake magnitude.

## FOCAL MECHANISM DETERMINATION DETAILS

Nineteen individual and composite event focal mechanisms were computed from the 1982-1983 earthquakes of this report. Hypocenters and moment tensor data are summarized in Appendix E, Table E1. The polarity readings and other details for each mechanism are shown in Appendix E, Figures E1 through E19. Focal mechanisms in this report are referenced by the earthquake date (for example, 830528); composite mechanisms are referenced by the date of the largest earthquake in the composite; the origin time (UTC) in both cases is included when necessary to avoid confusion.

Some of these mechanisms include observed and theoretical  $(SV/P)_s$  amplitude data (Kisslinger and others, 1981) as well as first-motion  $P$ -polarities. Six of the mechanisms presented in this report are relatively well-constrained by first-motion polarities alone; however, the  $(SV/P)_s$  amplitude ratios are used in conjunction with polarities to further constrain 13 solutions, that is, to help select the mechanism having the closest observed-to-theoretical amplitude ratios from all the possible solutions having a maximum allowed number of polarity inconsistencies (usually zero or one). In some instances, due to the small size of the earthquakes being analysed and due to the relative sparseness of station coverage, the  $(SV/P)_s$  ratios play a large role in constraining the solutions.

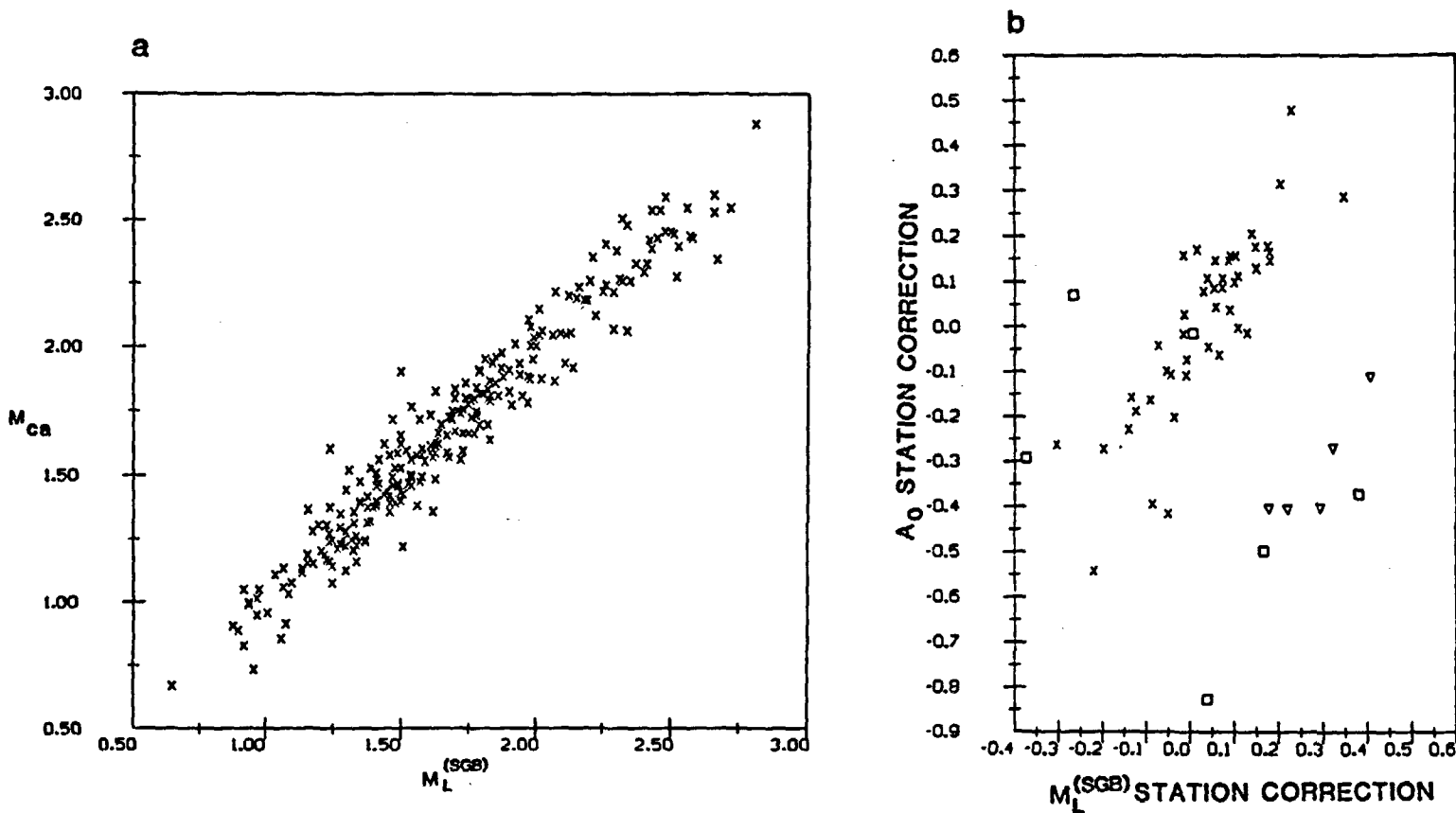


Figure 5.— (a), Scattergram of  $M_{ca}$  plotted as a function of  $M_L$  for 250 digitally recorded SGB earthquakes having at least five amplitude and five duration readings per event. Predetermined station corrections were applied. The product correlation coefficient,  $\rho(M_{ca}, M_L^{SGB})$ , equals 0.97, for this data set. (b), Comparison of the station corrections  $A_0(j)$ ,  $j = 1, \dots, n_{sta}$  with the  $M_L^{SGB}$  station corrections.  $\times$ ,  $\nabla$ , and  $\square$  represent L4C, S13O, and S13Y instruments, respectively. The  $\square$  stations on or above the  $\times$  station trend line are low gain stations. The  $\nabla$  and  $\square$  stations below the  $\times$  trend line are high gain stations.

Several assumptions, discussed in Kisslinger and others (1981), must be satisfied for the method to be valid. One assumption that was checked for the theoretical southern Great Basin velocity model is that the transmitted *P*-wave amplitude decays at a rate comparable to that of the transmitted *SV*-wave as the waves pass through crustal interfaces. The effect on the *S*- to *P*-ratio of one or two internal boundaries combined with the free surface is observed in Figure 6, in which the ratio of transmitted *S*-to-*P* body-wave amplitudes is plotted as a function of the rays' take-off angle, or angle of incidence, at the source. The compressional and torsional rays are assumed to follow identical paths. For earthquakes originating in the depth range one to three km below sea-level, the solid curve shows that the ratio is reasonably close to 1.0 for angles of incidence from 70° to 90°. For angles less than 55°, a nearly linear dependence of the ratio on angle of incidence is evident, and must be removed. This situation arises when the station's epicentral distance is on the order of 1 source depth or less. Also, for angles of incidence in the 55° to 70° range, no ratio data are usable, due to the instability resulting from free surface effects. For earthquakes originating at depths greater than three km below sea-level, the range of angles of incidence for which the *SV*-to-*P* ratio is near 1.0 is from about 77° to 90°. For angles less than 60°, the *SV*-to-*P* vertical component surface correction must be added to the observed ratio data. Because most stations are more than 3 to 4 source depths distant from the earthquakes being analysed, the majority of direct arrivals are in the range 75° to 90°, so the free surface effect is usually negligible for the data presented in this report. The relative constancy of the *SV*-to-*P* free surface particle-motion amplitude ratio over this fairly wide range of angles of incidence is a useful feature of the method, because the ray's angle of incidence is usually not very well resolved for most stations more than 2 to 3 source depths distant. Conversely, where the station is less than 1 to 2 source depths from the epicenter, the earthquake depth of focus is usually well-resolved, and the ray angle is less sensitive to errors in the velocity model; therefore, the correction for free-surface angle of incidence can be accurately determined.

Differences in anelastic attenuation for *P*- and *S*-waves could possibly affect the measured (*SV*/*P*)<sub>z</sub> ratios. Anelastic attenuation for compressional waves is not as great as for torsional waves, but this effect should be negligible for close-in (distance < 50 km) stations, since (a) the measured frequencies for the *P*-wavelet are frequently higher than for *S*, offsetting the effects of their higher velocity and *Q* (*Q<sub>P</sub>* ≈ 2*Q<sub>S</sub>* is often assumed) and (b) a recent investigation into the attenuation of shear waves in the SGB (Rogers and others, 1987) shows that the SGB is a high-crustal-*Q* region, in which neither *S* nor *P* will undergo much anelastic attenuation for stations within 50 km of the hypocenter. Quantitatively, we may assume *Q<sub>S</sub>* = 1000 and *Q<sub>P</sub>* = 2000, values appropriate to body wave propagation (geometric spreading coefficient, *n* = 1; Rogers and others, 1987, their Table 2). For *P*- and *S*-wavelets each having period 0.10 seconds (frequency 10 Hz), *α* = 6 km/sec, *β* =  $\frac{a}{1.7}$ , a plausible path correction for anelastic attenuation is

$$-\log_{10}(\exp[-10\pi r(\frac{1}{1000\beta} - \frac{1}{2000\alpha})]) = 0.0027r,$$

where *r* is the source-station distance (km). For the focal mechanism data of this report, we did not consider the anelastic attenuation path correction to be large enough, given the various uncertainties involved, to be applied.

The sparsity of seismometers in many parts of the southern Great Basin requires that we often rely on amplitude ratio data to limit the range of focal mechanisms that may be associated with a given earthquake. An example of the benefits and limitations of using amplitude ratio data to aid in the determination of the earthquake focal mechanism is shown in Appendix E, Figure E16. The *P*-wave first-motion polarities for that earthquake (831110 13:17) are inadequate to constrain nodal plane strike, dip, or rake angle: normal, strike-slip, and even oblique-thrust slip

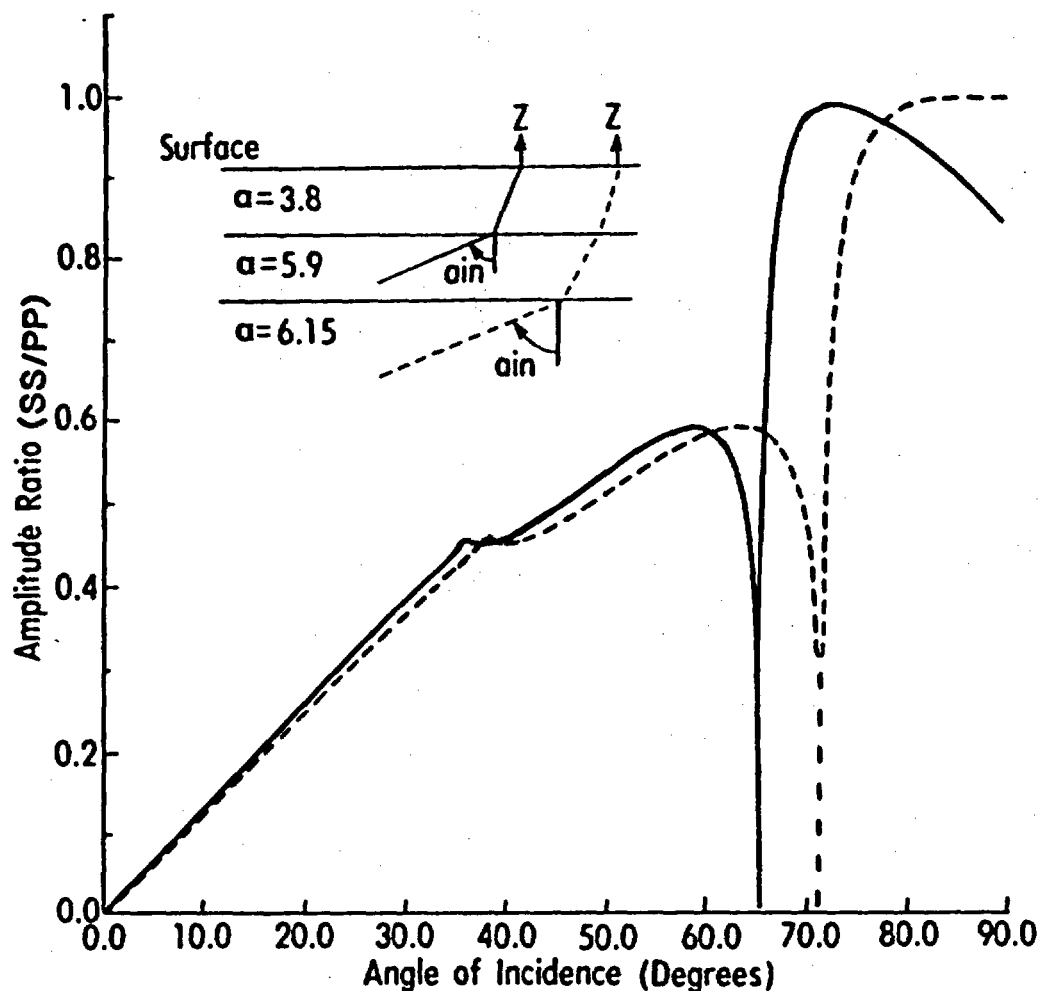


Figure 6.- The theoretical  $\dot{S}\dot{V}\dot{S}\dot{V}/\dot{P}\dot{P}$  ratio of vertical component amplitudes at the free surface is plotted as a function of angle of incidence of the  $\dot{S}\dot{V}$ - or  $\dot{P}$ -ray at the first layer boundary (solid curve), where the  $\dot{S}\dot{V}$ - and  $\dot{P}$ -waves have the same amplitudes in the second layer. The theoretical  $\dot{S}\dot{V}\dot{S}\dot{V}/\dot{P}\dot{P}$  ratio of vertical component amplitudes at the free surface is plotted as a function of angle of incidence of the  $\dot{S}\dot{V}$ - or  $\dot{P}$ -ray at the second layer boundary (dashed curve), where the  $\dot{S}\dot{V}$ - and  $\dot{P}$ -waves have the same amplitudes in the third layer. The inset shows the ray geometry involved, for earthquakes originating at depths corresponding to the second or third model layer, for velocity model M0. Anelastic attenuation effects have not been included in the calculations. The ratio of P to S velocity equals 1.71 in all layers in velocity model M0.

mechanisms are possible with no polarity inconsistencies. However, by adding 9 amplitude ratio readings, only two classes of mechanisms having 3 or fewer gross amplitude ratio errors remain, shown by the solid and dashed nodal plane solutions, respectively. For the solid-line solution, 7 of the 9 amplitude ratios are within tolerance of their theoretical values, whereas only 6 of the 9 are within tolerance for the other solution. Therefore, a weak preference may be assigned to the solid line solution. Although the solutions of Appendix E, Figure E16 imply that different geological structures are active, they have very similar T axes, and associated with other focal mechanisms, they may both be fit by the same stress field (discussed below). In summary, augmenting polarity data with  $SV/P$ , amplitude data may unambiguously constrain the most plausible solutions to extensional types, and may provide a quantitative method (minimum rms ratio error) to narrow the range to the one or two preferred solutions shown in Appendix E. In that the solution having minimum rms error is chosen from a class of solutions for which the rms error varies by about 10%, the preferred solutions should be thought of as approximations that are at least equally plausible as those for which strike, dip, or rake angles differ by about  $10^\circ$ .

## THE ASSOCIATION OF EARTHQUAKES AND MAPPED FAULTING

A question in regard to estimating seismic hazard at the proposed repository site is whether earthquakes in the region can be associated with specific known or suspected faults. This problem is considered in the paragraphs that follow as part of a discussion concerning the relationship between seismicity and the mapped geology of specific areas. Where possible we have compared seismicity with known Quaternary faults. The regional Quaternary record, however, is still under study and is incomplete. In many cases, then, we can only compare earthquake patterns with mapped pre-Quaternary structural grain, a comparison that is less desirable. Reactivation of old structures is not unusual, however, lending some credibility to these comparisons. In some cases observed relationships result in an improved understanding of the active deformational processes in the region. In light of certain limitations of the data that have been discussed above, however, the interpretations suggested must be considered tentative. Certainly, greater numbers of earthquakes should be located than currently available, and improved velocity models and earthquake location procedures should be attempted before accepting these interpretations in any definitive tectonic analysis. On the other hand, preliminary attempts to conduct joint velocity-hypocentral inversions for selected regions (Chang, written comm., 1987) seem not to materially affect our conclusions. These results will be presented in a future report. The main points in the following discussions are summarized in Table 2.

### Seismicity Overview

All earthquake epicenters (Appendix D) located by the SGB network through 1983 are plotted by magnitude range in Plate 1. Figure 7 shows the same epicenters plotted in Plate 1, with outlines of areas showing the locations of the detailed maps in Figures 9 through 14. Figure 8 shows the epicenters for 1982 and 1983 alone. Comparison of the 1982-83 (Figure 8) monitoring period with the period 1978-81 (Rogers and others, 1983) shows that many of the earlier active zones continue to produce clusters of earthquakes during this monitoring period. Comparison of the 1978-1983 monitoring period with the historic record (1868-1978; Figure 9) also leads to the conclusion that many of the earlier active regions continue to be active to 1983. In many cases, however, these zones are much more diffuse in the historic record because the accuracy of the locations is relatively low compared to the present data set. Both the historic and current seismicity maps show a band of seismicity crossing the SGB between roughly  $36^\circ\text{N}$  and  $38^\circ\text{N}$  that maybe somewhat discontinuous. That is, the east-west band may actually be the result of activity in a number of subzones across the SGB. The existence of earthquakes across this region before nuclear testing began suggests that this zone is not solely due to nuclear testing (Meremonte and Rogers, 1987). Although not



apparent in any of the figures in this report, the east-west seismic zone also exhibits a northerly extension into central Nevada at about  $116^{\circ}\text{N}$ .

Through 1983 Yucca Mountain has been within a zone of very low seismicity that extends to the west at least as far as  $117^{\circ}\text{W}$ . The historic and 1978-1983 records also show an apparent northeast-trending belt of seismicity that crosses Jackass Flats and Rock Valley about 20 km east of Yucca Mountain. This belt appears to be much more active in the 1978-1983 record, but this appearance is likely due to increased earthquake detection levels. The proposed site area at Yucca Mountain was seismically inactive during 1982-1983 (Figure 11).

Several new or previously unrecognized zones either became active or had significantly increased activity rates during 1982-83 compared to the 1978-81 monitoring period. Locations of the new activity are: earthquakes northwest of Alamo in the Pahrnagat Valley; events on the southwest side of Indian Springs Valley (Figure 14) and events in the valley to the east of the Pintwater Range; events between Mt. Dunfee and Gold Mountain and earthquakes to the east of Mt. Dunfee (Figure 13); and a cluster in Death Valley near Stovepipe Wells (between stations FMT and MCA, Figures 2 and 7). Several zones experienced increased seismicity in the 1981-82 period that may have been active only before 1978, for example: a zone of concentrated seismicity in a region of exposed bedrock between the northern end of the Hiko Range and the southern end of the North Pahroc Range (Figure 16); southwest of Alamo in the Tickaboo Valley (Figure 14); near the California-Nevada border (Figures 10 and 7).

Examination of Plate 1 shows that microseismicity in this region is largely uncorrelated with range front faults in spite of the likelihood that some of these faults, particularly in the Walker Lane belt, may be late Quaternary or younger in age (M. Reheis, personal comm., 1987). This lack of correlation suggests that these earthquakes reflect effects of deformation processes other than those directly related to the basin and range topography. Small earthquakes occurring in central Utah are also uncorrelated with the fault boundary between the Colorado Plateau and the Great Basin (Arabasz and Julander, 1986), although abundant Holocene fault scarps occur along that zone. Thus, this lack of correlation should not be taken as evidence that range front faults are unlikely to be associated with large earthquakes in the SGB.

The tectonics and seismicity for the period 1978-83 of selected regions are shown in Figures 10 through 16. Figure 17 shows the areas discussed below for which detailed maps and cross sections are presented. Appendix F contains stereo pairs for each of the active zones shown in Figure 17. A detailed discussion of focal mechanisms and active earthquake zones follows.

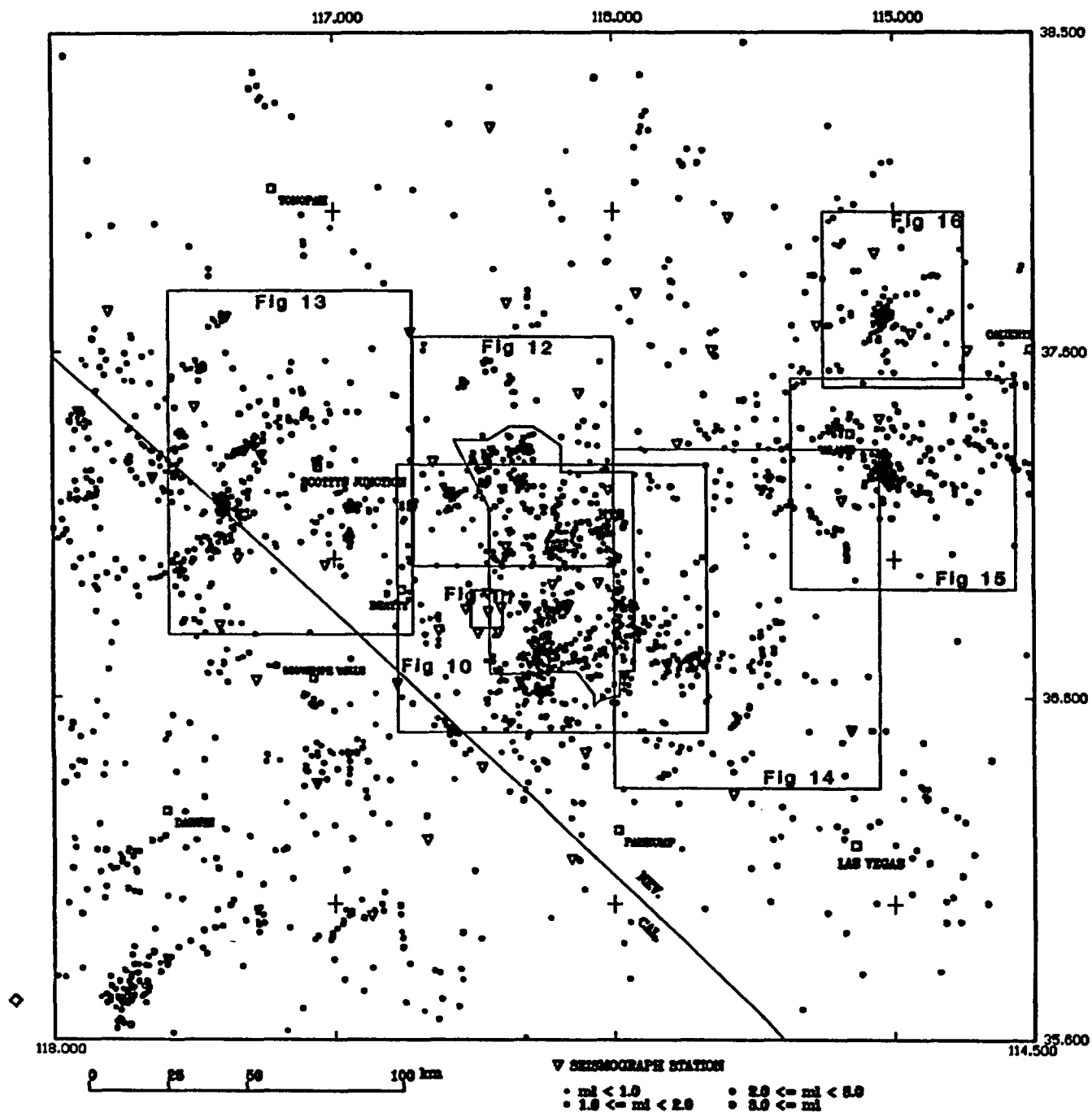


Figure 7.- Regional seismicity, August 1, 1978 through December 31, 1983. Boxes indicate the areas shown in figures 10 through 16.

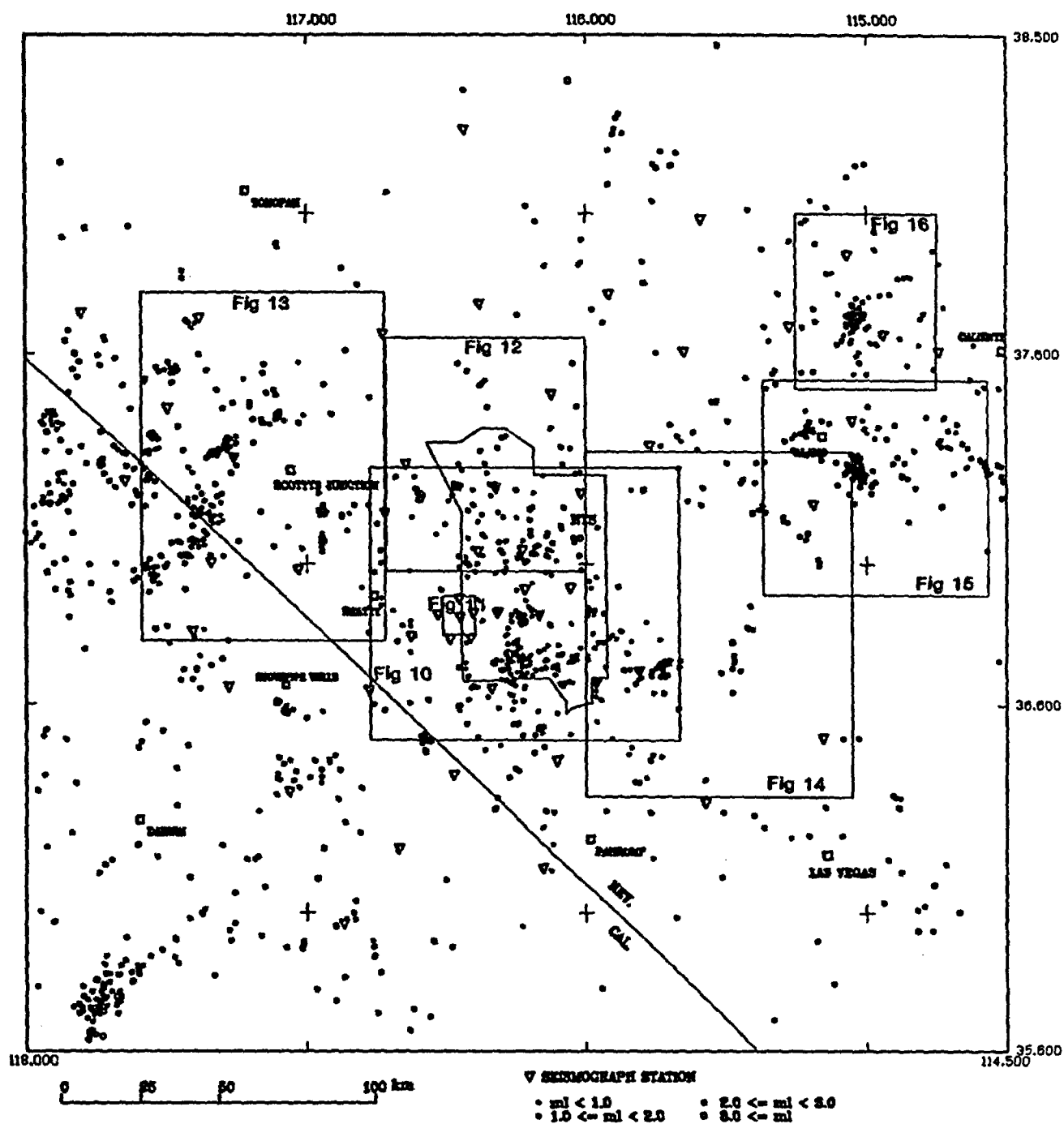


Figure 8.- Regional seismicity for the calendar years 1982 and 1983. Boxes indicate the areas shown in figures 10 through 16.

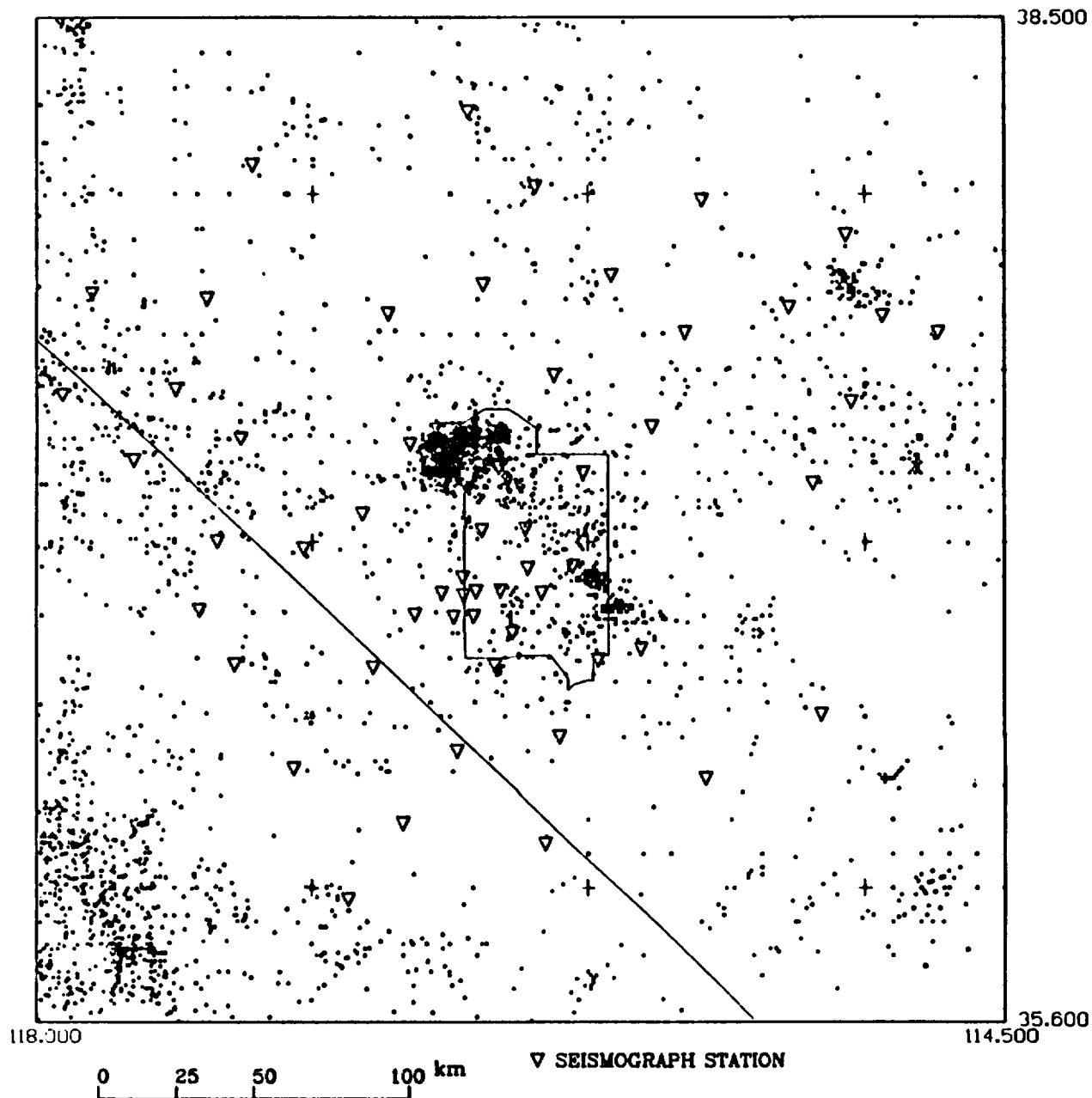


Figure 9.- Historical southern Great Basin seismicity spanning the time period 1868 through August, 1978. Because the locations in the historical record are often estimated to 0.1 degree, a single point on this plot often represents several dozen earthquakes.

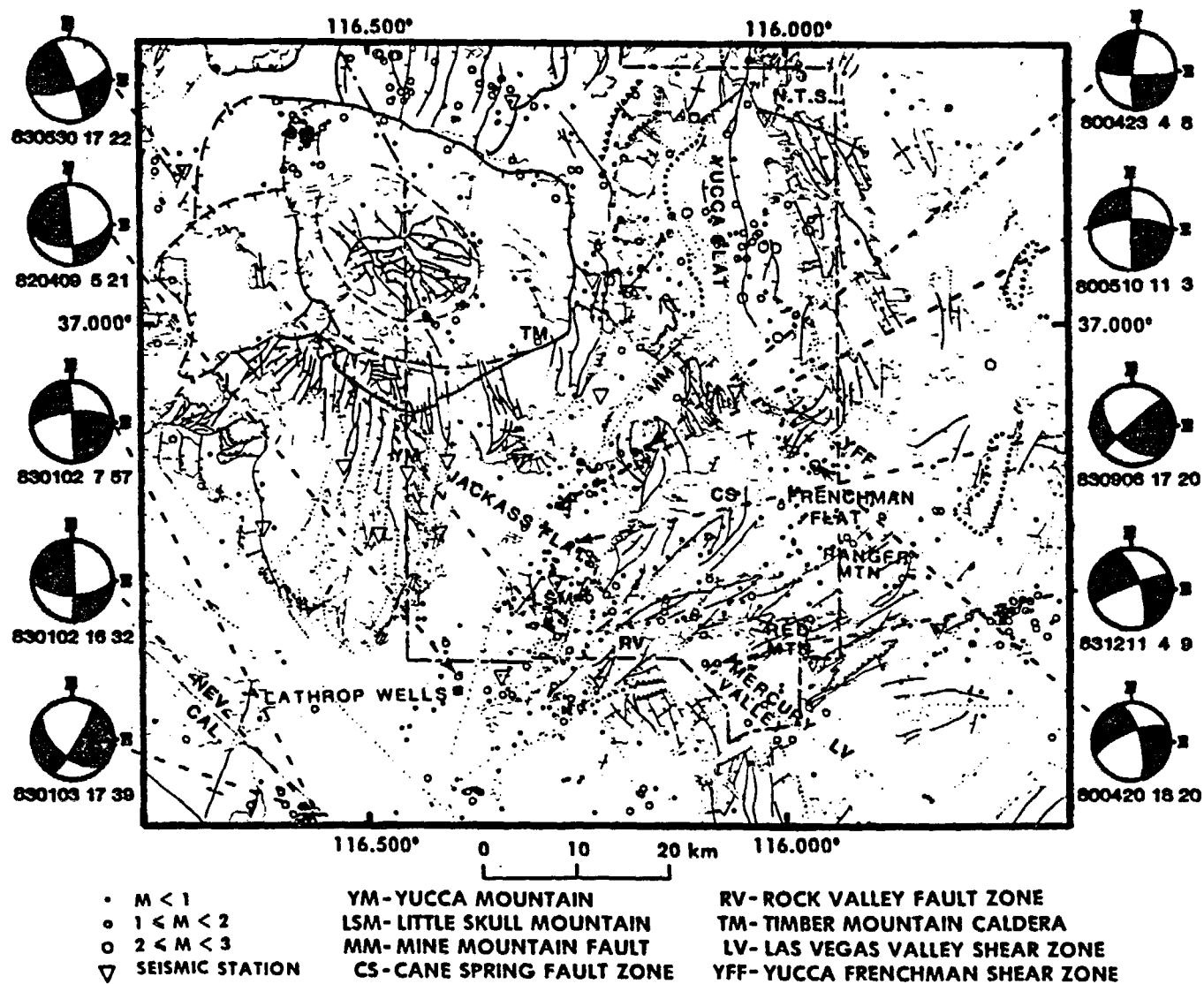


Figure 10.- Seismicity and focal mechanisms in the southern NTS region, for the time period August 1, 1978, through December 31, 1983. Faults from W. J. Carr (written comm., 1983).

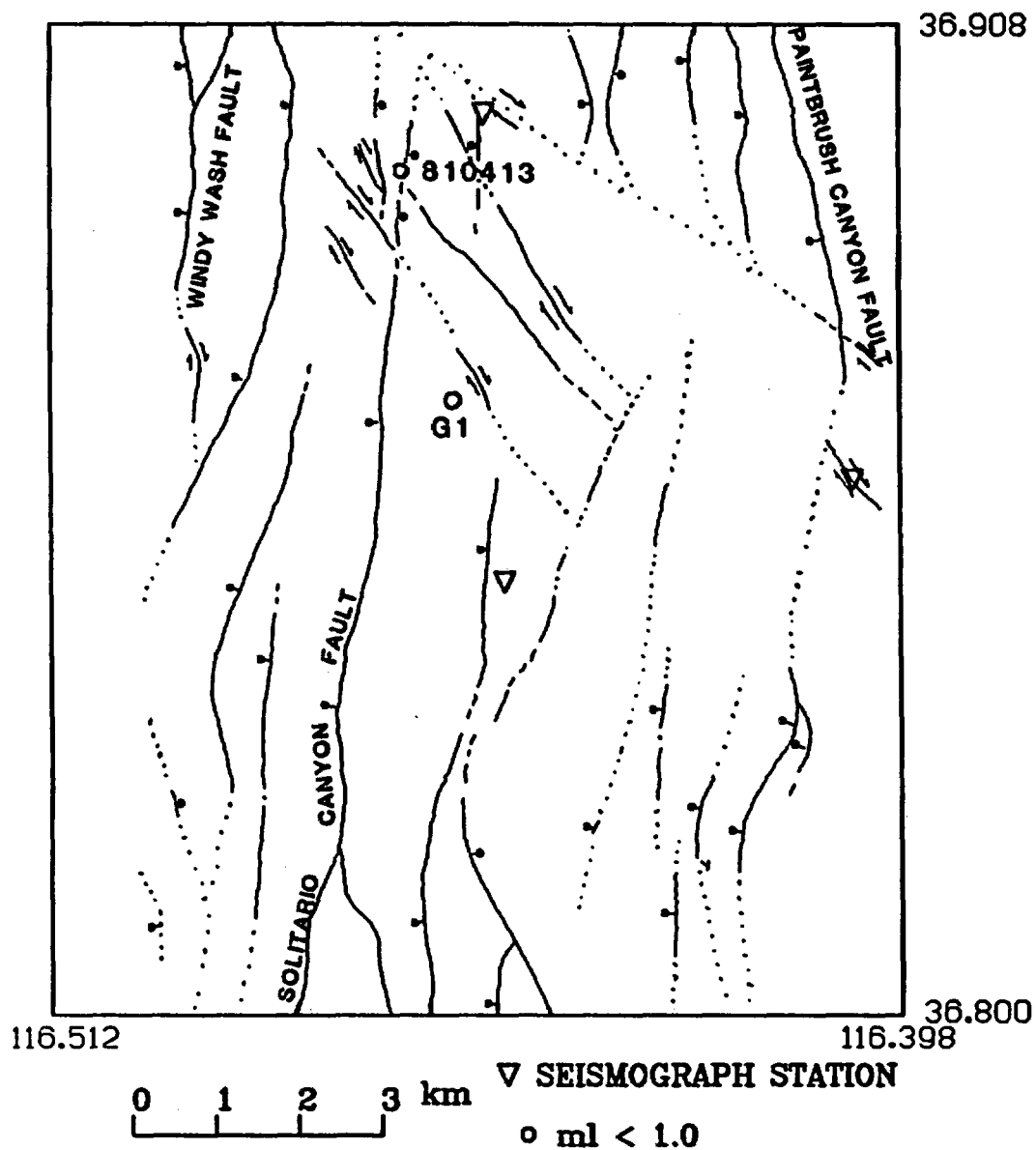


Figure 11.- Faults at Yucca Mountain (modified from USGS, 1984, their Figure 30). Solid lines indicate observed faults, whereas dashed and dotted lines indicate inferred faults. One earthquake (810413) was observed in this region during the time period August, 1978 through December, 1983. G1 - location of drillhole G1.

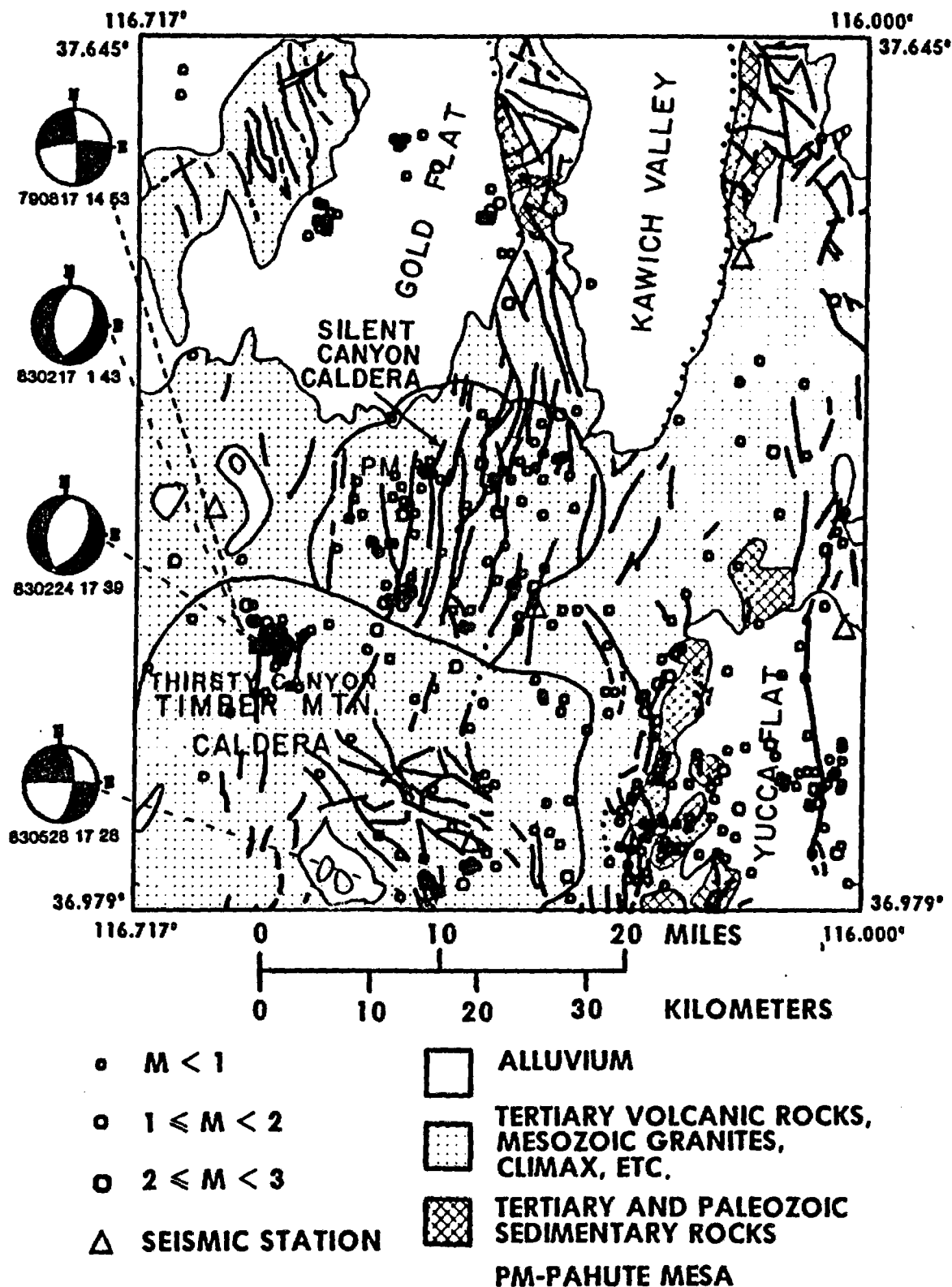


Figure 12.- Seismicity and focal mechanisms in the northern NTS region for the period August 1, 1978, through December 31, 1983. The geologic data are modified from Stewart and Carlson (1978).

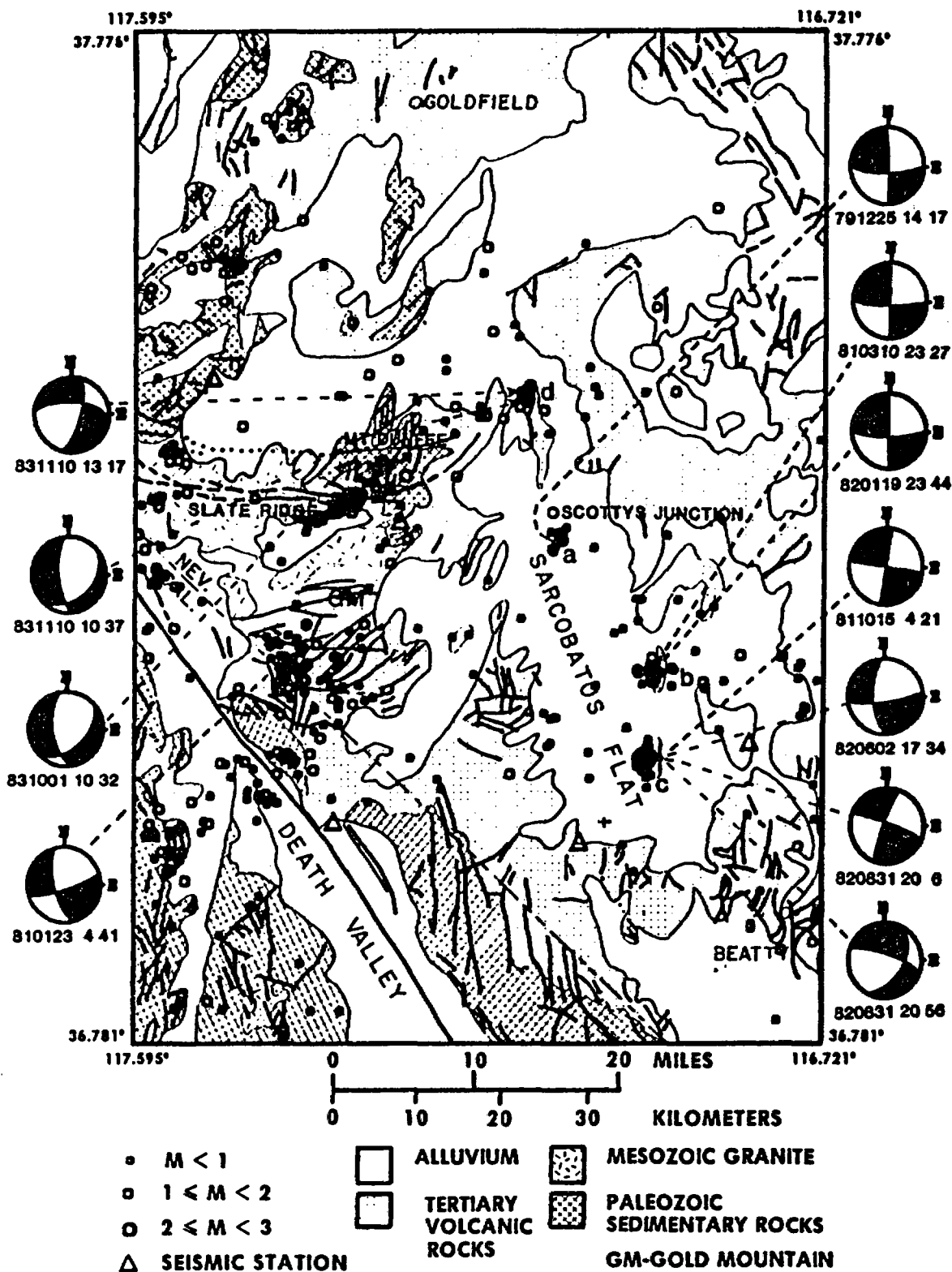


Figure 13.- Seismicity and focal mechanisms west of NTS for the time period August 1, 1978, through December 31, 1983. The geologic data are modified from Stewart and Carlson (1978).



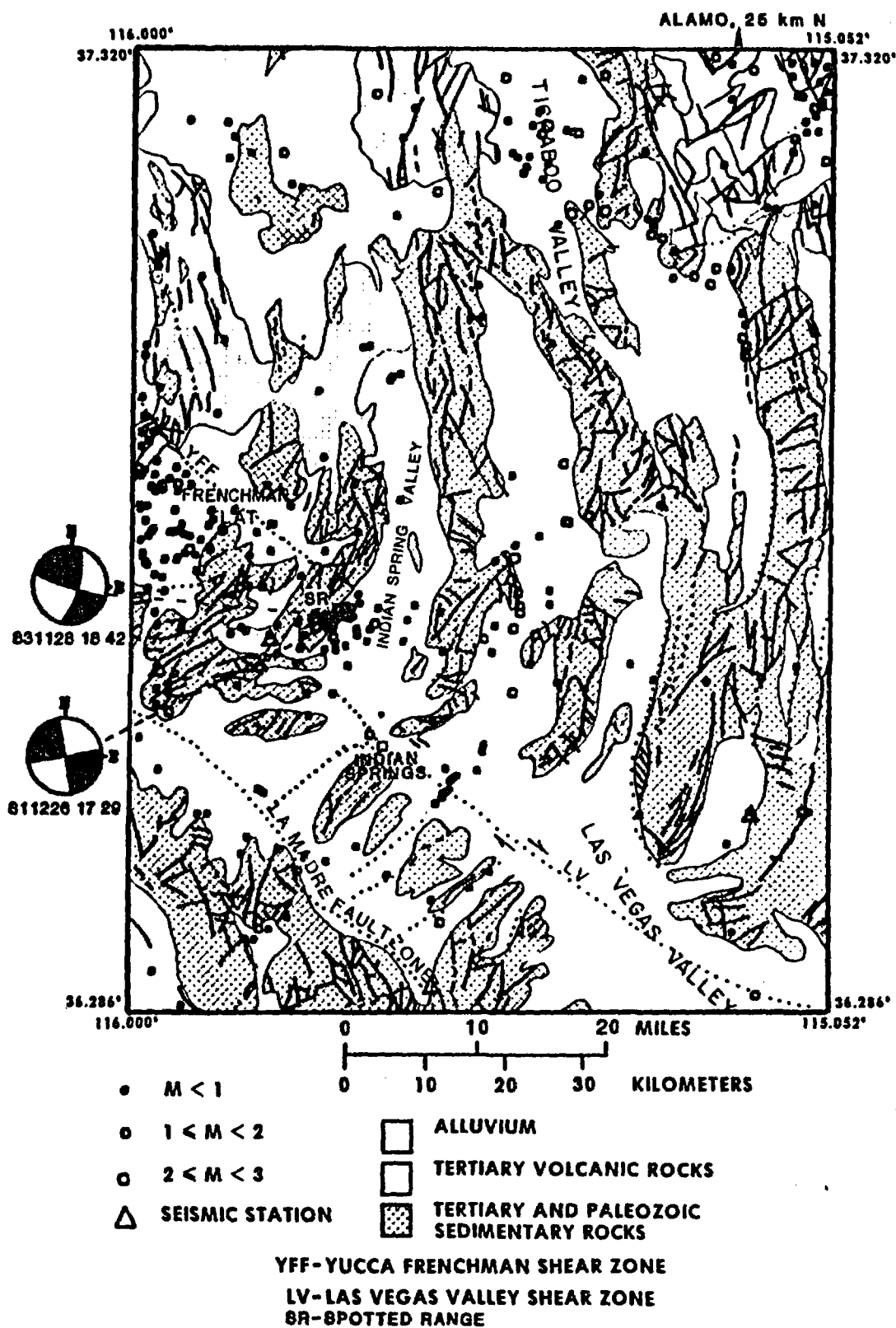


Figure 14.- Seismicity east of NTS for the time period August 1, 1978, through December 31, 1983. The geologic data are modified from Stewart and Carlson (1978).

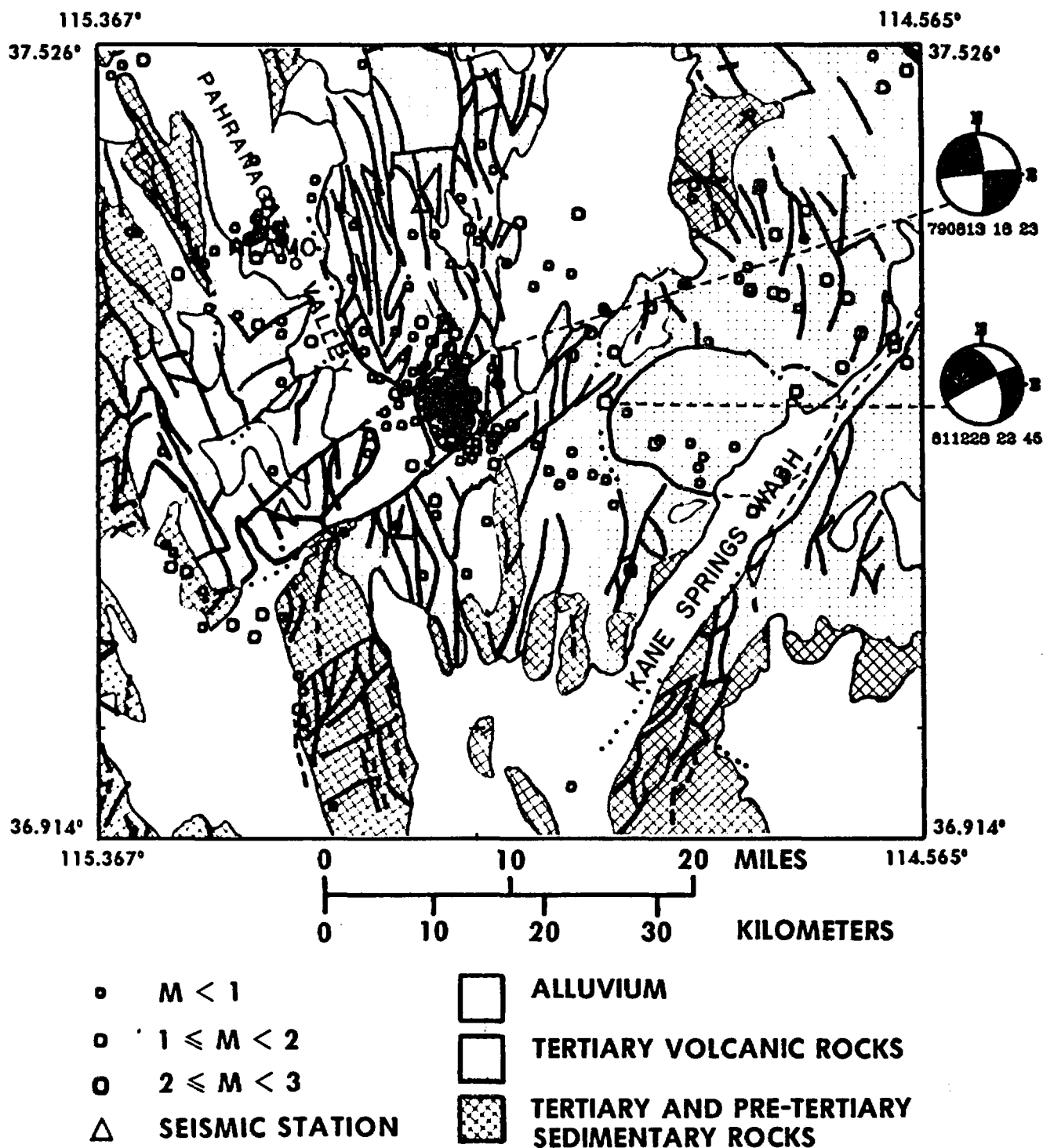


Figure 15.— Seismicity in the Pahranaagat shear zone area for the time period August 1, 1978, through December 31, 1983. The geologic data are modified from Stewart and Carlson (1978).

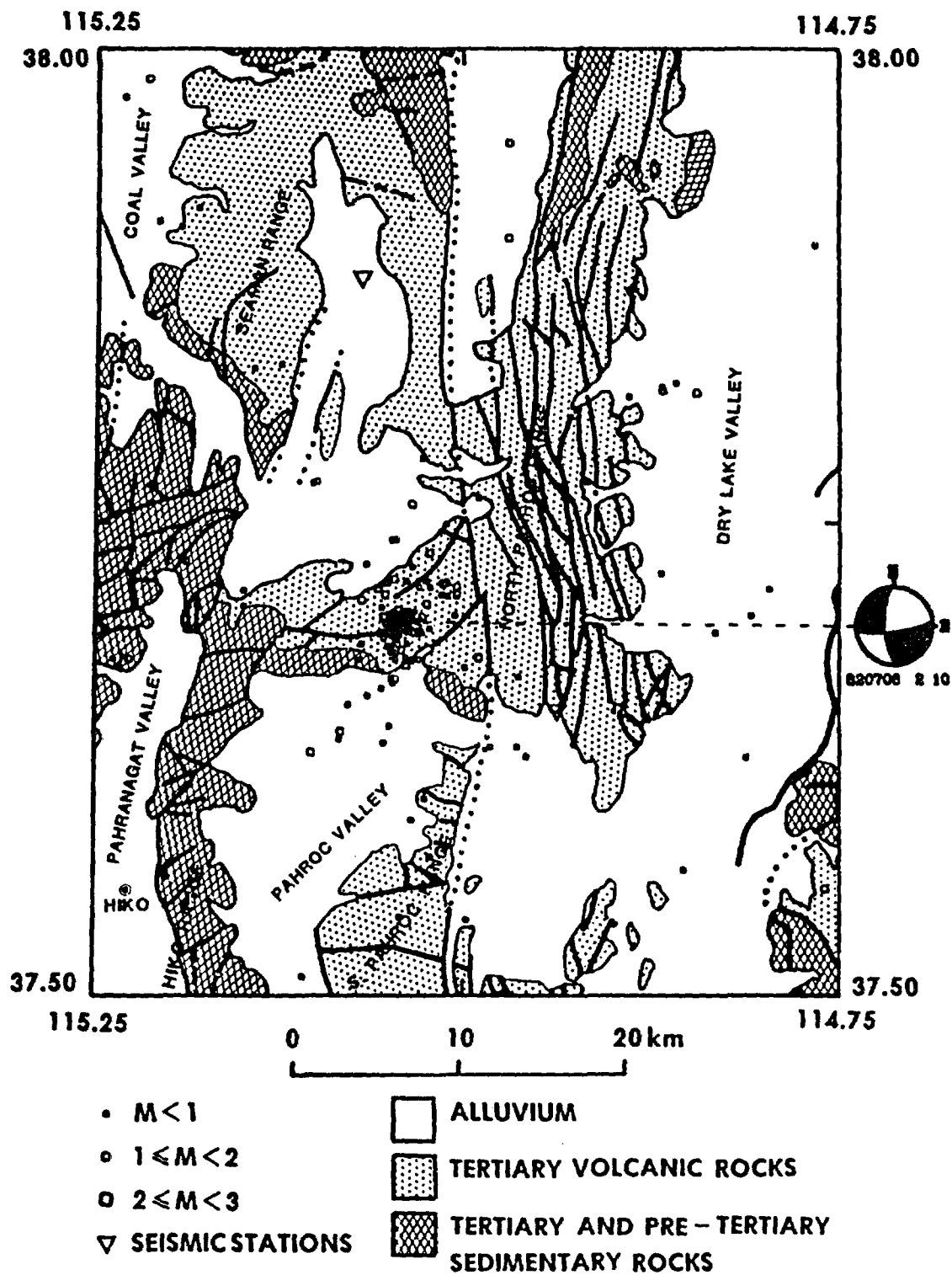


Figure 16.- Seismicity and focal mechanism in the vicinity of Pahroc Valley and North Pahroc Range for the period August 1, 1978, through December 31, 1983. The geologic data are modified from Stewart and Carlson (1978).

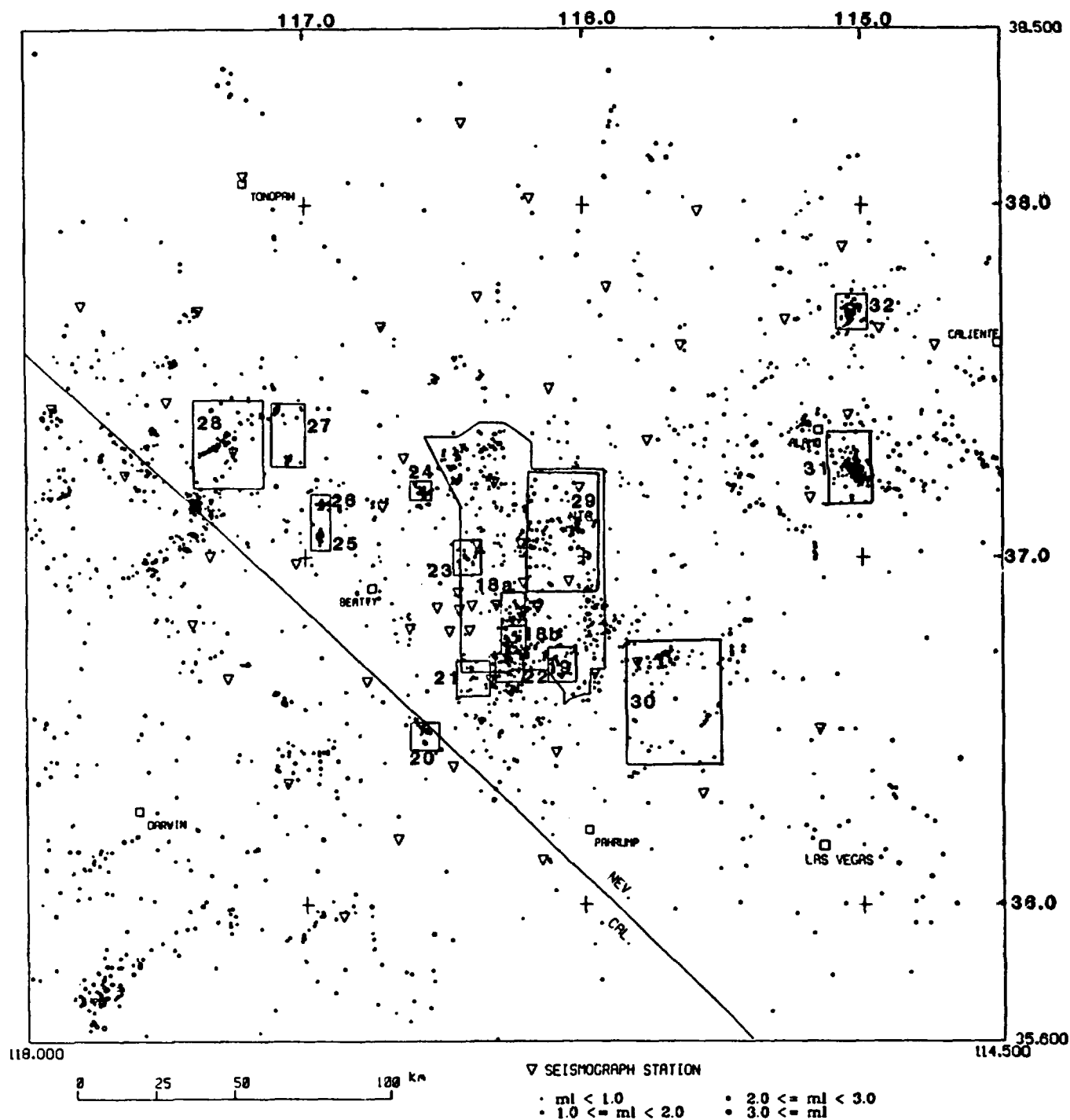


Figure 17.— Small rectangles enclose regions for which detailed epicenter and depth section plots are presented in the following figures. Numbers *within* or immediately *adjacent* to these rectangles correspond to figure numbers. The map shows the regional seismicity for the period August 1, 1978 through December 31, 1983.

Region	Activity	Trend, Dip, Slip	Data
Jackass Flats	1980 seismicity	E-W; -; - E-W; N; sinistral N-S; vertical; dextral	plan view seismicity focal mech. 800510 focal mech. 800510
	'80-'83 seismicity	NE-SW; -; - NE-SW; steep; oblique sinistral	depth section plot focal mech. 830906
	pre-Quaternary faults	NE-SW; -; -	geologic maps
Mercury Valley	'79-'83 seismicity	E-NE; steep; - E-NE; vertical; sinistral	depth section plots focal mech. 831211
Rock Valley & Cane Springs	Quaternary faults	E-NE; -; -	geologic map
Frenchman Flat & Massachusetts Mountain	'79-'83 Seismicity '71&'73 earthquakes	N; W; - N; steep; dextral	Stereo plots focal mechs. 710805 730219
Funeral Mountains	1983 seismicity  pre-Quaternary &	NW-SE; steep-NE?; - N-S; vertical; oblique dextral NE-SW; steep; oblique sinistral N-N45°; -; -	depth section plot focal mechs. 830102 focal mech. 830103 Geologic maps
Lathrop Wells	'79-'83 seismicity '82 earthquake	N-NE; -; - N; vertical; oblique dextral	Stereo plots focal mech. 820409
Striped Hills- Rock Valley	'79-'83 seismicity '83 earthquake Quaternary faults pre-Quaternary faults	E-NE; -; - E-NE; steep; sinistral E-NE; -; sinistral N20°E-N60°E; -; -	Stereo plots focal mech. 830530 Geologic map geologic map
Dome Mtn.	1983 seismicity '83 earthquake Quaternary? faults	NW; -; - N; E; dextral N; E; -	Depth sections focal mech. 830528 Geologic maps
Timber Mtn.	regional setting	NW; -; -	Walker Lane
Thirsty Canyon	1979 seismicity	N; -; - N; vertical; dextral	depth section plot & focal mech. 790817
	1983 seismicity	N-NE; W; normal	depth section plot & focal mechs. 830217, 830224
	pre-Quaternary fault	N; W; normal	geologic map
Sarcobatus Flat	earthquake series a 1979 earthquake	N; W; - N; steep; dextral	stereo plots focal mech. 791225
Sarcobatus Flat	earthquake series b 1982 earthquake Quaternary faults	N; W; - N; vertical; dextral NNW; W; -	depth section plot focal mech. 820119 unpublished mapping
Sarcobatus Flat	earthquake series c 1983 earthquakes  Quaternary faults	N; steep-W?; - N to N35°E; steep; oblique dextral NNW; W; -	depth section plot focal mechs. 830831 20:06 & 20:56 unpublished mapping
Sarcobatus Flat	earthquake series d 1983 earthquake  1983 earthquake pre-Quaternary faults	N; steep-E; - N; steep-E; oblique dextral NE; SE; oblique normal N; E; -	depth section plot focal mech. 831110 13:17 focal mech. 831110 10:37 geologic maps

Table 2. Summary of relationships of seismicity in the southern Great Basin to mapped faults (continued on next page). See the text for a complete discussion and references.

Region	Activity	Trend, Dip, Slip	Data
Slate Ridge	Feb.; '83 seismicity Feb.; '83 seismicity pre-Quaternary faults Oct.; '83 seismicity 1983 earthquakes Quaternary faults	N70°E; > 80°; - N70°E; 55°; - N10°E& E-W; -; - NE; -; - NE; E-SE; oblique normal NE; -; -	depth section plot depth section plot Geologic maps depth section plot focal mech. 831001 geologic maps
Yucca Flat	Yucca fault-Quaternary '79-'83 seismicity	N; steep-E; normal Varied (figure 26)	Geologic maps depth section & stereo plots
Indian Springs Valley & Spotted Range	'79-'83 seismicity  '81 & '83 earthquakes  pre-Quaternary faults '79-'83 seismicity  pre-Quaternary faults Las Vegas Valley Shear Zone	N; E; - N; -; -(rt. stepping <i>en echelon</i> ) ≈N; vert. to steep E; dextral  NNE; -; - NE; N-NW; -  N-NE; -; - NW; -; -	depth section fig. 30a stereo plots focal mechs. 811226 & 831128 geologic maps depth section fig. 30b  state geology map Quaternary geology maps
Pahrnagat Shear Zone	'79-'83 seismicity  1979 earthquake 1981 earthquake pre-Quaternary faults pre-Quaternary faults Quaternary faults	NE; -; -; left-stepping N; -; - N; steep; dextral E-NE; steep; oblique sinistral NE; -; - N; W; - N; -; dextral	stereo plots stereo plots focal mech. 790813 focal mech. 811228 geologic maps geologic maps prelim. reconn.
North Pahroc Range	1982 seismicity 1982 earthquake pre-Quaternary faults	N; W; -(diffuse) N; steep-W; dextral N; -; - & E; -; -	stereo plots focal mech. 820706 geology map

Table 2 (continued).

### Earthquakes in the Vicinity of Jackass Flats

The seismicity in the time period 1979-1983 in eastern Jackass Flats (see Figure 10) is plotted in depth sections in Figures 18a and b. A weak east-west lineation defined by events that occurred in 1980 (Figure 18a) includes the 800510 earthquake ( $M_d = 1.2$ ) for which a mechanism was previously prepared (Rogers and others, 1983, p. 29). That focal mechanism has an east-west striking nodal plane dipping  $70^\circ$  to the north and a vertical north-south nodal plane. Although the map view of this cluster appears to have a rough east-west lineation (Figure 18a), examination of the stereo-pair for this cluster (Appendix F, Figure F1a), suggests that this event could be interpreted as being near the southern end of the easternmost of two subparallel northerly-trending epicenter lineations.

About four km south of this 1980 activity a spatially diffuse set of earthquakes occurred from 1980 to 1983. A focal mechanism is also available for this group (event 830906; Figure 18b; Appendix E, Figure E1). The hypocenter depth sections shown in Figure 18b do not help to resolve the fault plane for this focal mechanism. The dip of the northwest-trending plane is not well-constrained by first motions, and the amplitude ratio data used to constrain the dip may have poorly modeled take-off angles; HYPO71 treats the rays as refractions from a velocity discontinuity at three km, whereas the radiation pattern model being fit assumes the rays are direct. Earthquake 830906 lies about 3 km west of Skull Mountain, where the majority of mapped pre-Quaternary faults have a northeast orientation (McKay and Williams, 1964). The mapped Pliocene faults at Skull Mountain (Ekren and Sargent, 1965) also have a northeast orientation. A weak northeast epicenter lineation (four or five events including event 830906) can be seen here, but a northwest lineation is also possible. If a choice of preferred nodal plane is made primarily on the basis of the geological structural grain, the northeast-trending nodal plane is preferred. The indicated slip on this plane is oblique sinistral motion. Additional discussion of these earthquakes follows in the next section.

### Earthquakes in the Vicinity of Mercury Valley

The Mercury Valley - Red Mountain - Ranger Mountain region produced few earthquakes ( $M_L \leq 2.0$ ) during the 1979-1983 monitoring period (Figure 9, Figures 19 a and b), but a focal mechanism for one earthquake (event 831211) was nevertheless computed. That shallow-focus earthquake ( $M_L = 1.6$ ), appearing in the center of AA' and BB' (Figure 19b), has a predominantly strike-slip focal mechanism (Appendix E, Figure E2). The earthquake occurred near the intersection of northeast-striking Quaternary faults and the northwest-striking Las Vegas Valley shear zone (Hinrichs, 1968). The left-lateral Rock Valley fault system, which trends east-northeast, is about 6 to 7 km north of the epicenter and is currently seismically active (Figure 19a). This earthquake is one of a weakly defined five-epicenter alignment that trends northeast (most easily seen in Figure 19 or Appendix F, figure F2), parallel to the Quaternary faults mapped by Hinrichs (1968). This lineation is subparallel to the group of earthquakes alining with the Rock Valley fault system to the north. Hence the northeast-striking nodal plane of earthquake 831211 is preferred. If these events, in fact, do lie on an east-northeast-trending fault, section BB' (Figure 19a) suggests that the fault dips steeply.

### Jackass Flats-Rock Valley-Mercury Valley areas

The southern quadrant of NTS includes Jackass Flats, Rock Valley (RV), and Mercury Valley (Figure 10). We have plotted, in Figure F15, a stereo-pair showing the seismicity for this area. This view shows the complexity of seismicity in the southern NTS, and also suggests several trends that are not readily apparent in the other detailed views. In spite of the fact that some of the complexity may be related to location errors, we believe that several significant features are present

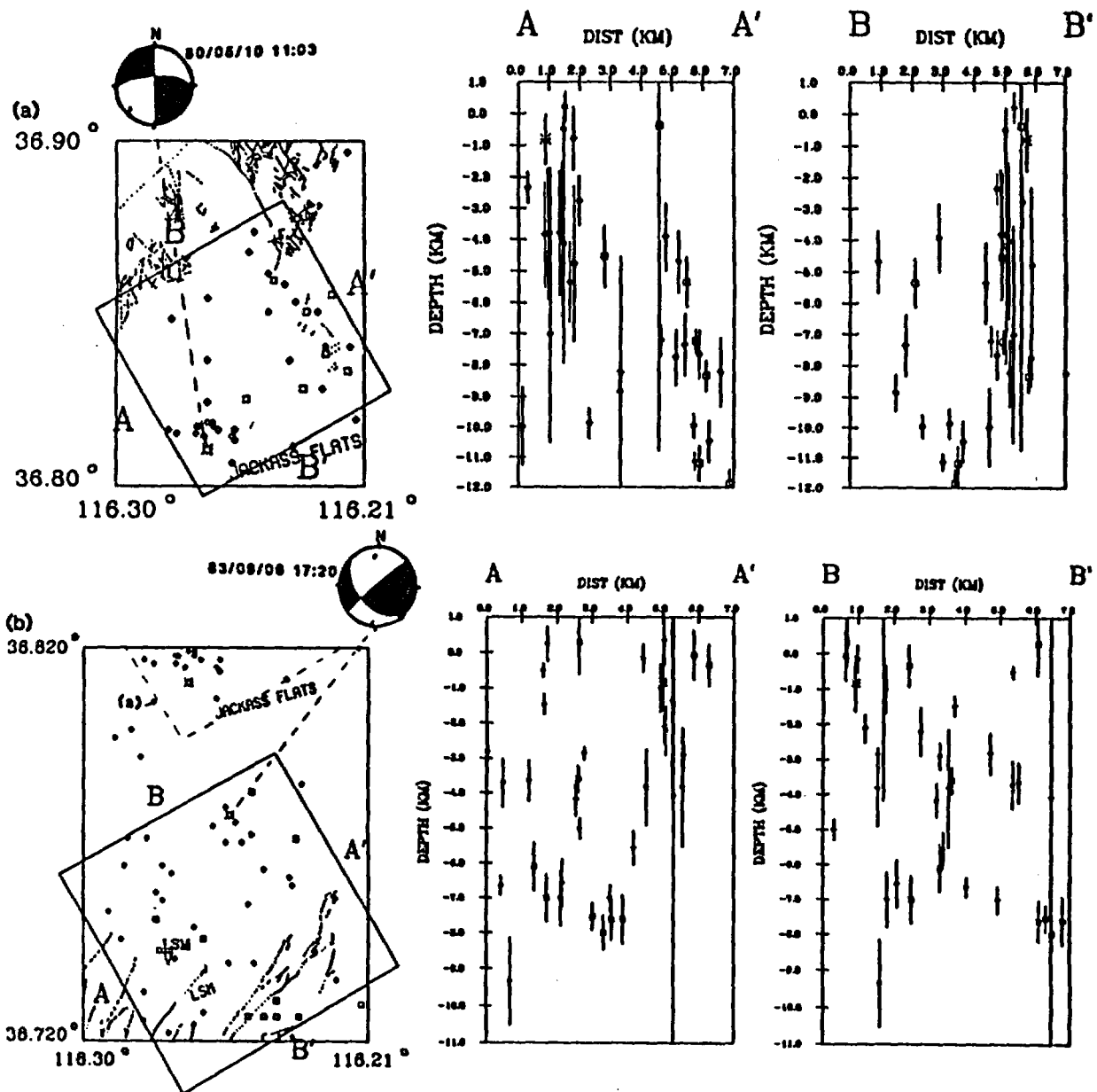


Figure 18.— (a) The 1979-1983 seismicity of eastern Jackass Flats is plotted with epicenter symbols keyed to magnitude. For this and all subsequent depth section plots, the magnitude symbols are *small diamonds* for  $M_L < 1.0$ , *small squares* for  $1.0 \leq M_L < 1.8$ , *small circles* for  $1.8 \leq M_L < 2.6$ , and *larger circles* for  $M_L \geq 2.6$ . Generally, hypocenters having focal mechanisms are plotted as *stars*. (b) The 1979-1983 earthquakes in the southern part of Jackass Flats and northern Little Skull Mountain (LSM). The vertical bar centered on each symbol in these and subsequent depth section plots represents  $\pm 1\sigma$  standard error in the depth estimate (HYPO71). Depths-of-focus are plotted in cross section if at least *five* phase readings are included in the hypocenter determination; otherwise, depth-of-focus errors are not estimable. Also, in this and the following figures the cross sections and maps are plotted at the same scale. Thus, the cross section axes can be used to scale map distances. Faults from Michael J. Carr (written commun., 1987).



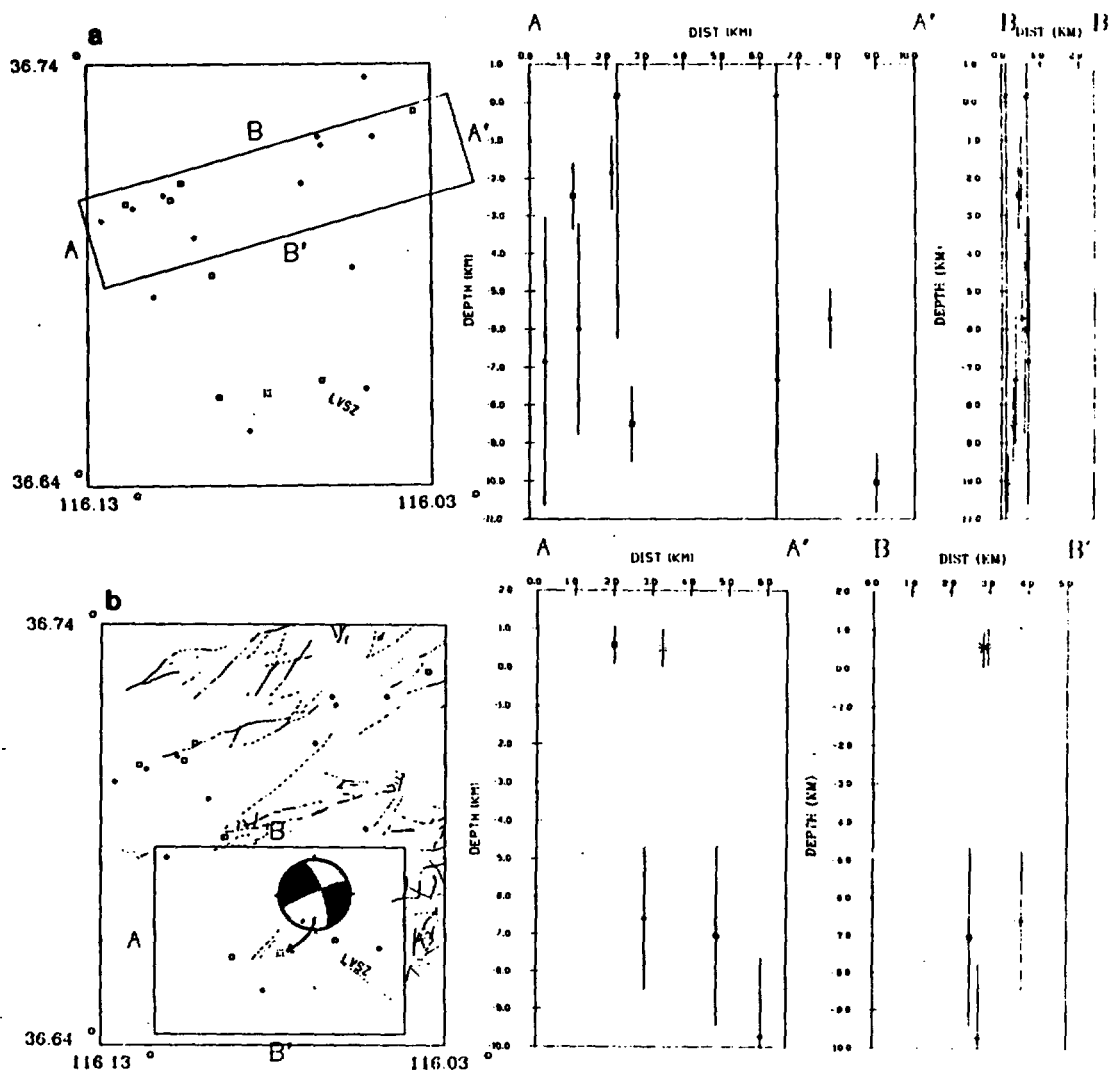


Figure 19.- (a) Maps and depth sections for 1979-1983 seismicity to the north of Mercury Valley. (b) 1979-1983 seismicity in the neighborhood of earthquake 831211 (Appendix E, Figure E2). LVSZ - northwest end of Las Vegas Shear Zone. Faults from Michael J. Carr (written comm., 1987).

in this map. In the southeastern part of this plot we recognize as many as 5 northeast- to east-northeast-trending zones of seismicity, which are at least partially confirmed on basis of mapped geology and focal mechanisms. These zones are sub-parallel to the Rock Valley and Cane Springs fault zones (Figure 10). The southwest terminus of these zones occurs in proximity to the inferred trace of the Las Vegas Valley shear zone or possibly the northern terminus of the Spring Mountain Range, giving the appearance of a diffuse northwest epicentral trend.

In the northeast quadrant of this stereo-pair map the earthquakes beneath Frenchman Flat form two sub-planar clusters that strike north along the east side of the flat. The easternmost cluster appears to be vertical or perhaps steeply dipping to the east. The westernmost cluster dips steeply to the west. These clusters appear to be discordant, however, with the structural trends that might be inferred to underlie Frenchman Flat, based on the general structural grain south of the Yucca-Frenchman flexure. Two earthquakes ( $M_L \approx 4$ ) in this zone yield focal mechanisms that suggest strike slip on faults trending north-south or east-west (Frenchman Lake, Feb. 19, 1973) to northeast-southwest (Massachusetts Mountain, August 5, 1971; Carr, 1974). There is no surface geologic evidence for north-south or east-west fault trends at Frenchman Flat, where the structural grain in the surrounding rock and alluvium trends about northeast-southwest. The Massachusetts Mountain aftershock locations, which were at depths greater than 6 km and occurred mostly south of the Cane Spring fault and the Yucca-Frenchman flexure, suggest a roughly north-northwest-trending fault plane. This orientation is also not corroborated by the geologic mapping. These data and our earthquake clustering suggest support for Carr's (1974) hypothesis that a buried north-northwest trending dextral slip fault zone could extend across the inferred trace of the Cane Spring fault. From the data of this study we further suggest that a series of deep-seated subparallel north-trending faults may extend south of the Yucca-Frenchman flexure beneath Frenchman Flat.

The activity in the western part of this stereo plot is even more complex than elsewhere in the area. The possibility that the seismicity in that region occurs on listric, shallow dipping, or detachment fault zones should be evaluated because such faults have been identified recently or suggested for some areas of the NTS (Scott, 1986; B. Meyers, personal commun., 1986). It appears, however, that no single gently dipping fault plane in this area can account for the observed distribution of seismicity which, instead, may represent slip within a shattered zone containing numerous faults. The distribution of earthquakes in the northern half of section BB' (Figure F15b) gives the appearance, possibly fortuitous, that the hypocenters are depth limited along a curved plane that dips to the southwest. As many as four faults may be indicated in the northern three-fourths of section BB', each having dip to the southwest. Focal mechanism 830906, which occurs at shallow depth (1.7 km) at the northern end of section BB' (Figure F15b), has a nodal plane that fits the strike and dip direction of this hypocentral trend. This result however, is at odds with the structural grain in the surrounding rocks, which mostly trends northeast to east-northeast. Furthermore, a focal mechanism about 12 km to the south (event 830530; Figure 10, 6.8 km depth) has nodal planes that strike north-northwest or east-northeast. The latter nodal plane is more nearly aligned with the structural grain. These two focal mechanisms are not necessarily inconsistent, but they do demonstrate the complexity of activity in this zone.

### Funeral Mountains Seismicity

Three groups of earthquakes were located during the period from January 1 through February 2, 1983 (figs. 10, 17, 20) about 2 km west of the California-Nevada border. The depth of focus for these earthquakes ranges from one km above sea level to twelve km below sea level (Appendix F, Figure F3), giving them the greatest depth range of any earthquake concentration in the study area. The southernmost cluster of earthquakes occurred contemporaneously with the northern groups. When plotted in depth sections (Figure 20), the southern group is seen to have deeper

average depth of focus, lying in a column suggesting steep southeasterly plunge (if these events lie on a common fault plane, the plane would dip steeply to the northeast). The two northern groups suggest a pair of *en echelon* northwest-trending alignments parallel to the Nevada-California border. Three composite focal mechanisms were computed from the two northern groups. For mechanism 830102 7:57 (Figure 20), first motion directions for the three most shallow-focus earthquakes in the two northern groups were combined (Appendix E, Figure E3). These events have depths of focus ranging from one km above to three km below sea level. Both nodal planes exhibit strike-slip motion on north-south- or east-west-trending nodal planes.

The composite mechanism 830102 16:32 (Figure 20; Appendix E, Figure E4) uses deeper focus earthquakes than mechanism 830102 7:57. Because pre-inspection of the first motion patterns from both the northern and southern groups revealed that many events in this zone had consistent focal mechanisms, first motion readings from two deeper earthquakes in both the southern and northern patches were combined. The resulting north-south or east-west nodal planes do not fit the northwest trend of the northern or southern earthquake groups.

Some earthquakes in this region, however, did demonstrate differing patterns. Mechanism 830103 17:39 (Figure 20; Appendix E, Figure E5) was constructed from four earthquakes whose epicenters lie within the easternmost of the northern earthquake clusters. The northwest-striking nodal plane approximately fits the epicentral trend, but the southwest dip of this plane does not coincide with the suggested steep northeast dip of the hypocentral cluster.

Interpretation of the stereo pairs (Appendix F, Figure F3) and focal mechanisms for this zone suggests that selection of the northerly-trending nodal planes would require activity on several parallel faults. These earthquakes occur in a region of the Funeral Mountains where that block exhibits numerous pre-Quaternary faults trending from  $N20^{\circ}-45^{\circ}$  E (Carr, 1984, fig. 19) and one northerly-trending inferred fault of unknown age (Jennings and others, 1973). On this basis, then, we tentatively argue that the northerly trending nodal planes are preferred over those of east-west or northwest trend. The three mechanisms, taken together, indicate the likelihood that the seismogenic structures in this area are steeply dipping *en echelon* north- to north-  $30^{\circ}$  east-trending faults in spite of the vague northwest epicentral trends.

### Earthquake Activity near Lathrop Wells

Few earthquakes occurred near Lathrop Wells during the 1979-1983 monitoring period (Figures 10 and 21), however, a focal mechanism solution for a small ( $M_L = 1.4$ ) earthquake in this region has been obtained (event 820409, Appendix E, Figure E5). Bedrock in this area is overlain by Quaternary alluvial deposits, and geologic maps (Swadley, 1983) provide few clues regarding fault orientations. The activity in this area (Figure 10; Appendix E, Figure E4) includes an event with a focal mechanism (820409) that is near the southern terminus of a group of 5 earthquakes forming a north-south trend, leading us to prefer the north-trending nodal plane. A more regional view of these events (Figure 9) suggests that this earthquake is within the northernmost lineation of two right-stepping epicentral alignments trending north-northeast. These alignments are parallel to the inferred fault that bounds the west side of Little Skull Mountain, although they are offset to the west of the inferred fault 2-3 km. The gravity data also support the interpretation of a north-trending fault to the east of Lathrop Wells (Healey and others, 1980).

### Striped Hills - Rock Valley Earthquakes

A group of earthquakes occurred in the Rock Valley area between the Striped Hills and Little Skull Mountain (fig 10 and 22; Appendix F, Figure F5). The east-northeast trending trace of the Rock Valley fault is just south of this group of events. These may be occurring on assumed northern splays or sub-parallel faults of the Rock Valley fault zone (Sargent and others, 1970). Most of the mapped faults exposed in the nearby Striped Hills, Specter Range, and on Little Skull Mountain,

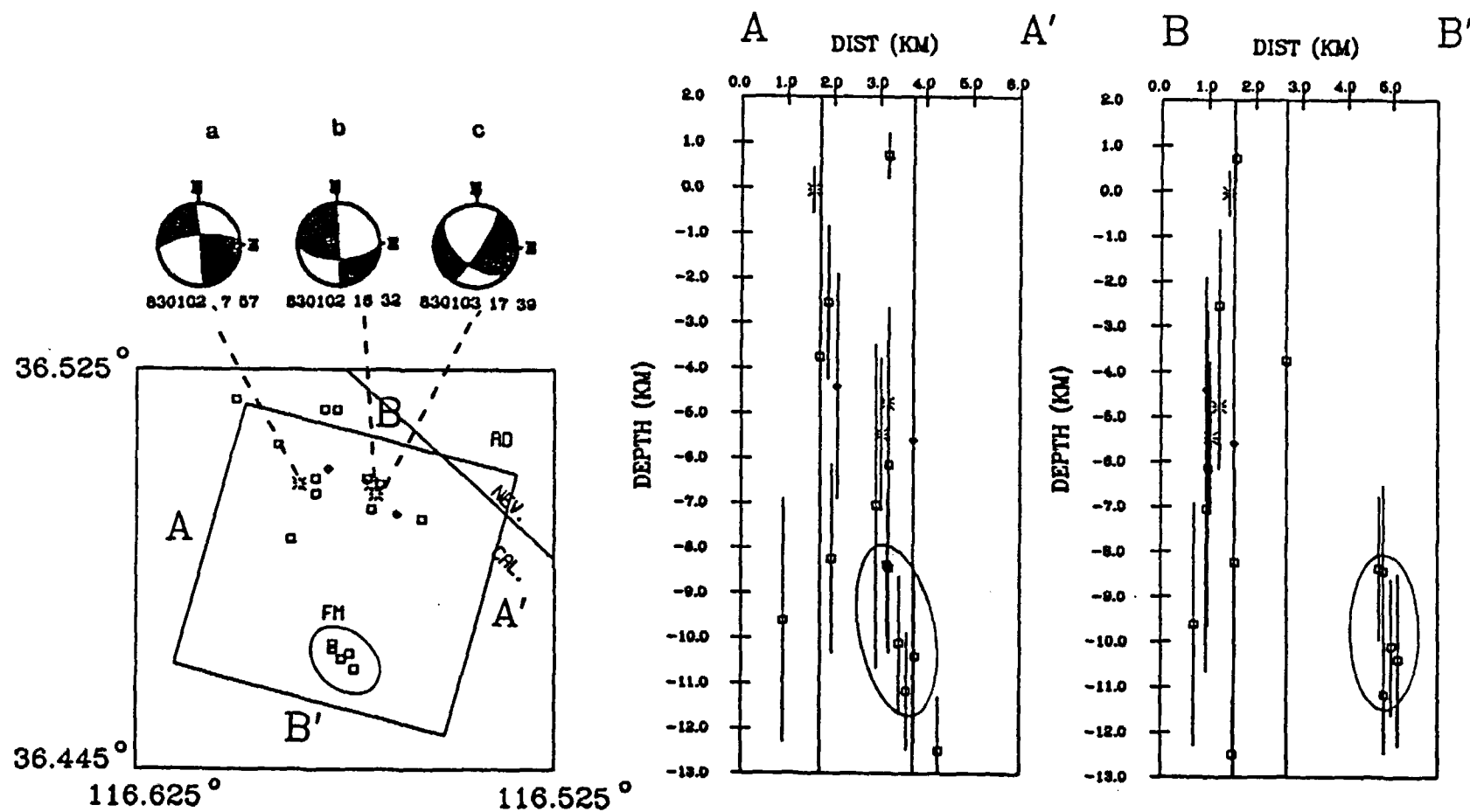


Figure 20.- The 1980-1983 Funeral Mountains seismicity in the vicinity of the earthquakes used to compute the three focal mechanisms shown. The events referred to as the "southern group" in the text are circled. FM - Funeral Mountains. AD - Amargosa Desert.

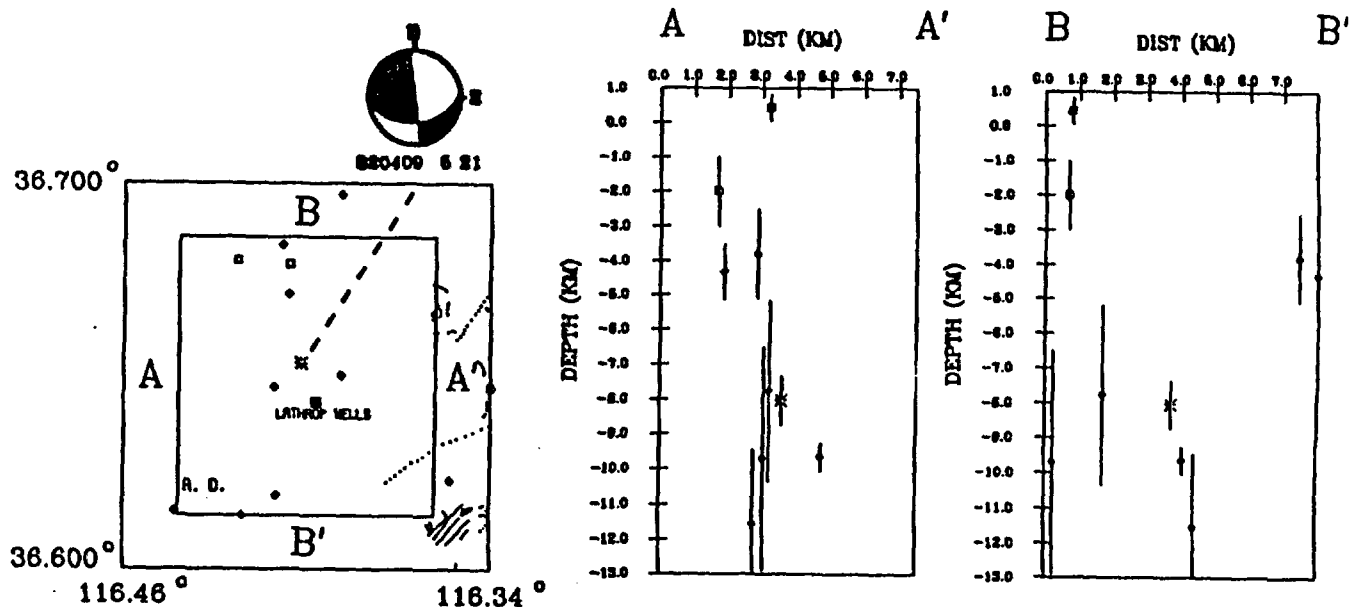


Figure 21.- 1979-1983 earthquake activity in the vicinity of the Lathrop Wells earthquake of 820409 (Appendix E, Figure E6). Faults from Michael J. Carr (written comm., 1987). A. D. - Amar-gosa Desert.

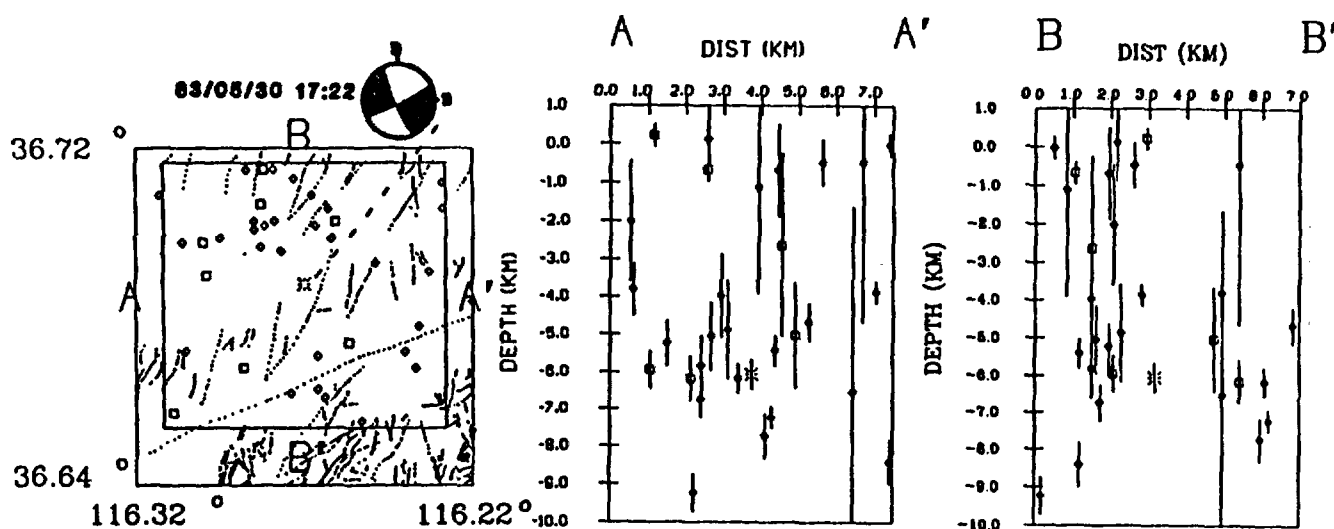


Figure 22.- Depth sections for 1979-1983 activity in the vicinity of the Striped Hills earthquake of 830530 (Appendix E, Figure E7). Faults from Michael J. Carr (written comm., 1987).

strike from about N 20° E to N 60° E. Association of these earthquakes with an east-northeast fault plane is supported by a focal mechanism (event 830530) from this group that exhibits an east-northeast trending nodal plane having sinistral strike slip (Figure 22 and Appendix E, Figure E7).

### Seismicity near Dome Mountain in 1983

From May 28 to May 30, 1983, a series of eight earthquakes occurred near Dome Mountain, at depths ranging from 7 to 10 km below sea level (Figures 10 and 12; Appendix F, Figure F6; several events shown in the plots occur outside this time window). These hypocenters, 15 km north of drill hole G1 on Yucca Mountain, are plotted in depth sections (Figure 23). The first and largest earthquake of the 1983 series, (event 830528  $M_L = 1.9$ ), was one of the shallowest (7.8 km below sea level) and the easternmost of the series. Its focal mechanism (Appendix E, Figure E8) has north-south and east-west striking nodal planes, having predominantly strike-slip motion. The epicenter of this event is within 1 km of a mapped east-dipping north-northwest striking fault (Byers and others, 1976), and the structural grain to the north and south of the earthquake activity is north-northwest trending. This event could be considered distinct from the other events in this sub-area, which appear to form a cylindrical group of events plunging to the northwest. Christiansen and others (1977, p. 955) suggest that "a fundamental, probably deep-seated structural zone to which both the Walker Lane and Las Vegas Valley shear zone are related extends through the region beneath the [Timber Mountain] volcanic field." Such a zone would have northwest strike. Both the epicenter alignment and the occurrence of deeper earthquakes is consistent with the presence of a deep seated structure. An alternative interpretation, however, would combine event 830528 and the mapped surficial grain to conclude that all these events are occurring on a series of deep seated north-trending *en echelon* faults. With regard to the repository site, it is noteworthy that this activity could lie on an *en echelon* extension of the Paintbrush Canyon fault.

### Earthquakes at Thirsty Canyon and Vicinity

The Thirsty Canyon region of Pahute Mesa experienced a swarm of small earthquakes in 1979 and another in February 1983 (Figure 12 and 24; Appendix F, Figure F7). The 1979 series appears to have a north-northeast-striking epicenter lineation, in agreement with a composite focal mechanism (event 790817; Rogers and others, 1983) for that swarm that has a north-trending dextral strike-slip nodal plane. Two composite mechanisms were constructed for the 1983 earthquakes (Figure 24 and Appendix E, Figures E9 and E10), both indicating normal faulting on either a west-dipping north-striking fault, or a southeast dipping northeast-striking fault. The two composite mechanisms are very similar and the separation into two mechanisms was based on slightly different amplitude ratio data. Depths of focus clustered in the range 4.2 to 6.6 km below sea level for the 5 earthquakes used in the composite mechanisms. The epicenters lie within one hundred meters of a mapped north-striking fault having a mapped length of about 9 km (O'Conner and others, 1966). The mapped dip on the segment of the fault nearest to the epicenters indicates that the west block is down. The geology, then, leads to a preference for the west dipping nodal plane. A slight westerly dip is also suggested in cross section AA' (Figure 24).

A variety of rupture styles in this region may be possible without requiring rotations of the principal stresses (Harmsen and Rogers, 1986). The same pattern of strike-slip and dip-slip mechanisms was observed for aftershocks of the Benham nuclear explosion along a fault striking north and bending to north-northeast, about 4 km east of these Thirsty Canyon earthquakes (Hamilton and Healy, 1969; McKeown, 1975). From the proximity of these 3 Thirsty Canyon mechanisms, we conclude that both dip slip and strike slip may occur on north- to northeast-trending faults, under the same regional stress conditions, depending upon the fault dip and strike.

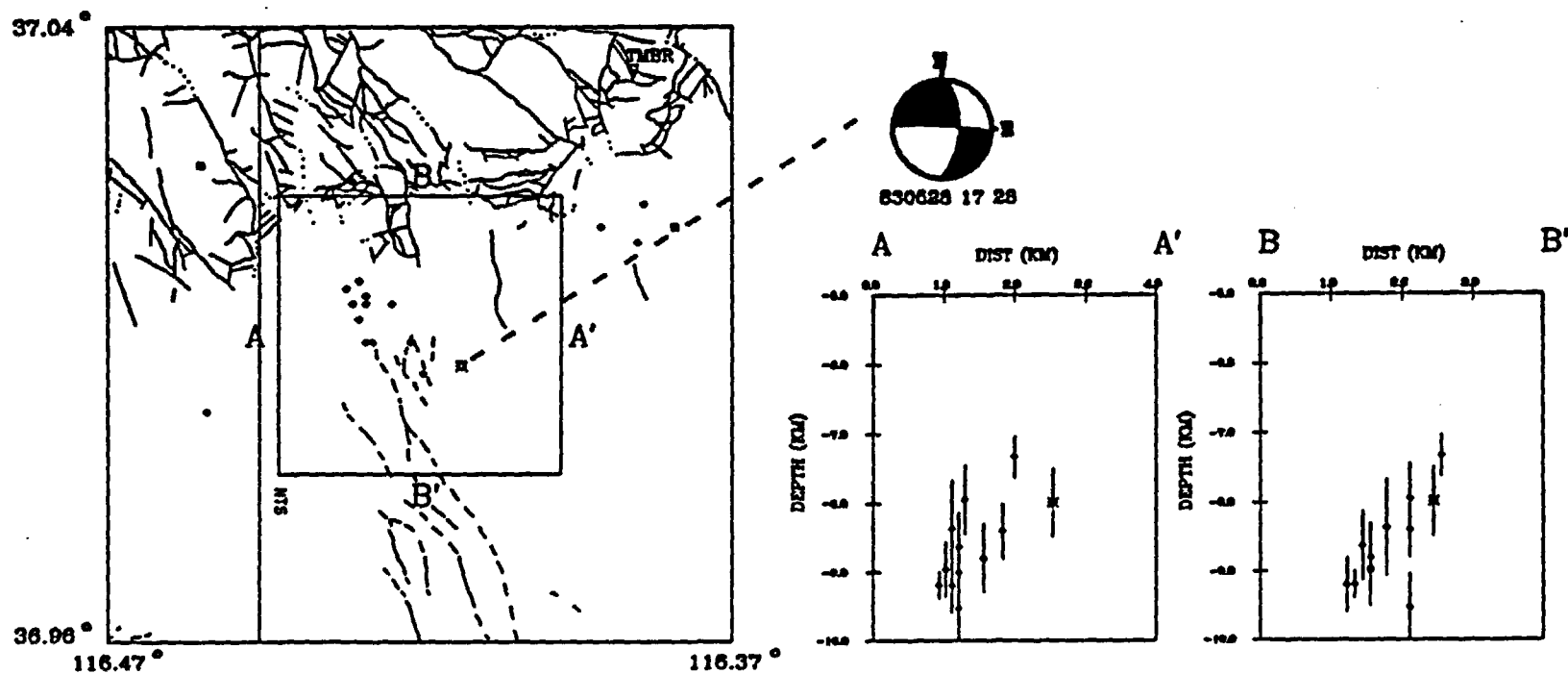


Figure 23.- 1979-1983 earthquakes in the vicinity of the Dome Mountain 830528 earthquake (Appendix E, Figure E8). Faults from Vergil Frizzell and Michael J. Carr (written comm., 1987). NTS - Nevada Test Site west boundary.

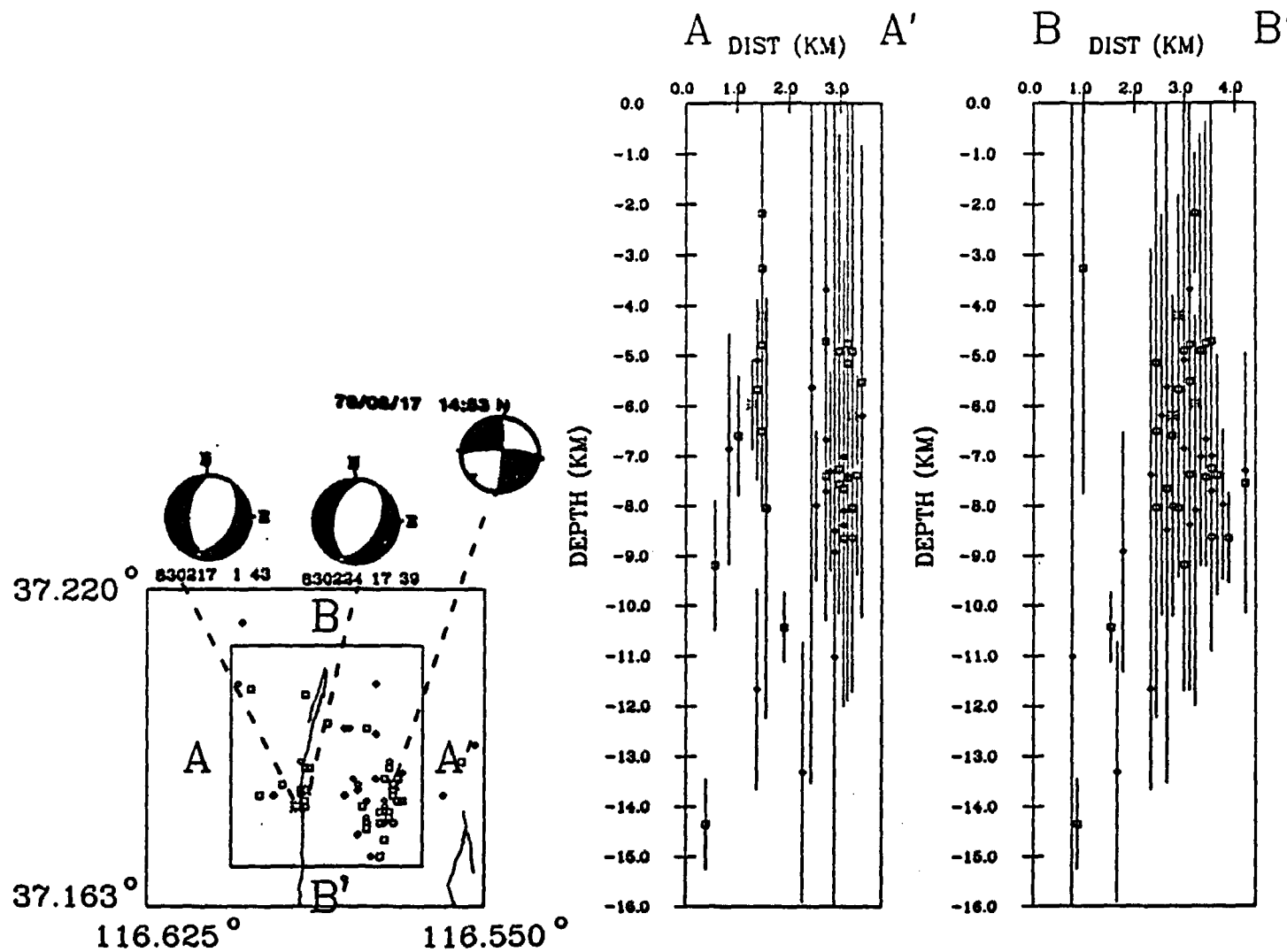


Figure 24.—1979-1983 earthquakes in the vicinity of Thirsty Canyon. The eastern concentration occurred in 1979, and the smaller western concentration occurred in February, 1983. Faults from O'Connor and others (1966).



### Seismicity at Sarcobatus Flat, 1981 through 1983

Four earthquake series (b,c, Figures 25, 26, a, d, Figure 27; Figure 13) have occurred in the Sarcobatus Flat region. Seismicity first noted by Rogers and others (1983) continued in the two southern clusters (b and c) in 1982 and 1983. The southernmost of these two series (c) that began October 15, 1981 and continued through November, 1981 began again with some intensity on August 31, 1982 and then decreased in 1983. The activity in this zone also tended to become shallower with time. The epicenter and hypocenter plots for cluster c activity in Figure 25 suggest that earthquakes there are occurring on short faults or short fault segments striking roughly north with nearly vertical dip (possibly west-dipping). These structures appear to maintain a steep dip to depths of about 11 km below sea level. Section AA' viewed along an assumed north strike shows that this zone has a width of about 2 km and, thus, may represent activity on more than one fault. Although other interpretations are possible, we suggest that these earthquakes are occurring on (Appendix F, Figure F8) a pair of right-stepping westerly dipping faults with the northern most segment striking north-northwest. Four focal mechanisms have been obtained for cluster c (Rogers and others, 1983; this report Appendix E, Figures E11, E12 and E13). The preferred nodal plane in these mechanisms trends from approximately north to N35E and indicates predominately right-lateral strike-slip motion. The mechanism in Appendix E (Figure E13), indicating a reversal in dip and oblique slip for the preferred nodal plane, suggests deformational complexity in this zone.

The Sarcobatus Flat earthquake cluster b occurs about 10 km north of cluster c (Figure 13, Figure 26). The activity in cluster b began in March, 1981, and intensified in January, 1982. Cluster b was mostly dormant in 1983. The cross sections (Figure 26) for this group of events suggest a steep (possibly west-dipping fault) plane in the depth range from near-surface to about 11 km. Although the composite focal mechanism for this group shows a vertical north-trending fault and is very similar to a previously determined mechanism (810310) for an earthquake in cluster b (Rogers and others, 1983), the dip of the north-trending nodal plane is not well constrained and may be west dipping (Appendix E, Figure E14).

The strike, dip, spatial position and focal mechanisms of clusters b and c could be interpreted as the occurrence of earthquakes on a common fault or fault system having a length of about 15-20 km. The occurrence of earthquakes near the end points of such a fault may have several differing implications. First, it is possible that this activity represents strain release due to stress concentrations occurring after slip on the central portion of the fault (Chinnery, 1963). This slip could have been the result of a main-shock earthquake or aseismic slip. Based on the distance between the two active zones, this interpretation suggests the possible occurrence of a pre-historic earthquake ( $M \approx 6$ ) with aftershocks continuing into the historic record. Second, Kellerher and Savino (1975) show that seismicity frequently occurs near the edges of the main rupture zone prior to the main shock suggesting the possible occurrence of such an event in the future. Both of these interpretations should be considered speculative. It is also possible that the occurrence of earthquakes in a steeply plunging cylindrical volume of rock, such as noted for these clusters and others in the region, could represent stress concentration that occurs at the intersection of two faults. This conclusion is likely to be correct in some active zones of the region, such as the activity that occurred on the eastern side of Lake Mead where cylindrical volumes of seismicity occurred near the intersection of the Indian Canyon and Fortification faults and the Mead Slope fault (Rogers and Lee, 1976). It is possible to speculate, for instance, that the activity in cluster c represents earthquakes occurring at the intersection of structures within the Walker Lane and younger more northerly-trending structures that may trend from the north into the Walker Lane (see Shawe, 1965, for instance).

Finally, it should be noted that recent but incomplete geologic studies in Sarcobatus Flat suggest that a north-northwesterly-trending Quaternary fault system may transect the eastern

side of the Flat (M. Reheis and J. Noller, personal commun., 1987). This system is composed of multiple strands of westerly dipping faults. Such a fault system would be consistent with most of the general patterns of seismicity that have been observed in Sarcobatus Flat (series b and c).

### Earthquakes near Scottys Junction

Earthquake series a (Figures 13 and 27a; Appendix F, Figure F9) in the northern area of Sarcobatus Flat, unlike b and c, occurred before 1981. A distinct northeast epicentral trend in this series is apparent in Figure 27a, but the focal mechanism of the mainshock of this series (event 791225; Rogers and others, 1983) exhibits north- and east-trending strike-slip nodal planes. In recognition of the focal mechanism result, the stereo pairs (Appendix F, Figure F9) permit the interpretation of two north-trending fault planes that dip to the west. The lateral extent of epicenters also supports an interpretation of multiple parallel faults or, perhaps, a right-stepping *en echelon* fault system.

An earthquake series (Sarcobatus Flat series d) about 15 km north-northwest of Scottys Junction occurred in November, 1983 (Figure 13, Figure 27b). The events occurred in an area of short pre-Quaternary mapped faults (Stewart and Carlson, 1978) having northerly trends and east dip (Figure 13). Focal mechanisms for two earthquakes (831110 10:37 and 831110 13:17) in this series have been computed; the first event is predominantly normal slip and the second is predominantly strike slip (Appendix E, Figures E15 and E16). The stereo pairs for this cluster (Appendix F, Figure F9) also suggest two parallel north-trending faults, where the most easterly events dip to the east. Thus, the 831110 10:37 focal mechanism seems to be at variance with the mapped geology and hypocenter patterns because its northerly-trending nodal plane dips to the west, whereas its easterly dipping nodal plane has a northwest strike. The northerly-trending nodal plane of focal mechanism 831110 13:17 dips east, in closer correspondence to mapped geology and the stereo pair hypocentral distribution. This localized mixture of normal and wrench faulting was also noted above at Thirsty Canyon and at Pahute Mesa (e.g., Hamilton and Healy, 1969).

### Seismicity in the vicinity of Slate Ridge

A series of 40 earthquakes was recorded from Feb 2, 1983 through Feb 5, 1983 about 25 km west of Scottys Junction and 10 km north of Gold Mountain (Figure 13). Figure 13 shows a northeast-trending epicenter lineation that crosses both the more easterly and the northerly-trending pre-Quaternary structural grain in the area. A small group of epicenters is located north of the east end of the main northeast-trending lineation. This entire group of earthquakes is plotted in depth sections along and perpendicular to the main northeast trend (fig 28; Appendix F, Figure F10). The depth distributions show that the small cluster of earthquake hypocenters is truly isolated from those of the main trend. The main trend of earthquakes may be described as a curved cylinder of events plunging N 70° E. The AA' depth section shows that the cylindrical volume has an elbow with a steeply plunging ( $> 80^\circ$ ) upper part from surface focus to about 5 km below sea level, and a lower part continuing to about 10 km below sea level, plunging  $\approx 55^\circ$ . Unfortunately, this series of earthquakes has not yielded a reliable focal mechanism.

It is possible that this cylinder of hypocenters represents failure near the intersection of two fault planes, where the rock is likely to be weaker. There are 2 mapped pre-Quaternary structural-grain orientations in the vicinity of the epicenters, one with strike of N 10° E and the other with strike approximately east-west. The intersection of 2 steeply-dipping planes ( $\geq 80^\circ$ ) could account for the steeply-plunging hypocentral cylinder with the observed strike, but not account for the more shallow plunging events. If we are unconstrained by the surficial geological structures, an infinite number of intersecting fault planes could possibly produce the upper section of events, from faults with northwesterly strike and northeast dip to faults with easterly strike and north dip. The elbow in the cylinder might also result from the intersection of a curved or listric north-dipping

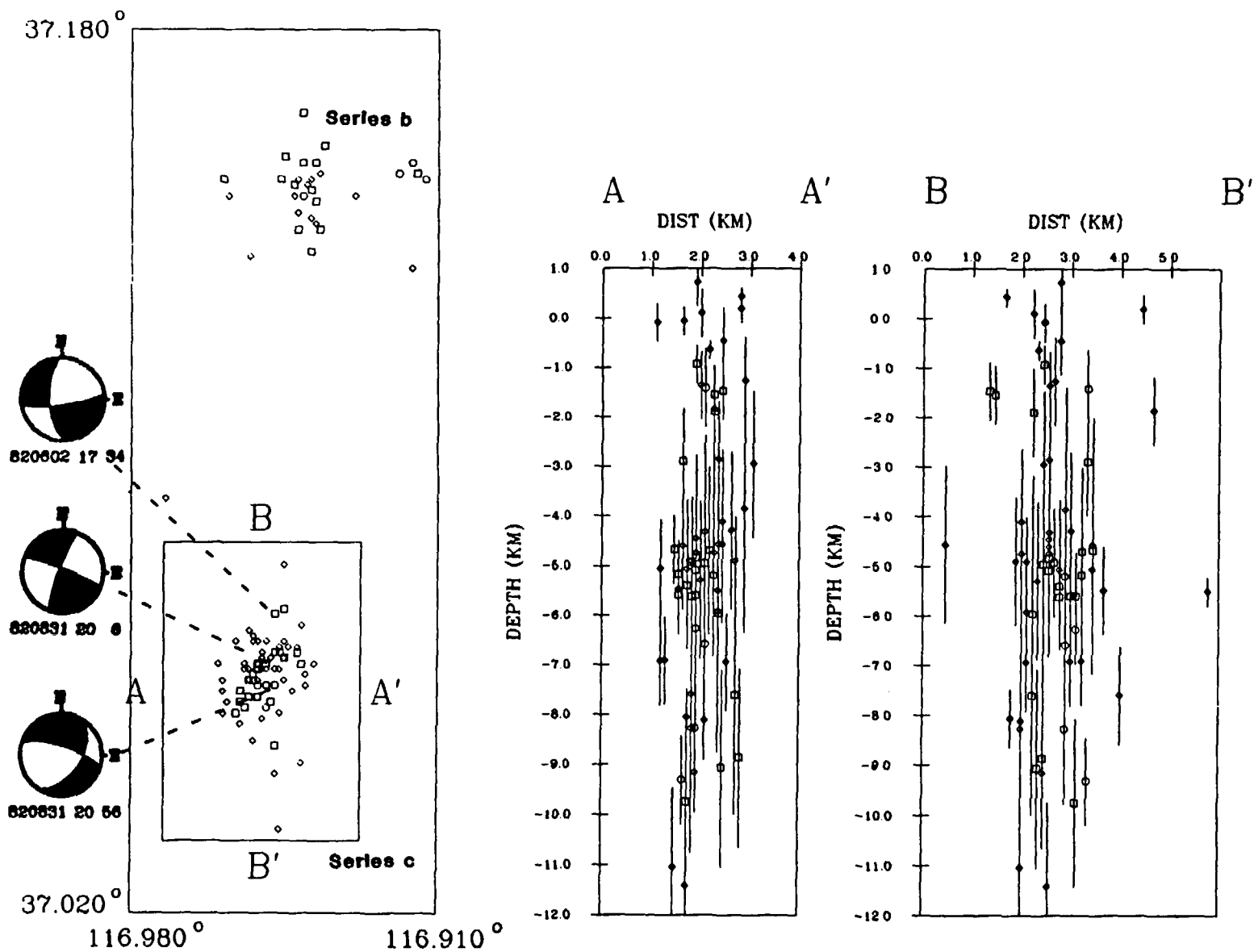


Figure 25.- Depth sections for activity during the monitoring period 1979-1983 in Sarcobatus Flats series c.

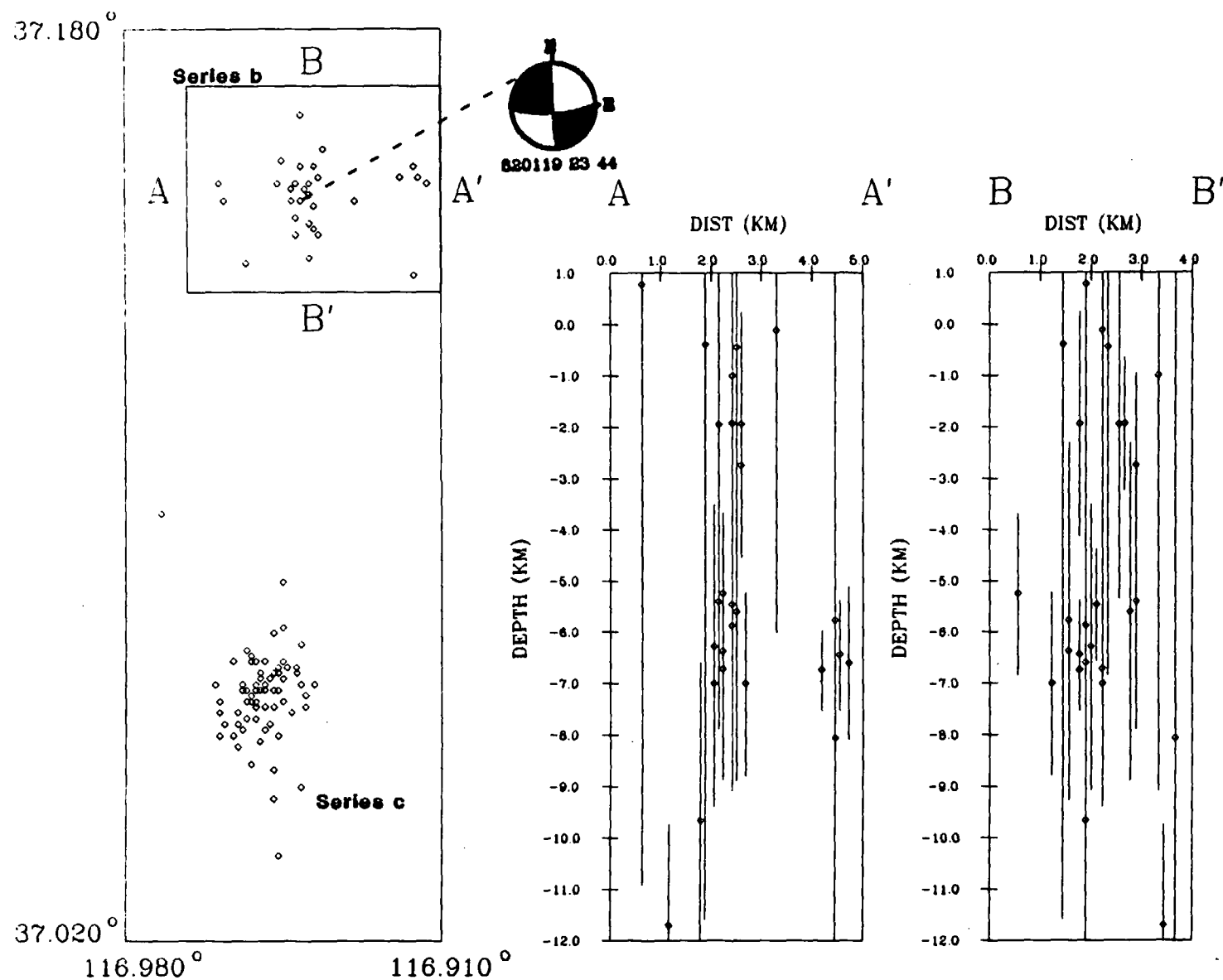


Figure 26. Depth sections and a focal mechanism for activity during the monitoring period 1979-1983 in Sarcobatus Flats series b.

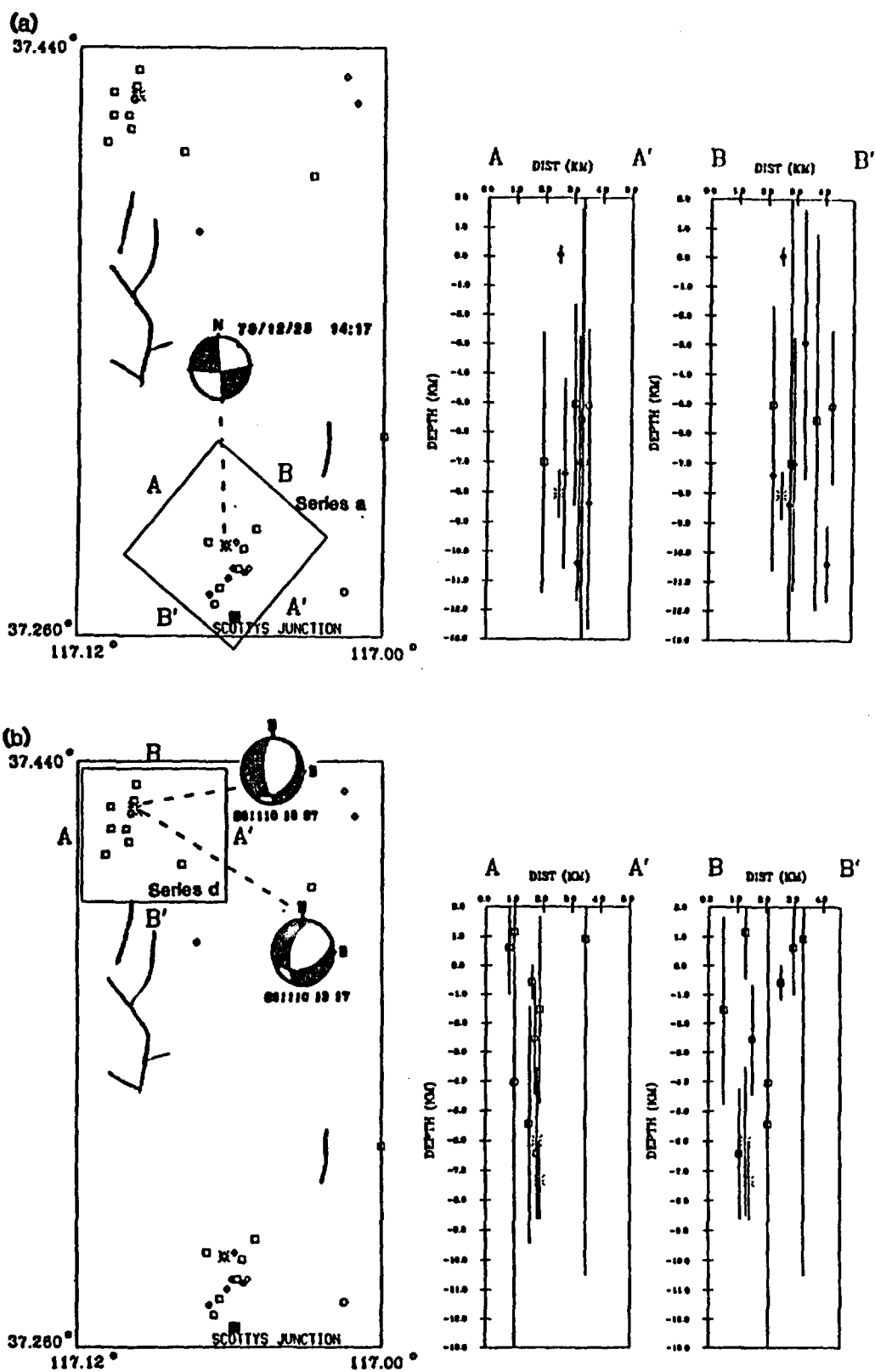


Figure 27.— (a) 1979-1983 earthquakes in Sarcobatus Flats series a, (b) and Sarcobatus Flats series d. Faults from Stewart and Carlson (1978).

east-striking fault with a vertical to southerly dipping northeast-striking fault. Recent preliminary mapping in this region (M. Reheis and J. Noller, personal comm., 1987) indicates the presence of northeast-trending Quaternary faults, lending credence to this last possibility. There are a number of other possibilities as well, but until a focal mechanism is obtained for earthquakes along this trend, full understanding of this cluster of events is not possible.

Seismicity along the main trend was dormant until October 1, 1983, at which time the group of 12 earthquakes commenced to the north of its northeast extent. These events were confined to depths greater than 4 km. As noted above, the depth sections show that the October series was spatially separate from the main trend. A composite mechanism (831001) of the first 4 of the events in this series (Appendix E, Figure E17) indicates oblique dip slip on both nodal planes. These events exhibit a weak northeast-epicenter lineation, having no distinct dip. Thus, we have a marginal preference for the nodal plane with northeast strike.

### Earthquakes near Yucca Flat

Earthquakes in the Yucca Flat region are shown in Figures 10, 12, and 29. Although roughly 7-10 earthquakes could be associated directly with the Yucca Flat fault trace, many other events occur in a diffuse pattern, mostly to the east of the fault trace. The stereo pairs for this area (Appendix F, Figure F11) indicate that these events occur downdip of the Yucca Flat fault trace. Continuation of activity to the southeast from the southern tip of the mapped section of the Yucca Flat fault suggests that the fault may continue in that direction and merge with or intersect the Yucca-Frenchman shear zone. A short epicenter lineation in the middle of Yucca Flat is probably associated with the Carpetbag Fault. A north-trending lineation of epicenters also occurs along the western margin of Yucca Flat suggesting that the bounding fault on that side of the valley is active. Earthquakes in the Eleana Range west of Yucca Flat are very diffuse in character and do not display patterns that can be associated with mapped structure.

Yucca Flat is a nuclear testing area, and it is reasonable to assume that many of the earthquakes shown are the result of the testing program. It is notable, however, that a high percentage of these events occur at depths greater than about 3 km (Figure 29, section AA'), which is considerably deeper than nuclear test depths. This behavior has also been noted in the Pahute Mesa testing area by Hamilton and others (1971) and Rogers and others (1977) and suggests that the nuclear tests act to relieve tectonic stress at depth by wave propagation effects. That is, elastic waves leaving the source produce enough additional shear stress or pore pressure on tectonically stressed faults that are near failure that this additional propagating wave-induced stress triggers fault rupture (Kisslinger, 1976).

### Earthquakes in Indian Spring Valley

Figures 30a and b show maps and cross sections for earthquakes in the Indian Springs Valley area (Figures 10 and 14). The two focal mechanisms of Figure 30a are predominantly strike-slip motion; we marginally prefer the the north-south nodal planes as the slip planes given the nearby pre-Quaternary north-northeast structural grain (Stewart and Carlson, 1978) in the rocks of the Spotted Range bounding the west side of Indian Spring Valley (Rogers and others, 1983; Appendix E, Figure E18), and because the stereo pairs (Appendix F, Figure F12) weakly suggest a pair of subparallel north-trending faults. Figure 30a (section AA') shows that the north-trending east-dipping nodal plane is in agreement with an east-dipping hypocentral trend. A right-step may occur at the northern extreme of the easternmost lineation. The group of events to the southeast (Figure 30b), near the town of Indian Springs, appears to occur on a northeast-striking fault that dips to the north-northwest. This fault appears to transect the concealed trace of the Las Vegas Valley shear zone (Figure 14) at nearly right angles.

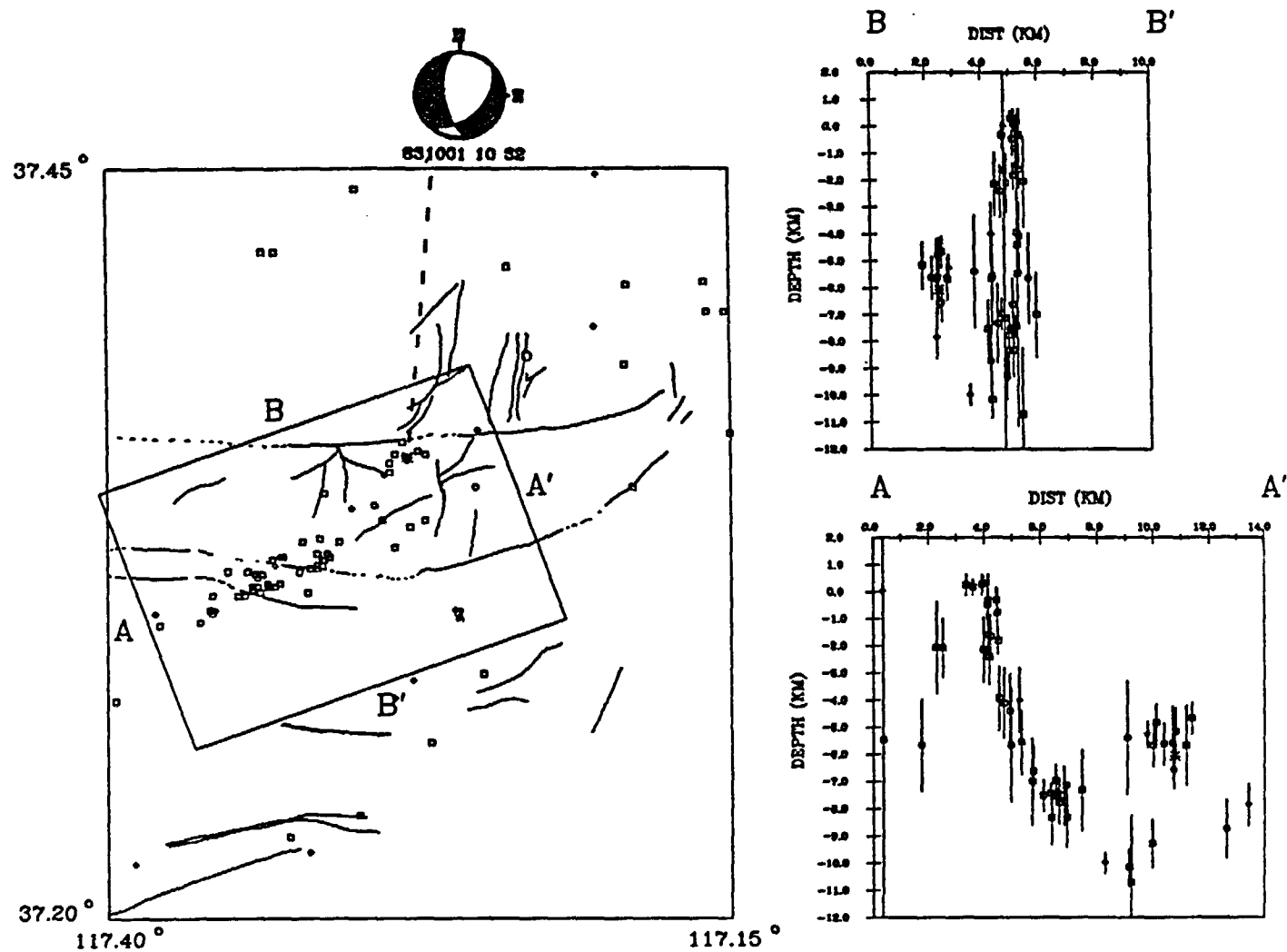


Figure 28.- 1979-1983 seismicity in the Slate Ridge region 25 km west of Scottys Junction. The western lineation occurred during February, 1983, and the northeast activity from which the mechanism of Appendix E, Figure E17 was computed, occurred during October, 1983. Faults (incomplete outside box AA'BB') from Albers and Stewart (1965).

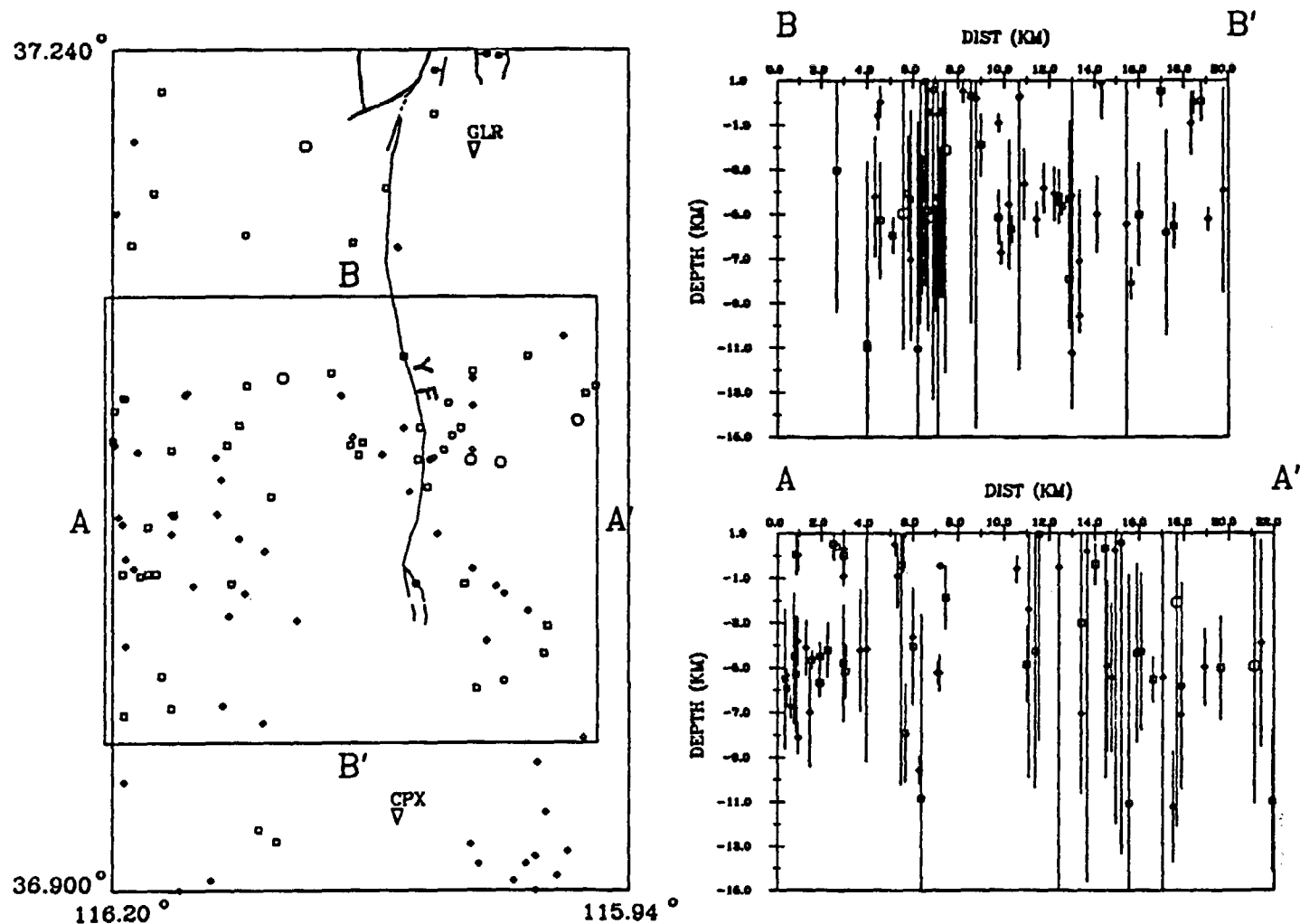


Figure 29.- Earthquakes in the vicinity of Yucca Flat, August, 1978 through December, 1983.  
Yucca fault (YF) from Stewart and Carlson (1978).



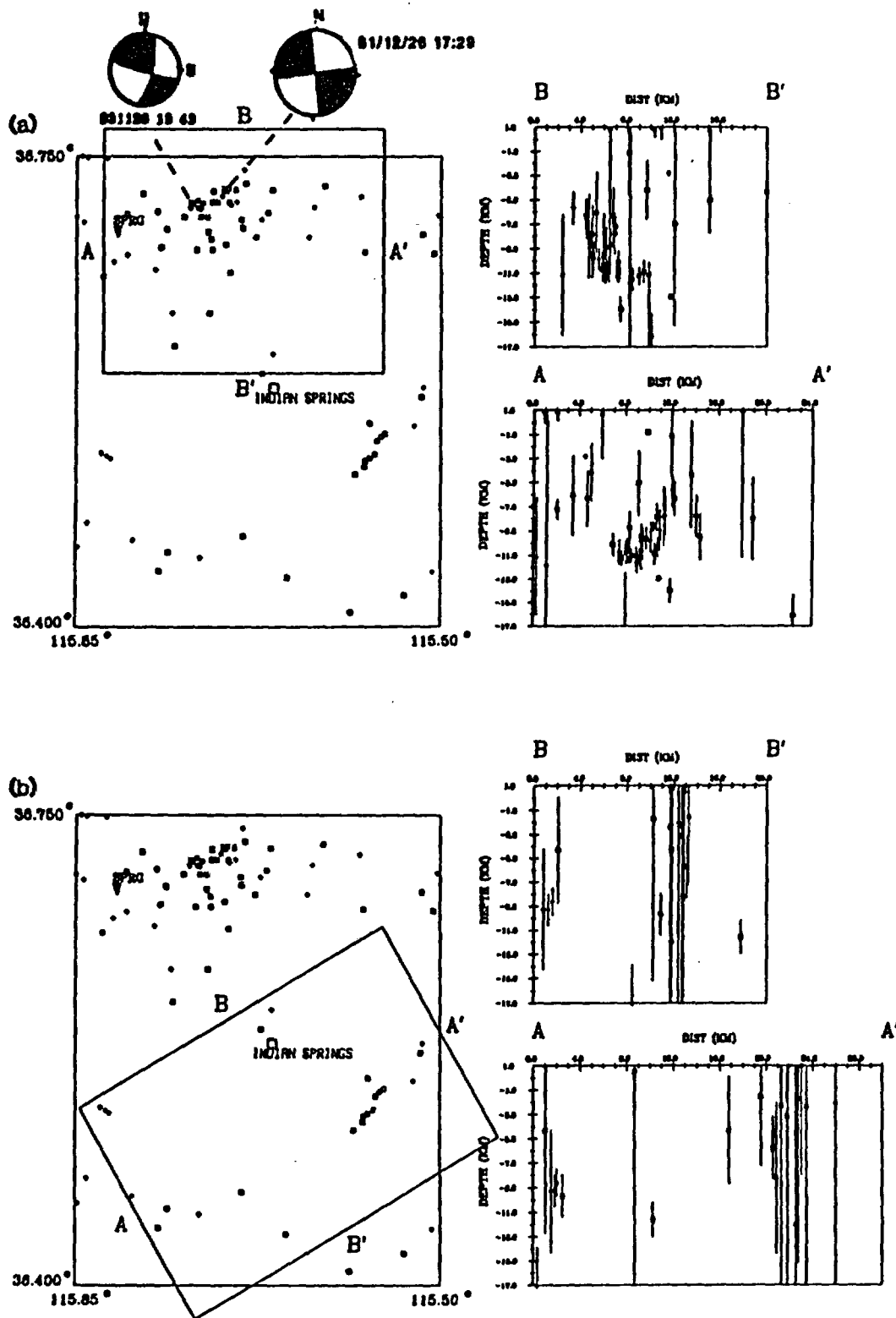


Figure 30.- (a) Depth sections and two focal mechanisms (Rogers and others, 1983; Appendix E, Figure E18) for earthquakes in the Indian Spring Valley and Spotted Range; (b) earthquakes in the vicinity of Indian Springs and Highway 95.

## Earthquakes in the Pahrnagat Region

Two different views of the seismicity in the Pahrnagat Shear Zone (Figure 15) are shown in Figures 31a and b. One of the views (Figure 31b, BB') is along the main northeast-striking structural trend and the other (Figure 31a, AA') is along the secondary north-striking structural trend; the secondary trend is also parallel to the nodal plane strikes for the 2 focal mechanisms. Because of the diffuse nature of the seismicity no clear relationship can be observed between the faulting and epicentral patterns in map view. If the north-trending faults are active, then the cross sections indicate that the zone is complex and must consist of many subparallel faults that are so closely spaced as to be indiscernible given the accuracy of the hypocenter locations in this region. View AA' (Figure 31b) suggests that the activity in this zone plunges steeply to the southwest. This behavior, however, may be the result of fortuitous juxtaposition of several active zones. The stereo pairs (Appendix F, Figure F13) are somewhat more helpful in the interpretation of these events. This plot suggests evidence for the presence of 3 or 4 northeast-trending lineaments that offset a north-trending lineation in a left-stepping pattern. A cursory field reconnaissance in this region disclosed several Pliocene to Quaternary strike-slip faults having potential north trends (R. E. Anderson, U. S. Geological Survey, personal comm., 1986).

## Earthquakes in North Pahroc Range

An earthquake series during July 1982 in the North Pahroc Range (Figure 16) is plotted in depth sections (Figure 32). Most of the earthquakes occur at depths less than 5 km below sea level. As this region is at the northeast edge of the network, location quality is not optimal. The mainshock ( $M_d = 3.1$ ) of this series (820706 02:10) occurred about 21 km northeast of Hiko, Nevada, where it was felt. A focal mechanism indicating predominant strike slip was obtained for this earthquake (Appendix E, Figure E19). The pre-Quaternary bedrock structures near the epicenter (Ekren and others, 1977) exhibit predominantly east-trending fault orientations; five to ten kilometers to the east of the epicenter, however, the longest and most abundant exposed faults trend from north-northwest to north-northeast. Some of these north-trending faults appear to bound Quaternary alluvial valleys. The stereo pairs (Appendix F, Figure F14) suggest 1-3 north-trending faults that may dip steeply to the west. The epicenters also have a more elongate north-south than east-west extent. Although the epicenter of the focal mechanism event (830607) is about 2 km due east of a prominent east-west striking fault, we have a slight preference for the north-trending dextral-slip nodal plane. This interpretation would require the presence of unmapped north-trending faults in this region.

## Earthquakes and Structure: Summary

The foregoing discussion demonstrates the difficulty of showing an unequivocal relationship between seismicity and known faults in this region. Because of the errors in the locations of the events and the unknown geometry of some faults at the depth of earthquake hypocenters, it is often difficult to directly associate given earthquakes and faults with any degree of confidence. The common association, however, of earthquake nodal planes with epicenter lineations and/or mapped structural grain in the surrounding rocks imparts some level of confidence that the faults that define the structural grain at the surface are likely to be active, and do, in fact, reflect the general structural pattern that exists at seismogenic depths. It is on the basis of these correlations that we suggest that faults in the region with azimuths ranging from about north to east-northeast should be considered favorably oriented for activation in the current stress regime. Exceptions to this conclusion are noted in the discussion section.

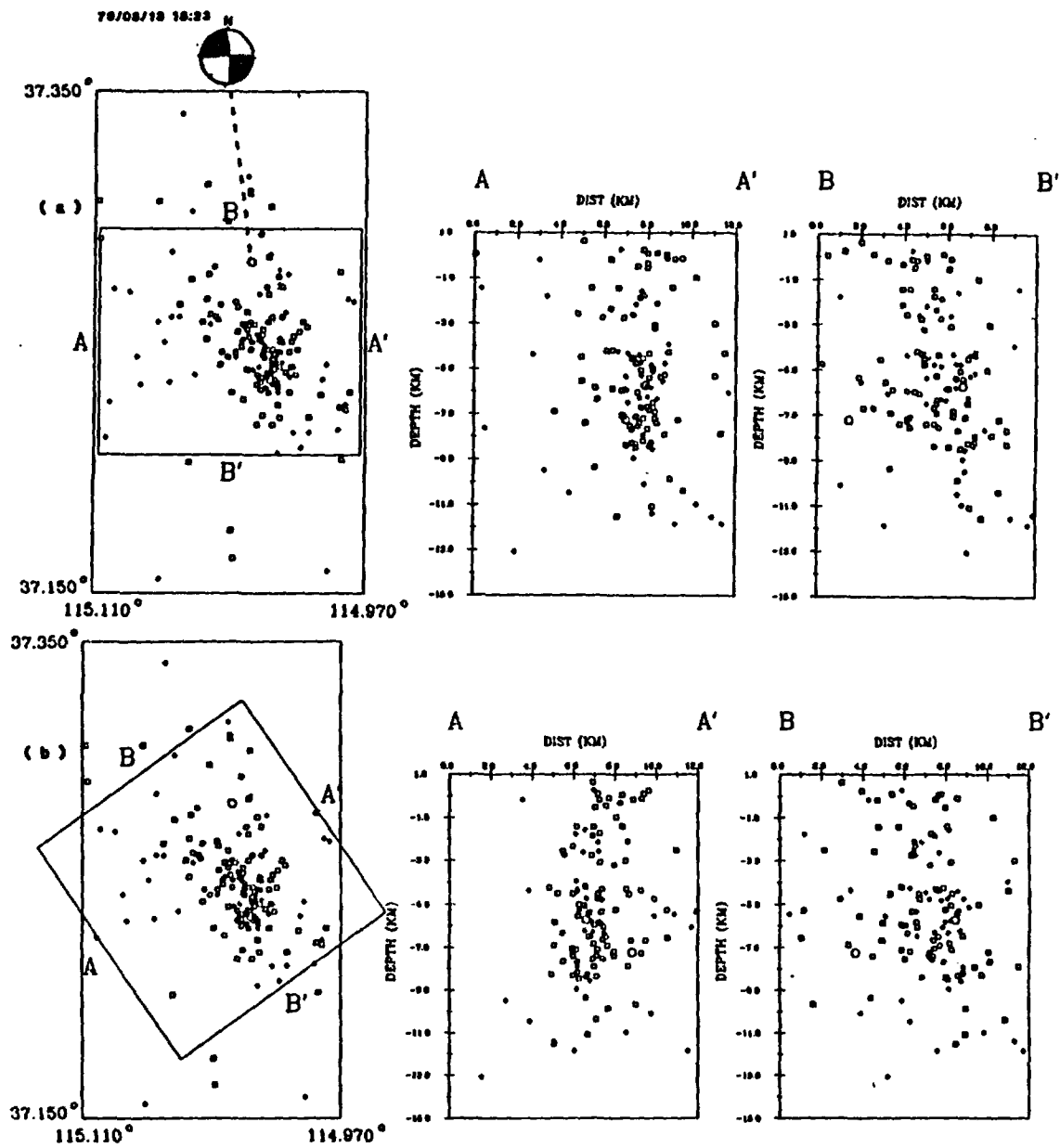


Figure 31.- (a) Pahrnagat Shear Zone earthquakes plotted in depth sections for the period August 1978 through December, 1983. (b) Same data, different projection planes.

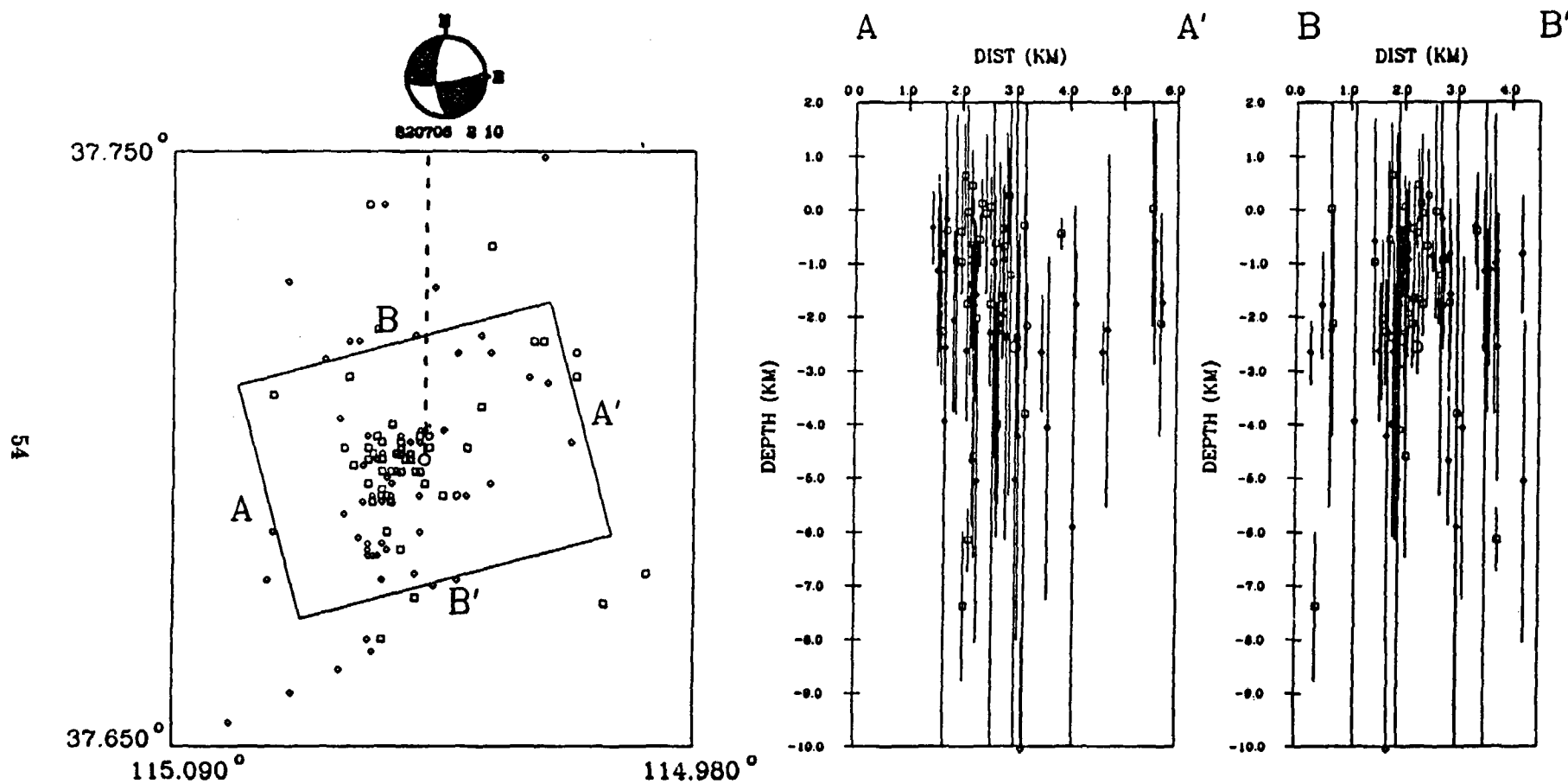


Figure 32.- Depth sections of 1979-1983 seismicity in the North Pahroc Range, including the series of July, 1982, from which the mechanism of Appendix E, Figure 19, was computed.

## DEPTH OF FOCUS DISTRIBUTION, 1982-1983

For the period January 1, 1982 through December 31, 1983, all earthquakes having HYPO71 "A" or "B" quality solutions, having estimated depth error  $< 4.0$  km, and located within the region  $114.8^\circ \text{ W} < \text{longitude} < 117.8^\circ \text{ W}$  and  $35.8^\circ \text{ N} < \text{latitude} < 38.2^\circ \text{ N}$ , are plotted in a depth histogram (Figure 33). There are 427 earthquakes meeting these criteria. The velocity model used to compute these locations (model M0) is plotted in Figure 34. The median depth is 4.9 km below sea level, and the median standard error is 0.9 km. The mean error in the depth of focus is plotted as a function of depth in Figure 35. The depth distribution appears to be bimodal, with peaks at about 1.0 km and 7.5 km below sea level, and with a pronounced minimum at 3.5 km below sea level. This pattern is similar to that for the period 1978 to 1981 reported by Rogers and others (1983). There is a moderate discontinuity in the velocity model at 3 km below sea level ( $P$ -velocity = 5.9 km/sec above that depth, 6.15 km/sec below), which could be a factor in producing the observed aseismicity just below that boundary. Others have noted (e.g., Caccamo and Neri, 1984) that the Geiger method, which is used to adjust hypocentral parameter estimates in the program HYPO71, is unstable for depths of focus that lie just above a velocity discontinuity.

We can combine the distribution of the standard error in depth and the distribution of depths to evaluate the probability density function of depth of focus (Figure 36). Here, depths are assumed to be random variables having normal distributions with means given by the estimated depths, and variances equal to the square of the depth error estimates. Comparing Figures 33 and 36 it can be seen that some of the irregularity in the depth distributions disappears when the depth is considered a random variable, however, the bimodality of the depth distribution is preserved. This result implies that the depth distribution of the hypocentral errors is not a factor in producing the observed bimodal behavior.

### 1982-1983 Relocations Using Velocity Gradient Models

All of the earthquakes for 1982-1983 period were relocated using the program HYPOELLIPSE (Lahr, 1979) and using velocity models containing a linear velocity gradient over a fixed halfspace velocity (Figure 34; models M1, M2) to determine if a gradient model would also produce a hypocentral depth distribution with a bimodal shape. The first velocity gradient model (M1) is specified by

$$v = \begin{cases} v_0 - kz, & \text{if } 0 \leq z_{sta} \text{ km (above sea level);} \\ v_0 + kz, & \text{if } 0 \leq z < 3 \text{ km (below sea level);} \\ v_h, & \text{if } z \geq 3 \text{ km (below sea level).} \end{cases}$$

Here  $v_0 = 3.2$  km/sec,  $v_h = 6.15$  km/sec,  $k = 0.783$  /sec, and  $z_{sta}$  = station elevation (km). Station residuals were obtained and used in the final locations. The depth histogram for A and B quality relocations having  $erz$  (standard error in depth)  $< 4$  km,  $35.8 < \text{latitude} < 38.2^\circ \text{ N}$ ,  $114.8 < \text{longitude} < 117.8^\circ \text{ W}$  (Figure 37) also shows the bimodal shape with a minimum 3.5 km below sea level. This result indicates that the depth distribution is not an artifact of the particular algorithm used to locate the earthquakes, nor is the result dependent on the presence of velocity discontinuities. The second velocity gradient model (M2) is specified by

$$v = \begin{cases} v_{shallow}, & \text{if } 0 \leq z_{sta} \text{ km (above sea level);} \\ v_0 + kz, & \text{if } 0 \leq z < 5 \text{ km (below sea level);} \\ v_h, & \text{if } z \geq 5 \text{ km (below sea level).} \end{cases}$$

Here,  $v_{shallow} = 3.2$  km/sec,  $v_0 = 4.4$  km/sec,  $v_h = 6.15$  km/sec, and  $k = 0.35$  /sec. The program HYPOELLIPSE was used to relocate the 1982-1983 earthquake data. The resulting depth distribution (Figure 38) shows a less pronounced seismicity minimum that has now shifted to depths

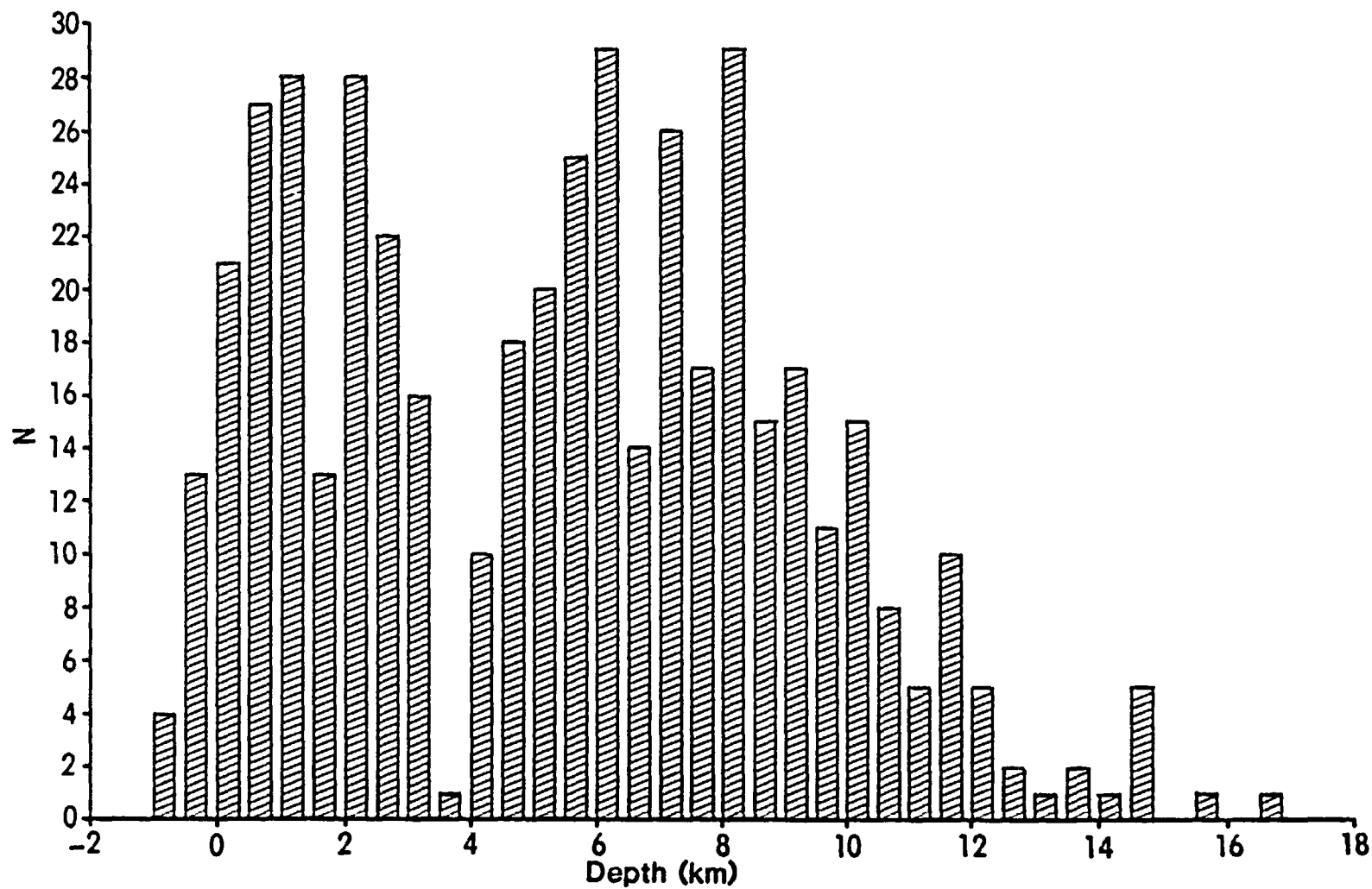


Figure 33.- Distribution of focal depths (  $< 0$  above sea level,  $> 0$  below) for well-located SGB earthquakes for the calendar years 1982 and 1983. The depth data are grouped into 0.5 km wide intervals.

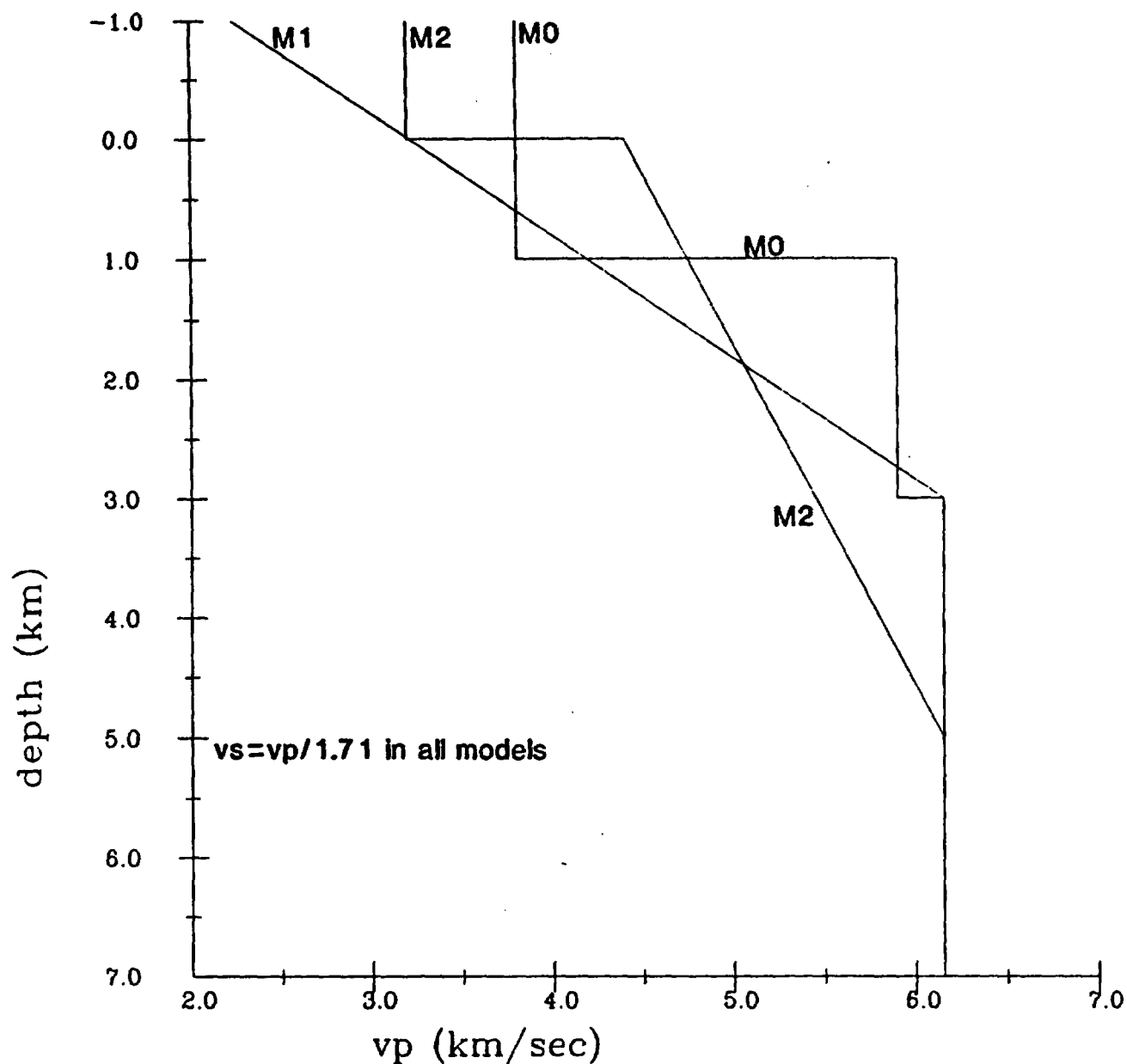


Figure 34.- *P*-wave velocity,  $v_p$ , versus depth for three velocity models that fit known average properties of SGB crustal rock. Model M0 is used routinely to locate SGB earthquakes, and models M1 and M2 are variants that were used with the computer program HYPOELLIPSE to investigate the sensitivity of depth of focus estimates to relatively small changes in the velocity model. For all models,  $v_s$ , the *S*-wave velocity, is assumed to equal  $v_p/1.71$  at a given depth.

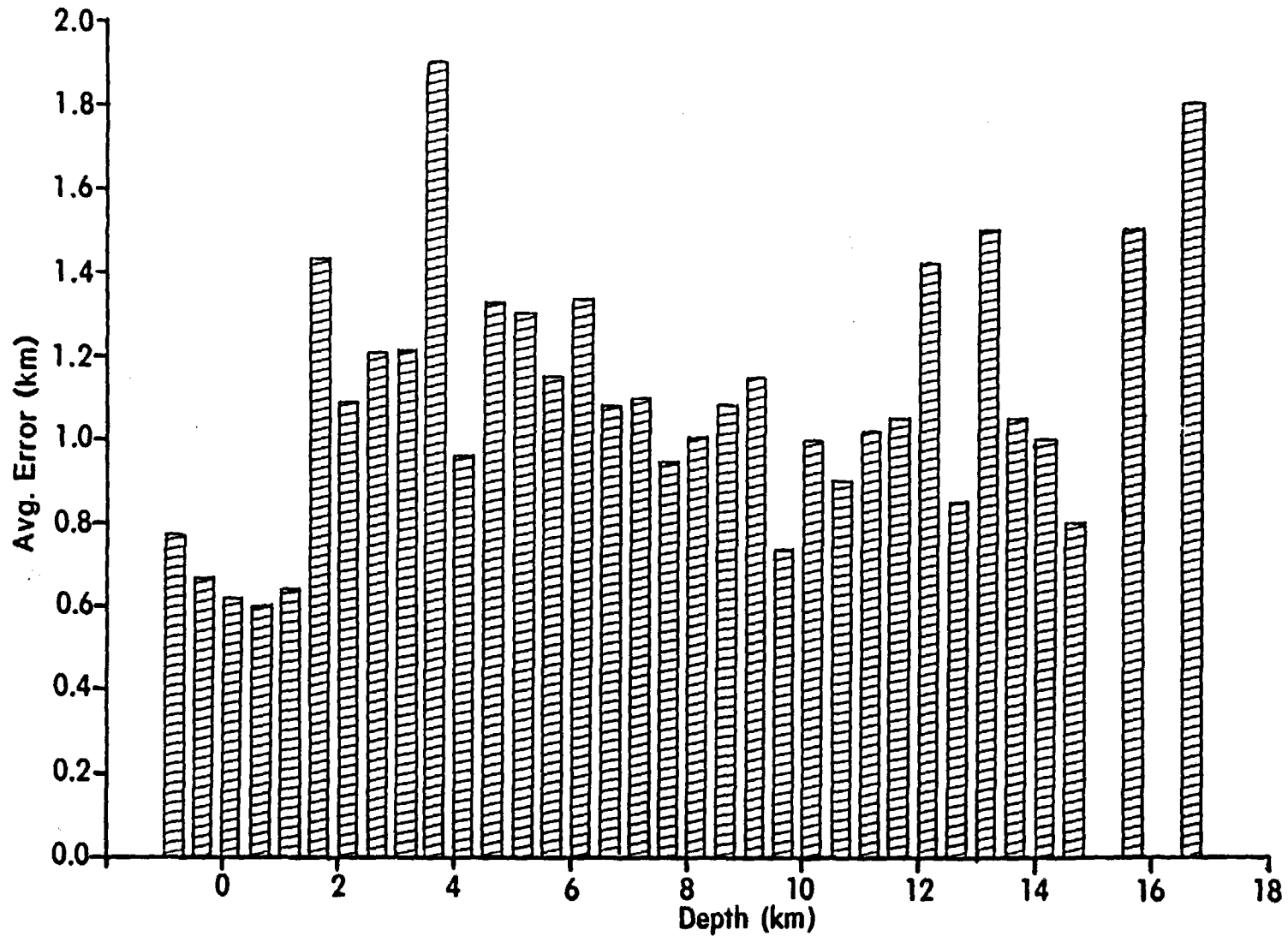


Figure 35.— Distribution of average standard error in depth-of-focus, as a function of estimated depth-of-focus, for the interval data plotted in figure 33.



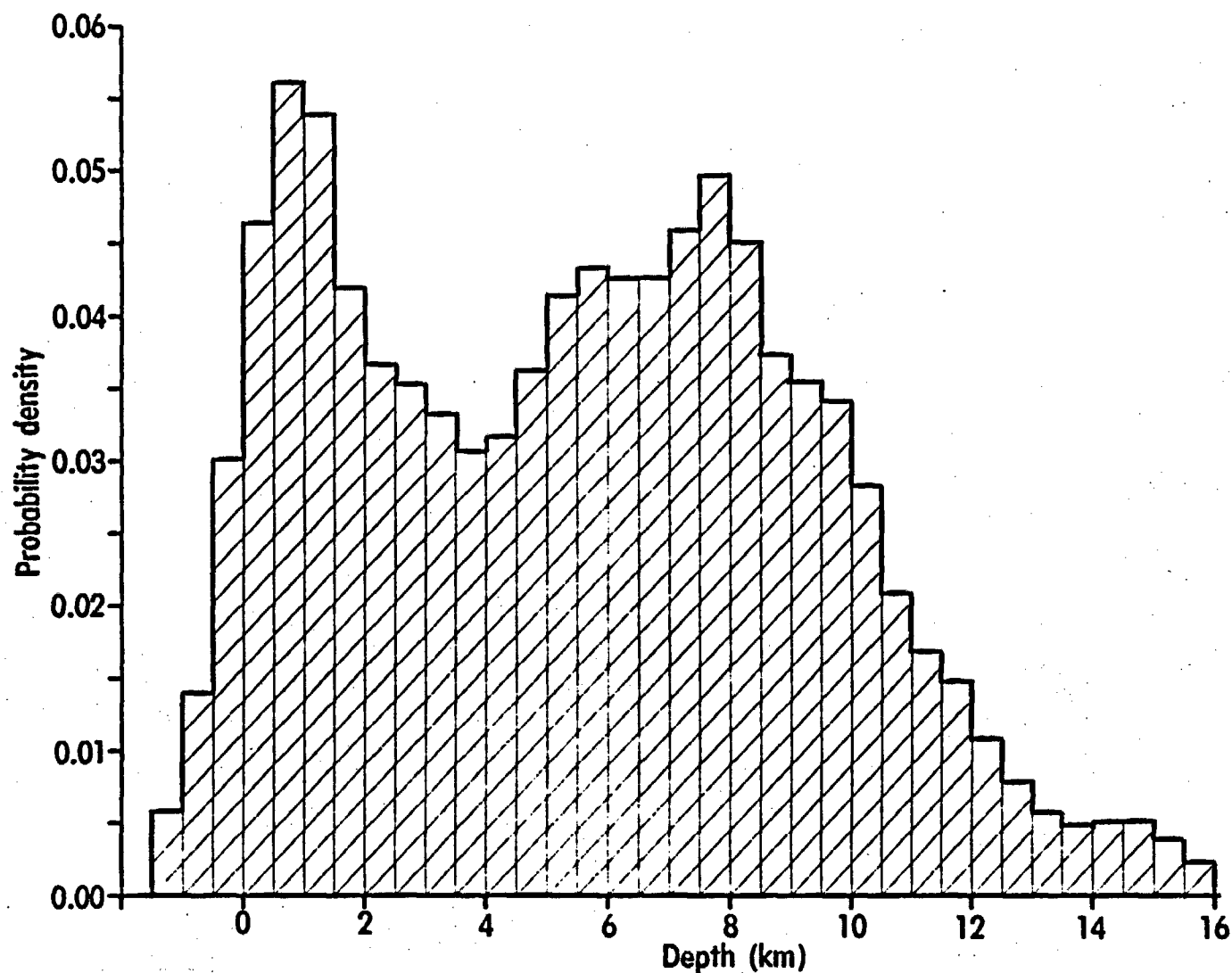


Figure 36.— Probability of an earthquake occurring at a depth  $z$  using velocity model M0, and the same data as in Figure 33. The calculations assume that each depth-of-focus estimate given by HYPO71 is a random variable having an independent gaussian distribution with mean and standard deviation equal to the depth estimate and depth error estimate, respectively. Probabilities within 0.5 km wide intervals were accumulated for depths from 1.5 km above sea level to 16 km below sea level. The total probability was then normalized to 1.0.

of 5-6 km, where the halfspace velocity begins. Thus, in all of the models, a relatively aseismic zone appears just below the last shallow refracting horizon. Earthquakes with hypocenters below this horizon are recorded by the local seismograph network as direct upgoing arrivals. These tests suggest two possible interpretations. First, perhaps, the velocity models suffer from some inherent inaccuracy relative to the true mean regional earth structure. For instance, if there were actually one or more refracting horizons at shallow depths below the 3 km level, then it is possible that the location scheme, using a velocity model without these layers, might force earthquake depths to higher or lower levels. Second, perhaps a true minimum in seismic activity exists at some depth in the upper 5 km of the crust, but that the location of the minimum shifts as a function of the velocity model used to locate the earthquakes. The first interpretation was partially tested by adding a number of artificial layers below 3 km and relocating the earthquakes. The result of this experiment was to modify the bimodal distribution somewhat, but a relative minimum remains at about 4 km. Thus, at present, the second interpretation is preferred.

### Geographic Variation In The Depth Distributions

For the period August 1, 1978 through December 31, 1983, the depth-of-focus distributions were plotted for three sub-regions of the southern Great Basin; the locations were obtained using velocity model M0 and the location program HYPO71. The depth distributions in these three regions (eastern, central, and western) are shown in Figure 39a, b, c. Although the general bimodal depth distribution and the full range of observed depths are found in each geographic region, the proportion of shallow-to-deep events is greater for the eastern region compared to the other two zones. The fact that the bimodal depth distribution occurs in all three regions leads to the conclusion that the shallow peak in the distribution can not be attributed solely to nuclear testing. The two most probable causes of the geographic variation in depth distribution are: (1) the effects of regional variations in velocity structure relative to the velocity model used to locate the earthquakes, and (2) the lack of sufficient observation time to determine the "true" geographic distribution of depths. The two western regions have similar depth distributions and are roughly contained within the broad Walker Lane Belt (Carr, 1984). In contrast, the eastern region, which has a different depth distribution, is contained largely within the basin and range subsection. In spite of the tentative conclusions above, this observation suggests the additional possibility that contrasting structural style or tectonic processes are related to the observed differences.

### FOCAL MECHANISMS AND THE REGIONAL STRESS FIELD

A method proposed by Angelier (1979) to extract stress direction information from sets of focal mechanisms has been applied to our focal mechanisms including those reported earlier (Rogers and others, 1983). The technique is to overlap the tension and pressure dihedral, independently, for all of the mechanisms on the focal sphere. If we assume that a regional stress field having constant principal stress directions activated all of the ruptures from which these mechanisms were derived, then the resulting focal area within the overlap of the tension dihedral must contain the direction of the minimum compressive stress,  $\sigma_3$ , and the focal area within the overlap of the pressure dihedral must contain the direction of the maximum compressive stress,  $\sigma_1$  (McKenzie, 1969).

The result of superposing the SGB mechanism pressure and tension dihedral for all mechanisms of Rogers and others (1983) and this report is plotted in Figure 40a. There is a finite region of overlap of all 29 tension dihedral areas, and 28 pressure dihedral shared a finite common region of overlap. The regional stress tensor may therefore be partially described as having maximum compressive stress orientation in the range N 20° E to N 35° E and minimum compressive stress orientation in the range N 50° W to N 70° W. The remarkable aspect of the dihedral intersection result is that it yielded zones of zero or one inconsistency given 29 focal mechanisms ranging from

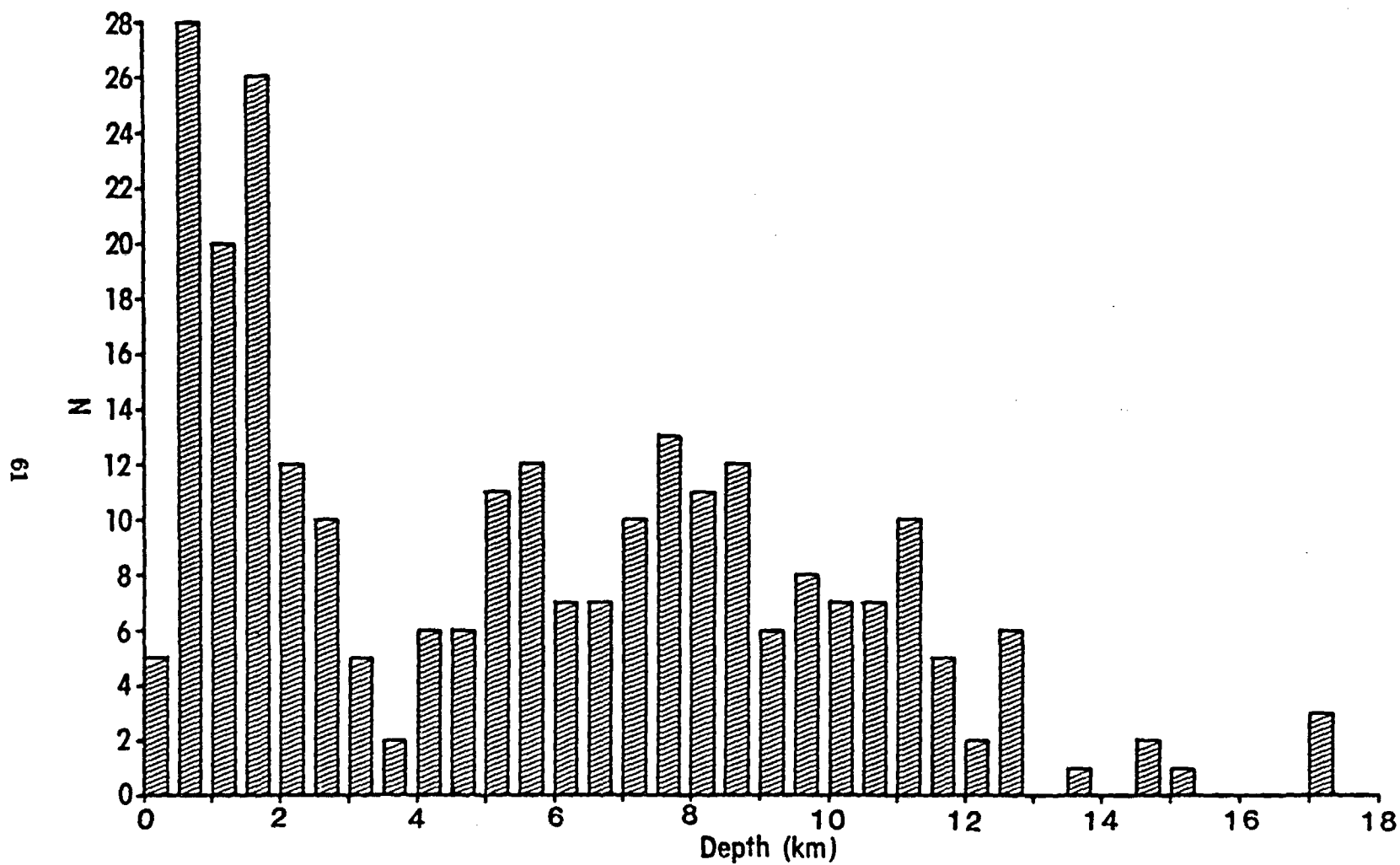


Figure 37.- Distribution of focal depths below mean station elevation ( $\approx 1.2$  km. above sea level) obtained using velocity model M1 and HYPOELLIPSE.

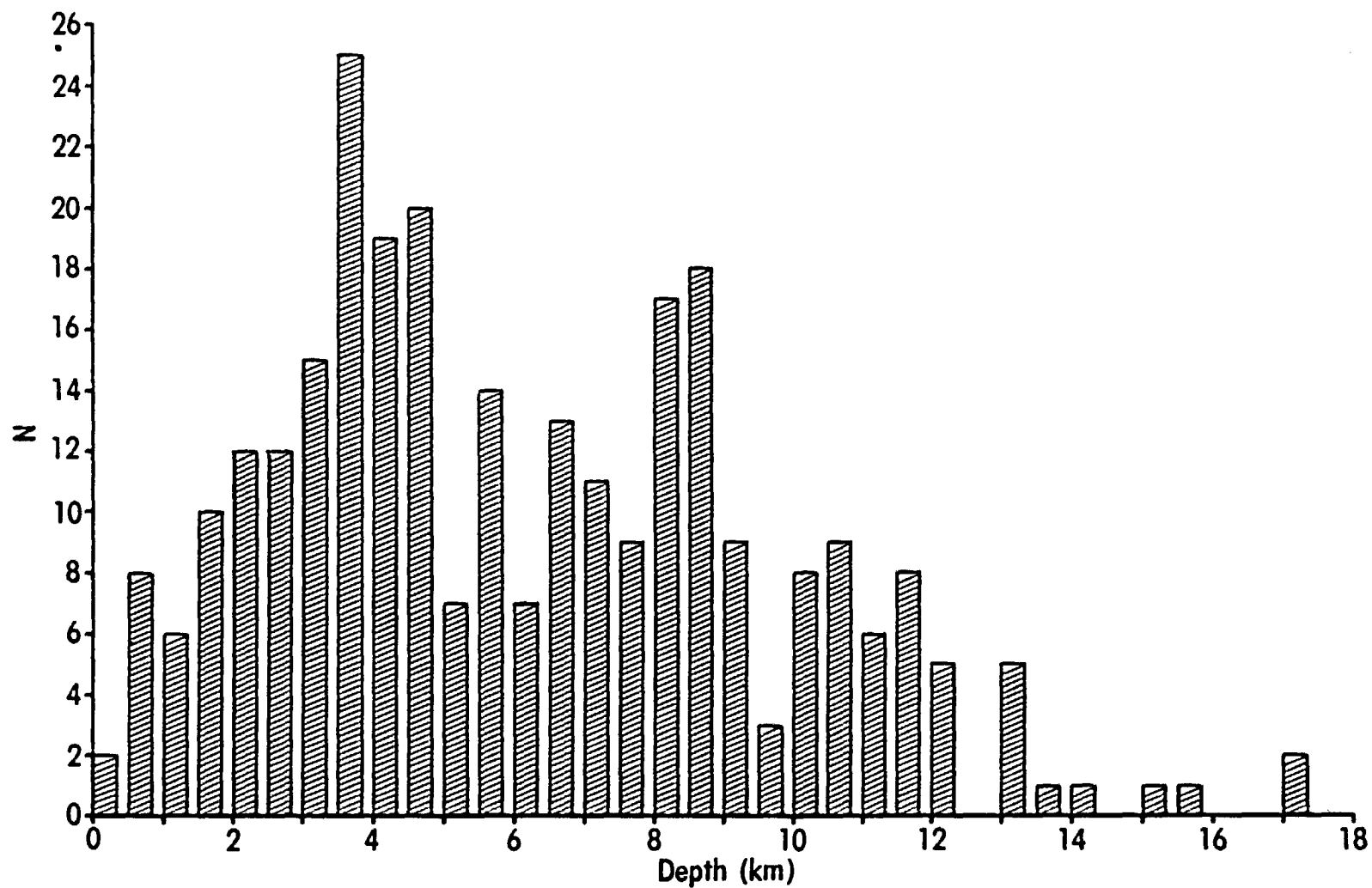


Figure 38.- Distribution of focal depths below mean station elevation obtained using velocity model M2 and HYPOELLIPSE.

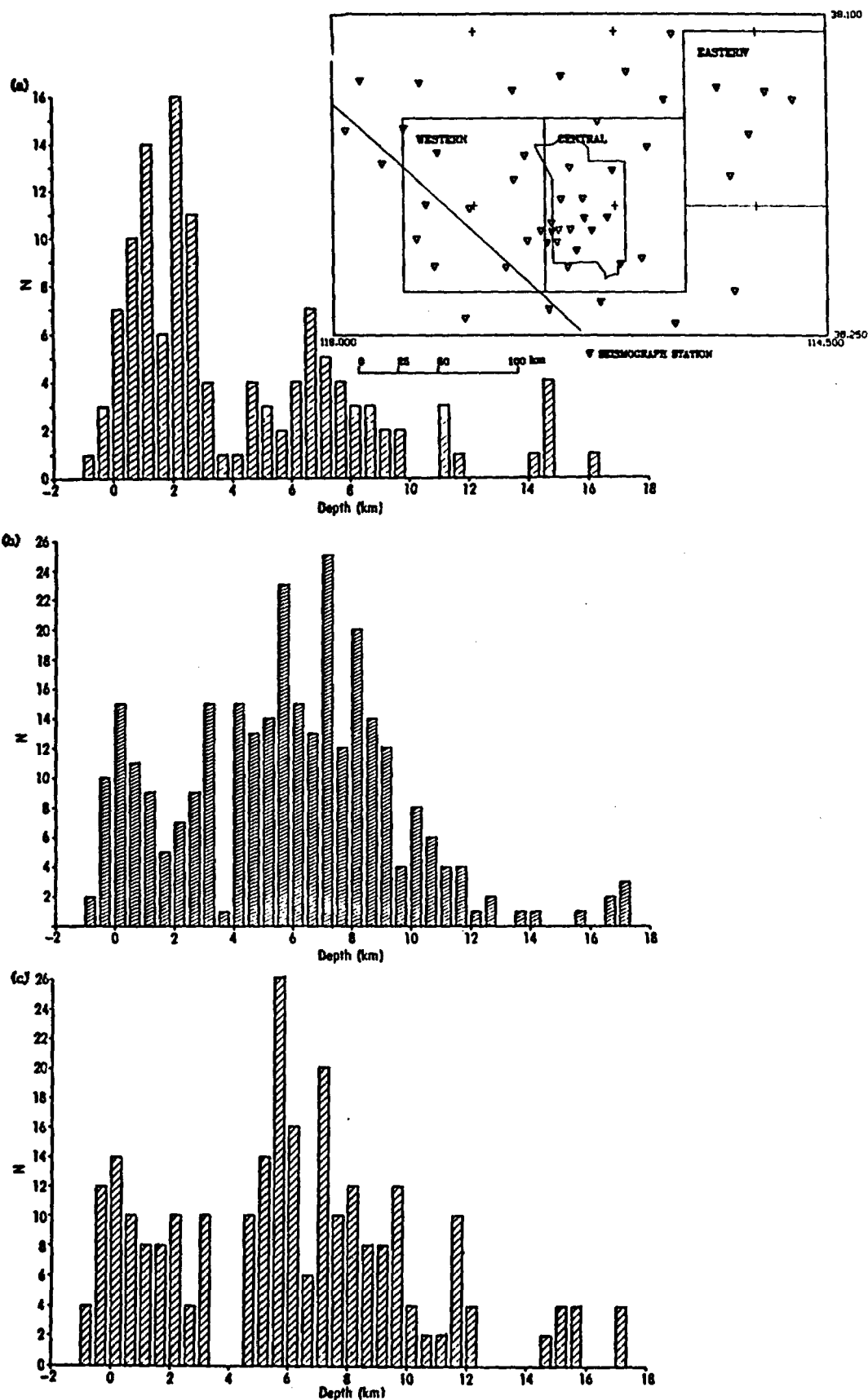


Figure 39.- Distribution of focal depths using velocity model M0 ( $< 0$  above sea level,  $> 0$  below) for three SGB regions for the period August 1, 1978, through December 31, 1983. The inset map outlines the three regions. (a) The *eastern* region is a one square degree area centered at 37°30' N, 115°0' W. (b) The *central* region is a one square degree area centered at 37°0' N, 116°0' W. (c) The *western* region is a one square degree area centered at 37°0' N, 117°0' W.

strike slip to normal slip. This degree of consistency for  $\hat{\sigma}_1$  and  $\hat{\sigma}_3$  directions is good evidence that these stress directions are fairly constant throughout the seismogenic portion of the crust. It is also notable that the full data set is most consistent with an orientation for these two stress directions that is oblique to the horizontal and vertical planes. This result suggests that the stress field may be modified by crustal geometry such as variable crustal thickness.

To explore the possibility that our focal mechanisms exhibit a systematic change with depth, we segregated them into those having depth of focus less than six km below sea level, and those having depth of focus greater than six km. Repeating the intersection of dihedra exercise described above on the 14 shallow-focus mechanisms resulted in the focal areas containing  $\hat{\sigma}_1$  and  $\hat{\sigma}_3$  shown in Figure 40b. For the 15 mechanisms from earthquakes at greater depths, the resulting focal areas containing  $\hat{\sigma}_1$  and  $\hat{\sigma}_3$  are shown in Figure 40c. These figures indicate orientations for  $\hat{\sigma}_3$  that are similar for shallow and deep events. Both shallow and deep data sets show  $\hat{\sigma}_1$  with a range of orientations between vertical and horizontal. Thus, these data provide no evidence that stress orientations giving rise to shallow earthquakes are different than the stress orientations giving rise to deep earthquakes.

In order to further evaluate the regional stress field from focal mechanism data we attempted to find a set of principal stress directions consistent with the slip directions  $\vec{X}$  or  $\vec{Y}$  of the focal mechanisms. Gephart (1985) showed that, in general, for a focal mechanism, at most one of the two slip vectors  $\vec{X}$  or  $\vec{Y}$  is consistent with a given set of principal stress directions. The method assumes that the direction of maximum shear on a given focal plane coincides with the slip direction and that the nodal plane orientations are known exactly. The method also assumes that microearthquakes are occurring on preexisting planes of weakness rather than breaking homogeneous, isotropic rock. From these assumptions, an important parameter  $R = \frac{\sigma_1 - \sigma_2}{\sigma_1 - \sigma_3}$  is computed for each slip direction  $\vec{X}$  and  $\vec{Y}$  by the coordinate transformation method of Gephart and Forsyth (1984). In this context,  $\sigma_1, \sigma_2$ , and  $\sigma_3$  represent the magnitude of the maximum, intermediate, and minimum principal compressive stresses, respectively. The nodal planes whose slip vectors produce  $R$  values such that  $0 \leq R \leq 1$  are selected as the preferred focal planes.

This analysis, which uses the directions

$$\hat{\sigma}_i, i = 1, 2, 3$$

and the focal mechanism directions,

$$\vec{X}_i, \vec{B}_i, \text{ and } \vec{Y}_i, i = 1, 2, \dots, 29$$

as input data, was performed for the mechanisms reported here and in Rogers and others (1983). We varied the directions  $\hat{\sigma}_1$  and  $\hat{\sigma}_3$  through the range of acceptable values indicated in Figure 40a and, for this analysis, ranked the quality of the assumed stress fields by the degree of similarity of the computed  $R$  values for the 29 mechanisms. Equivalently, for all allowable *orientations* of the principal stress ellipsoid implied by Figure 40a, we searched for that orientation for which the *shape* of the principal stress ellipsoid varied the least over the 29 mechanisms. Although this analysis is different from a formal inversion of mechanism data to obtain the stress tensor (as in Gephart and Forsyth, 1984), it provides a method to determine which nodal plane is the best choice for a given assumed stress field and, at the same time, gives an average value of  $R$  for all of the mechanisms, assuming constancy of principal stress directions.

The orientations of the principal stress components that minimize variance in  $R$  for the 1979-1983 southern Great Basin focal mechanisms are given in Table 3 below. For this stress field, whose principal axes are shown in Figure 41,  $\bar{R} = 0.34 \pm 0.21$ . This stress field gave  $R$  values in the physically acceptable range  $0 \leq R \leq 1$  for 28 of the 29 mechanisms, and had marginally

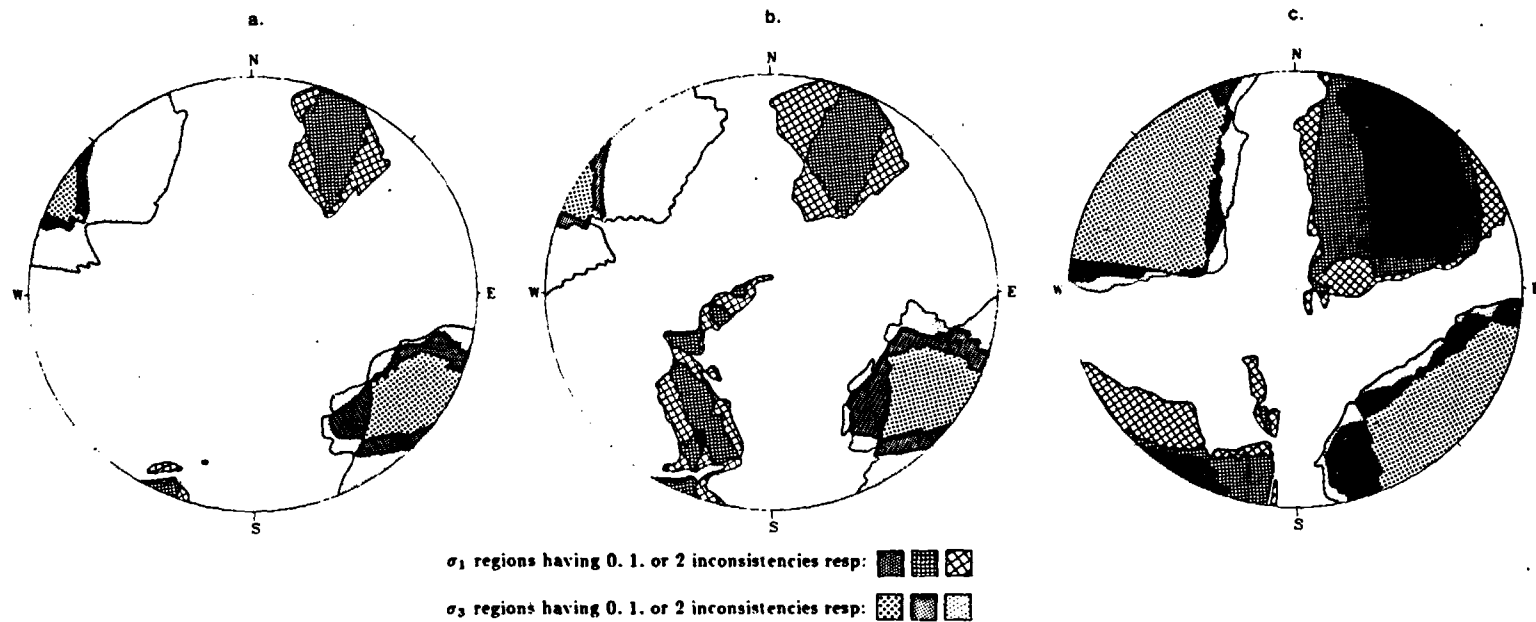


Figure 40- (a), Equal-area, lower hemisphere projection of the intersection of pressure dihedra and tension dihedra for 29 southern Great Basin earthquake focal mechanisms. Locations where all, all but one, and all but two, tension quadrants overlapped are designated by the "regions of inconsistency" in the legend. Locations where all but one and all but two pressure quadrants overlapped are designated by the  $\sigma_1$  "regions of inconsistency" in the legend. There was no common region of intersection of pressure dihedra for all of the mechanisms. The significance of these regions of intersection is discussed in the text. (b), Same as 40 (a) except that we intersect mechanism regions only for the 14 earthquakes having depth-of-focus,  $z \leq 6$  km. (c), Same as 40 (a) except that we intersect mechanism regions for the 15 earthquakes having  $z > 6$  km.

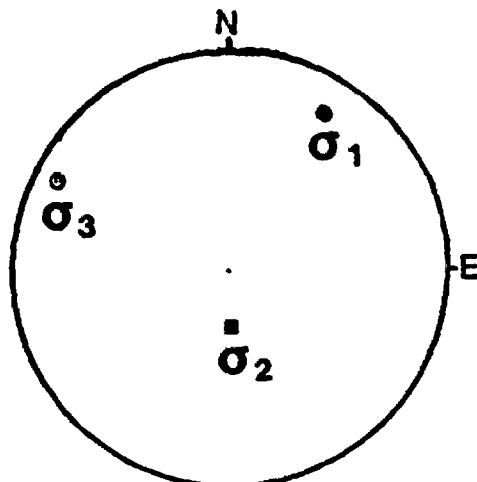


Figure 41.— Equal-area, lower hemisphere projection of the directions of the principal stress components,  $\sigma_1$ ,  $\sigma_2$ , and  $\sigma_3$ , obtained by the method discussed in the text, and shown in Table 3.

less variance in  $R$  than any other stress field that could be fit to this many mechanisms. Thus, it is possible to find principal stress component orientations that satisfy the original assumption of constant  $R$ -value reasonably well. This result does not constitute proof that  $R$  is nearly constant, or that principal stress directions are regionally unvarying, but suggests that such assumptions are plausible.

	Azimuth	Plunge
$\sigma_1$	32.0°	18.2°
$\sigma_2$	178.1°	68.0°
$\sigma_3$	298.0°	12.0°

Table 3. Principal stress directions resulting from the minimization of the variance of  $R = \frac{\sigma_1 - \sigma_2}{\sigma_1 - \sigma_3}$  for 28 southern Great Basin focal mechanisms.

Harmsen and Rogers (1986) have shown that if a fixed stress field is controlling seismic slip, then the most likely conditions for the proximate coexistence of strike-slip and normal fault earthquakes is that the stress field be approximately axially symmetric. That is,

$$0.8 \leq \sigma_2/\sigma_1 \leq 1.0$$

$$0.0 \leq R \leq 0.3$$

This conclusion is supported by the observation that both strike-slip and normal fault events are observed throughout the seismogenic portion of the crust (Figure 42) and is based on the assumption that slip will preferentially occur on pre-existing fault planes with orientations that are optimum for satisfying the Mohr-Coulomb criterion. An alternative interpretation suggested in the past—that the rate of increase in the vertical principal stress with depth is greater than the rate of increase of the greatest horizontal principal stress (Zoback and Zoback, 1980a, and Vetter and Ryall, 1983)—does not fit our observations. To satisfy this alternative, the focal mechanism types should display a depth dependence, such that strike-slip events would be restricted to shallow



depths and normal fault events would occur at greater depth. Hydrofrac data collected at Yucca Mountain (Stock and others, 1985) imply that

$$\sigma_H/\sigma_v \sim 0.65$$

$$\sigma_h/\sigma_v \sim 0.30$$

$$R > 0.5,$$

where  $\sigma_v$  is the effective vertical stress,  $\sigma_H$  is the maximum effective horizontal stress, and  $\sigma_h$  is the minimum effective horizontal stress. Harmsen and Rogers (1986) have shown that, under application of the Mohr-Coulomb criterion to these stress directions, assuming the relative stress magnitudes given by the hydrofrac data, strike-slip is not possible on north-south or east-west oriented fault planes. We infer, then, that the stress conditions measured by hydrofrac techniques do not reflect the general critical stress conditions throughout the region and/or the stress conditions at seismogenic depths. Most state of stress measurements at the Nevada Test Site indicate that  $\sigma_H \leq \sigma_v$ , the only exception being one measurement at the Spent Fuel Test-Climax site, where the maximum principal stress was determined to strike and plunge at N. 56° E. and 29°, respectively, and to have about 1.66 the amplitude of the intermediate principal stress (Ellis and Magner, 1982). In the vicinity of the Climax stock, no earthquakes catalogued through 1983 have been large enough to provide reliable focal mechanisms to compare stress associated with earthquakes with that from surface measurements. It is possible, however, that the peculiar stress conditions obtained by Ellis and Magner are local.

It is worth considering the implication of these results regarding the behavior of stress with depth. For instance, we can compare our results with several hypothetical models of stress-depth dependence. Figure 43 shows examples that have been discussed in the past. Jaeger and Cook (1969), among others, have suggested that the tectonic-gravitational model is a suitable model to explain tectonic behavior in an extensional regime. That is, normal dip-slip on faults trending perpendicular to the direction of least principal stress is driven by the gravitational (vertical) stress, which is assumed to be the maximum principal stress. The direction of least principal stress may vary over the region. This type of model would not generally permit strike-slip faulting unless coefficients of friction are very low on the wrench faults (Harmsen and Rogers, 1986; fig. 6). This model is similar to that suggested by the hydrofrac data collected at Yucca Mountain (Stock and others, 1985), in that horizontal stresses increase less rapidly with depth than the vertical stress,  $\sigma_z$ , which is assumed to equal the lithostatic load. The tectonic-gravitational model is based on the assumption of zero lateral displacement at the boundaries of the rock volume; thus, the tectonic stress release must occur slowly in order to avoid violating the principal assumption of the model. (If the boundary conditions are relaxed to allow material displacement through the boundary, the minimum compressive stress should decrease as the displacement occurs, so that model predicts increasing seismic slip with time.) Furthermore, the model predicts a large difference between the maximum and minimum principal stresses in dry rock at relatively shallow depths (when Poisson's ratio equals 0.25); this stress difference is more than adequate to initiate normal slip on steeply dipping surfaces whose stability is governed by the Mohr-Coulomb criterion. Because it is possible that fluid pore pressure is also high in an extensional tectonic regime, the tectonic-gravitational model suggests a degree of crustal instability that may not be plausible.

The Vetter and Ryall (1983) model requires a moderate amount of horizontal compressional tectonic stress in the direction parallel to the intermediate principal stress, such that  $\sigma_v \leq \sigma_H$  at depths less than about 10-15 km. Although this model permits both normal and strike-slip faulting, each mode is confined to certain sections of the crust as noted above.

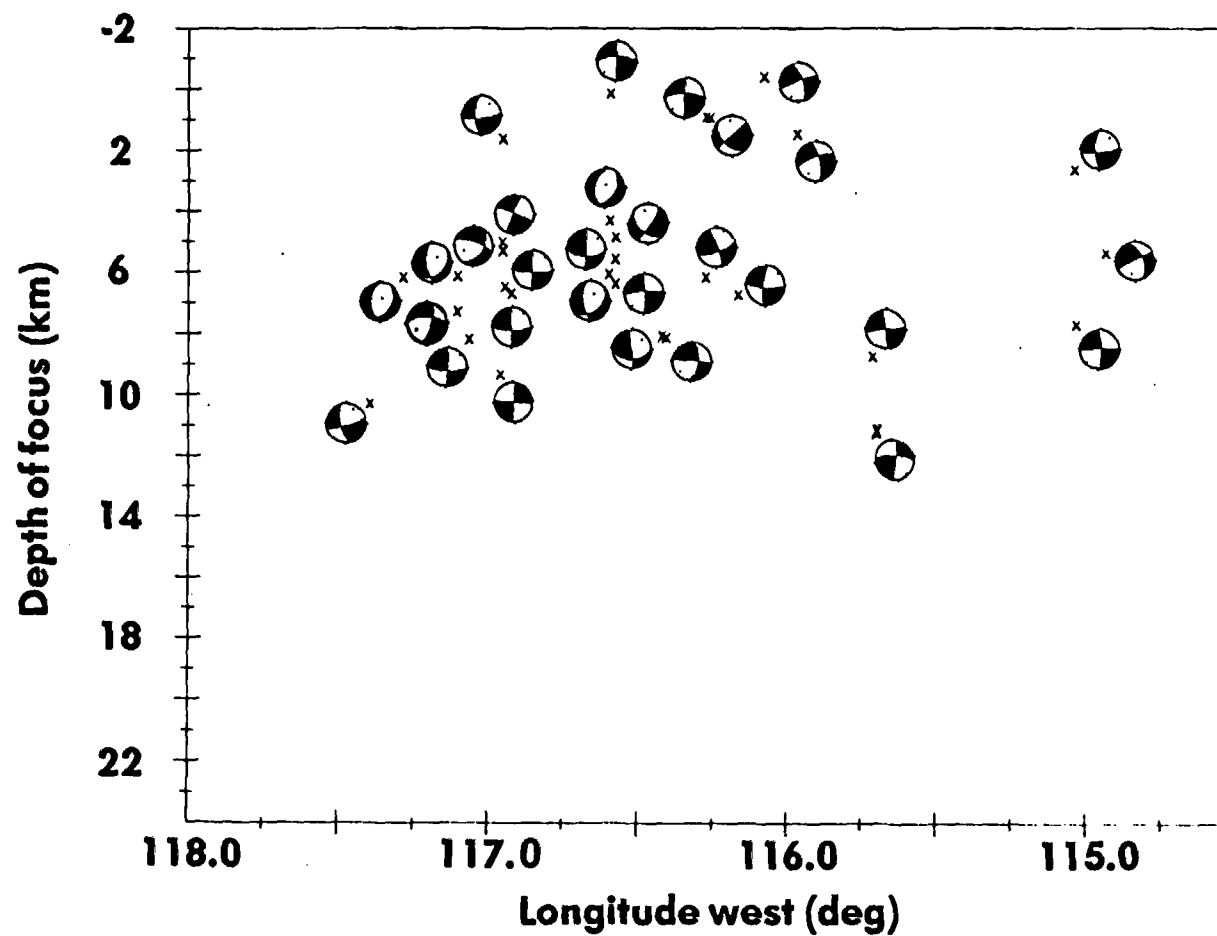
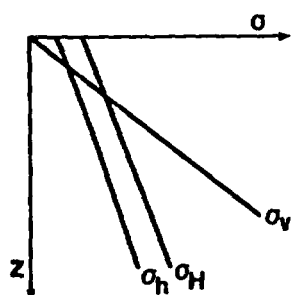


Figure 42.- Thirty southern Great Basin earthquake focal mechanisms plotted in depth section over the longitudinal range of the SGB network. Although this plot is in cross section, the focal mechanisms are lower hemisphere projections shown in map view.

## Models Of Stress Distribution With Depth

$$R = \frac{\sigma_1 - \sigma_2}{\sigma_1 - \sigma_3}$$

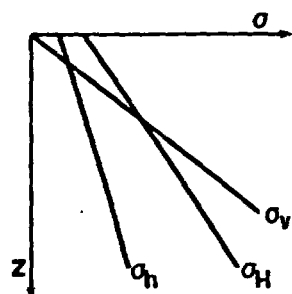


**R highly variable**

$$0 \leq R \leq 1$$

$$\sigma_v = \rho g z, \sigma_H = \sigma_r + \frac{\gamma}{1-\gamma} \sigma_z, \sigma_h = \gamma \sigma_r + \frac{\gamma}{1-\gamma} \sigma_z$$

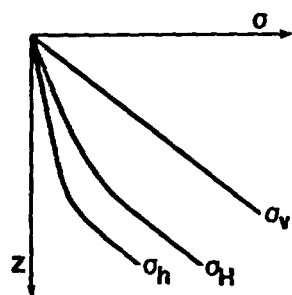
**Tectonic - Gravitational Model**  
(Jaeger and Cook, 1969)



**R highly variable**

$$0 \leq R \leq 1$$

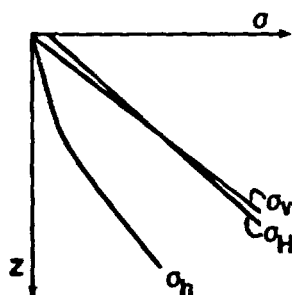
**Vetter and Ryall Model (1984)**



**At some shallow depth R becomes approximately constant**

$$R > 0.5$$

**Yucca Mountain Hydrofrac Data**  
(Stock and others, 1985)



**At some shallow depth R becomes approximately constant**

$$R \approx 0.0 - 0.3$$

**Hypothetical model accounting for the existence of both strike-slip and normal fault events throughout the seismogenic crust.**

Figure 43.- Four models showing how vertical and horizontal crustal stresses may be distributed with depth. Some consequences of such hypothetical stress distributions are discussed in the text. Symbols:  $\rho$  = rock density,  $g$  = acceleration of gravity,  $z$  = depth,  $\gamma$  = Poisson's constant,  $\sigma_v$  = magnitude of vertical stress,  $\sigma_H$  = magnitude of maximum horizontal stress,  $\sigma_h$  = magnitude of minimum horizontal stress, and  $\sigma_r$  = magnitude of regional horizontal tectonic stress, excluding its gravitational component.

Our focal mechanism data through 1983 are consistent with the interpretation that  $\sigma_v \approx \sigma_H$  throughout the upper 10-15 km of the crust, such that either minor stress perturbations or the presence of optimally oriented fault planes would permit both normal and strike-slip faulting. Furthermore, Harmsen and Rogers (1986) have demonstrated that, given axially symmetric stress conditions, dextral, sinistral, and normal slip are equally likely on north-, east-northeast-, and northeast-trending faults, respectively. A noteworthy implication of this model is that the horizontal component of tectonic stress increases with depth at a rate that consistently maintains the relationship between the vertical and horizontal principal stresses. This result is consistent with a basal shear acting horizontally along the base of the brittle crust or, perhaps, the lithosphere, as suggested by Hanks (1977).

### Earthquake Density in the Southern Great Basin

All of the earthquakes located in the region from August 1978 through December 31, 1983 within 150 km of the point 36°51' N, 116°27.5' W (Yucca Mountain proposed site) were combined into a histogram showing earthquake frequency per unit area as a function of distance to Yucca Mountain (Figure 44). This point, also referred to as the Site, is approximately one minute (1.8 km) south of drill hole G1 (see Figure 11). Figure 44 emphasizes the relatively low level of seismicity within several kilometers of Yucca Mountain, and reflects the relatively high earthquake density that occurs in the Jackass Flats-Rock Valley region, 10 to 20 kilometers east of the Site. The plot also shows the relatively higher rates of seismicity for much of the Nevada Test Site compared with the rest of the region. Some fraction of this earthquake activity is triggered by nuclear testing. Although at present there is no unequivocal method for establishing which earthquakes within the region are tectonic and which are triggered by testing, research is underway to try to establish such a method. Table 4 lists those active areas contributing the largest number of events to the computed densities. Table 4 was prepared by computing the number of earthquakes in each annulus of 5 km width centered at the distance given in the table, and then dividing that number by the area of the annulus to obtain the earthquake density. The earthquake energy densities within the same annuli have been computed and are shown in Figure 45. This figure indicates that Yucca Mountain is in a region of energy release that is about 2 to 3 orders of magnitude less than the regional level and 4 orders of magnitude less than the nuclear testing zones. This decrease occurs within about 30 km of the Site. The plot also shows that the maximum energy release occurs in the annulus that includes the nuclear testing areas.

An energy release contour map using the data from this study is shown in Figure 46. The principal features of this map are: (1) the east-west-trending pattern of energy release crossing the region at about latitude 37°; (2) a region paralleling the Nevada-California border that includes portions of the Furnace Creek-Death Valley fault system and Yucca Mountain where energy release

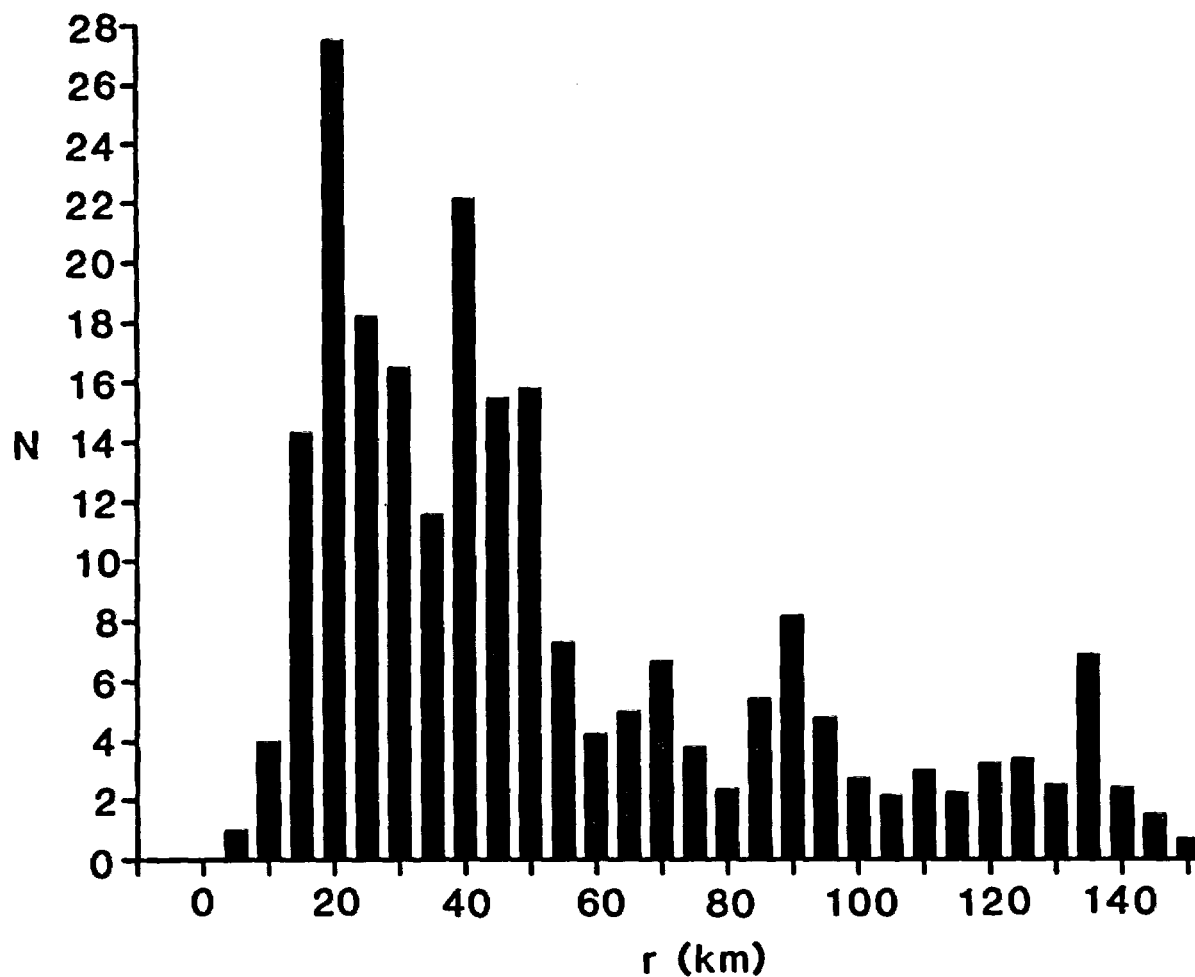


Figure 44.- Distribution of number of earthquakes per unit area as a function of distance from Yucca Mountain, from 0 to 150 km, for the time period August 1, 1978, through December 31, 1983 (Table 3). N is the earthquake frequency per unit area at epicentral distance r from Yucca Mountain.

distance (km)	no. eq.	normalized eq. density (no./unit area)	Active areas at that distance range
0.0	0	0.00	
5.0	1	1.00	Yucca Mtn. earthquake on 810413 at 20 21 (near YMT5)
10.0	8	4.00	Yucca Mountain, Crater Flat
15.0	43	14.33	Dome Mountain, Jackass Flats, Bare Mountain
20.0	110	27.50	Jackass Flats, Little Skull Mountain, Skull Mountain
25.0	91	18.20	Lookout Peak, Shoshone Mountain, Striped Hills
30.0	99	16.50	Rock Valley, Shoshone Mountain, Tippipah Spring
35.0	81	11.57	Rock Valley, Specter Range, Tippipah Spring
40.0	177	22.13	Thirsty Canyon, Funeral Mountains, Amargosa Desert
45.0	139	15.44	Frenchman Flat, Mercury Valley, Massachusetts Mountain
50.0	158	15.80	Sarcobatus Flat C, Pahute Mesa, Yucca Flat
55.0	80	7.27	Sarcobatus Flat B, Ranger Mountains
60.0	51	4.25	
65.0	65	5.00	Mesquite Flat, Stovepipe Wells
70.0	93	6.64	Indian Spring Valley
75.0	57	3.80	Sarcobatus Flat A (Scotty's Junction)
80.0	38	2.38	
85.0	92	5.41	Sarcobatus Flat D, Gold Mountain, Ubehebe Crater
90.0	147	8.17	Slate Ridge, Gold Mountain
95.0	91	4.79	
100.0	55	2.75	
105.0	45	2.14	
110.0	66	3.00	
115.0	52	2.26	
120.0	78	3.25	
125.0	85	3.40	
130.0	68	2.54	
135.0	185	6.85	Pahranagat Shear Zone
140.0	68	2.43	
145.0	44	1.52	
150.0	20	0.67	

Table 4. Seismogenic areas in the vicinity of Yucca Mountain and NTS for the period August, 1978 through 1983.

values are generally 2-3 orders of magnitude lower than the high energy release zones; this zone appears to be connected with low energy release in the eastern Mojave Desert; (3) a broad zone of high energy release roughly centered on northern NTS that is comparable in level to other high regions throughout the area; (4) significant zones of quiescence in the northern portion of the map area; and (5) a quiescent zone in the southeast corner of the map area that includes, among other features, the northwest-trending Spring Mountains and the Desert Game Range where that range displays a north-northwest structural trend. As noted earlier by Rogers and others (1983) faults with northwest trend are not favorably oriented for slip given the stress field orientation that has been inferred from earthquake focal mechanisms for the SGB. This interpretation does not seem appropriate, however, for the Furnace Creek-Death Valley fault zone or other areas to the west of Death Valley due to the presence of abundant Holocene fault scarps in that region. There is geological evidence indicating not only vertical displacements, but significant horizontal displacements as well (Carr, 1984). The geologic data suggest that the Death Valley region is subject to a more easterly to east-southeasterly least principal stress and a greatest principal stress that is vertical or perhaps roughly equal to the intermediate stress (Zoback and Zoback, 1980b). This stress orientation is similar to that generated at the North American-Pacific plate boundary. Thus, significantly lower energy release in the Furnace Creek-Death Valley fault zone may be the result of either low stress levels due to previous prehistoric seismic energy release or a kind of intraplate seismic gap where stresses are high and the fault zone is locked. Carr (1984) has suggested that the Furnace Creek-Death Valley fault zone relieves shear stress generated by relative motions along the continental plate boundary and acts as a tectonic buffer suppressing the accumulation of stresses generated by plate motions in regions to the east and northeast of this fault system. Comparison of the Holocene slip record on this fault system with the focal mechanism inferred stress orientations to the east of the system suggests that a clockwise stress rotation occurs at or just to the east of the Furnace Creek-Death Valley fault system. A stress rotation could be taken as evidence that a high-stress locked-fault scenario for this fault system is not as likely as a relieved stress state. Presumably, a locked fault state would carry significant amounts of slip to the east of the Furnace Creek-Death Valley fault system that would have an orientation and style more like that at the continental plate boundary.

Comparison of energy release in the current record (Figure 46) and in the historic record (Figure 47) reveals a pattern that is similar in its gross features, but differs in detail. For instance, the east-west zone of energy release is present, but has a considerably broader north-south extent than indicated in the current record. Some areas of early high-energy release (Figure 47) remain relatively high in the current monitoring period; for example, at the NTS testing regions, an area just to the west of the Death Valley fault zone, and the Lake Mead area. Other areas that are active in the early record are no longer active; for example, the areas north-northwest of Caliente in the northern section of the North Pahroc Range and the Kane Springs region to the south-southeast of Alamo were active in the historic record but are relatively inactive today. This change in activity has the appearance of gap-filling in some zones such as the North Pahroc Range-Paranaghat-Kane Springs region and, to a lesser extent, in the western border of the map between latitudes  $37.5^{\circ}N$  and  $38.5^{\circ}N$ . Another notable feature of Figures 46 and 47 is that averaged over decades the active zones tend to produce about the same mean annual energy release rate, including the zones of induced seismicity at Pahute Mesa and Lake Mead. This result implies a long-term constant strain release rate across the region. Several large regions of low energy release exist for both time periods: (1) the Death Valley-Spring Mountains-Desert Game Range region, and to the east between Kane Springs and Lake Mead; (2) the region between Gold Flat and the northwest corner of the map area; and (3) the northeast corner of the map area.

In this report we make no attempt to resolve differences in observed energy release rates

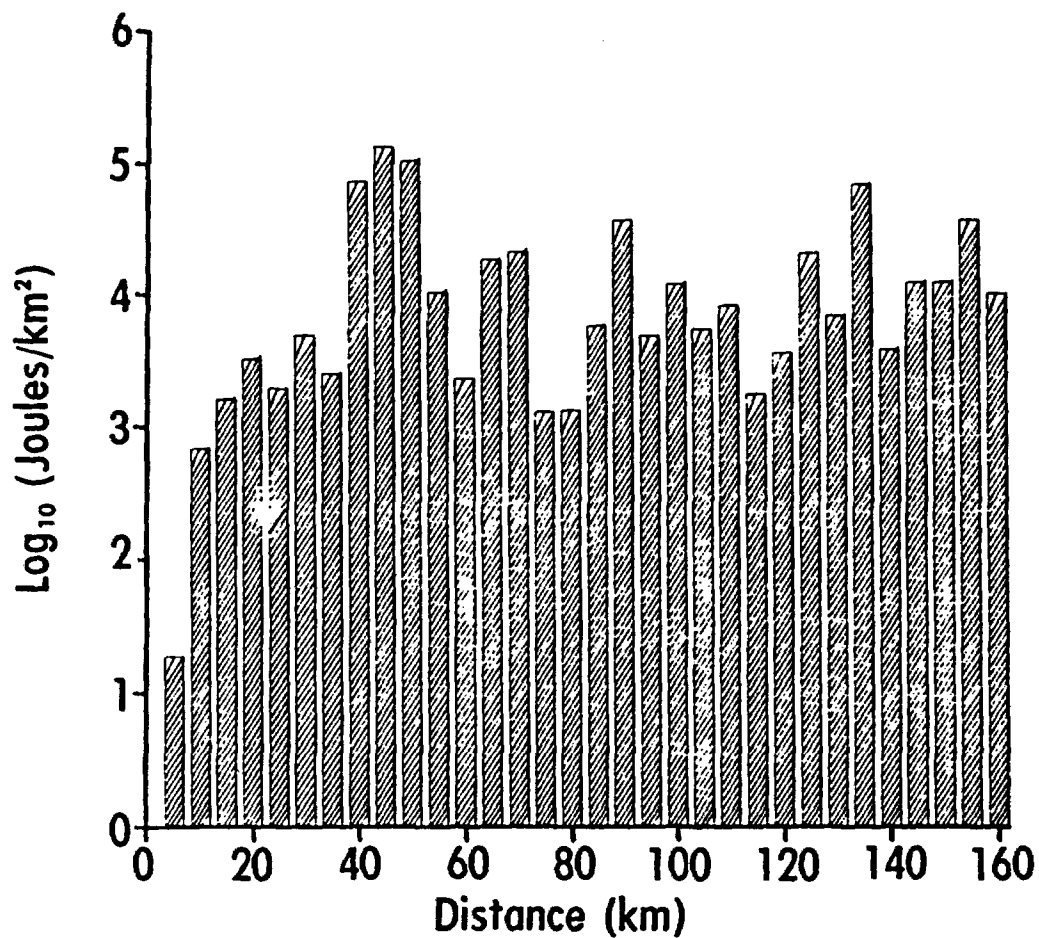


Figure 45.— Distribution of  $\log_{10}(E)$ , where  $E$  represents the cumulative energy release (*Joules/km<sup>2</sup>*) as a function of epicentral distance from Yucca Mountain, for the time period August 1, 1978, through December 31, 1983. The bars have width 5 km and are centered at the distances shown.



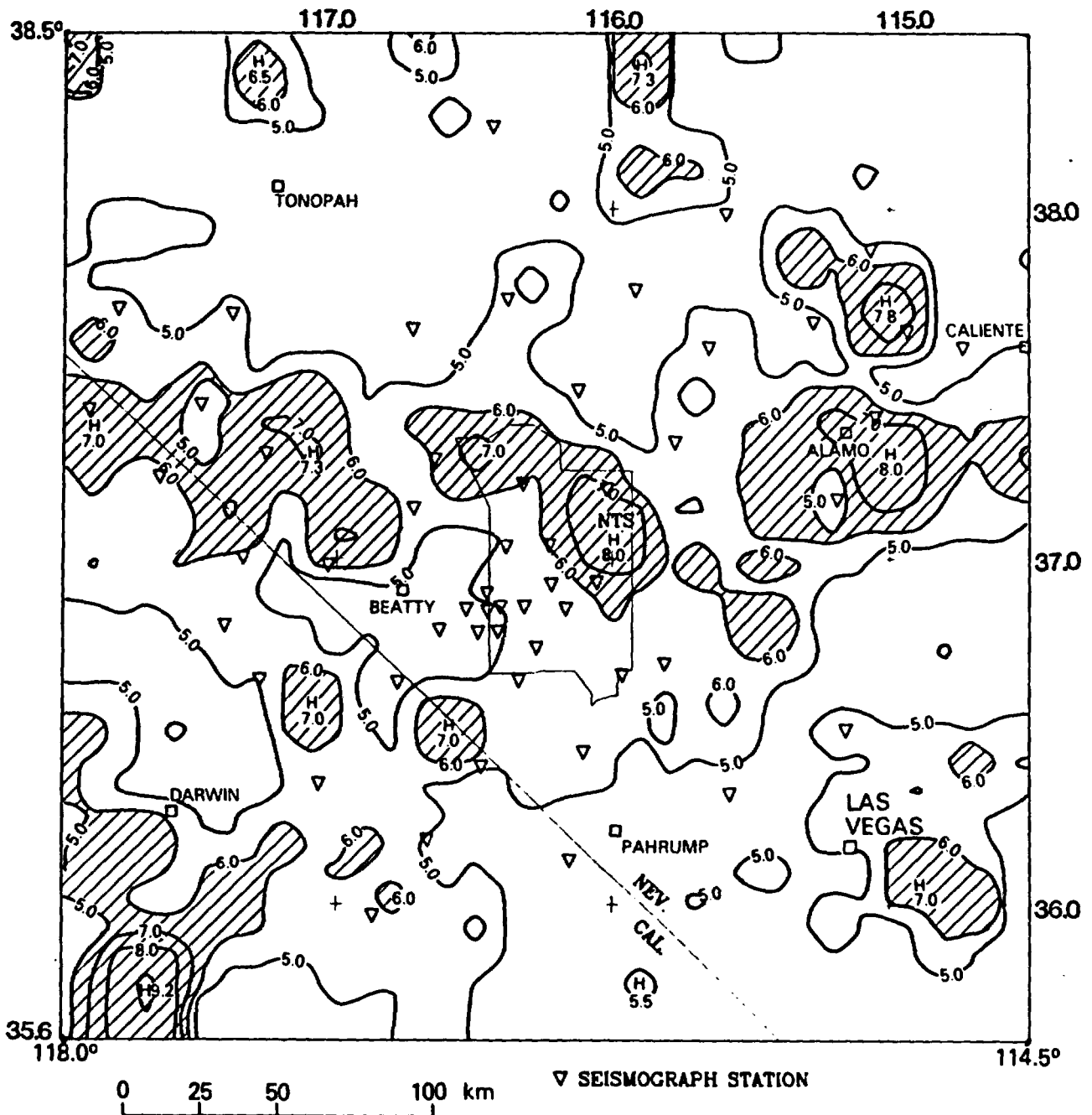


Figure 46.— The distribution of earthquake energy release in the southern Great Basin of Nevada and California is plotted as contours of energy release per unit area  $\log_{10}(\text{Joules}/80\text{km}^2)$  for the seismicity during the period August 1, 1978 through December 31, 1983. The cumulative energy in each  $0.1^\circ \text{EW} \times .08^\circ \text{NS}$  grid was tallied without regard to individual event depth-of-focus, and the gridded data were smoothed and contoured. All known nuclear tests were removed, but aftershocks of nuclear tests were not removed. This accounts for the remaining high rates of energy release in the Pahute Mesa-Yucca Flat-Rainier Mesa areas of NTS. Local magnitudes were converted to energy by the formula  $E = 10^{[1.90M_L + 2.20]}$ ,  $E$  in Joules.

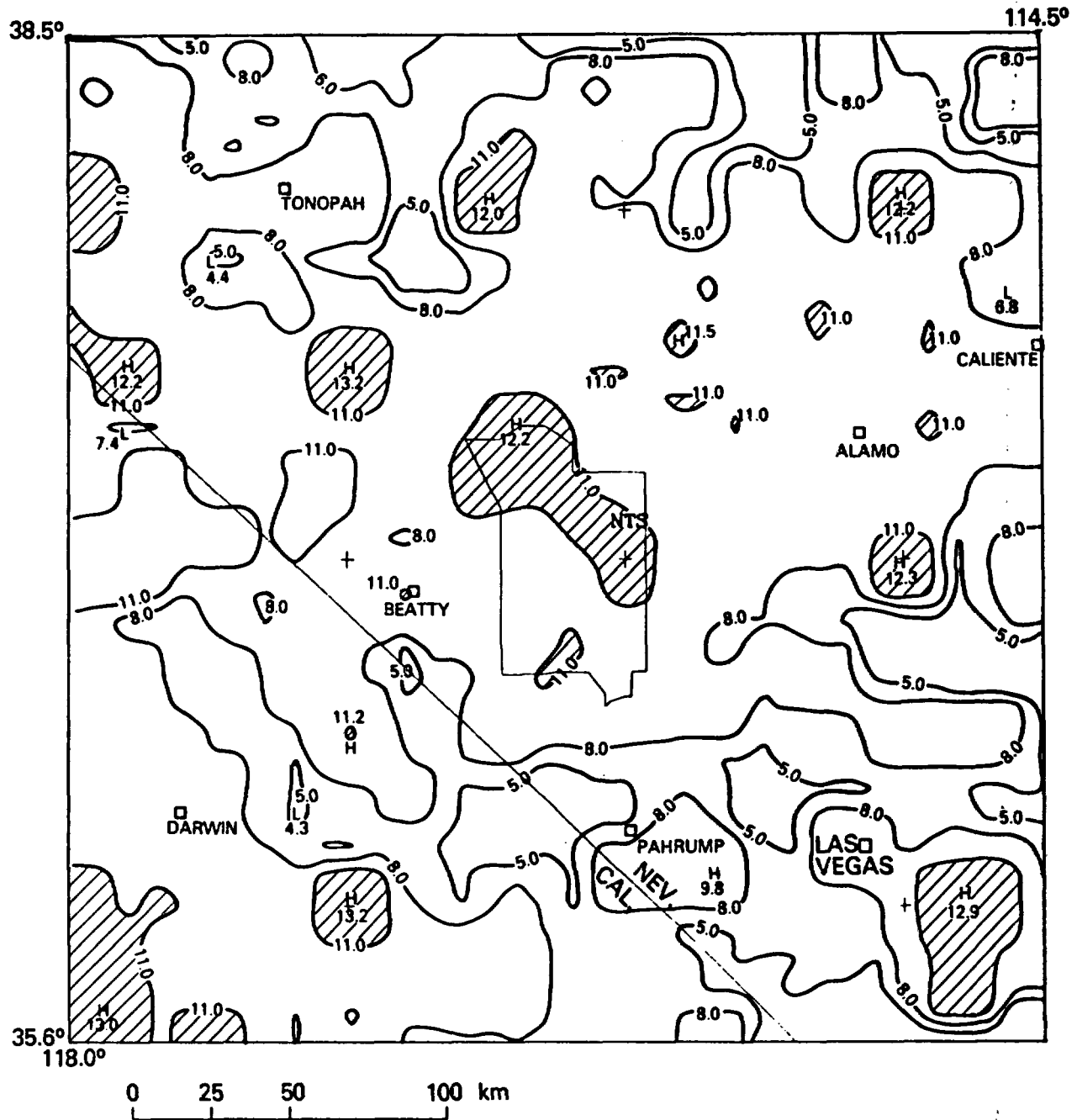


Figure 47.- The distribution of earthquake energy release in the southern Great Basin of Nevada and California based on a catalog of historical seismicity for the period 1865 through July, 1978 (Meremonte and Rogers, 1987). The contours are of the logarithm of the energy release per unit area ( $\log_{10}(\text{Joules}/80\text{km}^2)$ ). All magnitudes in the historical record were converted to equivalent  $M_S$ , and energy was computed by the formula  $E = 10^{[1.44M_S + 5.24]}$ ,  $E$  in Joules.

between the monitoring period and the historic period, which shows considerably higher levels of energy release per unit area per year. We defer until a future report a through discussion of earthquake recurrence rates. These topics require careful evaluation in order to understand and account for the intermix of tectonic and nuclear test related seismicity and to account for possible biases in the magnitudes of historic events compared to current events.

Figures 48a and b show a contour of earthquake energy release for the region projected onto a vertical east-west and north-south section, respectively. These figures show that seismic energy is released mostly between depths of 1 and 12 km, is patchy between 12 and 25 km, and is sparse below 25 km. There is a suggestion that energy-release boundaries increase slightly in depth to the southwest. If such a depth increase were taken as evidence of a thickening brittle crust to the southwest, it would be at variance with interpretations of refraction data that indicate that the crust thickens to the north (Prodahl, 1970; Johnson, 1965). Because the energy release patterns are greatly influenced by small numbers of the largest magnitude events (as can be seen by comparing the energy release cross sections with the hypocenter cross sections shown in Figures 49a and b) whose locations can be influenced by geographic variations in crustal properties, it is unlikely that the energy release patterns reflect contrasts in brittle crust thickness. Note that, because the minimum in earthquake frequency that occurs at about 4 km depth (Figure 33) has a small vertical extent, it is nearly obscured by the smoothing process that is used to produce these energy-release plots.

## DISCUSSION OF SEISMICITY AND STRUCTURE

In a review of the structural setting of the NTS region, Carr (1984) emphasized three structural subdivisions (called subsections), each having a different type of principal structure, structural fabric, and Neogene structural history. Structural complexity abounds in each subdivision. Principal Neogene structures include faults that bound cauldron complexes, range-bounding normal-slip and oblique-slip faults, dextral and sinistral strike-slip fault zones, and low-angle detachment faults. Though all types of principal structures may not exist in each subdivision, structural interactions along and across the structural zones that bound the subdivisions compound the structural complexity of the region as a whole. Crustal properties such as regional gravity gradients, heat flow, thickness, and  $Q$  are also variable in the region, and this variability adds an element of complexity to the structural framework. As a possible simplifying factor, not all types of structures in a subdivision are necessarily seismogenic. Nevertheless, it is within the context of an extraordinarily complex Neogene structural framework that the major aspects of seismicity must be understood. The most notable features of earthquakes in this region are: (1) An apparent east-west-trending zone of earthquakes, termed the East-West Seismic Belt or the Southern Nevada Seismic Belt (Smith and Lindh, 1978), crosses the SGB roughly between  $36^{\circ}$  and  $38^{\circ}$  N. Although this zone may be somewhat discontinuous, and the rates of seismicity and appearance are no doubt influenced by induced seismicity at NTS, comparison of the pre-nuclear testing period with the present-day record suggests that this seismic zone can be associated with natural tectonic stress release (Meremonte and Rogers, 1987). (2) Dextral slip on northerly-trending faults is preferred, with fewer occurrences of both sinistral slip on east-northeasterly-trending faults and normal slip on north-northeasterly-trending faults. All slip styles occur from near-surface to 10-15 km. The inferred least principal stress orientation is west-northwest, implying notable geographic uniformity in the stress axes across the SGB. (3) Microseismicity emanates from cylindrical volumes of rock that generally plunge steeply and tend to lie in north- to northeast-trending panels. (4) A seismicity minimum occurs between 3.5- to 4.0-km depth (Figures 33 and 49). (5) The association of earthquake clusters with specific faults is commonly difficult, although epicenters and nodal planes may align with nearby structural grain. Little correlation exists between range front faults and



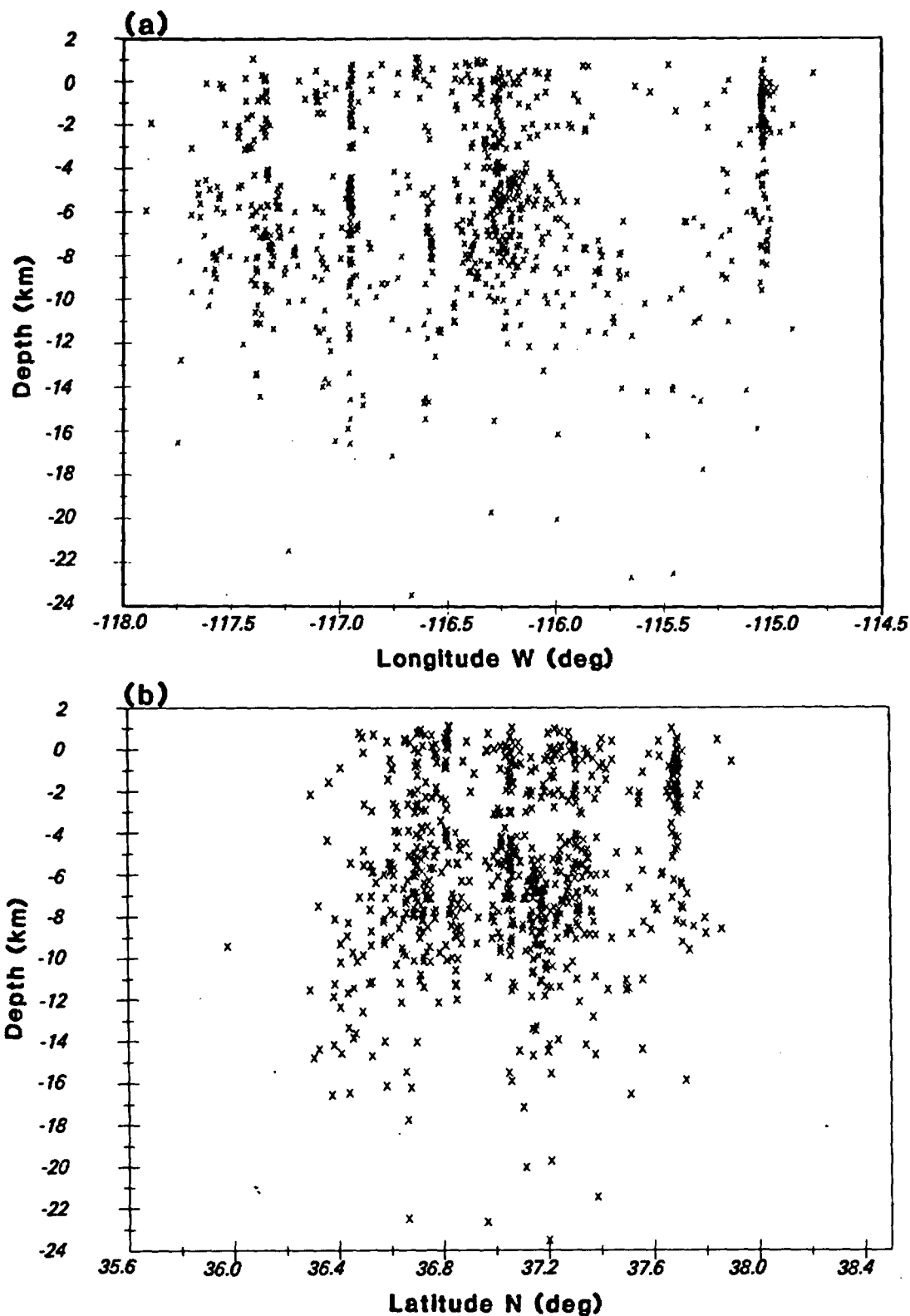


Figure 49.— (a) Depth-of-focus distribution for the period August, 1978 through December, 1983, for earthquakes having "A" or "B" location qualities and depth standard error estimates < 4.0 km, projected onto an east-west plane. (b) Depth-of-focus distribution for the same earthquakes projected onto a north-south plane.

contemporary seismicity. (6) Significantly lower seismic-wave attenuation than other regions of the Great Basin or California has also been noted (Rogers and others, 1987). These features may provide important evidence for evaluating suitable tectonic models that describe contemporary deformation in the SGB.

Given the varied and complex structural framework of the region, however, it is highly unlikely that a single tectonic model can explain all aspects of the Neogene geology and seismicity throughout the region. Deformation associated with extension, for example, is likely to be highly dependent on the position of lateral domain boundaries. Also, only in the past 15 years has it become clear that the continental crust can accommodate large-magnitude extension without rifting apart, and that low-angle normal faults or detachments play an important, if not fundamental, role in that extension. Only in the past few years has the concept of extensive large-displacement detachment faults in the SGB been recognized. Despite these advances, there is at present no consensus on the location or geometry of such faults or the nature of extensional accommodation in the deep crust. It is clear, therefore, that the modeling of deformation associated with extension is likely to be as dependent on one's choice of vertical domain boundaries as it is on lateral domain boundaries and that both must be prescribed in order to fully characterize the deformation.

The data reported herein may have some bearing on the resolution of these complex tectonic issues, but it would be unreasonable to expect a definitive tectonic model to evolve from these data alone. A complete review of all the geological, geophysical, and seismic data for this region is beyond the scope of this study, but some discussion regarding the relationship between seismicity and structure seems appropriate. Some of the following discussions are speculative and most involve considerable simplifications of the observations.

#### **SGB Microearthquakes and Their Relevance to the Occurrence of Larger Earthquakes**

Comparison of microearthquakes in the SGB with larger earthquakes and with induced seismicity reveal similarities. For example, it has been observed that the 1966 Clover Mountain earthquake ( $M = 6.1$ , USGS) occurred as a dextral strike-slip event on a north-trending fault similar to microseismicity in the study area (Smith and Lindh, 1978; Rogers and others, 1983; Wallace and others, 1983). Based on studies of both body and surface waves (Wallace and others, 1983; Lay and others, 1984; Wallace and others, 1985; Wallace and others, 1986) and geologic studies (Bucknam, 1969; Mckeown and Dickey, 1969) significant amounts of strike slip have occurred due to induced tectonic stress release associated with underground nuclear tests at NTS. This stress release is seen as surface displacements at the time of the event, as seismic energy release concurrent with the detonation, and as numerous aftershock earthquakes outside the zone of shattering (Hamilton and others, 1971; Rogers and others, 1977). At the Pahute Mesa nuclear test region and at Lake Mead (where increased pore pressures due to the lake impoundment acted to trigger tectonic stress release (Carder, 1945; Rogers and Lee, 1976)), focal mechanisms indicate that dextral strike slip occurred on north-trending faults, and normal faulting occurred on north-northeast-trending faults. In essence, the behavior at both Lake Mead and Pahute Mesa is typical of earthquake behavior throughout the monitored region and mimics, albeit at a smaller scale, the behavior of the Churchill Arc (Nevada Seismic Zone) in the northern Great Basin (Shawe, 1965). In the southern section of the Churchill Arc dextral strike slip is a significant component of the deformation where the structural fabric trends more northerly and intersects the central Walker Lane. The Fairview Peak, Cedar Mountain, and Rainbow Mountain earthquakes all exhibited geologic (Shawe, 1965) and seismic evidence (Doser, 1986; D. I. Doser, Univ. Texas, El Paso, 1987, unpublished manuscript and abstract) of dextral slip in this section of the Churchill Arc. The 1934 Excelsior Mountain earthquake exhibited geologic evidence for small amounts of sinistral strike

slip on a northeast-trending fault (Shawe, 1965), although seismic data indicate nearly pure normal faulting on a northeast-trending fault (D. I. Doser, Univ. Texas, El Paso, 1987, unpublished manuscript). Focal mechanisms from 1969 microearthquake activity in the Excelsior Mountains area, however, indicate strike-slip faulting (Gumper and Scholtz, 1971). In the northern section of the Churchill Arc, where structure trends more north-northeasterly, normal faulting also predominates (1915, Pleasant View earthquake). Other less compelling analogs in the two types of data are also present. For instance, the apparent coupling of adjacent seismic zones is observed in the southern Great Basin and the paleoseismic record of the Nevada seismic zone. These similarities were previously discussed by Rogers and others (1983). This comparison suggests that the driving mechanism producing crustal deformation is similar in at least some subprovinces of the Great Basin. We conclude that the similarities between microearthquakes in the study area and larger magnitude earthquakes in the Great Basin suggest a genetic association through the same or similar deformational processes and, thus, we consider the microseismicity to be of first-order tectonic significance.

This conclusion does not necessarily imply that large earthquakes ( $M > 7$ ) can occur in the SGB. Although in the Churchill Arc numerous large earthquakes have occurred historically ( $M \leq 7.8$ ), historic seismicity in our study area has been limited to  $M \leq 6.1$  (natural seismicity),  $M \leq 5.2$  (induced seismicity; Wallace and others, 1983). The conclusion that large earthquakes are possible in the SGB would require proof of the conditions needed for large events, such as the presence of stressed faults of sufficient length and favorable orientation for rupture in the contemporary stress field. It should be noted, in this regard, that Quaternary faults of sufficient length to produce large earthquakes include the Death Valley-Furnace Creek fault zone and various faults in the Mine Mountain-Spotted Range structural zone. The analogies between microearthquakes and the largest events in the Great Basin, thus, provide the basis for attempting to evaluate various models of Great Basin tectonic deformation in terms of the features of the earthquake data presented herein. In the discussions that follow, we consider these models and the extent to which the seismic data of this study support the application of a given model to the contemporary deformation of the SGB.

### Seismicity and Local Structure at Yucca Mountain

A model that incorporates block and listric faulting above low-angle detachment surfaces (i.e., Stewart, 1978) permits extension across a broad region with transport of some essentially intact sections of the upper plate over large distances. This model also attempts to account for other sections that are intensely extended on faults that are rooted in the detachment (Wernicke, 1981). Major lateral faults are postulated to bound these extended zones against zones of lesser extension (Anderson, 1971; Wernicke, 1981); the bounding faults are predicted to exhibit dextral motion at one side of a zone and sinistral motion at the opposite side. Anderson (1971) and Wernicke (1983), for instance, suggest that such deformation has occurred in the SGB along the Lake Mead fault system and the Garlock fault (Davis and Burchfiel, 1973). There is also evidence of this type of deformation at several scales. An example of considerable geographic extent, for instance, is the west-dipping Sevier Desert detachment in Utah which may penetrate to depths of about 15 km beneath eastern Nevada (Allmendinger and others, 1983). Shallower detachments of lesser geographic extent such as one that underlies the Bullfrog Hills west of NTS have also been recognized. At some locales at NTS local detachments have formed between the Tertiary section and Paleozoic rocks (W. B. Myers, U. S. Geol. Survey, written comm., 1986). A question of significance is whether the observed seismic quiescence at Yucca Mountain is related to the presence beneath Yucca Mountain of one or more detachment surfaces (Scott, 1986), and, if present, could such detachment surfaces uncouple Yucca Mountain from the regional stress field? For instance a vertical strike-slip fault might intersect a detachment surface from below in such a manner that strike-slip motion on the deep fault could occur without deforming the upper plate. A structure of

this type might be important for several reasons: (1) geologic evidence for detachments at Yucca Mountain has been noted by Scott (1986); (2) lower seismic energy release is observed at Yucca Mountain in spite of the presence of faults that are favorably oriented for slip in the contemporary stress field (Figure 11); (3) the fact that the state of stress inferred from hydrofrac measurements in the Yucca Mountain block can be explained solely on the basis of a topographic effect and does not require a tectonic stress component (Swolfs and Savage, 1985); (4) several earthquakes have been located beneath Yucca Mountain, but these events have all been located more than 4 km below sea level; and, (5) two of these events, which occurred after the time period discussed in this report, demonstrate predominantly strike-slip focal mechanisms. Taken together, these data are largely consistent with an interpretation that Yucca Mountain is uncoupled from the regional stress field.

Other interpretations, however, argue against the uncoupling hypothesis. For instance, the low level of seismicity at Yucca Mountain and a larger area to the west (item 2) could be the result of locked faults, or, alternatively, a stress shadow zone. Lack of energy release in the upper part of the brittle crust alone would be a more favorable condition for a detachment hypothesis. This zone demonstrates a low rate of energy release at all depths relative to surrounding regions. The lack of seismicity at depths below 5 km must be unrelated to possible shallow detachments. It is also possible that Yucca Mountain overlies a shallow detachment fault beneath which exists a zone of locked faults. Such a model would account for the geologic evidence for shallow detachment faults and the seismic evidence for low energy release.

Other evidence that could argue against uncoupling is the fact that the least principal stress determined from hydrofrac measurements within the Yucca Mountain block has approximately the same orientation as the least principal stress direction (west-northwest) deduced from the regional focal mechanisms. If Yucca Mountain is underlain by an active detachment, the stress orientation within the block would likely be determined by the dip direction of the detachment and possibly the orientation of the topography. This situation could give rise to stress orientations in the upper detached plate differing from that within the underlying brittle crust. On the other hand, as a detachment forms within the framework of the acting regional stresses, it is possible, and perhaps probable, that the least principal stress orientation within the detached block will have the same orientation as the regional stress direction.

#### **Regional Structure, Great Basin Tectonic Models, and the Characteristics of Contemporary Seismicity**

Arabasz (1984) proposed a model for the eastern margin of the Great Basin that incorporates a seismogenic upper crust that is composed of a stack of brittle plates separated by low-angle detachment surfaces. The model permits minor block interior motion generating diffuse low magnitude seismicity, moderate earthquakes on steeply dipping intraplate faults that do not cross plate boundaries, and major earthquakes on steeply dipping range front faults extending to 15 km that do cross plate boundaries and sole into deep detachment surfaces and/or the uncoupling zone. Application of this model to the SGB has some appeal, but is inconsistent in some critical aspects. For instance, in the SGB the general occurrence of dextral slip on north-south-trending faults from near-surface to the base of the seismogenic zone argues against a stack of plates that are uncoupled except at major range front boundaries. This inconsistency is reinforced by the fact that the steeply plunging cylinders of seismicity that we observe do not appear to occur in association with range-front faults. Furthermore, the predominance of lateral motion in the SGB may not support a model that requires a more mixed combination of deformation styles. Whereas, the seismic data suggest that much of the lateral slip occurs on north-trending faults, this model would predict the occurrence of lateral slip preferentially on faults subparallel to the spreading direction. The



spreading direction at present is likely to be west-northwest. For these reasons this model does not appear to be consistent with seismic observations in this region.

More generally, do the data of this study support or deny the widespread occurrence of detachments throughout the region, such as has been suggested by Hamilton (1987)? A detachment model might be consistent with the seismic data of this study under certain conditions. These conditions are: (1) that slip on the detachment is aseismic, or releases too little energy for the events to be considered for focal mechanism computation, or that the network geometry is inadequate to discern sub-horizontal slip; (2) that the over-riding plate is not stress uncoupled to the extent that small earthquakes are not possible in that plate; (3) that the current direction of transport of the over-riding plate is to the south; and (4) that the over-riding plate is geographically large enough that the zone accommodating sinistral slip occurs outside the study area. These conditions are reviewed in the following discussion.

Condition (1) is required because no focal mechanisms computed through 1983 have slip on nodal planes that are subhorizontal. Furthermore, given the stress orientations for this region and applying a Mohr-Coulomb failure criterion with a coefficient of friction  $\mu \approx 0.6$ , low angle faults might never be selectively preferred for failure in the contemporary stress regime (Harmsen and Rogers, 1986) unless special pore pressure or lithologic conditions existed. Considerable study and debate is currently ongoing concerning the formation of detachment surfaces and conditions for slip on such features (see, for example, Lucchitta, 1985; Davis, 1985; Power, 1985), and the application of simple failure criteria may be found to be unrealistic.

Condition (2) is required because we infer, from earthquake data, similar stress characteristics throughout the upper 10-15 km of the crust. One could postulate that the seismic quiet zone near 4 km depth is associated with a detachment surface. In one scenario, the quiet zone would demonstrate a low angle detachment surface dipping to the south in order to provide a mechanism for producing the widespread occurrence of dextral slip on north-trending faults (see below). This feature is nearly horizontal, however, as shown by the east-west and north-south cross sections shown in Figures 49a and 49b. In a second scenario a set of detachment zones is postulated to exist at this level in the crust that do not, on average, exhibit any primary dip direction, but serve as lensoid structures, similar to the model suggested by Hamilton (1987), absorbing extension on numerous shallow listric faults of varying orientation. One questions, however, whether such a set of structures could produce the notably consistent slip style that has been observed in the earthquake record. The principal argument against a set of active structures of this nature is associated with the fact that earthquakes occur with similar slip style from near-surface to depths as great as 10 to 15 km. This result, if it can be verified, suggests that stress coupling exists throughout this range of the brittle crust. Thus, the proposed upper plate (i.e., in this case the zone above about 4.0 km) and lower plate are not uncoupled. In fact, a plot of total energy release in the region as a function of depth shows that a sizable fraction of the total energy release occurs in the upper 4 km (Figure 50).

The hypothesis that a zone of uncoupling may separate brittle and ductile sections of the crust in the Great Basin is closely related to detachment faulting concepts. The existence of the uncoupling zone is primarily based on the fact that very few earthquakes occur below about 15 km throughout the Great Basin. One possible interpretation of our data is that the uncoupling zone acts as a detachment surface. In this model the entire brittle crust in the SGB is mechanically coupled, permitting lateral deformation throughout and across previously active shallow detachments. The existence of dextral motion on a series of subparallel faults across the zone suggests transport of the entire brittle crust in this region to the south. On the western margin of this zone where the transported blocks abut the Walker Lane the dextral motion is taken up along the northwest

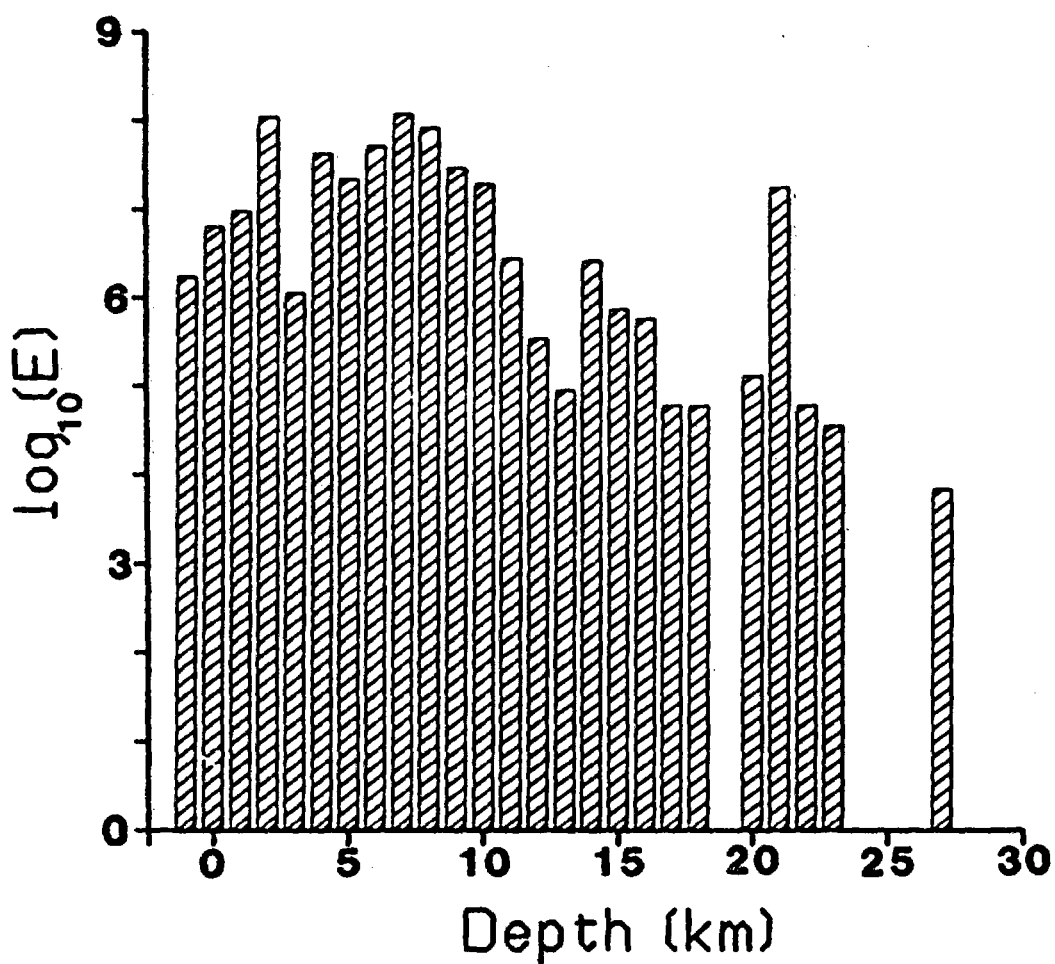


Figure 50.- Depth distribution of earthquake energy for August, 1978 through December, 1983 earthquakes having "A" or "B" location quality, and depth error estimates < 4.0 km. Energy release (joules) was computed from  $M_L$  by the formula  $E = 10^{1.90M_L + 3.20}$ .

trends of that zone. On the eastern margin of the zone, where the blocks adjoin the Colorado Plateau, one would expect sinistral motion along north to northeast-trending faults. Under this model one could hypothesize that previously active shallow detachments are now largely inactive due to the cooled crust (Lucchitta, 1985) in the SGB.

Conditions (3) and (4), above, are required in order to satisfy geographical constraints on the observed slip directions from SGB focal mechanisms that show dextral slip on north-trending faults. A schematic model demonstrating this concept is shown in Figure 51a. In fact, some evidence exists in both the current seismic record and the late Cenozoic geologic record that significant components of strike-slip movement have occurred or are occurring along the Great Basin-Colorado Plateau boundary (Arabasz and Julander, 1986; Anderson and Barnhard, 1987). A number of earthquakes in the Colorado Plateau-Great Basin transition zone can be interpreted as sinistral motion on northeast trending faults (Arabasz and Julander, 1986). Focal mechanisms from the Sevier Valley region, for instance, exhibit both dextral and sinistral slip on parallel nodal planes (Arabasz and Julander, 1986); in addition, Anderson and Barnhard (1987) find geologic evidence that they interpret as southwest-directed lateral transport or rafting of crustal blocks. They suggest, however, that these blocks are limited in vertical extent to about 5 km. The model shown in figure 51a would require infilling of late Cenozoic intrusive rocks along the zone's northern boundary. In fact, Late Cenozoic igneous rocks do occur in an east-west band across the upper third of the SGB (Stewart, 1978).

The deformation suggested in Figure 51a could be directly related to the tectonic activity that has taken place in the southern subsection of the SGB. Extrusion or transport of crustal material to the southwest along the Lake Mead and other northeast-trending shear zones could have been accompanied by north-south closure of the transport zone as material was removed. North-south closure further requires crustal stretching or southerly transport to replace the crustal block that was removed, perhaps in the generalized fashion shown in Figure 51a. This concept was first suggested by Anderson (1984). The deformation idealized in Figure 51a could also be the result of driving forces in the ductile lower section of the lithosphere and upper mantle that are essentially internal to the Great Basin. The counterclockwise rotation of the Sierra Nevada block (Hamilton and Myers, 1966) and the clockwise rotation of the Colorado Plateau (Wright, 1976) could also play a role in inducing externally acting stress on the Great Basin, although these motions are more likely to be passive response to either plate boundary or intraplate stress.

Cenozoic wrench faulting in the Great Basin has been widely discussed (i.e., Shawe, 1965; Hamilton and Myers, 1966; Wright, 1976; Hill, 1982; see Stewart, 1978 for an overview). These faults occur primarily as steeply dipping northeast- and northwest-trending structures. It is important to examine whether any of the concepts that have been proposed to explain wrench faulting in Basin and Range Cenozoic rocks are relevant to the transcurrent deformation that is observed in the contemporary seismic record. Atwater (1970) assumes that the Great Basin is a soft zone that is extending and shearing in response to plate motions along the continental boundary and that some fraction of the plate motion is absorbed on major continental fault zones subparallel to the San Andreas such as the Walker Lane, the Las Vegas Valley shear zone, and the Death Valley-Furnace Creek fault zones. Normal slip is postulated on faults rotated clockwise from these trends, resulting in Great Basin extension.

The stress orientations and magnitudes that we infer from hydrofrac and focal mechanism data in the SGB are rotated clockwise relative to those at the plate margin (Zoback and Zoback, 1980b). Although the source of such stress changes is unknown, they can result from the remote-stress distributed-deformation process itself. In this process complex passive intraplate response occurs leading to distributed inferred stress orientations in an otherwise simple remote stress environment. Alternatively, stress changes can also result from the superposition of remote plate margin stresses

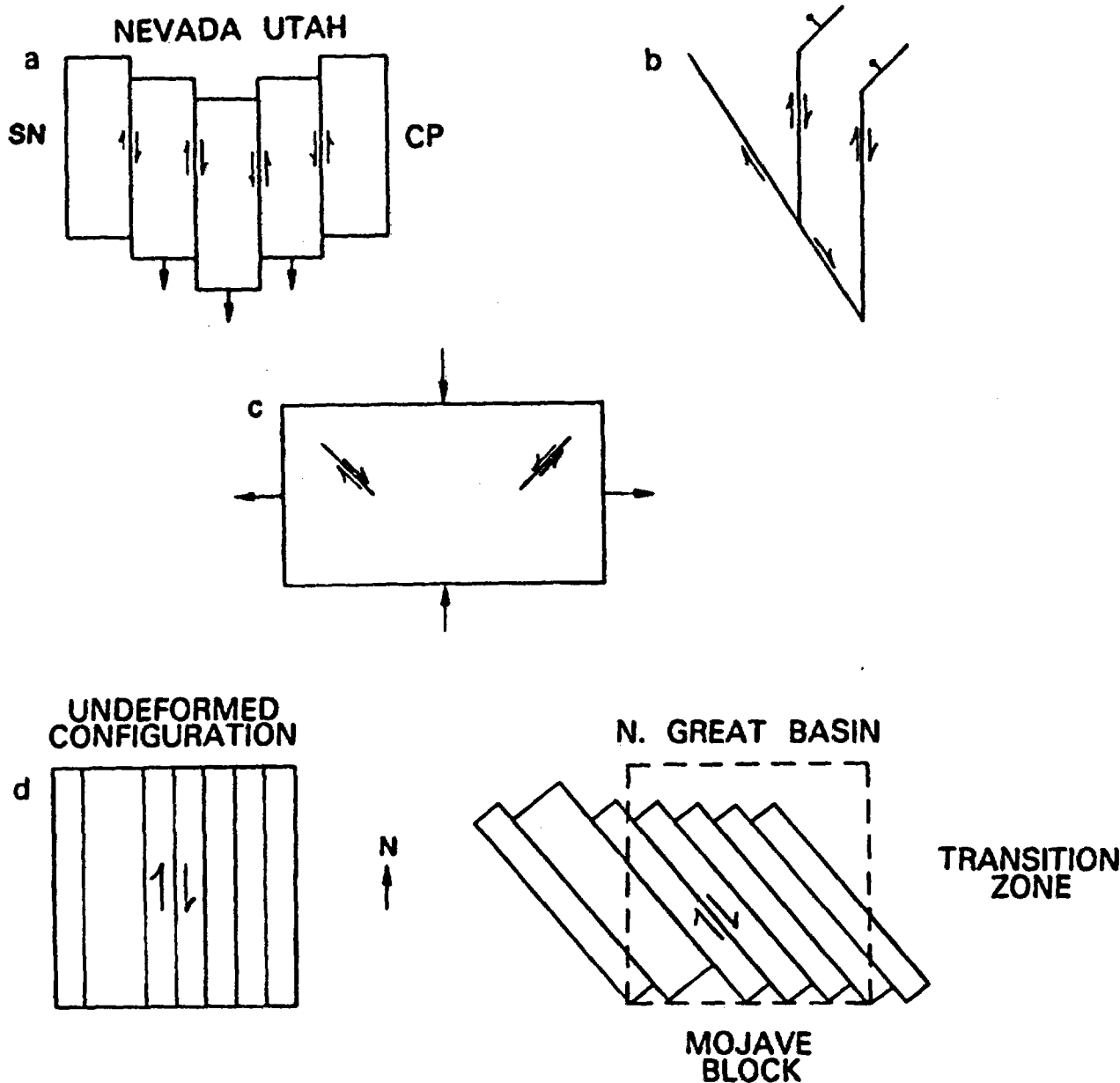


Figure 51. - (a) Schematic diagram depicting dextral slip along north-trending faults in the southern Great Basin, bounded by the Sierra Nevada block (SN), and sinistral slip along north-trending faults in the eastern margin of the Great Basin, bounded by the Colorado Plateau (CP). (b) Schematic diagram showing the relationship between dextral slip on north-trending faults and normal slip on north-northeast trending faults. The northwest-trending dextral slip fault could represent slip within the Walker Lane Belt and/or the Death Valley-Furnace Creek fault zones. (c) Schematic diagram showing how north-south shortening and east-west extension in the southern Great Basin may result in wrench faulting on northwest- and northeast-trending conjugate faults. (d) A schematic diagram showing one possible interpretation of Zoback and Zoback's (1980) suggestion that the SGB is a zone accommodating differential rates and amounts of extension between the northern Great Basin and the Mojave block. The drawing is adapted from the block-rotation models discussed in detail by Garfunkel and Ron (1985).

and stresses that are internal to the Great Basin. The concept depicted in Figure 51b is a modified version of Atwater's suggestion that would kinematically favor oblique strike slip on north-trending faults. However, because a clockwise rotation of the greatest principal stress does apparently occur in the Great Basin, relative to the plate margin stresses, pure dextral slip on north-trending faults is observed. Other kinematic inconsistency is apparent in this model that should lead to a wider range of slip style in the Great Basin than appears in the contemporary seismic record. Carrying components of strike slip into the Great Basin with a model of this type also requires significant rotations of crustal blocks across the region. Dextral slip requires counterclockwise rotation, and sinistral slip requires clockwise rotation (see for example, Figure 6b in Christie-Blick and Biddle, 1985; Garfunkel and Ron, 1985). At present evidence is lacking for block rotations across the Great Basin, although rotations are known to occur locally (Carr, 1984).

Other wrench models combine north-south shortening in response to compressional forces with east-west extension (Figure 51c) accommodated by lateral shear on conjugate faults trending roughly northwest and northeast in the directions of maximum shear stress. In other concepts it is assumed that wrench, detachment, normal and thrust faulting occur contemporaneously and are different manifestations of the same deformational processes (Anderson, 1971; Wernicke, 1984; King, 1983; Aydin and Nur, 1982).

Aydin and Nur (1982) suggest that transcurrent faulting is the principal mode of intraplate deformation and offsets in these transcurrent faults lead to secondary features such as basin and ridge formation. The basin formations have been termed pull-apart basins. This type of structure, for example, has been suggested as the mechanism leading to the formation of Death Valley (Burchfiel and Stewart, 1966; Hill and Troxel, 1966). The uniqueness of Aydin and Nur's (1982) model is that it permits faulting of virtually any style to occur in a predominantly strike-slip continental crust tectonic environment.

King (1983) also supports the view that in a continental crust setting, major strike-slip faults are the principal deformation mode, acting to accommodate lateral transport of crustal material and thereby thin the crust where disequilibrium occurs. King's (1983) model requires sets of primary and secondary faults of diverse orientations, from the smallest to the largest appropriate scale, to accommodate predominantly lateral motion. The fault orientation relative to the acting stress directions establishes the style of slip. A substantial fraction of the total deformation is taken up on the secondary faults. King's model, if applied to the SGB, would predict dextral faulting on a wide range of fault orientations; this feature, however, is not observed. We also see no evidence of reverse faulting or thrust events that would be expected on the basis of the Aydin and Nur model. Thus, the principal difficulty in relating the data of this study to these models is the uniformity of inferred contemporary fault orientations and slip modes that we observe across the entire region of our study. Such uniformity is not predicted by these models. On the other hand, the reverse and thrust faults predicted by these models might be much more infrequent, given that such faults, for instance, might store stress for greater periods of time and to higher stress levels before rupture. Some aspects of these models, however, are appropriate, as demonstrated by the probable pull-apart nature of Death Valley.

A wrench tectonic model suggested by Zoback and Zoback (1980b) for the SGB can be considered in relation to the seismic and geologic data of this region. This model would require differential rates of spreading between the northern Great Basin and the Mojave block as shown in Figure 51d. Figure 51d is adapted from Garfunkel and Ron (1985), who evaluated the general properties of such a model in detail. This model assumes that motion occurs on existing faults, with little internal block deformation, in response to north-south directed compressional forces. Thus, this representation is a special interpretation of the Zoback and Zoback (1980b) suggestion. They assumed the SGB has responded passively to extension to the north. This model's application to the

Cenozoic evolution of this region on the scale shown produces some shortcomings. These problems include the lack of significant counterclockwise rotation of crustal blocks in the central portion of the Great Basin compared to surrounding regions, the lack of a set of through-going north-trending lateral faults, the absence of contemporary sinistral faulting on east-west-trending faults, and the fact that the observed clockwise stress rotation in the SGB relative to surrounding regions (Rogers and others, 1986) is in a direction that is opposite to the predicted direction (Sbar, 1982). (Sbar's case, which was applied to the Great Basin as a soft zone deforming in response to motion on the plate boundary, can be applied on a smaller scale to the SGB by considering a mirror image of his model.) Zoback's wrench model, however, might be acceptable as a deformation mode of short duration and consequent, low-order block rotation. The appealing aspects of this model are the existence of limited dextral faulting on north-trending faults and the confinement of such events to an east-west zone.

The lack of observable north-trending transcurrent faults suggests that they would have to be deep-seated and hidden or that total slip is limited to the extent that it is not readily visible at the surface. In fact, for some regions of the Great Basin, evidence has been found suggesting that wrench faulting may be obscured by one or more overlying detachments (Hardyman, 1978; Molinari, 1984). Some of the larger earthquakes in the region demonstrate significant components of strike slip inferred from focal mechanisms and wave-form modeling (Doser, 1986), however, the surface faulting that accompanies these events frequently indicates a greater proportion of normal slip compared to strike slip. Similar behavior has been observed at Pahute Mesa in response to nuclear testing. As noted above, these events radiate significant components of strike-slip energy while producing surface scarps as great as 10 km long having maximum displacements exceeding 100 cm (Maldonado, 1977). Richter (1958) also noted slip inconsistency between geologic field observations and seismic data (indicating dextral slip along an north-northwest epicentral trend) for the 1947  $M = 6.4$  Mannix earthquake. In each case, this behavior is suggestive of contemporary deep-seated strike slip that produces sets of reidel shears in an overlying partially detached plate. Structure of this type could be an additional complicating aspect of any of the models shown in Figure 51.

Another means of coping with discordance between contemporary deformation style and that in the Late Cenozoic geologic record is to argue that the region is presently subjected to a short-lived regional stress field (Eaton and others, 1978). In principal, either the orientation or magnitudes of the principal stresses may exhibit temporal variation. Stress changes (i.e., orientation) within the Late Cenozoic have been inferred from the geologic record in selected locales (i.e., Frizzell and Zoback, 1987; Anderson and Ekren, 1977), lending some credence to this possibility. Such changes could be related to the stress build-up and stress release on segments of major faults between the Great Basin and the continental plate margin, for example, the Death Valley-Furnace Creek fault system, the Garlock fault, or even the plate margin itself.

Models 51c and d are closely related because, as drawn, they represent response to north-south directed compression. In 51c and d both sinistral and dextral faulting are possible in adjacent subzones as suggested by Garfunkel and Ron (1985). The significant differences between these two cases is that model c assumes the breaking of intact rock, while d assumes pre-existing faults. Furthermore, the faults in model c lie along the directions of maximum shear, whereas, in model d, the faults may rotate out of the direction of maximum shear. The consistency between the least principal stress direction determined from both focal mechanisms and hydrofrac measurements indicates that faults have not rotated out of the direction of maximum shear. To that extent, model d appears to be less plausible.

It is possible that certain aspects of each of the kinematic patterns shown in Figure 51a-d are present in rocks of the SGB. Given the complexity of observed structures in the region, this

hypothesis may be the only acceptable one. For instance, block rotations may occur locally, as has been noted in the southern section of Desert Game Ranges (see Carr, 1984 for an overview), in the Hampel Wash area of the NTS (Frizzell and Zoback, 1987), and in the Lake Mead area (Ron and others, 1986). Motion along the Walker Lane, as in Figure 51b, is not inconsistent with the observations of Figure 51a along the southwest boundary of the transported zone. Even though features of models 51b-d may be consistent with some aspects of the geologic and seismic data, as a whole the seismic data appear to be most consistent with the principal deformation modes described by Figure 51a.

If model 51a has validity, it could have important implications regarding the assessment of the seismic hazard in this region. For instance, if the initiating process that occurred along the southern end of the zone is essentially complete, one could postulate that the southern transport depicted in Figure 51a has been halted or at least temporarily impeded. In this case major lateral displacements on the set of subparallel north-trending faults across the SGB might not be expected. Given such conditions the microseismicity in this zone could represent release of residual stress remaining on completion of the process. On the other hand, if the potential exists in this region for the occurrence of significant strike-slip earthquakes, a hazard computation based solely on the extensional slip rates reflected by mapped scarps would be underestimated.

The presence of shallow active detachments would further complicate the assessment of the regional seismic hazard (Anderson and others, 1983; Arabasz and Julander, 1986), particularly in a zone undergoing substantial deep-seated strike slip. If active detachment surfaces exist in the upper crust of this region, motions in the lower plate might not be wholly reflected in the upper plate or they might be translated to the upper plate in a complex fashion (Hardyman, 1978). For example, the orientation of faults in the upper and lower plates could differ. Furthermore, if active shallow detachment faults are widespread in the region, then our suggested associations between seismicity and mapped surface faulting could be fortuitous. This scenario, if unrecognized, would produce misleading estimates of the seismic hazard. Upper plate faults that cut the surface, for example, might be of such limited vertical extent that they could only produce moderate or small earthquakes and the greatest hazard would be due to deep-seated faults. Also, listric faults that bottom in detachment zones and have strikes considered favorable for lateral slip or normal faulting could be kinematically unsuited for slip in the present stress regime and contemporary crustal conditions. This hypothesis is difficult to explore in detail, however, because little is known about the mechanics of detachment faulting. The principal characteristics of earthquakes in this region, however, do not seem to support the existence of active shallow detachment faults in the southern Great Basin.

## Summary

- Many earthquakes or earthquake clusters cannot be related to specific faults, and little correlation exists between range front faults and seismicity in the current monitoring period. In some cases, however, earthquake lineations and nodal planes appear to be associated with fault zones of certain orientations or with mapped structural grain.
- Earthquakes in some zones tend to occur in cylindrical rather than planar or tabular shaped clusters; other zones exhibit tabular north-south elongations. They plunge steeply and sometimes extend to 10-15 km depths. Two cylindrically-shaped clusters are curved or linearly segmented as a function of depth. We suggest that these distributions occur along the intersection of major faults; the concentration of seismicity along the locus of intersection is attributed to the presence of weaker rock in the vicinity of such fault intersections. Further testing of the location process, however, is required to establish that these distributions are not an artifact of the location process or the velocity model.
- For earthquakes for which focal mechanisms could be determined, a large percentage are strike-slip. Weak to fairly distinct north-south epicenter elongations suggest a preference for dextral strike slip on northerly-trending faults.
- The greatest number of earthquakes are confined to the upper 15 km; however, there appear to be two principal zones of energy release within the upper 25 km of the crust. The shallower zone occurs above about 15 km, and a deeper zone occurs below about 20 km. The energy release zones and the low between them appears to dip to the southwest. Zones of relatively high energy release in the upper 5 km compared to the regional values are not confined to the nuclear testing areas of the NTS.
- The depth distribution of earthquake foci is bimodal with maxima at 1.5 and 9 km, and a minimum at 4 km. Although several tests have been conducted to determine whether this effect is an artifact of the location process, this question is not yet satisfactorily resolved.
- There is no depth-dependent pattern for the occurrence of strike-slip or normal fault events. In some cases, strike-slip and normal fault events occur within the same cluster at about the same depth.
- Mapped faults of approximately north to east-northeast trend should be recognized as favorably oriented for slip in the current stress regime in spite of the apparent lack of association of specific earthquakes with specific faults. Listric faults could be an exception to this conclusion because, given the regional stress field orientation, such faults may not be favorable for slip even if they exhibit the requisite strike. At present too little is known about the mechanics of listric faulting to resolve this question.
- From a comparison of the late Quaternary geologic record along the Death Valley-Furnace Creek fault zone (DV-FC) and the contemporary seismic record to the east of DV-FC, we infer that a clockwise rotation of the principal stresses occurs in the SGB relative to areas to the west of the DV-FC. A speculative interpretation of this observation is that the SGB is partially uncoupled from the continental plate boundary stresses. This uncoupled state could be due to previous stress release along the DV-FC fault zone, but may also reflect some intrinsic or fundamental crustal boundary that exists at the DV-FC fault zone-Walker Lane boundary.
- Based on focal mechanisms, two zones of seismicity 25 km apart in Sarcobatus Flat could be interpreted as strain release at the end points of a common fault.



- Comparison of the energy release maps for the pre-1978 and post-1978 periods shows that, averaged over a given time period, the active zones appear to have about the same strain release rates across the region, including the areas of induced seismicity. The active zones also appear to shift with time in some areas, in a manner that has the appearance of gap filling.
- Energy release maps and seismicity maps for the current and the historic record show that seismicity in this region forms an east-west band of energy release across the SGB. The seismicity, however, occurs in distinct zones across the region that gives the east-west seismic zone a discontinuous appearance.
- Yucca Mountain lies within a seismic energy release low connected to the Furnace Creek-Death Valley and Mojave Desert lows.
- Focal mechanisms imply that  $\sigma_1$ , the maximum compressive stress, is roughly horizontal, but also that if a single fixed stress field is acting throughout the region, the principal stresses are rotated slightly out of the horizontal and vertical planes.
- The stress orientations inferred from the dihedral intersection method indicate that north-trending and east-northeast-trending nodal planes are the preferred fault planes for focal mechanisms having steeply dipping nodal planes. Dextral slip on steeply dipping north-trending planes, and sinistral slip on steeply dipping east-northeast-trending planes are consistent with the directions of maximum shearing stress on those planes. Normal and oblique slip are preferred on planes with strikes intermediate to these two directions.
- Continued low seismicity levels at Yucca Mountain and vicinity and the disparity of the Yucca Mountain hydrofrac stress measurements with the focal mechanism inferred principal stress attributes are consistent with the conclusion that Yucca Mountain is uncoupled from the regional stress field. Geologic data, which suggest that one or more detachments underlie Yucca Mountain, also support this conclusion. Alternate interpretations, however, are possible.
- While some of the data and interpretations may favor the existence of detachment faults at Yucca Mountain many of the characteristics of earthquakes in active zones throughout the region do not support an interpretation of detachment faulting as a regional pattern of deformation. The active zones indicate a predominance of lateral faulting on *en echelon* or parallel north-trending faults.
- The remarkable uniformity across the region in the occurrence of dextral, sinistral, and normal faulting on north-, east-northeast-, and northeast-trending faults, respectively, is interpreted to be consistent with an axially symmetric stress field having about equal intermediate and greatest principal stresses throughout the seismogenic crust. These slip styles are equally likely in this stress field if pre-existing faults of any orientation are available for slip. The observation that a preponderance of dextral slip on steeply dipping north trending faults occurs may reflect the fact that faults in this region have that preferential orientation. Also, it is important to note that this uniformity in deformation style occurs across a region that has experienced a variety of tectonic styles during the Cenozoic and that the contemporary style is markedly different from that of the recent geologic past.
- The uniformity in deformation style supports the conclusion that the driving mechanism producing crustal deformation is similar in at least some subprovinces of the Great Basin.
- Based on our interpretation from earthquake focal mechanisms of an axially symmetric regional stress field, we suggest that the stress conditions measured by hydrofrac techniques do not reflect the general critical stress conditions throughout the region and/or the stress conditions at seismogenic depths.

- We observe that the contemporary principal horizontal stresses are also rotated clockwise relative to the contemporary stress orientations to the north or east of the SGB.
- Our inference that the greatest and intermediate principal stresses are equal further implies that the horizontal component of tectonic stress is increasing with depth. This result may be consistent with a horizontal basal shear acting along the base of the brittle crust or, perhaps, the lithosphere.
- At present no single tectonic model satisfactorily accounts for all the critical features of the seismicity in the SGB.
- In another study, summarized in this report, we determined (Rogers and others, 1987) that attenuation of ground motion in the SGB is much lower than other parts of the Great Basin. This finding affects magnitude estimation for both current and pre-1978 earthquakes and also has an impact on the manner in which strong ground motion estimates will have to be computed in an earthquake hazard assessment of this region.

## References Cited

- Aki, K., and Chouet, B., 1975, Origin of coda waves: Source, attenuation, and scattering effects: *Journal of Geophysical Research*, v. 80, p. 3322-3342.
- Albers, J. P. and Stewart, J. H., 1965, Preliminary geologic map of Esmeralda County, Nevada: *U. S. Geological Survey Mineral Investigations Field Studies Map* MF-298.
- Allmendinger, R. W., Sharp, J. W., Tish, D. V., Serpa, L., Brown, L., Kaufman, S., Oliver, J., Smith, R. B., 1983. Cenozoic and Mesozoic structure of the eastern Basin and Range province, Utah, from Cocorp seismic-reflection data: *Geology*, v. 11, p. 532-536.
- Anderson, R. E., 1971, Thin-skinned distension in Tertiary rocks of southeastern Nevada: *Geological Society of America Bulletin*, v. 82, p. 43-58.
- Anderson, R. E., Zoback, M. L., and Thomson, G. A., 1983, Implications of selected subsurface data on the structural form and evolution of some basins in the Northern Basin and Range Province, Nevada and Utah: *Geological Society of America Bulletin*, v. 194, p. 1055-1072.
- Anderson, R. E. and Ekren, E. B., 1977, Late Cenozoic fault patterns and stress fields in the Great Basin and westward displacement of the Sierra Nevada block: *Geology*, v. 5, p. 388-389.
- Anderson, R. E., 1984, Strike-slip faults associated with extension in and adjacent to the Great Basin [abs.]: *Geologic Society of America Abstracts and Programs*, v. 16, no. 6, p. 429.
- Anderson, R. E. and Barnhard, T. P., 1987, Neotectonic framework of the central Sevier Valley area, Utah, and its relationship to seismicity, in Assessment of regional hazards and risk along the Wasatch Front, Utah, ed. P. L. Gori and W. W. Hays, *U. S. Geological Survey Open-File Report* 87-585, p. F1-134.
- Angelier, Jacques, 1979. Determination of the mean principal directions of stresses for a given fault population, *Tectonophysics*, v. 56, p. T17-T26.
- Arabasz, W. J., and Julander, D. R., 1986, Geometry of seismically active faults and crustal deformation within the Basin and Range–Colorado Plateau transition in Utah: *Geological Society of America Special Paper on Extensional Tectonics*, no. 208, p. 43-106.
- Atwater, T., 1970, Implications of plate tectonics for the Cenozoic tectonic evolution of western North America, *Geologic Society of America Bulletin*, v. 81, p. 3513-3536.
- Aydin, A., and Nur, A., 1982, Evolution of pull-apart basins and their scale independence: *Tectonics*, v. 1, p. 91-105.
- Bakun, W. H. and Lindh, A. G., 1977, Local magnitudes, seismic moments, and coda durations for earthquakes near Oroville, California: *Seismological Society of America Bulletin*, v. 67, p. 615-629.

- Bakun, W. H., and Joyner, W. B., 1984, The ML scale in Central California: *Seismological Society of America Bulletin*, v. 74, p. 1827-1843.
- Bucknam, R. C., 1969, Geologic effects of the Benham underground nuclear explosion, Nevada Test Site: *Seismological Society of America Bulletin*, v. 59, no. 6, p. 2209-2220.
- Burchfiel, B. C., and Stewart, J. C., 1966, "Pull-Apart" origin of the central segment of Death Valley, California: *Geological Society of America Bulletin*, v. 77, p. 439-442.
- Byers, F. M., Jr., Carr W. J., Christiansen, R. L., Lipman, P. W., Orkild, P. P., and Quinlivan, W. D., 1976, Geologic map of the Timber Mountain caldera area, Nye County, Nevada: *U.S. Geological Survey Miscellaneous Investigations Map I-891*.
- Caccamo, D. and Neri, G., 1984, A new analytic procedure to determine hypocentral parameters of local seismic events: *Seismological Society of America Bulletin*, v. 74, p. 669-688.
- Carr, W. J., 1974, Summary of tectonic and structural evidence for stress orientation at the Nevada Test Site: *U. S. Geological Survey Open-File Report 74-176*, 53 p.
- Carr, W. J., 1984, Regional structural setting of Yucca Mountain, southwestern Nevada, and late Cenozoic rates of tectonic activity in part of the southwestern Great Basin, Nevada and California: *U.S. Geological Survey Open-File Report 84-854*, 109 pages.
- Carder, D. S., 1945, Seismic investigation in the Boulder Dam area, 1940-1944, and the influence of reservoir loading on earthquake activity: *Seismological Society of America Bulletin*, v. 35, no. 4, p. 175-192.
- Chinnery, M. A. 1963. The stress changes that accompany strike slip faulting, *Seismological Society of America Bulletin*, v. 53, p. 921-932.
- Christiansen, R. L., Lipman, P.W., Carr, W.J., Byers, F. M., Jr., Orkild, P.P., and Sargent, K. A., 1977, Timber Mountain-Oasis Valley caldera complex of southern Nevada: *Geological Society of America Bulletin* v. 88, p. 943-959.
- Christie-Blick, N., and Biddle, K. T., 1985, Deformation and basin formation along strike-slip faults, in Biddle, K. T., and Christie-Blick, N., eds., Strike-slip deformation, basin formation, and sedimentation: *Society of Economic Paleontologists and Mineralogists Special Publication No. 37*, p. 1-34.
- Davis, G. A., and Burchfiel, B. C., 1973, Garlock fault: an intracontinental transform structure, southern California: *Geological Society of America Bulletin*, v. 84, p. 1407-1422.
- Davis, G. H., 1985, Metamorphic core complexes-expression of crustal extension by ductile-brittle shearing of the geologic column, in Conference on Heat and Detachment in Crustal Extension on Continents and Planets, 1985, Proc.: Houston, Texas, Lunar and Planetary Institute, Contribution No. 575.
- Doser, D. I., 1986, Earthquake processes in the Rainbow Mountain-Fairview Peak-Dixie Valley, Nevada region 1954-1959: *Journal of Geophysical Research*, v. 91, p. 12572-12586.

- Eaton, G. P., 1975, Harmonic magnification of the complete telemetered seismic system, from seismometer to film viewer screen, *U. S. Geological Survey Open-File Report* 75-99, 22 p.
- Eaton, G. P., Wahl, R. R., Prostka, H. J., Mabey, D. R., and Kleinkopf, M. D., 1978, Regional gravity and tectonic patterns--Their relation to late Cenozoic epeirogeny and lateral spreading in the Western Cordillera: in Smith, R. B., and Eaton, G. P., eds., *Cenozoic tectonics and regional geophysics of the Western Cordillera: Geological Society of America Memoir 152*, p. 51-91.
- Ekren, E. B., Orkild, P. P., Sargent, K. A., and Dixon, G. L., 1977, Geologic Map of Tertiary Rocks, Lincoln County, Nevada: *U.S. Geological Survey Miscellaneous Investigations Map I-1041*.
- Ekren, E. B., and Sargent, K. A., 1965, Geologic Map of the Skull Mountain Quadrangle, Nye County, Nevada: *U. S. Geological Survey Quadrangle Map GQ-387*.
- Ellis, W. L. and Magner, J. E., 1982, Determination of the in situ state of stress at the spent fuel test--Climax stock, Nevada Test Site: *U. S. Geological Survey Open-File Report* 82-458.
- Frizzell, V. A. and Zoback, M. L., 1987, Stress orientation determined from fault slip data in Hampel Wash area, Nevada, and its relation to contemporary regional stress field: *Tectonics*, v. 6, p. 89-98.
- Garfunkel, Z., and Ron, H., 1985, Block rotation and deformation by strike-slip faults. 2. The properties of a type of macroscopic discontinuous deformation: *Journal of Geophysical Research*, v. 90, p. 8589-8609.
- Gephart, J. W. and Forsyth, D. W., 1984, An improved method for determining the regional stress tensor using earthquake focal mechanism data: application to the San Fernando earthquake sequence: *Journal of Geophysical Research*, v. 89, p. 9305-9320.
- Gephart, J. W., 1985, Principal stress directions and the ambiguity in fault plane identification from focal mechanisms: *Seismological Society of America Bulletin*, v. 75, p. 621-626.
- Gumper, F. J. and Scholz, C., 1971, Microseismicity of the Nevada seismic zone: *Seismological Society of America Bulletin*, v. 61, p. 1413-1432.
- Hamilton, R. M., and Healy, J. H., 1969, Aftershocks of the Benham Nuclear Explosion: *Seismological Society of America Bulletin*, v. 59, p. 2271-2281.
- Hamilton, R. M., Smith, B. E., Fischer, F. G., and Papanek, P. J., 1971, Seismicity of the Pahute Mesa area, Nevada Test Site, 8 December 1968 through 31 December 1970: *U.S. Geological Survey Report USGS-GD-474-138*, 170 p.; available only from U.S. Department of Commerce National Technical Information Service, Springfield, VA 22161.
- Hamilton, W., and Myers, W. B., 1966, Cenozoic tectonics of the Western United States: *Reviews of Geophysics*, v. 4, p. 509-549.

- Hamilton, W., 1987, Crustal extension in the Basin and Range Province, southwestern United States: Geological Society London Special Publication 28.
- Hanks, T. C., 1977, Earthquake stress drops, ambient tectonic stresses and stresses that drive plate motions: *Pure and Applied Geophysics*, v. 115, p. 441-458.
- Hardyman, R. F., 1978, Volcanic stratigraphy and structural geology of Gillis Canyon quadrangle, northern Gillis Range, Mineral County, Nevada: Reno, Nevada, University of Nevada, unpub. Ph.D. thesis.
- Harmsen, S. C., and Rogers, A. M., 1986, Inferences about the local stress field from focal mechanisms: applications to earthquakes in the southern Great Basin of Nevada: *Seismological Society of America Bulletin*, v. 76, p. 1560-1572.
- Healey, D. L., Wahl, R. R., and Oliver, H. W., 1980, Death Valley sheet of complete Bouguer gravity map of Nevada: Nevada Bureau of Mines and Geology, Map sheet 68, scale 1:250,000.
- Herrmann, R. B., and Kijko, Andrzej, 1983, Modeling some empirical vertical component Lg relations: *Seismological Society of America Bulletin*, v. 73, p. 157-171.
- Hill, D. P., 1982, Contemporary block tectonics: California and Nevada: *Journal of Geophysical Research*, v. 87, p. 5433-5450.
- Hill, M. L., and Troxel, B. W., 1966, Tectonics of Death Valley Region, California: *Geological Society of America Bulletin*, v. 77, p. 435-438.
- Hinrichs, E. N., 1968, Geologic Map of the Camp Desert Rock quadrangle, Nye County, Nevada: *U.S. Geological Survey Geologic Quadrangle Map GQ-726*.
- Jaeger, J. C. and Cook, N. G. W., 1969, *Fundamentals of Rock Mechanics*: London, Methuen, 515 p.
- Jennings, Charles W., R. G. Strand, T. H. Rogers, M. C. Stinson, J. L. Burnett, J. E. Kahle and R. Streitz, 1973, *State of California Preliminary Fault and Geologic Map (South Half)*, California Division of Mines and Geology, Prelim. Report 13.
- Johnson, C. E., 1979, I. *CEDAR: An approach to the computer automation of short-period local seismic networks*. II. *Seismotectonics of the Imperial Valley of Southern California*, Pasadena, Calif., California Institute of Technology, unpub. Ph. D. thesis, 332 p.
- Johnson, L. R., 1965, Crustal structure between Lake Mead, Nevada, and Mono Lake, California: *Journal of Geophysical Research*, v. 70, p. 2863-2872.
- Johnston, Arch C., 1987, Air blast recognition and location using regional seismographic networks: *Seismological Society of America Bulletin*, v. 77, p. 1446-1456.
- Kellerher, J. and Savino, J., 1975, Distribution of seismicity before large strike slip and thrust-type earthquakes, *Journal of Geophysical Research*, v. 80, p. 260-271.

- King, G., 1983, The accommodating of large strains in the upper lithosphere of the earth and other solids by self-similar fault systems: The geometrical origin of b-value: *Pure and Applied Geophysics*, v. 121, p. 761-815.
- Kisslinger, C., 1976, A review of theories of mechanisms of induced seismicity: *Engineering Geology*, v. 10, p. 85-98.
- Kisslinger, C., Bowman, J. R., and Koch, Karl, 1981, Procedures for computing focal mechanisms from local ( $SV/P_z$ ) data: *Seismological Society of America Bulletin*, v. 71, p. 1719-1729.
- Lahr, John C., 1979, HYPOELLIPSE: A computer program for determining local earthquake hypocentral parameters, magnitude, and first motion pattern: *U.S. Geological Survey Open-File Report 79-431*, 53 p.
- Lancaster, D., 1975, *Active-filter cookbook*: Indianapolis, Indiana, H. W. Sams and Company, 240 p.
- Lay, T., Wallace, T. C., Helmberger, D. V., 1984, The effects of tectonic release on short-period P-waves from NTS explosions: *Seismological Society of America Bulletin* v. 74, p. 819-842.
- Lee, W. H. K., Bennett, R. E., and Meagher, K. L., 1972, A method of estimating magnitude of local earthquakes from signal duration: *U.S. Geological Survey Open-File Report*, 28 p.
- Lee, W. H. K., and Lahr, J. C., 1975, HYPO71 (revised): A computer program for determining hypocenter, magnitude, and first-motion pattern of local earthquakes: *U.S. Geological Survey Open-File Report 75-311*, p. 1-116.
- Lee, W. H. K., and Stewart, S. W., 1979. *Principles and applications of microearthquake networks*: New York City, N. Y., Academic Press, 293 p.
- Lucchitta, I., 1985, Heat and detachment in core-complex extension: in Conference on Heat and Detachment in Crustal Extension on Continents and Planets, 1985, Proc.: Houston, Texas, Lunar and Planetary Institute, Contribution No. 575.
- Maldonado, F., 1977, Composite postshot fracture map of Pahute Mesa, Nevada Test Site, June 1973 through March 1976: *U.S. Geological Survey Report USGS-474-243*, 8 p.; available only from U.S. Department of Commerce, National Technical Information Service, Springfield, Va. 22161.
- McKay, E. J. and Williams, W. P., 1964. Geology of the Jackass Flats quadrangle, Nye County, Nevada: *U.S. Geological Survey Geologic Quadrangle Map GQ-368*.
- McKenzie, D. P., 1969. The relation between fault plane solutions for earthquakes and the directions of the principal stresses: *Seismological Society of America Bulletin* v. 80, p. 591-601.
- McKeown, F. A. and Dickey, D. D., 1969, Fault displacements and motion related to nuclear explosions: *Seismological Society of America Bulletin*, v. 59, no. 6, p. 2253-2269.

- McKeown, F. A., 1975, Relation of geological structure to seismicity at Pahute Mesa, Nevada Test Site, *Seismological Society of America Bulletin*, v. 65, p. 747-764.
- Meremonte, M. E. and Rogers, A. M., 1987, Historical catalog of southern Great Basin earthquakes 1868-1978, *U.S. Geological Survey Open-File Report* 87-80, 203 p.
- Molinari, M. P., 1984, Late Cenozoic geology and tectonics of Stewart and Monte Cristo valleys, West-Central Nevada: Reno, Nevada, University of Nevada, unpub. M.S. thesis, 124 p.
- Navarro, R., and Overturf, D., 1970, Investigation of the shake-table calibration of the S-13 system and the L-4A system: Environmental Services Administration, Coast and Geodetic Survey Report CGS-746-6, March 12, 1970, 26 p.
- O'Conner, J. T., Anderson, R. E., and Lipman, P. W., 1966, Geologic map of the Thirsty Canyon quadrangle, Nye County, Nevada: U.S. Geological Survey Geologic Quadrangle Map GQ-524.
- Power, W. L., 1985, Low-angle normal faults—low differential stress at mid crustal levels? in Conference on Heat and Detachment in Crustal Extension on Continents and Planets, 1985, Proc.: Houston, Texas, Lunar and Planetary Institute, Contribution No. 575.
- Prodahl, C., 1970, Seismic refraction study of crustal structure in the Western United States: *Geological Society of America Bulletin*, v. 81, p. 2629-2646.
- Richter, C. F., 1958, *Elementary seismology*: San Francisco, Calif., Freeman, 768 p.
- Rogers, A. M., and Lee, W. H. K., 1976, Seismic study of earthquakes in the Lake Mead, Nevada-Arizona region: *Seismological Society of America Bulletin*, v. 66, p. 1651-1681.
- Rogers, A. M., Wuolett, G. M., and Covington, P. A., 1977, Seismicity of the Pahute Mesa area, Nevada Test Site, 8 October 1975 to 30 June 1976: U.S. Geological Survey Report USGS-474-184, 61 p.; available only from U.S. Department of Commerce, National Technical Information Service, Springfield, VA, 22161.
- Rogers, A. M., Harmsen, S. C., and Carr, W. J., 1981, Southern Great Basin Seismological Data Report for 1980 and Preliminary Data Analysis, *U. S. Geological Survey Open File Report* 81-1086, 148 p.
- Rogers, A. M., Harmsen, S. C., Carr, W. J., and Spence, W., 1983, Southern Great Basin Seismological Data Report for 1981 and Preliminary Data Analysis: *U.S. Geological Survey Open-File Report* 83-669. 240 p.
- Rogers, A. M., Anderson, R. E., and Harmsen, S. C., 1986, Strike slip seismicity in the Great Basin: *Transactions of the American Geophysical Union*, v. 67, p. 1236.
- Rogers, A. M., Harmsen, S. C., Herrmann, R. B., and Meremonte, M. E., 1987, A study of ground motion attenuation in the southern Great Basin, Nevada-California, using several techniques for estimates of  $Q_s$ ,  $\log A_0$ , and coda  $Q$ : *Journal of Geophysical Research*, v. 92, p. 3527-3540.



- Ron, H., Aydin, A., and Nur, A., 1986, Strike-slip faulting and block rotation in the Lake Mead fault system: *Geology*, vol. 14, no. 12, p. 1020-1023.
- Sargent, K. A., McKay, E. J., and Burchfiel, B. C., 1970, Geologic Map of the Striped Hills quadrangle, Nye County, Nevada: *U.S. Geological Survey Geologic Quadrangle Map GQ-882*.
- Sbar, M. L., 1982, Delineation and interpretation of seismotectonic domains in western North America: *Journal of Geophysical Research*, v. 87, p. 3919-3928.
- Scott, R. B., 1986, Extensional tectonics at Yucca Mountain, Southern Nevada: *Geological Society of America Abstracts with Programs*, v. 18, n. 5, p. 411.
- Shawe, D. E., 1965, Strike-slip control of Basin-Range structure indicated by historical faults in western Nevada: *Geological Society of America Bulletin*, v. 76, p. 1361-1378.
- Smith, R. B., and Lindh, A. G., 1978, Fault plane solutions of the Western United States: a compilation: in Smith, R. B., and Eaton, G. P., eds., *Cenozoic tectonics and regional geophysics of the Western Cordillera: Geological Society of America Memoir 152*, p. 107-109.
- Snoke, J. A., Munsey, J. W., Teague, A. G., and Bollinger, G. A., 1984, A program for focal mechanism determination by combined use of polarity and *SV-P* amplitude ratio data: *Earthquake Notes*, v. 55, p. 15.
- Stewart, J. H., 1978, Basin-range structure in western North America: A review, in Smith, R. B., and Eaton, G. P., eds., *Cenozoic tectonics and regional geophysics of the Western Cordillera: Geological Society of America Memoir 152*, p. 1-31.
- Stewart, J. H., and Carlson, J. E., 1978, Geologic map of Nevada: U.S. Geological Survey and Nevada Bureau of Mines and Geology map, MF-930, Scale 1:500,000.
- Stock, J. M., Healy, J. H., Hickman, S. H., and Zoback, M. D., 1985, Hydraulic fracturing stress measurements at Yucca Mountain, Nevada, and relationship to the regional stress field: *Journal of Geophysical Research*, v. 90, p. 8691-8706.
- Swadley, W. C., 1983, Map showing surficial geology of the Lathrop Wells quadrangle, Nye County, Nevada: U.S. Geological Survey Miscellaneous Investigations Map I-1361.
- Swolfs, H. S., and Savage, W. Z., 1985, Topography, stresses, and stability at Yucca Mountain, Nevada: *Proceedings, 26th U.S. Symposium on Rock Mechanics*, p. 1121-1129.
- USGS (U.S. Geological Survey) (comp.), 1984, A summary of geologic studies through January 1, 1983, of a potential high-level radioactive waste repository site at Yucca Mountain, Southern Nye County, Nevada: U.S. Geological Survey Open-File Report 84-792, U.S. Geological Survey, Menlo Park, California, 103 p.
- Vetter, U., and Ryall, A. S., 1983, Systematic change of focal mechanism with depth in the Western Great Basin: *Journal of Geophysical Research*, v. 88, p. 8237-8250.
- Wallace, T. C., Helmberger, D. V., and Engen, G. R., 1983, Evidence of tectonic release from underground nuclear explosions in long-period P- waves: *Seismological Society of America Bulletin* v. 73, p. 593-613.

- Wallace, T. C., Helmberger, D. V., and Engen, G. R., 1985, Evidence of tectonic release from underground nuclear explosions in long-period S-waves: *Seismological Society of America Bulletin*, v. 75, p. 157-174.
- Wallace, T. C., Helmberger, D. V., and Lay, J., 1986, Reply to comments by A. Douglas, J. B. Young, and N. S. Lyman and a note on the revised moments for Pahute Mesa tectonic release, *Seismological Society of America Bulletin*, v. 76, p. 313-318.
- Wernicke, B., 1981, Low-angle normal faults in the Basin and Range Province: Nappe tectonics in an extending orogen: *Nature*, v. 291, p. 645-648.
- Wernicke, B., Spencer, J. E., Burchfiel, B. C., and Guth, P. L., 1983, Magnitude of crustal extension in the southern Great Basin: *Geology*, v. 10, 497-502.
- Wright, Lauren, 1976, Late Cenozoic fault patterns and stress fields in the Great Basin and westward displacement of the Sierra Nevada block: *Geology*, v. 4, p. 489-414.
- Young, G. B. and Braile, L. W., 1976, A computer program for the application of Zoeppritz's amplitude equations and Knott's energy equations: *Seismological Society of America Bulletin*, v. 66, p 1983-2001, December 1976.
- Zoback, M. L., and Zoback, M. D., 1980a, Faulting patterns in north- central Nevada and strength of the crust: *Journal of Geophysical Research*, v. 85, p. 275-284.
- Zoback, M. L., and Zoback, M. D., 1980b, State of stress in the conterminous United States: *Journal of Geophysical Research*, v. 85, p. 6113-6156.

## **APPENDIX A**

### **System frequency response curves and calibrations**

## Appendix A

Derivations of the frequency response curves of the seismograph instrument packages used in this study are presented below. The individual components are first described as analog or digital filters. The complete systems are then described, and finally, figures of some representative southern Great Basin system calibrations, from seismometer to payout, are shown.

### Seismometer Response

For both S13 and L4C seismometers, the frequency response is written as the ratio of seismometer voltage out,  $E_s$ , to ground displacement (meters) input,  $Y_f$ . The complex transfer function  $H_1(f)$  is

$$H_1(f) = E_s/Y_f = 2\pi f_n G_{ls} \frac{f/f_n}{1 - (f_n/f)^2 + 2i\lambda(f_n/f)}$$

where  $i = \sqrt{-1}$ . The values of the effective loaded motor constants,  $G_{ls}$ , the seismometer natural frequencies,  $f_n$ , and the ratios of actual to critical damping,  $\lambda$ , corresponding to the different seismometers, which appear in the above equation, are shown in Table A1.

Seismometer	$G_{ls}$ (volts×sec meter)	$f_n$ (Hz)	$\lambda$
L4C	126.5	1.0	0.71
S130	377.8	1.0	0.70
S13Y	368.0	1.0	0.73

Table A1. The values of constants appropriate for SGB seismometers.

### Tricom 649 Amplifier/VCO

The frequency response of the Tricom 649 amplifier is modeled using a second-order Bessel low pass filter (-12 db/octave) cascaded with a third-order Butterworth high pass filter (-18 db/octave). Because this amplifier is broadband, it is designed by overlapping high and low pass filters. Letting  $H_L(f)$  = the low pass filter, and  $H_H(f)$  = the high pass filter, the complex transfer function  $H_2(f)$  is written as

$$H_2(f) = AH_L(f)H_H(f),$$

where  $A = 10^{(g/20)}$ ,  $g$  = amplifier gain (dB),

$$H_L(f) = \frac{1}{1 - (f/f_1)^2 + id_1(f/f_1)},$$

where  $f_0 = 16$  Hz (nominal -3 dB point),  $f_1 = 1.274f_0$ ,  $d_1 = 1.732$ , and

$$H_H(f) = \frac{f/f_2}{(1 + i(f/f_2))} \frac{(f/f_3)^2}{(1 - (f/f_3)^2 + id_2(f/f_3))},$$

where  $f_0 = 0.1$  Hz (nominal -3 dB point),  $f_2 = 1.0f_0$ ,  $f_3 = 1.0f_0$ , and  $d_2 = 1.0$ .

The filter design constants in these and the following formulas are from Lancaster (1975).

### Tricom 642 Discriminator

The Tricom 642 discriminator is analytically modeled by a fifth-order Bessel low pass filter having dropoff of 30 db/octave. This is factored into a first-order and two second-order filters, having the complex transfer function  $H_3(f)$  as follows:

$$H_3(f) = \frac{1}{(1 + i(f/f_1))(1 - (f/f_2)^2 + id_1(f/f_2))(1 - (f/f_3)^2 + id_2(f/f_3))},$$

where  $f_1 = 1.613f_0$ ,  $d_1 = 1.775$ ,  $f_2 = 1.819f_0$ ,  $d_2 = 1.091$ ,  $f_3 = 1.557f_0$ , and  $f_0 = 14.1$  Hz.

### Geotech 4250 Amplifier/VCO

The mathematical filter simulating this broadband amplifier is written as a second-order Bessel low pass filter (-12 db/octave) cascaded with a second-order Butterworth high pass filter (-12 db/octave). Letting  $H_L(f)$  and  $H_H(f)$  represent the low and high pass filters, respectively, and letting  $H_4(f)$  represent the amplifier response, we have

$$H_4(f) = AH_L(f)H_H(f),$$

where  $A = 10^{g/20}$ ,  $g$  = amplifier gain (db),

$$H_L(f) = \frac{1}{1 - (f/f_1)^2 + id_1(f/f_1)},$$

where  $f_c = 20$  Hz (nominal -3 db point),  $f_1 = 1.274f_c$ ,  $d_1 = 1.732$ , and

$$H_H(f) = \frac{(f/f_1)^2}{1 - (f/f_1)^2 + id_1(f/f_1)},$$

where  $f_c = 0.2$  Hz (nominal -3 db point),  $f_1 = 1.0f_c$ , and  $d_1 = 1.414$ .

### Geotech 4612 Discriminator

This component is modeled with a third-order Paynter low pass filter having a corner frequency,  $f_c$ , at 22.5 Hz. The complex frequency response,  $H_5(f)$ , is given by

$$H_5(f) = \frac{1}{(1 - (f/f_{01})^2 + id_1(f/f_{01}))(1 + i(f/f_{02}))},$$

where  $f_c = 22.5$  Hz (nominal 3 db point),  $f_{01} = 1.206f_c$ ,  $f_{02} = 1.152f_c$ , and  $d_1 = 1.203$ . This filter was preferred to that specified by the manufacturer (Butterworth third-order low pass with  $f_c = 25$  Hz), because the Paynter filter better approximated the observed response of the discriminator.

### Playout gain/shape - Analog Develocorder

The Develocorder is modeled as a second-order low pass filter having complex frequency response  $H_6(f)$  given by

$$H_6(f) = \frac{A}{1 - (f/f_1)^2 + 2id_1(f/f_1)},$$

where  $A = 17.730 \cdot 10^{-3}$  meters/volt,  $f_1 = 16$  Hz, and  $d_1 = 0.8$ .

### Playout gain/shape - Helicorder

The Helicorder has a variable gain,  $g$ , and is modeled as a fourth-order low pass filter. Its complex response,  $H_7(f)$ , may therefore be written as

$$H_7(f) = 10^{(g-g)/20} (H_6(f))^2$$

where  $g$  = Helicorder playout gain (dB), and  $H_6(f)$  is defined above, except that, for the Helicorder,  $f_1 = 35.0$  Hz, and  $d_1 = 0.48$ .

### The PDP 11/34 Digital Computer Response

The frequency response of the 12-bit analog to digital converter, PDP AD/11K, and the subsequent components on the digital computer, including magnetic tape and software, is flat for input signals having frequencies between 0 and 50 Hz, the Nyquist frequency. The system output is in digital counts, such that  $\pm 1$  volt input results in  $\pm 409.6$  counts output, respectively, for all frequencies below the Nyquist frequency. Letting  $H_8(f)$  be the system response of the PDP 11/34 computer, we have

$$H_8(f) = 409.6 \text{ counts/volt, } 0 \leq f \leq 50 \text{ Hz, and } -5 \leq \text{volts in} \leq 5.$$

### SGB Seismograph Systems

The entire system from ground motion input to payout has a frequency response,  $H(f)$ , that may be described by

$$H(f) = H_1(f)H_2(f)H_3(f)H_j(f) \quad \text{for system L4C,}$$

$$H(f) = H_1(f)H_2(f)H_3(f)H_j(f) \quad \text{for system S13O, and}$$

$$H(f) = H_1(f)H_4(f)H_5(f)H_j(f) \quad \text{for system S13Y,}$$

where  $j = 6, 7, \text{ or } 8$  depending on the medium on which the payout occurs (Develocorder, Helicorder, or digital computer, respectively) and the parameters  $G_{ie}$  and  $\lambda$  are chosen for the proper seismometer (Table A1). S13O refers to S13 instruments other than those on Yucca Mountain, and S13Y refers to S13 instruments on Yucca Mountain.

The constants,  $G_{ie}$ , are computed knowing the manufacturer's nominal motor constants, the circuit design, shunt resistance, and input impedance to the amplifier. The proper equations have been derived by Eaton (1975). The constants,  $\lambda$ , have been measured in the lab.

### Calibration

Although each component of these seismograph systems has been individually calibrated and compared with its ideal or theoretical performance, in the following we show only several representative examples of calibrations of the frequency response of complete systems. The first example, shown in Figure A1, is for the Mark Products L4C seismometer-Tricom amplifier system, having nominal gain of 43 dB, with payout being sampled by a DEC PDP 11/34 digital computer. The lack of agreement between the theoretical response (*solid curve*) and the observed system amplification ( $\times$  symbols) above about 10 Hz is believed to be due to interaction (induction) between the L4C calibration coil and main coil, and does not represent the actual system response. This interpretation is supported by the fact that shake table calibrations of the L4C do not show this discrepancy (R. Navarro and D. Overturf, 1970; S. Morrissey, written commun., 1986). That this difference arises in the seismometer and not in subsequent electronics-telemetry was established by examining the seismometer response alone. The second example, shown in Figure A2, compares theoretical (*solid curve*) and observed ( $\times$  symbols) frequency responses for the Teledyne Geotech S13 seismometer-Geotech amplifier system, with payout on a Helicorder paper record.

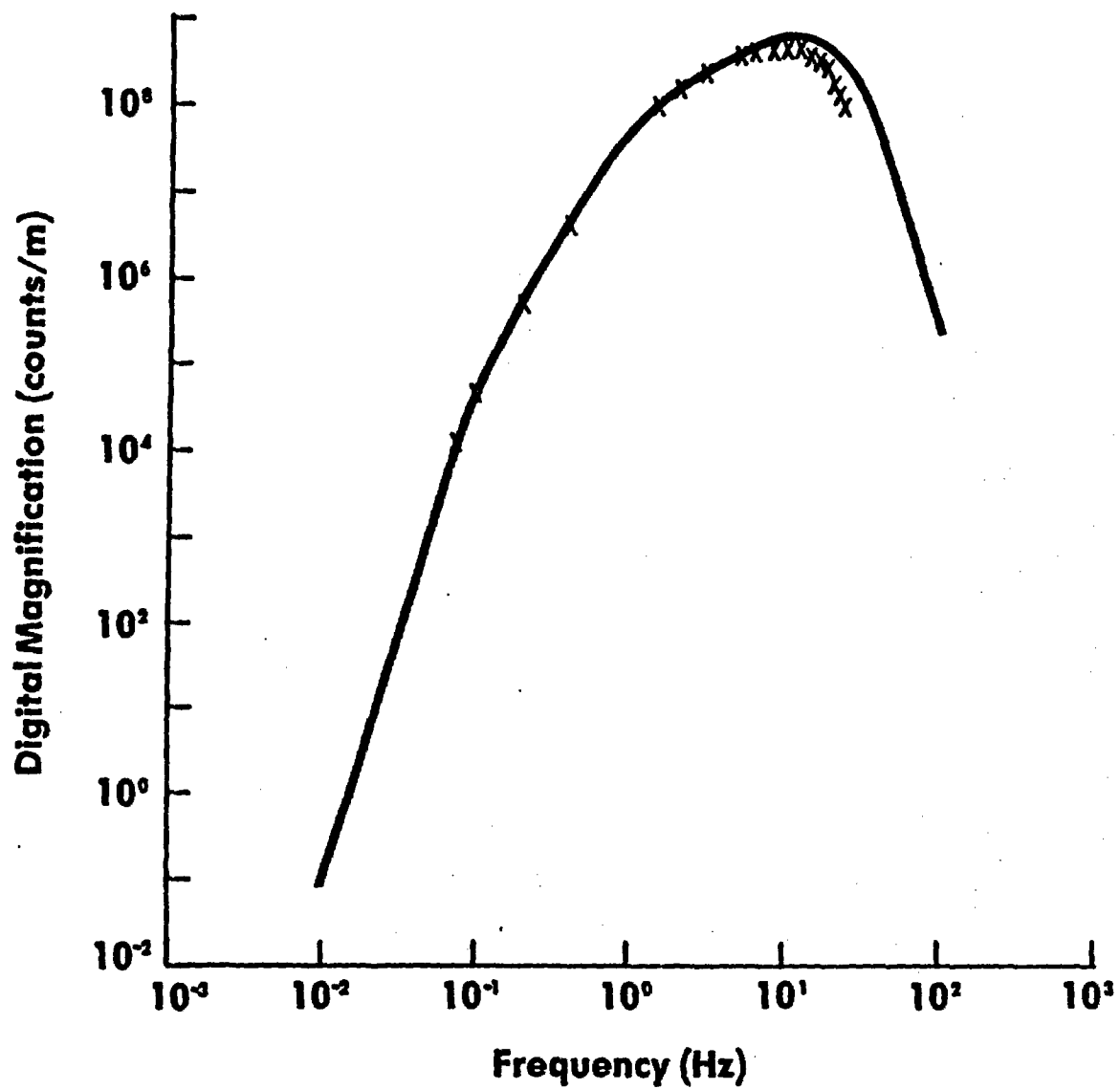


Figure A1. Amplitude response of L4C system into PDP 11/34 digital computer (theoretical, *solid curve*, observed *x's*) for a nominal amplifier gain of 48 db.

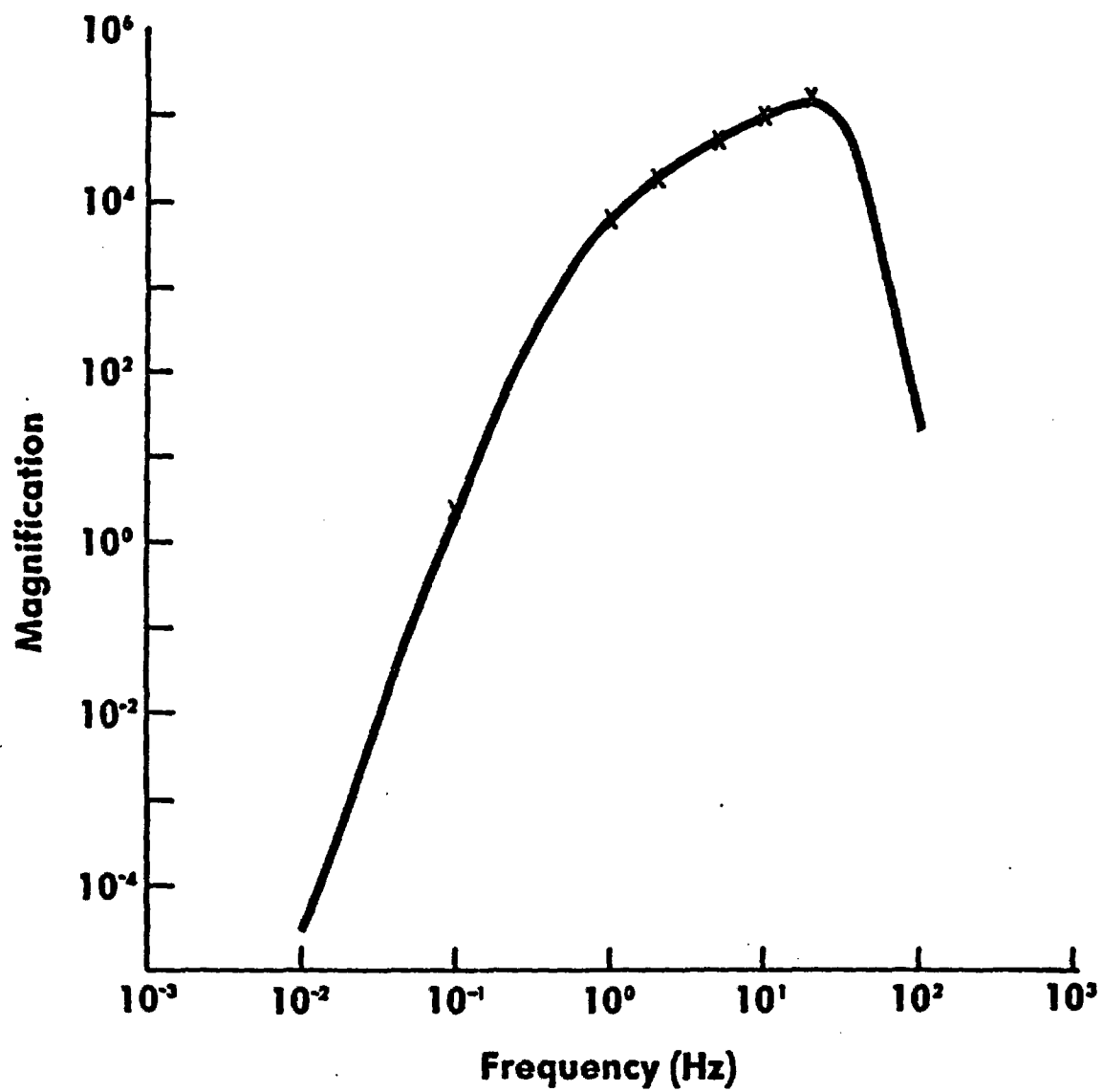


Figure A2. Amplitude response of S13Y system into helicorder for a nominal amplifier gain of 48 db.



## **APPENDIX B**

**Station codes, locations, instrumentation, and polarity reversals**

## STATION INFORMATION

CODE	STATION	PERIOD OF OPERATION (DAY/MONTH/YEAR)	LATITUDE (DEG MINUTES)	LONGITUDE (DEG MINUTES)	ELEVATION (METERS)	SEISMOMETER MODEL	GAIN (DB)
AMR	Amargosa, Cal.	24/07/78-present	36 23.86 N	116 28.45 W	720	L-4C	84
APK	Angels Peak, Nev.	15/06/75-05/08/83*	36 19.17 N	115 34.46 W	2680	S-13 to 21/3/81 L-4C 21/3/81-end	84
APKW	Angels Peak, Nev.	05/08/83-present*	36 19.19 N	115 35.22 W	2512	L-4C	84
BGB	Big Butte, Nev.	23/01/79-present	37 02.27 N	116 13.66 W	1720	L-4C	84
BLT	Belted Range, Nev.	30/05/79-present	37 28.93 N	116 07.35 W	1820	L-4C	84
BMT	Black Mountain, Nev.	26/02/80-01/04/83	37 17.02 N	116 38.74 W	2191	L-4C	84
BMTN	Black Mountain, Nev.	01/04/83-present	37 17.35 N	116 38.43 W	1900	L-4C	84
BRO	Bare Mountain, Nev.	28/11/78-08/04/81	36 45.76 N	116 37.52 W	920	L-4C	84
CDH1	Calico Hills, Nev.	06/02/80-18/11/81	36 51.62 N	116 19.05 W	1387	L-1-3DS (vert.) L-4C 18/11/81-pr	90 84
CDH5	Calico Hills, Nev.	06/02/80-18/11/81	36 51.62 N	116 19.05 W	1055	L-1-3DS (horiz.)	108
CPX	CP-1, Nev.	—/—/77-01/03/80*	36 55.80 N	116 03.33 W	1285	NGC-21 to 5/8/80 L-4C 5/8/80-pr.	84
CTS	Cactus Peak, Nev.	24/04/79-present	37 39.40 N	116 43.54 W	1890	L-4C	84
DLM	Delamar Mountains, Nev.	08/06/78-present*	37 36.35 N	114 44.33 W	1730	L-4C	84
EPN	Echo Peak, Nev.	02/09/75-present	37 12.85 N	116 19.42 W	2285	S-13 to 25/4/80 L-4C 25/4/80-pr.	84
EPNH	Echo Peak, Nev.	06/06/84-present	37 12.85 N	116 19.42 W	2285	L-4C horizontal	78
EPR	East Pahrnagat Rg, Nev	23/01/79-present*	37 10.12 N	115 11.19 W	1300	L-4C	84
FMT	Funeral Mountains, Cal.	28/11/78-present	36 38.38 N	116 46.73 W	1025	L-4C	84
GLR	Groom Lake Road, Nev.	20/11/75-present*	37 11.96 N	116 01.06 W	1435	L-4C	84
GMN	Gold Mountain, Nev.	13/07/79-present*	37 18.01 N	117 15.58 W	2155	L-4C	84
GMNH	Gold Mountain, Nev.	30/07/84-present	37 18.01 N	117 15.58 W	2155	L-4C horizontal	78

GMR	Groom Range, Nev.	23/01/79-present	37 20.03 N	115 46.27 W	1580	L-4C	84
GMRH	Groom Range, Nev.	09/09/84-present	37 20.03 N	115 46.27 W	1580	L-4C	84
GVN	Grapevine, Cal.	28/11/78-present	37 00.09 N	117 20.55 W	865	L-4C	84
GWV	Greenwater Valley, Cal.	24/07/78-present	36 11.20 N	118 40.24 W	1540	L-4C	84
HCR	Hot Creek Range, Nev.	21/07/81-present	38 14.02 N	116 26.18 W	2030	L-4C	84
JON	Johnnie, Nev.	24/07/78-present	36 26.39 N	116 06.18 W	920	L-4C	84
JONH	Johnnie, Nev.	22/06/84-present	36 26.39 N	116 06.18 W	920	L-4C horizontal	78
KRN	Kawich Range, Nev.	30/05/79-23/04/80	37 42.37 N	116 20.07 W	2570	L-4C	84
KRNA	Kawich Range, Nev.	23/04/80-present	37 44.47 N	116 22.80 W	1980	L-4C	84
LCH	Last Chance Range, Cal.	13/07/79-present	37 14.08 N	117 38.84 W	1455	L-4C	84
LEE	Leeds, Utah	01/01/71-01/06/80	37 14.58 N	113 22.60 W	1067	Benioff	
LOP	Lookout Peak, Nev.	23/01/79-present	36 51.25 N	116 10.05 W	1695	L-4C	84
LSM	Little Skull Mt., Nev.	13/12/79-present	36 44.40 N	116 16.37 W	1140	S-13	84
LSMH	Little Skull Mt., Nev.	17/07/84-present	36 44.40 N	116 16.37 W	1140	L-4C horizontal	78
LSME	Little Skull Mt., Nev.	17/07/84-present	36 44.40 N	116 16.37 W	1140	L-4C horizontal	78
LSN	Little Skull Mt., Nev.	19/02/79-13/12/79	36 45.21 N	116 15.57 W	1070	L-4C	84
MCA	Marble Canyon, Cal.	23/01/79-present	36 38.89 N	117 16.85 W	300	L-4C	84
MCX	Mercury, Nev.	15/06/77-07/03/80	36 39.37 N	115 59.45 W	1160	S-13	84
MCY	Mercury, Nev.	07/03/80-present	36 39.70 N	115 57.73 W	1285	S-13	84
MGM	Magruder Mountain, Nev.	13/07/79-present	37 26.47 N	117 29.79 W	2100	L-4C	84
MTI	Mount Irish, Nev.	08/06/79-present	37 40.60 N	115 16.36 W	1525	L-4C	84
MZP	Montezuma Peak, Nev.	13/07/79-present	37 42.04 N	117 22.98 W	2375	L-4C	84
NEL	Nelson, Nev.	01/01/71-01/06/80	35 42.73 N	114 50.62 W	1052	Benioff	
NNN	Nasa Mountain, Nev.	28/11/78-01/11/83	37 04.85 N	116 49.09 W	1500	L-4C	84
NOP	Nopah Range, Cal.	24/07/78-present	36 07.68 N	116 09.16 W	970	L-4C to 25/4/80 S-13 25/4/80-pr.	84 84

NPN	North Pahroc Rg, Nev.	08/06/79-present	37 39.16 N	114 56.22 W	1650	L-4C	84
PGE	Panamint Range, Cal.	28/11/78-present	36 20.93 N	117 03.95 W	1850	L-4C	84
PGEH	Panamint Range, Cal.	11/10/84-present	36 20.93 N	117 03.95 W	1850	L-4C horizontal	78
PPK	Piper Mountain, Cal.	13/07/79-present	37 25.58 N	117 54.43 W	1830	L-4C	84
PRN	Pahroc Range, Nev.	21/01/72-present	37 24.42 N	115 02.99 W	1470	NGC-21 to 19/6/80 S-13 19/6/80-pr.	84
PRNH	Pahroc Range, Nev.	28/08/84-present	37 24.42 N	115 02.99 W	1470	L-4C horizontal	78
QCS	Queen City Summit, Nev.	08/06/79-present	37 46.07 N	115 54.98 W	1890	L-4C	84
QSM	Queen of Sheba Mine, Ca	28/11/78-present	35 57.93 N	116 52.10 W	670	L-4C	84
RVE	Reveille Range, Nev.	08/06/79-20/07/81	38 01.18 N	116 11.51 W	2290	L-4C	84
SDH	Striped Hills, Nev.	24/07/78-present	36 38.73 N	116 20.29 W	1055	L-4C	84
SGV	South Grapevine Mts, Ca	28/11/78-15/06/81	36 58.87 N	117 01.94 W	1565	L-4C S-13 15/06/81-pr	84 84
SHRG	Sheep Range, Nev.	22/05/79-present	36 30.27 N	115 09.31 W	1645	L-4C	84
SPRG	Spotted Range, Nev.	28/05/79-present	36 41.64 N	115 48.56 W	1235	L-4C	84
SRG	Seaman Range, Nev.	08/06/79-present	37 52.93 N	115 04.08 W	1645	L-4C	84
SSP	Shoshone Peak, Nev.	10/10/73-present	36 55.50 N	116 13.11 W	2065	NGC-21 to 25/5/80 L-4C 27/5/80/pr.	84 84
SVP	Silver Peak Range, Nev.	13/07/79-present	37 42.90 N	117 48.05 W	2620	L-4C	84
TCN	Thirsty Canyon, Nev.	02/11/84-present	37 08.80 N	116 43.52 W	1469	L-4C	84
TMBR	Timber Mt., Nev.	19/02/82-present	37 02.05 N	116 23.13 W	1758	L-4C	84

TMO	Tin Mountain, Cal.	28/11/78-present	36 48.32 N	117 24.48 W	2195	L-4C	84
TNP	Tonopah, Nev.	31/08/64-02/19/82	38 04.92 N	117 13.08 W	1931	Benioff	
TPK	Tolicha Peak, Nev.	11/06/79-12/02/80*	37 16.11 N	116 48.26 W	2080	L-4C	84
TPU	Tempiute Mountain, Nev.	08/06/79-present*	37 38.30 N	115 38.95 W	1915	L-4C	84
WCT	Wildcat Mountain, Nev.	08/04/81-present	36 47.53 N	116 37.60 W	1000	L-4C	84
WRN	Worthington Mts., Nev.	08/06/79-present	37 58.90 N	115 35.30 W	1760	L-4C	84
YMT1	Yucca Mountain, Nev.	05/03/81-present*	36 51.20 N	116 31.80 W	1200	S-13	84
YMT2	Yucca Mountain, Nev.	05/03/81-present*	36 47.12 N	116 29.19 W	1220	S-13	84
YMT3	Yucca Mountain, Nev.	05/03/81-present*	36 47.23 N	116 24.79 W	1050	S-13	84
YMT4	Yucca Mountain, Nev.	01/04/81-present*	36 50.83 N	116 27.07 W	1256	S-13	84
YMAH	Yucca Mountain, Nev.	29/06/84-present	36 50.83 N	116 27.07 W	1256	L-4C horizontal	78
YMAE	Yucca Mountain, Nev.	29/06/84-present	36 50.83 N	116 27.07 W	1256	L-4C horizontal	78
YMT5	Yucca Mountain, Nev.	01/04/81-present*	36 53.90 N	116 27.23 W	1350	S-13	84
YMT6	Yucca Mountain, Nev.	01/04/81-present*	36 51.51 N	116 24.26 W	1150	S-13	84

\* INDICATES STATION HAVING POLARITY REVERSAL (SEE FOLLOWING TABLE).

POLARITY REVERSALS (PERTAINS TO DEVELOCORDER FILMS ONLY)

CODE	STATION	PERIOD OF REVERSE POLARITY (DAY/MONTH/YEAR)
APK	Angels Peak, Nev.	21/3/81 - 05/08/83
APKW	Angels Peak, Nev.	05/08/83 - present
CDH1	Calico Hills, Nev.	30/3/81 to 3/8/81; also 1/12/81 to present
CPX	CP-1, Nev.	5/8/80 to 13/12/80
DLM	Delamar Mts., Nev.	28/6/79 to 29/8/79
EPN	Echo Peak, Nev.	1/11/78 to 01/05/80
EPR	East Pahrnagat Range, Nev.	10/12/79 to 20/2/80
GLR	Groom Lake Road, Nev.	1/11/78 to 22/2/79
GMN	Gold Mountain, Nev.	28/6/79 to 29/8/79; also 5/8/80 to 17/12/80
JON	Johnnie, Nev.	1/11/78 to 22/2/79
LSM	Little Skull Mtn., Nev.	17/07/84 to present
LCH	Lost Change Range, Nev.	28/6/79 to 29/8/79
MGM	Magruder Mountain, Nev.	28/6/79 to 29/8/79
MTI	Mount Irish, Nev.	28/6/79 to 29/8/79
MZP	Montezuma Peak, Nev.	28/6/79 to 29/8/79
NPN	North Pahroc Range, Nev.	28/6/79 to 29/8/79
PGE	Panamint Range, Cal.	11/10/84 to present
PPK	Piper Mountain, Cal.	28/6/79 to 29/8/79
PRN	Pahroc Range, Nev.	10/12/79 to 20/2/80; also 28/08/84 to present
OCS	Queen City Summit, Nev.	28/6/79 to 29/8/79
QSM	Queen of Sheba Mine, Nev.	28/6/79 to 29/8/79
RVE	Reveille Range, Nev.	28/6/79 to 29/8/79
SRG	Seaman Range, Nev.	28/6/79 to 29/8/79
SSP	Shoshone Peak, Nev.	28/6/79 to 01/06/80
SVP	Silver Peak Range, Nev.	28/6/79 to 29/8/79
TPK	Tolicha Peak, Nev.	11/06/79 to 29/8/79
TPU	Tempiute Mountain, Nev.	28/6/79 to 29/8/79
WRN	Worthington Mts., Nev.	28/6/79 to 29/8/79
YMT1	Yucca Mountain, Nev.	05/03/81 to present
YMT2	Yucca Mountain, Nev.	05/03/81 to present
YMT3	Yucca Mountain, Nev.	05/03/81 to present
YMT3	Yucca Mountain, Nev.	05/03/81 to present
YMT4	Yucca Mountain, Nev.	01/04/81 to present
YMT5	Yucca Mountain, Nev.	01/04/81 to present
YMT6	Yucca Mountain, Nev.	01/04/81 to present

## **APPENDIX C**

### **Input parameters to HYPO71**

### Hypocenter Parameters Used for Earthquake Location Procedure

Routine earthquake location from phase data obtained from the southern Great Basin network is done using the computer program HYPO71 (Lee and Lahr, 1975). Their program has been modified to compute theoretical travel times of seismic rays to actual seismograph station locations, rather than to some mean reference ground level, as in the original computer program. This modification was necessary because SGB station elevations vary from 300 meters above sea level (station MCA) to 2620 meters above sea level (station SVP). Since most station elevations are greater than 1000 meters, we allow earthquake depth of focus to rise to -1.2 km, where negative depths (actually elevations) represent foci above sea level. Test variables 14 and 15 in HYPO71 have been assigned values to invoke the variable surface layer thickness option (see Table C2 below).

A second modification to the HYPO71 program computes local earthquake magnitudes according to the methods discussed in this report in the section "magnitude estimation details." Test variables 16 and 17 in HYPO71 have been assigned values for determining  $M_{ca}$ , the coda amplitude magnitude developed by Carl Johnson (1979). Three event magnitudes,  $M_L$ ,  $M_d$ , and  $M_{ca}$  may be obtained for each earthquake. The reported magnitude is computed from the formula

$$M = \frac{1}{2}[M_L + \frac{1}{2}(M_d + M_{ca})],$$

or by a similar average if fewer magnitude estimates are available for a given earthquake.

The P- and S-wave velocity model (in text, called M0) used to locate earthquakes is shown in table C1 below.

Depth to top of layer (km)	P-wave velocity (km/sec)	S-wave velocity (km/sec)
Station Elevation	3.8	2.22
1.0	5.9	3.45
3.0	6.15	3.60
24.0	6.9	4.04
32.0 (halfspace)	7.8	4.56

Table C1. Southern Great Basin P and S velocity model. Sea level = 0.0 km.

The values of test variables employed in HYPO71 are given in table C2 below.

TEST( 1) = 0.1 sec	TEST( 2) = 30.0 km	TEST( 3) = 0.5
TEST( 4) = 0.05 km	TEST( 5) = 5.0 km	TEST( 6) = 1.0
TEST( 7) = -1.276	TEST( 8) = 1.666	TEST( 9) = 0.00227
TEST(10) = 100.0 km	TEST(11) = 8.	TEST(12) = 0.5
TEST(13) = 1.0 km	TEST(14) = -1.2 km	TEST(15) = 999
TEST(16) = 0.852	TEST(17) = -1.766	

Table C2. HYPO71 test variables as discussed in Lee and Lahr (1975).

Pertinent control card options are ZTR = 5.0 km, XNEAR = 10.0 km, XFAR = 220 km, and POS = 1.71.



## APPENDIX D

### August 1978 through December 1983 hypocenter summary and quadrangle maps to which events are keyed

Hypocentral parameters for all local earthquakes cataloged by the U. S. G. S. for the period August 1, 1978, through December 31, 1983 are listed. Pre-1982 locations from previous open-file reports are repeated with revised magnitudes. The column headings for appendix D are nearly self-explanatory. For clarity, UTC is Universal Coordinated Time, azi gap is the azimuthal gap (HYPO71), horizontal error is the epicentral standard error,  $\sqrt{sdx^2 + sdy^2}$ , where  $sdx$  and  $sd_y$  are the standard errors in longitude and latitude (HYPO71), respectively, vertical error is the standard error in depth of focus,  $MD$  is duration magnitude, and  $Mblg$  is the local magnitude calibrated for southern Great Basin crustal paths and stations (Rogers and others, 1987). An asterisk after the depth estimate indicates that the depth-of-focus error estimate was very large ( $\geq 100$  km). Two asterisks after the depth estimate indicate that HYPO71 fixed the depth at 7.0 km (our default value, used when too few phase readings are available to provide a focal depth estimate). Pre-digital data (before October, 1981) tend to have fewer phase readings per event, and less precision, explaining the greater percentage of depth-of-focus problems for those hypocenters.

#### Chemical explosions at Bare Mountain and elsewhere

For the 1982-1983 reporting period, probable and possible blasts in the Bare Mountain quadrangle, just west of Yucca Mountain, are tagged in appendix D by a darkened circle (●) for probable blasts, and an open circle (○) for possible blasts, just to the left of the quadrangle name. Fourteen probable blasts and one possible blast were recorded in the Bare Mountain quadrangle in 1982-1983. The determination of probable blast was based on several factors. These include the fact that a mine was operating at Bare Mountain during 1982-1983, observations of only compressional first-motion polarities on local station seismograms, logical times for blasting (weekdays during standard working hours), shallow estimated depth of focus, and often the presence on several seismograms of an energetic phase at the time of a predicted sonic boom or air-coupled Raleigh wave (Johnston, 1987). Figure D5 shows digital seismograms that record a Bare Mountain chemical explosion of 820824. YMT1 and YMT2, on the west flank of Yucca Mountain, are usually the only SGB network stations that record the slow-moving ( $v \approx 0.32$  km/sec), air-coupled Raleigh wave generated from Bare Mountain blasts. Note that the Rayleigh wave is especially well-developed at YMT2, having greater amplitude than the body wave at that site (at YMT1 the relative amplitudes are unknown, since both arrivals are clipped). Station YMT4, only two km more distant from the epicenter than YMT2, did not visibly record the Raleigh wave, probably because YMT4 is topographically shielded from the advancing shock front. Most of these observations are possible on digital seismograms, but several are not clear on analog records such as deconvoluted films. Thus, we do not annotate potential Bare Mountain blasts before 1982. Event 831222 was a poorly recorded potential blast that may have been mislocated in the Bare Mountain mining region.

Although chemical blasts on Yucca Mountain occurred during 1982-1983, these events were confirmed as blasts by Department of Energy personnel and were not included in appendix D. A few Yucca Mountain blasts prior to 1982 are included here, but are tagged as blasts. Elsewhere in the southern Great Basin, known blasts are not included in appendix D, but some blasts may have been inadvertently included.

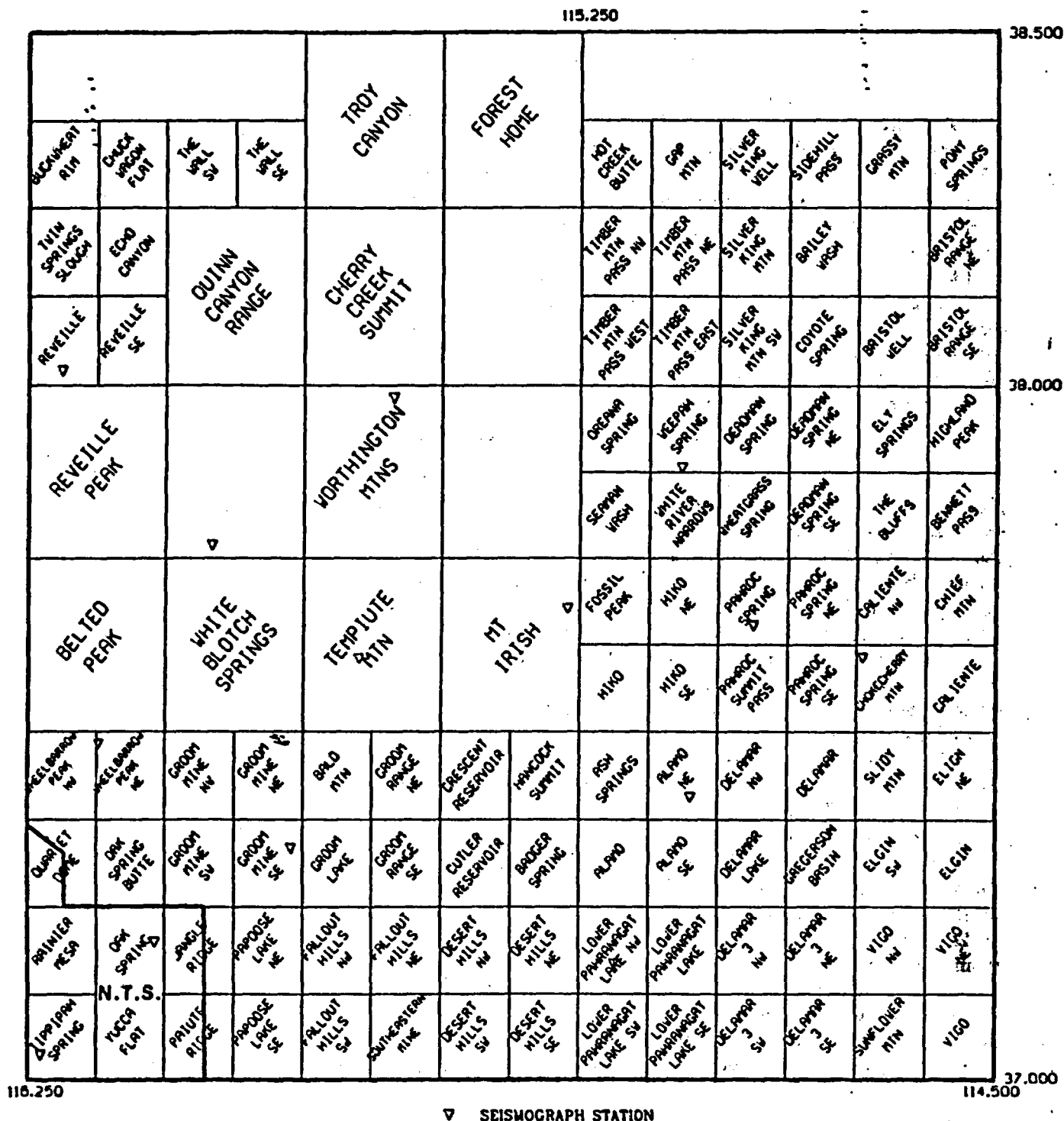


Figure D1. Quadrangle names in northeast quarter of southern Great Basin.

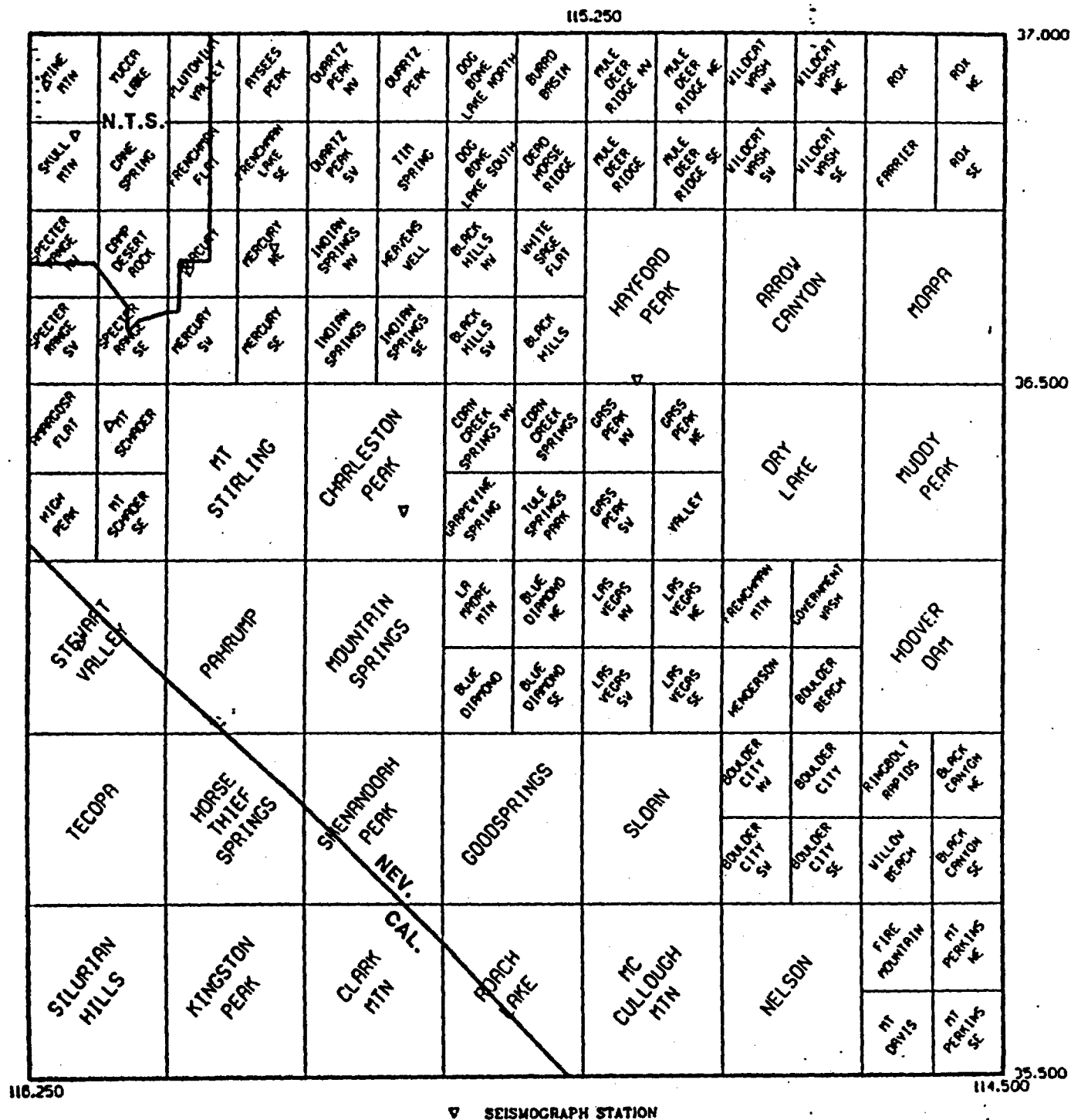


Figure D2. Quadrangle names in southeast quarter of southern Great Basin.

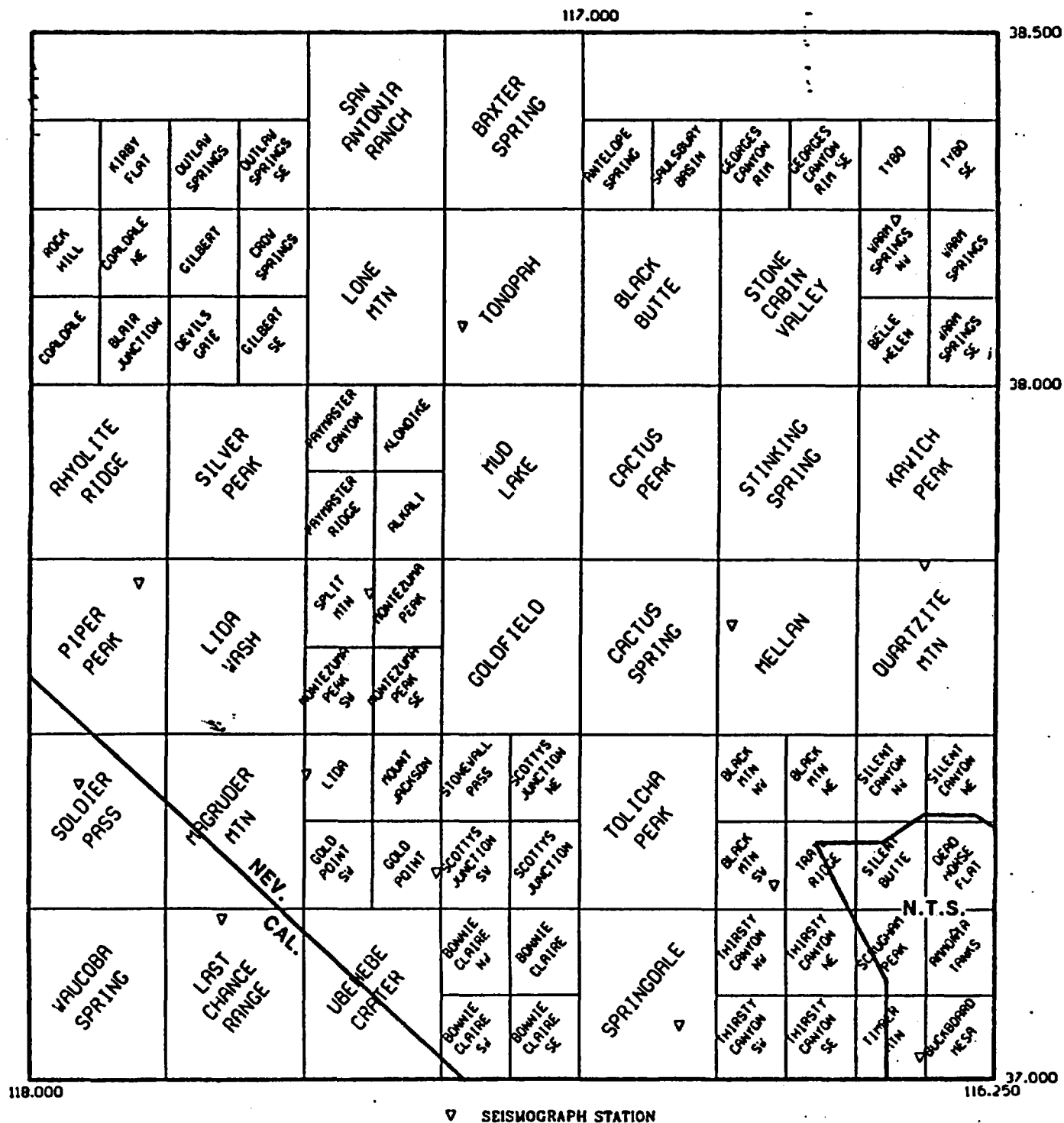


Figure D3. Quadrangle names in northwest quarter of southern Great Basin.

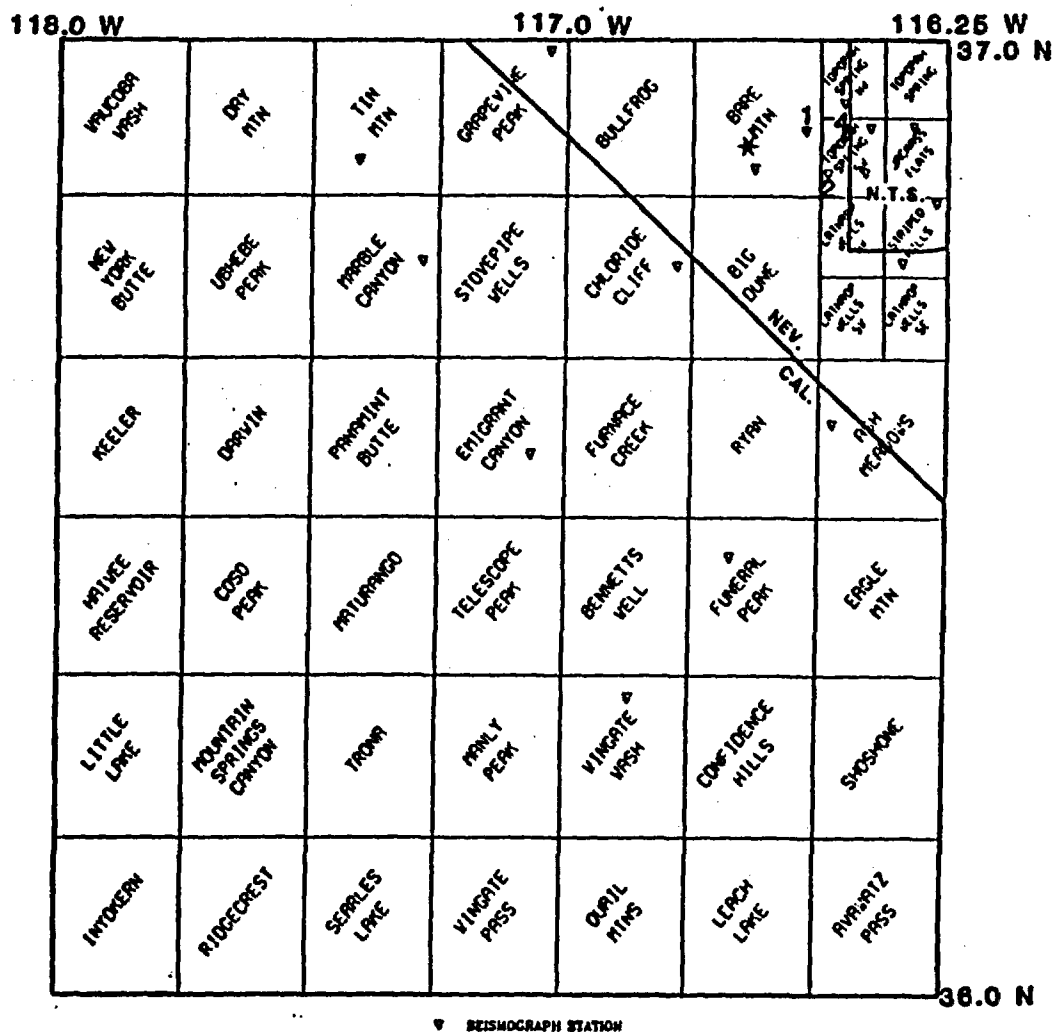


Figure D4.—Quadrangle names in the southwest quarter of the southern Great Basin. The star represents the location of the Bare Mountain chemical explosion of 820824 22:51, for which seismograms from stations YMT1, YMT2, and YMT4 (labeled) are shown below.

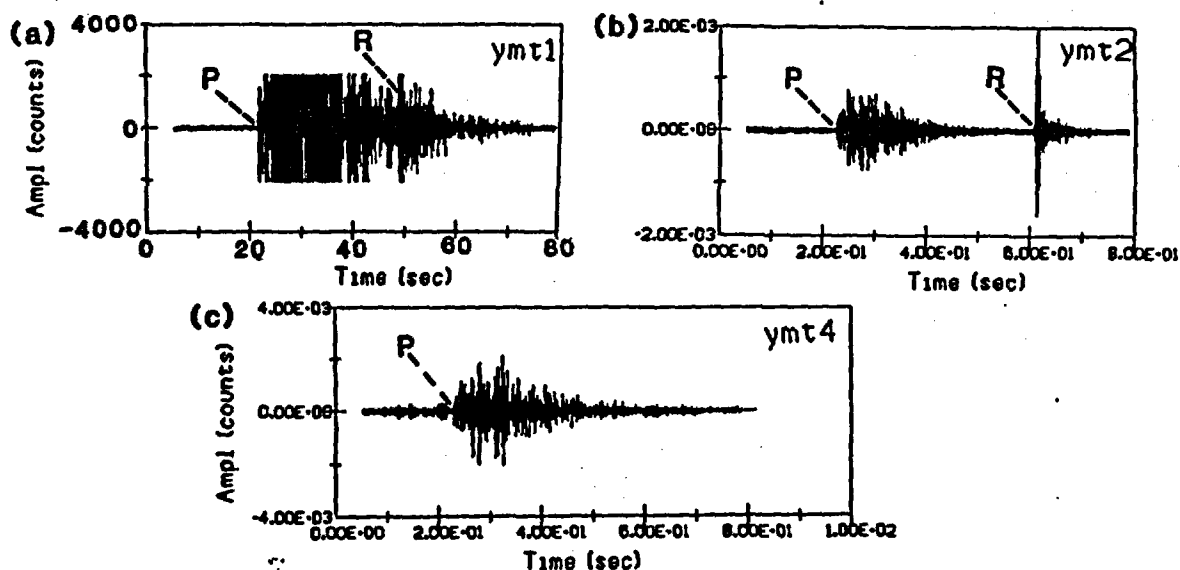


Figure D5.—Event 820824 22:51 seismograms, with compressional (P) and air-coupled Raleigh (R) phases labeled where evident, for (a), station YMT1, (b), station YMT2, and (c), station YMT4.

1978 LOCAL HYPOCENTER SUMMARY

DATE - TIME (UTC)	LATITUDE (DEG. N)	LONGITUDE (DEG. W)	HORIZ ERROR (KM)	DEPTH (KM)	VERT ERROR (KM)	AZI GAP (DEG)	QUAL	Md	Mbig	QUADRANGLE
AUG 3 0: 5: 7	36.572	115.519	---	7.00**	---	252	AD	1.4	---	INDIAN SPRINGS SE
3 15:36:12	37.474	114.730	0.6	-0.72	7.5	315	DD	1.5	---	SLIDY MTN
4 21:49:24	37.271	116.027	0.1	8.88	0.1	184	AD	1.0	---	OAK SPRING BUTTE
5 11:28:21	37.347	115.119	0.9	14.03	0.9	157	AC	1.2	---	ALAMO SE
6 10:45:50	38.238	115.230	---	7.00**	---	310	BD	1.5	---	TIMBER MTN PASS NW
10 19:34: 8	37.512	115.108	---	4.15	---	203	AD	1.7	---	HIKO SE
12 3: 9: 4	36.011	116.905	10.3	7.19	8.0	302	DD	0.9	---	BENNETTS WELL
14 16:10: 2	36.255	116.072	0.3	7.00	0.5	216	DD	2.0	---	RYAN
17 5: 8:45	37.358	116.468	2.0	3.06*	---	260	CD	1.5	---	SILENT BUTTE
17 8:51:37	37.319	116.325	7.9	7.00	5.5	284	DD	1.2	---	DEAD HORSE FLAT
17 8:55:43	37.302	116.371	---	7.00**	---	282	BD	1.4	---	DEAD HORSE FLAT
17 15:40:22	36.471	114.299	---	-0.75	---	294	BD	1.8	---	***REGIONAL***
25 8:42:49	36.737	116.170	0.8	2.81	2.0	77	AB	0.8	---	SPECTER RANGE NW
28 6: 3:29	36.829	116.225	0.5	7.74	0.9	142	AC	0.8	---	SKULL MTN
28 10:58: 3	36.742	116.175	1.2	7.13	3.2	142	BC	0.7	---	SPECTER RANGE NW
31 12:15:10	37.311	116.367	3.1	-0.75	2.5	267	CD	1.4	---	DEAD HORSE FLAT
31 12:18:18	37.309	116.363	---	7.00**	---	272	AD	1.2	---	DEAD HORSE FLAT
SEP 1 1: 7:23	37.988	116.567	---	7.00**	---	350	CD	1.4	---	STINKING SPRING
8 22:21:38	37.247	116.371	14.7	7.00*	---	332	DD	1.2	---	AMMONIA TANKS
13 22:34:44	37.310	116.419	6.2	1.19	6.9	271	DD	1.7	---	SILENT BUTTE
14 17:20:54	36.308	114.969	7.2	3.63*	---	263	DD	0.9	---	DRY LAKE
23 14: 0:54	35.887	115.908	4.3	2.96*	---	261	CD	1.1	---	HORSE THIEF SPRINGS
23 14:28:44	36.191	115.182	1.5	10.41	5.9	260	CD	1.4	---	LAS VEGAS NW
24 8:31:43	36.720	115.578	---	7.00**	---	148	AD	0.9	---	HEAVENS WELL
25 8:37:22	37.197	116.340	1.9	1.25	1.6	218	BD	---	0.2	AMMONIA TANKS
OCT 4 11:59: 1	36.616	116.243	1.3	2.50	3.3	102	BB	1.2	---	SPECTER RANGE SW
10 18:52:37	36.007	115.445	19.8	5.30*	---	300	DD	1.3	---	BLUE DIAMOND
14 16:12: 4	36.367	116.852	2.9	10.82	7.3	246	CD	1.3	---	FURNACE CREEK
NOV 29 8:34: 8	37.295	116.504	0.6	7.50	1.4	228	AD	2.1	---	TRAIL RIDGE
29 11:19:56	36.632	116.224	1.5	4.35	6.4	173	CC	0.5	---	SPECTER RANGE NW
29 16:19:22	37.174	116.190	1.6	4.16	7.7	149	CC	0.8	---	RAINIER MESA
30 13:50:27	37.073	117.445	3.9	9.23	1.3	295	CD	1.4	---	SPLIT MTN
30 14:38:23	36.040	117.885	18.3	2.09*	---	300	DD	1.3	---	HAIWEE RESERVOIR
30 22: 4:19	35.981	116.963	5.5	1.07*	---	270	DD	0.7	---	WINGATE WASH
DEC 1 17: 7:30	37.024	116.047	1.7	-0.86*	---	234	CD	2.5	---	YUCCA FLAT
2 12:41: 8	37.104	116.132	4.4	10.84	6.2	252	CD	1.2	---	TIPPICAH SPRING
3 0:43:30	36.129	117.426	5.5	3.88*	---	271	DD	1.1	---	MATURANGO
3 12:50:42	36.119	117.763	12.5	3.20*	---	293	DD	1.3	---	HAIWEE RESERVOIR
5 9:43: 8	37.339	116.326	2.5	5.15*	---	201	CD	1.3	---	DEAD HORSE FLAT
6 22:29:54	36.350	116.954	---	16.49	---	148	AD	1.2	---	FURNACE CREEK
8 21: 2: 2	35.986	117.283	1.8	3.43*	---	272	CD	1.1	---	TROMA
10 11:19:52	35.974	117.278	1.0	3.37*	---	261	CD	1.4	---	TROMA
10 13:35:30	36.401	116.105	---	5.64	---	264	AD	2.1	---	MT SCHADER
11 21:44:56	36.400	117.066	0.8	13.51	1.9	141	AC	1.1	---	EMIGRANT CANYON
12 6:37:35	36.684	116.408	0.6	9.70	3.2	174	BC	0.8	---	LATHROP WELLS NW
12 7: 7:15	36.679	116.406	0.4	-0.45	0.4	161	AC	1.4	---	LATHROP WELLS NW
13 4:19: 8	35.945	117.255	---	18.69	---	266	AD	1.1	---	TROMA
13 21:46:26	36.750	115.845	1.9	1.20*	---	269	CD	0.7	---	FRENCHMAN LAKE SE
13 23:29:17	35.948	115.943	6.6	3.28*	---	298	DD	0.7	---	HORSE THIEF SPRINGS
14 9:31:59	35.978	116.942	2.0	5.50	8.9	259	CD	1.4	---	WINGATE WASH
14 12:18:12	36.214	115.177	83.8	8.85*	---	329	DD	1.6	---	LAS VEGAS NW
15 20:17: 1	37.152	116.557	2.5	4.73*	---	262	CD	1.4	---	THIRSTY CANYON NE
17 20:51: 0	37.575	116.439	20.4	7.00*	---	315	DD	2.0	---	QUARTZITE MTN
18 6:43:28	37.360	116.378	6.3	-0.22*	---	292	DD	1.6	---	SILENT BUTTE
18 7:27:44	37.195	116.546	4.2	2.08*	---	272	CD	1.1	---	THIRSTY CANYON NE
22 1: 4:22	36.100	117.793	---	3.02	---	330	AD	1.0	---	HAIWEE RESERVOIR
23 2:35: 2	37.033	117.206	3.9	5.06	8.4	255	CD	0.6	---	BONNIE CLAIRE SW
23 12:12: 4	35.811	116.551	3.6	1.42*	---	277	CD	1.2	---	CONFIDENCE HILLS
23 23:49:48	36.219	117.397	5.5	11.96	8.5	266	DD	0.9	---	MATURANGO
25 23: 4:59	36.622	116.240	1.3	5.41	3.9	194	BD	1.0	---	SPECTER RANGE SW
26 22:18: 5	35.929	116.995	3.4	2.48*	---	278	CD	1.1	---	WINGATE WASH
27 5:25: 1	36.603	116.263	0.3	4.56	0.7	185	AD	1.5	---	LATHROP WELLS SE
29 4:27:53	36.964	117.566	8.0	11.40	3.9	292	DD	1.8	---	DRY MTN
30 1:30:22	36.021	117.597	8.0	10.80*	---	290	DD	1.3	---	COSO PEAK
31 15:54:53	36.136	114.940	---	3.50	---	335	AD	1.7	---	FRENCHMAN MTN

## 1979 LOCAL HYPOCENTER SUMMARY

	DATE - TIME (UTC)	LATITUDE (DEC. N)	LONGITUDE (DEC. W)	HORIZ ERROR (KM)	DEPTH (KM)	VERT ERROR (KM)	AZI GAP (DEG)	QUAL	Md	Mb1g	QUADRANGLE
JAN	3 16:22: 9	37.547	117.761	1.8	7.80	1.9	323	BD	1.2	---	PIPER PEAK
	5 11:45:26	36.389	116.888	0.8	14.78	1.8	161	AC	1.8	---	FURNACE CREEK
	8 13:48:54	37.283	116.496	2.3	3.34*	---	285	CD	1.1	---	SILENT BUTTE
	9 5:58:37	36.615	117.621	1.7	3.29*	---	298	CD	1.3	---	HAIWEE RESERVOIR
	10 16:36:21	36.413	117.893	2.0	8.77	1.5	302	BD	1.3	---	KEELER
	16 8:59:57	36.697	116.389	0.6	2.91	1.3	118	AB	0.5	---	LATHROP WELLS NW
	17 2:52:12	37.130	117.379	1.3	6.63	1.6	257	BD	1.4	---	UBEHEBE CRATER
	18 11:34:26	36.228	117.002	0.9	8.88	2.1	232	BD	1.0	---	TELESCOPE PEAK
	21 1: 5:24	35.966	116.951	3.8	2.86*	---	260	CD	1.4	---	WINGATE WASH
	22 18: 6:34	36.469	116.690	0.9	-0.52*	---	198	CD	1.8	---	CHARLESTON PEAK
FEB	3 19:16:13	37.321	114.872	22.2	4.55	7.5	310	DD	2.1	---	GREGGSON BASIN
	7 8: 4:56	36.615	116.807	0.9	2.15*	---	147	CC	1.1	---	FRENCHMAN LAKE SE
	7 10:19:36	36.437	117.006	2.4	10.30	4.7	106	BB	0.6	---	EMIGRANT CANYON
	8 1:38:32	36.163	117.924	1.8	5.74	3.3	302	BD	1.6	---	HAIWEE RESERVOIR
	8 23: 9:19	37.184	116.062	0.9	0.53	0.6	139	BC	1.4	---	OAK SPRING
	9 11:17:16	36.615	116.811	0.9	-0.76	1.8	147	BC	1.4	---	FRENCHMAN LAKE SE
	10 3:55:26	36.729	116.429	0.9	7.00	5.1	172	CC	1.4	---	BLACK HILLS NW
	15 4:23:11	37.172	116.887	0.7	2.11	1.4	216	AD	0.3	---	SPRINGDALE
	20 13:02:20	37.001	116.012	1.1	5.45*	---	136	CC	0.8	---	YUCCA FLAT
	1 0: 5:16	36.590	117.845	4.0	12.70	0.9	319	CD	0.7	---	NEW YORK BUTTE
MAR	3 15: 2:42	37.234	117.299	1.0	5.71	3.0	253	BD	1.4	---	UBEHEBE CRATER
	4 1: 8:31	35.941	116.976	2.4	6.14	2.5	264	BD	1.2	---	WINGATE WASH
	4 19:13: 3	37.280	116.509	1.0	7.79	4.0	227	BD	1.0	---	TRAIL RIDGE
	4 21:28:25	37.372	115.909	1.7	2.64	1.8	199	BD	1.3	---	GROOM MINE SW
	6 10:12:36	35.969	116.941	1.7	3.00*	---	260	CD	1.3	---	WINGATE WASH
	8 10:25:40	36.897	117.545	4.4	17.72	2.2	287	DD	1.8	---	DRY MTN
	9 15:27:17	36.472	114.897	0.8	3.35	2.3	259	BD	1.8	---	DRY LAKE
	9 16: 5:37	35.969	116.766	2.6	2.13	9.4	255	CD	0.8	---	WINGATE WASH
	9 23:50:16	36.613	117.332	0.7	9.25	1.4	153	AC	0.7	---	TIN MTN
	10 0:56:38	35.807	116.647	1.0	8.05	2.0	268	BD	1.9	---	CONFIDENCE HILLS
	10 1:29:20	36.703	116.261	0.3	2.64	2.4	118	BB	1.0	---	STRIPED HILLS
	11 4:20:30	36.726	116.248	0.4	-0.29	0.0	126	AC	1.2	---	SPECTER RANGE NW
	15 11:23:14	36.699	116.262	0.7	0.68	1.2	118	AB	0.5	---	STRIPED HILLS
	15 21: 3:41	37.221	117.509	1.0	6.58	3.1	295	BD	0.9	---	LAST CHANCE RANGE
	16 7:40:50	35.001	116.627	3.8	2.95	9.0	277	CD	1.2	---	CONFIDENCE HILLS
	17 23: 3:18	36.612	116.243	1.2	2.91	2.0	146	BC	0.2	---	SPECTER RANGE SW
	18 8: 8:45	36.943	117.653	3.1	23.49	0.0	297	CD	1.7	---	DRY MTN
	25 15:16:57	36.129	117.760	1.8	8.80	1.2	293	BD	1.6	---	HAIWEE RESERVOIR
	25 15:20:21	36.141	117.767	2.0	6.01*	---	293	CD	1.0	---	HAIWEE RESERVOIR
	25 16:32: 4	36.267	117.535	1.8	11.06	2.0	292	BD	1.3	---	DARWIN
	25 16:38:18	36.152	117.715	2.1	10.10	1.5	290	BD	1.1	---	COSO PEAK
	25 20:46:42	36.149	117.739	1.6	10.16	1.1	291	BD	1.3	---	COSO PEAK
	26 5:28: 0	36.085	117.344	2.3	2.12	6.0	268	CD	1.2	---	MATURANGO
	31 13: 0:38	36.466	115.795	1.0	17.04	3.2	245	BD	0.5	---	MT STIRLING
APR	2 3:27:36	36.756	116.672	1.1	1.03	4.5	124	BB	0.7	---	BARE MTN
	2 9:19:24	36.406	117.749	4.7	16.21	3.2	290	CD	0.9	---	DARWIN
	3 7:17: 1	37.021	118.028	4.7	3.96	3.0	325	CD	1.5	---	***REGIONAL***
	3 7:55:32	37.052	118.021	2.4	3.31	4.5	321	BD	1.0	---	***REGIONAL***
	3 9: 3: 6	37.043	118.002	14.7	1.90*	---	323	DD	1.0	---	***REGIONAL***
	4 11: 8: 5	36.158	117.737	2.1	9.69	2.0	291	BD	1.6	---	COSO PEAK
	5 7:55:47	36.429	117.063	0.6	4.21*	---	194	CD	0.6	---	EMIGRANT CANYON
	9 3:15:06	37.141	115.301	0.5	0.95	0.6	141	AC	1.2	---	DESERT HILLS NE
	9 17:47:31	35.729	117.690	2.1	11.18	1.5	300	BD	1.5	---	RIDGECREST
	10 7:40:22	37.026	118.022	3.0	3.42	4.2	321	CD	1.3	---	***REGIONAL***
	10 9:27:18	36.215	117.391	---	11.73	---	266	AD	1.3	---	MATURANGO
	11 21:38:17	37.211	116.388	0.8	4.50*	---	264	CD	1.2	---	SCRUGHAM PEAK
	15 19:43:36	37.170	117.383	1.5	6.80	6.6	275	CD	1.1	---	UBEHEBE CRATER
	15 20:51:59	37.178	117.411	3.2	2.82	9.7	269	CD	1.0	---	UBEHEBE CRATER
	16 3:23:26	37.163	117.393	1.2	5.90	2.9	265	BD	1.5	---	UBEHEBE CRATER
	16 10:30:30	37.159	117.378	1.5	11.69	4.5	275	BD	0.5	---	UBEHEBE CRATER
	16 17:13:59	37.164	117.393	0.6	6.95	3.5	265	BD	1.3	---	UBEHEBE CRATER
	16 18: 4:54	37.179	117.411	3.6	2.94*	---	260	CD	1.4	---	UBEHEBE CRATER
	16 19:24:47	37.156	117.377	2.2	5.30	3.4	258	BD	1.3	---	UBEHEBE CRATER
	18 23:54:34	36.106	117.800	1.5	5.54	1.1	290	BD	1.7	---	HAIWEE RESERVOIR
	18 23:58:14	36.434	117.241	9.2	7.00*	---	219	DD	1.1	---	EMIGRANT CANYON
	21 6: 3:24	37.182	117.415	2.9	2.71	8.7	283	CD	0.9	---	UBEHEBE CRATER

## 1979 LOCAL HYPOCENTER SUMMARY

	DATE - TIME (UTC)	LATITUDE (DEG. N)	LONGITUDE (DEG. W)	HORIZ ERROR (KM)	DEPTH (KM)	VERT ERROR (KM)	AZI GAP (DEG)	QUAL	Md	Mbiq	QUADRANGLE
APR	21 14:18:18	37.188	117.424	1.2	8.28	2.7	278	BD	1.8	---	UBEHEBE CRATER
	22 12:25:29	38.891	117.837	1.4	2.93	1.8	382	BD	1.9	---	HAIWEE RESERVOIR
	29 22:52:1	38.579	118.323	0.4	9.17	1.4	97	AB	1.0	---	LATHROP WELLS SE
MAY	1 19: 8:34	35.951	118.971	1.8	3.29	7.8	282	CD	1.4	---	WINGATE WASH
	2 8:44:28	35.789	118.545	1.5	19.51	3.8	263	BD	0.9	---	CONFIDENCE HILLS
	4 14:48: 8	38.918	117.443	1.1	7.18	2.1	288	BD	0.9	---	TIN MTN
	7 15:53: 8	38.415	117.912	0.9	3.13*	---	288	CD	0.8	---	KEELER
	7 18:28:12	38.737	118.178	0.3	4.95	2.8	148	AC	1.8	---	SPECTER RANGE NW
	9 12: 1:25	38.782	115.913	0.5	9.49	1.8	148	AC	1.2	---	FRENCHMAN FLAT
	11 3: 8:33	38.884	115.928	0.8	4.74	7.9	138	CC	1.1	---	FRENCHMAN FLAT
	15 1:20: 8	38.185	117.495	1.6	7.88*	---	287	CD	1.1	---	MATURANGO
	22 13:57:14	37.543	118.455	1.4	11.19	5.8	238	BD	1.2	---	QUARTZITE MTN
	24 8:12: 4	35.887	118.883	3.7	2.42*	---	287	CD	0.7	---	LEACH LAKE
	24 19: 5: 2	35.894	117.118	2.1	26.16	1.9	383	BD	1.3	---	WINGATE PASS
	28 17:33: 2	38.835	117.717	1.8	8.27	1.1	295	BD	1.4	---	COSO PEAK
	28 11:55:58	37.298	114.772	1.3	7.87	8.9	277	BD	1.8	---	GREGERSON BASIN
	30 13: 8:32	35.938	117.431	2.5	8.98	1.2	278	CD	2.1	---	TRONA
	30 20:23: 1	37.318	115.231	2.5	5.25*	---	148	CC	0.8	---	ALAMO
JUN	1 19: 1:28	38.814	115.895	0.5	0.79	1.5	181	AC	0.9	---	FRENCHMAN FLAT
	3 18:23:22	37.384	118.384	0.8	0.12	0.8	168	BC	0.8	---	DEAD HORSE FLAT
	5 1:21:52	35.753	118.824	1.8	7.88	1.1	388	BD	1.7	---	***REGIONAL***
	5 22:18: 4	35.257	115.439	3.3	4.56*	---	328	CD	1.1	---	***REGIONAL***
	8 4:12:33	38.849	117.818	2.7	4.31	5.1	287	CD	1.4	---	HAIWEE RESERVOIR
	8 22:41:11	37.159	114.989	2.1	3.11*	---	283	CD	1.8	---	DELAMAR 3 NW
	8 23:58:12	37.184	115.838	0.8	5.78	3.8	188	BC	1.4	---	LOWER PAHRANAGAT LAKE
	9 14:21:29	37.212	115.184	1.1	1.43	2.7	171	BC	1.8	---	LOWER PAHRANAGAT LAKE
	10 8:49: 8	37.277	115.818	1.2	5.54	5.8	155	CC	0.9	---	ALAMO SE
	11 16:11:23	37.293	118.455	0.4	-1.18*	---	93	CC	1.5	---	SILENT BUTTE
	11 17: 7:49	37.298	118.449	0.7	-8.85*	---	92	CC	1.7	---	SILENT BUTTE
	11 20:28:59	37.384	118.457	1.8	7.88*	---	189	CD	2.7	---	SILENT BUTTE
	12 19:55:28	38.775	115.583	0.9	7.88	7.9	181	CC	1.8	---	TIM SPRING
	14 7:45:34	35.789	117.987	2.5	-8.48	2.1	388	BD	1.7	---	LITTLE LAKE
	18 21:11:38	35.938	117.278	2.8	3.28*	---	288	CD	1.4	---	TRONA
	23 8:27:11	37.128	118.271	0.4	2.89	0.9	89	BB	1.4	---	BUCKBOARD MESA
	25 12:38:28	37.478	118.787	0.8	7.17	3.9	173	BC	1.2	---	TOLICHA PEAK
	27 5:38:28	37.588	118.488	0.5	5.32	7.3	175	CC	1.2	---	QUARTZITE MTN
	27 21:19:25	38.277	114.824	3.8	3.18*	---	287	CD	1.3	---	DRY LAKE
	28 1: 8: 8	38.851	115.937	0.7	8.48	1.8	57	BC	1.8	---	FRENCHMAN FLAT
	28 15:49:23	37.788	114.329	3.8	3.81*	---	318	CD	1.8	---	***REGIONAL***
	29 1:58:58	37.185	118.133	0.9	-8.87*	---	151	CC	1.9	---	RAINIER MESA
	29 2:11:48	37.281	118.183	0.4	7.88	5.8	99	BC	2.7	---	OAK SPRING
	30 12: 7:39	37.839	117.437	1.4	1.78	1.8	228	BD	1.8	---	UBEHEBE CRATER
JUL	1 21:57: 2	35.838	117.885	1.8	18.75	3.5	294	BD	1.3	---	MANLY PEAK
	4 8:59:33	37.274	117.581	1.7	11.31	7.8	255	CD	1.4	---	MAGRUDER MTN
	5 23:25:38	37.487	115.417	8.8	8.14	4.8	172	BC	0.9	---	CRESCENT RESERVOIR
	6 8:37:18	37.578	114.812	1.1	1.31	1.8	315	BD	0.3	---	CALIENTE
	6 8:38:34	37.784	115.828	0.1	1.82	0.4	148	AC	-0.5	---	WHITE RIVER NARROWS
	7 9:38:58	37.988	115.288	0.7	1.57	2.4	188	BC	0.4	---	OREANA SPRING
	7 11:37:58	37.341	115.885	0.6	4.22	2.8	185	AC	0.3	---	ALAMO SE
	9 57:25:35	38.442	115.588	2.4	2.18	7.2	283	CD	0.9	---	CHARLESTON PEAK
	10 3: 9:24	37.451	115.484	0.7	7.82	4.2	77	BC	1.1	---	CRESCENT RESERVOIR
	12 7:22:41	37.153	115.139	0.8	9.89	8.8	194	AD	1.1	---	LOWER PAHRANAGAT LAKE NW
	14 8:54:49	37.723	114.887	1.8	7.85	8.5	184	CD	0.2	---	PAHROC SPRING NE
	14 11:53:23	37.215	114.984	3.8	11.53	5.8	227	CD	0.8	---	DELAMAR 3 NW
	14 18:48:17	35.818	118.319	2.3	11.77*	---	288	CD	0.7	---	AYAWATZ PASS
	14 23: 7:19	37.154	117.418	---	7.88*	---	253	CD	1.1	---	UBEHEBE CRATER
	15 8:55:39	37.481	115.487	0.1	17.73	8.5	134	AD	0.4	---	CRESCENT RESERVOIR
	15 18:31:35	37.397	117.284	2.1	8.97	4.9	134	BC	0.7	---	STONEWALL PASS
	15 17:38:36	37.384	117.873	1.3	3.82*	---	281	CD	0.9	---	SCOTTYS JUNCTION NE
	18 21:28:28	38.955	114.988	1.8	2.18*	---	192	CD	1.8	---	WILDCAT WASH NW
	18 3:33:48	37.583	118.541	0.4	9.31	1.4	193	AD	0.5	---	MELLAN
	18 4:34:12	37.497	118.552	1.8	2.45	9.3	121	CC	0.4	---	BLACK MTN NE
	18 4:35:21	37.587	118.536	0.5	8.72	2.5	193	BC	0.8	---	MELLAN
	18 5:28:38	37.513	118.523	0.5	11.94	2.5	144	BC	0.8	---	MELLAN
	18 8:51:37	37.885	118.879	2.8	2.88	8.8	148	CC	0.8	---	MELLAN
	18 11:12:42	37.522	118.542	2.3	11.84	4.8	384	BD	0.4	---	MELLAN



# 1979 LOCAL HYPOCENTER SUMMARY

DATE - TIME (UTC)	LATITUDE (DEG. N)	LONGITUDE (DEG. W)	HORIZ ERROR (KM)	DEPTH (KM)	VERT ERROR (KM)	AZI CAP (DEG)	QUAL	Md	Mbiq	QUADRANGLE
JUL 18 13: 5: 4	37.508	116.543	0.3	1.94	2.9	107	BC	0.4	---	MELLAN
18 22:52:50	38.168	116.163	---	3.22	---	308	AD	1.6	---	TWIN SPRINGS SLOUGH
19 3:19:38	37.508	116.536	0.5	7.08	3.9	108	BC	0.8	---	MELLAN
19 3:21:12	37.509	116.835	0.3	8.72	2.2	108	BC	1.1	---	MELLAN
19 8:39:44	37.565	116.532	0.5	5.63	5.5	107	CC	0.8	---	MELLAN
19 23:28:26	37.561	115.362	1.2	14.27	3.0	111	BB	1.0	---	MT IRISH
26 10:39:35	37.379	116.731	4.1	19.65	6.6	284	CD	2.4	---	BLACK MTN NW
26 21:17:54	37.244	116.124	1.5	4.62	6.4	101	CC	---	0.1	OAK SPRING
27 5:39:47	36.523	116.855	0.9	7.55	1.7	164	AC	0.1	---	CHLORIDE CLIFF
AUG 2 18:34:39	37.306	115.108	0.7	1.43	2.5	138	BC	1.2	---	ALAMO SE
2 19:46:56	36.445	116.355	1.4	9.16	3.5	211	BD	0.7	---	ASH MEADOWS
3 12:37:45	36.940	115.139	0.2	4.87	2.7	156	BC	0.6	---	MULE DEER RIDGE NW
3 15:43:39	37.096	116.019	---	7.00**	---	189	BD	1.0	---	YUCCA FLAT
3 17:28:43	37.086	116.061	1.3	-1.28*	---	161	CC	1.1	---	YUCCA FLAT
3 22:38:35	37.110	116.019	---	7.00**	---	188	AD	1.1	---	YUCCA FLAT
4 11:48: 7	37.384	117.192	---	11.96	---	313	AD	1.3	---	STONEWALL PASS
4 17:48:22	37.572	116.467	0.6	6.91	5.8	181	CD	0.6	---	QUARTZITE MTN
6 10:13:55	37.199	116.395	0.7	5.25	1.0	184	AD	0.3	---	SCRUGHAM PEAK
6 21:55:54	36.255	114.777	2.3	0.18	1.2	262	BD	1.4	---	DRY LAKE
7 5: 1:21	37.561	117.882	---	2.32	---	233	AD	0.7	---	PIPER PEAK
8 23:21: 1	36.806	115.030	---	7.00**	---	227	AD	0.8	---	FRENCHMAN LAKE SE
9 3: 6:12	37.124	115.973	4.3	3.28*	---	271	CD	0.4	---	PAIUTE RIDGE
9 10: 1:25	37.281	114.783	3.1	3.23*	---	233	CD	0.8	---	DELMAR 3 NE
9 10:30: 6	36.702	116.267	0.6	-0.48*	---	84	CB	0.7	---	STRIPED HILLS
11 5:19: 3	37.692	114.838	---	1.26	---	165	AD	0.2	---	PAHROC SPRING NE
12 0: 0:29	37.042	116.322	---	7.00**	---	215	AD	1.0	---	BUCKBOARD MESA
12 4:14:52	37.013	115.891	0.5	5.00	1.7	218	AD	0.9	---	PAIUTE RIDGE
12 10:54:58	37.259	115.046	1.8	-0.46*	---	188	CD	1.7	---	ALAMO SE
12 11:31:20	37.251	115.014	0.9	3.21	2.4	216	BD	2.6	---	ALAMO SE
12 11:48:49	37.271	115.100	---	1.05	---	198	AD	0.9	---	ALAMO SE
12 11:50:16	37.260	115.047	1.5	1.44	3.4	188	BD	1.5	---	ALAMO SE
12 11:55:26	37.270	115.092	---	0.42	---	203	BD	0.8	---	ALAMO SE
12 12:18:46	37.250	115.034	---	7.00**	---	241	AD	0.8	---	ALAMO SE
12 12:19:49	37.258	115.054	1.4	2.57	3.4	185	BD	1.6	---	ALAMO SE
12 12:53: 2	37.246	115.037	0.8	2.35	1.6	191	AD	2.0	---	LOWER PAHRANAGAT LAKE
12 13:47:14	37.248	115.034	2.4	2.78*	---	192	CD	1.4	---	LOWER PAHRANAGAT LAKE
12 14:14:10	37.262	115.011	---	7.00**	---	248	CD	0.6	---	ALAMO SE
12 15:29:11	37.239	115.031	0.5	7.05	2.1	155	BC	1.2	---	LOWER PAHRANAGAT LAKE
12 15:46:36	37.119	115.009	4.0	1.12	6.6	265	CD	2.5	---	LOWER PAHRANAGAT LAKE SE
12 15:51: 7	37.225	115.015	1.0	5.01	3.9	200	BD	1.4	---	LOWER PAHRANAGAT LAKE
12 15:55:16	37.362	115.188	---	7.00**	---	211	DD	---	0.2	ALAMO
12 16:18: 7	37.242	115.016	1.6	5.62	4.3	198	BD	1.1	---	LOWER PAHRANAGAT LAKE
12 17:19:14	37.260	115.070	---	1.52	---	220	AD	0.9	---	ALAMO SE
12 17:50:35	36.472	116.898	0.5	6.24	3.9	81	BC	0.4	---	FURNACE CREEK
12 18: 3:52	37.375	115.188	---	7.00**	---	218	DD	0.7	---	ASH SPRINGS
12 18:18: 8	37.233	115.016	0.7	8.26	1.5	199	AD	1.2	---	LOWER PAHRANAGAT LAKE
12 18:32:17	37.235	115.025	1.1	8.05	1.9	211	BD	1.0	---	LOWER PAHRANAGAT LAKE
12 19:49:10	37.302	115.060	---	7.00**	---	213	DD	0.6	---	ALAMO SE
12 20:53:37	37.264	115.036	0.6	5.87	3.1	152	BC	1.3	---	ALAMO SE
12 22:21:43	37.244	115.016	1.4	4.82	6.6	210	CD	0.8	---	LOWER PAHRANAGAT LAKE
12 23: 7:59	37.244	115.022	1.5	6.29	3.9	197	BD	0.8	---	LOWER PAHRANAGAT LAKE
13 0: 0:13	37.236	115.024	0.9	6.49	1.8	198	AD	1.3	---	LOWER PAHRANAGAT LAKE
13 6:43:40	37.262	115.031	0.8	2.61*	---	153	CC	1.2	---	ALAMO SE
13 6:15:30	37.257	115.030	0.5	7.10	2.4	154	BC	1.9	---	ALAMO SE
13 8:30: 8	37.177	116.572	0.3	5.84	2.4	56	BC	1.6	---	THIRSTY CANYON NE
13 9: 0:59	36.376	115.179	---	10.72	---	254	CD	1.0	---	GASS PEAK NW
13 9:13:37	37.241	115.017	0.6	8.40	1.3	198	AD	1.6	---	LOWER PAHRANAGAT LAKE
13 9:50: 2	37.245	115.023	0.3	7.54	1.4	156	AC	2.1	---	LOWER PAHRANAGAT LAKE
13 10:33:19	37.253	115.023	0.4	6.05	2.5	155	BC	1.5	---	ALAMO SE
13 15: 8: 5	37.246	115.015	0.7	6.50	2.0	198	AD	1.3	---	LOWER PAHRANAGAT LAKE
13 16:38:50	37.247	115.022	1.0	7.39	2.2	197	BD	1.3	---	LOWER PAHRANAGAT LAKE
13 16:44:54	37.232	115.015	1.5	11.06	2.5	199	BD	1.3	---	LOWER PAHRANAGAT LAKE
13 17:35: 5	37.304	115.188	---	7.00**	---	227	AD	0.5	---	ALAMO
13 18:23:38	37.238	115.029	0.4	7.60	1.0	174	AC	2.7	---	LOWER PAHRANAGAT LAKE
13 18:35:10	37.220	114.999	1.4	10.37	2.3	223	BD	1.3	---	DELMAR 3 NW
13 19:21:18	37.233	115.026	0.9	4.52	3.0	212	BD	1.6	---	LOWER PAHRANAGAT LAKE

## 1979 LOCAL HYPOCENTER SUMMARY

DATE - TIME (UTC)	LATITUDE (DEG. N)	LONGITUDE (DEG. W)	HORIZ ERROR (KM)	DEPTH (KM)	VERT ERROR (KM)	AZI GAP (DEG)	QUAL	Md	Mbig	QUADRANGLE
AUG 13 20:33:34	37.189	116.555	0.4	8.75	2.4	106	BD	1.4	---	THIRSTY CANYON NE
13 20:56: 8	37.381	115.039	---	4.66	---	281	AD	1.0	---	ALAMO NE
13 22:42:19	36.888	117.485	7.7	-0.18	4.7	282	DD	1.0	---	TIN MTN
13 23:28:24	37.177	116.576	0.4	7.40	2.4	102	BC	1.5	---	THIRSTY CANYON NE
13 23:32:29	37.247	115.029	1.0	8.38	2.0	196	BD	2.0	---	LOWER PAHRANAGAT LAKE
13 23:37:45	37.184	116.578	---	7.00**	---	200	AD	0.4	---	THIRSTY CANYON NE
13 23:37:58	37.227	115.033	1.6	11.52	3.0	213	BD	1.3	---	LOWER PAHRANAGAT LAKE
14 1:19:44	37.233	115.080	3.4	13.07	2.4	195	CD	0.8	---	LOWER PAHRANAGAT LAKE
14 1:35:38	37.241	115.018	0.4	0.52*	---	157	CC	1.8	---	LOWER PAHRANAGAT LAKE
14 2:54:58	37.269	115.020	1.0	4.54	0.8	154	CC	1.0	---	ALAMO SE
14 3: 3:14	37.235	115.019	0.5	5.72	1.7	175	AC	2.8	---	LOWER PAHRANAGAT LAKE
14 3:12:48	37.175	116.572	0.3	8.65	0.9	58	AC	1.7	---	THIRSTY CANYON NE
14 3:53:21	37.178	116.573	0.3	7.28	1.4	83	AC	1.2	---	THIRSTY CANYON NE
14 4:18:27	37.083	116.381	---	7.00**	---	160	DD	0.3	---	TIMBER MTN
14 4:13:47	37.153	116.565	---	11.26	---	182	AD	0.0	---	THIRSTY CANYON NE
14 4:31:21	37.182	116.576	0.4	3.69	6.6	198	CD	0.4	---	THIRSTY CANYON NE
14 4:31:56	37.186	116.574	0.8	8.49	4.6	106	BC	0.8	---	THIRSTY CANYON NE
14 4:35:17	37.195	116.580	---	7.00**	---	200	AD	0.3	---	THIRSTY CANYON NE
14 4:51:55	37.539	114.170	9.6	11.50	2.8	209	DD	2.0	---	***REGIONAL***
14 4:55: 5	37.220	115.014	0.9	7.20	2.1	201	BD	1.3	---	LOWER PAHRANAGAT LAKE
14 5:12:42	37.176	116.578	0.3	7.99	1.5	109	AC	0.7	---	THIRSTY CANYON NE
14 5:43:34	37.230	115.039	1.8	4.24	0.4	210	CD	1.4	---	LOWER PAHRANAGAT LAKE
14 5:49: 8	37.178	116.576	0.2	7.71	1.2	109	AC	0.6	---	THIRSTY CANYON NE
14 6:22:10	37.238	115.018	0.7	5.78	2.2	198	BD	0.9	---	LOWER PAHRANAGAT LAKE
14 7:15:20	37.178	116.576	0.4	4.71	4.9	169	BC	1.3	---	THIRSTY CANYON NE
14 8:22:54	37.183	116.559	---	10.18	---	197	AD	0.5	---	THIRSTY CANYON NE
14 8:41:57	37.008	116.820	26.5	39.11*	---	184	DD	0.7	---	SPRINGDALE
14 8:53:25	37.189	116.571	0.7	7.39	4.5	100	BC	0.7	---	THIRSTY CANYON NE
14 9: 3:26	37.257	115.050	1.5	-0.12*	---	192	CD	1.0	---	ALAMO SE
14 9: 4:33	37.240	115.014	0.5	3.09*	---	158	CC	1.8	---	LOWER PAHRANAGAT LAKE
14 10:29: 3	37.182	116.572	0.6	8.39	3.3	108	BC	0.5	---	THIRSTY CANYON NE
14 11:39:52	37.180	116.571	0.3	2.89*	---	111	CC	1.7	---	THIRSTY CANYON NE
14 11:45:13	37.179	116.571	0.4	7.43	1.8	58	AC	1.2	---	THIRSTY CANYON NE
14 12:59:11	37.188	116.581	0.3	0.73	1.1	192	BD	0.4	---	THIRSTY CANYON NE
14 14:58:57	37.213	115.304	---	3.99	---	208	BD	0.8	---	DESERT HILLS NE
14 16:55:29	37.172	116.573	0.5	7.56	2.6	110	BC	1.7	---	THIRSTY CANYON NE
14 19:15:49	37.195	116.576	---	11.05	---	205	AD	1.0	---	THIRSTY CANYON NE
14 22:58: 5	37.185	116.578	1.4	0.69*	---	133	CC	1.0	---	THIRSTY CANYON NE
15 2:11:30	36.810	114.921	7.9	2.61	4.1	204	DD	2.3	---	***REGIONAL***
15 16: 3:17	37.188	116.579	0.8	5.03	7.9	106	CC	0.7	---	THIRSTY CANYON NE
15 16:47:44	37.225	114.980	---	1.03	---	248	AD	0.7	---	DELAMAR 3 NW
15 17: 1:42	37.230	115.015	0.6	5.13	2.3	200	BD	0.0	---	LOWER PAHRANAGAT LAKE
15 20: 5:28	37.244	115.022	0.4	1.86	1.0	156	AC	2.0	---	LOWER PAHRANAGAT LAKE
15 21:13: 5	37.230	115.020	0.7	8.18	1.5	199	AD	1.2	---	LOWER PAHRANAGAT LAKE
15 21:50:33	37.233	115.016	1.4	2.97*	---	221	CD	1.1	---	LOWER PAHRANAGAT LAKE
16 1: 8:49	37.233	115.018	1.2	0.24	3.1	214	BD	1.1	---	LOWER PAHRANAGAT LAKE
16 2:41:15	37.178	116.570	0.4	8.64	1.5	58	AC	1.9	---	THIRSTY CANYON NE
16 2:47:25	37.179	116.576	0.3	6.68	1.8	108	AC	0.9	---	THIRSTY CANYON NE
16 3: 3:21	37.182	116.569	0.5	7.38	2.0	138	AC	1.3	---	THIRSTY CANYON NE
16 3: 4:39	37.250	115.013	0.6	7.39	1.4	197	AD	1.3	---	ALAMO SE
16 3:37:46	37.244	115.041	0.6	2.74	4.6	207	BD	2.3	---	LOWER PAHRANAGAT LAKE
16 4: 5: 2	37.234	115.024	1.5	7.11	2.6	220	BD	1.4	---	LOWER PAHRANAGAT LAKE
16 5:26: 8	37.232	115.022	0.6	4.39	2.6	235	BD	1.0	---	LOWER PAHRANAGAT LAKE
16 5:31:52	37.241	114.990	2.9	0.34*	---	217	CD	0.7	---	DELAMAR 3 NW
16 5:57:40	37.195	116.581	1.5	13.32	2.6	206	BD	0.4	---	THIRSTY CANYON NE
16 10:57:28	37.233	115.015	0.8	6.49	2.2	199	BD	1.3	---	LOWER PAHRANAGAT LAKE
16 12:52:59	37.192	116.552	1.3	11.33	3.1	206	BD	0.8	---	THIRSTY CANYON NE
16 13:20:51	37.239	115.017	0.9	8.83	2.4	198	BD	1.4	---	LOWER PAHRANAGAT LAKE
16 15:49:57	37.258	115.029	0.5	5.94	2.3	154	BC	2.3	---	ALAMO SE
16 16: 2: 9	37.240	115.025	1.5	2.63*	---	232	CD	1.1	---	LOWER PAHRANAGAT LAKE
16 19:10: 4	37.247	115.022	0.7	4.70	3.1	197	BD	1.0	---	LOWER PAHRANAGAT LAKE
16 23:47:12	37.072	116.222	---	17.65	---	209	AD	1.4	---	TIPPICAH SPRING
16 23:47:19	37.143	116.442	---	7.00**	---	272	AD	---	0.2	SCRUGHAM PEAK
17 0: 1: 7	37.250	115.024	0.5	2.16	0.9	196	AD	1.1	---	ALAMO SE
17 0:39:13	37.187	116.568	0.5	6.20	4.0	106	BC	1.0	---	THIRSTY CANYON NE
17 1:32:34	37.240	115.007	---	7.07	---	236	AD	0.9	---	LOWER PAHRANAGAT LAKE

## 1979 LOCAL HYPOCENTER SUMMARY

DATE - TIME (UTC)	LATITUDE (DEG. N)	LONGITUDE (DEG. W)	HORIZ ERROR (KM)	DEPTH (KM)	VERT ERROR (KM)	AZI CAP (DEG)	QUAL	Md	Mbiq	QUADRANGLE
AUG 17 1:37:23	37.250	115.029	0.6	5.34	2.1	195	BD	1.1	---	ALAMO SE
17 2:37:30	37.184	116.570	0.3	8.05	1.4	57	AC	1.5	---	THIRSTY CANYON NE
17 2:39:45	37.183	116.581	---	7.00*	---	200	AD	0.6	---	THIRSTY CANYON NE
17 2:39:48	37.188	116.571	0.6	5.15	5.6	106	CC	1.3	---	THIRSTY CANYON NE
17 4:11: 8	37.180	116.573	0.4	4.91	4.3	108	BC	1.5	---	THIRSTY CANYON NE
17 4:31:29	37.181	116.577	0.3	2.83*	---	88	CC	1.4	---	THIRSTY CANYON NE
17 8: 1:34	37.172	116.575	0.3	7.31	2.0	111	AC	0.5	---	THIRSTY CANYON NE
17 8:58:57	37.186	116.569	0.5	2.92*	---	106	CC	1.2	---	THIRSTY CANYON NE
17 10:28:43	37.194	116.574	0.6	6.92	2.4	104	BC	0.8	---	THIRSTY CANYON NE
17 13:41:33	37.181	116.572	0.8	8.10	3.9	108	BC	0.4	---	THIRSTY CANYON NE
17 14:53: 7	37.185	116.570	0.3	6.20	2.2	57	BC	1.9	---	THIRSTY CANYON NE
17 16:10:29	37.230	115.021	1.9	4.74	3.7	220	BD	1.1	---	LOWER PAHRANAGAT LAKE
17 22:36:50	37.230	115.020	1.3	7.91	1.9	221	BD	1.0	---	LOWER PAHRANAGAT LAKE
18 2:22:23	37.260	115.066	---	7.00*	---	221	AD	0.7	---	ALAMO SE
18 2:40: 9	37.238	115.011	0.8	5.37	2.9	199	BD	1.3	---	LOWER PAHRANAGAT LAKE
18 4:48:14	37.246	115.009	0.9	5.26	2.2	221	BD	1.3	---	LOWER PAHRANAGAT LAKE
19 20:56:10	37.180	116.572	0.2	7.03	1.2	108	AC	0.8	---	THIRSTY CANYON NE
19 21:21:21	37.182	116.568	0.4	5.52	4.7	57	BC	1.4	---	THIRSTY CANYON NE
19 22:14:58	37.324	114.875	0.8	7.35	2.7	217	BD	1.4	---	DELAMAR LAKE
20 10:37: 9	37.183	116.570	0.6	4.91	6.8	107	CC	1.1	---	THIRSTY CANYON NE
20 11:28:35	37.078	116.019	5.7	3.63*	---	191	DD	0.8	---	YUCCA FLAT
20 12:17:56	37.053	117.443	0.5	2.82*	---	145	CC	0.9	---	UBEHEBE CRATER
20 14:33:46	37.178	116.572	0.6	7.01	3.9	109	BC	0.9	---	THIRSTY CANYON NE
20 15:21:42	37.186	116.572	0.5	7.66	3.0	65	BC	1.1	---	THIRSTY CANYON NE
20 15:29:35	37.234	115.015	1.3	8.56	1.7	221	BD	1.1	---	LOWER PAHRANAGAT LAKE
20 15:51:11	37.179	116.571	0.3	4.76	4.4	56	BC	1.3	---	THIRSTY CANYON NE
20 23:55: 9	37.246	115.014	1.1	6.91	1.2	221	BD	1.2	---	LOWER PAHRANAGAT LAKE
22 14:20:37	37.044	116.200	0.5	7.00	1.0	83	AA	1.0	---	TIPPIPAH SPRING
25 8:54:53	37.040	116.209	0.5	7.00	0.9	73	AA	2.2	---	TIPPIPAH SPRING
25 23:33:43	37.047	116.205	0.7	7.00	1.2	90	AA	0.6	---	TIPPIPAH SPRING
26 1:22:50	37.051	116.197	0.3	6.74	0.5	93	AB	0.7	---	TIPPIPAH SPRING
27 5:17:31	37.217	115.018	0.8	7.66	1.7	201	AD	1.3	---	LOWER PAHRANAGAT LAKE
27 23:52: 3	37.235	114.992	9.9	10.96*	---	202	DD	1.0	---	DELAMAR 3 NW
28 21:17: 6	36.386	114.970	---	7.00*	---	342	CD	1.2	---	DRY LAKE
29 4:17:52	37.678	115.236	0.9	7.00	1.4	126	AB	1.4	---	FOSSIL PEAK
29 7:45:57	37.143	116.733	---	0.25	---	229	BD	0.1	---	THIRSTY CANYON NW
29 10:45:11	37.164	116.728	0.6	0.25*	---	66	CC	1.1	---	THIRSTY CANYON NW
29 14:18: 9	37.149	116.244	---	7.00*	---	210	AD	1.2	---	RAINIER MESA
29 15:45:45	37.116	116.053	1.7	3.02*	---	135	CB	1.5	---	YUCCA FLAT
31 2:55:51	37.160	116.754	0.8	6.13	3.0	131	BB	0.7	---	SPRINGDALE
31 12:57:24	37.251	115.024	0.3	4.75	2.4	155	BC	1.2	---	ALAMO SE
31 13: 3: 2	37.242	115.013	1.0	6.34	1.7	221	AD	0.9	---	LOWER PAHRANAGAT LAKE
SEP 31 23:45: 5	37.177	115.784	0.8	10.51	1.8	218	AD	0.8	---	PAPOOSE LAKE NE
3 4:36:40	37.214	114.999	1.5	3.17*	---	203	CD	1.0	---	DELAMAR 3 NW
3 18:19:16	37.174	115.771	1.4	5.32*	---	184	CD	0.8	---	PAPOOSE LAKE NE
4 11: 3:48	36.900	115.987	---	6.80	---	150	AD	0.6	---	PLUTONIUM VALLEY
4 13:57:54	36.906	115.976	0.4	6.19	1.3	154	AC	0.7	---	PLUTONIUM VALLEY
5 6:16:42	37.230	115.009	1.2	7.90	2.7	200	BD	1.3	---	LOWER PAHRANAGAT LAKE
6 15:30: 7	37.087	116.045	0.8	0.80*	---	113	CC	1.6	---	YUCCA FLAT
10 12:29:32	37.261	115.050	1.2	7.39	3.0	186	BD	1.4	---	ALAMO SE
10 21: 4:58	37.049	116.203	1.0	6.31	1.5	90	AB	0.6	---	TIPPIPAH SPRING
11 7:47:36	36.856	116.205	2.3	0.72	0.4	258	BD	0.6	---	SKULL MTN
13 12: 6:10	37.047	116.214	0.7	7.00	1.0	102	AB	1.1	---	TIPPIPAH SPRING
13 17: 2:14	37.351	114.906	3.3	10.58	6.7	203	CD	0.7	---	DELAMAR LAKE
16 14: 5:45	37.083	116.651	14.0	7.00*	---	154	DD	1.0	---	THIRSTY CANYON SW
18 3:35: 2	37.070	117.020	---	6.47	---	134	AD	0.3	---	BONNIE CLAIRE SE
20 15:35:10	37.209	116.880	---	7.00*	---	307	AD	0.4	---	SPRINGDALE
22 2:38:54	37.176	117.386	0.3	11.00	0.9	117	AB	1.2	---	UBEHEBE CRATER
23 3:19:38	36.351	117.068	8.5	7.00	4.1	173	DC	1.0	---	EMIGRANT CANYON
24 2: 5:23	36.351	117.068	14.6	7.00*	---	173	DD	0.7	---	EMIGRANT CANYON
25 10:13:10	37.107	116.019	---	5.69	---	188	AD	0.7	---	YUCCA FLAT
25 15:22:16	37.058	117.477	0.6	5.85	3.3	155	BC	0.8	---	UBEHEBE CRATER
26 3:49:36	37.404	117.935	0.6	5.14	3.1	240	BD	1.2	---	SOLDIER PASS
26 19:15:57	37.238	116.337	0.9	11.29	2.5	103	BC	1.3	---	AMMONIA TANKS
27 8:35:29	36.860	117.384	6.5	0.24*	---	296	DD	2.0	---	TIN MTN
28 3:13:32	36.823	117.534	0.7	6.79	1.5	206	AD	1.2	---	DRY MTN

## 1979 LOCAL HYPOCENTER SUMMARY

	DATE - TIME (UTC)	LATITUDE (DEG. N)	LONGITUDE (DEG. W)	HORIZ ERROR (KM)	DEPTH (KM)	VERT ERROR (KM)	AZI CAP (DEG)	QUAL	Md	Mb1g	QUADRANGLE
SEP	28 17:23:58	37.229	118.345	0.7	8.93	0.4	89	AA	1.1	---	AMMONIA TANKS
	28 20:38:17	38.735	118.220	1.0	4.07*	---	84	CC	0.7	---	SPECTER RANGE NW
	29 9:25:52	37.293	118.338	0.8	3.11*	---	119	CC	1.0	---	DEAD HORSE FLAT
OCT	1 14:34:53	37.144	115.641	0.6	4.95*	---	111	CC	0.7	---	FALLOUT HILLS NW
	2 4:59:41	37.198	118.392	0.5	8.39	1.4	98	AB	0.6	---	SCRUGHAM PEAK
	2 5:42:18	37.198	118.389	0.4	7.43	1.0	98	AB	0.7	---	SCRUGHAM PEAK
	2 14:3:53	38.488	117.903	2.1	2.92	0.2	274	CD	1.3	---	KEELER
	2 17:51:38	38.389	115.842	0.5	11.73	2.4	150	BC	0.8	---	MT STIRLING
	2 20:43:14	37.197	118.394	0.6	0.29	1.3	98	AB	1.0	---	SCRUGHAM PEAK
	3 2:21:00	37.288	118.288	5.0	4.40	2.7	285	DD	1.4	---	DEAD HORSE FLAT
	4 2:22:1	37.222	118.347	0.6	0.48	0.5	67	BA	1.5	---	AMMONIA TANKS
	4 3:31:20	38.368	115.830	0.2	1.47	0.8	152	AC	0.8	---	MT STIRLING
	4 9:38:4	37.229	118.343	0.8	8.12	0.5	76	AA	1.0	---	AMMONIA TANKS
	5 9:52:27	38.874	118.182	0.5	7.00	0.7	75	AA	0.6	---	SKULL MTN
	7 2:39:2	37.078	115.288	2.4	0.60	0.4	193	CD	0.7	---	DESERT HILLS SE
	7 19:54:24	37.255	115.447	0.8	2.79*	---	100	CC	0.8	---	CUTLER RESERVOIR
	9 9:48:30	38.919	118.020	1.3	9.57	1.4	188	BD	0.3	---	YUCCA LAKE
	9 17:32:42	37.145	118.757	0.4	7.00	0.6	45	CC	1.2	---	SPRINGDALE
	10 17:8:2	37.813	115.876	1.0	2.91*	---	135	CC	0.6	---	PAIUTE RIDGE
	10 21:22:9	37.251	115.825	1.9	4.53	3.2	227	BD	1.3	---	ALAMO SE
	11 17:29:17	37.251	115.852	0.8	4.49	2.3	186	BD	1.6	---	ALAMO SE
	13 8:11:54	37.208	115.803	1.0	11.84	1.3	227	BD	0.8	---	LOWER PAHRANAGAT LAKE
	14 8:20:12	37.078	118.064	0.4	9.53*	---	135	CC	0.6	---	YUCCA FLAT
	15 8:3:31	37.075	118.038	0.6	5.48	3.3	146	BC	0.6	---	YUCCA FLAT
	15 10:41:12	37.874	118.040	1.0	4.94	3.8	177	BC	0.6	---	YUCCA FLAT
	15 14:33:3	37.151	115.128	1.9	5.10	2.4	214	BD	1.2	---	LOWER PAHRANAGAT LAKE NW
	16 10:47:9	38.908	118.168	0.4	7.41	0.5	119	AB	0.8	---	MINE MTN
	16 21:8:54	37.844	115.812	0.7	4.43	4.0	185	BD	0.8	---	***QUAD. NOT LISTED***
	17 1:9:15	37.730	118.305	0.6	2.83*	---	168	CC	---	0.2	QUARTZITE MTN
	17 15:25:51	38.740	115.873	0.5	-0.84	0.6	120	AB	0.6	---	MERCURY NE
	17 15:55:45	38.739	115.862	0.9	2.18	2.2	129	BB	0.5	---	MERCURY NE
	21 1:14:10	37.905	115.688	0.7	14.77	3.2	143	BC	0.9	---	FALLOUT HILLS SW
	24 17:13:8	37.244	115.037	---	2.05	---	329	AD	1.0	---	LOWER PAHRANAGAT LAKE
	24 20:47:36	37.905	115.191	0.3	4.51	0.8	207	AD	1.4	---	OREANA SPRING
	25 22:17:59	38.508	115.157	---	7.00**	---	136	BD	0.8	---	HAYFORD PEAK
	27 17:13:5	37.258	115.074	0.8	8.17	10.0	210	CD	0.8	---	ALAMO SE
NOV	2 19:51:11	37.241	115.045	1.0	5.83	3.2	188	BD	1.7	---	LOWER PAHRANAGAT LAKE
	3 18:48:45	37.152	117.403	0.8	7.18	1.8	186	AD	2.0	---	UBEHEBE CRATER
	3 17:44:7	37.124	117.398	4.5	14.84	5.5	267	CD	1.8	---	UBEHEBE CRATER
	4 1:8:59	37.145	117.401	0.7	5.48	3.3	207	BD	1.7	---	UBEHEBE CRATER
	4 8:53:52	37.154	117.405	0.7	1.94	1.4	205	AD	1.1	---	UBEHEBE CRATER
	4 20:27:53	37.180	117.405	0.6	5.89	3.5	184	BD	1.3	---	UBEHEBE CRATER
	4 22:18:15	37.144	117.403	0.3	7.88	1.0	189	AD	1.6	---	UBEHEBE CRATER
	5 13:4:33	37.152	117.401	0.5	5.84	3.3	186	BD	1.7	---	UBEHEBE CRATER
	5 13:18:18	37.188	117.403	0.7	5.54	3.7	182	BD	1.3	---	UBEHEBE CRATER
	5 22:50:44	37.239	115.828	1.8	4.32	8.4	231	CD	0.9	---	LOWER PAHRANAGAT LAKE
	6 1:22:59	37.290	118.393	0.4	8.59	1.5	85	AB	1.1	---	SILENT BUTTE
	6 9:21:42	37.288	118.923	1.7	8.54	4.2	274	BD	0.1	---	TOLICHA PEAK
	6 9:27:49	37.223	118.955	0.6	8.23	3.1	148	BC	---	0.2	SPRINGDALE
	7 3:35:2	37.588	118.483	0.2	8.97	1.8	131	AC	1.2	---	QUARTZITE MTN
	8 15:42:13	37.488	115.383	0.7	2.25*	---	81	CC	1.6	---	CRESCENT RESERVOIR
	8 19:10:5	38.844	118.341	---	1.02	---	231	AD	0.5	---	JACKASS FLATS
	9 8:5:58	38.835	118.330	0.3	3.84	0.5	100	AB	0.6	---	STRIPED HILLS
	9 3:2:37	38.488	117.818	1.8	11.78	1.6	250	BD	0.9	---	KEELER
	9 11:35:58	38.690	117.210	0.3	7.68	0.7	73	AB	1.2	---	STOVEPIPE WELLS
	9 23:13:4	38.691	117.234	0.8	10.81	1.4	88	AA	0.4	---	STOVEPIPE WELLS
	10 9:52:9	38.772	118.088	0.5	7.95	1.8	100	AB	0.5	---	CANE SPRING
	10 1:38:59	38.689	117.208	0.8	5.89	1.5	74	AB	1.0	---	STOVEPIPE WELLS
	10 15:43:31	37.823	118.159	1.6	4.17	5.0	188	CD	0.5	---	TIPPINAH SPRING
	14 23:24:18	37.679	118.268	0.9	5.96*	---	168	CD	0.9	---	QUARTZITE MTN
	15 22:51:34	37.484	118.368	---	7.00**	---	193	AD	---	0.2	SILENT CANYON NE
	18 4:38:18	38.894	117.207	0.5	7.81	1.1	72	AB	1.7	---	STOVEPIPE WELLS
	18 18:22:44	38.891	117.204	0.3	7.48	0.7	73	AB	2.1	---	STOVEPIPE WELLS
	18 18:48:21	38.889	117.213	0.2	7.87	0.5	73	AA	0.9	---	STOVEPIPE WELLS
	20 2:13:54	37.217	115.028	0.8	8.27	1.8	280	AD	1.8	---	LOWER PAHRANAGAT LAKE
	20 3:8:49	37.214	118.038	1.3	1.97	1.5	125	BD	1.3	---	OAK SPRING

## 1979 LOCAL HYPOCENTER SUMMARY

	DATE - TIME (UTC)	LATITUDE (DEG. N)	LONGITUDE (DEG. W)	HORIZ ERROR (KM)	DEPTH (KM)	VERT ERROR (KM)	AZI GAP (DEG)	QUAL	Md	Mblg	QUADRANGLE
NOV	20 3:38:16	37.234	115.071	1.8	9.48	2.1	199	BD	0.9	---	LOWER PAHRANAGAT LAKE
	20 6:43:19	37.237	115.058	0.7	10.48	1.0	202	AD	0.9	---	LOWER PAHRANAGAT LAKE
	20 10:28:21	37.244	115.068	---	10.72	---	188	AD	0.9	---	LOWER PAHRANAGAT LAKE
	20 10:42:20	37.214	115.097	2.8	3.93*	---	224	CD	0.9	---	LOWER PAHRANAGAT LAKE
	20 11:14:57	37.340	116.122	0.5	3.88*	---	164	CD	0.6	---	OAK SPRING BUTTE
	20 16:35:23	37.106	115.265	---	0.51	---	182	AD	0.9	---	DESERT HILLS SE
	21 3: 6:49	36.690	117.223	0.4	6.72	1.0	99	AB	0.9	---	STOVEPIPE WELLS
	22 18:45: 5	36.655	115.939	0.6	2.93*	---	142	CC	0.6	---	MERCURY
	25 0: 2:17	37.341	114.943	0.3	0.39*	---	197	CD	0.3	---	DELMAR LAKE
	27 11:41:58	36.802	115.444	1.6	7.06*	---	206	CD	0.7	---	DOG BONE LAKE SOUTH
	28 16:24:18	37.837	116.427	5.1	2.25*	---	257	DD	1.0	---	KAWICH PEAK
	29 2:41:24	37.065	116.227	1.0	8.19	0.8	219	BD	0.4	---	TIPPIPAH SPRING
	29 16:37: 4	36.985	116.003	0.6	5.83	4.6	147	BC	2.5	---	YUCCA LAKE
	30 2: 8:50	37.285	115.019	1.6	10.88	1.6	204	BD	0.9	---	ALAMO SE
	30 14: 0:37	37.501	116.533	0.5	11.40	1.2	106	AC	1.5	---	MELLAN
DEC	1 8:47:35	37.232	115.021	3.3	5.29	7.2	237	CD	0.9	---	LOWER PAHRANAGAT LAKE
	2 1: 6: 3	36.709	116.268	0.7	1.11	2.8	129	BB	0.3	---	STRIPED HILLS
	2 8:47:36	37.267	114.979	2.9	11.84	3.2	211	CD	1.1	---	DELMAR LAKE
	3 13:31:50	37.624	116.677	3.2	12.19	5.0	127	CB	0.9	---	MELLAN
	9 8:28: 4	37.431	117.015	0.7	0.46*	---	195	CD	0.6	---	SCOTTYS JUNCTION NE
	11 12:26:31	37.501	116.534	0.4	6.05	4.0	106	BC	1.6	---	MELLAN
	13 14:38: 0	38.023	116.638	11.0	4.16	8.1	241	DD	1.0	---	CHERRY CREEK SUMMIT
	14 11:45: 9	36.632	116.237	1.6	6.32	5.8	71	CB	0.4	---	SPECTER RANGE NW
	17 8:48:34	37.174	116.467	0.4	10.93	1.1	109	AB	0.3	---	SCRUGHAM PEAK
	17 12:53:35	37.451	117.022	0.5	10.82	3.5	140	BC	0.5	---	SCOTTYS JUNCTION NE
	19 14:59: 5	37.506	116.532	0.7	2.91*	---	107	CC	1.0	---	MELLAN
	21 19:13:49	36.124	117.471	12.7	2.08*	---	256	DD	0.9	---	MATURANGO
	22 2:29:12	36.516	116.339	---	-0.87	---	201	AD	0.4	---	LATHROP WELLS SE
	22 9:53:56	37.206	115.015	2.1	11.38	2.3	226	BD	1.0	---	LOWER PAHRANAGAT LAKE
	23 12:41:54	37.509	116.543	0.3	11.31	1.3	127	AC	0.9	---	MELLAN
	23 16:34:53	37.048	116.195	1.6	4.57	2.0	154	BC	0.3	---	TIPPIPAH SPRING
	24 14:54:52	36.678	115.507	7.7	17.73	6.8	152	DC	1.0	---	HEAVENS WELL
	25 14:17:12	37.288	117.062	0.3	8.00	0.8	67	AC	2.8	---	SCOTTYS JUNCTION
	25 14:24:11	37.270	117.066	0.7	5.09	2.6	92	BC	1.9	---	SCOTTYS JUNCTION
	25 14:27:41	37.280	117.054	0.2	2.04*	---	102	CC	0.8	---	SCOTTYS JUNCTION
	25 14:29:33	37.281	117.057	1.0	7.00*	---	67	CC	1.1	---	SCOTTYS JUNCTION
	25 15:19:18	37.281	117.059	0.3	7.00	4.3	89	BC	0.9	---	SCOTTYS JUNCTION
	25 15:24:11	37.275	117.064	0.5	5.57	6.4	88	CC	1.1	---	SCOTTYS JUNCTION
	25 16:15: 2	37.278	117.061	0.5	2.92	4.6	175	BC	0.9	---	SCOTTYS JUNCTION
	25 17:36:59	37.273	117.068	0.2	10.38	1.3	173	AC	0.6	---	SCOTTYS JUNCTION
	25 23:36:21	37.280	117.055	0.3	8.37	4.3	67	BC	0.9	---	SCOTTYS JUNCTION
	26 2:13:45	37.236	115.021	0.4	5.06	2.1	157	BC	1.7	---	LOWER PAHRANAGAT LAKE
	26 6:25:59	37.243	115.016	1.5	-0.10	1.6	108	BD	1.2	---	LOWER PAHRANAGAT LAKE
	26 14: 7:10	37.281	117.053	0.3	2.60*	---	75	CC	0.7	---	SCOTTYS JUNCTION

## 1980 LOCAL HYPOCENTER SUMMARY

	DATE - TIME (UTC)	LATITUDE (DEG. N)	LONGITUDE (DEG. W)	HORIZ ERROR (KM)	DEPTH (KM)	VERT ERROR (KM)	AZI CAP (DEG)	QUAL	Md	Mb1g	QUADRANGLE
JAN	6 4:22:19	36.533	116.384	0.8	2.84*	---	166	CC	0.7	---	LATHROP WELLS SW
	8 15:11:59	37.292	117.021	0.4	8.31	0.5	100	AB	1.3	---	MAGRUDER MTN
	8 16: 6: 8	37.297	117.024	0.8	7.00	1.7	103	AB	1.1	---	MAGRUDER MTN
	8 16:37:58	36.762	115.849	0.8	-0.80	1.4	144	AC	0.8	---	FRENCHMAN LAKE SE
	8 18:51: 2	36.749	115.849	1.6	4.18	4.7	146	BC	0.7	---	MERCURY NE
	9 4:34:22	37.206	116.340	0.7	0.23	0.4	140	AC	0.6	---	AMMONIA TANKS
	9 19: 8:20	37.159	117.397	0.4	5.98	2.9	113	BC	0.8	---	UBEHEBE CRATER
	11 11:36:23	36.668	116.237	4.4	0.46	4.2	309	CD	0.4	---	SPECTER RANGE NW
	11 21:48:31	37.577	114.279	15.7	0.24*	---	298	DD	1.1	---	***REGIONAL***
	11 23:21:44	36.815	116.268	2.7	7.00	3.5	185	CD	---	0.1	JACKASS FLATS
	12 11:40:00	36.815	116.258	0.5	0.77	1.0	186	AB	0.9	---	JACKASS FLATS
	12 19:13:26	36.819	116.265	1.0	4.14	3.8	189	BB	0.8	---	JACKASS FLATS
	13 4:40:00	36.819	116.265	0.3	0.47	0.7	189	AB	0.4	---	JACKASS FLATS
	13 4:44:44	36.816	116.278	0.3	2.32	0.5	174	AC	---	0.2	JACKASS FLATS
	13 7:14:23	36.814	116.257	1.5	4.78	2.5	165	BC	0.6	---	JACKASS FLATS
	13 7:48:50	37.098	117.354	3.9	7.00	5.7	300	CD	---	0.1	UBEHEBE CRATER
	14 2: 4:33	37.240	115.457	0.3	13.81	2.3	99	BB	0.8	---	DESERT HILLS NW
	15 8:49:53	37.289	117.069	0.3	7.00	4.4	89	BC	1.2	---	SCOTTYS JUNCTION
	15 12:21:21	37.061	116.050	0.6	-0.19*	---	113	CC	0.6	---	YUCCA FLAT
	15 14:21:11	37.533	116.371	0.3	0.13*	---	123	CC	0.5	---	QUARTZITE MTN
	15 20:28:21	36.183	117.054	3.3	5.06	2.5	251	CD	2.6	---	COSO PEAK
	16 17:58:42	37.280	117.062	0.2	-0.66	0.3	142	AC	0.9	---	SCOTTYS JUNCTION
	20 19: 4:53	36.874	116.180	---	7.00**	---	215	AD	---	0.2	SKULL MTN
	21 20:48:46	37.267	115.188	---	7.00**	---	208	AD	0.4	---	ALAMO
	23 23:50:24	37.207	115.477	0.5	-0.87	2.0	107	AC	1.4	---	DESERT HILLS NW
	24 0:34: 1	37.196	115.465	0.5	5.01	0.1	117	CC	0.7	---	DESERT HILLS NW
	24 8:59:40	37.070	115.529	2.2	24.87	1.4	253	BD	0.7	---	SOUTHEASTERN MINE
	25 11:40:11	36.810	116.305	1.0	10.55	1.3	187	BD	---	0.2	LATHROP WELLS SE
	26 3: 7:11	36.721	116.234	0.5	5.18	1.1	65	AA	0.8	---	SPECTER RANGE NW
	26 3:27:53	36.533	116.363	0.6	-1.16*	---	104	CC	0.7	---	LATHROP WELLS SE
	28 17:22:21	37.223	117.858	2.7	13.65	3.7	210	CD	0.8	---	WAUCOBA SPRING
	28 18: 4: 1	36.740	116.271	0.3	1.47	0.3	115	AB	0.9	---	STRIPED HILLS
	30 0:33: 5	37.165	117.407	0.9	10.50	3.7	127	BD	0.4	---	UBEHEBE CRATER
	30 9: 2:29	36.820	115.880	0.7	15.57	1.2	313	AD	0.3	---	FRENCHMAN FLAT
	30 11:31: 8	36.593	115.305	0.7	0.20*	---	144	CC	1.3	---	BLACK HILLS
	30 14:28:33	36.629	116.280	0.5	7.50	0.8	209	AD	0.5	---	STRIPED HILLS
	31 14:28:48	37.281	117.649	0.4	5.09	0.8	128	AB	1.4	---	MAGRUDER MTN
FEB	1 15:47:49	37.578	117.895	0.2	4.17	1.4	205	AD	0.4	---	PIPER PEAK
	2 4:49:36	37.161	117.400	0.7	11.03	1.8	187	AD	0.7	---	UBEHEBE CRATER
	2 7:37: 9	36.820	116.213	3.0	9.92	4.2	183	CD	0.2	---	SKULL MTN
	4 5:58:34	36.619	116.257	0.8	4.60	0.3	275	AD	0.5	---	LATHROP WELLS SE
	4 14: 5:55	37.190	115.469	0.8	6.37	7.1	113	CC	1.0	---	DESERT HILLS NW
	4 16:21:19	36.629	116.326	0.4	2.99	0.7	126	AB	1.3	---	STRIPED HILLS
	5 4:36:15	37.089	116.201	---	3.98	---	120	AD	0.3	---	TIPPICAN SPRING
	5 5:58:16	37.203	116.574	0.6	11.02*	---	209	DD	---	0.2	THIRSTY CANYON NE
	6 8:49:16	37.203	116.605	---	19.43	---	261	AD	0.1	---	THIRSTY CANYON NE
	6 9: 8:55	36.620	116.326	0.4	2.62	0.7	127	AB	0.9	---	STRIPED HILLS
	6 11:49:15	36.624	116.317	0.6	2.44	0.8	182	AD	0.5	---	LATHROP WELLS SE
	17 2:42:24	37.160	116.056	0.9	13.14	1.4	169	AC	0.3	---	OAK SPRING
	19 23:42:50	37.273	117.285	1.7	6.30	2.7	152	BD	0.6	---	GOLD POINT
	20 1:41:33	37.728	115.066	0.8	15.77	1.3	116	AB	0.4	---	HIKO NE
	20 2:52:52	37.279	117.278	1.0	7.00	1.6	84	BA	0.4	---	GOLD POINT
	21 4:44:18	36.957	117.809	0.4	11.88	0.5	259	AD	1.0	---	WAUCOBA WASH
	21 4:51:00	36.964	117.746	2.1	-1.08	2.7	214	BD	0.8	---	DRY MTN
	22 3:37:52	37.372	115.038	0.8	4.37	0.3	118	CC	0.9	---	GROOM LAKE
	24 5:56:24	36.425	116.337	2.8	4.33	7.3	211	CD	---	0.2	ASH MEADOWS
	24 10:23:58	37.026	117.497	1.5	18.82	2.9	188	BD	---	0.2	UBEHEBE CRATER
	24 20:36:57	37.253	117.600	0.9	7.51	1.6	139	AD	0.1	---	MAGRUDER MTN
MAR	26 4: 5:27	37.180	117.172	0.2	9.99	0.8	143	AD	0.8	---	BONNIE CLAIRE NW
	28 12:27:19	36.786	117.460	0.8	7.57	0.9	208	AD	0.8	---	TIN MTN
	28 19: 3:48	37.185	117.193	0.3	8.36	1.0	94	AB	1.3	---	BONNIE CLAIRE NW
	1 7:36:13	37.258	115.617	0.9	3.05*	---	92	CC	0.6	---	GROOM RANGE SE
	3 3:18:51	37.517	117.717	0.9	3.13*	---	132	CC	0.3	---	LIDA WASH
	3 16:59:55	37.515	116.530	0.9	8.41	5.5	143	CC	1.0	---	MELLAN
	6 7:45:27	35.629	117.173	3.2	9.38	0.9	292	CD	---	0.2	WINGATE PASS
	7 16:50: 7	37.336	117.302	0.2	9.99	0.4	192	AD	0.0	---	GOLD POINT

## 1980 LOCAL HYPOCENTER SUMMARY

	DATE - TIME (UTC)	LATITUDE (DEG. N)	LONGITUDE (DEG. W)	HORIZ ERROR (KM)	DEPTH (KM)	VERT ERROR (KM)	AZI CAP (DEG)	QUAL	Md	Mbiq	QUADRANGLE
MAR	7 18:12:11	37.759	115.795	0.1	-0.71	3.8	121	BC	1.1	---	***QUAD. NOT LISTED***
	8 18: 4:15	37.511	115.342	0.5	10.04	2.0	129	BD	---	0.2	MT IRISH
	12 10:28:48	37.242	117.149	1.0	11.09	1.1	176	BC	-0.1	---	BONNIE CLAIRE NW
	14 1:34:21	36.544	116.392	1.5	6.13	---	115	CC	0.7	---	LATHROP WELLS SW
	14 11:12:39	37.204	116.664	0.4	23.39	1.8	105	AB	1.0	---	THIRSTY CANYON NW
	14 20:52:52	36.612	116.264	1.3	7.00	2.3	157	BC	0.4	---	LATHROP WELLS SE
	15 3:39:48	37.517	117.743	1.3	16.42	3.1	124	BB	---	0.2	LIDA WASH
	15 4:46:25	36.816	115.999	0.5	1.77	1.7	118	BC	2.1	---	FRENCHMAN FLAT
	17 19:17:16	36.364	116.573	0.7	5.01	4.3	112	BB	0.7	---	RYAN
	18 12:56:47	37.874	117.103	1.8	7.00	---	313	CD	1.1	---	MUD LAKE
	19 4:24:53	37.307	117.615	0.5	-0.03	0.9	108	AB	0.4	---	MAGRUDER MTN
	22 3: 5:54	37.286	117.546	0.5	1.51	1.3	209	AD	0.2	---	MAGRUDER MTN
	25 22:48:44	37.599	117.649	0.8	3.23	---	194	CD	0.9	---	LIDA WASH
	26 3:13: 7	36.868	116.177	1.0	7.00	2.1	119	BD	---	0.2	SKULL MTN
	26 6:15:42	37.240	117.646	0.4	22.92	0.2	251	AD	0.4	---	LAST CHANCE RANGE
	27 20: 1: 7	37.113	117.367	0.6	7.03	2.1	129	BB	0.0	---	UBEHEBE CRATER
	28 2: 8:44	36.328	116.375	0.2	7.38	0.7	102	AB	1.1	---	ASH MEADOWS
	28 21: 3:37	36.706	116.263	0.2	5.41	0.4	127	AB	0.4	---	STRIPED HILLS
APR	31 13: 3:57	36.871	116.171	0.4	8.37	0.7	73	AA	0.8	---	SKULL MTN
	2 14:15:11	36.893	116.319	---	36.89	---	290	AD	0.8	---	TOPOPAH SPRING
	2 17:56:30	36.904	115.998	1.2	10.78	4.6	150	BC	0.5	---	PLUTONIUM VALLEY
	2 18:13: 5	36.836	115.959	3.5	10.66	9.1	216	CD	0.4	---	FRENCHMAN FLAT
	2 18:20:41	36.860	115.961	0.3	1.30	---	85	CC	2.2	---	FRENCHMAN FLAT
	2 21:14:54	36.874	115.982	0.6	8.71	1.9	54	BB	1.2	---	FRENCHMAN FLAT
	3 2:18: 9	36.899	115.999	0.7	10.56	3.1	176	BC	0.7	---	PLUTONIUM VALLEY
	3 6:40:44	36.851	115.967	0.5	6.26	4.5	161	BC	0.7	---	FRENCHMAN FLAT
	3 15:22:36	36.857	115.961	0.2	5.39	1.4	151	AC	0.9	---	FRENCHMAN FLAT
	3 17:15:13	36.855	115.957	0.4	-0.07	---	126	CC	0.9	---	FRENCHMAN FLAT
	3 23:47: 9	37.052	116.169	0.7	5.15	1.2	175	AC	1.2	---	TIPPIPAH SPRING
	4 18: 0:49	36.976	115.636	1.0	15.19	4.7	164	BC	0.5	---	QUARTZ PEAK NW
	5 2:27:45	36.853	115.957	0.6	0.92	---	91	CC	1.2	---	FRENCHMAN FLAT
	5 2:29: 6	36.864	115.948	0.1	0.99	1.4	199	AD	0.6	---	FRENCHMAN FLAT
	5 17:29:58	36.830	115.891	0.1	15.44	0.2	207	AD	0.2	---	FRENCHMAN FLAT
	6 1:35:21	36.554	116.342	0.9	2.82	3.2	94	BC	0.7	---	LATHROP WELLS SE
	8 2:11:31	36.877	115.939	0.6	7.63	3.1	164	BC	1.0	---	PLUTONIUM VALLEY
	10 7:39:22	37.289	117.058	0.9	7.39	3.2	204	BD	0.3	---	SCOTTYS JUNCTION
	11 9:48: 4	36.862	116.319	---	7.00	---	241	DD	0.8	---	JACKASS FLATS
	14 13:54:23	37.200	116.307	0.4	2.97	---	114	CC	1.0	---	AMMONIA TANKS
	14 16:55: 4	37.164	117.421	0.8	7.00	3.5	189	BD	0.4	---	UBEHEBE CRATER
	15 10:24:43	37.514	117.716	0.6	2.99	---	101	CD	0.8	---	LIDA WASH
	15 12:42:57	36.920	116.117	---	7.00	---	216	AD	1.3	---	YUCCA LAKE
	15 12:44:56	36.619	115.981	---	3.60	---	235	AD	0.7	---	FRENCHMAN FLAT
	15 21:38: 2	36.911	115.992	0.8	1.93	1.5	123	AB	0.7	---	PLUTONIUM VALLEY
	16 11:25:35	37.207	115.461	0.4	14.02	1.7	61	AB	2.2	---	DESERT HILLS NW
	16 21:41:27	37.211	115.484	0.5	-0.64	---	84	CC	1.3	---	DESERT HILLS NW
	21 2:27:39	37.310	116.317	0.4	5.15	2.3	85	BC	1.4	---	DEAD HORSE FLAT
	23 4: 8:40	36.874	116.162	0.5	6.60	0.9	65	BA	1.3	---	SKULL MTN
	23 5:24:30	36.817	116.257	0.5	2.75	0.8	99	AB	1.0	---	JACKASS FLATS
	23 11:37:37	36.826	116.253	0.4	4.52	1.0	58	AB	1.8	---	JACKASS FLATS
	23 16:43:20	37.301	117.381	0.4	-0.03	---	124	CC	0.7	---	GOLD POINT SW
	24 6: 2:28	36.818	116.271	0.7	3.79	2.1	121	BB	0.6	---	JACKASS FLATS
	24 6: 2:60	36.818	116.270	0.7	3.79	2.1	121	BB	0.5	---	JACKASS FLATS
	24 7:20:50	36.819	116.267	0.6	3.78	2.0	117	AB	0.6	---	JACKASS FLATS
	24 11: 9:49	37.332	114.598	0.6	9.67	0.5	231	AD	1.7	---	ELGIN
	25 3:48:39	36.042	116.107	1.9	3.53	---	229	CD	1.4	---	STEWART VALLEY
	25 10:40:30	37.326	116.299	0.3	-0.26	---	77	CC	2.0	---	DEAD HORSE FLAT
	26 2:13: 7	36.816	116.271	0.5	3.82	1.7	122	AB	0.3	---	JACKASS FLATS
	27 13: 1:55	37.045	117.471	1.0	2.61	3.2	205	BD	0.8	---	UBEHEBE CRATER
	27 21:15:17	37.254	116.417	0.4	-0.95	0.4	149	AC	1.2	---	SILENT BUTTE
	29 4:12:48	36.830	115.860	0.3	7.87	1.8	155	AC	0.7	---	FRENCHMAN LAKE SE
	29 17:53:31	36.817	116.263	0.4	-0.22	0.5	116	AB	0.5	---	JACKASS FLATS
	30 9:33:59	36.641	115.999	0.5	12.05	1.0	132	AB	0.8	---	MERCURY
MAY	2 7:38:28	36.818	116.265	0.8	4.00	2.5	116	BB	0.5	---	JACKASS FLATS
	3 10:31:19	36.459	117.049	0.7	13.74	1.6	133	AB	0.7	---	EMIGRANT CANYON
	8 11:36:39	37.167	117.410	0.2	5.02	2.4	128	BC	0.8	---	UBEHEBE CRATER
	10 11: 3:33	36.874	116.267	0.6	0.88	0.8	58	BB	1.2	---	JACKASS FLATS

## 1980 LOCAL HYPOCENTER SUMMARY

	DATE - TIME (UTC)	LATITUDE (DEG. N)	LONGITUDE (DEG. W)	HORIZ ERROR (KM)	DEPTH (KM)	VERT ERROR (KM)	AZI GAP (DEG)	QUAL	Md	Mblg	QUADRANGLE
MAY	11 9:28:54	36.576	116.344	0.4	8.13	1.4	136	AC	0.7	---	LATHROP WELLS SE
	13 2:33:43	36.789	116.090	2.0	8.61	4.2	178	BC	---	0.1	CANE SPRING
	14 8:33:32	36.845	116.206	0.6	7.00	1.0	145	AC	0.5	---	SKULL MTN
	15 1:30:38	36.504	115.894	1.5	7.00	4.1	230	BD	0.5	---	MERCURY SW
	16 16:49: 8	37.087	116.053	0.7	7.07	3.6	162	BC	0.9	---	YUCCA FLAT
	18 1:43:11	36.812	116.236	1.3	8.23	3.7	149	BC	0.4	---	SKULL MTN
	18 17:50:25	36.911	116.016	2.4	32.46	4.3	196	BD	0.3	---	YUCCA LAKE
	19 4:16:35	37.076	117.072	0.9	11.24	2.5	64	BA	1.8	---	BONNIE CLAIRE SE
JUN	3 9: 4:28	36.886	116.003	0.5	7.98	3.5	149	BC	0.7	---	YUCCA LAKE
	4 19:54:36	37.572	116.458	0.9	4.59*	---	88	CC	1.1	---	QUARTZITE MTN
	6 19:43:17	36.888	115.739	1.5	2.49*	---	200	CD	0.6	---	QUARTZ PEAK NW
	7 2: 8:55	36.977	116.977	---	8.00	---	151	BD	1.1	---	BULLFROG
	7 12: 0:33	36.617	116.264	0.3	7.74	0.0	152	AC	0.8	---	LATHROP WELLS SE
	7 12: 1:41	36.617	116.256	0.2	5.53	0.6	148	AC	0.5	---	LATHROP WELLS SE
	7 12:21:54	36.614	116.261	---	5.17	---	153	AD	0.2	---	LATHROP WELLS SE
	8 11:40: 4	37.343	114.794	1.5	8.09	1.0	302	BD	1.0	---	GREGORSON BASIN
	9 7:53:32	36.781	115.984	1.1	7.00	5.2	155	CC	1.0	---	FRENCHMAN FLAT
	9 12:29:10	36.872	116.334	---	7.00**	---	181	AD	---	0.2	JACKASS FLATS
	10 15:19: 5	37.156	117.339	0.4	7.00	1.3	186	AD	1.0	---	UBEHEBE CRATER
	15 1:17:38	36.823	115.999	1.1	0.23	3.7	192	BD	0.4	---	FRENCHMAN FLAT
	18 17:57:11	36.712	115.623	0.3	-0.31*	---	116	CC	1.0	---	HEAVENS WELL
	19 2:33:21	36.697	116.283	0.8	-0.13	1.0	139	BB	0.8	---	STRIPED HILLS
	19 4: 4: 8	36.535	116.374	0.8	1.18	3.3	108	BC	0.6	---	LATHROP WELLS SE
	20 20:40:56	36.671	116.406	1.2	7.75	2.6	182	BD	0.5	---	LATHROP WELLS NW
JUL	3 2:52:10	36.873	116.181	1.4	11.38	5.8	153	CD	0.3	---	SKULL MTN
	3 21:15:42	36.317	114.893	2.3	4.14	2.4	254	BD	1.2	---	DRY LAKE
	4 7: 3: 3	36.696	116.277	0.5	4.86	1.3	69	AA	0.6	---	STRIPED HILLS
	4 8:21:39	36.820	116.085	0.4	4.19	3.3	97	BB	0.6	---	BARE MTN
	5 13:28: 8	36.785	116.027	2.7	8.25	3.0	106	CD	0.7	---	BARE MTN
	7 15:13:14	36.748	115.821	2.0	11.15	4.9	191	BD	0.7	---	MERCURY NE
	9 0:36:58	36.935	118.452	23.8	7.00	8.0	334	DD	1.4	---	***REGIONAL***
	9 2:13:48	37.252	115.030	1.5	2.75	6.2	186	CD	1.7	---	ALAMO SE
	9 15: 5:51	36.856	116.169	2.1	10.73	3.1	154	BC	0.4	---	SKULL MTN
	11 13:22: 4	36.750	116.277	0.3	7.00	0.6	50	AA	1.2	---	JACKASS FLATS
	11 13:28:10	36.757	116.277	0.5	7.00	0.8	71	AA	0.3	---	JACKASS FLATS
	11 13:37:58	36.750	116.277	0.4	7.00	0.7	67	AA	0.7	---	JACKASS FLATS
	11 14:53: 2	36.755	116.275	0.4	6.55	0.7	70	AA	0.5	---	JACKASS FLATS
	11 15:10:21	37.099	115.046	0.4	1.59	1.3	116	AC	1.1	---	HICO NE
	12 17:10:20	36.702	116.282	0.4	5.05	0.9	63	AA	1.0	---	STRIPED HILLS
	13 13:58:20	37.397	115.210	0.8	0.44	3.3	134	BC	1.2	---	ASH SPRINGS
	13 16: 2:10	36.808	115.934	0.4	5.66	2.3	175	BC	1.0	---	FRENCHMAN FLAT
	13 16:51: 8	36.774	115.980	---	12.48	---	224	AD	0.8	---	FRENCHMAN FLAT
	14 2:18:23	36.772	115.978	---	7.00**	---	235	AD	0.3	---	FRENCHMAN FLAT
	14 2:51:48	36.814	115.932	1.8	7.23	6.2	199	CD	0.9	---	FRENCHMAN FLAT
	14 2:57:15	36.758	115.957	---	24.98	---	234	AD	0.6	---	FRENCHMAN FLAT
	14 12: 4:29	37.115	116.205	2.3	14.86	3.4	200	BD	0.9	---	TIPPIPAH SPRING
	14 12:12:42	37.099	116.193	0.5	-0.03	0.7	113	AB	0.7	---	TIPPIPAH SPRING
	14 12:44:29	37.052	116.147	---	0.18	---	160	AD	0.7	---	TIPPIPAH SPRING
	14 16:42:50	36.806	115.947	1.0	8.89	1.9	193	AD	0.4	---	FRENCHMAN FLAT
	15 12: 3:21	36.743	115.954	2.4	26.29	2.2	162	BC	---	0.2	MERCURY
	15 14:23:33	36.802	115.921	0.2	11.60	0.5	203	AD	0.2	---	FRENCHMAN FLAT
	15 23:18:18	36.896	116.815	0.5	-0.05*	---	123	CC	1.3	---	BULLFROG
	16 6:37:38	36.190	115.435	1.7	2.33	1.9	295	BD	1.3	---	LA MADRE MTN
	17 14:16: 3	36.765	115.911	0.8	0.69	1.3	188	AD	0.4	---	FRENCHMAN FLAT
	17 22: 3:14	37.086	115.188	---	7.46	---	228	BD	0.5	---	LOWER PAHRANAGAT LAKE SW
	18 12:13:41	37.099	116.194	0.7	5.28	2.6	93	BB	1.2	---	TIPPIPAH SPRING
	18 15:18:53	36.752	116.292	0.7	9.33	1.2	150	AC	0.2	---	JACKASS FLATS
	18 15:39:44	36.759	116.303	---	7.21	---	228	AD	---	0.1	JACKASS FLATS
	19 10: 1:46	36.872	116.177	0.5	7.50	0.7	154	AC	0.1	---	SKULL MTN
	19 21:49: 4	37.408	114.457	---	7.00**	---	327	CD	1.3	---	***REGIONAL***
	19 21:49:36	36.836	115.281	5.5	6.98*	---	246	DD	0.6	---	DEAD HORSE RIDGE
	20 1:49:59	37.030	116.019	---	7.00**	---	234	AD	0.5	---	YUCCA FLAT
	20 9: 7:55	37.023	116.007	0.5	11.24	2.5	157	BC	0.8	---	YUCCA FLAT
	20 9:47:19	37.020	116.003	0.4	7.12	3.2	158	BC	0.8	---	YUCCA FLAT
	20 23: 4:18	36.709	116.313	3.0	7.00	2.4	201	CD	0.2	---	STRIPED HILLS
	21 2: 8:40	36.832	115.988	---	7.00**	---	254	AD	-0.2	---	FRENCHMAN FLAT



## 1988 LOCAL HYPOCENTER SUMMARY

DATE - TIME (UTC)	LATITUDE (DEG. N)	LONGITUDE (DEG. W)	HORIZ ERROR (KM)	DEPTH (KM)	VERT ERROR (KM)	AZI GAP (DEG)	QUAL	Md	Mb1g	QUADRANGLE
JUL 21 4: 7:59	37.077	116.187	1.5	6.99	2.4	142	BC	0.7	---	TIPPIPAH SPRING
22 10:50:14	36.976	115.649	1.5	22.54	3.0	126	BB	1.2	---	QUARTZ PEAK NW
22 14:11:42	36.806	115.691	---	16.36	---	208	AD	0.8	---	QUARTZ PEAK SW
22 20: 0:48	37.383	115.556	---	7.00**	---	193	AD	1.0	---	GROOM RANGE NE
22 20:28:13	36.973	115.646	---	21.01	---	125	AD	0.9	---	QUARTZ PEAK NW
23 10: 3:50	36.709	115.772	0.4	6.30	2.3	165	BC	1.9	---	MERCURY NE
23 10: 5:49	36.703	115.673	---	12.49	---	185	AD	0.8	---	INDIAN SPRINGS NW
23 13:18:49	37.037	115.524	13.6	15.47*	---	105	DD	1.0	---	SOUTHEASTERN MINE
24 11:39:43	37.057	116.236	0.4	6.59	0.6	175	AC	0.8	---	TIPPIPAH SPRING
25 20:30:50	37.261	116.469	0.4	0.03*	---	48	CC	2.3	---	SILENT BUTTE
25 21:14:10	37.261	116.465	0.3	-0.26*	---	50	CC	2.2	---	SILENT BUTTE
25 23:10:40	37.262	116.487	0.8	2.83*	---	77	CC	2.8	---	SILENT BUTTE
26 5: 0: 4	37.242	116.315	---	31.05	---	164	AD	0.5	---	AMMONIA TANKS
26 17:19:58	36.698	115.678	0.6	6.35*	---	166	CC	1.2	---	INDIAN SPRINGS NW
26 18:33: 7	37.006	115.677	1.0	16.92*	---	109	CD	1.0	---	FALLOUT HILLS SW
27 9:42: 9	36.649	115.287	2.9	9.51*	---	129	CC	1.1	---	WHITE SAGE FLAT
27 13:00:28	36.668	115.482	---	7.00**	---	226	AD	0.5	---	DOG BONE LAKE SOUTH
28 5: 0:29	36.914	115.967	0.6	4.33	6.1	188	CD	0.7	---	PLUTONIUM VALLEY
28 14:48:47	37.200	115.436	---	7.00**	---	263	AD	0.6	---	DESERT HILLS NW
28 16:55:56	36.721	115.967	1.8	-0.61	0.6	227	BD	0.6	---	MERCURY
28 19:38:11	37.234	115.404	0.5	2.63*	---	154	CC	1.6	---	DESERT HILLS NW
31 3:48:10	36.707	115.801	0.4	7.18	0.6	95	AB	1.0	---	MERCURY NE
31 19:22:16	37.097	116.031	2.8	7.00*	---	141	CC	2.0	---	YUCCA FLAT
31 19:26:16	37.073	116.005	1.3	2.12	10.0	121	CC	2.7	---	YUCCA FLAT
AUG 6 3:42: 4	37.066	116.145	0.6	-0.52	0.5	148	AD	0.7	---	TIPPIPAH SPRING
6 9:37:34	37.262	116.485	0.7	6.71*	---	74	CC	1.5	---	SILENT BUTTE
7 3:21:59	36.438	115.648	0.6	11.54	1.4	87	AB	1.2	---	CHARLESTON PEAK
7 9:53:37	37.313	116.291	0.8	2.56	3.2	120	BC	1.2	---	DEAD HORSE FLAT
8 9:51:35	37.038	116.476	---	22.57	---	167	DD	0.9	---	TIMBER MTN
9 2:21:22	36.535	116.396	---	4.14	---	271	AD	0.7	---	LATHROP WELLS SW
9 2:21:40	36.617	116.281	1.1	11.41	2.2	161	BD	0.4	---	LATHROP WELLS SE
11 8:14:30	37.149	117.409	0.7	6.21	4.0	134	BC	0.5	---	UBEHEBE CRATER
11 8:19:44	37.143	116.294	0.3	7.61	0.7	170	AC	0.2	---	AMMONIA TANKS
12 4:53:14	36.487	116.806	0.4	-0.89	1.0	67	AC	1.1	---	FURNACE CREEK
14 8:20:27	36.329	116.239	0.4	6.67	3.5	129	BC	0.7	---	HIGH PEAK
15 9: 0: 1	37.100	116.163	---	7.00**	---	274	AD	0.7	---	TIPPIPAH SPRING
15 18:15:37	35.975	115.241	3.5	4.29	3.5	256	CD	1.7	---	SLOAN
15 23: 9:50	36.477	116.920	0.6	10.04	2.6	78	BB	1.1	---	FURNACE CREEK
17 17:48: 9	36.996	117.534	0.8	6.75	1.6	186	AD	1.5	---	DRY MTN
18 0: 0:43	37.198	115.197	---	1.28	---	140	AD	1.3	---	LOWER PAHRANAGAT LAKE NW
19 8:33: 4	36.916	115.971	0.9	3.50*	---	186	CD	0.5	---	PLUTONIUM VALLEY
20 11:58:16	36.728	115.613	0.3	7.94	3.4	133	BC	1.0	---	HEAVENS WELL
20 16: 5:20	36.702	116.282	---	7.00**	---	165	AD	0.3	---	JACKASS FLATS
21 3:24: 2	37.200	116.528	0.3	11.23	6.6	112	AB	1.7	---	THIRSTY CANYON NE
21 12:30:48	36.810	115.970	---	1.37	---	252	AD	0.0	---	FRENCHMAN FLAT
22 1:11: 2	36.511	116.466	1.2	13.67	3.6	291	BD	0.6	---	LATHROP WELLS SW
23 3:37:51	37.137	117.012	0.6	4.62	6.4	114	CC	1.2	---	BONNIE CLAIRE
24 10:34:23	36.807	115.973	0.3	5.24	0.5	250	AD	-0.1	---	FRENCHMAN FLAT
24 11:40: 8	36.873	116.154	1.1	10.37	0.6	230	BD	---	0.2	SKULL MTN
24 23: 7: 2	36.635	116.000	0.5	8.44	1.0	134	AB	0.7	---	CAMP DESERT ROCK
25 8: 7:49	37.317	116.437	0.3	5.44	2.7	91	BC	1.0	---	SILENT BUTTE
25 8: 9:29	37.303	116.438	0.1	11.80	0.1	193	AD	0.7	---	SILENT BUTTE
25 8:32:36	37.316	116.435	0.3	6.77	1.8	91	AC	0.9	---	SILENT BUTTE
25 9:27: 4	37.314	116.433	0.3	5.16	2.6	90	BC	1.4	---	SILENT BUTTE
25 13:32:26	37.314	116.432	0.3	6.70	1.9	90	AC	0.8	---	SILENT BUTTE
25 15:12:22	37.317	116.432	0.3	4.81	3.5	91	BC	0.8	---	SILENT BUTTE
26 1: 0:10	37.314	116.432	0.4	6.91	2.3	90	BC	0.6	---	SILENT BUTTE
26 1:28:56	37.314	116.427	0.4	8.20	2.1	90	BB	0.9	---	SILENT BUTTE
26 2:40:29	37.296	116.466	1.1	10.05	2.1	135	BB	0.8	---	SILENT BUTTE
26 10:15:45	37.324	116.430	0.4	5.18	2.9	214	BD	0.8	---	SILENT BUTTE
26 11:18:14	36.413	116.289	0.1	0.78	0.4	105	AC	0.4	---	ASH MEADOWS
26 11:18:58	36.807	116.258	---	7.00**	---	213	AD	0.5	---	JACKASS FLATS
28 2:10:26	36.746	115.977	---	7.00**	---	227	AD	0.4	---	MERCURY
28 17:12:28	36.807	116.024	1.0	2.86*	---	92	CC	0.7	---	CANE SPRING
29 5: 1:30	36.989	116.729	0.4	8.92	1.2	92	AB	1.1	---	BARE MTN
29 5:54:32	36.835	115.979	1.5	5.70	5.5	208	CD	0.3	---	FRENCHMAN FLAT

## 1988 LOCAL HYPOCENTER SUMMARY

	DATE - TIME (UTC)	LATITUDE (DEG. N)	LONGITUDE (DEG. W)	HORIZ ERROR (KM)	DEPTH (KM)	VERT ERROR (KM)	AZI GAP (DEG)	QUAL	Md	Mb1g	QUADRANGLE
AUG	29 20:48:3	36.898	117.712	1.1	1.29	2.1	262	BD	1.7	---	COSO PEAK
	30 19:18:7	37.138	117.411	0.7	7.78	3.2	142	BC	1.3	---	UBEHEBE CRATER
SEP	3 1:31:18	37.192	117.579	0.5	7.98	0.9	148	AC	1.1	---	LAST CHANCE RANGE
	5 5:11:51	36.712	118.342	0.8	5.11	1.2	191	AD	---	0.2	STRIPED HILLS
	5 11:42:38	36.849	118.280	---	1.98	---	210	AD	0.8	---	JACKASS FLATS
	11 14:59:60	36.974	118.170	0.8	-0.02	0.5	133	AB	1.6	---	MINE MTN
	11 20:58:3	36.593	118.140	3.2	11.09	---	143	CC	0.9	---	SPECTER RANGE SW
	11 22:19:6	36.828	118.338	0.4	4.59	1.1	184	AB	1.2	---	STRIPED HILLS
	12 2:21:34	36.744	115.429	0.6	4.89	---	171	CC	1.9	---	BLACK HILLS NW
	12 7:41:56	37.278	114.983	1.1	5.33	2.8	196	BD	1.8	---	DELAMAR LAKE
	13 5:54:25	37.143	118.314	0.7	8.32	1.7	181	AC	1.3	---	AMMONIA TANKS
	13 10:48:38	37.564	115.882	2.5	4.81	---	102	CC	1.3	---	WHITE BLOTCH SPRINGS
	13 14:58:19	37.183	115.443	0.7	8.89	1.6	139	BC	1.5	---	DESERT HILLS NW
	14 14:19:18	36.830	115.941	0.5	4.31	---	135	CC	0.9	---	FRENCHMAN FLAT
	17 4:48:40	36.858	118.227	1.4	3.28	---	270	CD	1.4	---	REVEILLE
	18 11:13:47	36.978	118.559	1.8	7.81	6.7	211	CD	0.8	---	BARE MTN
	19 18:0:44	36.789	118.942	0.5	-0.88	1.1	154	AC	1.8	---	CHLORIDE CLIFF
	19 18:0:48	36.432	118.953	5.2	2.34	---	214	DD	1.7	---	FURNACE CREEK
	22 17:22:51	37.254	118.479	0.8	8.04	---	78	CC	1.8	---	SILENT BUTTE
	22 19:8:49	36.980	118.815	0.5	4.18	8.5	110	CC	1.2	---	BULLFROG
	22 21:28:40	37.257	118.521	0.8	1.57	2.9	155	BC	1.4	---	TRAIL RIDGE
	23 12:28:38	36.858	115.919	1.3	11.21	3.5	206	BD	0.8	---	FRENCHMAN FLAT
	24 8:17:26	36.759	115.769	---	7.80	---	183	CD	1.1	---	FRENCHMAN LAKE SE
	25 9:33:50	35.476	118.979	---	7.80	---	360	DD	1.8	---	***REGIONAL***
	26 18:59:58	36.783	118.438	0.2	2.98	---	188	CD	0.3	---	LATHROP WELLS NW
	27 9:18:48	36.863	115.964	18.3	7.80	8.8	182	DD	1.8	---	MERCURY
	28 15:8:15	36.884	115.988	---	2.88	---	236	BD	0.5	---	PLUTONIUM VALLEY
	29 21:25:54	36.854	118.813	2.9	8.88	---	192	CD	0.7	---	CANE SPRING
OCT	2 1:48:15	37.274	117.815	1.4	9.81	0.9	254	BD	2.0	---	SCOTTYS JUNCTION
	2 8:13:41	36.998	115.983	0.4	5.83	2.3	129	BB	1.8	---	PLUTONIUM VALLEY
	2 20:15:47	36.447	114.485	8.8	2.94	3.7	298	DD	1.9	---	***REGIONAL***
	2 20:15:57	37.818	114.793	---	20.58	---	289	DD	1.5	---	DELAMAR 3 SE
	3 5:25:3	37.238	118.348	0.5	-0.14	0.4	94	AB	1.5	---	AMMONIA TANKS
	3 11:50:55	37.318	115.885	3.7	10.82	3.8	169	CD	0.6	---	GROOM MINE SW
	3 17:52:8	37.489	114.787	---	3.89	---	254	BD	1.1	---	DELAMAR
	3 17:52:41	36.788	115.818	---	7.80	---	291	DD	0.3	---	FRENCHMAN LAKE SE
	4 2:23:46	35.622	117.580	2.2	6.18	0.9	299	BD	1.8	---	RIDGECREST
	6 19:48:31	37.287	117.855	0.3	5.83	3.4	87	BC	1.1	---	SCOTTYS JUNCTION
	8 21:45:52	37.324	114.884	4.5	11.40	1.3	305	CD	2.1	---	ELGIN SW
	9 2:19:22	36.778	115.937	0.7	-0.22	---	180	CC	1.8	---	FRENCHMAN FLAT
	9 18:3:39	36.783	115.927	0.2	2.88	0.7	168	AC	0.7	---	FRENCHMAN FLAT
	12 2:47:41	37.284	117.188	---	2.43	---	282	AD	2.2	---	BONNIE CLAIRE
	12 5:40:44	36.841	115.634	---	18.82	---	324	AD	1.3	---	QUARTZ PEAK SW
	12 14:52:14	37.843	117.211	---	2.83	---	273	BD	1.2	---	BONNIE CLAIRE SW
	12 16:27:31	37.483	118.184	0.4	29.57	0.3	183	AD	1.1	---	WHEELBARROW PEAK NE
	13 18:57:31	37.258	118.481	0.9	8.89	---	99	CC	1.8	---	SILENT BUTTE
	13 14:52:15	37.879	117.888	0.8	5.87	3.2	135	BC	0.9	---	BONNIE CLAIRE SE
	13 18:27:24	37.582	115.358	0.5	18.91	2.1	95	BB	0.9	---	MT IRISH
	15 4:53:22	37.229	114.993	1.8	8.99	8.8	228	CD	1.4	---	DELAMAR 3 NW
	15 12:21:52	37.317	118.357	1.7	4.78	6.5	192	CD	0.9	---	DEAD HORSE FLAT
	15 12:29:6	37.235	118.447	---	8.85	---	141	AD	1.2	---	SCRUGHAM PEAK
	17 19:21:37	35.934	117.484	5.1	8.98	1.7	283	DD	1.3	---	TRONA
	17 19:21:54	37.216	118.884	---	38.12	---	185	DD	0.7	---	SPRINGDALE
	19 8:33:18	37.358	118.184	---	2.88	---	195	AD	1.4	---	QUARTET DOME
	20 11:38:12	37.488	118.888	1.9	7.80	---	287	CD	1.1	---	BLACK MTN NW
	20 11:41:38	37.324	118.348	0.8	1.87	2.2	118	BC	1.3	---	DEAD HORSE FLAT
	21 4:1:54	36.783	115.892	0.8	13.95	1.8	143	AC	1.4	---	INDIAN SPRINGS NW
	23 1:32:14	36.248	114.748	4.5	12.95	2.8	284	CD	1.7	---	HOOVER DAM
	23 2:31:19	37.461	118.272	1.7	7.37	---	184	CC	1.2	---	SILENT CANYON NE
	24 13:27:47	37.887	115.981	---	4.89	---	138	CD	1.3	---	PAIUTE RIDGE
	24 19:25:38	37.118	115.991	1.2	19.91	1.9	92	BB	1.5	---	PAIUTE RIDGE
	24 19:27:45	37.887	118.825	0.8	4.35	4.8	134	BC	1.3	---	YUCCA FLAT
	25 8:27:38	38.358	117.287	3.2	4.81	1.4	258	CD	1.8	---	SAN ANTONIA RANCH
	25 8:38:60	37.758	118.388	0.3	8.34	0.8	173	AC	2.4	---	KAWICH PEAK
	25 1:8:45	37.343	114.797	9.5	2.52	9.5	288	DD	1.7	---	GREGSON BASIN
	27 13:22:51	36.795	118.311	0.3	3.34	3.4	129	BB	1.3	---	JACKASS FLATS

## 1980 LOCAL HYPOCENTER SUMMARY

	DATE - TIME (UTC)	LATITUDE (DEG. N)	LONGITUDE (DEG. W)	HORIZ ERROR (KM)	DEPTH (KM)	VERT ERROR (KM)	AZI GAP (DEG)	QUAL	Md	Mb1g	QUADRANGLE
OCT	27 20: 2:28	36.004	115.066	2.0	2.16	1.8	274	BD	1.5	---	LAS VEGAS SE
	31 0:40:33	36.767	115.964	1.6	8.50	2.1	99	CB	1.4	---	MERCURY
	31 18:11: 9	37.223	116.175	0.4	0.78*	---	146	CC	1.2	---	RAINIER MESA
	31 18:11:49	37.182	116.179	1.3	0.70*	---	170	CD	1.2	---	RAINIER MESA
	31 18:15:51	37.211	116.282	1.4	15.43	2.7	101	BB	1.1	---	AMMONIA TANKS
	31 18:40:57	37.149	116.253	1.3	8.18	2.8	103	BB	1.3	---	AMMONIA TANKS
	31 16:43: 3	37.211	116.297	1.9	19.61	2.5	109	BB	1.3	---	AMMONIA TANKS
	31 19:18:11	37.101	115.962	12.0	7.00*	---	238	DD	1.2	---	PAIUTE RIDGE
	31 19:46:11	37.184	116.252	0.9	2.29*	---	95	CC	---	0.2	AMMONIA TANKS
	2 23:59:37	37.293	117.050	1.6	1.00*	---	125	CD	1.1	---	SCOTTYS JUNCTION
NOV	3 2:17:27	37.541	115.302	---	15.98	---	129	AD	1.1	---	MT IRISH
	3 3:30:26	36.637	116.276	---	24.32	---	195	AD	1.2	---	STRIPED HILLS
	3 8:10:24	36.566	116.005	2.4	17.67	1.5	239	BD	2.1	---	SPECTER RANGE SE
	3 14: 8:38	36.690	116.004	---	2.95	---	153	AD	1.3	---	CAMP DESERT ROCK
	4 6:49:50	37.669	114.963	1.6	2.20	1.5	131	BB	1.7	---	PAHROC SPRING
	4 7:39:51	36.255	117.115	1.3	12.74	0.6	264	BD	1.5	---	EMIGRANT CANYON
	4 8: 6:41	36.798	116.070	1.3	4.55	5.5	123	DC	1.1	---	CANE SPRING
	5 9:46:12	37.217	114.747	---	3.07	---	348	AD	1.2	---	VIGO NW
	6 5:52:32	36.798	115.988	1.9	4.20*	---	194	CD	0.7	---	FRENCHMAN FLAT
	6 10:41:21	36.702	115.931	1.3	7.00	2.2	119	BB	0.6	---	MERCURY
	8 22:27:18	37.243	115.871	1.3	14.17	3.4	136	BC	1.1	---	PAPOOSE LAKE NE
	9 2:25:29	36.130	116.129	---	7.00**	---	261	BD	1.4	---	STEWART VALLEY
	9 7: 8:45	37.777	116.303	0.9	0.91*	---	202	CD	1.7	---	KAWICH PEAK
	9 13:58:36	36.788	115.998	---	7.00**	---	231	AD	0.7	---	FRENCHMAN FLAT
	11 1:43:51	36.739	116.254	---	7.00**	---	186	AD	0.5	---	STRIPED HILLS
	11 6:33: 3	37.313	116.464	0.9	10.86**	1.4	125	AB	1.8	---	SILENT BUTTE
	11 11: 4:59	37.308	116.501	0.9	8.47	5.2	128	CC	1.3	---	TRAIL RIDGE
	11 12:36:13	36.715	116.279	---	7.00**	---	156	AD	0.9	---	STRIPED HILLS
	12 9:44:44	37.322	116.442	0.8	6.55*	---	96	CC	1.1	---	SILENT BUTTE
	13 19: 7:44	37.004	116.229	1.3	5.09	1.7	167	BC	0.9	---	TIPPIPAH SPRING
	14 17:10:26	37.084	116.029	2.7	11.07*	---	144	CC	2.0	---	YUCCA FLAT
	14 17:15:35	37.090	115.966	1.4	4.96	6.1	91	CC	3.0	---	PAIUTE RIDGE
	19 3:15: 9	37.143	116.564	0.5	14.55	2.7	87	BB	1.3	---	THIRSTY CANYON NE
	19 8:43:56	37.227	115.633	0.6	11.65	5.3	106	CC	1.2	---	FALLOUT HILLS NW
	19 9: 2:41	36.609	116.275	4.8	10.48	8.7	220	CD	0.9	---	LATHROP WELLS SE
	20 2:50:19	37.673	116.346	15.9	17.89	3.9	311	DD	0.8	---	QUARTZITE MTN
	21 3:35:28	37.381	115.060	---	7.00**	---	310	AD	1.2	---	ALAMO NE
	21 3:52:56	37.426	116.952	---	2.70	---	208	AD	1.3	---	TOLICHA PEAK
	22 4:58:54	36.517	116.580	0.4	2.89*	---	163	CC	1.1	---	BIG DUNE
	22 19:16:26	36.519	116.643	1.1	5.00	3.3	265	BD	1.2	---	BIG DUNE
	22 22: 6:32	36.531	115.826	0.9	9.28	5.0	118	CC	0.9	---	MERCURY SE
	23 1:11:45	37.196	114.699	3.2	7.00*	---	212	CD	1.0	---	VIGO NW
	23 2:57:25	36.530	115.564	0.3	3.12*	---	98	CC	1.3	---	INDIAN SPRINGS SE
	23 4:48:29	36.521	115.574	0.6	5.69	2.6	136	BC	1.2	---	INDIAN SPRINGS SE
	23 12:13:22	36.540	115.562	2.7	12.00*	---	86	CC	1.1	---	INDIAN SPRINGS SE
	23 15:15:28	36.551	115.526	0.7	2.07*	---	157	CC	0.9	---	INDIAN SPRINGS SE
	25 0:38:31	36.679	115.574	0.6	16.09	1.8	149	AC	1.3	---	HEAVENS WELL
	26 4: 7: 5	37.099	117.336	1.1	-0.88*	---	123	CD	0.9	---	USENEBE CRATER
	26 11:12:42	36.013	117.547	15.7	-0.46*	---	292	DD	1.4	---	COSO PEAK
	26 11:24:34	37.484	116.351	---	7.00**	---	150	BD	0.9	---	SILENT CANYON NE
	27 10:15:13	36.411	115.887	0.6	10.08	1.2	107	AB	1.0	---	CHARLESTON PEAK
	27 22: 2: 2	36.674	116.250	---	5.17	---	222	AD	0.5	---	JACKASS FLATS
	28 11: 8:20	36.869	115.926	2.9	4.24*	---	231	CD	0.5	---	FRENCHMAN FLAT
	29 4:56:53	36.782	116.272	0.2	2.85	0.2	198	AD	0.6	---	JACKASS FLATS
	29 8:21:31	36.857	115.816	---	7.00**	---	302	AD	---	-0.1	FRENCHMAN LAKE SE
	29 9:17:14	36.713	116.273	---	8.37	---	143	AD	0.2	---	STRIPED HILLS
	30 6: 0:48	36.203	117.071	14.6	17.56	7.8	207	DD	1.1	---	TELESCOPE PEAK
	1 23:16:11	36.666	115.319	0.5	17.62	0.7	123	AB	1.4	---	WHITE SAGE FLAT
	2 6:31: 3	36.791	115.894	3.5	4.30*	---	219	CD	0.8	---	FRENCHMAN FLAT
	4 0:40:35	36.264	117.144	1.4	7.00	1.5	240	BD	1.8	---	BAXTER SPRING
DEC	6 6:46:35	37.388	115.117	1.0	5.89	2.0	112	BB	1.5	---	ALAMO NE
	8 20: 5:13	36.792	115.476	---	7.00**	---	158	AD	0.7	---	DOG BONE LAKE SOUTH
	10 19:34:46	36.311	117.205	7.8	7.00	3.7	260	DD	1.6	---	SAN ANTONIA RANCH
	10 21:44:34	36.766	114.774	---	7.00**	---	281	CD	1.7	---	WILDCAT WASH SE
	14 0:21:40	37.385	116.060	0.6	0.96	1.4	75	BC	1.2	---	WHEELBARROW PEAK NE
	14 6: 5:58	37.108	116.754	0.5	17.02	1.8	105	BB	1.4	---	SPRINGDALE

# 1980 LOCAL HYPOCENTER SUMMARY

	DATE - TIME (UTC)	LATITUDE (DEG. N)	LONGITUDE (DEG. W)	HORIZ ERROR (KM)	DEPTH (KM)	VERT ERROR (KM)	AZI CAP (DEG)	QUAL	Md	Mb1g	QUADRANGLE
DEC	14 11:12:54	36.541	116.631	1.0	-0.82	2.0	103	AC	1.1	---	BIG DUME
	15 2:34:47	36.646	115.417	0.3	9.41	1.0	105	AC	1.3	---	BLACK HILLS NW
	16 21:17:41	37.205	115.869	---	7.80**	---	303	AD	0.9	---	PAPOOSE LAKE NE
	17 7:28:51	37.036	116.211	---	2.04	---	196	AD	1.1	---	TIPPIPAH SPRING
	17 15:23:52	37.326	116.304	0.7	-0.30*	---	48	CC	2.2	---	DEAD HORSE FLAT
	17 15:25:45	37.353	116.319	0.4	2.15*	---	54	CC	2.3	---	DEAD HORSE FLAT
	17 15:51:31	37.387	117.232	0.3	21.35	0.3	83	AA	2.7	---	STONEWALL PASS
	17 16: 1:18	36.958	115.747	0.0	4.86*	---	84	CC	2.5	---	QUARTZ PEAK NW
	18 9:30:11	36.967	116.838	3.2	15.14	1.9	220	CD	1.0	---	BLACK BUTTE
	19 14:47:33	36.354	116.308	---	7.00**	---	137	AD	1.2	---	ASH MEADOWS
	19 19:10:34	36.939	116.713	0.2	7.94	1.2	119	AC	1.1	---	BARE MTN
	20 9:37:59	36.546	117.528	0.3	0.51	7.8	310	DD	2.3	---	***REGIONAL***
	20 8:47:54	36.527	115.569	1.1	2.27*	---	165	CC	1.3	---	INDIAN SPRINGS SE
	20 1:46:17	36.525	115.573	1.0	8.18	0.2	87	CC	1.3	---	INDIAN SPRINGS SE
	20 6:24:28	36.751	116.006	0.3	0.17	1.1	124	AB	1.0	---	CANE SPRING
	20 18:18:43	36.515	115.583	1.0	1.51	5.7	80	CC	1.4	---	INDIAN SPRINGS SE
	20 18:32:27	36.553	115.569	1.2	1.70*	---	152	CC	1.1	---	INDIAN SPRINGS SE
	21 14:54:45	37.431	114.982	1.4	0.47*	---	178	CC	1.3	---	DELAMAR NW
	21 22:13:45	36.785	116.231	1.1	0.32*	---	100	CD	0.3	---	SKULL MTN
	22 1:34:17	36.545	115.554	0.4	2.34*	---	151	CC	1.1	---	INDIAN SPRINGS SE
	22 1:35:27	37.009	115.430	---	9.71	---	221	AD	0.6	---	DESERT HILLS SW
	22 11:42:54	37.317	116.333	1.3	-0.23*	---	86	CC	1.2	---	DEAD HORSE FLAT
	22 14:42:25	37.222	114.820	3.6	15.17	1.3	203	CD	1.9	---	DELAMAR 3 NE
	23 1:14: 4	36.770	115.991	1.9	0.73*	---	227	CD	0.4	---	FRENCHMAN FLAT
	23 9: 5:25	36.969	117.748	2.1	2.61	3.6	265	BD	1.8	---	DRY MTN
	23 17:35:58	37.354	116.369	1.4	2.14*	---	80	CC	1.7	---	DEAD HORSE FLAT
	26 3:21:45	36.663	115.094	22.1	7.00*	---	202	DD	1.4	---	HAYFORD PEAK
	26 7: 1:18	36.668	115.454	0.6	22.38	0.6	103	AB	1.4	---	BLACK HILLS NW
	26 8:46:31	36.692	116.329	---	3.97	---	191	AD	0.8	---	STRIPED HILLS
	30 12: 9:23	36.616	116.289	---	13.08	---	167	AD	0.5	---	LATHROP WELLS SE
	30 19:45:27	37.316	115.031	0.8	5.45	2.5	200	BD	1.0	---	ALAMO SE

## 1981 LOCAL HYPOCENTER SUMMARY

	DATE - TIME (UTC)	LATITUDE (DEG. N)	LONGITUDE (DEG. W)	HORIZ ERROR (KM)	DEPTH (KM)	VERT ERROR (KM)	AZI GAP (DEG)	QUAL	Md	Mblg	QUADRANGLE
JAN	2 15: 3: 8	35.975	118.345	8.4	8.58	3.9	283	DD	2.5	---	***REGIONAL***
	3 6: 3:57	36.786	115.583	0.8	1.88	3.7	218	BD	1.0	---	HEAVENS WELL
	3 16:18:44	37.479	115.676	23.6	14.38*	---	257	DD	2.4	---	BALD MTN
	3 16:19:36	37.821	115.283	0.5	3.37	3.0	127	BC	2.6	---	***QUAD. NOT LISTED***
	3 18: 4:52	36.697	115.691	0.5	1.12	3.5	73	BC	1.4	---	INDIAN SPRINGS NW
	4 7: 2:41	37.811	115.251	1.2	3.63	6.9	158	CC	1.6	---	***QUAD. NOT LISTED***
	4 11:38:52	37.821	115.297	1.4	-0.01*	---	189	CD	1.3	---	***QUAD. NOT LISTED***
	5 0:34: 2	36.448	116.516	0.3	0.38	5.0	111	BB	2.0	---	RYAN
	5 0:38:14	36.437	116.535	0.6	5.51	3.3	111	BC	1.1	---	RYAN
	5 11:57:23	37.156	116.757	0.6	4.86	5.0	135	BC	1.7	---	SPRINGDALE
	6 2:21: 4	37.318	116.349	3.0	2.34*	---	194	CD	1.3	---	DEAD HORSE FLAT
	6 6: 8:26	37.159	116.936	0.6	7.08	1.8	176	AD	1.6	---	SPRINGDALE
	6 20:49:45	38.389	117.283	2.2	2.98	2.2	267	BD	2.4	---	SAN ANTONIA RANCH
	9 5:26:35	36.102	117.778	4.6	0.68*	---	281	CD	1.5	---	HAIWEE RESERVOIR
	9 22:29:50	36.771	116.286	1.6	0.97*	---	181	CD	0.7	---	JACKASS FLATS
	10 5:29:25	37.439	117.566	4.6	0.58*	---	238	CD	2.3	---	MAGRUDER MTN
	12 17:16:29	36.421	114.654	5.1	7.08	2.0	289	DD	2.5	---	MUDDY PEAK
	16 0:14:40	37.231	115.024	0.3	8.32	1.1	157	AC	2.7	---	LOWER PAHRANAGAT LAKE
	23 4:41:12	37.148	117.387	0.2	10.28	0.5	110	AB	2.7	---	UBEHEBE CRATER
	28 1: 5:22	37.152	117.386	0.6	9.23	2.0	125	BB	1.7	---	UBEHEBE CRATER
	28 6:55:58	37.156	117.386	0.4	5.89	1.3	123	AC	1.7	---	UBEHEBE CRATER
FEB	8 8:21:21	36.472	115.187	3.1	1.88	2.3	229	CD	1.9	---	GASS PEAK NW
	12 0:39:14	38.302	117.203	9.6	4.18	8.0	272	DD	1.9	---	BAXTER SPRING
	13 18: 0: 0	36.971	116.194	0.6	-0.07	0.9	67	BB	1.7	---	MINE MTN
	15 20: 0:47	36.318	117.259	1.7	5.86	0.7	281	BD	2.0	---	SAN ANTONIA RANCH
	16 20:12:18	36.275	114.268	5.4	-0.86	8.7	288	DD	2.2	---	***REGIONAL***
	22 14:47: 0	36.241	115.058	3.3	7.08	2.1	259	CD	1.8	---	LAS VEGAS NE
	22 18:37: 2	35.804	114.839	4.6	0.28	4.0	304	CD	1.9	---	BOULDER CITY SE
	26 22:21: 8	36.506	115.076	9.1	5.86	2.4	241	DD	1.8	---	HAYFORD PEAK
	28 3:23:54	37.189	114.781	1.1	5.68*	---	199	CD	1.9	---	DELMAR 3 NE
MAR	2 15:26:24	37.185	117.846	0.7	5.29	2.2	223	BD	1.6	---	WAUCOBA SPRING
	3 23:14:32	37.267	115.052	2.4	5.55	4.5	182	BD	1.8	---	ALAMO SE
	5 19:41:52	36.532	116.364	0.4	-1.14*	---	184	CC	1.5	---	LATHROP WELLS SE
	10 23:27:56	37.155	116.917	0.3	6.58	8.8	51	AC	2.2	---	SPRINGDALE
	14 1: 9: 5	36.534	116.369	0.4	0.81*	---	186	CC	1.4	---	LATHROP WELLS SE
	16 13:10:59	36.543	115.558	0.3	-0.92	8.9	87	CC	2.4	---	INDIAN SPRINGS SE
	28 23:11:16	37.078	116.178	0.9	4.78	2.6	97	BB	1.6	---	TIPPIPAH SPRING
APR	29 11:19:45	36.538	117.974	3.0	2.56	3.6	241	CD	1.8	---	NEW YORK BUTTE
	2 19:40: 2	38.343	117.296	3.2	2.74	3.3	257	CD	2.3	---	SAN ANTONIA RANCH
	3 0:53:43	38.293	117.239	6.0	2.56	6.1	257	DD	2.0	---	BAXTER SPRING
	3 10:43:58	37.571	116.465	2.1	6.64*	---	127	CC	1.7	---	QUARTZITE MTN
	5 16:34:17	36.042	117.740	7.9	2.58*	---	272	DD	2.0	---	COSO PEAK
	6 18:19:48	36.448	114.473	4.1	3.55	2.2	273	CD	2.2	---	***REGIONAL***
	7 23: 3:28	37.155	116.919	0.2	7.74	2.1	75	BC	2.0	---	SPRINGDALE
	8 4:38:32	37.156	116.914	0.3	5.83	1.7	79	AC	1.9	---	SPRINGDALE
	8 4:44:53	37.155	116.911	0.5	6.08	1.6	75	AC	2.0	---	SPRINGDALE
	9 13:36: 6	36.825	116.267	0.4	5.34	1.3	72	AB	0.9	---	JACKASS FLATS
	9 23:44:36	37.062	116.051	0.7	-1.12*	---	113	CC	1.7	---	YUCCA FLAT
	10 11:56:59	36.925	116.126	0.8	1.05	2.8	99	BB	1.2	---	MINE MTN
	11 1:37:48	36.532	116.379	0.5	4.38	6.9	135	CC	1.6	---	LATHROP WELLS SW
	12 5:33: 9	36.603	116.041	0.3	5.33	1.3	127	AB	1.3	---	SPECTER RANGE SE
	12 8:15:24	36.771	116.233	0.5	0.33	0.6	61	AA	1.8	---	SKULL MTN
	13 20:21:28	36.895	116.471	0.5	4.49	0.7	135	AC	0.7	---	TOPOPAH SPRING NW
	17 1:23:48	37.590	115.634	1.3	0.10	0.8	112	BB	2.1	---	TEMPIUTE MTN
	17 1:42:10	36.524	116.374	0.6	-0.15*	---	181	CC	1.5	---	LATHROP WELLS SE
	17 2:15:25	37.614	115.636	1.0	0.20	0.7	137	BC	1.8	---	TEMPIUTE MTN
	17 5:31: 1	37.155	117.379	---	11.68	---	121	AD	0.8	---	UBEHEBE CRATER
	17 8:38:33	37.287	116.728	0.4	2.60*	---	89	CC	1.3	---	BLACK MTN SW
	19 2: 3:32	37.423	115.155	---	5.83	---	194	BD	1.1	---	ASH SPRINGS
	20 12:29:50	36.944	117.633	0.8	2.64	2.3	221	BD	1.5	---	DRY MTN
	20 18: 7:24	37.658	115.651	---	7.00**	---	250	CD	1.0	---	TEMPIUTE MTN
	21 9: 3: 9	36.666	115.774	0.9	2.81	0.2	267	AD	0.9	---	MERCURY NE
	21 11:10:43	37.735	115.736	1.9	8.65	4.4	176	CC	1.1	---	TEMPIUTE MTN
	22 16: 2: 2	37.067	117.406	0.5	5.49	1.2	169	AC	2.2	---	UBEHEBE CRATER
	24 16:35: 5	36.719	116.141	0.4	1.42	1.3	72	AC	1.4	---	SPECTER RANGE NW
	24 16:39:19	36.725	116.140	0.4	-0.23*	---	71	CC	1.6	---	SPECTER RANGE NW

# 1981 LOCAL HYPOCENTER SUMMARY

DATE - TIME (UTC)	LATITUDE (DEG. N)	LONGITUDE (DEG. W)	HORIZ ERROR (KM)	DEPTH (KM)	VERT ERROR (KM)	AZI CAP (DEG)	QUAL	Md	Mbig	QUADRANGLE
APR 25 15:28:49	36.788	116.087	0.5	0.00*	---	86	CC	1.8	---	CANE SPRING
28 20:34:29	36.714	116.141	0.4	5.22	2.1	43	BC	1.8	---	SPECTER RANGE NW
28 19:13:39	36.905	116.254	2.4	16.07	3.2	191	BD	0.8	---	TOPOPAH SPRING
30 16:55:23	36.717	116.144	---	-0.01	---	172	AD	1.0	---	SPECTER RANGE NW
MAY 2 21:53:43	37.120	117.334	0.4	7.07	1.5	111	AB	1.6	---	UBEHEBE CRATER
3 14:47:34	37.387	117.358	0.5	2.09	1.1	132	AB	1.8	---	GOLD POINT
3 15:38:12	36.647	116.340	1.3	7.00	1.6	178	BC	1.2	---	STRIPED HILLS
3 16:49:50	37.382	117.357	---	7.00**	---	180	BD	1.0	---	GOLD POINT
3 16:56:42	37.272	117.397	---	0.95	---	164	CD	1.2	---	GOLD POINT SW
3 17: 0:17	37.298	117.363	0.5	5.65	1.7	110	BB	2.0	---	GOLD POINT
3 17: 8:52	37.325	117.322	---	1.92	---	333	AD	1.6	---	GOLD POINT
3 17:16:08	37.341	117.313	---	5.69	---	178	AD	1.2	---	GOLD POINT
4 1:29:48	36.991	115.702	---	7.00**	---	191	AD	1.7	---	QUARTZ PEAK NW
5 7:52: 9	37.297	117.379	1.8	5.47	5.7	121	CB	1.7	---	GOLD POINT SW
5 13:59: 6	36.377	118.092	3.7	4.65	1.7	203	CD	2.7	---	***REGIONAL***
5 14:34:53	36.387	118.062	1.8	3.05	1.8	253	BD	2.6	---	***REGIONAL***
5 20: 9:17	37.315	117.352	---	2.54	---	143	AD	1.1	---	GOLD POINT
5 20:38:17	37.302	117.359	---	7.00**	---	181	BD	1.1	---	GOLD POINT
7 4:29:58	37.122	117.337	0.8	5.01	3.0	156	BC	1.4	---	UBEHEBE CRATER
7 14:48:27	37.417	117.240	0.5	0.33*	---	215	CD	1.5	---	STONEWALL PASS
10 17:28:48	37.139	117.415	0.8	7.66	2.1	149	BC	2.0	---	UBEHEBE CRATER
12 0:40:55	35.951	117.322	2.0	6.16	2.6	261	BD	1.8	---	TRONA
12 11:55: 4	37.139	116.600	0.5	5.68	6.5	174	CC	1.3	---	THIRSTY CANYON NE
12 13:20:36	37.029	117.445	0.8	2.68	2.3	182	BD	1.8	---	UBEHEBE CRATER
18 18:48:18	36.690	116.299	0.4	-0.23	0.3	115	AB	1.1	---	STRIPED HILLS
19 12:35:58	36.671	116.266	---	4.77	---	251	AD	0.8	---	STRIPED HILLS
20 6:50:17	36.621	116.021	5.1	2.74	9.6	226	DD	1.5	---	SPECTER RANGE SE
23 13:34:36	36.756	116.221	---	7.00	---	226	AD	0.8	---	SKULL MTN
23 18:50:22	36.150	117.848	3.5	8.90	1.4	265	CD	2.5	---	HAIWEE RESERVOIR
25 4:59:20	36.102	117.934	2.7	5.97	0.8	285	CD	2.5	---	HAIWEE RESERVOIR
25 19:39: 1	36.154	117.818	7.6	8.38	3.2	260	DD	2.3	---	HAIWEE RESERVOIR
28 13:22:54	37.132	117.286	---	2.71	---	132	AD	1.6	---	UBEHEBE CRATER
29 5:22:54	36.664	115.703	0.3	12.93	0.2	293	AD	1.0	---	INDIAN SPRINGS NW
29 9:13:16	37.149	117.403	0.7	5.42	4.6	132	BC	1.6	---	UBEHEBE CRATER
29 11: 7:55	36.655	116.329	---	2.56	---	120	AD	1.0	---	STRIPED HILLS
30 6:15:16	37.322	115.399	0.5	6.38	2.9	145	BC	2.5	---	CUTLER RESERVOIR
JUN 31 2:55: 3	37.320	115.377	0.6	2.45*	---	134	CC	2.5	---	CUTLER RESERVOIR
2 0:31:19	37.990	117.112	0.9	28.57	0.6	216	AD	1.3	---	MUD LAKE
3 13:19:50	37.134	115.422	1.1	21.68	0.3	196	BD	1.3	---	DESERT HILLS NW
4 3: 0: 2	36.585	115.991	0.5	16.32	0.4	173	AC	1.9	---	MERCURY SW
4 11: 5:23	36.707	116.203	0.3	0.66	0.3	75	AA	1.4	---	STRIPED HILLS
4 12:53:41	37.346	115.414	0.7	3.13*	---	172	CC	2.0	---	CUTLER RESERVOIR
6 13: 5: 8	36.462	116.025	2.1	-0.09*	---	259	CD	1.1	---	MT SCHADER
6 15:39:57	37.194	117.236	---	3.99	---	153	AD	0.8	---	BONNIE CLAIRE NW
7 18:24: 0	36.631	116.279	38.4	4.39*	---	265	DD	0.8	---	STRIPED HILLS
8 14:44:20	36.951	116.962	0.5	-0.31	0.4	148	AD	1.3	---	BULLFROG
10 7:31:35	36.414	117.246	0.3	0.67	3.1	227	BD	1.4	---	EMIGRANT CANYON
10 19:52:10	37.156	117.408	1.3	7.98	7.1	131	CD	1.4	---	UBEHEBE CRATER
11 0:30:34	37.164	117.399	---	5.28	0.2	125	AD	1.1	---	UBEHEBE CRATER
11 18: 0:19	38.380	115.898	2.1	16.40	1.7	254	BD	2.8	---	***QUAD. NOT LISTED***
13 17:47: 2	37.308	116.302	1.5	4.04	7.4	114	CC	1.1	---	DEAD HORSE FLAT
15 17:57:58	36.742	116.276	0.4	6.09	0.7	73	AA	1.2	---	STRIPED HILLS
16 5:25:29	36.770	116.255	0.4	3.81	1.1	91	AB	1.0	---	JACKASS FLATS
17 1:46:52	36.770	116.250	0.3	0.98	0.7	77	AA	0.6	---	JACKASS FLATS
17 3:28:35	36.775	116.252	0.2	2.11	0.4	90	AA	1.0	---	JACKASS FLATS
17 9: 4:41	36.727	116.262	0.3	9.50	0.2	104	AB	0.5	---	STRIPED HILLS
18 15: 1:20	37.361	117.150	0.6	0.46*	---	163	CC	1.3	---	SCOTTYS JUNCTION SW
18 17: 0: 0	36.987	116.175	0.5	-0.53	0.7	77	BB	1.7	---	MINE MTN
19 4:48:28	36.769	115.398	0.4	3.43*	---	113	CC	1.2	---	DOG BONE LAKE SOUTH
21 4:51:35	37.011	116.141	1.7	-0.68	1.6	208	BD	1.0	---	TIPPICAN SPRING
22 5:33:42	36.849	117.470	1.0	5.60	1.5	197	AD	1.2	---	TIN MTN
22 9:22:39	37.387	115.630	---	3.93	---	151	BD	1.1	---	BALD MTN
22 18:31:44	36.748	116.265	0.4	4.17	0.5	174	AD	0.6	---	STRIPED HILLS
23 15:17:31	37.122	117.047	---	7.00**	---	219	AD	0.7	---	BONNIE CLAIRE SE
24 1:11:49	37.577	116.455	0.4	9.22	2.4	90	BC	1.1	---	QUARTZITE MTN
25 15:46: 5	36.477	115.887	0.6	9.64	2.4	136	BC	1.2	---	MT STIRLING

## 1981 LOCAL HYPOCENTER SUMMARY

DATE - TIME (UTC)	LATITUDE (DEG. N)	LONGITUDE (DEG. W)	HORIZ ERROR (KM)	DEPTH (KM)	VERT ERROR (KM)	AZI GAP (DEG)	QUAL	Md	Mb1g	QUADRANGLE
JUN 26 7:15:11	36.615	116.259	---	7.00**	---	216	AD	0.4	---	LATHROP WELLS SE
27 13:44:33	36.634	116.190	1.1	6.29	1.2	236	BD	0.5	---	SKULL MTN
27 20:43:21	36.662	116.197	0.6	4.17	0.9	61	BA	1.2	---	SKULL MTN
27 21:50:5	36.736	116.169	---	0.35	---	302	A	0.6	---	SPECTER RANGE NW
27 23:50:29	37.148	116.943	2.6	2.09	3.9	226	CD	1.1	---	SPRINGDALE
28 2:42:9	36.968	115.903	0.4	4.98	5.4	148	CC	1.3	---	PLUTONIUM VALLEY
28 23:49:3	36.691	117.708	2.4	7.00	1.5	262	BD	1.6	---	COSO PEAK
29 7:9:43	37.321	117.000	0.3	-0.30*	---	72	CC	1.5	---	SCOTTYS JUNCTION
29 22:17:50	36.722	115.766	2.7	6.93	3.3	213	CD	1.2	---	MERCURY NE
30 0:1:1	36.584	116.186	---	7.00**	---	333	BD	0.3	---	SPECTER RANGE SW
30 6:29:37	36.604	115.662	---	7.00**	---	342	BD	0.6	---	INDIAN SPRINGS
30 12:6:59	36.613	116.320	0.6	7.43	0.6	201	AD	0.8	---	LATHROP WELLS SE
JUL 3 10:31:52	37.148	116.590	0.3	8.62	4.2	103	BC	1.5	---	THIRSTY CANYON NE
4 0:4:46	37.327	116.298	0.3	2.86	1.6	76	AC	1.7	---	DEAD HORSE FLAT
4 5:2:29	37.153	116.946	0.7	9.66	3.1	116	BC	1.8	---	SPRINGDALE
4 5:31:55	37.167	116.707	5.4	34.52	6.9	212	DD	0.6	---	THIRSTY CANYON NW
4 5:53:24	37.154	116.937	0.5	1.93	2.2	121	BC	0.6	---	SPRINGDALE
4 11:25:38	37.137	116.916	1.7	8.66*	---	63	CC	0.6	---	SPRINGDALE
5 16:10:44	36.610	115.756	0.3	-0.33*	---	118	CC	1.1	---	MERCURY SE
9 17:36:14	36.113	115.423	1.5	0.23*	---	272	CD	1.7	---	BLUE DIAMOND
12 2:42:31	37.150	116.943	0.3	7.00	2.4	120	BC	1.1	---	SPRINGDALE
14 15:47:36	37.161	117.407	0.4	5.99	2.1	129	BC	1.5	---	UBEHEBE CRATER
14 17:8:49	37.159	117.405	0.3	6.04	0.8	111	AC	1.5	---	UBEHEBE CRATER
15 1:41:4	36.531	116.606	0.2	14.59	0.9	121	AB	1.8	---	BIG DUNE
15 2:23:31	36.519	116.601	0.9	2.45*	---	235	CD	1.6	---	BIG DUNE
15 4:37:16	36.532	116.607	0.2	11.03	0.7	120	AB	1.5	---	BIG DUNE
15 5:12:31	36.536	116.611	0.5	0.53	2.5	120	BC	0.9	---	BIG DUNE
16 15:11:34	37.415	117.703	---	11.07	---	167	AD	1.2	---	MAGRUDER MTN
16 15:15:4	37.078	116.033	1.1	-0.58*	---	232	CD	2.0	---	YUCCA FLAT
18 21:22:8	35.813	117.901	11.6	7.00	4.9	289	DD	1.6	---	LITTLE LAKE
21 15:36:30	36.723	116.063	0.4	-0.16*	---	124	CC	0.9	---	CAMP DESERT ROCK
22 2:31:20	37.228	115.862	0.3	2.06	0.7	154	AC	0.6	---	PAPOOSE LAKE NE
22 4:7:59	37.190	116.989	0.3	6.61	2.0	87	AC	1.6	---	SPRINGDALE
24 12:2:20	37.355	117.697	0.8	1.09	3.2	132	BC	2.3	---	MAGRUDER MTN
24 20:47:59	36.712	116.068	0.8	0.23*	---	124	CC	1.0	---	CAMP DESERT ROCK
27 10:45:31	36.705	115.850	2.3	0.19*	---	271	CD	0.7	---	MERCURY NE
27 20:20:32	36.424	115.535	1.7	5.04	6.1	122	CC	1.3	---	CHARLESTON PEAK
28 0:3:56	37.677	116.286	2.1	14.98	6.0	269	CD	0.7	---	QUARTZITE MTN
28 7:49:10	36.636	115.949	0.8	0.46	1.2	149	AC	0.6	---	MERCURY
AUG 1 4:26:41	36.703	116.285	0.4	5.83	0.8	78	AA	0.8	---	STRIPED HILLS
2 12:37:35	37.079	115.900	0.6	4.19*	---	146	CC	0.6	---	PAIUTE RIDGE
2 21:52:2	37.222	117.319	---	0.12	---	136	AD	1.0	---	UBEHEBE CRATER
5 16:56:11	35.346	116.602	11.1	7.00	3.0	290	DD	2.2	---	***REGIONAL***
6 11:25:31	36.835	116.179	0.5	4.89	2.8	141	BC	0.9	---	SKULL MTN
6 18:57:48	36.626	116.255	1.5	5.11*	---	220	CD	1.3	---	STRIPED HILLS
7 9:39:48	37.156	116.323	0.3	-0.62*	---	132	CC	1.1	---	AMMONIA TANKS
7 18:57:49	36.657	116.309	---	0.47	---	316	AD	1.2	---	STRIPED HILLS
13 20:31:56	37.224	116.962	---	11.79	---	244	AD	1.7	---	SPRINGDALE
16 0:16:9	36.710	116.325	0.8	2.60	1.4	111	AB	---	0.2	STRIPED HILLS
16 11:24:9	36.499	116.300	---	0.86	---	175	AD	1.3	---	ASH MEADOWS
23 2:9:17	37.156	116.941	0.3	6.37	2.5	60	BC	1.5	---	SPRINGDALE
25 18:43:30	36.670	117.102	2.2	4.87	1.4	284	BD	2.0	---	***REGIONAL***
26 4:10:21	36.716	117.326	2.9	1.53	6.1	172	CD	-0.1	---	MARBLE CANYON
26 5:18:35	36.692	116.053	0.3	-0.44*	---	143	CC	0.9	---	CAMP DESERT ROCK
26 16:10:6	36.384	117.566	0.1	24.62*	---	250	DD	1.3	---	DARWIN
26 16:37:40	36.672	116.240	1.7	6.53	4.9	97	BB	1.0	---	SPECTER RANGE NW
27 0:30:18	37.245	115.922	1.0	5.31	3.6	157	BC	-0.2	---	JANGLE RIDGE
SEP 1 0:3:19	37.655	115.651	---	7.00**	---	249	CD	1.4	---	TEMPUTE MTN
1 16:19:36	37.422	117.338	0.4	4.84	2.3	156	BC	1.2	---	MOUNT JACKSON
7 3:51:52	37.358	115.023	2.1	3.62	3.2	203	BD	1.3	---	ALAMO SE
9 18:46:11	36.752	117.065	4.2	4.08	3.0	278	CD	2.0	---	***REGIONAL***
12 1:1:55	36.764	116.275	---	39.08	---	172	BD	---	0.2	JACKASS FLATS
12 21:23:35	35.995	116.768	4.9	14.27	5.3	200	CD	2.3	---	WINGATE WASH
15 4:56:48	37.012	116.305	0.2	5.34	1.6	116	AC	0.6	---	TIMBER MTN
15 6:17:27	37.017	116.384	0.3	7.64	1.6	106	AB	0.6	---	TIMBER MTN
15 6:44:50	37.013	116.388	0.2	4.94	2.1	107	BC	0.7	---	TIMBER MTN

# 1981 LOCAL HYPOCENTER SUMMARY

	DATE - TIME (UTC)	LATITUDE (DEG. N)	LONGITUDE (DEG. W)	HORIZ ERROR (KM)	DEPTH (KM)	VERT ERROR (KM)	AZI GAP (DEG)	QUAL	Md	Mbig	QUADRANGLE
SEP	15 7:52:49	37.015	116.385	0.3	2.70	0.7	117	AC	0.8	---	TIMBER MTN
	16 4:15:55	37.011	116.388	0.2	4.09	2.8	108	BC	0.7	---	TIMBER MTN
	16 11: 8:23	37.014	116.391	0.5	7.51	3.1	160	BC	0.6	---	TIMBER MTN
	21 4:59:25	37.014	116.379	0.3	5.97	1.5	117	AC	1.0	---	TIMBER MTN
	21 5:16:18	37.016	116.384	0.8	4.56	3.7	224	BD	---	0.2	TIMBER MTN
	23 9:35:40	37.109	117.077	0.3	8.26	1.0	121	AB	0.9	---	BONNIE CLAIRE SE
	24 2:24:43	37.223	116.909	---	20.23	---	206	AD	0.5	---	SPRINGDALE
	24 2:35:55	37.194	116.978	0.4	5.82	4.5	88	BC	1.3	---	SPRINGDALE
	25 17:59:44	37.885	116.925	6.9	1.24*	---	263	DD	1.4	---	CACTUS PEAK
	26 10:48:53	36.899	115.628	4.2	-0.38*	---	282	CD	0.9	---	INDIAN SPRINGS NW
	28 17:32:36	37.702	117.402	0.9	7.00	1.0	183	BD	1.5	---	SPLIT MTN
	28 17:48:31	37.711	117.399	0.9	8.44	1.1	177	BC	1.4	---	SPLIT MTN
OCT	28 18:18:00	37.702	117.385	2.8	6.12	2.4	229	CD	1.4	---	SPLIT MTN
	5 20:17:31	37.134	116.213	0.3	4.34	2.2	76	BC	---	2.0	RAINIER MESA
	5 20:42: 7	37.147	116.214	0.2	5.76	0.8	124	AC	---	0.8	RAINIER MESA
	5 21:12: 4	37.143	116.215	0.2	4.62	1.0	121	AC	0.6	0.9	RAINIER MESA
	5 21:31:20	37.144	116.218	0.2	5.20	0.7	121	AC	---	0.9	RAINIER MESA
	6 1:24: 4	37.185	117.309	21.5	7.00*	---	214	DD	0.8	---	UBEHEBE CRATER
	6 5:42:31	36.807	115.942	---	2.94	---	318	CD	1.0	---	FRENCHMAN FLAT
	6 21:24: 0	36.847	115.215	---	7.00**	---	246	AD	1.2	---	HAYFORD PEAK
	7 2:28:16	37.133	117.338	0.6	5.86	2.0	190	BD	0.3	---	UBEHEBE CRATER
	7 12:54: 3	37.101	116.162	0.9	4.21	2.7	150	BC	0.2	---	TIPPICAH SPRING
	8 12:19:27	36.019	113.255	---	2.90	---	336	AD	1.8	---	***REGIONAL***
	8 16:48:58	36.409	116.717	86.4	7.00*	---	350	DD	0.8	---	RYAN
	9 2:27:30	36.784	115.984	0.6	11.27	0.8	237	AD	0.3	---	FRENCHMAN FLAT
	9 3:27: 0	36.173	114.999	2.7	13.22	0.9	276	CD	1.0	---	FRENCHMAN MTN
	9 15:11:59	37.339	114.731	1.1	10.61	1.2	246	BD	0.6	---	ELGIN SW
	9 18:58:43	37.376	115.691	84.6	2.01*	---	107	DC	0.3	---	BALD MTN
	10 12:21:56	37.126	117.470	52.5	1.94*	---	288	DD	0.3	---	UBEHEBE CRATER
	13 14:47:54	37.061	116.951	0.3	8.27	1.5	142	AC	2.6	---	SPRINGDALE
	13 14:51:58	37.064	116.947	0.4	4.73	2.1	94	BC	1.1	---	SPRINGDALE
	13 14:56:14	37.062	116.945	0.4	0.45	0.7	94	AC	1.0	---	SPRINGDALE
	13 15: 8:16	37.067	116.950	0.3	-0.11	0.5	95	AC	0.7	---	SPRINGDALE
	13 19:51:12	37.059	116.951	0.2	6.27	0.7	45	AB	2.2	---	SPRINGDALE
	14 2:33:12	37.061	116.940	0.4	3.86	2.5	147	BC	0.4	---	SPRINGDALE
	14 3:11:42	37.062	116.951	0.3	-0.73	0.5	94	AC	0.7	---	SPRINGDALE
	14 4:31:59	37.064	116.951	0.3	5.08	1.2	63	AC	1.5	---	SPRINGDALE
	14 8:45:47	37.059	116.951	0.2	5.59	0.9	62	AC	1.9	---	SPRINGDALE
	14 9:15:16	37.065	116.951	0.2	0.92	0.4	63	AC	1.9	---	SPRINGDALE
	14 12:28:46	37.058	116.958	0.2	6.90	0.9	118	AB	1.0	---	SPRINGDALE
	14 15:51:34	37.064	116.951	0.2	4.45	1.2	63	AC	0.9	---	SPRINGDALE
	14 21:57: 4	36.682	115.769	60.6	7.00*	---	322	DD	-0.2	---	MERCURY NE
	14 22:23:10	37.054	116.955	0.3	5.47	0.9	72	AB	1.1	---	SPRINGDALE
	15 0:27:19	36.442	118.493	---	7.00**	---	256	AD	---	0.2	ASH MEADOWS
	15 0:52:50	37.095	116.972	0.2	5.25	0.9	106	AC	0.8	---	SPRINGDALE
	15 2:23:49	37.068	116.945	0.4	9.06	2.0	50	BB	1.6	---	SPRINGDALE
	15 4:21: 9	37.055	116.955	0.3	9.20	0.9	64	AB	2.5	---	SPRINGDALE
	15 7:19: 5	37.062	116.959	0.3	15.78	1.2	109	AC	0.9	---	SPRINGDALE
	15 7:22:50	37.069	116.949	0.3	8.11	0.8	64	AB	1.1	---	SPRINGDALE
	15 18:43:13	37.058	116.955	0.2	5.17	0.7	52	AC	1.3	---	SPRINGDALE
	15 19:24: 3	36.904	116.150	72.6	2.03*	---	220	DD	0.2	---	MINE MTN
	15 21:59:36	36.612	116.855	64.6	7.00*	---	345	DD	0.1	---	CHLORIDE CLIFF
	16 1:47:42	37.065	116.960	0.2	0.08	0.4	66	AC	1.1	---	SPRINGDALE
	16 2:33:41	36.529	115.821	0.4	9.25	1.3	133	AB	0.3	---	MERCURY SE
	16 5: 9:13	37.047	116.941	0.3	-0.19	0.3	143	AC	1.0	---	SPRINGDALE
	16 13:37:39	36.243	116.583	1.6	2.91	5.4	264	CD	1.9	---	STONE CABIN VALLEY
	17 1:12: 1	37.051	116.952	0.4	7.58	1.0	88	BB	0.8	---	SPRINGDALE
	17 17:59:50	36.440	116.937	0.3	8.20	0.9	78	AB	1.3	---	FURNACE CREEK
	17 21:16: 4	36.442	116.954	0.6	13.23	1.4	84	AB	1.0	---	FURNACE CREEK
	18 0:51:33	37.069	116.956	0.2	11.04	1.6	84	AC	0.8	---	SPRINGDALE
	19 0:16: 9	36.615	116.256	0.3	5.07	0.9	150	AC	0.5	---	LATHROP WELLS SE
	19 1:43:48	37.064	116.953	0.3	11.41	1.7	93	AC	0.8	---	SPRINGDALE
	19 18:34:48	37.203	116.317	0.3	6.08	0.9	74	AB	0.6	---	DEAD HORSE FLAT
	19 22:42:30	37.118	115.051	45.4	7.00*	---	268	DD	-0.5	---	LOWER PAHRANAGAT LAKE SE
	19 23:30:30	36.987	116.401	82.7	3.00*	---	146	DC	-0.5	---	TOPOPAH SPRING NW
	20 0:53: 6	36.525	116.683	1.3	-0.91	1.1	268	BD	2.3	---	***REGIONAL***



## 1981 LOCAL HYPOCENTER SUMMARY

DATE - TIME (UTC)	LATITUDE (DEG. N)	LONGITUDE (DEG. W)	HORIZ ERROR (KM)	DEPTH (KM)	VERT ERROR (KM)	AZI GAP (DEG)	QUAL	Md	Mb1g	QUADRANGLE
OCT 20 5:12:45	37.041	115.172	0.4	5.01	2.4	147	BC	2.0	---	LOWER PAHRANAGAT LAKE SW
20 9:28:53	37.029	115.168	0.4	5.30	2.7	148	BC	1.2	---	LOWER PAHRANAGAT LAKE SW
21 22:18:19	35.478	116.333	99.9	16.61*	---	348	DD	0.7	---	***REGIONAL***
22 19:10:4	37.064	116.946	0.4	2.85	1.2	94	AC	1.0	---	SPRINGDALE
22 23:35:29	35.452	118.194	1.8	2.61	1.1	309	BD	1.8	---	***REGIONAL***
23 6:16:45	37.706	115.149	0.6	5.47	2.3	127	BC	0.8	---	FOSSIL PEAK
24 1:45:14	37.071	116.953	0.2	8.05	0.6	120	AB	0.9	---	SPRINGDALE
24 4:45:15	36.579	115.517	---	12.77	---	312	AD	---	0.1	INDIAN SPRINGS SE
24 16:29:11	37.823	115.533	0.2	-0.81	5.7	99	CD	1.2	---	WORTHINGTON MTNS
24 16:56:15	36.715	116.287	0.6	9.23	0.5	249	AD	0.1	---	STRIPED HILLS
24 21:34:46	37.061	116.949	0.3	6.58	0.9	94	AB	2.0	---	SPRINGDALE
25 22:18:31	37.000	117.505	0.5	7.87	2.1	176	BC	0.7	---	LAST CHANCE RANGE
26 1:25:8	36.748	116.192	0.3	0.84*	---	164	CB	---	0.2	SPECTER RANGE NW
26 4:50:29	36.759	116.234	0.7	3.82	1.7	103	AB	0.1	---	SKULL MTN
26 15:18:15	37.656	116.727	---	7.00**	---	289	DD	-0.1	---	MELLAN
26 15:23:26	37.663	115.632	---	2.09	---	173	AD	0.0	---	TEMPIUTE MTN
27 0:24:14	37.068	116.944	0.2	6.93	1.0	64	AB	1.0	---	SPRINGDALE
27 0:27:4	36.696	115.811	48.8	11.84*	---	104	DB	1.0	---	MERCURY NE
27 0:31:18	36.859	115.697	0.5	2.07	3.3	179	BD	0.3	---	QUARTZ PEAK SW
27 3:16:8	36.186	117.626	0.7	5.97*	---	266	CD	1.4	---	COSO PEAK
27 15:24:14	37.521	116.537	---	7.00**	---	190	AD	-0.4	---	MELLAN
28 5:9:56	36.999	116.193	0.3	8.11	0.7	148	AC	0.2	---	MINE MTN
28 15:8:47	37.953	117.009	---	7.00**	---	294	AD	0.0	---	MUD LAKE
29 1:47:42	36.858	116.163	0.5	8.43	0.6	120	AB	0.4	---	SKULL MTN
29 13:50:00	36.592	116.218	0.4	-0.48	0.6	78	AC	0.3	---	SPECTER RANGE SW
29 17:49:34	38.005	115.165	0.6	10.24	1.3	237	AD	1.0	---	TIMBER MTN PASS WEST
30 6:42:00	37.078	116.221	0.9	7.12	0.8	184	AD	0.7	---	TIPPICAH SPRING
30 12:27:56	37.253	117.566	0.4	7.77	0.6	92	AB	1.2	---	WAGRUDE MTN
30 15:19:14	36.787	117.087	---	7.00**	---	350	DD	0.7	---	GRAPEVINE PEAK
NOV 2 5:50:30	35.986	117.063	4.0	17.10	2.2	277	CD	1.7	---	MANLY PEAK
5 1:39:42	36.032	117.698	0.5	5.99	0.5	266	AD	1.5	---	COSO PEAK
5 2:11:42	36.947	116.404	3.7	20.88	1.4	313	CD	0.7	---	TOPOPAH SPRING NW
5 8:42:50	37.156	115.076	0.7	7.17	0.7	265	AD	0.7	---	LOWER PAHRANAGAT LAKE
6 6:52:30	37.500	118.029	1.2	5.23	1.8	268	BD	1.0	---	***REGIONAL***
6 21:12:24	37.116	117.337	0.3	9.54	1.1	113	AB	0.6	---	UBEHEBE CRATER
7 13:26:14	36.373	117.917	0.5	13.50	0.6	245	AD	1.5	---	KEELER
8 6:9:43	36.335	115.988	0.2	4.51	3.7	123	BC	1.1	---	MT STIRLING
8 14:42:3	37.057	116.954	0.4	2.69	1.1	85	AC	1.3	---	SPRINGDALE
9 0:24:55	37.026	116.216	0.7	4.39	1.0	84	BA	0.9	---	TIPPICAH SPRING
9 3:34:37	37.105	117.062	0.5	8.47	2.1	100	BB	1.1	---	BONNIE CLAIRE SE
9 15:48:16	36.521	118.003	1.6	2.64	4.5	262	CD	2.1	---	***REGIONAL***
10 15:45:39	37.277	115.051	1.0	-0.65	0.9	211	CD	1.4	---	ALAMO SE
10 23:42:20	37.076	116.952	0.3	4.89	1.3	64	BC	1.0	---	SPRINGDALE
11 1:34:19	37.069	116.952	0.2	8.27	2.5	64	BC	0.7	---	SPRINGDALE
11 6:49:13	37.044	116.170	0.3	-0.30	0.5	103	AC	---	0.1	TIPPICAH SPRING
11 20:15:52	37.083	116.079	0.6	2.42	7.5	106	CC	0.7	---	YUCCA FLAT
11 20:24:31	37.044	116.036	0.4	-0.22*	---	173	CD	0.6	---	YUCCA FLAT
11 20:37:16	37.076	116.076	0.3	4.27	6.1	107	CC	1.3	---	YUCCA FLAT
11 21:29:55	37.286	116.019	0.3	4.33	2.0	99	BB	0.4	---	OAK SPRING BUTTE
12 2:24:45	37.081	116.074	0.3	-0.98	9.2	107	CC	1.5	---	YUCCA FLAT
12 15:23:2	37.422	117.333	0.5	-1.11*	---	72	CC	1.3	---	MOUNT JACKSON
12 21:28:10	37.080	116.060	0.3	4.67	1.7	106	AC	1.4	---	YUCCA FLAT
13 6:47:54	36.814	117.480	0.5	7.85	0.7	206	AD	0.7	---	TIN MTN
13 20:15:11	36.696	116.365	4.9	29.87	3.0	287	CD	0.6	---	TOPOPAH SPRING
13 21:16:43	37.209	114.776	0.6	11.45	2.0	199	BD	1.2	---	DELMAR 3 NE
14 5:45:53	36.619	116.410	0.3	3.79	1.3	110	AB	0.9	---	LATHROP WELLS SW
14 12:13:39	36.615	116.443	0.3	6.27	2.6	134	BC	0.8	---	LATHROP WELLS SW
14 14:17:6	37.714	115.149	0.4	2.76	1.5	126	AC	0.5	---	FOSSIL PEAK
14 20:17:40	37.511	114.526	1.3	8.08	0.8	281	BD	1.4	---	CALIENTE
14 20:24:6	37.537	114.567	---	7.00**	---	321	AD	1.1	---	CALIENTE
15 4:33:55	37.564	115.201	0.4	10.90	1.1	134	AB	---	0.1	HIKO
15 14:30:20	37.062	116.953	0.2	5.06	1.4	63	AC	1.0	---	SPRINGDALE
16 0:04:27	37.512	114.565	0.8	5.90	2.9	278	BD	1.6	---	CALIENTE
17 3:18:8	37.518	114.610	1.3	8.78	2.0	282	BD	0.7	---	CALIENTE
18 0:45:16	37.220	114.790	1.2	15.58	1.9	255	BD	0.9	---	DELMAR 3 NE
18 18:39:44	37.235	115.411	0.5	8.62	2.1	179	BC	0.8	---	DESERT HILLS NW

## 1981 LOCAL HYPOCENTER SUMMARY

	DATE - TIME (UTC)	LATITUDE (DEG. N)	LONGITUDE (DEG. W)	HORIZ ERROR (KM)	DEPTH (KM)	VERT ERROR (KM)	AZI GAP (DEG)	QUAL	Md	Mbig	QUADRANGLE
NOV	19 10:10:44	37.386	115.877	0.4	8.04	1.7	178	AC	1.9	---	ALAMO SE
	19 19:56:31	36.660	116.603	0.4	15.33	1.1	155	AC	0.9	---	BIG DUNE
	19 21:40:53	37.057	116.949	0.2	1.41	0.8	82	AC	2.5	---	SPRINGDALE
	19 21:44:20	37.059	116.953	0.3	9.74	1.7	69	AB	1.2	---	SPRINGDALE
	19 21:56:52	37.065	116.951	0.3	9.15	0.8	68	AB	1.0	---	SPRINGDALE
	19 22:1:55	37.060	116.955	0.2	5.59	0.8	68	AB	1.4	---	SPRINGDALE
	19 23:1:43	37.060	116.959	0.3	8.92	0.9	87	AB	0.8	---	SPRINGDALE
	20 1:31:45	36.527	115.817	0.3	8.59	1.1	135	AC	0.7	---	MERCURY SE
	20 4:10:51	36.197	115.407	1.3	8.73*	---	230	CD	0.5	---	LA MADRE MTN
	20 4:20:58	37.668	115.849	0.3	1.57	1.1	104	AC	0.7	---	HIKO NE
	20 8:42:17	37.849	114.540	1.3	7.82	1.4	294	BD	1.4	---	BENNETT PASS
	20 9:8:4	37.064	116.954	0.3	4.60	1.3	63	AC	0.7	---	SPRINGDALE
	21 1:50:58	36.444	117.018	0.8	18.35	1.8	112	AB	0.8	---	EMIGRANT CANYON
	21 4:44:19	37.065	116.954	0.2	0.06	0.3	63	AC	0.8	---	SPRINGDALE
	21 18:44:20	37.066	116.950	0.2	5.28	1.0	84	BC	1.0	---	SPRINGDALE
	21 22:29:17	37.542	114.658	0.5	1.70	0.8	245	AD	1.2	---	CHOCHECHERRY MTN
	21 23:59:50	37.062	116.952	0.2	5.61	0.9	83	AC	1.2	---	SPRINGDALE
	22 12:50:12	37.145	117.523	0.7	1.97	2.2	177	BC	0.5	---	LAST CHANCE RANGE
	22 18:27:10	37.245	115.491	0.5	11.67	2.2	143	BC	0.9	---	DESERT HILLS NW
	22 22:23:49	36.670	116.327	0.4	2.54	0.5	129	AB	0.4	---	STRIPED HILLS
	22 22:51:26	37.322	115.901	0.5	5.39	1.0	143	AC	0.4	---	GROOM MINE SW
	23 1:0:27	37.064	116.950	0.2	1.35	0.7	63	AC	1.1	---	SPRINGDALE
	23 3:18:49	37.056	116.959	0.2	5.05	1.0	62	AC	1.0	---	SPRINGDALE
	23 4:35:58	36.812	117.778	0.8	1.66*	---	222	CD	1.0	---	WAUCOBA WASH
	23 8:14:42	37.337	115.563	0.3	0.38	0.4	88	AC	1.3	---	GROOM RANGE SE
	23 8:28:13	37.317	115.567	0.7	2.66	0.0	184	CC	0.8	---	GROOM RANGE SE
	23 9:5:10	36.681	117.893	1.3	11.66	5.0	253	CD	1.3	---	NEW YORK BUTTE
	23 18:26:4	37.014	116.360	0.3	8.65	0.8	99	AB	0.4	---	BUCKBOARD MESA
	23 19:10:14	37.066	116.948	0.1	0.63	0.2	95	AC	0.7	---	SPRINGDALE
	23 23:29:51	37.236	115.009	0.0	4.78	2.7	214	BD	1.0	---	LOWER PAHRANAGAT LAKE
	24 12:14:50	37.036	114.549	1.6	11.00	0.5	293	CD	1.6	---	BENNETT PASS
	24 20:49:30	37.084	116.949	0.3	4.32	1.5	83	AC	0.9	---	SPRINGDALE
	25 4:2:50	37.084	116.951	0.2	4.83	1.1	83	AC	1.4	---	SPRINGDALE
	26 3:48:30	37.468	117.600	0.2	4.85	1.0	72	AB	1.0	---	MAGRUDER MTN
	28 1:15:40	37.680	114.905	0.5	1.89	1.2	152	AC	0.9	---	PAHROC SPRING
	29 10:11:21	36.784	116.120	0.2	12.03	0.7	90	AA	0.5	---	CANE SPRING
DEC	30 16:39:56	36.498	116.307	0.2	9.74	0.6	62	AB	1.1	---	ASH MEADOWS
	30 17:43:53	36.417	117.198	0.5	8.55	1.1	195	AD	0.7	---	EMIGRANT CANYON
	1 19:49:33	36.827	116.437	0.3	-8.13BL	0.3	141	AC	0.8	---	● TOPOPAH SPRING SW
	2 23:6:49	37.062	116.953	0.2	5.39	1.3	52	AC	1.7	---	SPRINGDALE
	3 3:36:50	37.063	116.952	0.2	4.92	1.1	83	BC	1.3	---	SPRINGDALE
	4 7:22:48	37.619	115.862	0.3	7.55	1.0	71	AC	1.1	---	WHITE BLOTCH SPRINGS
	5 13:43:38	37.620	115.869	0.3	7.52	1.3	70	AC	1.0	---	WHITE BLOTCH SPRINGS
	7 2:51:56	37.771	115.182	0.5	2.12	1.6	138	AC	0.5	---	WHITE RIVER NARROWS
	7 20:58:53	37.027	116.227	0.5	5.37	0.5	128	AB	0.6	---	TIPPICAH SPRING
	8 8:24:49	37.074	116.370	0.5	8.24	1.2	103	AB	0.4	---	BUCKBOARD MESA
	8 12:34:56	37.659	115.065	0.4	1.92	1.0	99	AC	0.7	---	HIKO NE
	9 15:52:42	36.545	117.814	1.4	5.05*	---	244	CD	1.6	---	NEW YORK BUTTE
	9 23:21:17	36.636	116.492	2.4	27.31BL	1.7	125	BB	0.9	---	● TOPOPAH SPRING SW
	10 0:49:19	37.383	115.335	0.3	10.75	1.5	111	AC	0.9	---	HANCOCK SUMMIT
	10 1:28:12	36.703	116.126	0.7	6.84	3.8	111	BC	0.3	---	SPECTER RANGE NW
	10 2:25:10	37.075	116.148	1.4	20.80	0.6	304	BD	0.0	---	TIPPICAH SPRING
	10 23:30:53	37.056	116.956	0.2	4.67	0.7	82	AC	1.3	---	SPRINGDALE
	11 4:4:38	37.069	116.951	0.5	4.74	2.0	64	BC	1.0	---	SPRINGDALE
	12 0:19:49	36.630	116.635	0.3	-1.19BL	0.4	129	AB	1.0	---	● BARE MTN
	13 1:20:6	38.435	117.956	4.9	9.29	1.5	282	CD	2.9	---	***QUAD. NOT LISTED***
	15 23:17:38	37.145	116.938	0.5	5.60	3.3	77	CC	1.1	---	SPRINGDALE
	16 21:5:0	37.187	116.114	0.5	0.12*	---	129	CC	2.9	---	YUCCA FLAT
	17 6:19:24	37.382	115.328	0.4	14.50	1.6	110	AB	1.0	---	HANCOCK SUMMIT
	19 14:13:36	36.764	116.287	0.5	-0.25	0.5	116	BB	0.9	---	JACKASS FLATS
	19 18:21:51	37.321	115.446	0.9	16.52	2.7	146	BC	0.8	---	CUTLER RESERVOIR
	19 20:46:33	37.284	116.444	0.3	5.21	2.0	59	BC	1.1	---	SILENT BUTTE
	20 19:3:59	36.725	115.698	0.7	7.80	2.4	85	CB	1.2	---	INDIAN SPRINGS NW
	21 7:14:17	37.184	117.389	0.4	9.25	1.1	113	AB	1.0	---	UBEHEBE CRATER
	22 16:44:56	37.256	115.032	0.4	-0.27	0.7	154	AC	---	0.2	ALAMO SE
	22 19:11:59	36.740	115.690	0.5	5.65	1.3	185	AD	0.7	---	INDIAN SPRINGS NW

# 1981 LOCAL HYPOCENTER SUMMARY

DATE - TIME (UTC)	LATITUDE (DEG. N)	LONGITUDE (DEG. W)	HORIZ ERROR (KM)	DEPTH (KM)	VERT ERROR (KM)	AZI GAP (DEG)	QUAL	Md	Mbiq	QUADRANGLE
DEC 22 21:55: 1	36.821	116.463	0.1	-0.64BL	2.3	94	BB	0.5	---	● TOPOPAH SPRING SW
23 0:32:19	36.730	115.688	0.4	6.29	1.4	75	BB	1.1	---	INDIAN SPRINGS NW
23 1: 8:32	37.333	115.488	0.7	5.06	8.6	128	CC	1.0	---	CUTLER RESERVOIR
23 7:14:20	37.233	116.362	0.4	-1.06	0.4	43	BA	1.3	---	AMMONIA TANKS
23 22: 8:42	36.716	115.697	0.7	7.76	1.6	74	BB	0.6	---	INDIAN SPRINGS NW
23 23: 6:49	36.819	116.465	0.4	-0.24BL	6.7	96	AB	0.5	---	● TOPOPAH SPRING SW
25 9:44:41	36.719	116.025	0.5	4.09	2.1	97	BB	0.7	---	CAMP DESERT ROCK
25 15:22:22	36.714	115.782	1.2	8.92	1.7	114	BB	0.9	---	INDIAN SPRINGS NW
26 5:42:55	37.175	117.379	0.3	6.61	1.1	169	AC	1.0	---	UBENEKE CRATER
26 6: 4:10	37.899	117.512	0.9	5.44	7.4	229	CD	1.8	---	SILVER PEAK
26 17:29:44	36.725	115.708	0.2	8.60	0.4	73	AB	1.7	---	INDIAN SPRINGS NW
28 11:57:19	36.528	116.129	0.3	5.40	0.9	109	AB	1.1	---	SPECTER RANGE SW
28 22:45:43	37.222	114.928	0.6	5.20	1.6	129	BC	2.1	---	DELAMAR 3 NW
29 0:41:25	37.195	114.866	0.4	5.67	1.6	161	AD	1.7	---	DELAMAR 3 NW
29 9:16:13	37.191	114.873	0.4	6.99	6.7	218	AD	1.6	---	DELAMAR 3 NE
29 10:42:52	37.188	114.918	1.2	6.16	5.1	216	CD	1.4	---	DELAMAR 3 NW
30 0: 5:13	37.196	114.906	0.6	2.81	2.1	214	BD	2.2	---	DELAMAR 3 NW
30 9:56:29	37.213	114.966	0.3	11.25	1.2	177	AC	1.3	---	DELAMAR 3 NW
30 10:46:56	37.172	114.865	0.7	10.39	1.6	225	AD	1.2	---	DELAMAR 3 NE
30 16: 9:13	37.196	114.929	0.6	5.28	4.7	174	BC	1.7	---	DELAMAR 3 NW
30 16:44: 0	37.386	115.233	0.3	8.77	1.1	89	AB	1.1	---	ASH SPRINGS
31 3:18:34	37.256	115.020	0.3	7.18	1.4	155	AC	1.6	---	ALAMO SE
31 13:10:24	35.986	117.269	0.8	6.61	4.0	265	BD	1.3	---	TRONA

## 1982 LOCAL HYPOCENTER SUMMARY

	DATE - TIME (UTC)	LATITUDE (DEG. N)	LONGITUDE (DEG. W)	HORIZ ERROR (KM)	DEPTH (KM)	VERT ERROR (KM)	AZI GAP (DEG)	QUAL	Md	Mb1g	QUADRANGLE
JAN	3 9:14:48	37.115	116.748	0.3	-1.14*	---	185	CC	1.1	1.1	THIRSTY CANYON SW
	4 19:29:38	36.389	115.147	2.9	10.53	2.1	268	DD	1.3	1.5	CASS PEAK SW
	5 4:25:42	36.727	115.470	0.4	9.88	1.3	98	AC	1.9	1.9	BLACK HILLS NW
	5 4:42:3	36.436	116.922	0.8	8.81	3.2	92	BB	0.8	1.0	FURNACE CREEK
	5 5:8:1	36.635	115.478	1.8	8.09*	---	157	CC	1.2	1.4	BLACK HILLS NW
	5 5:38:22	37.282	117.726	1.6	1.93	3.1	182	BD	1.0	1.1	MAGRUDER MTN
	5 15:31:37	36.741	115.472	0.5	11.26	3.9	107	BC	1.0	1.3	BLACK HILLS NW
	5 20:9:57	36.720	115.469	2.0	2.60*	---	207	CD	1.0	1.4	BLACK HILLS NW
	8 1:47:22	36.726	115.705	0.3	7.81	1.1	73	AB	1.1	1.2	INDIAN SPRINGS NW
	8 8:32:1	36.461	115.848	0.4	11.32	1.8	115	AC	0.4	1.1	MT STIRLING
	8 9:0:18	37.973	115.229	---	-1.02	---	214	AD	0.8	0.9	OREANA SPRING
	8 13:41:1	37.280	117.729	1.1	0.97*	---	164	CC	1.3	1.5	MAGRUDER MTN
	8 22:23:0	36.777	116.429	---	0.31	---	230	AD	0.6	---	TOPOPAH SPRING SW
	9 12:10:32	37.288	117.735	0.8	4.87	2.5	164	BC	1.4	1.5	MAGRUDER MTN
	10 9:30:34	36.301	116.328	0.3	-0.45*	---	107	CC	1.4	1.5	ASH MEADOWS
	10 4:15:49	37.329	116.057	0.9	4.52	6.0	112	CC	0.9	1.0	OAK SPRING BUTTE
	11 8:37:14	35.901	116.760	1.6	-0.76*	---	241	CD	1.3	1.3	WINGATE WASH
	11 23:52:14	36.333	116.320	0.8	1.07	2.2	172	BC	1.2	1.1	ASH MEADOWS
	12 6:47:54	37.880	115.237	0.8	7.78	1.4	193	AD	1.3	1.4	LOWER PAHRANAGAT LAKE SW
	12 9:31:12	35.692	115.331	9.2	2.06*	---	316	DD	1.5	1.6	ROACH LAKE
	12 20:43:11	37.156	116.938	0.2	2.30*	---	80	CC	1.1	1.3	SPRINGDALE
	13 5:53:33	36.989	116.286	0.3	6.48	0.7	168	AC	0.9	1.0	TOPOPAH SPRING
	14 4:22:3	37.250	115.028	1.2	8.47	3.9	204	BD	0.8	1.0	ALAMO SE
	14 8:35:40	37.812	117.861	2.4	5.69*	---	268	CD	1.2	1.4	WAUCOBA SPRING
	14 19:43:55	36.303	116.320	0.5	2.82*	---	92	CC	1.6	1.8	ASH MEADOWS
	14 21:9:56	36.879	116.207	1.5	4.12	3.0	141	BC	0.8	0.8	MINE MTN
	15 2:36:15	37.234	117.702	1.2	5.04*	---	201	CD	1.2	1.3	LAST CHANCE RANGE
	16 5:47:44	37.507	114.578	2.8	5.33	4.5	281	CD	1.7	1.6	CALIENTE
	16 11:56:30	36.639	115.964	0.6	11.07	1.0	143	AC	0.4	0.9	MERCURY
	17 5:2:10	37.186	117.427	0.6	1.60	1.9	126	AC	0.9	1.0	UBENESE CRATER
	18 17:38:0	37.831	115.141	0.3	-0.20	9.4	115	CB	1.1	1.1	SEAMAN WASH
	19 11:53:56	37.556	117.839	1.6	4.88	9.8	163	CC	1.3	1.2	PIPER PEAK
	19 14:24:16	37.438	115.214	---	7.00**	---	206	AD	0.5	0.8	ASH SPRINGS
	19 14:45:51	37.262	116.021	0.6	11.97	4.7	126	BB	0.8	---	OAK SPRING BUTTE
	19 15:24:4	37.257	116.037	0.7	-0.27	0.6	120	AB	1.3	1.2	OAK SPRING BUTTE
	19 23:44:43	37.151	116.940	0.2	6.39	0.6	69	AB	2.1	2.3	SPRINGDALE
	20 11:8:10	37.151	116.939	0.2	5.46	1.1	89	AC	1.7	2.1	SPRINGDALE
	20 11:14:3	37.153	116.939	0.3	5.87	2.0	79	AC	0.9	1.1	SPRINGDALE
	20 18:46:25	37.149	116.938	0.2	0.44	6.4	75	CC	1.7	1.7	SPRINGDALE
	20 22:47:16	37.152	116.943	0.4	6.28	2.8	76	BC	1.2	1.3	SPRINGDALE
	21 2:7:42	37.146	116.939	0.3	1.92	1.3	75	AC	1.2	1.1	SPRINGDALE
	21 11:40:12	37.152	116.940	0.2	0.54*	---	176	CC	1.0	1.1	SPRINGDALE
	21 15:34:41	37.147	116.942	0.5	1.94	3.4	172	BC	1.1	1.0	SPRINGDALE
	22 23:7:54	36.847	116.222	0.4	4.84	2.4	114	BC	0.3	1.0	SPECTER RANGE NW
	23 0:7:17	36.822	116.847	0.4	-0.31BL	0.5	92	AB	1.1	---	● BARE MTN
	23 7:30:48	37.080	116.142	0.3	0.41	9.8	96	CB	1.1	1.0	TIPPICAH SPRING
	23 11:45:41	37.322	116.378	0.4	5.47	7.5	113	CC	1.2	1.2	SILENT BUTTE
	24 15:43:59	37.402	117.941	0.7	9.70	0.3	231	AD	2.9	2.1	SOLDIER PASS
	24 15:48:45	37.419	117.931	1.1	8.26	0.8	233	BD	1.3	1.6	SOLDIER PASS
	24 16:11:13	37.247	115.018	1.5	6.67	3.8	208	BD	1.5	1.5	LOWER PAHRANAGAT LAKE
	24 16:24:38	37.423	117.894	1.6	5.64	1.3	139	BC	1.5	1.8	SOLDIER PASS
	24 16:48:21	37.375	117.921	1.0	4.58	0.9	228	BD	2.1	2.3	SOLDIER PASS
	24 20:6:44	37.425	117.892	0.9	5.84	1.0	129	AB	1.5	1.7	SOLDIER PASS
	25 2:38:46	37.397	117.937	1.2	6.79	0.8	234	BD	2.3	2.5	SOLDIER PASS
	25 14:27:20	37.866	116.945	0.4	3.03*	---	183	CD	0.9	1.2	SPRINGDALE
	25 20:27:20	37.394	117.905	2.5	3.44	1.8	268	BD	1.6	1.4	SOLDIER PASS
	26 11:20:5	37.396	117.871	0.5	1.83	1.1	166	AC	1.4	1.8	SOLDIER PASS
	27 7:39:34	37.159	114.408	2.2	6.41	1.4	273	BD	2.3	2.2	***REGIONAL***
	27 8:29:58	37.191	114.515	1.1	8.64	0.6	240	BD	2.0	2.1	VIGO NE
	29 13:16:14	37.109	116.090	0.5	-0.12*	---	73	CC	1.6	1.4	YUCCA FLAT
	29 14:17:12	37.157	116.945	0.3	0.38*	---	181	CC	1.4	1.1	SPRINGDALE
	29 14:33:43	37.218	115.582	0.4	1.20	4.6	180	BC	1.7	1.4	FALLOUT HILLS NE
	31 21:6:43	37.246	117.557	0.5	5.25	1.4	96	AB	1.1	1.6	LAST CHANCE RANGE
	31 22:19:33	37.249	117.565	1.0	4.73	2.5	94	BB	1.2	1.4	LAST CHANCE RANGE
	31 22:25:53	37.239	117.570	0.4	8.91	0.6	103	AB	0.3	1.0	LAST CHANCE RANGE
FEB	1 1:19:38	36.298	115.929	2.0	1.35	3.8	231	BD	1.1	0.7	MT STIRLING

## 1982 LOCAL HYPOCENTER SUMMARY

DATE - TIME (UTC)	LATITUDE (DEG. N)	LONGITUDE (DEG. W)	HORIZ ERROR (KM)	DEPTH (KM)	VERT ERROR (KM)	AZI CAP (DEG)	QUAL	Md	Mb19	QUADRANGLE
FEB 1 7: 0:50	37.238	117.567	0.3	8.07	0.6	109	AB	1.4	1.6	LAST CHANCE RANGE
1 9:16: 4	36.125	116.126	7.0	2.26	3.9	265	DD	1.5	1.3	STEWART VALLEY
2 2:51:58	37.253	117.567	0.4	5.74	0.9	90	AB	1.4	1.5	MAGRUDER MTN
2 16:13:31	37.409	117.909	1.3	6.33	1.1	218	BD	1.6	1.6	SOLDIER PASS
3 10:26:17	36.391	116.993	0.3	8.02	1.6	154	AC	1.3	1.5	FURNACE CREEK
4 10:24:13	37.190	117.870	0.5	6.93	1.1	214	AD	1.4	1.2	WAUCOBA SPRING
4 14:32: 6	37.297	117.725	0.7	0.46*	---	160	CC	1.3	1.1	MAGRUDER MTN
5 9:19:12	36.634	115.723	0.4	8.02	2.7	124	BC	1.2	0.9	INDIAN SPRINGS NW
5 21:25: 9	37.260	114.686	6.3	11.86	4.9	213	DD	---	1.4	ELGIN SW
6 10:39:29	37.383	117.887	0.7	2.81	1.0	192	AD	---	2.0	SOLDIER PASS
7 8:10:42	36.098	116.962	0.7	16.81	0.6	191	AD	1.8	2.6	BENNETTS WELL
7 9:36:25	35.931	117.165	1.8	9.80	1.2	266	BD	1.8	1.8	MANLY PEAK
9 2:22:47	36.867	116.692	0.8	-0.38*	---	148	CC	0.4	0.7	● BARE MTN
9 18:46:26	37.065	116.938	0.5	2.94	1.5	76	AC	1.1	1.2	SPRINGDALE
9 18:52:51	37.063	116.940	0.2	1.26	0.9	85	AC	0.8	1.0	SPRINGDALE
9 19:41:16	36.202	116.118	---	6.41	---	198	AD	0.7	1.2	STEWART VALLEY
9 20:18:42	36.742	116.180	0.8	6.54	2.1	91	BC	0.6	1.0	CAMP DESERT ROCK
11 20:24:42	36.839	116.650	1.0	1.06BL	4.5	135	BB	0.7	0.7	● BARE MTN
11 23:43:58	37.741	115.046	0.1	9.43	0.4	126	AD	0.8	1.1	HIKO NE
12 17:14:12	37.360	116.301	0.3	-0.10*	---	59	CC	---	1.5	DEAD HORSE FLAT
12 18:33:19	37.226	116.452	0.3	-0.70*	---	123	CC	1.3	1.1	SCRUGHAM PEAK
12 18:51:19	37.229	116.472	0.2	3.00*	---	93	CC	1.4	1.1	SCRUGHAM PEAK
12 20:57:52	37.211	115.839	---	7.00**	---	193	AD	1.0	0.6	PAPOOSE LAKE NE
12 23:23:27	37.216	116.473	0.5	-1.09*	---	103	CC	---	1.5	SCRUGHAM PEAK
13 1:43:15	37.224	116.447	0.4	5.16	1.6	89	AC	1.5	1.2	SCRUGHAM PEAK
13 2: 7:13	37.220	116.452	0.3	-0.26*	---	87	CC	1.5	1.3	SCRUGHAM PEAK
13 2:10:12	37.225	116.459	0.3	-0.25	9.5	72	CC	1.4	---	SCRUGHAM PEAK
13 3:24:53	37.268	116.444	1.2	9.54	2.2	204	BD	1.3	1.1	SILENT BUTTE
13 12:58:37	36.146	115.089	2.0	5.39	1.7	243	BD	1.4	1.2	TIMBER MTN PASS NE
14 0:32:59	37.173	117.940	1.6	6.03	0.7	264	BD	1.5	2.7	WAUCOBA SPRING
14 3: 5:47	37.291	115.107	0.6	-0.86*	---	164	CC	1.3	1.0	ALAMO SE
15 11: 2:33	36.477	117.603	5.6	1.54*	---	275	DD	1.0	1.3	DARWIN
15 20:55: 4	37.321	117.565	0.2	-0.82	4.6	74	BC	1.9	1.8	MAGRUDER MTN
16 0:11:33	37.322	117.562	0.3	-0.53	8.0	73	CC	1.3	1.7	MAGRUDER MTN
16 0:20:40	37.313	117.564	1.0	0.27*	---	115	CC	1.4	1.5	MAGRUDER MTN
16 0:26:55	37.320	117.572	0.2	-0.43	5.3	76	CC	1.5	1.9	MAGRUDER MTN
16 1:27: 8	37.397	115.699	1.9	8.00*	---	190	CD	0.8	1.3	BALD MTN
16 5:23: 8	38.104	115.070	2.9	5.52	4.0	235	CD	1.6	1.8	TIMBER MTN PASS EAST
16 6:23:54	37.196	117.844	0.6	5.93	2.6	232	BD	1.0	1.4	WAUCOBA SPRING
16 10:23:34	37.178	117.878	0.8	0.60*	---	209	CD	0.9	1.6	WAUCOBA SPRING
16 20:27: 4	36.304	116.324	0.5	-0.65*	---	105	CC	1.7	1.7	ASH MEADOWS
16 23: 4:51	37.316	117.648	---	3.00	---	116	AD	0.6	---	MAGRUDER MTN
17 9:53:42	37.319	117.568	0.2	0.59	4.4	75	BC	1.7	1.9	MAGRUDER MTN
18 5: 6: 7	35.754	117.723	2.5	6.84	0.8	282	BD	2.3	2.7	MOUNTAIN SPRINGS CANYON
18 6:18: 2	36.661	115.824	0.5	7.00	8.3	141	CC	0.9	1.2	MERCURY NE
18 8:58:45	36.708	116.106	0.2	-0.16	6.4	49	CC	1.7	1.7	CAMP DESERT ROCK
18 19:31:24	36.900	116.388	---	7.00**	---	242	BD	0.6	---	TOPOPAH SPRING NW
18 19:52:42	37.325	117.541	0.9	-0.96*	---	79	CC	0.8	1.1	MAGRUDER MTN
18 21:15:40	36.692	115.518	2.7	4.88*	---	258	CD	1.3	1.1	HEAVENS WELL
19 0:35:53	37.207	117.847	0.6	6.03	0.9	207	AD	0.7	1.2	WAUCOBA SPRING
19 1:24:57	36.659	117.766	1.5	5.33	1.0	289	BD	2.0	2.5	INYOKERN
19 1:56:28	36.677	115.801	1.3	-0.77	0.6	224	BD	0.5	0.5	MERCURY NE
19 2:24:40	36.392	115.785	---	14.87	---	168	AD	0.9	---	MT STIRLING
19 4:26:41	35.663	116.631	3.1	2.63*	---	275	CD	1.6	1.7	LEACH LAKE
20 0:29:40	36.868	116.252	0.4	4.07	1.0	96	AB	0.7	1.1	JACKASS FLATS
20 1:46:59	36.634	115.758	0.8	-0.63	3.6	280	DD	0.9	---	MERCURY NE
20 1:56:33	36.672	115.814	0.8	-0.79	0.8	135	BC	0.3	---	MERCURY NE
20 12:12:50	36.002	117.949	71.9	7.00*	---	296	DD	0.7	1.5	HAIWEE RESERVOIR
20 16:18: 0	37.327	117.528	0.2	-0.14	5.3	95	CC	0.4	1.3	MAGRUDER MTN
20 21:20:16	37.983	115.213	1.6	5.77	1.6	221	BD	0.6	1.2	OREANA SPRING
21 15:21:51	37.926	116.015	0.4	5.64	6.0	128	CC	1.2	1.6	REVEILLE PEAK
21 23:14:47	38.038	115.197	---	10.25	---	247	AD	0.5	1.1	TIMBER MTN PASS WEST
21 23:21:59	37.286	115.070	1.8	1.78	5.5	179	CD	1.0	1.0	ALAMO SE
23 2:41:31	36.548	116.242	0.2	2.92*	---	97	CC	0.6	0.6	SPECTER RANGE SW
23 14:57:39	36.707	116.119	0.3	2.47	0.9	80	AC	1.0	1.1	CAMP DESERT ROCK
23 18:29: 9	36.706	116.117	0.5	5.99	2.8	108	BC	0.8	0.7	CAMP DESERT ROCK

## 1982 LOCAL HYPOCENTER SUMMARY

DATE - TIME (UTC)	LATITUDE (DEG. N)	LONGITUDE (DEG. W)	HORIZ ERROR (KM)	DEPTH (KM)	VERT ERROR (KM)	AZI GAP (DEG)	QUAL	Md	Mb1g	QUADRANGLE
FEB 23 22:53:38	35.918	115.177	2.5	8.43	1.0	268	CD	1.9	2.0	SLOAN
25 5:19:58	35.918	118.548	1.0	14.08	1.1	224	AD	---	2.3	CONFIDENCE HILLS
26 4:39:48	37.788	114.951	0.8	4.57	3.0	173	BC	1.1	1.0	WHEATGRASS SPRING
26 23:59:14	37.888	118.946	0.4	5.92	1.7	66	BB	1.0	1.2	SPRINGDALE
27 28:48:37	37.926	118.015	0.8	5.80*	---	128	CC	1.3	1.1	REVELLE PEAK
28 17:31:48	37.139	118.953	0.4	11.78	2.0	118	AB	1.0	1.0	SPRINGDALE
MAR 1 8: 9:22	35.849	117.758	3.8	8.35	1.4	288	CD	2.0	2.0	INYO KERN
2 18:52: 1	37.343	117.189	0.3	-0.13	0.4	87	AB	1.1	1.3	SCOTTYS JUNCTION SW
2 22:17:47	35.797	115.117	12.2	8.74	3.8	380	DD	1.5	1.5	SLOAN
3 4: 3: 7	37.552	118.198	1.6	0.41	5.3	280	CD	2.0	---	***REGIONAL***
4 2:44:38	38.997	117.777	0.9	0.34*	---	288	CD	1.3	1.5	WAUCOBA WASH
4 15: 8:54	37.587	117.735	0.5	8.13	1.2	116	AC	1.5	1.3	LIDA WASH
5 22:21:28	36.344	114.987	3.4	8.89	1.9	259	CD	1.2	1.8	DRY LAKE
6 3:48: 4	35.898	117.074	5.5	2.82*	---	275	DD	1.2	1.4	MANLY PEAK
6 9:15:27	37.978	118.179	0.4	2.91*	---	128	CC	1.2	1.5	REVELLE PEAK
7 7:43:56	38.874	118.832	0.8	0.38	4.8	238	BD	1.4	1.3	***REGIONAL***
7 8:42:12	38.919	117.783	0.9	5.82	2.3	197	BD	1.3	1.8	DRY MTN
7 8:52: 8	37.788	115.835	0.7	8.18*	---	135	CC	1.5	1.5	WHITE RIVER NARROWS
7 21:44:38	35.889	117.768	7.7	7.39	2.4	385	DD	1.7	1.5	INYO KERN
7 22:29: 7	35.728	117.833	7.8	2.72	4.5	292	DD	1.8	2.3	INYO KERN
8 2:25: 7	37.215	118.455	0.3	1.19	1.6	83	AC	1.2	1.2	SCRUGHAM PEAK
8 4:23:56	37.338	118.317	0.5	2.48*	---	138	CC	1.2	0.9	DEAD HORSE FLAT
8 5:18:23	35.784	117.731	3.1	7.78	1.8	281	CD	1.8	2.5	MOUNTAIN SPRINGS CANYON
8 7: 1:45	35.848	117.687	8.8	11.78	3.5	291	DD	1.8	---	MOUNTAIN SPRINGS CANYON
8 14:41:45	35.845	117.731	2.2	8.51	0.8	288	BD	3.7	---	RIDGECREST
8 19:32:38	37.113	117.988	0.8	3.88*	---	244	CD	0.9	1.1	WAUCOBA SPRING
8 21: 8:47	38.774	117.492	2.7	9.12	1.5	281	CD	0.8	1.1	TIM MTN
9 8:46:19	35.828	117.688	5.3	10.98	1.5	295	DD	1.3	1.5	MOUNTAIN SPRINGS CANYON
9 12:26:28	35.823	117.782	3.8	7.59	1.6	284	CD	1.7	1.6	MOUNTAIN SPRINGS CANYON
9 17: 8:32	38.627	118.282	1.1	5.58	2.4	142	BC	0.7	0.8	STRIPED HILLS
9 19:39:49	37.594	115.835	---	-0.68	---	189	DD	0.9	---	MIKO SE
9 21:29:39	35.747	117.748	2.5	7.88	0.9	283	CD	1.4	2.7	RIDGECREST
10 3:36:27	37.279	114.641	2.7	2.88*	---	251	CD	1.2	1.3	ELGIN SW
10 17:25:37	38.882	115.977	0.4	2.85*	---	112	CC	0.9	---	FRENCHMAN FLAT
10 28:13:33	37.894	115.188	---	7.88**	---	184	AD	1.0	---	FOSSIL PEAK
10 22:32:52	38.185	115.513	2.2	18.49	2.8	237	BD	1.7	1.9	MOUNTAIN SPRINGS
11 8:56:38	38.947	118.198	1.9	8.87	0.7	283	BD	1.4	1.2	***REGIONAL***
11 11:52: 7	37.248	114.589	2.8	8.87	1.1	289	BD	2.2	---	VIGO NE
11 23:59:53	38.439	118.974	0.8	9.85	4.4	129	BC	1.4	1.4	FURNACE CREEK
13 9:19: 1	38.267	115.892	1.3	3.89	2.8	215	BD	1.9	1.9	THE WALL SW
13 18:14:47	35.595	117.812	8.4	5.34	2.3	298	DD	2.0	2.1	INYO KERN
13 11: 9:52	38.585	118.579	0.3	4.48	2.5	188	BC	0.8	0.7	BIG DUNE
13 19:44: 7	38.789	118.188	0.3	1.88	1.8	138	AC	0.4	0.7	CAMP DESERT ROCK
13 22:17:53	37.422	118.318	3.2	0.83	8.9	282	CD	1.5	1.3	***REGIONAL***
14 8:14:59	38.885	118.111	1.7	3.89*	---	98	CC	0.8	0.7	CAMP DESERT ROCK
14 9:35:13	37.678	115.228	0.3	3.91	1.8	148	AC	1.2	1.4	FOSSIL PEAK
14 12:12:18	38.897	115.448	---	7.15	---	228	AD	1.0	1.2	BLACK HILLS NW
14 18:11:52	35.897	117.785	4.3	8.78	1.5	383	CD	1.9	2.0	INYO KERN
14 18:31:55	35.799	117.787	7.2	7.52	3.1	288	DD	2.0	2.3	MOUNTAIN SPRINGS CANYON
14 22:18:55	38.342	117.111	---	34.27	---	219	AD	1.5	1.9	EMIGRANT CANYON
15 1:58:49	35.848	117.687	8.9	13.18	2.4	293	DD	1.7	2.0	MOUNTAIN SPRINGS CANYON
15 17: 2:18	37.248	115.437	0.4	5.33	2.8	53	BC	1.9	2.2	DESERT HILLS NW
15 17:33:48	38.785	118.458	0.3	4.88	1.4	73	AB	1.1	1.1	LATHROP WELLS NW
15 17:58: 9	37.231	115.444	0.5	1.28	1.9	188	AC	1.4	1.4	DESERT HILLS NW
15 28:42:53	36.577	117.888	0.3	5.89	2.8	117	AC	1.8	1.9	STOVEPIPE WELLS
15 23:28:34	37.161	117.484	0.3	5.79	2.2	118	BC	1.8	1.8	UBEHEBE CRATER
16 7: 8:13	36.588	117.882	0.3	8.98	0.8	118	AC	2.8	---	STOVEPIPE WELLS
16 7:20: 8	36.595	117.877	0.3	1.35	1.3	118	AC	1.4	1.3	STOVEPIPE WELLS
16 7:21:25	36.583	117.884	0.3	7.88	1.8	118	AC	1.2	---	STOVEPIPE WELLS
16 7:23:18	38.581	117.888	0.4	8.67	2.1	117	BC	1.4	---	STOVEPIPE WELLS
16 8:47: 1	38.588	117.881	0.2	7.99	0.7	118	AC	2.5	1.3	STOVEPIPE WELLS
16 9: 1:47	38.581	117.875	1.1	-8.84*	---	114	CD	1.1	1.3	STOVEPIPE WELLS
16 9:17: 4	38.585	117.884	1.9	3.17*	---	115	CD	0.7	1.1	STOVEPIPE WELLS
16 13:35:58	38.588	117.883	0.3	5.47	2.4	118	BC	1.7	1.7	STOVEPIPE WELLS
16 13:44:57	38.582	117.873	0.3	-0.19	9.2	113	CC	1.1	1.3	STOVEPIPE WELLS
17 28: 6:43	38.583	117.882	0.4	2.98*	---	115	CC	1.2	1.2	STOVEPIPE WELLS

## 1982 LOCAL HYPOCENTER SUMMARY

DATE - TIME (UTC)	LATITUDE (DEG. N)	LONGITUDE (DEG. W)	HORIZ ERROR (KM)	DEPTH (KM)	VERT ERROR (KM)	AZI GAP (DEG)	QUAL	Md	Mbiq	QUADRANGLE
MAR 18 10:38:4	36.829	116.232	0.3	0.35*	---	49	CB	1.2	1.4	SKULL MTN
18 12:17:3	37.050	116.947	0.4	3.04*	---	91	CC	1.4	1.2	SPRINGDALE
18 16:13:21	36.726	115.698	0.5	-0.92*	---	122	CC	1.0	1.0	INDIAN SPRINGS NW
18 20:55:33	37.730	115.188	---	7.00**	---	163	DD	1.2	1.6	FOSSIL PEAK
19 0:33:48	37.155	115.381	0.4	2.40*	---	142	CC	1.6	1.7	DESERT HILLS NW
19 1:32:59	37.167	115.367	0.8	0.85*	---	130	CC	1.2	0.9	DESERT HILLS NE
19 3:4:1	37.412	117.160	0.5	0.33*	---	187	CD	1.1	1.1	STONEWALL PASS
19 3:7:38	37.118	117.318	0.8	0.18*	---	104	CC	1.5	1.2	UBEHEBE CRATER
19 14:22:21	37.060	117.453	0.2	4.65	1.0	146	AC	1.1	1.2	UBEHEBE CRATER
19 15:9:52	36.457	115.761	0.4	9.63	1.7	92	AC	1.1	1.0	MT STIRLING
20 3:42:47	37.063	117.462	0.6	2.93*	---	149	CC	1.2	1.0	UBEHEBE CRATER
20 8:2:51	36.136	115.039	4.5	1.67	7.7	241	CD	1.5	1.4	TIMBER MTN PASS NE
21 1:46:4	36.644	117.382	0.4	7.52	0.7	183	AD	1.6	1.9	MARBLE CANYON
21 10:27:7	37.503	115.353	0.4	2.24*	---	51	CC	1.3	1.0	MT IRISH
21 10:47:36	37.144	116.937	0.3	2.74	1.8	75	AC	1.5	1.5	SPRINGDALE
21 11:12:38	37.144	116.942	0.3	5.40	2.5	76	BC	1.4	1.2	SPRINGDALE
21 15:26:38	35.655	117.779	16.5	3.99	4.6	315	DD	1.7	1.7	INYO KERN
21 22:19:44	37.140	116.939	0.3	0.99	8.1	188	CC	1.5	1.5	SPRINGDALE
22 2:46:39	36.279	115.880	1.3	3.86	3.4	216	BD	1.5	1.7	THE WALL SW
22 5:43:11	36.614	115.946	0.3	6.52	0.7	80	AA	1.1	1.3	MERCURY SW
22 20:1:32	36.974	116.325	0.2	0.88*	---	90	CB	0.5	0.7	TOPOPAH SPRING
24 19:8:23	37.155	116.201	0.4	-0.66*	---	122	CC	1.0	1.2	RAINIER MESA
25 3:21:35	36.506	115.031	11.9	13.64	6.3	254	DD	1.7	1.5	HAYFORD PEAK
25 4:23:58	37.133	116.250	0.3	1.88	1.1	106	AC	1.0	0.9	AMMONIA TANKS
25 19:37:27	37.549	115.229	---	17.72	---	226	AD	1.0	1.3	HIKO
25 22:3:24	35.592	115.606	5.5	14.04	1.9	297	DD	1.6	1.5	CLARK MTN
29 22:32:23	37.041	114.569	3.6	2.45*	---	264	CD	1.5	1.6	VIGO
30 18:5:36	36.756	117.792	2.3	6.03*	---	249	CD	1.4	1.7	WAUCOBA WASH
31 15:47:10	36.036	115.762	0.4	-0.60*	---	175	CC	1.3	1.5	QUINN CANYON RANGE
APR 1 23:49:6	36.726	116.232	0.2	7.60	0.7	67	AA	1.3	1.3	SPECTER RANGE NW
2 8:13:26	36.726	116.239	0.2	7.98	0.5	66	AA	1.0	1.3	SPECTER RANGE NW
2 13:57:28	36.730	116.239	0.2	7.61	0.6	59	BA	1.2	1.2	SPECTER RANGE NW
3 2:6:25	37.177	117.876	0.6	6.64	2.4	216	BD	0.9	1.5	WAUCOBA SPRING
3 8:45:45	35.786	117.962	2.2	5.79	0.9	327	BD	1.7	1.5	LITTLE LAKE
3 10:31:7	36.851	116.245	0.4	3.90	1.1	83	AB	0.4	0.5	SKULL MTN
3 13:17:49	37.175	117.879	0.5	6.12	1.2	221	AD	1.7	1.8	WAUCOBA SPRING
3 17:13:9	36.731	115.992	1.3	4.65	3.6	118	BB	1.0	0.9	MERCURY
4 1:29:2	37.172	117.884	0.7	6.00	1.6	232	BD	1.8	1.7	WAUCOBA SPRING
4 8:22:14	37.168	117.913	1.1	1.88	4.3	227	BD	1.8	1.9	WAUCOBA SPRING
4 8:25:27	37.186	117.859	0.6	6.00	1.4	212	AD	1.7	1.5	WAUCOBA SPRING
4 12:19:37	37.250	115.008	0.5	-0.05	0.7	158	AC	1.7	1.9	ALAMO SE
4 16:27:26	37.176	117.878	0.5	6.89	1.2	217	AD	1.4	1.4	WAUCOBA SPRING
4 23:8:11	37.712	115.053	0.4	7.37	1.4	117	AB	1.3	1.4	HIKO NE
5 8:13:47	35.803	117.746	5.0	0.41	3.6	367	DD	1.8	1.8	MOUNTAIN SPRINGS CANYON
5 14:38:23	37.852	116.146	0.3	-0.58	0.7	105	AC	1.5	1.6	REVELLE PEAK
6 15:13:7	37.405	115.200	0.3	-0.18	0.4	88	AC	1.4	1.4	ASH SPRINGS
8 8:52:58	37.226	117.863	2.2	14.32	1.8	232	BD	0.8	0.9	WAUCOBA SPRING
9 5:21:16	36.653	116.402	0.4	6.03	0.7	61	BA	1.5	1.4	LATHROP WELLS NW
9 7:6:29	37.026	116.195	0.2	4.48	0.4	83	AA	1.0	1.1	TIPPIPAH SPRING
9 9:23:33	37.237	115.021	1.4	1.58	2.6	211	BD	0.8	1.0	LOWER PAHRANAGAT LAKE
10 2:11:14	35.749	117.751	1.6	5.82	0.9	301	BD	1.4	1.8	INYO KERN
10 18:48:54	37.028	116.178	0.3	4.20	1.2	98	AB	1.2	1.1	TIPPIPAH SPRING
10 21:32:4	37.573	116.045	0.5	4.05	3.3	99	BC	1.0	1.0	BELTED PEAK
12 9:24:7	37.773	115.312	0.9	3.02*	---	163	CD	1.4	1.4	***QUAD. NOT LISTED***
12 10:23:26	37.376	114.996	0.4	1.18	1.4	175	AC	0.9	1.0	DELAMAR NW
13 5:5:31	36.943	117.778	0.7	10.54	1.5	226	AD	1.1	1.0	WAUCOBA WASH
13 9:20:22	37.734	115.023	0.4	6.79	0.7	133	AB	1.5	1.7	HIKO NE
14 20:10:13	35.723	116.619	1.3	1.76	3.5	277	BD	1.4	1.0	LEACH LAKE
15 1:3:24	37.385	115.005	0.4	2.26	0.7	170	AC	1.0	1.6	ALAMO NE
15 4:40:6	36.739	116.246	0.3	7.00	0.4	115	AB	0.9	0.6	SPECTER RANGE NW
15 16:54:20	37.034	116.193	0.6	3.83	1.1	215	AD	0.7	0.9	TIPPIPAH SPRING
16 6:15:24	37.232	115.395	0.3	6.34	1.3	98	AC	1.7	1.8	DESERT HILLS NW
16 11:54:11	37.027	116.186	0.3	4.63	0.4	110	AB	1.2	1.1	TIPPIPAH SPRING
16 13:18:11	37.047	116.182	0.5	5.67	0.6	234	AD	1.1	1.0	TIPPIPAH SPRING
16 21:39:57	37.281	117.250	0.7	8.45	0.7	143	AC	1.1	1.4	GOLD POINT
17 2:15:57	36.694	117.395	1.1	0.74	1.0	238	BD	0.6	0.7	MARBLE CANYON

## 1982 LOCAL HYPOCENTER SUMMARY

DATE - TIME (UTC)	LATITUDE (DEG. N)	LONGITUDE (DEG. W)	HORIZ ERROR (KM)	DEPTH (KM)	VERT ERROR (KM)	AZI GAP (DEG)	QUAL	Md	Mbi9	QUADRANGLE
APR 17 14:52:48	37.028	116.182	0.3	4.49	0.6	87	AA	0.9	1.1	TIPPIPAH SPRING
17 18:48:33	37.024	116.023	0.8	4.39	3.5	119	BC	1.3	1.4	YUCCA FLAT
17 19:44: 9	37.030	116.189	0.5	4.89	1.2	94	BB	0.8	1.1	TIPPIPAH SPRING
19 13:52:13	35.722	117.776	1.5	5.81	1.6	302	BD	1.6	1.5	INYO KERN
19 20:32:46	36.669	117.452	2.3	0.56	1.9	246	BD	0.9	1.2	MARBLE CANYON
20 12:19:19	36.136	115.696	1.7	5.39	2.2	233	BD	1.9	2.5	CHERRY CREEK SUMMIT
21 8:25:52	37.218	117.682	0.3	9.58	0.6	169	AC	1.4	1.8	LAST CHANCE RANGE
21 23:14:15	37.318	117.846	1.3	14.58	1.0	298	BD	1.4	1.3	SOLDIER PASS
22 11:32:55	36.712	116.229	0.2	9.02	0.3	141	AC	0.9	0.8	SPECTER RANGE NW
22 13:22:50	37.049	116.238	0.8	2.93	0.7	241	AD	0.9	0.7	TIPPIPAH SPRING
23 10:12: 3	37.113	116.505	0.4	9.18	2.8	89	BC	0.7	0.9	THIRSTY CANYON SE
23 10:56:37	36.982	116.017	0.5	5.53	1.0	172	AC	1.2	0.9	YUCCA LAKE
24 0:17:48	35.773	117.700	0.6	7.58	0.4	292	AD	2.2	2.8	MOUNTAIN SPRINGS CANYON
24 13:13:24	37.958	117.788	0.8	0.47	0.6	245	AD	2.1	2.0	RHYOLITE RIDGE
24 14:14:59	38.128	115.746	0.8	0.19	0.8	194	BD	1.5	1.8	CHERRY CREEK SUMMIT
25 2:49:38	36.728	117.304	0.3	11.25	0.4	146	AC	1.4	1.3	MARBLE CANYON
25 3: 3:33	36.510	117.937	1.3	0.72	1.1	256	BD	1.7	2.0	NEW YORK BUTTE
25 3:45:21	36.588	117.877	0.4	13.88	1.0	115	AB	1.3	1.4	STOVEPIPE WELLS
25 4:13:24	35.655	117.777	0.9	0.51	0.4	293	AD	2.8	3.4	INYO KERN
25 4:26:25	35.708	117.742	0.5	7.46	0.4	304	AD	1.8	1.9	RIDGECREST
25 8: 1:21	37.627	114.810	0.8	-0.51	1.0	149	AC	0.9	0.9	PAHROC SPRING NE
25 23:56:12	36.739	115.994	0.3	9.58	0.5	157	AC	0.3	0.5	MERCURY
27 15:42:37	35.597	117.881	1.0	8.60	0.6	296	AD	2.3	3.3	INYO KERN
27 17:34: 1	35.741	117.740	0.6	7.00	0.6	290	AD	2.3	2.4	RIDGECREST
28 10:21:33	36.942	117.529	0.5	4.78	3.2	196	BD	1.3	1.5	DRY MTN
28 12: 8:38	38.019	115.140	1.0	-0.12	0.8	221	AD	1.2	1.7	TIMBER MTN PASS WEST
28 17: 3:10	37.332	118.090	0.2	4.72	1.0	112	AC	1.0	1.2	OAK SPRING BUTTE
28 19:41: 2	37.042	118.136	0.4	3.67	1.0	178	AC	1.1	0.9	TIPPIPAH SPRING
28 21:17:18	36.337	114.899	1.4	5.05	3.2	263	BD	1.6	1.9	DRY LAKE
28 22:58:26	37.202	115.061	---	15.24	---	330	AD	1.1	1.4	LOWER PAHRANAGAT LAKE
28 23:23: 4	38.139	115.768	0.6	2.46	2.7	195	BD	1.3	1.6	QUINN CANYON RANGE
28 23:35:29	38.132	115.751	0.5	4.97	3.9	219	BD	1.4	1.4	QUINN CANYON RANGE
29 4: 0: 1	36.874	116.777	0.3	9.19	0.9	49	AB	1.4	1.4	BULLFROG
MAY 1 1:12:41	37.161	116.190	0.3	7.89	0.7	103	AB	1.2	1.3	RAINIER MESA
2 7:19:42	35.728	117.743	0.6	8.61	0.5	295	AD	2.3	2.5	RIDGECREST
2 10: 2:23	36.190	117.929	0.6	3.39	---	281	CD	1.5	1.5	HAIWEE RESERVOIR
5 7:31:50	37.093	116.856	0.2	-0.43	0.3	88	AA	1.0	1.0	SPRINGDALE
5 20:28:21	36.822	117.499	0.8	5.99	0.9	197	AD	1.2	1.3	TIN MTN
6 11:35:48	37.288	114.905	2.3	9.30	3.0	288	BD	1.2	1.4	DELAMAR LAKE
6 18:37:43	35.970	117.901	0.5	2.92	0.5	289	AD	2.0	2.3	LITTLE LAKE
7 0:12:14	35.828	117.826	3.1	10.43	4.0	296	CD	1.6	2.1	MOUNTAIN SPRINGS CANYON
7 8:58:30	36.723	116.047	0.2	5.72	0.6	96	AB	0.8	0.8	CAMP DESERT ROCK
7 14:45: 4	35.987	115.679	0.8	7.09	0.9	270	AD	1.0	1.9	SHENANDOAH PEAK
7 15:43:44	35.959	116.897	---	7.00	---	266	AD	2.1	1.9	WINGATE WASH
7 18: 6:43	36.293	115.771	0.3	11.41	0.9	162	AC	1.2	1.5	MT STIRLING
8 12:52:17	36.174	115.731	0.8	0.34	0.9	203	AD	1.7	1.5	CHERRY CREEK SUMMIT
8 18:40: 0	36.371	116.061	---	5.86	1.2	0	0	0.0	---	CHUCK WAGON FLAT
8 21:49:41	35.728	117.775	1.9	5.93	0.9	312	BD	1.9	2.2	INYO KERN
9 2:12:29	37.531	115.428	0.5	5.16	5.0	113	BC	1.1	1.1	MT IRISH
9 8:58:20	37.074	116.046	0.5	0.39	0.9	130	AC	1.2	1.4	YUCCA FLAT
10 6:22:37	35.783	117.730	2.4	7.00	2.4	299	CD	2.0	2.1	MOUNTAIN SPRINGS CANYON
12 0: 5:20	35.733	117.710	1.1	7.59	0.8	302	BD	2.1	2.6	RIDGECREST
12 1:22:58	35.760	117.798	2.0	3.06	---	310	CD	2.1	2.2	LITTLE LAKE
12 19:29:25	37.282	115.029	0.3	7.24	0.6	169	AC	3.0	3.3	ALAMO SE
12 19:33:25	37.293	115.024	0.5	4.75	2.6	152	BC	2.0	2.0	ALAMO SE
12 19:50:51	37.272	115.021	0.4	8.69	0.7	192	AD	2.0	---	ALAMO SE
12 20: 7:37	37.309	115.030	1.0	5.27	1.3	179	AC	1.3	1.8	ALAMO SE
12 20: 9:10	37.253	115.026	0.2	2.59	---	227	DD	1.0	0.8	ALAMO SE
12 20:26: 3	37.266	115.037	1.3	0.17	1.6	152	BC	1.5	1.6	ALAMO SE
12 20:27:37	37.234	114.984	2.1	3.88	---	247	CD	1.1	1.1	DELAMAR 3 NW
12 22: 8:60	37.237	115.006	1.1	9.85	2.2	215	BD	1.0	1.5	LOWER PAHRANAGAT LAKE
12 22:15:20	37.223	114.980	2.3	7.87	4.1	225	BD	1.3	1.3	DELAMAR 3 NW
12 22:33:11	37.258	115.077	2.0	4.36	5.5	187	CD	1.1	1.2	ALAMO SE
12 23: 4:13	37.254	115.004	1.0	0.16	1.1	158	CC	1.7	1.6	ALAMO SE
13 0:12:27	37.280	115.048	5.8	2.09	---	181	DD	2.4	---	ALAMO SE
13 11:25:29	37.246	115.044	2.1	6.34	7.4	153	CC	2.3	---	LOWER PAHRANAGAT LAKE



## 1982 LOCAL HYPOCENTER SUMMARY

	DATE - TIME (UTC)	LATITUDE (DEG. N)	LONGITUDE (DEG. W)	HORIZ ERROR (KM)	DEPTH (KM)	VERT ERROR (KM)	AZI GAP (DEG)	QUAL	Md	Mb19	QUADRANGLE
MAY	13 15:42:54	37.252	115.007	0.5	4.29	2.1	209	BD	1.2	1.3	ALAMO SE
	13 17:37:48	37.240	115.008	2.4	0.09	1.7	213	BD	1.2	1.1	LOWER PAHRANAGAT LAKE
	13 21:24:53	37.256	115.000	0.3	0.12	0.4	159	BC	1.8	2.0	ALAMO SE
	14 3:11:28	37.247	115.020	1.3	1.75	2.4	208	BD	1.4	1.1	LOWER PAHRANAGAT LAKE
	14 5: 0:34	37.260	115.018	0.2	0.32	0.3	156	AC	1.8	2.1	ALAMO SE
	14 8: 0:23	37.226	115.102	1.7	7.64	2.7	213	BD	1.1	1.1	LOWER PAHRANAGAT LAKE
	14 19: 6:56	36.033	116.026	1.8	6.76	5.1	127	CB	2.0	1.6	BENNETTS WELL
	14 19:40:25	35.749	117.784	0.7	6.15	0.6	302	AD	2.1	2.1	INYOKERN
	14 20: 5: 6	35.773	117.768	0.8	5.64	0.8	284	AD	2.0	2.5	LITTLE LAKE
	15 0:24:58	37.276	115.015	0.4	6.69	1.6	155	AC	1.5	1.5	ALAMO SE
	15 5:50:52	37.715	115.058	0.3	6.36	1.1	116	AB	1.0	1.3	HIKO NE
	15 18:12:10	37.275	115.060	1.1	17.09	1.6	186	BD	1.4	---	ALAMO SE
	15 21:41:37	37.313	115.052	0.7	4.55	1.4	184	AD	1.4	1.4	ALAMO SE
	15 22:49:56	37.272	115.013	0.6	-0.10	0.6	186	AD	1.3	1.6	ALAMO SE
	16 2:10:31	37.015	115.172	0.7	5.32	1.9	191	AD	1.4	1.6	LOWER PAHRANAGAT LAKE SW
	16 21:23:30	37.224	114.983	0.7	3.00	3.0	204	BD	1.2	1.6	DELAMAR 3 NW
	16 23:33: 3	36.771	116.280	0.2	5.01	0.3	75	AA	0.9	0.9	JACKASS FLATS
	17 12:16: 1	37.063	116.041	0.3	-0.32	---	146	CC	1.4	1.4	YUCCA FLAT
	17 12:55:44	37.310	115.030	0.4	6.56	0.7	209	AD	1.5	1.5	ALAMO SE
	17 14: 2:56	37.251	115.033	1.4	4.25	4.7	203	BD	1.0	1.2	ALAMO SE
	17 22:14:57	37.264	115.020	0.7	-0.25	0.6	183	AD	1.7	1.6	ALAMO SE
	17 23: 8:29	36.756	116.152	0.2	4.44	1.1	98	AC	0.6	0.8	SKULL MTN
	18 2:55:58	37.298	115.041	0.5	9.66	0.7	184	AD	1.3	1.2	ALAMO SE
	18 3:51: 6	37.255	115.023	0.4	0.46	0.4	199	AD	1.2	1.3	ALAMO SE
	22 21:55:12	36.362	117.031	0.4	4.25	0.4	84	AA	1.2	1.3	EMIGRANT CANYON
	23 8:35:15	35.716	117.784	1.0	5.13	0.9	302	BD	1.9	2.2	INYOKERN
	23 13:57:47	36.650	116.369	0.3	9.65	0.4	111	AB	1.0	1.0	LATHROP WELLS NW
	24 15: 9:56	37.408	115.493	1.0	4.87	---	146	CC	1.3	1.4	CRESCENT RESERVOIR
	24 17:33:58	36.546	116.428	0.2	6.26	1.3	94	AC	1.2	1.2	LATHROP WELLS SW
	25 23:50:37	37.203	116.456	0.2	6.50	0.9	60	AC	1.0	1.3	SILENT BUTTE
	26 17:17: 1	37.269	115.025	---	1.95	---	198	AD	1.2	1.1	ALAMO SE
	27 8:32:44	37.268	114.978	1.0	6.05	2.5	203	BD	---	1.0	DELAMAR LAKE
	27 10:57: 3	36.712	116.103	0.3	6.50	1.0	137	AC	1.3	---	CAMP DESERT ROCK
	28 12:33:28	37.052	116.170	0.3	0.92	0.4	92	AB	---	0.9	TIPPIPAH SPRING
	29 10:38:53	37.255	115.031	1.8	5.96	2.6	225	BD	1.1	1.3	ALAMO SE
	30 1:26:52	35.763	115.945	0.7	3.61	2.3	242	BD	1.8	2.0	HORSE THIEF SPRINGS
	30 8:29:44	37.124	115.296	0.4	2.00	1.0	152	AC	1.6	1.8	DESERT HILLS SE
	30 14:28:20	37.265	115.066	1.3	6.69	1.7	186	BD	1.3	1.0	ALAMO SE
	30 18:24:34	37.346	114.656	1.9	5.28	---	284	CD	1.2	1.3	ELGIN SW
	31 3:27:31	37.245	115.017	0.8	4.34	3.6	209	BD	1.3	1.3	LOWER PAHRANAGAT LAKE
	31 15:42: 2	35.598	118.411	9.1	7.98	---	315	DD	2.5	3.0	***REGIONAL***
JUN	1 2: 8: 9	35.717	117.746	1.5	4.65	3.0	302	BD	---	1.8	RIDGECREST
	1 8:37:29	37.254	115.036	2.0	4.19	7.1	201	CD	---	1.2	ALAMO SE
	1 11: 2: 1	35.948	114.819	1.9	5.23	0.9	260	BD	1.7	2.3	BOULDER CITY
	2 10:59:24	37.368	115.253	0.4	10.79	2.4	105	BD	---	1.0	BADGER SPRING
	2 11:21:19	38.237	115.897	0.7	3.38	2.5	227	BD	---	1.4	QUINN CANYON RANGE
	2 13:31:39	35.981	117.421	1.6	5.96	1.8	269	BD	---	1.4	TRONA
	2 17:29: 1	37.068	116.942	0.3	4.90	0.9	135	AC	1.0	1.2	SPRINGDALE
	2 17:34:54	37.074	116.947	0.2	1.54	0.6	53	AC	---	1.5	SPRINGDALE
	4 7:41:53	37.135	115.294	0.6	7.64	1.0	160	AC	---	0.8	DESERT HILLS NE
	5 0:57:39	37.260	115.013	0.3	2.12	1.1	156	AC	2.4	---	ALAMO SE
	5 2:40:33	37.247	115.005	0.7	1.41	1.4	211	AD	---	1.4	LOWER PAHRANAGAT LAKE
	5 9:54:53	37.637	117.850	1.9	7.15	2.3	200	BD	2.5	---	PIPER PEAK
	5 23: 6:40	37.855	116.950	0.5	15.36	1.5	146	AC	---	0.8	SPRINGDALE
	6 4:32: 5	37.003	116.945	0.2	4.56	1.6	66	AC	---	0.9	SPRINGDALE
	6 9:44:32	37.636	115.064	0.3	5.87	1.5	112	AC	---	1.0	HIKO NE
	6 12:32:15	37.640	115.083	0.3	5.77	1.1	81	AC	---	1.3	HIKO NE
	6 23:45:57	37.269	117.617	0.4	4.41	0.6	88	AA	---	1.1	MAGRUDER MTN
	7 0:17: 2	37.249	115.022	1.0	4.45	3.7	206	BD	---	1.1	LOWER PAHRANAGAT LAKE
	8 8: 7:21	37.230	114.978	1.1	4.35	6.2	246	CD	---	1.3	DELAMAR 3 NW
	8 18:15:42	35.615	116.867	0.9	2.65	1.9	272	AD	---	1.9	WINGATE WASH
	9 4: 8:24	36.500	117.860	1.2	5.68	---	254	CD	---	1.4	NEW YORK BUTTE
	9 4:28:56	36.967	117.549	0.3	0.50	0.4	182	AD	---	1.4	DRY MTN
	9 18:45:23	36.932	116.803	0.5	9.19	1.2	144	AC	---	0.8	BULLFROG
	12 0:53:54	37.142	116.851	0.5	0.30	0.9	121	AB	---	0.8	SPRINGDALE
	12 1:38:51	37.135	116.875	0.3	0.00	9.2	48	CB	1.9	---	SPRINGDALE

# 1982 LOCAL HYPOCENTER SUMMARY

	DATE - TIME (UTC)	LATITUDE (DEG. N)	LONGITUDE (DEG. W)	HORIZ ERROR (KM)	DEPTH (KM)	VERT ERROR (KM)	AZI GAP (DEG)	QUAL	Md	Mbiq	QUADRANGLE
JUN	13 23:39:40	36.869	116.195	0.4	4.36	0.8	58	AA	1.5	---	SKULL MTN
	14 6:11:36	37.203	114.982	1.0	11.49	1.7	232	AD	---	1.3	DELAMAR 3 NW
	14 10:22:41	36.397	117.935	0.8	6.30	1.2	259	AD	---	1.7	KEELER
	15 1:26:25	36.968	116.124	0.2	5.23	0.5	104	AB	---	0.5	YUCCA LAKE
	16 6:38:43	35.870	117.475	11.3	6.10	0.5	292	DD	---	1.5	TROMA
	17 16:55:50	37.072	116.941	0.2	-0.43	0.2	84	AC	---	1.0	SPRINGDALE
	18 9:14:55	37.335	117.686	0.3	6.02	0.9	134	AB	---	1.3	MAGRUDER MTN
	18 9:48:21	37.334	117.684	0.2	2.96	1.5	134	AC	---	1.4	MAGRUDER MTN
	18 18:52:42	37.121	116.387	0.4	8.58	1.4	185	AD	---	0.8	TIMBER MTN
	18 20:5:13	37.077	116.302	0.7	7.03	2.0	161	AC	---	0.7	BUCKBOARD MESA
	19 9:36:29	35.751	117.756	7.8	-1.08	4.6	301	DD	---	1.8	LITTLE LAKE
	19 22:50:13	36.605	117.112	0.3	5.72	1.7	116	AC	---	1.4	STOVEPIPE WELLS
	20 0:3:1	36.611	117.110	0.3	5.90	2.0	113	BC	---	1.0	STOVEPIPE WELLS
	20 1:51:28	36.199	117.603	0.5	6.77	0.8	203	AD	---	1.7	COSO PEAK
	20 3:34:47	36.663	116.266	0.4	7.72	0.6	127	AB	---	0.7	STRIPED HILLS
	20 3:36:2	36.661	116.264	0.2	7.23	0.3	106	AB	---	0.6	STRIPED HILLS
	20 11:46:53	36.101	117.418	4.1	15.44	1.0	292	CD	2.1	---	MATURANGO
	21 10:31:57	36.606	117.106	0.2	0.82	0.3	113	AC	---	1.2	STOVEPIPE WELLS
	22 9:22:53	37.141	116.877	0.3	2.11	1.7	49	AB	---	1.4	SPRINGDALE
	22 15:29:59	36.604	117.106	0.4	7.59	1.6	115	AC	---	1.0	STOVEPIPE WELLS
	22 19:44:13	37.075	116.945	0.2	1.46	0.6	65	AC	---	1.2	SPRINGDALE
	22 21:14:48	37.085	116.372	0.4	0.63	0.7	107	AB	---	0.7	BUCKBOARD MESA
	22 21:59:45	37.168	116.830	0.3	9.79	1.1	128	AC	---	1.2	SPRINGDALE
	23 13:27:53	36.604	117.114	0.2	8.85	0.7	117	AB	---	1.4	STOVEPIPE WELLS
JUL	23 13:31:56	36.605	117.111	0.2	0.36	0.3	115	AC	---	1.2	STOVEPIPE WELLS
	23 14:9:49	36.605	117.109	0.3	5.66	1.4	115	AC	---	1.4	STOVEPIPE WELLS
	23 15:20:14	36.607	117.104	0.5	4.09	0.1	113	CC	---	1.2	STOVEPIPE WELLS
	23 22:43:21	36.607	117.101	0.3	4.78	2.7	112	BC	---	1.2	STOVEPIPE WELLS
	24 7:7:00	36.610	117.099	0.2	0.80	0.4	111	AC	---	0.8	STOVEPIPE WELLS
	25 19:10:41	37.084	117.358	0.2	0.84	0.3	120	AB	---	1.2	UBENEZE CRATER
	28 10:41:35	37.509	117.054	0.3	3.12	---	83	CC	---	1.4	LIDA WASH
	28 12:51:40	36.837	116.267	0.3	9.85	0.5	105	AB	---	0.4	JACKASS FLATS
	30 16:5:10	37.718	115.051	0.3	7.49	1.1	119	AB	---	0.9	HIKO NE
	3 6:7:36	36.081	115.918	11.2	7.00	---	186	DD	2.5	---	QUINN CANYON RANGE
	3 9:10:57	37.009	116.107	0.4	2.71	---	141	CC	0.9	---	YUCCA FLAT
	3 12:27:51	37.265	115.045	2.9	9.34	5.5	180	CD	2.2	---	ALAMO SE
	4 7:23:24	37.699	115.043	0.3	-0.05	0.6	117	AC	---	1.4	HIKO NE
	4 7:30:59	37.698	115.046	0.3	0.74	0.6	116	AC	---	1.2	HIKO NE
	4 7:38:8	37.654	115.078	1.5	11.71	5.0	103	CB	---	0.8	HIKO NE
	4 8:0:28	37.846	114.460	3.1	3.50	---	308	CD	---	1.4	***REGIONAL***
	4 12:44:3	35.757	117.717	4.4	8.38	1.4	284	CD	---	2.8	MOUNTAIN SPRINGS CANYON
	4 14:34:18	35.773	117.672	10.1	2.96	5.8	267	DD	2.1	2.0	MOUNTAIN SPRINGS CANYON
	5 7:8:49	37.906	117.106	0.3	0.48	0.4	107	AC	---	1.6	MUD LAKE
	5 17:54:3	35.400	116.447	4.0	0.50	3.1	310	CD	---	1.7	***REGIONAL***
	5 21:30:45	37.252	116.153	0.2	4.11	1.3	112	AC	---	0.8	QUARTET DOME
	5 23:45:7	37.219	114.825	1.7	2.22	7.0	229	CD	---	1.2	DELAMAR 3 NE
	6 2:18:43	37.698	115.037	0.2	2.56	0.6	119	AC	3.1	---	HIKO NE
	6 2:15:43	37.668	115.046	0.6	0.70	0.9	154	AC	---	1.3	HIKO NE
	6 2:19:26	37.686	115.045	0.7	0.40	1.1	113	BC	---	1.2	HIKO NE
	6 2:38:0	37.691	115.048	0.4	0.93	0.6	114	AC	---	1.2	HIKO NE
	6 2:33:16	37.677	115.035	0.8	-1.11	0.9	114	BB	---	1.0	HIKO NE
	6 2:36:52	37.678	115.039	0.6	3.19	5.1	160	CC	---	0.9	HIKO NE
	6 2:37:17	37.701	115.038	0.6	5.03	9.3	119	CC	---	1.0	HIKO NE
	6 2:43:6	37.699	115.040	1.0	0.93	1.5	118	BC	---	0.9	HIKO NE
	6 2:49:49	37.683	115.045	0.6	1.00	2.8	113	BC	---	1.1	HIKO NE
	6 2:51:25	37.694	115.037	0.9	1.22	4.1	118	BB	---	1.3	HIKO NE
	6 2:53:27	37.691	115.050	0.7	0.17	1.0	113	AC	---	0.8	HIKO NE
	6 4:5:22	37.696	115.038	0.5	-0.26	0.9	118	BC	---	1.4	HIKO NE
	6 4:8:16	37.691	115.044	0.5	0.83	0.9	115	AC	---	0.9	HIKO NE
	6 4:17:57	37.702	115.038	0.7	2.38	1.8	119	AC	---	1.2	HIKO NE
	6 4:26:42	37.699	115.042	0.7	2.52	2.1	118	BC	---	0.9	HIKO NE
	6 4:29:6	37.692	115.028	0.6	4.05	3.2	120	BB	---	0.8	HIKO NE
	6 4:36:16	37.696	115.046	0.3	1.67	0.9	116	AC	---	1.3	HIKO NE
	6 4:47:39	37.682	115.049	0.3	1.13	1.2	112	AC	---	0.8	HIKO NE
	6 4:56:31	37.696	115.039	0.6	0.69	1.0	118	AC	---	1.4	HIKO NE
	6 5:0:55	37.684	115.049	0.4	1.15	1.5	112	AC	---	1.1	HIKO NE

## 1982 LOCAL HYPOCENTER SUMMARY

	DATE - TIME (UTC)	LATITUDE (DEG. N)	LONGITUDE (DEG. W)	HORIZ ERROR (KM)	DEPTH (KM)	VERT ERROR (KM)	AZI CAP (DEG)	QUAL	Md	Mblg	QUADRANGLE
JUL	6 5:10:11	37.692	115.045	0.4	0.93	0.5	115	AC	---	1.2	HIKO NE
	6 5:11:55	37.678	115.046	0.7	0.83	1.1	111	BC	---	0.8	HIKO NE
	6 5:19:51	37.694	115.044	0.2	0.87	0.3	116	AC	---	0.9	HIKO NE
	6 5:24:53	37.682	115.048	0.4	0.79	0.7	112	AC	0.8	1.1	HIKO NE
	6 5:29:27	37.692	115.033	1.2	3.76	6.6	119	CB	1.2	1.2	HIKO NE
	6 5:38:40	37.727	115.035	0.7	1.84	2.3	127	BC	0.5	0.8	HIKO NE
	6 5:49:56	37.699	115.043	0.3	2.29	1.0	117	AC	0.9	1.2	HIKO NE
	6 6:14:29	37.698	115.040	0.3	1.65	1.1	116	AC	1.2	1.5	HIKO NE
	6 6:42:58	37.386	116.124	9.7	7.00*	---	169	DC	1.5	---	WHEELBARROW PEAK NE
	6 6:56:54	36.815	117.540	---	7.00**	---	325	BD	2.0	---	DRY MTN
	6 9:40:41	37.136	117.331	8.1	-0.14*	---	107	DC	1.1	---	UBEHEBE CRATER
	6 10: 5:19	37.674	114.999	6.3	7.00	5.3	274	DD	1.9	---	PAHROC SPRING
	6 14:58: 7	37.698	115.049	0.3	0.97	0.6	115	AC	---	1.4	HIKO NE
	7 0:21:15	37.678	115.070	2.1	3.13*	---	176	CC	0.9	1.0	HIKO NE
	7 10:14:31	37.067	116.942	0.5	7.60	2.4	96	BB	---	1.3	SPRINGDALE
	7 16:40:27	37.700	115.049	0.6	-0.65	1.0	116	AC	---	1.3	HIKO NE
	7 19:43:35	37.273	115.069	0.7	3.01*	---	128	CC	---	1.1	GROOM LAKE
	8 1:50:49	37.702	115.036	0.3	2.16	0.6	120	AC	---	2.0	HIKO NE
	8 2:33: 8	37.701	115.046	0.4	0.56	0.5	117	AC	---	1.2	HIKO NE
	8 6: 6:37	37.277	117.644	0.4	0.12	0.6	121	AB	---	1.2	MAGRUDER MTN
	8 19:32:40	37.696	115.044	0.3	-0.12	0.5	116	AC	---	1.3	HIKO NE
	9 13:23:19	37.450	114.993	0.8	0.40	1.2	174	AC	---	1.0	DELAMAR NW
	9 18:37:17	36.336	114.884	1.0	6.43	1.6	263	BD	---	1.5	DRY LAKE
	10 6:31:15	36.721	116.203	0.2	1.62	4.5	128	BB	---	0.4	SPECTER RANGE NW
	10 8:57:21	37.386	115.190	0.0	5.79	3.0	154	BC	---	1.4	ASH SPRINGS
	10 18: 5:46	37.363	115.212	1.6	9.58	3.4	165	BC	---	1.2	ALAMO
	11 10: 2:26	35.795	117.727	3.7	0.60	3.0	298	CD	---	1.5	MOUNTAIN SPRINGS CANYON
	13 21:31:39	37.699	115.040	0.3	1.94	0.8	118	AC	---	2.3	HIKO NE
	14 10: 9:27	37.227	117.327	0.3	7.45	0.7	89	AB	---	1.1	UBEHEBE CRATER
	14 22: 2:32	37.696	115.042	0.2	1.76	0.6	117	AC	---	1.4	HIKO NE
	15 5:24:51	37.691	115.044	0.4	1.73	1.4	115	AC	---	1.4	HIKO NE
	15 19:35:32	37.073	116.423	0.3	0.17	0.1	261	AD	---	0.9	TIMBER MTN
	15 19:45:58	36.129	115.750	1.1	1.01	2.5	236	BD	---	1.6	QUINN CANYON RANGE
	16 16:11:43	37.698	115.047	0.4	1.38	1.7	116	AC	---	1.1	HIKO NE
	17 8:58:15	37.065	116.941	0.4	8.86	1.8	96	AB	---	1.2	SPRINGDALE
	17 9:53:56	36.709	116.213	0.3	0.52	0.4	135	AB	---	1.0	SPECTER RANGE NW
	17 11:26: 9	37.700	115.036	0.4	0.20	0.6	120	AC	---	1.3	HIKO NE
	17 16: 8:38	36.178	115.920	1.3	5.44	3.2	221	BD	---	1.6	QUINN CANYON RANGE
	19 7:36:51	37.347	114.742	1.9	5.71	2.8	232	BD	1.8	---	ELGIN SW
	19 7:51:50	37.336	114.708	1.3	1.85	3.4	209	BD	---	1.6	ELGIN SW
	19 11:35:53	37.487	117.645	---	7.00**	---	150	AD	1.8	---	SOLDIER PASS
	20 20:20:54	37.716	115.014	0.6	-0.02	2.2	132	BB	---	1.9	HIKO NE
	21 9:14:44	36.526	117.931	10.8	32.23*	---	257	DD	2.3	---	NEW YORK BUTTE
	21 10:54:31	37.038	116.736	2.1	25.92	2.1	222	BD	1.5	---	THIRSTY CANYON SW
	22 9:24:52	37.122	114.849	0.7	5.53	4.8	232	BD	---	1.4	DELAMAR 3 SE
	23 23:47:57	36.137	117.722	1.5	3.75	3.9	250	BD	2.0	2.2	COSO PEAK
	24 0: 5:24	36.152	117.698	1.0	2.47	2.9	247	BD	1.6	1.6	COSO PEAK
	24 0:18:13	37.696	115.046	0.4	-0.46	0.7	115	AC	1.5	1.7	HIKO NE
	24 3:36:12	37.001	117.901	1.3	1.16	4.3	225	BD	1.6	1.5	WAUCOBA SPRING
	24 22:54:27	36.562	117.002	0.3	9.67	1.5	97	BC	---	1.3	STOVEPIPE WELLS
	25 1:21: 2	37.699	115.042	0.5	0.63	0.9	118	BC	---	1.3	HIKO NE
	25 1:52:46	35.821	117.678	4.7	-0.47	3.6	295	CD	---	1.6	MOUNTAIN SPRINGS CANYON
	25 7:59:16	37.009	116.211	0.3	4.75	0.4	83	AA	---	1.0	TIPPICAH SPRING
	25 9:34:56	37.609	116.862	0.3	7.36	0.6	175	AC	---	1.3	CACTUS SPRING
	27 12:17:52	36.231	117.839	1.3	1.32	2.2	260	BD	---	1.5	HAIWEE RESERVOIR
	27 12:47:36	37.716	115.005	1.0	4.33	4.3	134	BB	1.8	2.1	HIKO NE
	29 1:31:27	36.604	116.633	0.6	10.51	1.1	203	BD	---	0.5	BIG DUNE
	29 4:35:18	37.595	117.744	0.4	0.05	1.5	171	BC	---	1.5	LIDA WASH
	29 4:42:31	37.576	117.808	1.8	1.36	5.6	154	CC	---	1.1	PIPER PEAK
	29 15:52:33	37.372	115.232	0.0	0.37	3.4	93	BC	---	1.3	ALAMO
	30 22:35:41	37.895	114.764	1.1	3.60*	---	258	CD	---	0.9	DEADMAN SPRING NE
	31 0:57:57	35.663	117.770	2.3	5.29	1.3	293	BD	---	2.2	INYOKERN
	31 6:42:18	35.428	116.301	1.3	6.66	2.1	307	BD	2.2	2.3	***REGIONAL***
	31 10:10:37	37.377	115.219	0.3	0.32	0.4	95	AC	1.7	1.8	ASH SPRINGS
	31 17:55:12	35.756	117.663	6.9	0.57	5.7	267	DD	---	1.6	MOUNTAIN SPRINGS CANYON
	31 19:48:20	36.506	115.085	2.4	-1.15	1.1	248	BD	---	1.3	HAYFORD PEAK

## 1982 LOCAL HYPOCENTER SUMMARY

DATE - TIME (UTC)	LATITUDE (DEG. N)	LONGITUDE (DEG. W)	HORIZ ERROR (KM)	DEPTH (KM)	VERT ERROR (KM)	AZI CAP (DEG)	QUAL	Md	Mblg	QUADRANGLE
JUL 31 22:17:29	37.357	114.928	---	0.88	---	268	DD	1.0	1.0	DELMAR LAKE
AUG 1 9:53:36	37.227	117.920	0.7	2.19	2.2	224	BD	---	1.6	WAUCOBA SPRING
1 17:23:17	36.919	117.565	0.4	4.95	3.4	288	BD	---	1.1	DRY MTN
1 21:30:00	37.692	115.038	0.4	1.38	1.2	117	AB	---	1.1	HIKO NE
2 6:3:40	35.773	117.738	3.8	0.66	2.8	288	CD	---	1.8	MOUNTAIN SPRINGS CANYON
2 9:38:54	37.628	114.614	0.9	-0.98	0.7	292	AD	---	0.8	CHIEF MTN
2 11:56:55	37.679	115.039	0.8	5.08	3.0	114	BB	---	0.3	HIKO NE
2 16:58:58	36.753	118.189	0.5	10.03	1.0	118	AB	0.5	0.9	SKULL MTN
3 8:45:51	35.918	117.274	1.9	2.23	6.2	276	CD	---	1.8	TRONA
6 7:57:11	37.718	115.012	0.9	2.12	2.1	133	BB	---	1.4	HIKO NE
6 8:46:4	37.632	114.982	0.3	0.22	0.2	151	AC	0.6	0.5	PAHROC SPRING
6 10:26:19	37.692	115.048	---	-0.76	---	294	AD	---	1.0	HIKO NE
6 10:58:22	37.605	115.026	---	-0.72	---	200	BD	---	0.7	HIKO SE
6 15:50:17	37.716	115.023	1.4	2.23	3.3	145	BD	---	1.0	HIKO NE
6 16:2:50	37.719	115.025	0.2	2.65	0.6	145	AD	---	0.7	HIKO NE
6 17:33:6	37.719	115.039	---	0.98	---	232	AD	---	0.9	HIKO NE
6 17:49:7	37.704	115.044	0.6	0.97	1.1	118	AC	---	1.2	HIKO NE
7 9:0:2	36.891	117.697	0.8	2.70	2.4	198	BD	1.4	1.4	DRY MTN
7 13:30:59	36.722	118.273	0.3	3.71	0.7	76	AA	---	0.7	STRIPED HILLS
8 14:49:30	36.724	118.265	0.3	3.84	0.8	72	AA	---	1.0	STRIPED HILLS
9 17:37:13	37.698	115.046	0.3	4.58	1.9	116	AC	---	1.2	HIKO NE
9 18:36:22	37.189	117.866	2.7	9.42	4.4	245	CD	---	1.0	WAUCOBA SPRING
9 20:58:55	37.338	114.731	1.8	3.31	---	235	CD	---	1.4	ELGIN SW
9 21:59:15	37.683	115.049	0.3	1.11	1.8	112	AC	0.9	0.8	HIKO NE
9 23:6:38	37.024	116.369	0.2	8.93	0.2	134	AB	0.4	0.8	BUCKBOARD MESA
10 6:21:38	37.703	115.033	0.4	2.66	1.1	121	AC	---	0.6	HIKO NE
10 15:54:44	36.897	118.218	0.6	-0.49	0.4	141	AC	---	0.7	MINE MTN
11 21:4:11	37.114	117.336	0.8	8.93	1.7	196	AD	---	0.9	UBEHEBE CRATER
12 8:55:48	36.597	116.450	0.4	5.37	1.4	105	AC	---	0.8	LATHROP WELLS SW
13 5:44:10	37.164	117.338	0.2	5.61	1.4	104	AC	---	1.3	UBEHEBE CRATER
13 14:47:30	37.117	118.749	0.4	4.03	1.4	123	BB	1.0	1.0	THIRSTY CANYON SW
13 17:38:40	37.700	115.042	0.2	4.10	1.3	144	AC	1.1	1.2	HIKO NE
13 19:44:2	36.725	118.281	0.4	2.81	0.8	113	AB	---	0.8	STRIPED HILLS
13 22:1:49	36.748	118.630	0.6	3.85	0.6	191	AD	---	0.5	BIG DUNE
14 3:11:58	37.203	118.189	---	3.09	---	281	AD	---	0.8	RAINIER MESA
14 4:6:52	37.022	118.455	0.2	9.39	0.3	157	AC	---	1.0	TIMBER MTN
14 4:26:27	36.296	118.147	0.8	2.06	1.8	159	AC	---	1.0	HIGH PEAK
14 7:41:11	36.294	118.117	1.1	0.98	1.2	171	BC	---	1.2	MT SCHADER SE
14 7:45:2	36.295	118.143	1.1	5.55	2.7	161	BC	---	0.9	HIGH PEAK
15 18:45:21	37.401	114.240	2.9	3.88	2.4	298	CD	---	2.1	***REGIONAL***
15 19:37:57	37.515	114.497	2.4	2.56	2.3	298	BD	---	1.4	***REGIONAL***
16 4:14:21	35.711	117.676	5.7	4.04	3.2	300	DD	---	1.7	RIDGECREST
16 4:19:46	37.175	117.908	1.2	2.28	4.7	228	BD	---	1.3	WAUCOBA SPRING
16 6:26:29	37.692	115.046	0.3	1.02	---	150	CC	---	1.2	HIKO NE
16 22:7:12	36.959	117.603	0.7	3.29	---	183	CD	---	1.5	DRY MTN
17 7:22:12	36.903	116.733	0.3	5.02	1.5	146	AC	---	0.9	BARE MTN
19 6:1:24	36.760	118.019	1.2	6.34	4.0	207	BD	---	0.3	CANE SPRING
19 7:31:35	36.222	115.269	5.7	1.95	---	306	DD	---	0.8	BLUE DIAMOND NE
19 15:13:57	37.199	117.376	0.5	10.18	1.5	123	AB	---	1.0	UBEHEBE CRATER
20 6:43:00	35.349	116.472	2.5	3.75	3.3	314	CD	---	1.6	***REGIONAL***
20 10:32:56	35.949	114.766	1.1	3.53	0.7	299	BD	---	1.3	BOULDER CITY
20 11:11:40	36.021	114.794	2.0	3.30	0.9	284	BD	---	1.8	BOULDER BEACH
20 22:13:49	37.666	117.848	2.1	6.73	1.4	206	BD	2.0	---	PIPER PEAK
21 20:7:8	37.219	118.460	0.4	10.27	0.7	158	AC	---	0.8	SCRUGHAM PEAK
21 21:10:27	36.770	118.201	1.2	3.09	1.8	265	BD	---	1.6	***REGIONAL***
22 0:41:7	37.100	118.085	0.4	0.60	0.6	102	AC	---	1.0	YUCCA FLAT
22 4:57:5	36.479	115.839	1.0	15.39	0.7	253	AD	---	0.9	MT STIRLING
22 13:46:32	35.780	116.987	1.1	8.98	0.9	279	BD	---	1.9	WINGATE WASH
22 15:39:58	36.161	115.762	0.7	5.11	5.3	220	CD	---	0.9	PAHRUMP
23 16:8:42	36.778	115.478	0.3	3.00	2.0	101	BC	---	2.5	DOG BONE LAKE SOUTH
24 15:17:41	37.474	116.778	0.3	4.79	2.4	86	BC	---	1.6	TOLICHA PEAK
24 22:51:19	36.825	116.651	0.5	-0.488L	0.7	79	BA	---	1.0	● BARE MTN
25 18:28:1	37.196	116.480	0.2	0.36	0.3	46	AC	1.5	1.1	SCRUGHAM PEAK
25 23:32:45	35.874	117.717	1.7	4.79	1.7	280	BD	---	1.9	MOUNTAIN SPRINGS CANYON
26 5:6:39	37.194	117.544	0.2	5.50	3.1	144	BC	1.8	1.7	LAST CHANCE RANGE
27 1:9:45	37.228	117.831	0.5	7.47	1.2	202	AD	---	1.4	WAUCOBA SPRING

## 1982 LOCAL HYPOCENTER SUMMARY

DATE - TIME (UTC)	LATITUDE (DEG. N)	LONGITUDE (DEG. W)	HORIZ ERROR (KM)	DEPTH (KM)	VERT ERROR (KM)	AZI GAP (DEG)	QUAL	Md	Mb1g	QUADRANGLE
AUG 27 20: 0:14	37.058	116.948	0.4	4.69	1.7	79	BC	1.5	1.3	SPRINGDALE
27 20:43:43	35.727	117.760	4.7	10.39	3.4	310	CD	---	2.4	INYOKERN
29 17:12:44	35.296	116.584	---	2.00	---	344	AD	1.4	0.4	***REGIONAL***
29 18:17: 6	37.527	117.225	1.1	2.53	0.5	154	CC	1.0	-0.6	GOLDFIELD
30 16:46:42	37.147	117.349	0.1	6.99	0.5	112	AC	---	0.9	UBEHEBE CRATER
31 0: 3:57	36.158	114.925	0.4	2.40*	---	273	DD	1.4	1.6	FRENCHMAN MTN
31 1:14:44	36.009	114.817	1.7	0.37	1.3	280	BD	---	1.7	BOULDER BEACH
31 19:23: 8	37.772	115.099	0.3	3.03*	---	137	CC	---	0.6	WHITE RIVER NARROWS
31 20: 6:27	37.066	116.948	0.4	4.91	2.6	55	BC	1.5	1.3	SPRINGDALE
31 20:56:36	37.061	116.947	0.2	5.19	0.7	45	AC	1.9	2.4	SPRINGDALE
31 21:15:35	37.035	116.946	0.1	5.49	0.3	140	AC	---	1.1	SPRINGDALE
SEP 1 2:29:34	37.409	116.475	1.4	7.00	3.1	292	BD	---	1.8	***REGIONAL***
2 14:32:27	37.691	115.044	0.2	4.67	1.2	151	AC	1.2	1.0	HIKO NE
2 18: 6:18	36.732	116.261	0.3	6.64	0.3	90	AA	---	0.9	STRIPED HILLS
3 12:19:45	37.586	117.682	0.4	2.67	2.3	100	BC	1.1	0.9	LIDA WASH
3 14:28:10	37.949	114.970	3.2	15.34	3.0	306	CD	1.3	1.2	DEADMAN SPRING
3 23: 4:11	37.069	116.945	0.5	4.11	1.5	185	AD	---	1.1	SPRINGDALE
5 2:35: 5	37.137	117.311	0.2	9.47	0.5	99	AB	---	0.8	UBEHEBE CRATER
12 12:26:13	37.366	116.454	---	2.94	---	330	AD	---	1.5	***REGIONAL***
12 18:24: 2	36.516	116.057	2.2	1.97	4.7	163	DC	---	0.5	SPECTER RANGE SE
12 18:52:55	37.698	115.040	0.5	0.36	0.8	118	AC	---	1.5	HIKO NE
14 17: 9:57	37.409	115.013	---	5.60	---	219	AD	---	0.8	ALAMO NE
14 20:49:28	36.829	116.648	0.4	-1.98L	0.5	110	AB	1.0	0.9	BARE MTN
16 13:10:26	37.174	117.920	0.9	0.27	0.7	227	AD	---	1.6	WAUCOBA SPRING
17 6: 7: 6	35.746	116.898	1.3	3.12*	---	283	CD	---	1.6	QUAIL MTNS
19 13:48: 1	35.744	117.668	2.1	9.66	1.1	299	BD	---	1.9	RIDGECREST
19 22: 9:27	37.409	118.113	1.3	1.54	1.3	279	BD	---	1.9	***REGIONAL***
19 22:17:20	37.403	117.866	7.9	0.22	0.5	177	DD	---	1.3	SOLDIER PASS
19 23:49:47	36.763	116.243	0.4	2.19	0.7	113	AB	---	0.6	SKULL MTN
20 23:39:26	37.456	114.066	---	2.09	---	328	BD	---	1.6	***REGIONAL***
22 10:13:21	35.925	117.646	1.3	1.30	3.2	286	BD	---	1.7	MOUNTAIN SPRINGS CANYON
23 12:34:46	37.712	115.005	0.5	6.23	1.1	133	AB	---	1.6	HIKO NE
23 23:14: 5	37.253	114.494	1.2	8.15	0.8	244	BD	2.6	---	***REGIONAL***
23 23:20:16	37.359	114.969	0.5	8.24	0.6	270	AD	---	1.0	DELAMAR LAKE
23 23:28:51	37.258	114.484	1.7	2.26	4.7	274	BD	---	1.5	***REGIONAL***
24 0:55:31	37.282	114.579	0.5	0.02	4.0	278	BD	---	1.4	ELGIN
24 4:42:26	37.358	115.263	2.1	2.02	3.5	239	BD	---	1.0	BADGER SPRING
25 8:19:32	37.847	118.149	1.7	7.26	2.3	304	BD	---	1.4	***REGIONAL***
25 8:30:55	36.927	117.436	0.8	1.68	2.2	162	BC	---	1.0	TIN MTN
25 8:40:16	37.254	114.510	2.2	4.97*	---	316	CD	---	1.3	ELGIN
25 16:34:32	37.060	116.943	0.3	4.28	1.6	117	AC	---	1.1	SPRINGDALE
25 16:56:11	37.295	114.590	0.8	6.25*	---	261	CD	---	1.4	ELGIN
25 20:33:18	37.286	114.529	0.7	9.79	0.6	240	BD	---	1.5	ELGIN
25 22:54:43	36.485	116.308	0.4	0.97	1.8	179	AC	---	0.7	ASH MEADOWS
25 23:29:45	36.352	117.961	2.2	2.97	7.3	286	CD	---	2.4	KEELER
25 23:34:13	36.483	117.426	0.7	7.70	4.2	232	BD	---	1.5	PANAMINT BUTTE
26 1:10: 6	37.263	114.554	0.9	13.43	1.9	297	AD	---	1.2	ELGIN
27 8:19:43	37.924	118.156	---	1.46	---	328	DD	0.9	---	***REGIONAL***
29 8:11:17	36.454	116.902	0.4	5.55	3.5	71	BC	---	1.8	FURNACE CREEK
29 10:14:34	37.697	115.052	0.5	0.39	0.8	114	AC	---	1.3	HIKO NE
30 6:49:13	35.636	117.779	0.9	5.11	0.5	298	AD	---	2.1	INYOKERN
30 9:54:30	36.574	117.071	---	-0.73	---	200	AD	---	1.2	STOVEPIPE WELLS
30 13:54:27	37.168	116.402	0.2	8.64	0.5	113	AB	---	1.3	SCRUGHAM PEAK
30 22:10:57	36.841	116.224	0.4	7.64	0.8	71	BA	---	1.0	SKULL MTN
OCT 1 6:24:59	35.717	117.729	6.6	5.33	2.0	301	DD	---	2.3	RIDGECREST
1 6:36:35	36.055	117.259	18.3	7.00*	---	252	DD	---	1.5	MATURANGO
1 9:21:19	35.831	117.601	4.9	9.02	1.6	300	CD	---	2.3	MOUNTAIN SPRINGS CANYON
1 10:34:44	37.284	114.531	1.9	-1.00*	---	240	CD	---	1.8	ELGIN
1 11: 4:51	36.196	117.305	3.6	17.04	0.7	289	CD	---	1.3	MATURANGO
1 12:19:35	35.802	117.624	4.2	10.05	1.0	284	CD	---	2.4	MOUNTAIN SPRINGS CANYON
1 12:31:45	36.262	116.867	3.6	21.98	0.6	296	CD	---	1.4	FURNACE CREEK
1 13:12: 4	35.845	117.888	6.9	11.93	2.5	291	DD	---	1.9	MOUNTAIN SPRINGS CANYON
1 14:29: 3	35.780	117.680	6.6	8.11	2.0	288	DD	3.8	---	MOUNTAIN SPRINGS CANYON
1 14:33: 7	35.736	117.661	13.1	7.61	4.5	301	DD	---	2.5	RIDGECREST
2 4: 3:39	35.891	117.519	10.5	16.58	3.5	292	DD	---	2.0	MOUNTAIN SPRINGS CANYON
2 4: 8:35	35.836	117.605	0.2	21.12	---	300	AD	---	2.0	MOUNTAIN SPRINGS CANYON

# 1982 LOCAL HYPOCENTER SUMMARY

	DATE - TIME (UTC)	LATITUDE (DEG. N)	LONGITUDE (DEG. W)	HORIZ ERROR (KM)	DEPTH (KM)	VERT ERROR (KM)	AZI GAP (DEG)	QUAL	Md	Mb1g	QUADRANGLE
OCT	2 10:17:28	37.282	114.517	3.2	2.82*	---	269	CD	---	1.9	ELGIN
	2 10:27:51	37.276	114.566	4.0	2.31*	---	264	CD	---	1.1	ELGIN
	2 13:42:29	35.855	117.461	2.7	20.95	0.7	286	CD	---	1.8	TRONA
	2 14: 2: 5	35.785	117.729	3.0	7.03	1.1	287	CD	---	2.6	MOUNTAIN SPRINGS CANYON
	2 16: 1:27	35.996	117.375	13.8	7.98*	---	272	DD	---	2.8	TRONA
	3 7:17:30	37.252	114.453	2.3	8.19	1.0	276	BD	---	2.2	***REGIONAL***
	3 9:47:47	35.922	117.471	3.1	18.49	1.0	287	CD	---	2.1	TRONA
	3 12:47: 8	37.899	118.054	3.5	-0.64*	---	298	DD	---	1.5	***REGIONAL***
	3 16:10:00	37.298	114.572	---	2.31	---	309	AD	---	1.4	ELGIN
	4 0: 6:38	36.711	117.343	---	0.90	---	189	AD	---	1.2	MARBLE CANYON
	4 15:33:35	37.823	118.067	3.8	-1.13*	---	270	CD	2.0	---	***REGIONAL***
	7 3:36:11	37.336	115.731	0.9	6.40	0.9	211	AD	---	1.4	GROOM LAKE
	9 0:35:15	37.304	115.019	1.1	2.52	2.0	214	BD	---	1.7	ALAMO SE
	12 8:22:47	35.824	117.717	5.8	6.96	1.9	294	DD	---	2.7	MOUNTAIN SPRINGS CANYON
	13 2:47:45	37.787	118.012	3.5	9.00*	---	263	CD	---	1.9	***REGIONAL***
	15 4: 4:29	37.246	118.615	0.4	5.06	0.5	136	AC	---	1.0	THIRSTY CANYON NE
	15 6:13:13	36.623	115.964	0.5	19.20	1.1	151	AC	---	1.0	MERCURY SW
	17 3: 9:54	37.334	114.699	---	4.21	---	291	AD	---	1.3	ELGIN SW
	17 9:10:26	37.846	118.874	1.2	2.91*	---	225	CD	---	1.4	CACTUS PEAK
	18 1:59:31	36.073	117.152	---	2.16	---	259	BD	---	1.5	TELESCOPE PEAK
	18 8: 0:16	36.250	118.154	---	7.00**	---	193	BD	0.9	0.9	HIGH PEAK
	19 19:33:14	37.301	114.592	---	3.08	---	307	AD	---	1.2	ELGIN
	20 12:53:47	36.703	118.279	0.5	3.98	1.1	89	AA	---	1.0	STRIPED HILLS
	21 0:31:24	37.691	115.046	---	0.55	---	204	AD	---	1.1	HIKO NE
	21 8:56:10	36.504	115.907	---	4.20	---	264	BD	---	0.3	MERCURY SW
	21 9:11:52	36.284	115.402	7.9	5.27*	---	333	DD	---	1.3	GRAPEVINE SPRING
	22 5:34:33	37.695	115.045	---	0.14	---	148	AD	---	1.1	HIKO NE
	22 5:39:56	36.704	118.145	---	8.47	---	183	AD	---	1.2	SPECTER RANGE NW
	24 18:10:24	37.024	118.140	0.6	7.91	2.2	157	BC	1.4	---	TIPPIPAH SPRING
	24 18:11:24	37.020	118.133	0.3	9.58	0.6	102	AB	1.4	-0.4	TIPPIPAH SPRING
	25 7:48:55	37.859	114.741	---	7.00**	---	265	AD	0.7	-0.8	THE BLUFFS
	27 18:21:28	36.738	116.201	0.6	0.61*	---	98	CB	1.4	---	SPECTER RANGE NW
	30 1:43:39	36.876	115.990	0.8	0.93*	---	121	CB	---	1.4	PLUTONIUM VALLEY
	30 3:26: 9	37.216	118.325	0.5	23.13	0.7	259	BD	---	1.0	AMMONIA TANKS
	30 20:48:52	37.305	114.623	---	2.37	---	304	AD	---	1.3	ELGIN
NOV	2 4:54:43	37.236	117.880	---	7.00**	---	235	AD	---	1.5	WAUCOBA SPRING
	4 3:54:52	36.825	118.125	0.2	0.72	9.2	113	CB	---	1.0	SKULL MTN
	4 6:24:49	36.828	118.130	0.9	-0.85*	---	192	CD	---	1.1	SKULL MTN
	4 16:35:12	36.794	118.614	7.9	1.87BL	0.2	193	DD	---	0.8	● BARE MTN
	4 16:39:14	36.582	118.173	0.9	2.25	2.6	137	BD	---	0.8	SPECTER RANGE SW
	7 5:22:14	37.816	117.444	---	6.17	---	205	AD	---	1.4	PAYMASTER RIDGE
	7 6:29:26	37.837	117.444	0.6	4.17	3.5	221	BD	---	1.4	PAYMASTER RIDGE
	8 7:45:25	37.511	116.375	0.3	5.05	3.8	74	BC	---	1.4	QUARTZITE MTN
	10 0:11:33	37.511	116.379	0.6	6.29	7.0	132	CD	---	1.2	QUARTZITE MTN
	11 4:40:14	37.632	114.964	---	0.27	---	150	AD	---	0.8	PAHROC SPRING
	11 12:22:28	36.737	116.049	0.7	-0.76*	---	134	CC	---	0.9	CAMP DESERT ROCK
	11 14: 0:39	37.381	114.706	---	3.23	---	275	AD	---	1.8	SLIDY MTN
	12 20:48:26	37.153	116.942	---	0.38	---	289	AD	---	1.0	SPRINGDALE
	12 21:46:34	37.511	116.373	0.2	2.69*	---	74	CC	---	1.5	QUARTZITE MTN
	13 1:43:57	37.150	118.958	1.0	0.14*	---	237	CD	---	1.1	SPRINGDALE
	14 1:12:52	37.153	118.959	1.0	-0.78*	---	237	CD	---	1.3	SPRINGDALE
	14 5:25:50	35.601	116.660	21.5	2.03*	---	323	DD	---	1.6	LEACH LAKE
	14 21:38:58	36.952	115.986	0.7	-0.34	0.6	182	AD	---	0.9	PLUTONIUM VALLEY
	16 7: 2:58	36.513	116.227	1.0	4.91	5.6	200	CD	---	1.1	SPECTER RANGE SW
	16 7:20:49	36.251	115.364	46.5	-0.57*	---	335	DD	---	1.3	TULE SPRINGS PARK
	16 9:14:56	37.689	115.054	---	0.36	---	115	AD	---	1.1	HIKO NE
	16 18:22:20	37.707	115.025	---	7.00**	---	139	AD	---	1.3	HIKO NE
	16 23:35:25	36.031	114.940	27.1	2.87*	---	314	DD	---	1.6	HENDERSON
	17 7:56:55	37.494	114.601	0.4	6.37	0.2	300	AD	---	1.5	ELGIN NE
	18 2:14:20	36.698	117.440	---	18.29	---	262	AD	---	1.4	MARBLE CANYON
	18 9:16:51	37.086	-116.026	0.6	0.39*	---	73	---	---	1.9	***REGIONAL***
	19 3:32:18	37.428	117.909	---	7.00**	---	351	AD	---	1.3	SOLDIER PASS
	19 14: 5:12	37.221	115.023	---	7.00**	---	239	AD	---	1.5	LOWER PAHRANAGAT LAKE
	20 22:56:14	35.873	117.560	0.6	19.95	0.2	290	BD	---	1.7	MOUNTAIN SPRINGS CANYON
	21 5:25:31	37.698	115.041	0.3	2.13	0.8	118	AD	---	1.5	HIKO NE
	21 9:28:32	35.730	117.728	3.5	7.00	1.3	302	CD	---	2.3	RIDGECREST

# 1982 LOCAL HYPOCENTER SUMMARY

DATE - TIME (UTC)	LATITUDE (DEG. N)	LONGITUDE (DEG. W)	HORIZ ERROR (KM)	DEPTH (KM)	VERT ERROR (KM)	AZI GAP (DEG)	QUAL	Md	Mbiq	QUADRANGLE
NOV 21 16: 6:34	35.761	117.667	---	5.02	---	367	AD	---	1.7	MOUNTAIN SPRINGS CANYON
22 4: 0:52	37.332	114.636	---	14.18	---	254	AD	---	1.4	ELGIN SW
22 5:44: 4	36.145	114.718	3.4	6.05	1.3	296	CD	---	1.9	HOOVER DAM
22 16:57:12	36.962	115.963	0.9	3.93	4.6	190	BD	0.7	0.7	PLUTONIUM VALLEY
22 18:11:24	37.693	115.046	0.1	0.04	2.0	123	BD	---	1.9	HIKO NE
23 10:30:56	37.575	115.023	---	7.00..	---	256	AD	1.1	---	HIKO SE
23 18:13: 4	36.701	115.843	1.1	-0.96	1.8	172	BD	---	0.9	MERCURY NE
25 10:35: 7	37.716	115.036	0.3	1.77	1.0	126	AD	---	0.8	HIKO NE
25 18:30:15	36.799	116.285	0.6	2.25	1.3	95	AB	---	1.0	JACKASS FLATS
26 8:24:11	37.715	114.794	---	7.00..	---	294	AD	---	1.1	PAHROC SPRING NE
26 10:31:22	37.700	115.054	0.4	2.26	1.0	114	AD	---	1.2	HIKO NE
27 5:12:56	37.638	115.344	---	7.53	---	267	AD	---	0.9	MT IRISH
27 19:13:38	37.250	115.014	0.7	3.17.	---	208	CD	---	1.5	ALAMO SE
29 6:14:59	37.258	115.002	1.1	7.26	2.5	208	BD	---	1.4	ALAMO SE
29 8:14:23	36.979	116.398	0.3	-0.86	0.4	84	AB	---	1.1	TOPOPAH SPRING NW
30 4:17:25	36.678	116.236	0.4	-0.11.	---	154	CC	---	0.6	SPECTER RANGE NW
30 5:34:56	37.692	115.030	0.9	0.27.	---	119	CB	---	2.1	HIKO NE
30 5:55:58	37.679	114.990	---	12.17	---	153	AD	---	1.2	PAHROC SPRING
30 6: 0:13	37.663	115.055	---	7.00..	---	178	AD	---	1.0	HIKO NE
DEC 1 1:41: 8	37.701	115.042	0.3	3.99	2.1	118	BD	---	1.5	HIKO NE
2 8:47:20	37.350	115.269	0.6	4.94	8.7	100	CC	---	1.5	BADGER SPRING
2 13:41:12	35.979	116.828	---	7.00..	---	173	AD	1.1	1.1	WINGATE WASH
3 6:23:59	37.298	115.159	---	7.00..	---	197	AD	---	1.2	ALAMO
3 14:17: 8	37.259	114.567	1.0	3.47	3.6	234	BD	---	1.8	ELGIN
3 18:26:53	36.380	116.072	3.4	3.97	3.4	254	CD	---	2.0	...REGIONAL...
3 18:30:25	37.923	115.274	---	7.00..	---	284	AD	---	1.2	...QUAD. NOT LISTED...
5 2:25:48	37.059	117.484	0.7	2.73	2.3	151	BC	---	1.5	UBEHEBE CRATER
5 19:57:56	37.634	115.054	---	7.00..	---	205	AD	---	1.1	HIKO NE
5 22:33:00	37.176	117.422	---	8.25	---	128	AD	---	1.1	UBEHEBE CRATER
6 15:39:17	37.796	116.818	1.0	2.38.	---	244	CD	---	1.4	CACTUS PEAK
7 1:48:24	36.680	116.423	0.4	1.99	1.0	145	AC	---	1.1	LATHROP WELLS NW
7 2:40:49	37.122	117.303	---	7.00..	---	177	AD	---	0.8	UBEHEBE CRATER
7 9:43:52	36.120	114.676	2.8	6.04	1.0	275	CD	---	2.7	HENDERSON
7 10:11:17	36.552	115.961	---	29.67	---	185	BD	---	0.8	MERCURY SW
10 20: 0: 7	36.854	116.395	0.4	7.88BL	0.7	69	AA	---	1.1	● TOPOPAH SPRING SW
13 10:59:00	36.393	116.950	0.7	5.86	2.5	144	BC	---	1.4	FURNACE CREEK
14 2: 4:20	38.471	115.529	10.0	11.77	4.2	286	DB	---	2.1	TROY CANYON
14 20:21:16	37.124	117.344	0.4	6.69	1.8	115	AC	---	1.3	UBEHEBE CRATER
15 10:54:38	37.802	116.057	9.9	2.90.	---	295	DD	---	1.6	...REGIONAL...
16 8:15:15	37.163	117.969	---	3.24	---	263	AD	---	1.1	WAUCOBA SPRING
17 20:17:47	36.725	116.304	---	7.00..	---	141	AD	---	0.9	STRIPED HILLS
18 4: 8:24	37.459	117.203	0.6	3.07.	---	93	CC	---	1.1	STONEWALL PASS
19 4:31:15	37.074	116.020	1.0	0.79.	---	47	DC	3.1	---	YUCCA FLAT
19 17:38:48	36.819	115.423	0.4	3.61	5.7	117	CC	2.5	---	DOG BONE LAKE SOUTH
19 17:41:54	36.861	115.412	---	7.00..	---	295	AD	---	1.6	DOG BONE LAKE NORTH
19 18:14:19	36.817	115.405	0.6	7.00.	---	113	CC	---	1.7	DOG BONE LAKE SOUTH
19 19:18:55	36.672	117.410	---	25.30	---	221	BD	---	1.4	MARBLE CANYON
19 22:21:47	36.817	115.409	0.4	2.93.	---	113	CC	---	1.8	DOG BONE LAKE SOUTH
20 18:14:50	37.709	115.069	0.8	0.97.	---	111	CD	---	1.6	HIKO NE
20 19:47:47	37.375	115.614	0.6	0.35.	---	114	CC	---	1.7	GROOM RANGE NE
20 20:14:59	37.214	116.610	1.4	-0.17	1.8	113	BB	---	1.3	THIRSTY CANYON NE
21 9: 3:51	36.443	115.770	0.6	4.29	8.4	97	CC	---	1.6	MT STIRLING
21 19:14:30	37.180	115.634	1.1	4.88.	---	115	CD	---	1.2	FALLOUT HILLS NW
21 22:38:26	36.813	117.369	---	7.00..	---	150	AD	0.7	1.1	TIN MTN
22 5: 2:26	36.869	115.988	0.4	4.05	3.0	145	BC	---	1.7	FRENCHMAN FLAT
22 14:47:49	36.188	116.941	---	24.45	---	313	AD	---	2.4	BENNETTS WELL
22 16:10:53	36.869	115.960	---	3.48	---	227	AD	---	1.0	FRENCHMAN FLAT
23 18:19:00	35.603	117.930	4.2	2.62.	---	319	CD	---	2.1	INYOKERN
24 0: 2:55	37.558	114.787	---	2.03	---	220	AD	---	1.3	PAHROC SPRING SE
24 3:58:55	35.530	117.960	---	6.67	---	315	AD	---	2.3	INYOKERN
26 1:54:44	35.728	117.803	6.1	3.26	2.9	292	DD	---	2.5	INYOKERN
26 9:43: 7	35.822	117.681	4.4	13.81	1.3	301	CD	---	2.2	MOUNTAIN SPRINGS CANYON
26 12: 8:54	37.696	115.043	---	0.07	1.5	116	AD	---	1.4	HIKO NE
26 12:13: 9	37.694	115.049	---	1.91	---	149	AD	---	1.5	HIKO NE
26 16:45:30	36.701	117.395	---	4.07	---	234	AD	---	1.0	MARBLE CANYON
27 8:40:28	37.629	115.103	---	7.00..	---	187	AD	---	1.2	HIKO NE

# 1982 LOCAL HYPOCENTER SUMMARY

DATE - TIME (UTC)	LATITUDE (DEG. N)	LONGITUDE (DEG. W)	HORIZ ERROR (KM)	DEPTH (KM)	VERT ERROR (KM)	AZI GAP (DEG)	QUAL	Md	Mb1g	QUADRANGLE
DEC 27 8:56:33	37.448	117.203	0.1	0.89	4.1	133	BD	---	1.0	STONEWALL PASS
27 23:22:25	36.822	116.628	---	-0.54BL	---	244	AD	---	0.7	BAKE MTH
27 23:38:14	36.715	116.282	---	7.00**	---	197	AD	---	1.0	STRIPED HILLS
28 0:36:45	36.855	115.994	---	7.00**	---	205	AD	---	1.0	FRENCHMAN FLAT
28 1:18: 4	36.777	115.938	0.4	4.36	3.8	169	BC	---	1.1	FRENCHMAN FLAT
28 2:26:43	37.258	117.864	1.0	5.39	3.7	207	BD	---	1.8	SOLDIER PASS
28 7:20:22	35.736	117.815	3.9	6.81	1.4	303	CD	---	2.5	INYO KERN
28 8:42:23	36.591	116.318	5.6	1.65	1.1	312	DD	---	0.8	LATHROP WELLS SE
28 20: 8:54	36.698	116.182	2.3	12.25	3.4	243	BD	---	1.0	SPECTER RANGE NW
28 20:39:13	35.711	117.814	39.1	-1.05*	---	330	DD	---	2.4	INYO KERN
28 23:27:43	35.967	117.259	---	11.32	---	292	CD	---	1.0	TRONA
29 13:12: 0	37.552	117.463	---	1.93	---	124	AD	---	1.4	MONTEZUMA PEAK SW
29 14:52:55	37.552	117.467	0.2	4.76	1.1	109	AC	---	1.5	MONTEZUMA PEAK SW
29 16:17: 1	37.553	117.466	0.6	1.94	1.4	109	AC	---	1.8	MONTEZUMA PEAK SW
29 19: 8:22	37.575	117.493	---	3.89	---	195	AD	---	1.4	MONTEZUMA PEAK SW
29 22: 0:20	37.555	117.476	0.4	-0.89*	---	114	CC	---	1.0	MONTEZUMA PEAK SW
29 22: 6:30	37.564	117.465	0.3	5.67	1.6	86	AC	---	1.9	MONTEZUMA PEAK SW
29 22:11: 9	37.552	117.508	---	7.00**	---	217	AD	---	1.2	LIDA WASH
29 22:15:20	37.555	117.469	0.4	0.38*	---	110	CC	---	1.3	MONTEZUMA PEAK SW
29 22:55:32	37.551	117.466	0.2	4.30	1.5	109	AD	---	1.4	MONTEZUMA PEAK SW
29 23:23:13	37.553	117.460	0.4	2.46	1.0	106	AD	---	1.4	MONTEZUMA PEAK SW
30 6:18:58	37.554	117.462	1.1	4.01	9.2	124	CD	---	1.3	MONTEZUMA PEAK SW
30 7:31:26	37.553	117.467	0.2	2.17	0.6	110	AC	---	1.3	MONTEZUMA PEAK SW
30 7:36:51	37.558	117.467	0.3	-0.82	7.9	84	CC	---	1.0	MONTEZUMA PEAK SW
30 7:54: 6	37.561	117.537	6.5	10.83	6.6	237	DD	---	1.1	LIDA WASH
30 8:29: 5	37.559	117.483	1.3	5.27	4.1	187	BD	---	1.4	MONTEZUMA PEAK SW
30 9:27:28	37.545	117.475	0.5	4.07	3.1	107	BC	---	1.2	MONTEZUMA PEAK SW
30 9:36:20	37.749	115.012	---	4.00	---	233	AD	---	1.1	HIKO NE
30 10:39:36	37.686	115.069	---	-0.37	---	159	AD	---	1.1	HIKO NE
30 14:12: 3	37.551	117.467	0.4	2.46	0.9	110	AC	---	1.4	MONTEZUMA PEAK SW
30 15:11: 1	37.549	117.524	7.4	11.16	7.7	228	DD	---	1.4	LIDA WASH
30 15:20:10	37.545	117.483	1.5	5.03	3.8	184	BD	---	1.4	MONTEZUMA PEAK SW
30 16: 5:56	37.555	117.478	4.8	5.37*	---	200	CD	---	1.4	MONTEZUMA PEAK SW
30 16: 9:29	37.517	117.482	---	7.00**	---	195	AD	---	1.1	MONTEZUMA PEAK SW
30 16:13:17	37.560	117.484	---	7.00**	---	205	AD	---	1.5	MONTEZUMA PEAK SW
30 18:19:32	37.549	117.465	---	1.37	---	123	AD	---	1.5	MONTEZUMA PEAK SW
30 18:45:41	37.550	117.479	---	7.00**	---	199	AD	---	1.1	MONTEZUMA PEAK SW
31 1:27:24	37.554	117.462	---	3.95	---	124	AD	---	1.4	MONTEZUMA PEAK SW
31 2: 8:10	35.787	117.802	---	5.03	---	309	AD	---	1.9	LITTLE LAKE
31 15:43:16	37.174	117.307	0.4	5.17	2.5	93	BC	---	1.0	UBEHEBE CRATER
31 16:30:57	36.009	117.384	---	7.00**	---	270	AD	---	1.7	MATURANGO
31 19:50: 7	35.717	117.802	7.0	8.18	2.1	303	DD	3.0	---	INYO KERN
31 19:52:33	35.859	117.649	0.2	2.66	4.1	292	DD	3.2	0.8	MOUNTAIN SPRINGS CANYON
31 23:57:15	36.781	115.839	---	11.95	---	239	AD	0.3	-0.7	FRENCHMAN LAKE SE



## 1983 LOCAL HYPOCENTER SUMMARY

DATE - TIME (UTC)	LATITUDE (DEG. N)	LONGITUDE (DEG. W)	HORIZ ERROR (KM)	DEPTH (KM)	VERT ERROR (KM)	AZI GAP (DEG)	QUAL	Md	Mb1g	QUADRANGLE
JAN 1 21:47:55	36.467	116.576	0.5	10.11	1.5	269	AD	---	1.4	RYAN
1 22:21:19	35.850	117.725	1.6	4.03*	---	304	CD	---	1.9	MOUNTAIN SPRINGS CANYON
2 0:38:27	36.465	116.573	0.9	10.40	1.9	270	AD	---	1.6	RYAN
2 0:46:27	36.503	116.570	0.5	7.06	3.6	105	BC	---	1.4	BIG DUNE
2 3:51:58	36.468	116.574	0.5	11.16	1.3	269	AD	---	1.6	RYAN
2 5:16:39	36.503	116.582	0.3	2.54	1.7	186	AC	---	1.3	BIG DUNE
2 5:35:10	36.491	116.588	1.1	3.75*	---	262	CD	---	1.1	RYAN
2 7:57:58	36.502	116.586	0.3	0.85**	0.5	109	AC	---	1.4	BIG DUNE
2 16:32:20	36.502	116.569	0.2	5.47	1.7	95	AC	---	2.6	BIG DUNE
2 19:36:35	36.502	116.567	0.4	6.15	3.5	152	BC	---	1.4	BIG DUNE
3 5:58:00	36.517	116.577	1.6	4.44	9.8	233	CD	---	1.1	BIG DUNE
3 7:21:46	35.903	117.011	0.8	4.37	4.2	282	BD	---	1.7	MANLY PEAK
3 9: 9:58	35.915	117.013	1.8	8.75	7.8	271	CD	---	1.7	MANLY PEAK
3 10:31:47	35.903	117.014	0.8	1.77	1.1	262	AD	---	1.8	MANLY PEAK
3 17:39:44	36.500	116.568	0.2	4.77	1.4	80	AC	---	2.4	BIG DUNE
3 19:18:41	36.716	116.327	0.7	-0.95	0.7	128	AB	---	1.1	STRIPED HILLS
4 6:38: 4	35.707	117.761	6.1	-1.18	4.4	312	DD	0.0	---	INYOKERN
4 6:38:31	36.143	117.872	3.0	13.10	---	0	D	0.0	---	COALDALE NE
4 13:17:43	37.408	117.079	0.3	-0.92*	---	133	CD	---	1.2	SCOTTYS JUNCTION NE
4 14:58:12	36.500	116.582	0.3	8.23	2.1	119	BC	---	1.3	BIG DUNE
4 20: 2: 7	37.006	116.289	0.6	6.81	0.8	106	AD	0.6	-1.3	BUCKBOARD MESA
5 6:45:45	37.218	117.389	1.9	10.40	1.7	240	BD	0.9	---	UBEHEBE CRATER
5 9:17:15	37.601	117.825	1.0	7.71	2.2	169	BC	1.2	3.2	PIPER PEAK
7 17:59:49	37.899	114.970	0.7	4.20	1.1	250	AD	---	1.2	DEADMAN SPRING
8 3:37:19	37.446	116.353	0.2	8.92	0.9	102	AC	---	1.8	SILENT CANYON NE
8 6:52: 1	37.063	116.311	0.5	6.21	0.8	226	AD	---	1.1	BUCKBOARD MESA
8 14:54:10	36.497	116.569	0.3	-0.71	0.5	106	AC	---	1.6	RYAN
8 19:31: 6	36.661	116.092	0.3	-0.59	0.5	99	AC	---	1.5	CAMP DESERT ROCK
8 20:57:51	37.165	116.941	0.2	5.24	1.6	130	AC	---	1.3	SPRINGDALE
9 23:12:28	36.495	116.557	0.4	12.49	1.2	126	AC	---	1.4	RYAN
10 15:12:54	36.409	117.040	0.3	12.25	0.5	124	AB	---	1.6	EMIGRANT CANYON
10 19:51:41	36.851	116.194	0.7	8.78	0.9	130	AB	---	1.1	SKULL MTN
10 19:53:57	36.720	116.334	0.9	-1.85	1.2	135	AB	---	1.0	STRIPED HILLS
10 22:51: 3	37.153	117.386	0.5	13.35	1.2	124	AB	---	1.3	UBEHEBE CRATER
10 23:27:46	36.083	114.759	3.9	3.48	2.6	272	CD	---	2.3	BOULDER BEACH
11 18:36:11	36.196	117.608	6.3	7.11*	---	279	DD	---	1.5	COSO PEAK
11 23:28:45	36.583	116.722	1.2	9.45	4.3	331	BD	---	1.0	BIG DUNE
12 6:36: 5	37.357	117.551	0.3	0.81	0.7	71	AC	---	1.5	MAGRUDER MTN
13 6:51:30	37.183	116.591	0.2	5.10	1.1	105	AC	---	0.9	THIRSTY CANYON NE
13 8: 2: 4	37.357	117.551	0.4	5.08	1.1	71	AC	---	1.7	MAGRUDER MTN
13 8:58: 6	37.369	117.549	0.5	7.68	1.1	180	AC	---	1.3	MAGRUDER MTN
16 7:33:43	37.370	117.555	0.5	6.93	1.0	185	AD	---	1.0	MAGRUDER MTN
16 19:12:58	37.666	115.048	1.1	1.99	1.7	252	BD	---	0.9	HICO NE
17 19:57:32	36.529	116.169	0.4	6.92	1.4	161	AC	---	0.9	SPECTER RANGE SW
17 20: 0:13	36.863	116.319	---	7.00**	---	319	AD	---	0.8	JACKASS FLATS
17 20:20:20	36.521	116.180	0.6	11.07	1.2	172	AC	---	1.4	SPECTER RANGE SW
20 21: 6:47	36.976	116.756	0.7	10.80	1.0	142	AC	---	1.2	BULLFROG
21 7:13:18	37.178	117.364	0.6	10.99	1.7	140	AC	0.9	1.3	UBEHEBE CRATER
21 8:40:35	37.286	117.590	0.4	10.79	0.6	164	AD	---	1.1	MAGRUDER MTN
24 12: 5:40	36.537	116.168	0.2	3.05*	---	157	CC	---	1.5	SPECTER RANGE SW
24 12:19:20	36.533	116.174	0.5	2.83	1.7	162	AC	---	0.8	SPECTER RANGE SW
24 12:28: 1	36.533	116.170	0.4	5.76	1.5	160	AC	---	1.3	SPECTER RANGE SW
24 22:16: 2	36.537	116.152	0.4	5.73	1.8	176	AC	0.6	1.0	SPECTER RANGE SW
25 5:22:14	36.514	116.183	2.7	0.86	1.5	280	CD	---	1.2	SPECTER RANGE SW
25 21: 4:58	37.087	117.833	0.9	3.88*	---	250	CD	---	1.6	WAUCOBA SPRING
26 20:31:39	37.711	116.244	---	7.00**	---	231	AD	---	1.5	BELTED PEAK
28 2:31:55	36.096	116.501	8.7	23.54*	---	302	DD	---	1.8	FUNERAL PEAK
28 23: 2:55	36.725	116.323	3.4	-0.49	2.0	227	CD	---	1.0	STRIPED HILLS
30 2: 7:52	38.021	116.215	0.6	7.00	5.6	134	CC	---	1.7	REVEILLE
31 16:13:10	36.228	115.206	8.3	6.13*	---	338	DD	---	2.0	LAS VEGAS NW
FEB 1 8:24:11	37.175	115.039	1.4	4.97	4.1	238	BD	---	1.6	LOWER PAHRANAGAT LAKE
1 17:48:48	35.806	117.752	2.8	5.89	1.0	286	CD	---	2.0	LITTLE LAKE
1 20:47:52	36.496	116.563	0.3	5.59	9.3	104	CC	1.5	0.3	RYAN
1 23:24: 9	36.815	116.628	0.6	0.66BL	0.4	114	AB	1.0	0.4	● BARE MTN
1 23:42:14	36.944	116.194	---	7.00**	---	214	AD	---	1.0	MINE MTN
2 2:57:29	36.469	116.578	0.7	8.43	1.9	269	AD	---	1.4	RYAN

## 1983 LOCAL HYPOCENTER SUMMARY

DATE - TIME (UTC)	LATITUDE (DEG. N)	LONGITUDE (DEG. W)	HORIZ ERROR (KM)	DEPTH (KM)	VERT ERROR (KM)	AZI CAP (DEG)	QUAL	Md	Mblg	QUADRANGLE
FEB 2 3: 4:53	36.478	116.578	0.6	8.37	1.8	269	AD	---	1.4	RYAN
2 13:29:23	37.308	117.320	1.1	7.00	1.8	145	BC	---	1.2	GOLD POINT
2 13:32:11	37.315	117.344	0.5	2.14	1.2	99	AB	---	1.4	GOLD POINT
2 13:33:20	37.307	117.345	0.3	-0.16	0.3	135	AB	---	1.3	GOLD POINT
2 13:39:20	37.320	117.330	0.8	5.56	1.2	141	AC	---	1.4	GOLD POINT
2 13:44: 8	37.088	115.208	0.6	4.92	1.7	154	AC	---	2.1	LOWER PAHRANAGAT LAKE SW
2 13:46:14	37.088	115.167	0.6	2.49*	---	291	DD	---	1.5	LOWER PAHRANAGAT LAKE SW
2 14:28:17	37.310	117.340	0.3	0.48	0.8	98	AB	---	1.4	GOLD POINT
2 14:35: 0	37.310	117.316	0.3	7.44	0.4	158	AC	---	1.3	GOLD POINT
2 14:39: 5	37.311	117.336	0.2	1.82	0.5	128	AB	---	1.7	GOLD POINT
2 15:18:21	37.330	117.279	1.0	9.28	0.9	210	BD	---	1.3	GOLD POINT
2 15:59:50	37.308	117.339	0.5	0.33	1.0	136	AC	---	1.3	GOLD POINT
2 16:10:41	36.996	115.168	---	-0.48	---	292	AD	---	1.5	MULE DEER RIDGE NW
2 16:14: 8	37.332	117.273	---	5.81	---	220	AD	---	1.3	GOLD POINT
2 16:29:55	37.310	117.333	0.5	4.10	1.3	144	AC	---	1.7	GOLD POINT
2 17:15:56	37.302	117.261	---	7.00**	---	195	DD	---	0.9	GOLD POINT
2 18: 9:41	37.399	117.151	0.6	17.96	0.8	285	AD	---	1.4	STONEWALL PASS
2 19:10:23	37.350	117.875	1.0	8.38	1.6	196	AD	---	1.8	SOLDIER PASS
2 19:22:12	37.311	117.331	0.8	4.40	1.4	146	AC	---	1.3	GOLD POINT
2 20:42:54	37.314	117.341	0.3	2.41	1.0	99	AB	---	1.8	GOLD POINT
2 21:22: 9	37.320	117.331	0.5	4.00	1.2	156	AC	---	0.9	GOLD POINT
2 21:40:48	37.443	117.627	---	7.00**	---	207	DD	---	1.1	MAGRUDER MTN
2 21:54:52	37.332	117.290	0.8	10.16	0.7	199	AD	---	1.2	GOLD POINT
2 22:16:35	37.321	117.312	0.1	7.14	0.1	167	AD	---	1.3	GOLD POINT
3 2:29:40	37.319	117.334	1.0	5.65	2.1	154	BC	---	1.2	GOLD POINT
3 3: 5:26	37.317	117.333	---	2.85	---	152	AD	---	0.8	GOLD POINT
3 3: 7: 6	37.274	117.424	4.9	0.84	7.1	98	DC	---	1.0	GOLD POINT SW
3 3:54:53	37.313	117.340	0.3	1.65	0.8	99	AB	---	1.5	GOLD POINT
3 4: 5:32	37.316	117.319	0.5	7.52	0.6	156	AC	---	1.2	GOLD POINT
3 4:47:22	37.320	117.311	0.9	8.32	1.1	167	AC	---	1.3	GOLD POINT
3 5: 7:37	37.319	117.314	0.6	7.77	0.6	163	AC	---	1.4	GOLD POINT
3 5:25:42	37.314	117.338	0.3	0.33	0.5	100	AB	---	1.7	GOLD POINT
3 5:48:51	37.326	117.315	0.7	7.52	1.1	172	AC	---	1.4	GOLD POINT
3 5:47:10	37.310	117.336	0.5	0.80	0.9	99	AB	1.3	1.4	GOLD POINT
3 7: 1:10	37.319	117.313	0.2	7.50	0.2	164	AC	---	1.0	GOLD POINT
3 7: 4:14	37.308	117.339	0.2	1.60	0.7	98	AB	---	1.7	GOLD POINT
3 7:51:22	37.301	117.350	0.7	2.00	1.7	129	BB	---	1.4	GOLD POINT
3 8:14:21	37.325	117.307	0.9	7.33	1.5	176	AC	---	1.4	GOLD POINT
3 10: 3:12	37.317	117.314	0.2	7.58	0.3	160	AC	---	1.3	GOLD POINT
3 10:22:16	37.310	117.342	0.3	-0.30	0.3	73	AB	---	1.7	GOLD POINT
3 15:31:31	37.310	117.335	0.6	3.94	1.2	143	AC	---	1.1	GOLD POINT
3 17:48:29	36.777	115.954	0.4	7.56	1.2	153	AC	---	1.1	FRENCHMAN FLAT
3 18:19:43	37.321	117.316	0.5	6.98	0.6	165	AC	---	1.0	GOLD POINT
3 19:39:33	37.315	117.323	0.9	6.63	1.0	154	AD	---	1.0	GOLD POINT
3 20:55: 2	37.309	117.342	0.4	-0.26	0.4	96	AB	---	1.3	GOLD POINT
4 19:23:32	37.311	115.211	0.7	8.94	2.4	123	BB	---	1.5	ALAMO
4 21:18:29	37.268	114.569	---	27.59	---	312	AD	---	1.4	ELGIN
5 9:34:18	37.317	117.316	0.7	8.34	1.0	160	AC	---	1.1	GOLD POINT
5 19:13:29	37.307	117.348	0.4	-0.25	0.4	134	AB	---	1.0	GOLD POINT
5 20:47:53	37.015	116.229	0.7	2.99	0.8	161	AC	---	0.6	TIPPIPAH SPRING
6 5:14:59	37.542	114.998	---	7.00**	---	278	AD	---	1.0	PAHROC SUMMIT PASS
6 11:14:13	37.568	114.852	---	7.00**	---	317	BD	---	0.6	PAHROC SPRING SE
6 12:31:57	37.781	114.806	---	7.00**	---	294	AD	---	0.6	PAHROC SPRING NE
7 7:45:55	36.543	116.246	0.4	4.12	4.4	193	BD	---	0.8	SPECTER RANGE SW
7 14: 3:49	37.049	117.941	2.2	11.44	7.4	237	CD	---	1.7	WAUCOBA SPRING
7 16:46:24	37.170	115.586	0.4	2.47	2.8	150	BC	---	1.4	FALLOUT HILLS NE
8 9: 2:36	37.084	117.953	1.2	1.54	4.8	244	BD	---	1.6	WAUCOBA SPRING
8 9:54:29	37.252	114.873	0.9	15.08	0.8	231	AD	---	2.6	GREGERSON BASIN
8 14:41:19	37.684	115.846	4.7	2.06	1.7	200	CD	---	0.8	HIKO NE
9 20:14:58	36.713	116.204	---	15.76	---	302	AD	---	1.1	SPECTER RANGE NW
10 21: 9:51	37.932	117.869	5.0	2.75*	---	293	DD	---	1.5	RHYOLITE RIDGE
10 22:44:14	36.548	117.577	3.5	8.14*	---	267	CD	---	1.2	UBHEBE PEAK
11 7:39:56	36.413	116.243	0.4	9.20	1.3	120	AB	---	1.5	AMARGOSA FLAT
11 21:11:11	37.143	117.380	0.4	13.25	0.9	136	AC	---	1.2	UBHEBE CRATER
11 23:43: 0	36.950	117.551	1.0	11.96	1.4	201	AD	---	1.5	DRY MTN
12 8:20:35	36.418	116.254	0.3	7.08	1.1	185	AD	---	1.7	ASH MEADOWS

## 1983 LOCAL HYPOCENTER SUMMARY

DATE - TIME (UTC)	LATITUDE (DEC. N)	LONGITUDE (DEC. W)	HORIZ ERROR (KM)	DEPTH (KM)	VERT ERROR (KM)	AZI GAP (DEG)	QUAL	Md	Mbiq	QUADRANGLE
FEB 12 0:24:54	36.113	117.744	6.9	-0.29	5.7	311	DD	---	1.6	COSO PEAK
13 10:39:0	37.184	116.591	0.4	5.68	1.8	106	AC	---	1.1	THIRSTY CANYON NE
13 17:20:24	36.656	116.222	0.3	11.88	0.5	107	AB	---	1.3	SKULL MTN
13 17:34:19	37.181	116.590	0.4	2.18	1.2	105	AC	---	1.2	THIRSTY CANYON NE
13 23:41:8	37.196	116.585	0.3	10.43	0.7	168	AC	---	1.2	THIRSTY CANYON NE
14 1:41:15	36.394	116.276	0.5	4.49	1.8	272	AD	---	1.2	ASH MEADOWS
14 2:56:5	37.148	117.166	0.5	9.94	2.0	130	AB	---	1.0	BONNIE CLAIRE NW
14 19:17:4	37.261	116.590	0.6	3.27	---	256	CD	---	1.3	THIRSTY CANYON NE
16 1:21:26	36.655	116.253	0.3	4.66	0.5	243	AD	---	0.7	STRIPED HILLS
16 8:26:6	36.084	114.689	3.7	3.15	1.5	293	CD	---	2.6	HOOVER DAM
16 15:19:56	36.227	115.069	6.1	-0.58	---	296	DD	---	1.6	LAS VEGAS NE
17 1:43:5	37.181	116.592	0.2	5.97	0.9	96	AC	---	1.5	THIRSTY CANYON NE
17 5:2:35	37.088	116.136	0.2	4.06	2.6	117	BB	---	1.1	TIPPICAH SPRING
17 8:23:20	37.182	116.590	0.4	4.79	2.3	105	BC	---	1.0	THIRSTY CANYON NE
17 12:48:12	36.481	116.151	0.1	5.68	0.2	203	AD	---	1.0	AMARGOSA FLAT
17 22:6:46	37.185	116.595	0.3	6.60	1.2	105	AB	---	1.2	THIRSTY CANYON NE
17 23:32:16	36.684	116.220	1.5	5.82	1.2	285	BD	---	0.6	SPECTER RANGE NW
18 0:37:45	36.825	116.649	0.7	-0.94BL	0.5	215	AD	---	1.2	BARE MTN
18 8:38:48	36.838	116.372	0.4	6.81	0.7	111	AB	---	0.4	JACKASS FLATS
18 8:58:7	37.420	114.785	---	7.29	---	288	AD	---	1.4	DELAMAR
20 0:3:56	36.481	117.105	---	17.00	---	182	AD	---	1.2	EMIGRANT CANYON
20 14:20:59	37.071	115.215	6.1	0.65	4.1	279	DD	---	1.4	LOWER PAHRANAGAT LAKE SW
20 21:17:31	36.782	117.283	---	31.98	---	235	CD	---	1.3	TIN MTN
21 22:53:57	37.064	117.245	2.3	2.10	2.1	210	BD	---	1.1	BONNIE CLAIRE SW
21 23:52:5	37.133	116.625	---	2.05	---	282	AD	---	0.7	THIRSTY CANYON NW
22 2:46:41	37.183	116.597	0.5	6.86	2.3	103	BB	---	0.6	THIRSTY CANYON NE
22 16:12:32	37.643	115.050	1.3	1.94	2.9	182	BD	---	0.9	HIKO NE
22 18:47:13	37.804	115.794	0.3	8.68	0.6	148	AC	---	1.4	***QUAD. NOT LISTED***
23 3:49:51	37.801	115.786	0.3	7.93	0.7	138	AC	1.3	-0.1	***QUAD. NOT LISTED***
23 7:12:36	37.805	115.791	0.6	5.18	4.2	92	BC	1.5	0.3	***QUAD. NOT LISTED***
23 15:45:39	36.856	115.973	2.7	4.10	---	231	CD	---	0.7	FRENCHMAN FLAT
23 22:28:15	37.691	115.044	0.6	1.58	1.8	115	AC	---	0.8	HIKO NE
24 4:6:25	37.697	115.050	0.6	0.61	1.0	115	BC	---	0.7	HIKO NE
24 10:0:40	37.188	116.590	0.5	6.51	1.6	142	AC	---	1.0	THIRSTY CANYON NE
24 13:20:57	36.964	116.425	0.4	1.96	2.1	167	BC	---	0.4	TOPOPAH SPRING NW
24 17:39:22	37.184	116.590	0.4	4.21	2.4	186	BC	---	1.4	THIRSTY CANYON NE
24 19:26:14	36.691	116.233	0.2	3.86	0.3	264	AD	---	0.9	SPECTER RANGE NW
25 19:42:5	36.848	117.847	2.1	3.02	---	269	CD	---	1.3	WAUCOBA WASH
27 23:19:31	36.576	116.103	---	10.80	---	276	AD	0.8	---	SPECTER RANGE SE
28 12:59:46	38.000	116.714	---	8.23	---	311	CD	1.8	0.3	STONE CABIN VALLEY
MAR 2 16:48:51	35.959	116.228	---	1.03	---	254	AD	0.7	-0.1	TECOPA
5 18:27:54	36.953	117.546	0.6	1.48	1.1	184	AD	---	1.4	DRY MTN
5 23:57:9	36.951	117.550	0.6	4.16	4.4	182	BD	---	1.6	DRY MTN
7 5:6:27	36.797	116.290	0.3	5.77	0.6	124	AB	---	0.8	JACKASS FLATS
7 10:56:5	37.214	116.604	0.4	1.97	1.1	173	AC	---	1.0	THIRSTY CANYON NE
9 9:31:37	36.380	115.823	1.5	8.37	3.1	208	BD	---	1.2	MT STIRLING
9 20:51:13	37.705	115.055	0.7	3.93	---	115	CC	1.1	0.9	HIKO NE
10 8:38:16	36.754	116.248	0.4	5.56	0.5	123	AB	---	1.0	SKULL MTN
11 0:3:18	37.702	115.049	0.2	2.03	1.3	116	AC	---	1.0	HIKO NE
11 1:36:21	36.374	117.824	3.5	6.46	---	274	CD	---	1.7	KEELER
11 9:59:46	36.814	117.542	2.0	6.49	2.6	272	BD	---	1.0	DRY MTN
11 11:59:23	37.515	115.321	0.3	6.53	1.5	92	AC	---	1.5	MT IRISH
11 22:6:51	36.742	116.227	---	5.35	---	348	AD	---	1.0	SPECTER RANGE NW
13 23:33:52	36.855	116.267	0.6	8.84	0.6	165	AC	---	0.8	JACKASS FLATS
16 9:21:43	37.147	116.316	0.6	6.73	0.8	149	AC	---	0.9	AMMONIA TANKS
16 9:41:21	37.226	116.325	0.3	2.69	0.3	126	AB	---	1.4	AMMONIA TANKS
16 17:33:46	36.717	116.327	1.4	-0.95	1.0	269	BD	---	0.4	STRIPED HILLS
17 9:47:40	37.900	115.370	---	11.48	0.1	237	BD	---	1.2	***QUAD. NOT LISTED***
18 9:40:37	36.745	116.087	0.2	8.38	0.6	122	AB	---	1.2	CAMP DESERT ROCK
20 7:10:10	38.011	115.421	0.6	4.81	3.8	217	BD	---	1.5	***QUAD. NOT LISTED***
21 0:45:2	37.250	116.355	0.7	2.74	0.4	325	AD	---	0.9	DEAD HORSE FLAT
21 10:7:46	36.859	116.239	0.2	9.94	0.4	92	AB	---	0.7	SKULL MTN
22 15:55:20	37.319	117.928	0.9	4.62	1.6	312	AD	---	1.9	SOLDIER PASS
28 4:37:16	37.400	114.676	1.3	11.10	1.6	248	BD	---	1.4	SLIDY MTN
28 14:26:57	37.570	117.151	0.9	3.18	---	294	CD	---	1.6	GOLDFIELD
29 23:1:7	37.127	116.203	0.3	6.20	1.4	112	AB	---	1.1	RAINIER MESA

## 1983 LOCAL HYPOCENTER SUMMARY

DATE - TIME (UTC)	LATITUDE (DEG. N)	LONGITUDE (DEG. W)	HORIZ ERROR (KM)	DEPTH (KM)	VERT ERROR (KM)	AZI GAP (DEG)	QUAL	Md	Mbiq	QUADRANGLE
MAR 30 16:58:58	36.525	117.518	1.3	2.93	4.2	261	BD	---	1.3	UBHEBE PEAK
31 3:15: 2	36.767	116.137	0.3	7.68	0.8	142	AC	---	0.6	SKULL MTN
31 3:48:48	37.516	116.371	0.2	1.90	0.9	191	AC	---	1.2	QUARTZITE MTN
APR 1 17:59:28	37.037	116.123	0.3	5.23	0.8	126	AB	---	0.8	YUCCA FLAT
2 0:45:38	37.419	117.107	0.7	4.04	---	138	CC	---	1.3	SCOTTYS JUNCTION NE
2 13:45: 1	37.402	117.152	0.3	4.54	2.5	85	BC	---	1.5	STONEWALL PASS
4 11:30: 3	36.510	116.591	0.7	9.61	2.7	118	BC	---	1.5	BIG DUNE
4 18: 2: 5	37.167	116.778	0.6	10.43	0.7	202	AD	---	1.2	SPRINGDALE
5 0:23:47	37.166	117.341	0.1	9.22	0.4	105	AB	---	1.5	UBEHEBE CRATER
5 1:10:14	36.699	116.295	0.4	5.23	0.6	115	AB	---	0.9	STRIPED HILLS
5 1:35:55	37.419	117.101	0.5	5.44	4.0	137	BC	---	1.4	SCOTTYS JUNCTION NE
5 11: 5:18	37.211	115.795	0.2	7.63	1.3	80	AB	---	2.1	PAPOOSE LAKE NE
6 23: 9:14	37.522	116.363	0.3	8.69	1.7	121	AC	---	1.6	QUARTZITE MTN
13 10: 8: 8	37.482	117.159	0.3	0.71	0.4	137	AC	---	1.2	STONEWALL PASS
13 15:15:51	36.348	116.259	0.6	6.78	1.0	197	AD	---	1.0	LATHROP WELLS SE
14 14:38:32	37.701	115.040	0.5	2.39	1.6	110	AC	1.0	1.2	HIKO NE
14 18:56:17	36.826	116.627	0.6	-0.55BL	0.6	116	AB	1.2	0.9	● BARE MTN
15 8:38:40	35.895	117.017	0.6	4.54	2.1	284	BD	---	1.2	MANLY PEAK
15 15: 7:39	37.197	117.596	0.3	9.54	0.6	154	AC	---	1.8	LAST CHANCE RANGE
15 15:31:27	37.195	117.602	0.5	10.19	0.7	159	AC	---	1.8	LAST CHANCE RANGE
15 15:37:59	37.197	117.601	0.4	9.78	0.7	155	BC	---	1.7	LAST CHANCE RANGE
15 15:48:48	37.205	117.610	0.7	11.20	1.2	180	BC	---	1.3	LAST CHANCE RANGE
15 15:53:30	37.197	117.595	0.3	9.55	0.7	153	AC	---	1.5	LAST CHANCE RANGE
15 16: 4: 3	37.326	117.673	3.9	12.22	7.2	156	CC	---	1.1	MAGRUDER MTN
15 16:46:45	37.702	115.042	0.9	2.28	3.2	141	BC	---	0.9	HIKO NE
15 21:10: 9	36.997	117.574	0.4	2.99	1.5	182	AD	---	1.4	DRY MTN
16 4:33:49	36.724	116.148	0.5	8.09	1.4	107	AC	---	0.5	SPECTER RANGE NW
16 9: 0:44	37.449	116.031	0.3	-0.52	0.3	103	AB	---	1.4	WHEELBARROW PEAK NE
16 10: 6: 1	37.067	116.946	0.3	5.96	2.8	93	BB	---	1.5	SPRINGDALE
16 10:46:52	37.056	116.946	0.5	4.57	2.6	146	BC	---	1.0	SPRINGDALE
17 15:38:58	37.283	117.738	9.0	0.83	5.8	279	DD	---	1.0	MAGRUDER MTN
17 17:32: 5	37.292	117.732	0.3	0.39	0.5	162	BC	---	1.9	MAGRUDER MTN
19 21:39: 6	36.389	117.107	0.3	11.12	0.8	174	AC	---	2.0	EMIGRANT CANYON
20 3:36: 8	36.544	116.263	0.3	9.28	0.8	200	AD	---	1.0	LATHROP WELLS SE
20 11:51:29	37.374	117.732	0.6	12.69	1.5	140	AC	---	1.0	MAGRUDER MTN
21 2:46: 8	36.698	116.300	0.2	5.94	0.5	100	AB	---	1.2	STRIPED HILLS
21 18:13:37	35.712	116.748	---	2.05	---	303	BD	---	2.0	LEACH LAKE
21 22:37:28	37.278	117.734	1.5	4.33	4.8	166	BD	---	1.6	MAGRUDER MTN
21 22:38:53	37.284	117.785	---	0.98	---	207	AD	1.2	1.1	SOLDIER PASS
21 22:50:37	37.257	117.721	---	7.00**	---	208	AD	---	1.1	MAGRUDER MTN
22 18:17:39	37.529	114.628	---	7.00**	---	299	AD	---	1.4	CHOCHECHERRY MTN
22 23: 9:40	36.826	116.657	---	-0.44BL	---	282	AD	1.0	0.9	● BARE MTN
23 1:25:57	37.504	114.523	0.2	6.71	0.6	316	AD	---	1.5	CALIENTE
23 6: 8:51	36.590	115.672	1.4	4.30	4.4	334	BD	---	1.2	INDIAN SPRINGS
23 9:49:57	36.431	117.085	1.1	18.63	2.1	155	BC	---	1.2	EMIGRANT CANYON
25 2:20:55	35.872	116.759	1.1	4.29	4.8	304	BD	---	1.2	WINGATE WASH
25 3:21:26	35.827	116.735	---	7.00**	---	314	BD	---	1.5	CONFIDENCE HILLS
25 5:40:25	35.998	116.834	1.3	4.56	2.2	185	BD	---	1.2	WINGATE WASH
25 11:19:53	37.550	115.188	8.4	3.02	---	216	DD	---	1.0	HIKO
25 13:36:50	37.550	116.425	0.1	2.63	3.2	279	BD	---	1.2	QUARTZITE MTN
26 0:44: 4	35.918	116.765	0.8	3.95	2.5	284	BD	---	0.8	WINGATE WASH
26 12:14:38	36.860	116.243	0.3	5.34	0.8	146	AC	---	1.3	SKULL MTN
26 13: 1:00	36.862	116.245	0.5	7.34	1.0	111	AB	---	0.6	SKULL MTN
26 14: 5:21	37.087	117.999	0.3	7.00	---	245	DD	---	1.6	WAUCOBA SPRING
MAY 1 20:58:29	37.833	115.123	---	5.24	---	185	AD	---	1.0	WHITE RIVER NARROWS
2 6:53:48	37.140	116.374	4.8	1.56	0.9	327	CD	---	0.9	AMMONIA TANKS
2 8:23:55	36.614	116.565	1.0	7.01	5.0	152	CC	---	1.3	BIG DUNE
6 1:17:49	37.378	114.678	---	7.00**	---	288	AD	---	0.9	SLIDY MTN
6 4:42:59	37.771	114.917	0.2	4.81	0.9	187	AD	---	1.1	WHEATGRASS SPRING
6 8:21:49	36.699	116.699	---	7.00**	---	177	AD	---	0.6	CAMP DESERT ROCK
6 11: 1:13	37.426	117.107	1.1	-1.15	1.6	197	BD	---	1.4	SCOTTYS JUNCTION NE
7 1:55:56	37.415	117.100	0.4	0.56	0.6	89	AC	---	1.4	SCOTTYS JUNCTION NE
7 2: 4:51	37.411	117.109	0.8	-0.62	1.6	119	AC	---	1.2	SCOTTYS JUNCTION NE
7 3:18:49	36.830	116.052	0.2	7.90	0.3	245	AD	---	0.7	CANE SPRING
7 17:41:10	37.134	117.482	2.0	8.89	3.2	170	BC	---	1.3	UBEHEBE CRATER
7 23:47:53	36.788	115.892	1.1	13.48	3.2	187	BD	---	0.8	FRENCHMAN FLAT

## 1983 LOCAL HYPOCENTER SUMMARY

DATE - TIME (UTC)	LATITUDE (DEG. N)	LONGITUDE (DEG. W)	HORIZ ERROR (KM)	DEPTH (KM)	VERT ERROR (KM)	AZI CAP (DEG)	QUAL	Md	Mb19	QUADRANGLE
MAY 8 13:51:46	36.441	117.062	0.8	10.57	0.9	169	AD	---	1.2	EMIGRANT CANYON
8 17:36:31	37.698	115.047	0.2	0.63	0.3	116	AC	---	0.7	HIKO NE
10 3: 3:41	37.158	116.929	8.7	0.11	5.9	277	DD	---	0.9	SPRINGDALE
13 12:14:36	37.699	115.046	0.3	1.75	1.2	116	AC	---	1.2	HIKO NE
13 14:56:29	36.761	115.968	---	7.80**	---	237	AD	---	0.9	FRENCHMAN FLAT
14 3:18:21	37.164	117.576	0.6	9.82	1.3	198	AD	---	1.3	LAST CHANCE RANGE
15 6: 7:46	37.700	115.042	0.5	2.92	1.2	118	AC	---	0.9	HIKO NE
15 11:55: 1	36.964	117.536	0.6	5.88	5.9	195	CD	---	1.5	DRY MTN
17 7:54: 6	35.781	116.559	1.8	3.86*	---	279	CD	---	1.9	LEACH LAKE
17 20:51:49	37.667	116.947	0.3	1.89	0.9	64	AC	---	1.6	SPRINGDALE
17 22:39:38	36.604	116.782	1.9	1.83	2.6	319	BD	1.1	1.1	BULLFROG
18 1:59:10	37.682	115.047	0.9	2.56	2.5	114	BD	---	0.7	HIKO NE
18 5:28:19	37.543	115.043	---	3.87	---	268	BD	---	0.7	HIKO SE
18 6:57:44	37.148	117.850	0.7	9.41	2.3	217	BD	---	1.8	WAUCOBA SPRING
18 7:55:53	37.703	115.037	0.6	10.05	2.1	130	BD	---	1.0	HIKO NE
18 21: 7:25	37.183	116.688	0.4	8.19	1.3	183	AB	---	1.1	THIRSTY CANYON NE
19 6:42:54	36.233	116.811	---	7.08**	---	173	AD	---	1.1	BENNETTS WELL
19 6:49:43	37.355	117.530	0.6	1.86	1.5	94	AC	---	1.4	MAGRUDER MTN
20 3:37: 9	37.108	117.489	0.3	6.03	1.6	150	AD	---	1.5	UBEHEBE CRATER
20 9:51: 5	37.647	114.876	0.7	3.86	0.8	194	AD	---	1.1	PAHROC SPRING
20 14:56:41	37.370	117.550	1.1	7.44	2.0	181	BD	---	1.0	MAGRUDER MTN
21 11: 2:36	36.161	117.178	0.4	8.02*	---	216	CD	2.5	---	TELESCOPE PEAK
21 11:33:33	36.156	117.187	2.1	3.26*	---	225	CD	---	1.4	TELESCOPE PEAK
21 18: 5:55	37.137	117.347	0.2	6.13	1.0	114	AC	---	0.6	UBEHEBE CRATER
22 2:21: 2	36.154	117.215	1.5	3.13*	---	268	CD	---	1.3	TELESCOPE PEAK
22 18:48: 1	36.910	117.841	1.4	7.00	9.6	234	CD	---	1.7	WAUCOBA WASH
23 19: 8:45	36.927	116.250	2.1	4.29	3.3	150	CC	---	0.5	TOPOPAH SPRING
24 8:53: 1	35.875	116.758	---	7.00**	---	392	AD	1.0	1.0	WINGATE WASH
24 11:13:33	36.386	115.576	0.4	14.68	0.5	168	AB	---	1.7	CHARLESTON PEAK
26 8:36:00	36.443	116.922	0.8	9.79	2.2	159	BC	---	1.1	FURNACE CREEK
26 17:28:38	36.996	116.414	0.2	7.99	0.5	34	AA	---	1.9	TOPOPAH SPRING NW
26 17:33:20	37.002	116.430	0.6	8.37	0.7	199	AD	---	0.4	TIMBER MTN
26 17:45:41	36.999	116.428	0.5	7.95	0.5	194	AD	---	0.4	TOPOPAH SPRING NW
26 17:47:38	36.999	116.422	0.5	8.40	0.4	205	AD	---	0.3	TOPOPAH SPRING NW
26 17:51:51	36.999	116.429	0.5	9.53	0.5	196	AD	---	0.6	TOPOPAH SPRING NW
26 17:54:44	37.006	116.432	0.2	9.19	0.2	223	AD	---	0.7	TIMBER MTN
26 18: 0:27	37.005	116.429	0.5	8.83	0.5	193	AD	0.7	1.0	TIMBER MTN
26 18: 6:49	37.004	116.431	0.3	8.96	0.4	202	AD	---	0.8	TIMBER MTN
26 18:19:45	37.004	116.429	0.4	9.00	0.5	201	AD	---	0.9	TIMBER MTN
26 19:25:41	36.995	116.420	0.2	7.33	0.3	51	AA	0.7	0.9	TOPOPAH SPRING NW
26 19:53:53	37.007	116.430	0.3	9.20	0.4	205	AD	---	0.9	TIMBER MTN
26 20:18:49	37.004	116.425	0.3	6.60	0.5	197	AD	---	0.8	TIMBER MTN
JUN 30 17:22: 9	36.688	116.270	0.2	6.85	0.4	81	AA	---	1.5	STRIPED HILLS
1 19:58:29	36.584	117.052	0.4	7.93	2.5	107	BC	---	1.4	STOVEPIPE WELLS
3 13:17:44	36.719	116.433	0.2	7.03	0.4	193	AD	---	0.7	LATHROP WELLS NW
3 17: 5:32	36.629	116.273	0.5	6.29	0.8	205	AD	---	0.6	STRIPED HILLS
4 1:23: 4	36.991	117.537	1.1	14.11	1.9	189	BD	---	1.2	DRY MTN
4 3:26:59	37.381	115.196	0.7	6.74	1.9	101	AB	---	2.2	ASH SPRINGS
4 3:28:52	37.383	115.207	0.5	5.50	3.6	97	BC	---	1.6	ASH SPRINGS
4 11:37:41	37.389	115.207	0.3	4.12	1.6	94	AC	---	2.9	ASH SPRINGS
4 11:49:45	37.378	115.216	3.2	1.76*	---	104	CC	---	1.6	ASH SPRINGS
4 11:52: 8	37.409	115.158	---	15.65	---	198	BD	1.2	---	ASH SPRINGS
4 12:19: 5	37.385	115.210	---	7.00**	---	183	AD	1.0	---	ASH SPRINGS
4 13:15:00	37.380	115.211	0.3	4.89	2.6	96	BC	1.5	1.7	ASH SPRINGS
4 15:28:48	37.149	115.359	0.6	6.15	1.8	136	AC	---	2.5	DESERT HILLS NE
4 16:45:53	37.377	115.187	0.7	8.12	1.9	106	AB	1.6	1.6	ASH SPRINGS
8 1:11:24	37.083	116.735	---	7.00**	---	191	DD	0.5	---	THIRSTY CANYON SW
8 12:53:29	36.707	115.930	---	7.00**	---	202	AD	0.6	---	MERCURY
9 1:27:37	36.612	116.227	0.9	2.80	1.1	307	AD	---	1.1	SPECTER RANGE SW
9 1:29:24	36.614	116.421	0.4	4.31	0.8	297	AD	---	0.7	LATHROP WELLS SW
9 11:51:48	36.701	116.161	0.2	5.52	1.1	145	AC	---	0.8	SPECTER RANGE NW
10 15:45:35	37.292	115.380	0.6	7.65	3.1	86	BC	---	1.2	BADGER SPRING
12 2:56: 6	37.017	116.247	---	7.04	---	179	AD	---	0.6	TIPPIPAH SPRING
14 16:56:44	37.045	116.947	0.3	1.84	0.7	143	AC	---	1.0	SPRINGDALE
16 8:34:42	36.882	116.736	0.2	0.47BL	0.3	104	AC	---	1.3	BARE MTN
16 10:56:53	37.504	118.081	---	7.00**	---	261	AD	1.0	---	***REGIONAL***

# 1983 LOCAL HYPOCENTER SUMMARY

DATE - TIME (UTC)	LATITUDE (DEG. N)	LONGITUDE (DEG. W)	HORIZ ERROR (KM)	DEPTH (KM)	VERT ERROR (KM)	AZI GAP (DEG)	QUAL	Md	Mblg	QUADRANGLE
JUN 16 19:34: 8	36.388	117.099	---	23.79	---	185	AD	1.9	---	EMIGRANT CANYON
17 5:18:37	36.788	115.736	---	7.00**	---	292	AD	0.5	---	QUARTZ PEAK SW
17 6: 7:54	37.482	115.131	---	7.00**	---	280	AD	1.1	---	ASH SPRINGS
18 5: 8:38	37.189	116.591	0.8	11.87	2.0	106	AB	---	0.9	THIRSTY CANYON NE
18 12:35:18	37.202	116.802	0.5	14.35	0.9	106	AB	---	1.1	THIRSTY CANYON NE
18 15:17:10	37.260	117.409	---	7.00**	---	191	AD	0.7	---	GOLD POINT SW
18 23:45:48	37.351	115.859	---	7.00**	---	159	AD	0.8	---	GROOM LAKE
20 0:43:15	36.453	115.731	---	15.29	---	178	AD	0.7	---	CHARLESTON PEAK
22 5: 0:28	36.729	116.035	0.4	10.04	0.8	141	AC	---	1.3	CAMP DESERT ROCK
22 12: 4:56	37.392	115.211	0.3	2.78*	---	114	CC	1.3	---	ASH SPRINGS
23 7:24:14	36.898	115.811	---	4.71	---	198	BD	1.2	---	MERCURY NE
23 7:54: 2	36.726	114.526	---	7.00**	---	356	CD	1.5	---	MOAPA
24 3:52:14	36.898	115.884	---	0.23	---	152	DD	1.0	---	MERCURY NE
24 3:59:53	36.898	115.783	---	7.00**	---	342	BD	1.0	---	MERCURY NE
24 4:44:32	37.648	117.720	---	7.00**	---	183	AD	1.3	---	LIDA WASH
24 10:56:38	37.020	117.298	---	11.90	---	153	BD	0.9	---	UBENEDE CRATER
25 2:37:44	36.898	116.308	0.5	2.01	1.6	109	AB	0.7	---	STRIPED HILLS
25 12:54:14	36.984	117.216	4.5	1.28	7.3	219	CD	1.1	---	GRAPEVINE PEAK
26 3:54:32	36.883	115.768	3.0	4.16	2.4	228	CD	1.3	---	MERCURY NE
27 5:12:46	37.915	115.179	---	7.00**	---	273	AD	1.1	---	OREANA SPRING
28 4: 1:38	37.181	116.490	---	-1.00	---	334	AD	0.9	---	SCRUGHAM PEAK
JUL 4 2:32:54	37.235	117.543	0.2	0.14	0.4	104	AB	---	1.5	LAST CHANCE RANGE
5 9:26:25	37.152	116.423	0.5	11.87	0.5	216	AD	---	1.0	SCRUGHAM PEAK
7 0:12:57	37.210	115.798	2.2	0.69	1.7	227	BD	---	1.1	PAPOOSE LAKE NE
7 7: 4:40	36.672	116.305	0.4	3.60	0.7	134	AB	---	0.6	STRIPED HILLS
7 11:28:29	36.653	116.220	1.0	3.50	3.0	292	BD	---	0.6	SPECTER RANGE NW
7 15:23:58	37.020	117.528	0.7	4.84	0.9	177	CC	---	1.2	LAST CHANCE RANGE
7 15:58:25	37.238	117.572	0.5	7.91	1.0	110	AB	---	1.4	LAST CHANCE RANGE
10 7:39:39	37.390	114.956	0.9	0.97	0.8	181	AD	---	1.2	DELAMAR NW
10 18:42:57	37.864	115.798	0.3	8.47	0.9	160	AC	---	1.1	***QUAD. NOT LISTED***
10 19:31:57	37.688	117.397	0.5	2.59	0.5	128	AB	---	1.6	SPLIT MTN
11 4:32:14	37.914	117.107	0.8	0.23	0.7	217	AD	---	1.3	MUD LAKE
11 22:34:41	36.826	116.649	0.3	-0.72BL	0.3	93	AB	---	1.0	●BARE MTN
12 5:44:19	37.689	115.937	0.8	1.87	2.6	98	BB	---	1.4	WHITE BLOTCH SPRINGS
13 14:55:19	36.728	116.243	0.2	7.53	0.4	70	AA	---	1.3	SPECTER RANGE NW
15 18:52:57	37.298	114.864	0.8	5.89	3.2	226	BD	---	1.9	GREGERSON BASIN
15 22:26:58	37.639	117.717	1.1	2.06	3.8	180	BC	---	1.1	LIDA WASH
16 1:51:56	36.834	116.216	0.3	8.32	0.5	143	AC	---	1.1	SKULL MTN
16 3:19:53	36.452	116.089	0.9	5.32	0.7	163	AC	---	0.7	MT SCHADER
16 8:53:44	37.236	117.537	1.9	1.60	7.8	122	CB	---	1.0	LAST CHANCE RANGE
16 9:44:44	36.841	116.215	1.0	8.20	1.1	278	BD	---	0.3	SKULL MTN
16 15:13:28	36.449	117.102	---	-0.73	---	166	AD	---	1.1	EMIGRANT CANYON
16 19:13: 0	37.094	116.199	0.3	5.94	0.8	148	AC	---	1.0	TIPPIPAH SPRING
16 19:56:57	37.257	115.833	0.9	1.44	1.4	200	AD	---	1.8	ALAMO SE
17 1:33:29	36.980	117.618	0.7	8.26	2.2	219	BD	---	1.0	DRY MTN
18 2:21:20	37.741	115.049	0.5	9.48	0.8	141	AC	2.4	---	HIKO NE
18 18:53:32	37.689	117.421	0.6	1.68	1.0	153	AD	---	1.0	SPLIT MTN
18 20:33:10	36.980	116.632	---	0.98BL	---	343	AD	---	0.5	●BARE MTN
19 9: 9:15	37.284	116.083	0.3	2.38	0.8	146	AC	---	0.9	OAK SPRING BUTTE
19 10:55:28	37.675	117.411	0.8	9.15	4.3	108	BC	---	0.8	SPLIT MTN
19 12: 0: 7	36.587	116.265	0.8	-0.06	0.9	241	AD	---	0.5	LATHROP WELLS SE
20 10:48:11	37.482	117.111	0.5	3.28	8.1	105	CC	2.4	---	SCOTTYS JUNCTION NE
20 10:51:15	37.494	117.117	1.5	2.91*	---	102	CC	1.5	---	SCOTTYS JUNCTION NE
20 10:54:43	37.481	117.028	---	3.23	---	198	AD	1.3	---	SCOTTYS JUNCTION NE
20 13: 8:11	37.162	116.079	---	3.02	---	216	AD	1.1	---	OAK SPRING
21 15:33: 1	37.700	115.028	0.2	0.44	0.3	122	AB	---	1.6	HIKO NE
22 16:26:51	37.391	116.159	1.3	4.15	1.2	280	BD	---	1.7	***REGIONAL***
23 0:23:58	36.742	116.033	0.4	0.85	0.8	172	AC	---	1.0	CAMP DESERT ROCK
23 23:43:42	36.693	116.249	0.8	0.47	0.6	255	AD	---	0.5	SPECTER RANGE NW
24 1:51:13	37.104	117.068	0.3	0.52	0.8	100	AC	---	1.0	BONNIE CLAIRE SE
24 21:38:42	37.783	114.999	0.7	0.24	0.7	187	AD	---	0.9	WHEATGRASS SPRING
25 1:17:33	36.975	117.924	0.8	11.37	5.5	249	CD	---	2.2	WAUCOBA WASH
25 2:24: 0	36.737	117.384	---	4.73	---	198	AD	---	0.7	MARBLE CANYON
25 5:32:19	37.069	117.965	3.8	2.81*	---	207	CD	---	1.4	WAUCOBA SPRING
25 18:10:19	37.686	115.038	0.3	2.56*	---	206	DD	---	0.6	HIKO NE
25 19: 4:23	37.675	115.039	0.3	3.46	1.9	112	AB	---	1.2	HIKO NE

## 1983 LOCAL HYPOCENTER SUMMARY

DATE - TIME (UTC)	LATITUDE (DEG. N)	LONGITUDE (DEG. W)	HORIZ ERROR (KM)	DEPTH (KM)	VERT ERROR (KM)	AZI GAP (DEG)	QUAL	Md	Mbig	QUADRANGLE
JUL 25 22:27:31	37.572	116.456	0.3	7.68	2.6	99	BC	---	1.0	QUARTZITE MTN
26 23:53:50	37.142	117.359	0.3	10.59	0.8	117	AB	---	1.0	UBEHEBE CRATER
27 0:14:2	36.729	116.212	0.3	4.83	0.9	70	AB	---	1.2	SPECTER RANGE NW
28 9:43:25	37.324	115.259	1.1	1.85	3.8	112	BC	1.5	---	BADGER SPRING
28 22:44:58	36.859	115.937	0.8	5.34	1.5	257	AD	---	1.1	FRENCHMAN FLAT
29 11:30:31	36.809	115.876	0.6	7.96	1.5	205	AD	---	1.4	FRENCHMAN FLAT
29 17:46:3	36.382	117.049	0.7	11.75	0.8	122	AB	---	1.3	EMIGRANT CANYON
29 23:24:31	36.798	115.906	0.4	3.02	---	185	CD	---	0.8	FRENCHMAN FLAT
30 16:31:38	37.257	115.027	0.6	7.53	1.6	225	AD	---	1.5	ALAMO SE
31 4:39:38	37.701	115.040	2.0	2.34	3.8	209	BD	---	0.7	HIKO NE
31 13:41:6	37.314	115.186	9.0	7.00	---	130	DC	---	1.0	ALAMO
AUG 1 7:35:53	36.647	116.411	2.3	11.54	2.1	268	BD	---	0.6	LATHROP WELLS NW
1 18:28:3	37.198	117.377	0.3	7.93	1.1	108	BB	1.4	1.6	UBEHEBE CRATER
1 21:21:41	37.712	115.015	---	5.39	---	233	AD	---	0.8	HIKO NE
2 0:21:1	37.663	115.042	0.2	6.14	0.6	116	AB	---	1.4	HIKO NE
3 12:11:1	36.975	116.144	1.7	0.91	1.4	236	BD	---	0.6	MINE MTN
3 14:17:56	37.313	117.644	0.5	5.50	1.4	116	AB	---	1.2	MAGRUDER MTN
3 18:17:47	37.393	115.213	1.5	2.77	0.8	249	CD	---	1.1	ASH SPRINGS
5 3:22:46	36.623	116.353	1.3	6.15	0.6	267	BD	---	0.9	LATHROP WELLS SE
5 16:23:19	37.316	117.654	0.4	4.56	1.4	122	AB	---	1.3	MAGRUDER MTN
6 2:14:41	37.062	117.404	0.6	2.94	2.1	131	BB	1.7	---	UBEHEBE CRATER
6 2:17:39	37.062	117.391	0.3	2.35	0.9	127	AD	1.2	---	UBEHEBE CRATER
6 4:42:10	37.023	117.344	---	0.98	---	232	BD	1.1	---	UBEHEBE CRATER
6 7:26:9	36.360	116.805	0.5	5.74	5.7	119	CC	1.6	---	FURNACE CREEK
6 10:47:42	37.046	117.386	---	3.52	---	151	AD	1.0	---	UBEHEBE CRATER
6 11:23:41	36.310	117.466	4.0	2.15	---	265	CD	1.5	---	PANAMINT BUTTE
6 14:29:15	37.056	117.393	---	-1.06	---	154	AD	0.9	---	UBEHEBE CRATER
6 15:37:58	37.067	117.406	0.6	1.45	2.9	131	BB	1.3	---	UBEHEBE CRATER
6 16:6:46	37.062	117.389	0.3	-0.02	8.1	128	CB	1.2	---	UBEHEBE CRATER
6 16:7:32	37.065	117.393	0.4	4.19	1.9	127	AB	1.2	---	UBEHEBE CRATER
6 6:53:29	36.745	116.262	0.3	3.58	0.4	103	AB	---	1.1	STRIPED HILLS
8 18:48:48	37.545	117.156	0.4	8.84	2.5	127	BC	---	1.1	GOLDFIELD
8 19:16:55	37.315	117.586	0.4	10.39	0.5	242	AD	---	0.9	MAGRUDER MTN
9 15:20:58	36.986	117.575	0.5	8.50	2.2	202	BD	---	1.8	DRY MTN
9 15:47:43	37.692	115.044	0.2	1.79	0.6	115	AC	---	1.1	HIKO NE
9 18:32:50	37.701	115.006	0.1	1.73	0.4	147	AD	---	1.0	HIKO NE
10 18:36:16	36.835	115.784	1.6	16.42	2.1	275	BD	---	0.8	FRENCHMAN LAKE SE
10 21:34:30	37.718	115.053	0.2	9.11	0.5	118	AB	---	0.9	HIKO NE
11 14:30:28	36.788	117.403	1.0	7.00	0.7	191	AD	---	1.1	TIN MTN
11 17:26:15	37.964	117.635	0.5	3.83	0.7	255	CD	---	1.8	SILVER PEAK
11 17:57:47	37.067	117.421	0.9	0.44	0.8	288	AD	---	0.9	UBEHEBE CRATER
12 6:37:44	37.487	117.144	0.5	5.89	4.3	105	BC	---	1.4	STONEWALL PASS
12 7:38:21	36.379	115.809	0.6	8.43	2.4	177	BC	---	1.1	MT STIRLING
13 3:39:58	37.159	117.376	0.2	0.77	0.4	105	AC	---	1.5	UBEHEBE CRATER
13 6:8:52	37.070	117.412	---	-0.07	---	132	AD	---	1.0	UBEHEBE CRATER
13 9:37:32	37.000	116.392	0.5	-0.12	0.4	152	AC	---	1.3	TIMBER MTN
13 14:1:25	37.045	116.404	2.4	0.97	1.8	267	BD	---	0.9	TIMBER MTN
14 13:23:24	37.366	117.537	0.5	5.91	1.4	170	AC	---	0.9	MAGRUDER MTN
14 21:0:49	37.068	117.371	0.6	1.75	2.2	137	BC	---	1.1	UBEHEBE CRATER
15 6:41:24	36.783	116.247	0.6	0.06	0.7	88	AB	1.1	---	SKULL MTN
16 16:42:58	37.356	117.546	0.6	0.19	1.0	99	BB	---	1.5	MAGRUDER MTN
16 19:2:46	37.031	116.297	2.2	-1.01	1.3	237	BD	---	1.0	BUCKBOARD MESA
17 9:44:21	37.734	114.723	---	7.00	---	260	AD	---	0.8	CALIENTE NW
17 16:17:23	37.040	116.307	1.4	2.70	1.6	278	BD	---	0.7	BUCKBOARD MESA
17 20:38:23	37.372	117.547	0.6	7.57	1.4	180	AC	---	1.3	MAGRUDER MTN
17 23:40:29	37.720	115.047	0.5	8.21	1.2	121	AB	---	1.3	HIKO NE
18 2:8:25	36.851	116.227	0.4	10.45	0.7	112	AB	---	0.8	SKULL MTN
18 7:43:25	37.194	117.605	0.6	7.75	0.2	181	AD	---	1.0	LAST CHANCE RANGE
18 15:16:50	36.774	116.259	0.4	0.14	0.4	97	AB	---	0.7	JACKASS FLATS
18 20:55:51	37.065	116.266	1.0	2.65	1.0	267	AD	---	1.1	BUCKBOARD MESA
19 15:50:33	36.854	116.235	0.2	11.13	0.3	165	AC	---	0.6	SKULL MTN
19 18:5:59	36.851	116.231	0.4	11.19	0.6	120	AB	---	1.0	SKULL MTN
22 5:52:50	37.146	115.404	0.3	6.29	1.8	80	AC	2.4	2.5	DESERT HILLS NW
22 6:32:54	36.706	116.229	0.6	8.41	0.6	217	AD	---	0.6	SPECTER RANGE NW
22 9:7:38	37.529	117.575	2.0	2.65	0.3	272	CD	---	1.2	LIDA WASH
22 23:46:0	37.159	117.407	0.2	9.03	0.5	130	AC	0.8	1.0	UBEHEBE CRATER

## 1983 LOCAL HYPOCENTER SUMMARY

DATE - TIME (UTC)	LATITUDE (DEG. N)	LONGITUDE (DEG. W)	HORIZ ERROR (KM)	DEPTH (KM)	VERT ERROR (KM)	AZI GAP (DEG)	QUAL	Md	Mb19	QUADRANGLE
AUG 23 2:43:15	37.522	117.578	---	7.00**	---	391	AD	1.1	1.2	LIDA WASH
23 3:3:19	37.335	117.802	1.3	24.87	0.8	188	BC	0.9	1.2	SOLDIER PASS
23 19:40:33	37.695	117.429	0.6	8.05	0.9	168	AC	---	1.3	SPLIT MTN
25 16:22:40	36.418	117.466	5.5	-0.13	3.8	283	DD	---	1.3	PANAMINT BUTTE
26 10:43:6	36.643	115.854	1.6	8.99	1.2	332	BD	---	0.8	MERCURY NE
28 1:4:34	37.085	116.536	0.6	12.88	0.6	300	AD	---	1.0	THIRSTY CANYON SE
28 18:14:45	38.226	115.869	0.6	2.81	2.6	227	BD	---	1.1	QUINN CANYON RANGE
29 4:56:35	38.222	115.992	0.7	7.00	5.6	259	CD	---	1.8	QUINN CANYON RANGE
29 8:37:36	38.682	118.274	0.5	8.18	9.4	252	AD	0.8	0.7	STRIPED HILLS
29 15:46:24	38.725	115.663	2.5	9.44	1.9	328	CD	---	1.1	INDIAN SPRINGS NW
29 17:22:23	37.134	116.297	0.5	5.97	0.8	294	AD	---	0.7	AMMONIA TANKS
29 19:38:39	38.414	116.949	0.3	14.45	0.5	100	AB	---	1.7	FURNACE CREEK
30 10:23:31	37.048	117.413	0.9	4.48	3.6	185	BD	---	1.1	UBEHEBE CRATER
30 10:26:36	37.080	117.400	0.3	-1.15	0.5	129	AB	---	1.3	UBEHEBE CRATER
31 7:44:47	38.663	115.964	2.4	7.00	1.3	182	BD	---	0.6	MERCURY
31 10:20:50	37.627	114.958	---	6.44	---	244	AD	---	0.9	PAHROC SPRING
31 22:46:37	38.839	116.224	0.2	7.23	0.4	58	AA	---	1.3	SKULL MTN
SEP 1 8:28:25	37.685	115.051	0.5	0.32	0.7	158	AC	---	0.7	HIKO NE
1 23:2:10	37.198	117.304	0.2	7.92	0.6	89	AB	---	1.7	UBEHEBE CRATER
2 2:5:1	36.701	116.285	0.3	6.74	0.5	119	AB	---	0.7	STRIPED HILLS
3 8:37:52	36.986	117.548	0.6	2.75	3.2	194	BD	---	1.1	DRY MTN
3 1:6:13	36.970	117.558	0.5	5.28	4.5	200	BD	---	1.6	DRY MTN
5 15:40:56	36.837	116.237	0.3	7.21	0.5	123	AB	---	0.8	SKULL MTN
5 16:18:8	37.491	114.299	2.3	5.98	2.3	295	BD	---	1.7	***REGIONAL***
5 17:9:20	37.456	114.294	1.5	7.12	5.8	333	CD	---	1.7	***REGIONAL***
5 18:31:25	37.305	114.887	1.5	16.58	2.9	269	BD	---	1.2	DELAMAR LAKE
5 20:4:57	36.761	116.235	0.4	2.90	0.4	185	AD	---	0.5	SKULL MTN
5 23:34:29	36.772	116.247	0.3	1.37	2.8	172	BC	---	0.7	SKULL MTN
6 2:21:26	37.091	117.366	0.6	14.32	1.0	134	AB	---	1.0	UBEHEBE CRATER
6 17:20:16	36.777	116.254	0.3	0.83	0.8	82	AA	---	1.6	JACKASS FLATS
10 12:45:42	35.900	116.479	5.4	11.67*	---	252	DD	1.9	---	SHOSHONE
11 23:15:24	37.080	116.199	0.5	5.35	0.3	281	AD	---	0.9	TIPPIPAH SPRING
12 7:38:42	38.595	118.459	0.7	4.61	2.0	285	AD	---	1.0	LATHROP WELLS SW
12 8:28:3	37.844	117.019	0.5	0.20	0.7	177	AC	---	0.8	BONNIE CLAIRE SE
12 12:27:55	37.235	115.017	0.5	5.40	2.6	213	BD	---	1.6	LOWER PAHRANAGAT LAKE
13 6:4:54	36.946	117.844	0.8	2.82	2.1	231	BD	---	1.3	WAUCOBA WASH
14 13:38:34	37.552	117.358	0.3	2.88*	---	84	CC	1.4	---	MONTEZUMA PEAK SE
15 12:13:43	37.324	115.602	2.0	0.07	1.3	257	BD	---	1.2	GROOM RANGE SE
16 8:39:15	37.764	118.116	2.2	4.75*	---	302	CD	---	1.3	***REGIONAL***
16 19:28:48	37.202	118.959	0.7	5.90	2.9	251	BD	---	1.0	SPRINGDALE
16 19:56:37	37.076	118.113	2.9	2.22*	---	280	CD	---	1.7	***REGIONAL***
17 8:41:46	37.191	117.322	0.4	1.90	1.0	95	AC	1.3	---	UBEHEBE CRATER
19 8:57:8	37.288	115.391	2.0	2.46*	---	201	CD	1.3	---	CUTLER RESERVOIR
20 0:48:59	37.188	116.589	1.3	8.04	4.2	254	BD	---	1.1	THIRSTY CANYON NE
21 1:16:32	37.694	115.023	1.3	5.90	6.0	144	CD	---	1.1	HIKO NE
21 7:3:26	36.998	117.499	0.7	6.10	3.5	174	BC	---	1.4	TIN MTN
21 15:52:50	36.494	117.592	0.5	19.71	4.3	266	DD	---	1.7	DARWIN
22 0:30:59	37.616	114.889	1.4	9.45	2.5	215	BD	---	1.0	WHEATGRASS SPRING
23 18:47:29	37.244	114.852	---	7.00**	---	264	BD	1.6	---	DELAMAR J NE
25 2:40:53	37.821	114.866	1.3	9.14	3.8	224	BD	---	1.1	DEADMAN SPRING SE
25 19:51:40	37.416	114.723	1.5	4.19*	---	272	CD	---	1.0	SLIDY MTN
26 7:2:25	37.597	117.385	0.7	8.50	1.4	161	AC	---	1.5	MONTEZUMA PEAK SW
26 11:42:52	37.534	117.817	1.2	10.45	2.3	152	BC	---	1.3	PIPER PEAK
27 16:55:45	36.990	117.508	0.7	7.93	2.0	179	AC	---	1.1	DRY MTN
28 1:37:42	37.852	117.367	0.6	4.13	1.6	140	AD	---	1.2	UBEHEBE CRATER
29 5:26:41	36.703	115.478	5.6	2.46*	---	317	DD	---	1.7	BLACK HILLS NW
29 10:17:50	36.601	116.769	1.7	10.29	0.8	289	BD	0.7	1.2	CHLORIDE CLIFF
30 21:23:26	37.167	114.729	1.2	10.62	2.3	258	BD	---	2.0	VIGO NW
OCT 1 10:32:54	37.353	117.280	0.2	0.07	0.7	58	AA	2.4	2.5	GOLD POINT
1 10:33:59	37.343	117.253	0.7	8.74	1.1	116	AB	2.1	2.4	GOLD POINT
1 10:47:46	37.352	117.280	0.2	8.57	0.7	50	AA	---	2.4	GOLD POINT
1 10:51:47	37.348	117.287	0.3	5.68	0.8	61	AB	---	1.8	GOLD POINT
1 10:54:58	37.337	117.293	0.5	5.39	2.1	95	BB	---	1.0	GOLD POINT
1 11:0:30	37.353	117.281	0.5	5.61	1.4	69	BB	---	1.6	GOLD POINT
1 19:5:37	37.362	117.252	0.9	7.85	0.8	254	AD	0.9	0.9	GOLD POINT
1 19:55:53	37.354	117.285	0.6	5.63	0.8	187	AD	---	1.0	GOLD POINT



## 1983 LOCAL HYPOCENTER SUMMARY

	DATE - TIME (UTC)	LATITUDE (DEG. N)	LONGITUDE (DEG. W)	HORIZ ERROR (KM)	DEPTH (KM)	VERT ERROR (KM)	AZI GAP (DEG)	QUAL	Md	Mblg	QUADRANGLE
OCT	1 20:35:12	37.347	117.289	0.3	5.25	0.5	211	AD	---	0.9	GOLD POINT
	1 21:20:34	37.351	117.287	0.2	4.82	0.7	117	AB	---	1.4	GOLD POINT
	1 21:40:35	37.321	117.442	0.7	11.96	1.8	144	AC	---	1.2	GOLD POINT SW
	1 23:30:12	37.443	117.308	3.5	1.56	4.9	258	CD	---	1.2	MOUNT JACKSON
	2 5:20:47	37.001	117.682	1.0	6.83	5.6	199	CD	---	1.4	LAST CHANCE RANGE
	3 14:17:59	36.668	116.288	0.3	6.16	0.6	94	AB	---	1.3	STRIPED HILLS
	3 21:56:26	37.354	117.273	0.2	4.68	0.6	119	AB	1.4	---	GOLD POINT
	4 2: 4:44	37.355	117.276	0.6	5.68	1.5	119	AB	1.4	---	GOLD POINT
	5 10:18: 1	37.419	114.721	0.6	3.69*	---	272	CD	---	1.1	SLIDY MTN
	5 12:57: 4	37.496	117.321	1.2	18.88	1.8	179	BC	---	1.4	MOUNT JACKSON
	6 9: 1:33	37.702	115.047	0.4	2.03	1.5	117	AC	---	1.4	HIKO NE
	9 12: 6:55	37.167	117.623	1.3	10.05	1.6	207	BD	---	1.3	LAST CHANCE RANGE
	11 9:30:50	37.140	117.411	0.6	6.37	2.0	136	BC	---	1.0	UBEHEBE CRATER
	11 9:38:41	37.137	117.385	0.7	8.00	3.0	129	BB	---	1.3	UBEHEBE CRATER
	11 13:17:52	37.134	117.399	0.6	5.10	4.2	136	BC	---	1.7	UBEHEBE CRATER
	12 9:25:54	37.187	117.400	0.3	6.67	1.4	118	AC	---	1.1	UBEHEBE CRATER
	12 13:54:15	36.295	117.174	0.9	3.94	2.4	241	BD	---	0.4	EMIGRANT CANYON
	12 15:27:30	36.922	117.851	0.8	11.13	3.4	267	BD	---	1.5	WAUCOBA WASH
	12 18: 9:36	37.323	117.285	2.6	10.72	2.5	194	CD	---	1.2	GOLD POINT
	13 6:40:40	37.285	116.362	0.4	-0.94	0.6	74	AC	---	1.7	DEAD HORSE FLAT
	13 8:34:42	36.926	117.896	3.1	7.00*	---	252	CD	---	1.2	WAUCOBA WASH
	13 8:51: 8	37.227	116.344	1.1	7.92	2.3	317	BD	---	0.9	AMMONIA TANKS
	14 13:20:22	36.978	116.294	0.9	5.42	2.2	193	BD	---	1.4	TOPOPAH SPRING
	14 20:10:38	37.290	115.495	1.9	1.26	4.2	257	BD	---	1.7	CUTLER RESERVOIR
	15 10:33:30	37.857	116.024	0.9	2.97	5.8	111	CC	---	1.1	REVEILLE PEAK
	17 3:24:32	36.780	116.677	0.3	4.72	0.8	113	AB	1.1	1.1	BARE MTN
	17 6:23:36	36.674	116.257	0.4	5.02	1.4	120	AB	---	1.3	STRIPED HILLS
	19 1:14:13	36.472	116.364	2.6	4.03*	---	327	CD	---	0.8	ASH MEADOWS
	19 12:36:21	36.970	117.546	0.7	3.17*	---	196	CD	---	1.1	DRY MTN
	19 19: 6:35	37.553	115.323	0.6	5.22	3.4	157	BC	---	1.5	MT IRISH
	20 0:14:45	37.465	115.531	0.8	8.53	2.7	134	BC	---	1.6	GROOM RANGE NE
	20 6:59:43	37.703	115.036	0.6	4.22	3.8	120	BC	---	1.1	HIKO NE
	20 8: 6:22	37.542	115.333	0.8	0.86	1.2	163	BC	---	0.7	MT IRISH
	21 2:25:43	37.462	115.534	1.1	2.49*	---	122	CC	1.4	---	GROOM RANGE NE
	22 9: 5:24	37.059	117.982	1.3	5.21*	---	287	CD	---	1.3	WAUCOBA SPRING
	23 21:13:20	37.365	117.560	1.0	8.95	2.3	186	BD	---	1.0	MAGRUDER MTN
	24 5:26:29	37.001	117.438	0.5	3.00	1.1	151	AC	---	1.1	UBEHEBE CRATER
	25 18:45: 9	36.294	115.511	1.7	10.48	9.3	296	CD	---	1.4	CHARLESTON PEAK
	26 11:44:14	36.653	116.083	0.5	6.58	1.9	104	AB	---	0.5	CAMP DESERT ROCK
	27 11:37:48	37.195	116.342	0.9	7.75	1.9	314	AD	---	0.8	AMMONIA TANKS
	27 15:57:31	37.397	114.899	2.3	6.04*	---	255	CD	---	1.5	DELAMAR NW
	27 22: 5:36	37.211	116.405	1.5	3.78*	---	325	CD	---	0.8	SCRUGHAM PEAK
	28 8:27:13	37.462	115.549	1.2	8.15	5.3	136	CC	---	1.3	GROOM RANGE NE
	29 11: 4:51	37.019	117.413	1.5	-0.96	1.6	146	CC	---	0.9	UBEHEBE CRATER
	29 11: 9:40	37.025	117.419	0.5	2.88	1.1	141	AC	---	0.8	UBEHEBE CRATER
	29 15:39:17	37.023	117.433	0.5	0.80	0.6	146	AC	---	1.4	UBEHEBE CRATER
	29 15:42: 1	37.026	117.435	0.3	-0.26	0.5	146	AC	---	1.3	UBEHEBE CRATER
	29 16:38:54	37.027	117.427	0.7	5.05	3.2	144	BC	---	1.2	UBEHEBE CRATER
	29 20:33:36	37.066	116.227	1.9	13.67	2.7	271	BD	---	1.0	TIPPICAH SPRING
	30 6: 9:51	37.512	116.938	2.5	6.66*	---	179	CC	---	1.3	CACTUS SPRING
	30 7:22: 6	37.728	115.976	1.0	2.95	4.8	183	BD	---	1.3	WHITE BLOTCH SPRINGS
	30 13:39:54	37.023	117.450	2.2	5.32	6.9	152	CC	1.2	---	UBEHEBE CRATER
	30 13:52:30	36.162	117.536	21.9	1.18*	---	267	DD	1.4	---	COSO PEAK
	30 21:24:15	37.018	117.425	0.6	2.95	1.1	144	AC	---	1.0	UBEHEBE CRATER
NOV	2 16:39:34	36.817	116.281	1.0	9.98	1.3	151	AC	---	0.5	JACKASS FLATS
	3 8:19:47	36.745	116.288	1.1	1.11*	---	277	CD	---	0.8	STRIPED HILLS
	4 16:36:16	37.350	117.282	0.4	5.16	0.9	120	AB	---	1.2	GOLD POINT
	5 9:41:38	37.356	114.733	1.1	4.90*	---	244	CD	---	1.0	ELGIN SW
	7 16:11:45	35.948	117.278	2.4	3.35*	---	273	CD	---	1.2	TROMA
	7 16:24:22	37.618	114.843	3.2	11.13	6.9	229	CD	---	1.1	DEADMAN SPRING SE
	7 20:32:12	37.623	114.857	1.3	4.04*	---	227	CD	---	1.0	DEADMAN SPRING SE
	7 21:38:51	37.411	117.191	0.4	-0.01	0.7	84	CC	---	1.4	STONEWALL PASS
	9 16:31:15	36.721	116.062	0.6	7.33	1.7	159	AC	---	0.6	CAMP DESERT ROCK
	10 10:37:15	37.426	117.098	0.2	6.01	2.5	92	AC	1.9	2.0	SCOTTYS JUNCTION NE
	10 12:22:26	37.424	117.099	0.4	2.54	1.9	100	BC	---	2.2	SCOTTYS JUNCTION NE
	10 13:17:33	37.425	117.097	0.2	7.33	1.3	92	AB	1.7	1.5	SCOTTYS JUNCTION NE

## 1983 LOCAL HYPOCENTER SUMMARY

DATE - TIME (UTC)	LATITUDE (DEG. N)	LONGITUDE (DEG. W)	HORIZ ERROR (KM)	DEPTH (KM)	VERT ERROR (KM)	AZI GAP (DEG)	QUAL	Md	Mblg	QUADRANGLE
NOV 11 5:29:51	36.583	116.453	1.3	6.48	2.5	297	BD	0.4	0.7	LATHROP WELLS SW
11 17:56:49	37.345	118.139	1.0	6.39	3.2	263	BD	1.0	1.8	***REGIONAL***
12 4:16:43	38.171	115.678	4.4	4.87*	---	303	CD	---	1.5	CHERRY CREEK SUMMIT
12 4:31:48	37.184	115.957	1.6	10.97	3.2	157	BC	---	1.1	PAIUTE RIDGE
12 15:23:51	37.819	114.868	2.3	1.16	4.9	223	BD	---	1.2	DEADMAN SPRING SE
13 3: 9:41	36.856	116.169	1.7	3.90	2.4	171	BC	---	0.9	SKULL MTN
13 3:21:42	36.378	116.949	1.0	16.47	1.8	124	BB	---	0.8	FURNACE CREEK
13 7:46:52	37.433	117.897	0.7	1.55	3.2	93	BC	---	1.0	SCOTTYS JUNCTION NE
14 21: 0:51	37.678	115.360	1.4	-0.25	1.1	97	CB	---	1.5	MT IRISH
15 1:37:27	37.059	118.120	1.0	1.89	1.4	255	BD	---	1.4	YUCCA FLAT
16 2:29:23	36.837	116.628	2.4	4.01	3.1	248	BD	---	0.3	BAKE MTN
18 16:15:28	37.860	116.818	0.7	3.28*	---	183	CD	---	1.4	REVELLE PEAK
19 3:58:53	36.618	116.257	0.4	5.39	1.0	154	AC	---	0.9	LATHROP WELLS SE
19 11:58:28	36.414	116.883	2.8	15.62	0.6	343	CD	---	1.3	FURNACE CREEK
20 10:54:33	36.716	115.704	1.0	10.30	0.8	282	AD	---	1.3	INDIAN SPRINGS NW
20 11: 2:37	36.705	115.731	0.7	11.28	0.4	278	AD	---	1.1	INDIAN SPRINGS NW
20 13:17:10	36.716	115.715	1.3	9.80	0.9	281	BD	---	1.2	INDIAN SPRINGS NW
21 2: 7:17	36.682	116.193	2.6	-0.44	1.8	282	CD	---	0.7	SPECTER RANGE NW
21 4:51:25	36.705	115.747	1.3	10.10	0.9	275	BD	---	1.3	INDIAN SPRINGS NW
21 5:22:12	36.711	115.731	1.4	8.70	1.3	278	BD	---	1.2	INDIAN SPRINGS NW
21 9:28:25	36.932	115.982	1.5	7.41	2.3	268	BD	---	0.6	PLUTONIUM VALLEY
21 13:55:42	36.712	115.741	1.0	10.70	1.0	276	BD	---	1.0	INDIAN SPRINGS NW
21 14:50:18	36.720	115.711	0.8	9.80	0.9	281	AD	---	1.0	INDIAN SPRINGS NW
22 0: 2: 8	37.020	116.431	3.0	5.85	3.1	252	CD	---	0.3	TIMBER MTN
22 15:31:48	37.391	117.459	1.4	7.00	2.5	144	BC	---	1.1	LIDA
22 19:42:57	36.580	116.948	1.4	8.40	1.9	284	BD	---	0.8	CHLORIDE CLIFF
23 1: 2:52	37.458	117.284	0.3	5.29	2.7	88	BC	---	1.6	MOUNT JACKSON
24 11:35:17	37.258	117.271	0.6	7.06	0.8	120	AB	---	1.1	GOLD POINT
27 0:21:54	36.329	116.892	0.7	14.27	1.1	150	AC	---	1.2	FURNACE CREEK
27 2:58:29	36.708	115.687	1.3	7.76	1.7	287	BD	---	1.3	INDIAN SPRINGS NW
27 9:54: 5	36.716	115.720	0.9	9.42	1.0	280	AD	---	1.3	INDIAN SPRINGS NW
27 14:32:28	36.724	115.719	1.3	9.72	1.0	280	BD	---	1.4	INDIAN SPRINGS NW
27 23:39:33	36.705	115.731	0.6	10.63	0.7	191	BD	---	1.3	INDIAN SPRINGS NW
28 0:36:39	36.713	115.722	0.8	10.26	0.6	279	AD	---	1.3	INDIAN SPRINGS NW
28 5:58:48	37.142	117.378	0.5	8.03	1.8	173	AC	---	1.2	UBEHEBE CRATER
28 18:42: 5	36.715	115.739	0.3	11.22	1.0	117	AB	---	1.7	INDIAN SPRINGS NW
28 18:43:47	36.681	115.720	2.3	11.16	1.0	329	BD	---	1.0	INDIAN SPRINGS NW
28 19:25: 1	37.199	117.914	1.8	4.72*	---	254	CD	---	1.1	WAUCOBA SPRING
28 19:29: 2	36.712	115.733	0.7	10.23	0.6	295	AD	---	1.1	INDIAN SPRINGS NW
29 20: 5:58	36.747	115.853	0.8	9.40	1.1	188	AD	---	1.4	MERCURY NE
30 5: 4: 1	37.363	115.672	0.5	8.74	1.0	185	AC	---	1.2	GROOM LAKE
30 5:44:30	36.703	116.432	0.3	1.04	1.2	205	AD	---	0.9	LATHROP WELLS NW
30 17:19:33	36.308	114.885	2.4	-0.79	1.6	265	BD	---	2.1	DRY LAKE
DEC 1 12:45: 2	36.716	115.720	0.7	10.59	0.7	280	AD	---	1.2	INDIAN SPRINGS NW
2 8:14:27	37.082	116.200	0.7	5.50	3.1	250	BD	---	1.1	TIPPIPAH SPRING
2 9:44: 7	37.165	117.338	0.5	7.77	2.1	159	BC	---	0.7	UBEHEBE CRATER
2 21:47:46	36.935	115.884	0.9	6.30	1.3	330	AD	---	1.0	PLUTONIUM VALLEY
4 0:38:13	36.681	115.735	4.4	24.00*	---	74	DA	1.7	---	INDIAN SPRINGS NW
5 4:48:19	37.272	117.581	0.4	8.75	0.7	71	AA	---	2.0	MAGRUDER MTN
5 10:52:35	36.705	115.725	0.6	11.03	0.7	219	AD	---	1.5	INDIAN SPRINGS NW
7 18:46:21	36.728	118.140	0.7	1.54*	---	128	CC	---	0.9	SPECTER RANGE NW
9 2:40: 6	36.779	116.255	0.5	-0.36	0.7	157	AC	---	0.8	JACKASS FLATS
11 4: 9:30	36.662	116.078	0.3	-0.51	0.5	95	AC	1.8	1.8	CAMP DESERT ROCK
11 6:14:48	36.715	115.729	0.3	10.96	0.6	172	AC	---	1.6	INDIAN SPRINGS NW
12 4:43:47	36.665	116.062	0.8	7.04	2.4	105	BB	---	1.1	CAMP DESERT ROCK
12 12:23:23	37.048	117.119	0.9	7.18	0.5	202	AD	---	1.1	BONNIE CLAIRE SE
12 19: 3:59	37.120	115.281	0.6	8.72	0.8	241	AD	---	1.4	DESERT HILLS SE
12 23:42:50	37.256	117.882	1.6	4.93	6.7	241	CD	---	1.1	SOLDIER PASS
13 0:52:21	37.029	116.237	4.0	0.90	3.2	304	CD	---	0.8	TIPPIPAH SPRING
13 1:40:57	37.003	116.220	1.7	5.36	1.7	298	BD	---	0.9	TIPPIPAH SPRING
13 6:31:22	37.211	116.251	9.1	23.70*	---	317	DD	---	1.1	AMMONIA TANKS
14 18:40:46	37.603	115.748	---	38.53	---	195	AD	---	1.5	TEMPIUTE MTN
15 21:54:39	37.711	115.011	1.3	0.58	2.3	131	BB	---	1.0	HIKO NE
17 21:32:30	37.379	117.725	2.6	15.00	1.1	187	CD	---	1.0	MAGRUDER MTN
18 4:23:20	35.982	116.860	0.3	9.32	0.4	166	AC	---	0.8	WINGATE WASH
18 14:17:18	37.325	114.829	0.8	0.26	0.7	220	BD	---	1.8	GREGERSON BASIN

# 1983 LOCAL HYPOCENTER SUMMARY

DATE - TIME (UTC)	LATITUDE (DEG. N)	LONGITUDE (DEG. W)	HORIZ ERROR (KM)	DEPTH (KM)	VERT ERROR (KM)	AZI GAP (DEG)	QUAL	Md	Mbiq	QUADRANGLE
DEC 20 0:14:6	36.663	116.040	1.4	9.73	2.1	118	BB	0.8	0.5	CAMP DESERT ROCK
20 12:44:51	37.363	116.285	0.9	11.20	3.8	295	BD	---	1.0	DEAD HORSE FLAT
20 23:28:32	37.574	117.028	0.5	5.82	2.5	217	BD	---	1.0	GOLDFIELD
21 10:23:4	36.950	117.618	1.0	7.99	2.5	217	BD	---	1.1	DRY MTN
21 22:58:47	36.694	115.724	1.6	11.49	0.9	326	BD	---	1.3	INDIAN SPRINGS NW
21 22:58:55	36.689	115.721	1.4	11.22	0.7	327	BD	---	1.1	INDIAN SPRINGS NW
22 1:56:47	36.685	115.707	1.3	10.83	0.9	303	BD	---	1.1	INDIAN SPRINGS NW
22 16:39:22	36.926	116.518	---	34.478L	---	237	BD	---	1.6	OBARE MTN
22 17:40:57	36.990	116.454	0.8	6.42	1.3	207	AD	---	0.8	TOPOPAH SPRING NW
22 21:10:56	36.691	116.212	1.7	0.68	1.7	233	BD	---	0.7	SPECTER RANGE NW
23 5:12:7	37.368	114.420	0.9	2.18	---	299	DD	---	1.6	***REGIONAL***
23 23:43:35	37.427	116.913	0.4	0.84	0.5	121	AC	---	1.5	TOLICHA PEAK
24 6:9:56	36.989	117.547	0.8	1.56	2.4	178	BC	---	1.5	DRY MTN
24 6:27:4	36.345	116.435	3.5	0.34	2.6	301	CD	---	1.6	TYBO
24 10:8:6	36.464	116.186	0.8	0.84	0.9	216	AD	---	1.1	AMARGOSA FLAT
25 10:29:15	36.986	117.567	0.6	5.40	4.9	183	BD	---	1.4	DRY MTN
26 8:38:47	36.988	117.570	0.6	4.33	7.5	201	CD	---	1.4	DRY MTN
26 10:8:27	36.986	117.578	0.7	2.94	3.2	204	BD	---	1.6	DRY MTN
26 10:3:12	37.012	117.561	1.2	2.05	4.6	236	BD	---	1.1	LAST CHANCE RANGE
26 19:56:32	37.188	117.861	0.4	3.17	---	215	CD	---	1.8	WAUCOBA SPRING
26 22:20:35	37.188	117.838	1.2	1.36	2.6	230	BD	---	1.3	WAUCOBA SPRING
27 18:39:25	37.428	117.098	0.3	6.43	2.2	92	BC	---	1.4	SCOTTYS JUNCTION NE
29 3:23:52	35.819	117.332	1.3	3.22	---	291	CD	---	1.7	TRONA
30 2:36:15	37.247	116.682	0.6	11.23	1.8	129	AB	---	1.4	THIRSTY CANYON NW
30 20:26:36	36.769	116.099	0.8	5.56	1.8	166	AC	---	0.8	CANE SPRING
30 23:34:30	36.507	116.387	1.2	0.81	0.8	276	BD	---	1.0	LATHROP WELLS SW
30 23:55:10	37.423	117.011	0.3	2.02	2.2	132	BC	---	0.9	SCOTTYS JUNCTION NE
31 14:52:00	36.708	115.920	0.4	9.63	1.2	147	AC	---	1.3	FRENCHMAN FLAT

## APPENDIX E

### 1982-1983 Focal mechanisms with table summarizing mechanisms computed 1979-1983

The fault plane solutions of Appendix E were obtained by selecting the best-fitting solution(s) from the application of the computer program "FOCMEC" (Snoke and others, 1984) to the ray data generated by HYPO71, and in some instances, to amplitude data. We plot data on the lower focal hemisphere using the equal-area projection (Lee and Stewart, 1979). The symbols represent first-motion *P*-polarities, and their positions represent the points where the HYPO71-determined raypaths intersect the focal hemisphere. The darkened circles represent impulsive compressional arrivals, the + symbols represent emergent compressional, the open circles represent impulsive dilatational, the - symbols represent emergent dilatational, and the × symbols represent indeterminate or nodal readings. In the following figures the *P* and *T* symbols represent the pressure and tension axes, respectively. The *X* and *Y* symbols represent slip vectors for each nodal plane, and *B* is the null axis. Primed symbols are the respective vectors for alternate (dashed) solutions when they are presented. Some mechanisms are composited using data from several events that are clustered in time and space. Composite solutions are noted in each figure.

For several mechanisms, the information contained in *P*-wave polarities was not adequate to effectively constrain the nodal planes. In these instances, first motion *P*- and *SV*- amplitude data were gathered at selected stations, indicated by a large  $\square$  symbol around the polarity symbol. The observed and theoretical  $\log_{10}(SV/P)_z$  ratios and the difference between the logarithms of observed and theoretical ratios are computed for hundreds of potential solutions whose nodal planes conform to *P*-wave first-motion polarities. The theoretical values shown in each figure are for the "optimum" solution shown, having the lowest rms error and fewest polarity inconsistencies. If the difference between observed and theoretical values is greater than a specified limit,  $err_{max}$ , that station's amplitude data are not used in the solution and an asterisk is placed by its name in the solution table. We always set  $err_{max} \leq 0.3$ , corresponding to a maximum factor between theoretical and observed amplitude ratios of 2.0.

We reiterate here that the use of amplitude ratios obtained from vertical-component seismograph records is a procedure that is fraught with difficulties, especially that of correctly identifying the *S*-wave onset. A second difficulty is that observed *P*-wavelet amplitudes for raypaths approximately parallel to a nodal plane are rarely as weak or "nodal" as is suggested by simple radiation pattern theory (for example, see Figure E13). One possible explanation of the larger-than-expected *P*-wave amplitudes near nodal planes is that near-source heterogeneity may be significant, resulting in a smearing or averaging of compressional energy that heavily samples the fault zone (thus increasing nodal and near-nodal *P*-amplitudes and decreasing slightly less nodal *P*-amplitudes). Those mechanisms which rely on amplitude ratio information to constrain nodal plane locations are identified in the captions.

# Southern Great Basin Focal Mechanisms 1979-1983

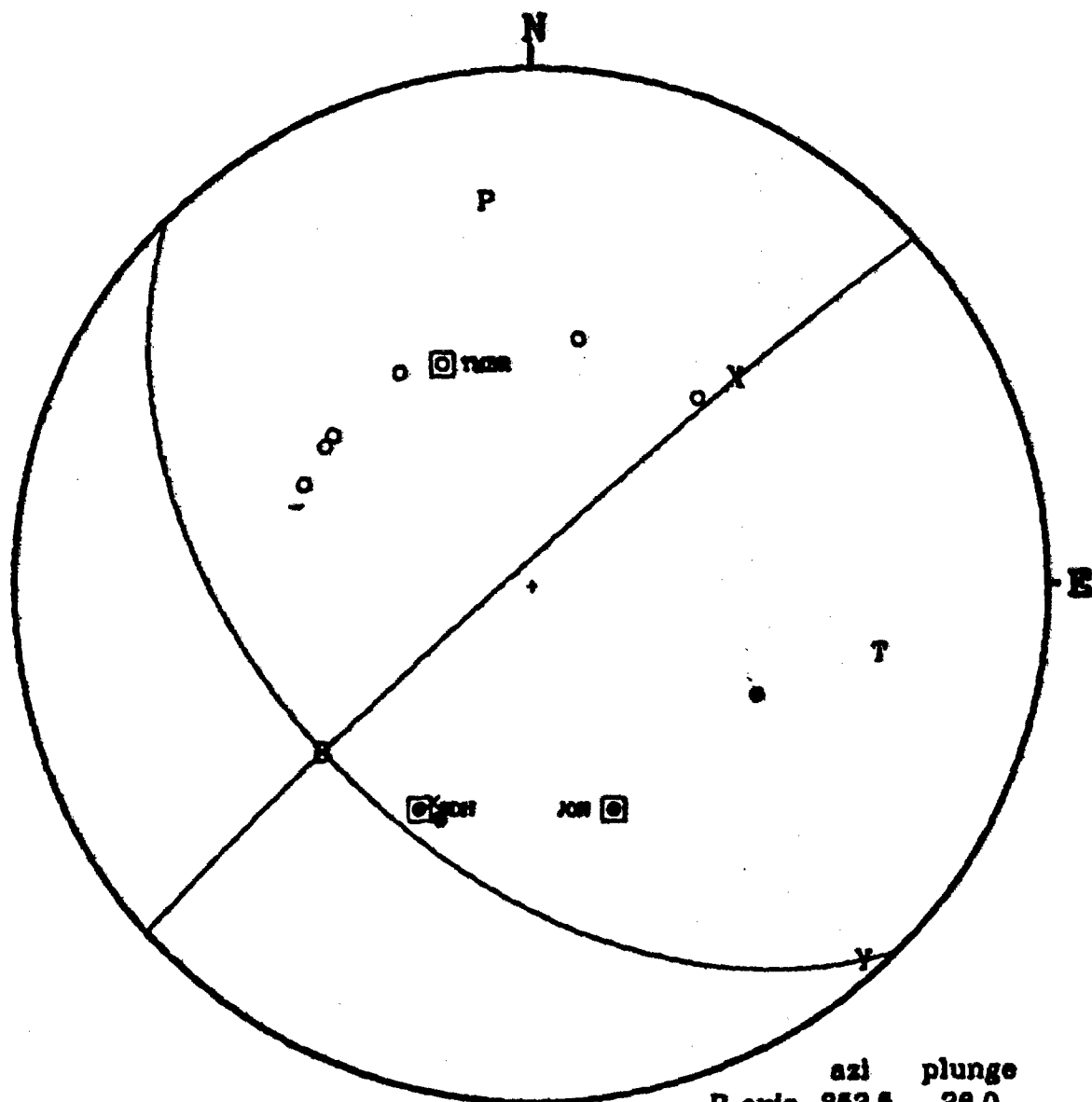
St, strike of nodal plane; Dp, dip of nodal plane; Rk, rake of slip vector; Tr, trend of axis; Pl, plunge of axis. ML, local (SGB) magnitude; Other, D=coda duration magnitude calibrated against ML(SGB); Tsm, type of source mechanism: 1, single event focal mechanism; 2, composite focal mechanism. Nodal planes: \*, designates inferred fault plane. Rmk: Remarks, designated by \*, means that (SV/P)  $\pm$  amplitude ratios were used to constrain or help determine the focal mechanism. Ref, Reference: 1, Rogers and others (1983).

## Southern Great Basin Focal Mechanisms 1979-1981

Cata- log/ Index	Origin time (UTC)		North latitude	West longitude	Focal depth (km)	mb	MS	Magnitude		Moment (dyne-cm)	T s	Nodal planes						Principal axes						R m
	Date	Time						ML	Oth			1st			2nd			P		T		B		
												St	Dp	Rk	St	Dp	Rk	Tr	Pl	Tr	Pl	Tr	Pl	
1	1979-08-13	1823:38	37.238	116.029	7.6	...	...	...	2.7D	.....	2	355	80	-177°	264	87	-10	219	9	310	5	68	80	1
2	1981-12-28	2246:42	37.222	114.928	5.2	...	...	...	2.1D	.....	1	339	54	-172	244	84	-37°	195	30	297	20	57	53	1
3	1981-12-26	1729:44	36.725	115.708	8.6	...	...	...	1.7D	.....	2	80	90	0	170	90	180°	35	0	125	0	0	90	1
4	1979-08-17	1453:07	37.185	116.570	6.2	...	...	...	1.9D	.....	2	266	79	-6	357	84	-169°	222	12	131	4	25	78	1
5	1980-04-02	1820:41	36.860	115.961	1.3	...	...	...	2.2D	.....	1	248	70	-20	345	71	-159	207	28	116	1	25	62	1
6	1980-04-23	0408:40	36.874	116.162	6.6	...	...	...	1.3D	.....	1	92	80	-10	184	80	-170	48	14	318	0	227	76	1
7	1980-05-10	1103:33	36.811	116.267	0.8	...	...	...	1.2D	.....	1	269	70	0	359	90	-160	226	14	132	14	359	70	1
8	1981-01-23	0441:12	37.148	117.387	10.2	...	...	...	2.7D	.....	1	166	68	-169	72	80	-22°	27	23	121	8	227	66	1
9	1979-12-25	1417:12	37.288	117.062	8.0	...	...	...	2.8D	.....	1	88	74	3	357	87	-164°	44	9	312	13	167	74	1
10	1981-03-10	2327:56	37.155	116.917	6.5	...	...	...	2.2D	.....	1	89	80	0	179	90	-170°	44	7	314	7	179	80	1
11	1981-10-15	0421:09	37.055	116.955	9.2	...	...	...	2.5D	.....	2	188	90	180°	98	90	0	53	0	143	0	0	90	1

## Southern Great Basin Focal Mechanisms 1982-1983

Cata- log/ Index	Origin time (UTC)		North latitude	West longitude	Focal depth (km)	mb	MS	Magnitude		Moment (dyne-cm)	s	Nodal planes						Principal axes						R m	
	Date	Time						ML	Oth			1st			2nd			P		T		B			
												St	Dp	Rk	St	Dp	Rk	Tr	Pl	Tr	Pl	Tr	Pl		Ref
1	1983-09-08	1720:16	36.777	116.254	0.83	...	...	1.6	...	.....	1	135	47	175	228	87	43°	354	26	101	32	232	47	....	•
2	1983-12-11	0409:30	36.662	116.078	-0.51	...	...	1.8	1.8D	.....	1	341	71	-7	249	83	-161°	204	18	296	8	50	70	....	•
3	1983-01-02	0757:58	36.502	116.586	0.05	...	...	1.4	...	.....	2	265	70	-177	356	87	-20°	222	16	129	12	4	70	....	•
4	1983-01-02	1632:20	36.502	116.569	5.47	...	...	2.6	...	.....	2	91	60	3	359	87	150°	49	19	310	23	175	60	....	•
5	1983-01-03	1739:44	36.500	116.568	4.77	...	...	2.4	...	.....	2	129	52	-12	32	80	-141°	343	34	86	19	200	50	....	•
6	1982-04-09	0521:18	36.653	116.402	8.03	...	...	1.4	1.5D	.....	1	84	45	0	174	90	-45	49	30	299	30	174	45	....	•
7	1983-05-30	1722:09	36.688	116.270	6.05	...	...	1.5	...	.....	1	71	71	7°	339	83	161	26	8	294	18	140	70	....	•
8	1983-05-28	1728:38	36.996	116.414	7.99	...	...	1.9	...	.....	1	5	62	-5°	273	85	-152	226	23	322	16	140	70	....	•
9	1983-02-17	0143:05	37.181	116.592	5.97	...	...	1.5	...	.....	2	32	42	-113°	183	52	-71	34	74	286	5	195	15	....	•
10	1983-02-24	1739:22	37.184	116.590	4.21	...	...	1.4	...	.....	2	30	46	-104°	190	46	-76	20	80	290	0	200	10	....	•
11	1982-06-02	1734:54	37.074	116.947	1.54	...	...	1.5	...	.....	2	178	63	-14	82	78	-152°	37	28	133	10	240	60	....	•
12	1982-08-31	2006:27	37.066	116.948	4.91	...	...	1.3	1.5D	.....	1	200	82	174°	291	84	8	65	2	155	10	324	80	....	•
13	1982-08-31	2056:36	37.061	116.947	5.19	...	...	2.4	1.9D	.....	1	34	49	-24°	288	72	-137	242	43	346	14	90	44	....	•
14	1982-01-19	2344:43	37.151	116.940	6.39	...	...	2.3	2.1D	.....	2	88	76	-179	178	89	-14°	44	11	312	9	90	44	....	•
15	1983-11-10	1037:15	37.426	117.098	6.01	...	...	2.0	1.9D	.....	2	48	35	-138	175	68	-63	47	58	285	18	186	26	....	•
16	1983-11-10	1317:33	37.425	117.097	7.33	...	...	1.5	1.7D	.....	1	274	62	-22°	15	71	210	237	34	143	6	45	55	....	•
17	1983-10-01	1032:54	37.353	117.280	6.07	...	...	2.6	2.4D	.....	2	46	45	-135°	171	60	-155	29	59	285	9	190	30	....	•
18	1983-11-28	1842:05	36.715	115.739	11.22	...	...	1.7	...	.....	2	13	71	175°	105	85	19	237	10	331	17	118	70	....	•
19	1982-07-06	0210:43	37.698	115.037	2.56	...	...	...	3.1D	.....	1	177	69	-167	83	78	-22	39	24	131	6	235	65	....	•



# JACKASS FLATS

DATE/TIME: 830908 17 20 16.09

LAT: 36.777 LONG: 116.254

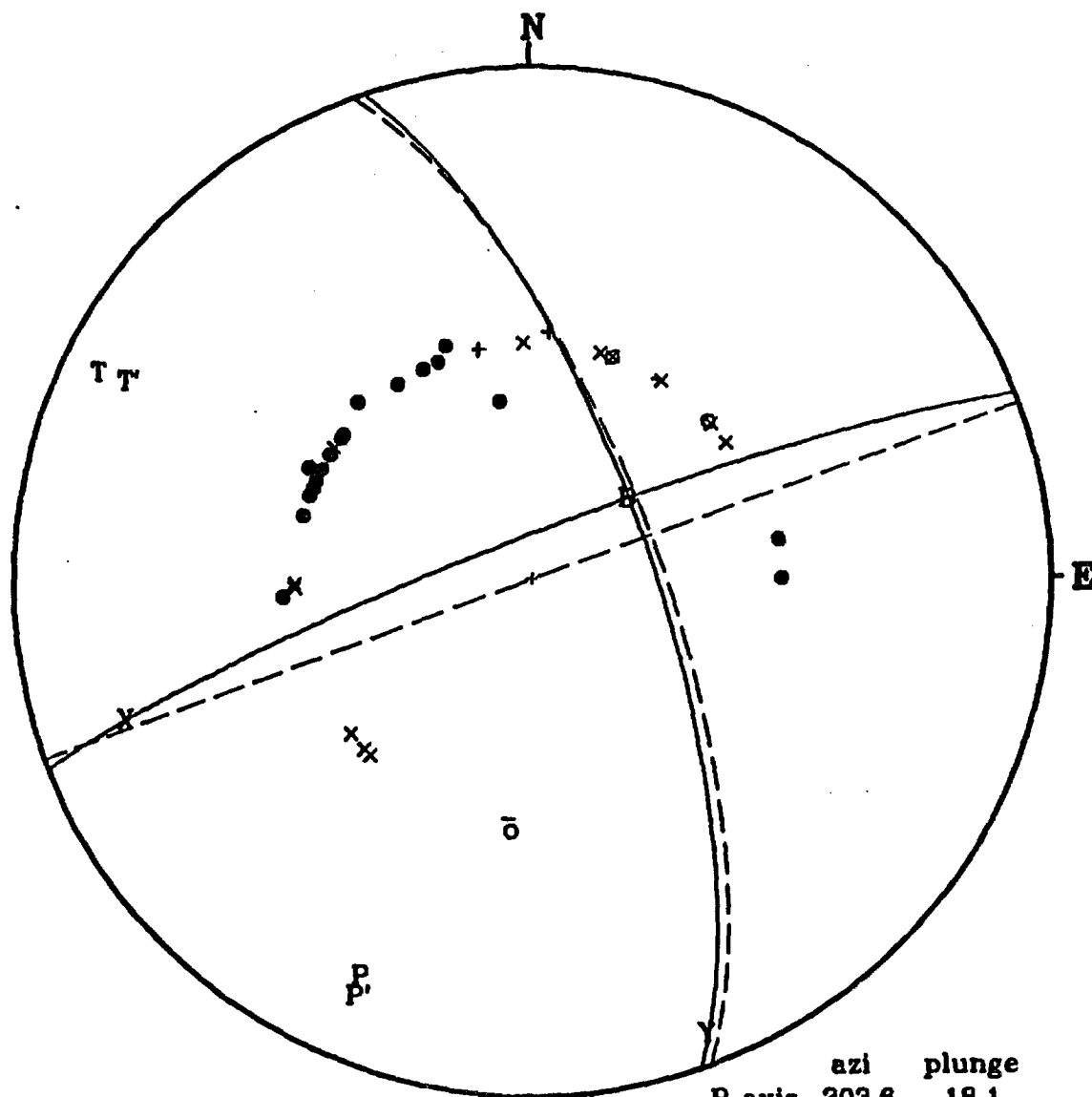
DEPTH, km: 0.83 +/- 0.4 ML: 1.6

	azi	plunge
P axis	353.5	26.0
T axis	100.9	31.5
B axis	232.0	47.0
X axis	45.2	42.8
Y axis	138.3	3.4

Observed	Theoretical	Difference	Station
1.4828	1.4963	-0.0135	GDH
0.3479	0.4729	-0.1250	THOR
0.3188	0.2946	0.0242	JON

The rms error is 0.073

Figure E1. This focal mechanism is not well-constrained without the the  $(SV/P)_s$  amplitude ratio data shown. Because 830908 17:20 is a very shallow-focus earthquake, the phase arrivals shown are probably refractions. No path corrections for potentially different SV-to-P attenuation along refractor interfaces have been applied, adding to the uncertainty of this solution.

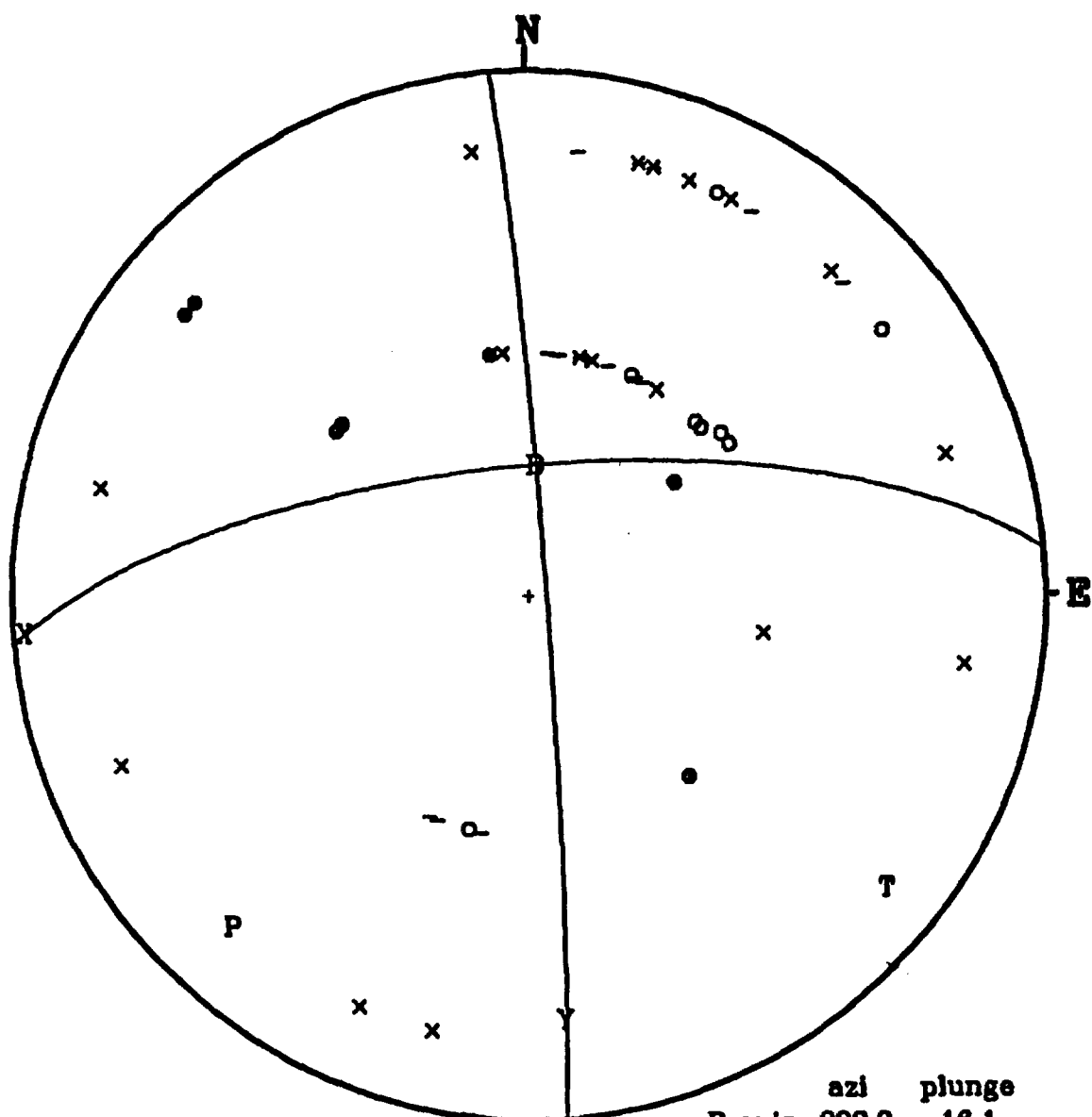


CAMP DESERT ROCK  
 DATE/TIME: 831211 4 9 30.36  
 LAT: 36.662 LONG: 116.078  
 DEPTH, km: -0.51 +/- 0.5 ML: 1.8

	azi	plunge
P axis	203.6	18.1
T axis	296.3	8.3
B axis	50.0	70.0
X axis	251.2	18.7
Y axis	158.9	6.7

Dashed Solution	Azi	Plunge
P axis	203.22	14.00
T axis	296.78	14.00
B axis	70.00	70.00
X axis	250.00	20.00
Y axis	160.00	0.00

Figure E2. Only first motion P-polarities were used for this mechanism. The *dashed-line* nodal planes represent an equally suitable solution.

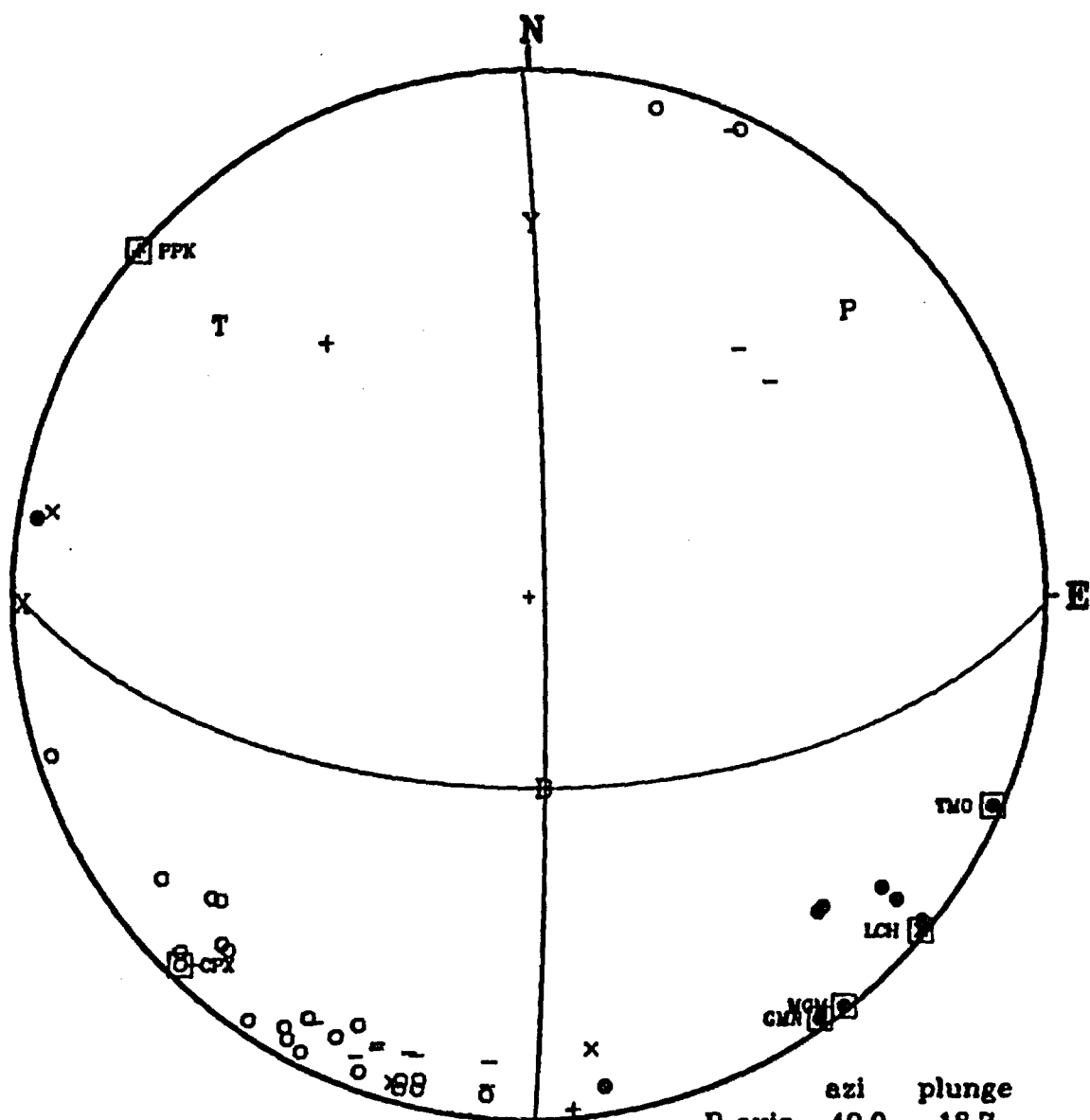


BIG DUNE  
 DATE/TIME: 830102 7 57 58.38  
 LAT: 36.502 LONG: 116.586  
 DEPTH, km: 0.05 +/- 0.5 ML: 1.4  
 COMPOSITE WITH 830108 14 54 10.06  
 830102 5 16 39.45

	azi	plunge
P axis	222.3	16.1
T axis	128.8	12.0
B axis	3.7	69.8
X axis	266.0	2.8
Y axis	175.0	20.0

Figure E3. This focal mechanism uses data from several shallow Funeral Mountains earthquakes.





BIG DUNE

DATE/TIME: 830102 18 32 20.19

LAT: 36.502 LONG: 116.569

DEPTH, km: 5.47 +/- 1.7 ML: 2.6

COMPOSITE WITH 830101 21 47 54.87

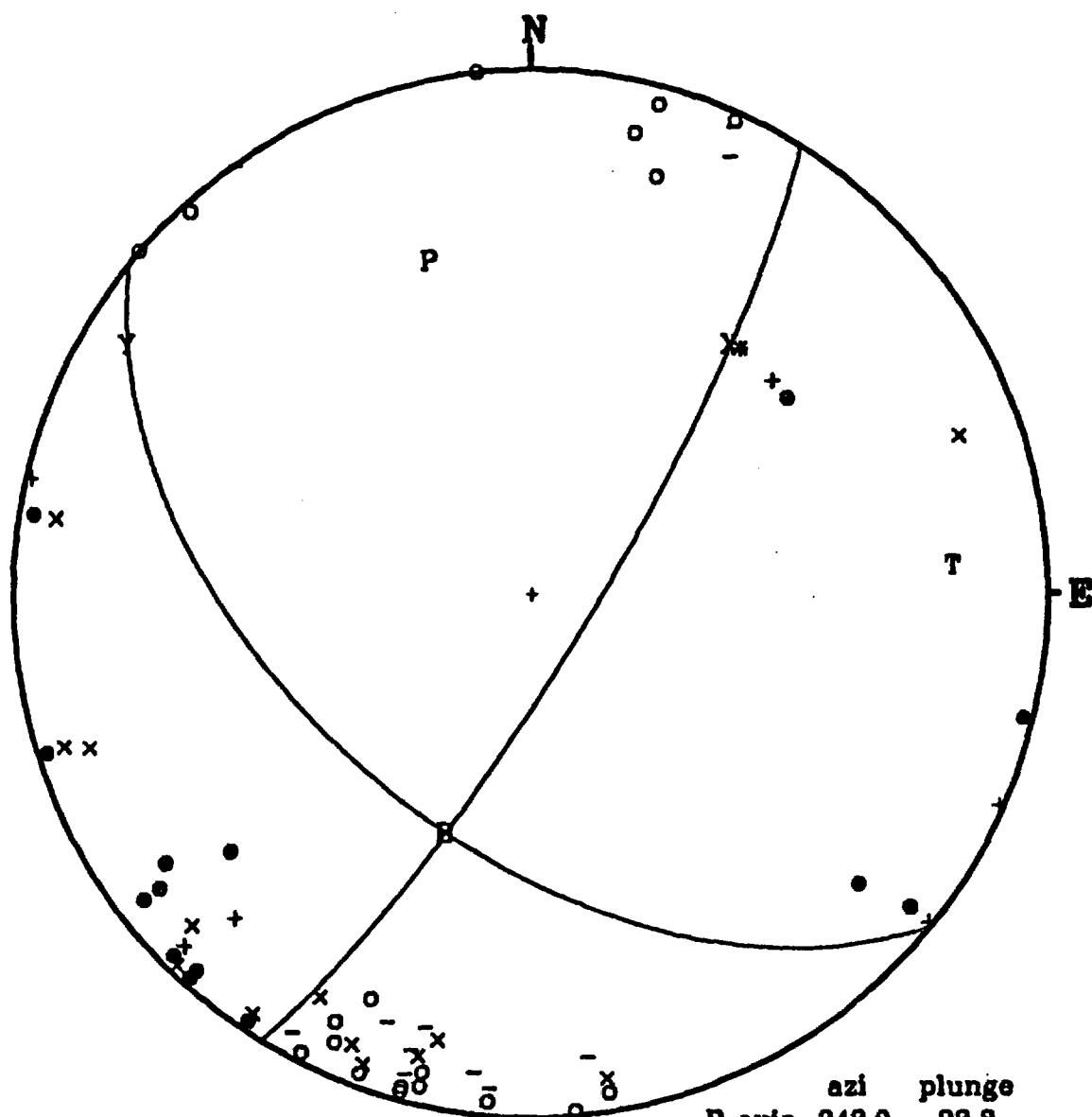
830102 00 38 26.86 830102 00 46 26.55

	azi	plunge
P axis	49.0	18.7
T axis	310.9	22.5
B axis	175.0	60.0
X axis	269.3	2.5
Y axis	0.8	29.9

Observed	Theoretical	Difference	Station
0.3724	0.3362	0.0362	CPX
0.4414	0.6165	-0.1751	TMO
0.2860	0.3396	-0.0536	GMM
0.6760	0.4047	0.2713	LCH
0.9490	0.3292	0.6198	MGM
0.4160	0.3747	0.0413	PPK

The average (rms) ratio error = .148

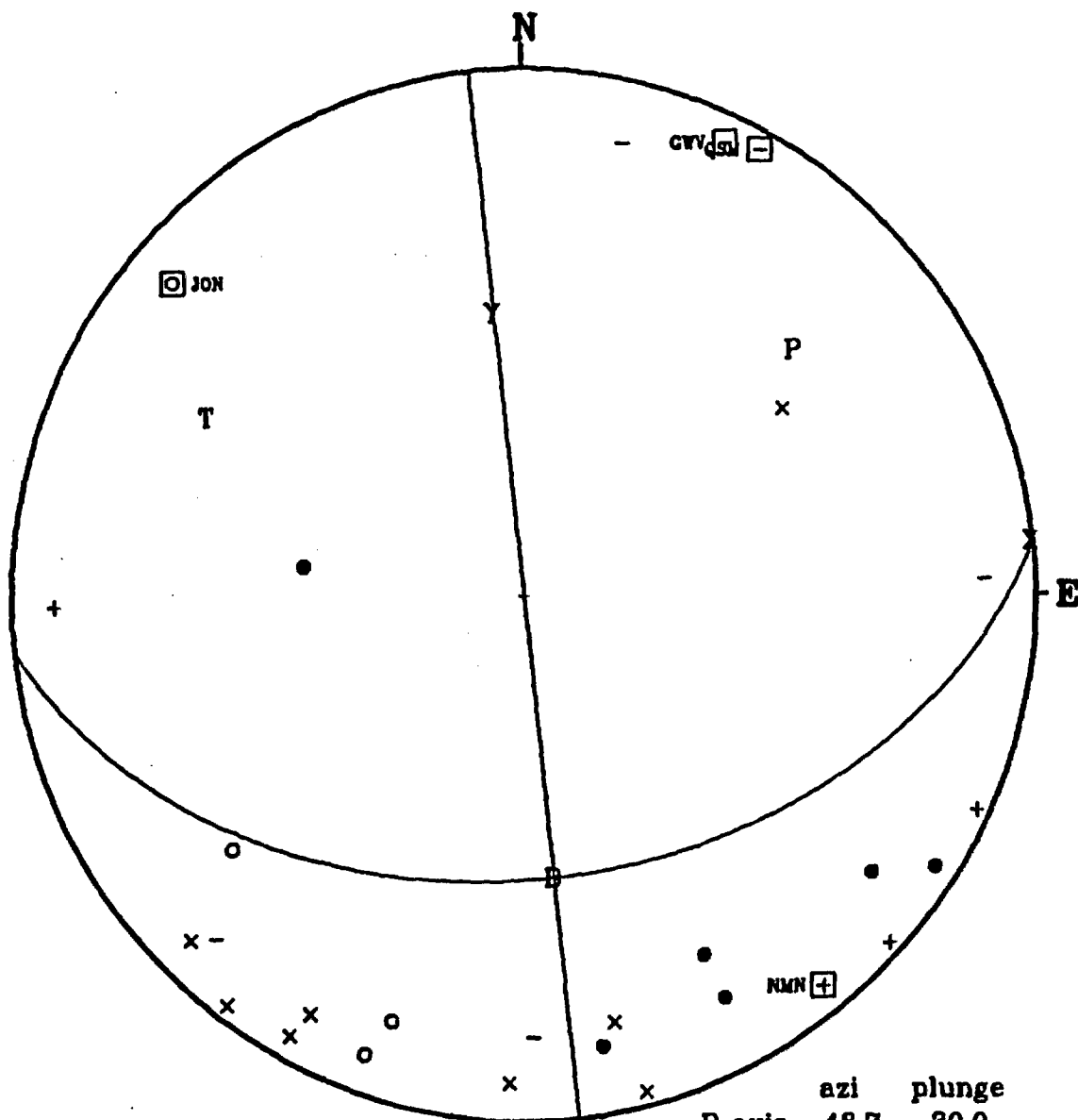
Figure E4. This focal mechanism uses amplitude ratio data from one of the component Funeral Mountains earthquakes.



	azi	plunge
P axis	343.0	33.8
T axis	86.1	18.7
B axis	200.0	50.0
X axis	39.3	38.4
Y axis	301.6	9.8

**BIG DUNE**  
 DATE/TIME: 830103 17 39 44.35  
 LAT: 36.500 LONG: 116.568  
 DEPTH, km: 4.77 +/- 1.4 ML: 2.4  
 COMPOSITE WITH 830102 19 38 35.48  
 830104 14 58 11.59 830109 23:12:28.43

Figure E5. Data from four Funeral Mountains earthquakes were used for this focal mechanism.



LATHROP WELLS NW

DATE/TIME: 820409 5 21 18.24

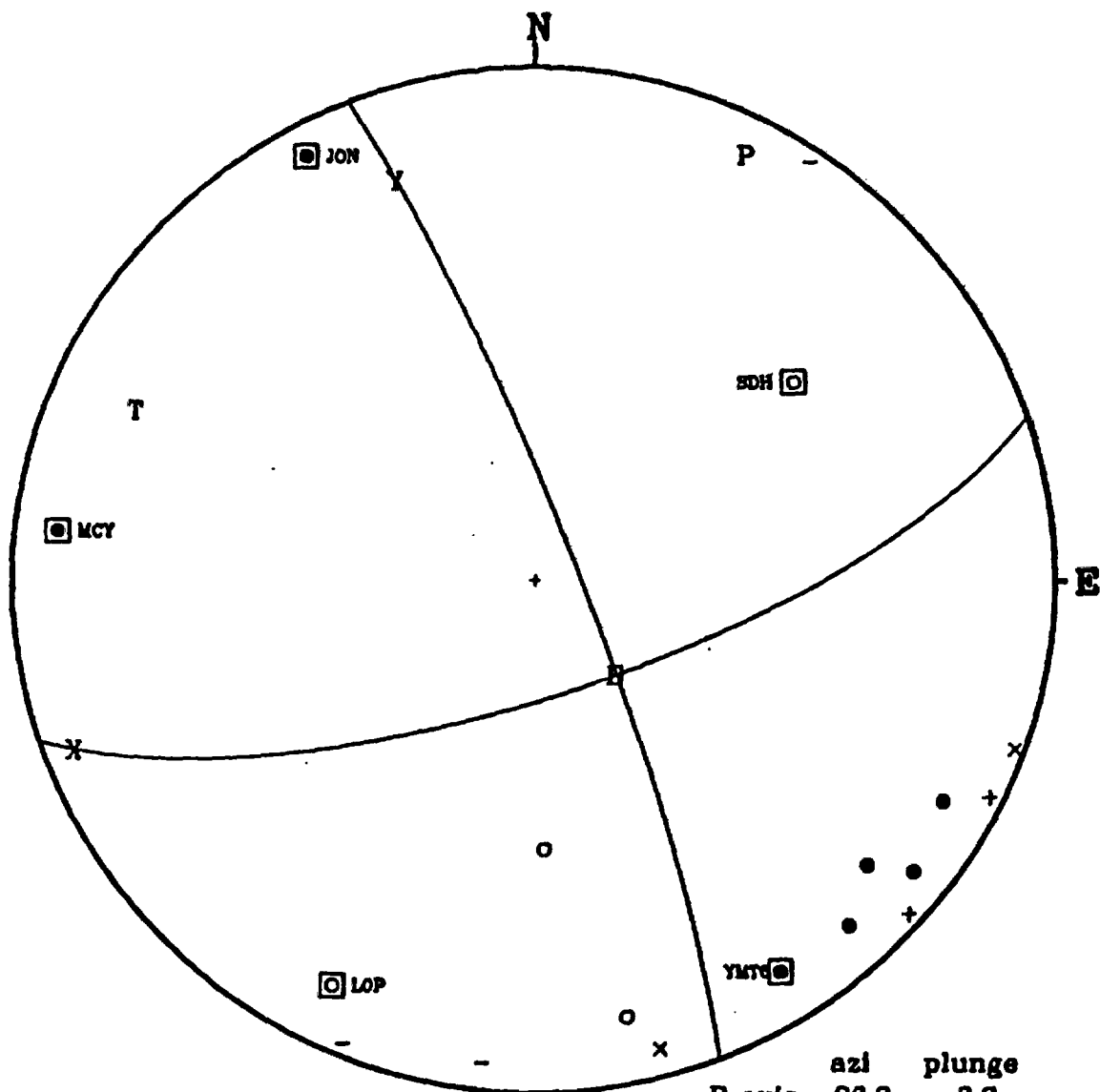
LAT: 38.653 LONG: 116.402

DEPTH, km: 8.03 +/- 0.7 ML: 1.4

	azi	plunge
P axis	48.7	30.0
T axis	299.3	30.0
B axis	174.0	45.0
X axis	84.0	0.0
Y axis	354.0	45.0

Log10(SV/P) <sub>z</sub>			Station
Observed	Theoretical	Difference	
0.4785	0.3003	0.1782	JON
0.2686	0.3175	-0.0489	GMV
0.4909	0.5989	-0.1080	NMN
0.4611	0.3883	0.0728	OSM
The average rms error = .113			

Figure E6. This focal mechanism requires the information contained in the amplitude ratios to be well-constrained.



# **STRIPED HILLS**

DATE/TIME: 830530 17 22 9.36

LAT: 36.688 LONG: 116.270

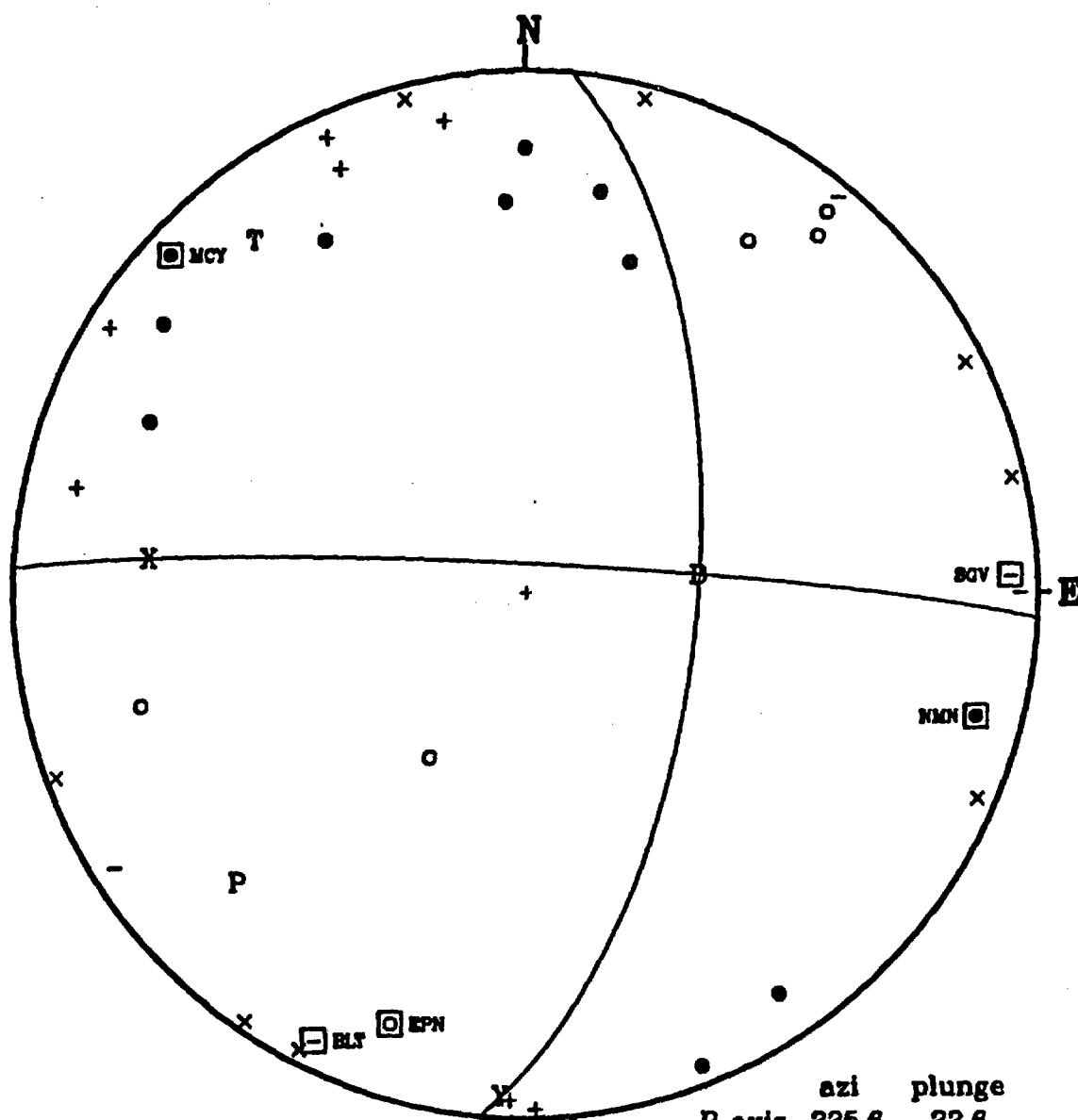
DEPTH, km: 6.05 +/- 0.5 ML: 1.5

	azi	plunge
P axis	26.3	8.3
T axis	293.6	18.1
B axis	140.0	70.0
X axis	248.9	8.7
Y axis	341.2	18.7

Log10(SV/P)z			Station
Observed	Theoretical	Difference	
0.0853	0.3059	-0.2206	SDH
0.5161	0.3350	0.1811	LOP
0.3831	0.5780	-0.1949	YMT6
0.1274	0.1388	-0.0114	MCY
0.5902	0.3890	0.2012	JON

The average (rms) ratio error = .179

Figure E7. This focal mechanism requires the information contained in the amplitude ratios to be well-constrained.



TOPOPAH SPRING NW

DATE/TIME: 830528 17 28 37.83

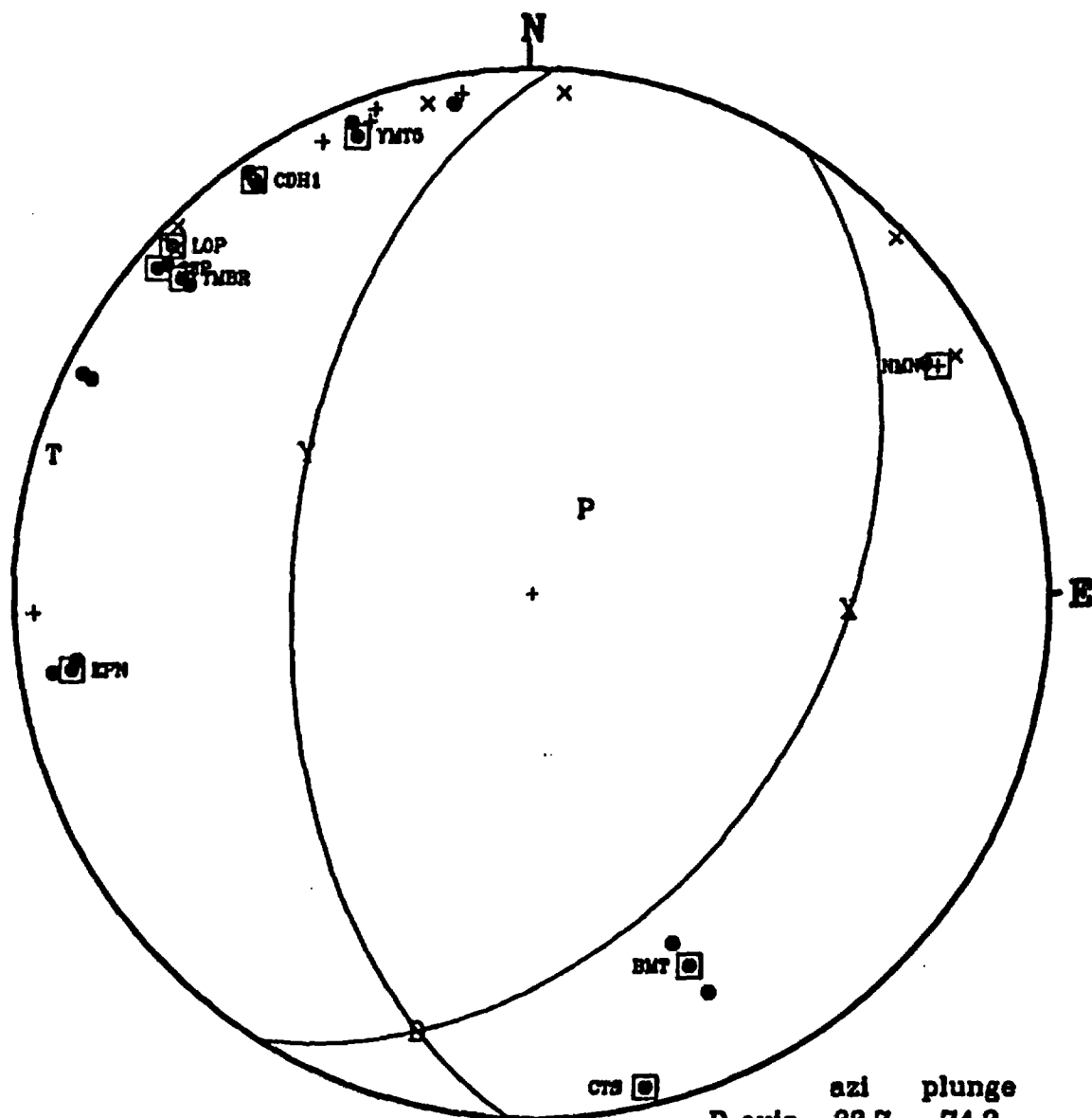
LAT: 38.996 LONG: 118.414

DEPTH, km: 7.99 +/- 0.6 ML: 1.9

	azi	plunge
P axis	225.6	22.6
T axis	322.3	15.6
B axis	84.0	62.0
X axis	275.3	27.5
Y axis	182.8	4.7

Log10(SV/P)			Station
Observed	Theoretical	Difference	
0.1485	0.4420	-0.2935	EPN
0.1899	0.1608	-0.0509	NMN
0.1568	-0.1503	0.3071	NCY
0.6511	0.6679	-0.0168	SGV
0.3522	0.4661	-0.1139	BLT
Average (rms) ratio error = 0.19			

Figure E8. This focal mechanism is for an earthquake on Dome Mountain, on the south flank of Timber Mountain. The strike and dip of the north-south plane are well-constrained on the basis of polarity data alone. The amplitude data help constrain the dip of the alternate east-west nodal plane.



# **THIRSTY CANYON NE**

DATE/TIME: 830217 1 43 4.68

LAT: 37.181 LONG: 116.592

DEPTH, km: 5.97 +/- 0.9 ML: 1.5

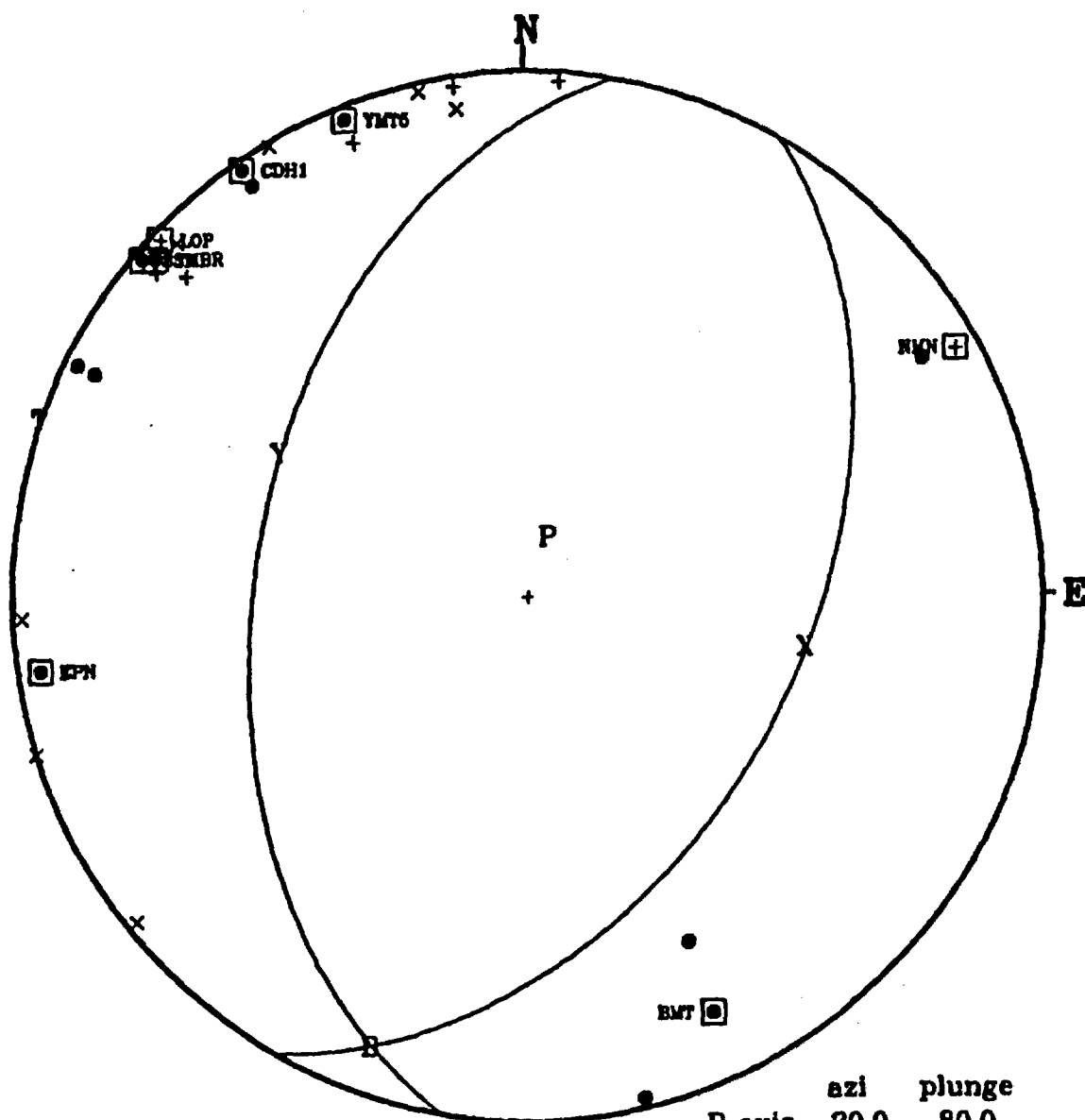
COMPOSITE WITH 830217 8 23 19.75

830217 22 8 46.10

	azi	plunge
P axis	33.7	74.2
T axis	286.3	4.8
B axis	195.0	15.0
X axis	92.7	38.4
Y axis	302.1	47.7

Log10(SV/P) <sub>z</sub>			
Observed	Theoretical	Difference	Station
0.2682	0.9625	-0.6943	BMT
2.2976	0.9797	1.3179	EPN
-0.1142	-0.2917	0.1775	TMR
0.0391	0.2289	-0.1897	YMTS
0.4653	0.6242	-0.1589	CDH1
-0.0317	0.1667	-0.1984	SSP
0.0282	-0.1748	0.2031	LOP
0.4777	-0.2300	0.7076	CTS
0.2675	0.1356	0.1319	
The average (rms) ratio error = .178			

Figure E9. Although all P-wave first-motion polarities are compressional, S-wave amplitudes are larger than P-wave amplitudes for this event, indicating that it is probably a predominantly normal-slip earthquake, not an explosion. (SV/P)<sub>z</sub> amplitude ratio data are helpful in constraining the strike and dip of nodal planes.



THIRSTY CANYON NE

DATE/TIME: 830224 17 39 22.22

LAT: 37.184 LONG: 116.590

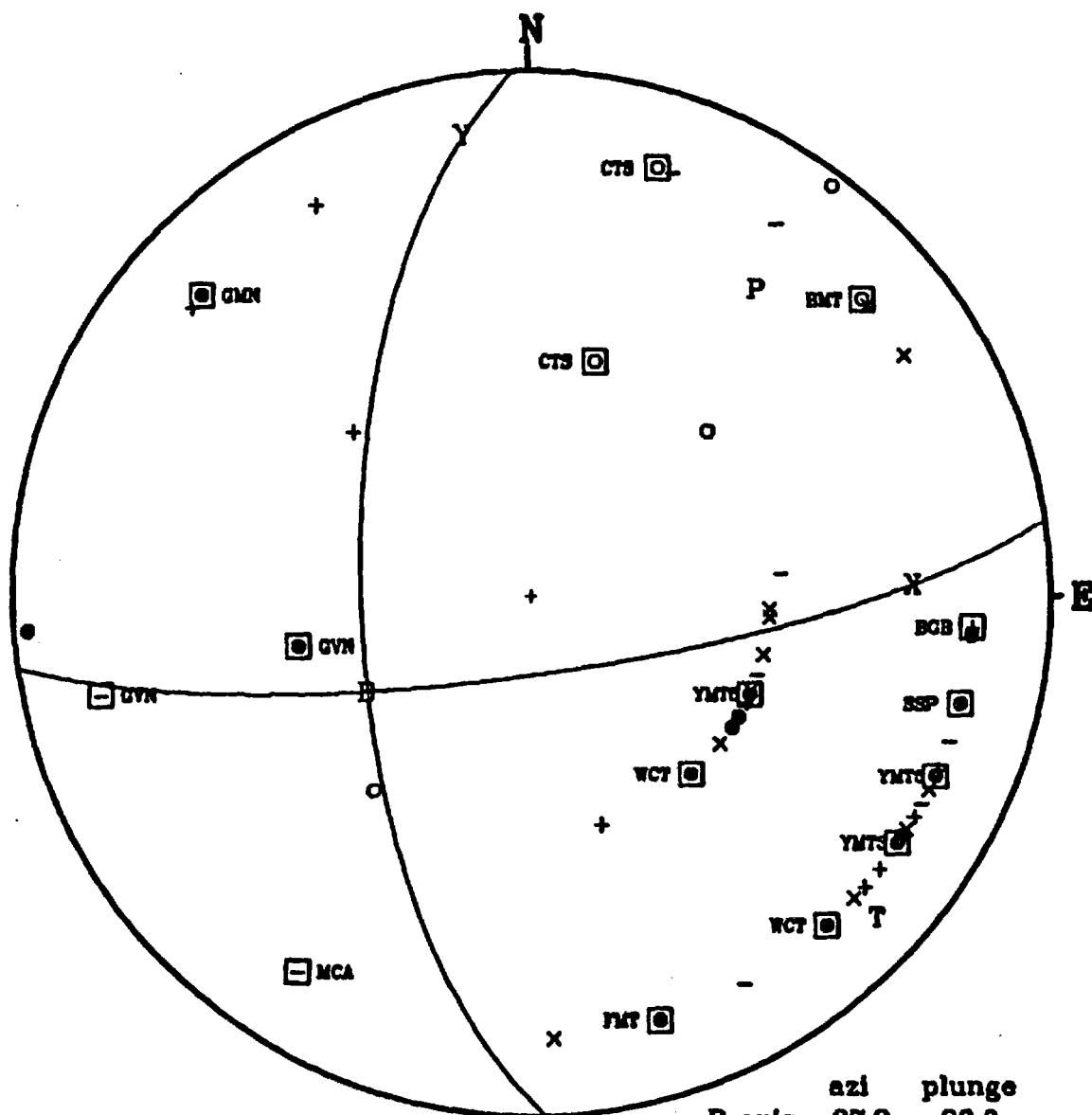
DEPTH, km: 4.21 +/- 2.4 ML: 1.4

COMPOSITE WITH 830224 10 0 39.87

	azi	plunge
P axis	20.0	80.0
T axis	290.0	0.0
B axis	200.0	10.0
X axis	100.2	44.1
Y axis	299.8	44.1

Observed	Theoretical	Difference	Station
0.4180	0.4141	0.0049	BMT
1.7547	0.5119	1.2428	EPN
-0.6131	-0.3307	-0.2824	LOP
0.1045	0.0557	0.0488	TMBR
0.6511	0.4038	0.2473	YMT5
-0.0962	0.0908	-0.1870	CDH1
-0.1345	-0.1384	0.0039	SSP
0.4714	-0.0951	0.5665	LOP
The average (rms) error = .172			

Figure E10. As in Figure E9, all P-wave first motions are compressional, and  $(SV/P)_s$  wavelet amplitude ratios are helpful in constraining the strike and dip of the nodal planes.



SPRINGDALE

DATE/TIME: 820602 17 34 53.86

LAT: 37.074 LONG: 116.947

DEPTH, km: 1.54 +/- 0.8 ML: 1.5

COMPOSITE WITH 820617 16 55 50.30

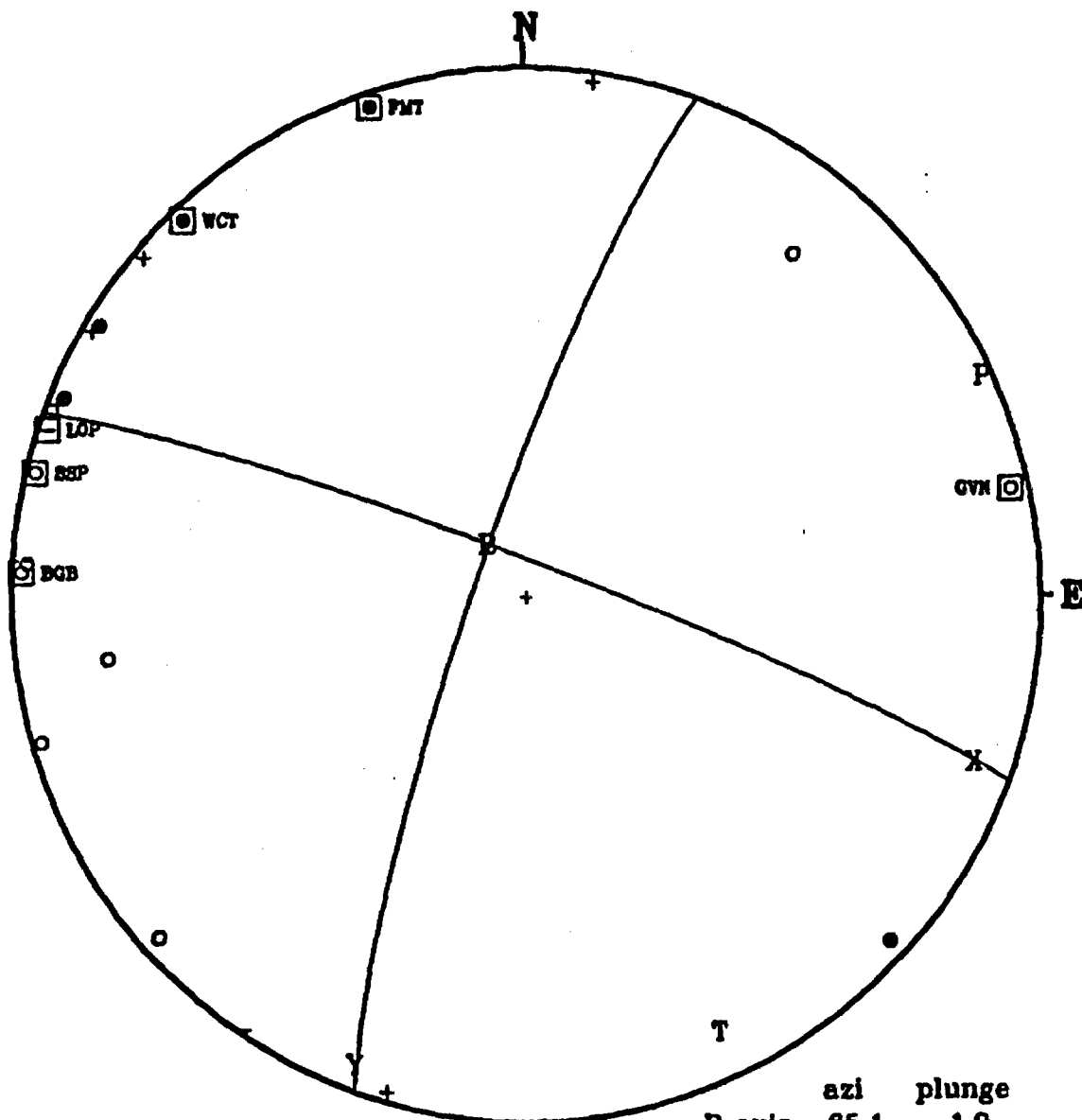
	azi	plunge
P axis	37.2	28.0
T axis	132.5	9.8
B axis	240.0	60.0
X axis	88.3	28.9
Y axis	352.0	12.2

Log10(SV/P)z		Difference	Station
Observed	Theoretical		
0.1130	0.0113	0.1017	BHT
1.3350	1.4229	-0.0879	GVN
-0.2424	0.4928	-0.7352	*GVN
-0.4416	-0.3364	-0.1052	WCT
-0.0262	0.1366	-0.1628	YMT5
0.3276	0.1112	0.2163	FNT
1.3014	0.7503	0.5512	*MCA
0.2294	-0.0172	0.2466	YMT3
0.4655	0.6266	-0.1611	BGB
0.0861	0.3145	-0.2285	SSP
0.0894	0.3262	-0.2368	CTS
0.2583	0.0812	-0.7230	*GVN
-0.2456	0.8060	-1.0516	*WCT
0.1509	0.9342	-0.8433	*YMT5
0.0423	0.2278	-0.1855	CTS

The average (rms) ratio error = .182

Figure E11. Composite of first motions and  $(SV/P)_z$  amplitude ratios are required to constrain these earthquake nodal planes. Note, however, as in Figure E1, HYPO71 modeled the arrivals as refractions, but the amplitude ratio method assumes they are direct.





SPRINGDALE

DATE/TIME: 820831 20 6 26.85

LAT: 37.088 LONG: 116.948

DEPTH, km: 4.91 +/- 1.1 ML: 1.3

	azi	plunge
P axis	65.1	1.9
T axis	155.4	9.8
B axis	324.2	80.0
X axis	109.8	8.3
Y axis	200.6	5.6

Observed	Theoretical	Difference	Station
0.8148	-0.3913	1.3062	GVN
0.0444	0.0930	-0.0485	WCT
0.0257	0.0728	-0.0471	FMT
-0.6800	-0.5594	-0.1206	BGB
0.3781	0.2143	0.1558	SSP
0.8028	0.9229	-0.1202	LOP
Average (rms) ratio error = 0.0580			

Figure E12. Fault plane strikes are better constrained than their respective dips from first motions; amplitude ratio data are helpful in constraining the dip of the nodal planes.

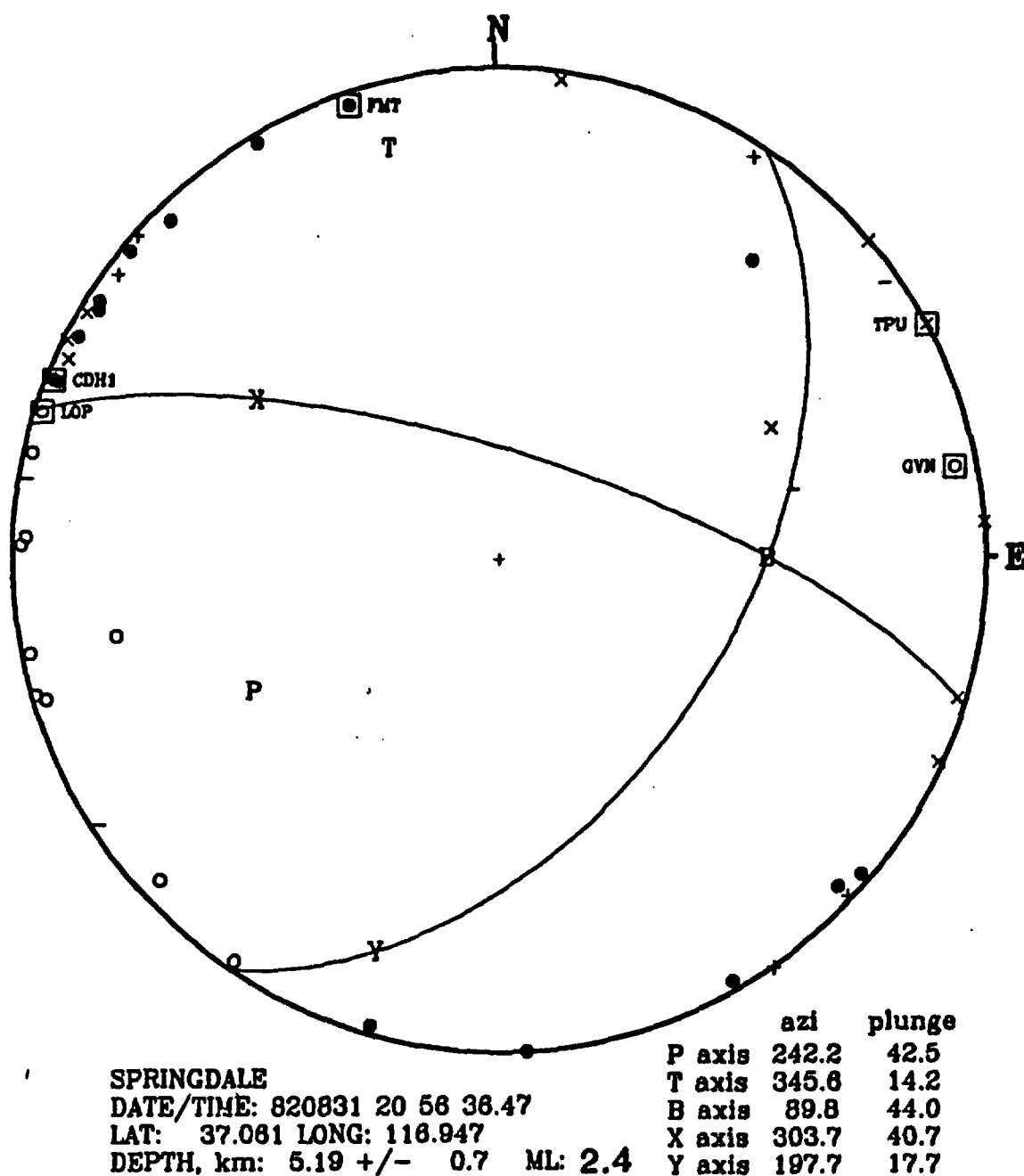


Figure E13. This focal mechanism does not require the information contained in the amplitude ratios to be well-constrained. The amplitude ratio data are included as a check on the method. The two stations that appear to have inconsistent amplitude data, CDH1 and LOP, are near a nodal plane.

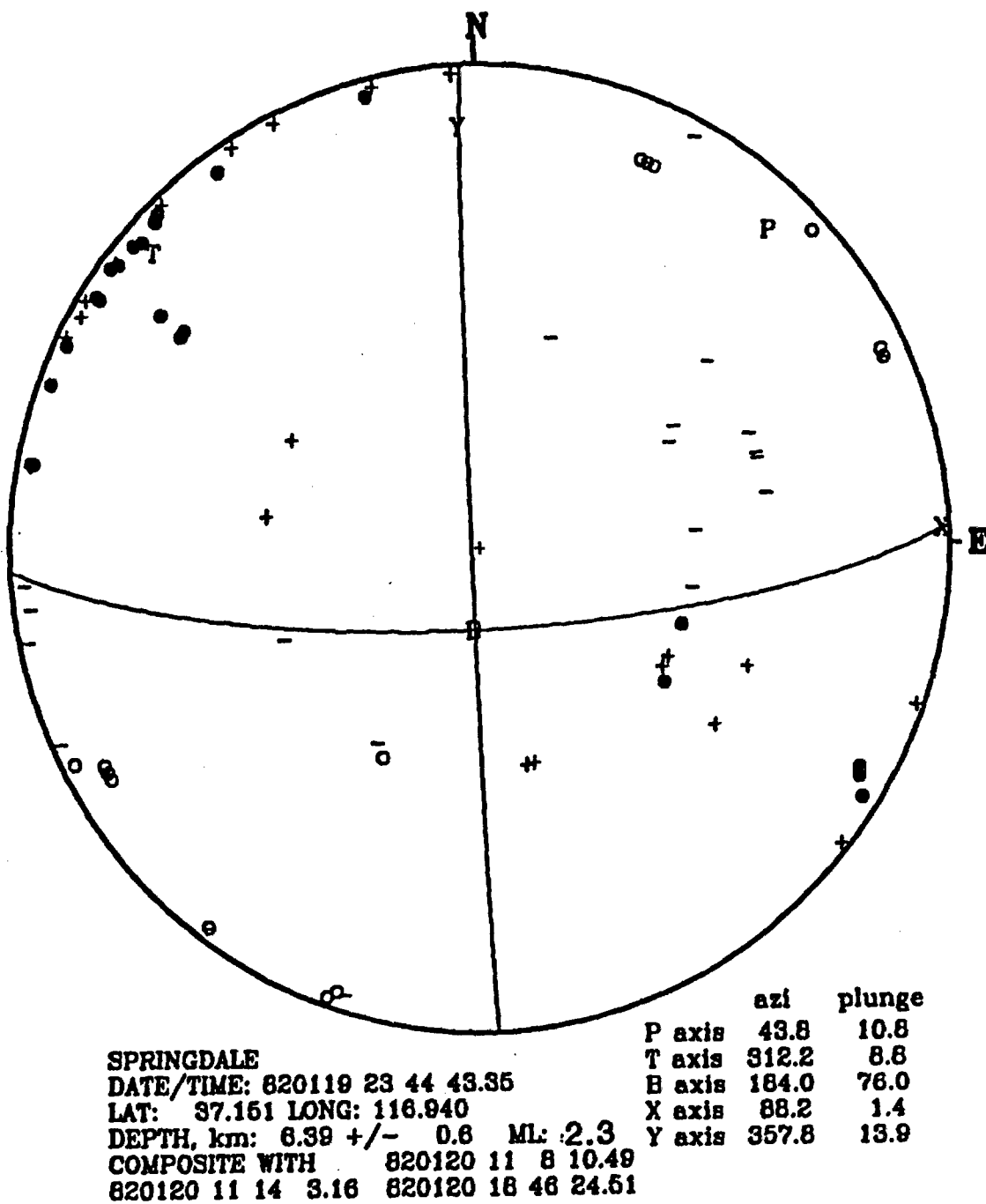
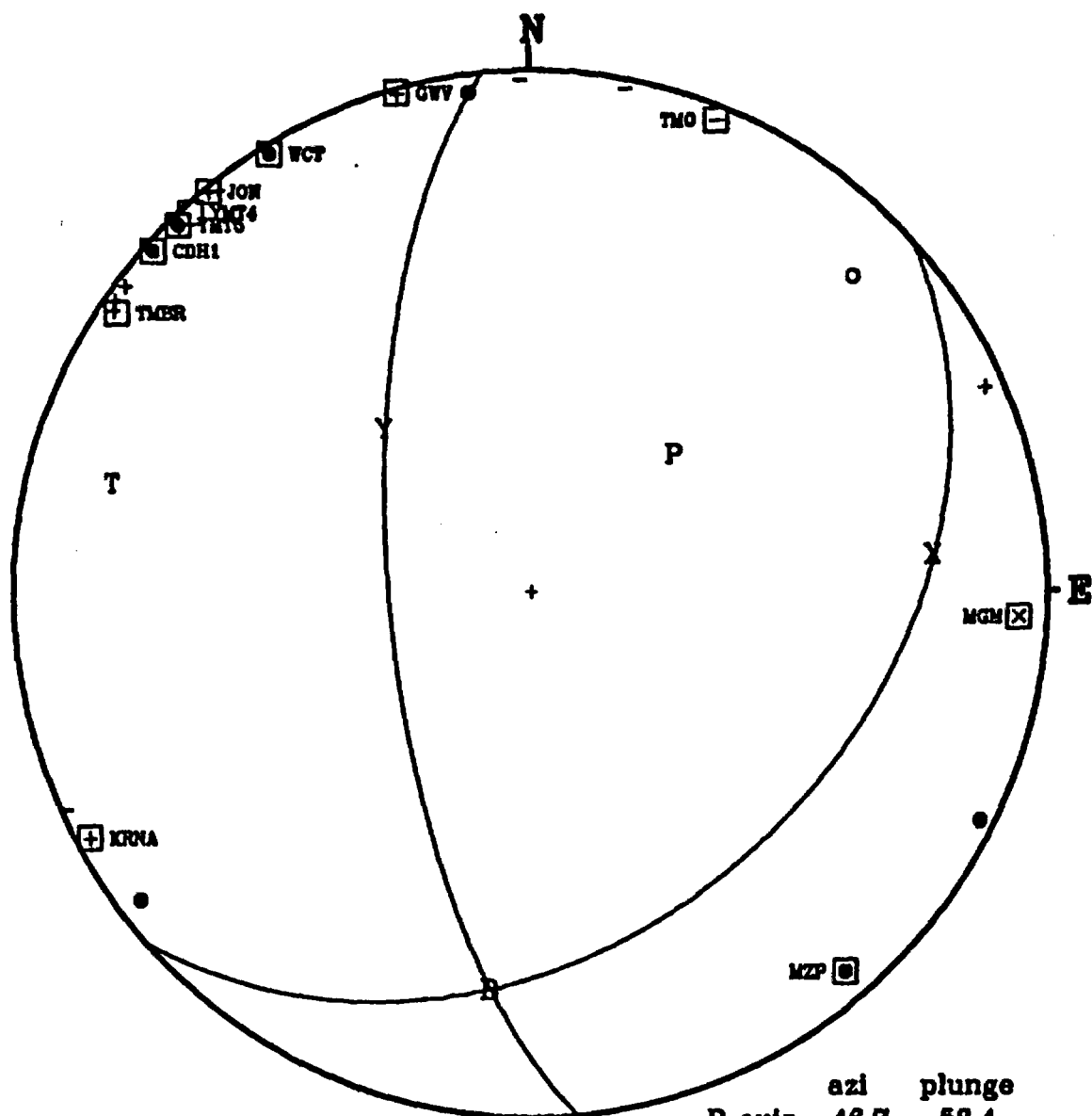


Figure E14. This Sarcobatus Flat composite focal mechanism is well constrained on the basis of polarities alone.



SCOTTYS JUNCTION NE

DATE/TIME: 831110 10 37 14.85

LAT: 37.428 LONG: 117.098

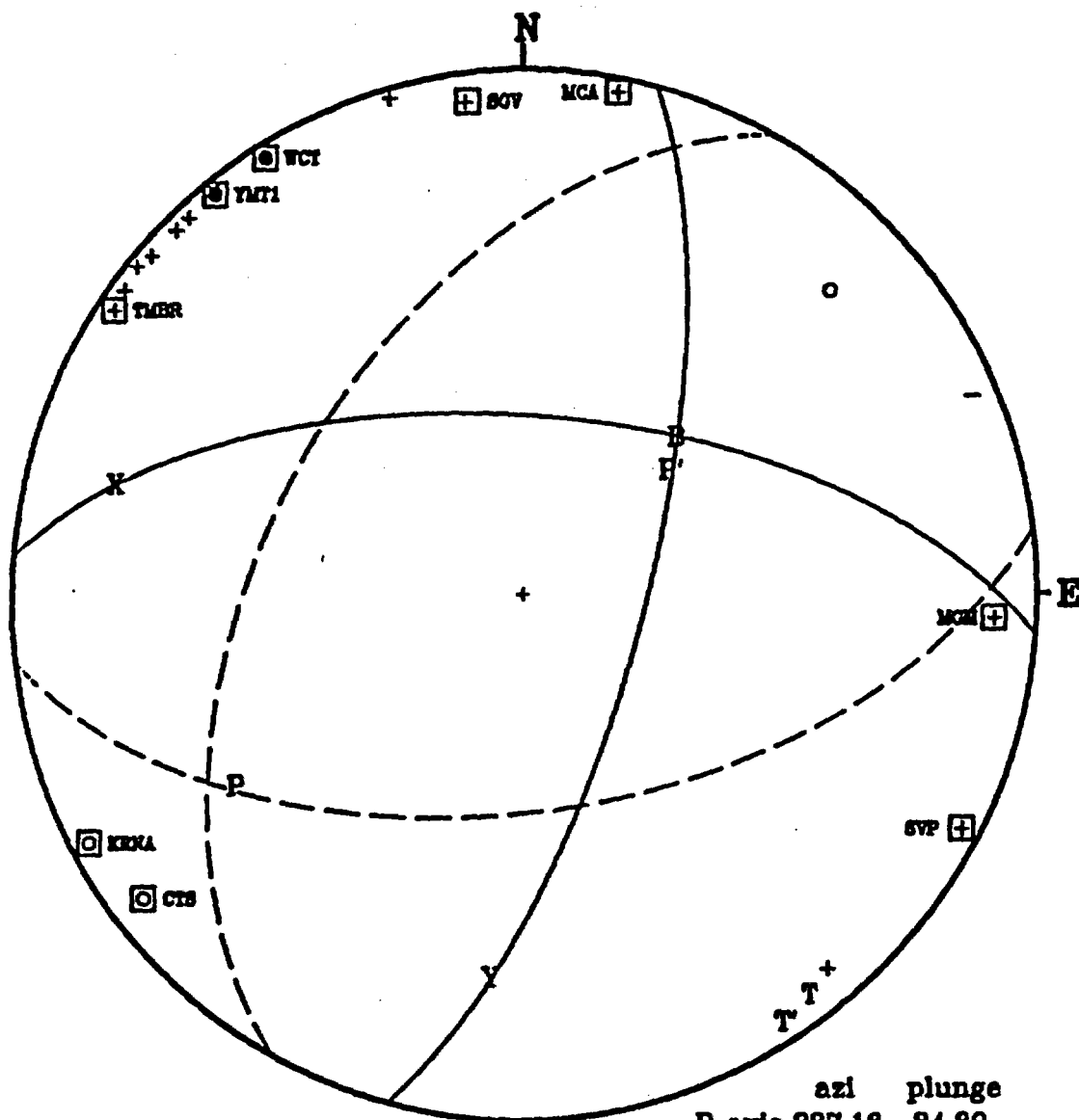
DEPTH, km: 8.01 +/- 2.5 ML: 2.0

	azi	plunge
P axis	46.7	58.4
T axis	284.8	18.1
B axis	186.0	25.0
X axis	84.9	22.5
Y axis	318.2	55.2

Observed	Log10(S/P)Z	Theoretical	Difference	Station
0.8661	0.7845	0.7845	0.1816	MGM
0.2951	0.4832	0.4832	-0.1981	MZP
0.8400	0.8493	0.8493	-0.1893	TMO
0.0577	0.1887	0.1887	-0.1310	JON
0.6511	0.3963	0.3963	0.2548	GVV
0.9578	1.0302	1.0302	-0.0724	KRNA
0.4553	0.2137	0.2137	0.2416	TMBR
0.3353	0.1949	0.1949	0.1404	YNT5
0.0972	-0.0682	-0.0682	0.1654	VCT
0.2537	0.1715	0.1715	0.0822	YNT4
0.2817	0.2349	0.2349	-0.0332	CDH1

The average rms ratio error = 0.161.

Figure E15. Amplitude ratios are helpful in constraining the strike and dip of the nodal planes.



# SCOTTYS JUNCTION NE

DATE/TIME: 831110 13 17 32.85

LAT: 37.425 LONG: 117.097

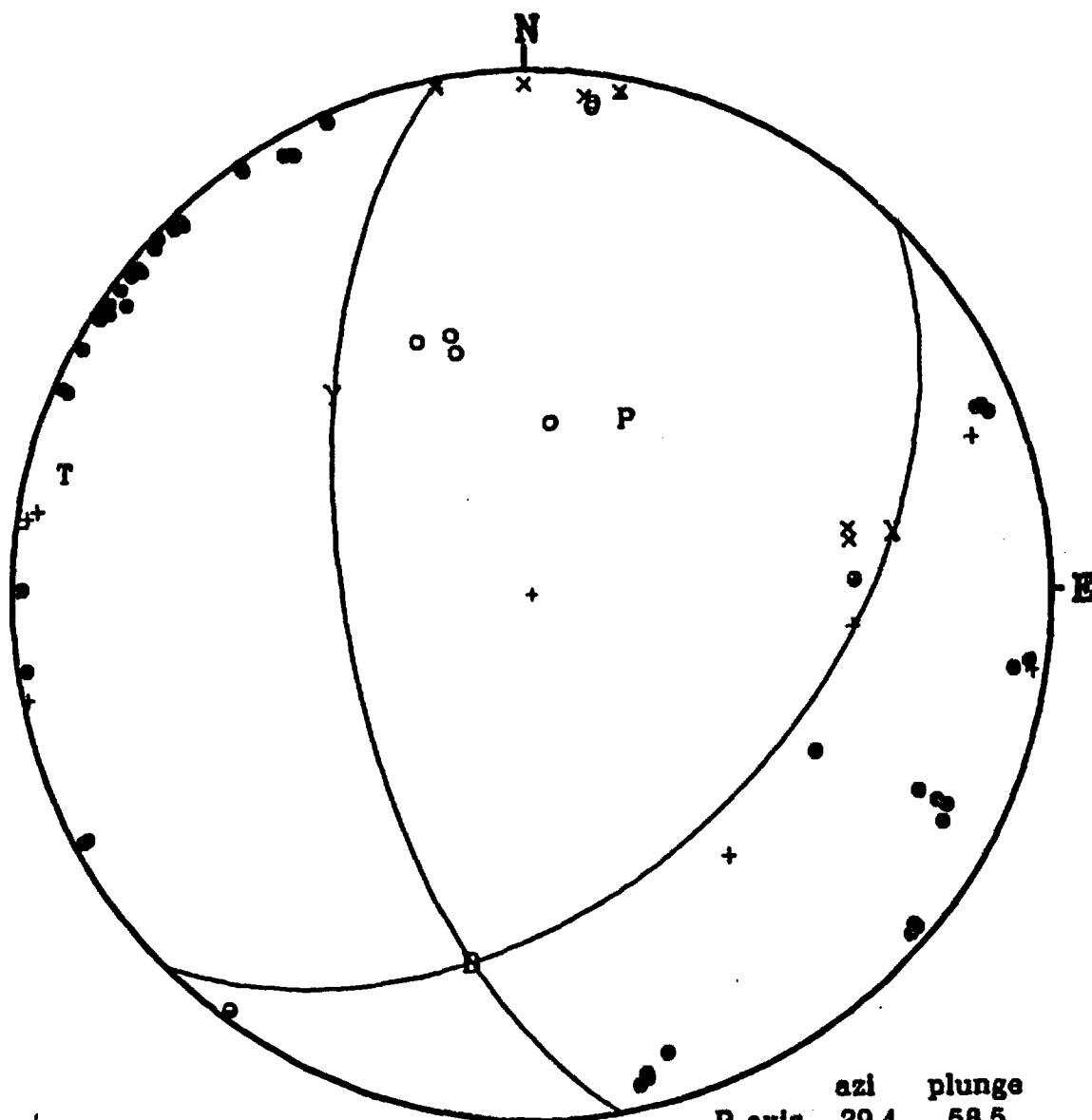
DEPTH, km: 7.33 +/- 1.3 ML: 1.6

	azi	plunge
P axis	237.18	34.39
T axis	143.25	5.69
B axis	45.07	55.01
X axis	285.19	19.23
Y axis	184.50	28.00

		strike		dip	rake
		Soln 1	274.50	62.00	-21.90
		Soln 2	82.80	58.20	-53.00
Observed	Log10(SV/P)z				
	Theoretical				
		Difference			
		Solid	Dash		
1.3448	1.3398	0.0042	-.83	Station	
0.4227	0.4052	0.0175	-.69	MGH	
0.4727	-0.7331	1.2118	-.87	CTS*	
0.1284	0.2671	-0.1467	-.86	SGV	
-0.3287	0.4916	-0.8203	-1.34	SVP	
0.5687	0.3591	0.2016	1.05	KRNA*	
0.1438	0.0316	0.1114	0.18	TMBR*	
-0.1382	-0.1892	-0.0298	-.22	YMT1	
0.7826	0.8015	-0.1889	-.14	WCT	
				MCA	

The rms error for the 7/8 acceptable solutions is 0.128 (solid)  
The rms error for the 6/8 acceptable solutions is 0.133 (dashed)  
ASTERISK placed before poorly fit station using solid sol.,  
after poorly fit station using dashed solution.

Figure E16. These focal mechanisms require the information contained in the amplitude ratios to constrain the solutions to the range shown by the solid-line and dashed-line nodal plane solutions.



**GOLD POINT**

DATE/TIME: 831001 10 32 53.88

LAT: 37.353 LONG: 117.280

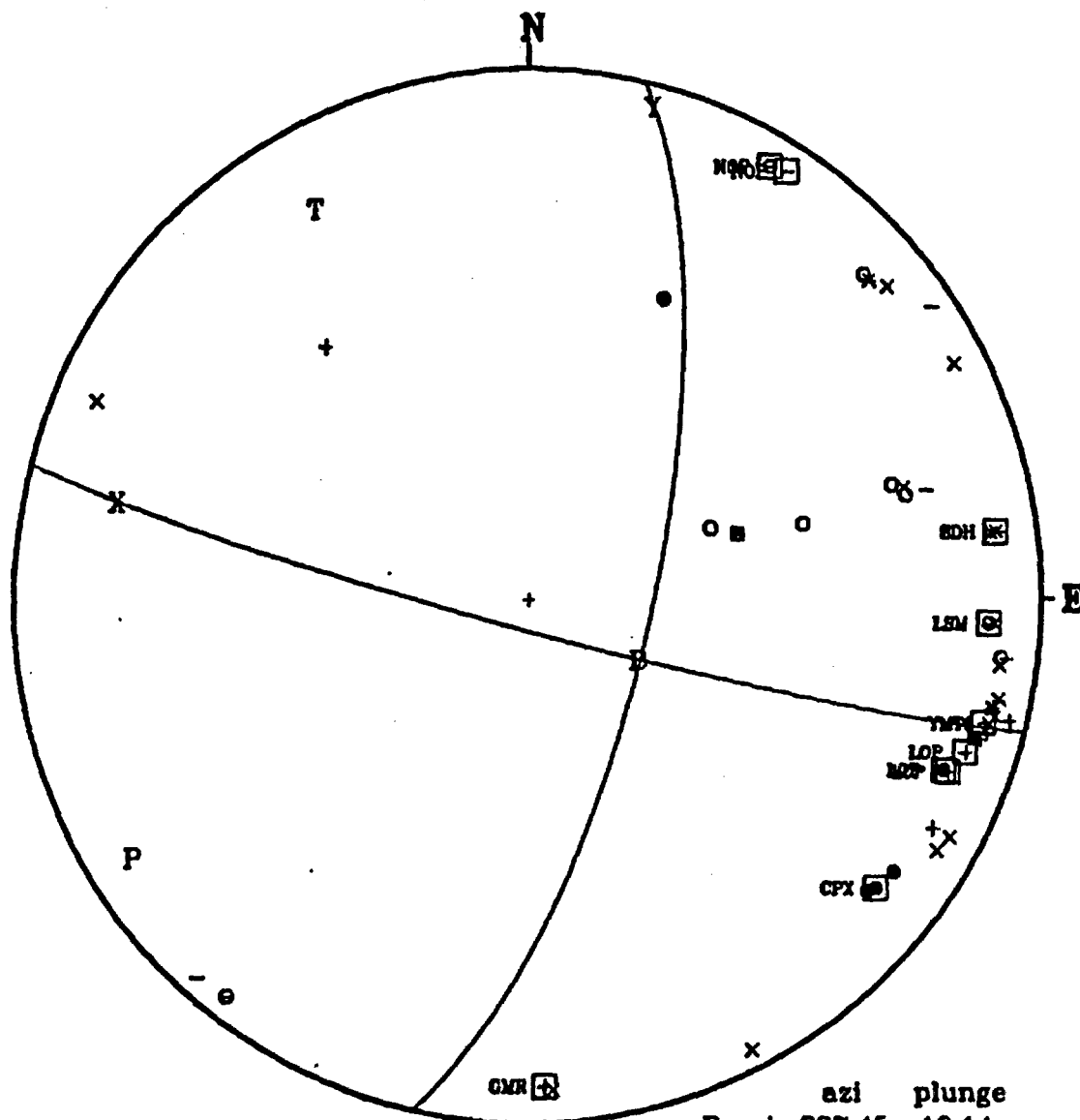
DEPTH, km: 6.07 +/- 0.7 ML: 2.5

COMPOSITE WITH 831001 10 33 59.49

831001 10 47 45.74 831001 10 51 47.04

	azi	plunge
P axis	29.4	58.5
T axis	285.0	8.7
B axis	190.0	30.0
X axis	80.7	29.8
Y axis	315.5	45.2

Figure E17. Although this mechanism is a composite, the wide range of azimuths of compressional arrivals for the mainshock (831001 10:32) constrain the solution to predominantly normal slip.



INDIAN SPRINGS NW

DATE/TIME: 831128 18 42 5.27

LAT: 36.715 LONG: 115.739

DEPTH, km: 11.22 +/- 0.6 ML: 1.7

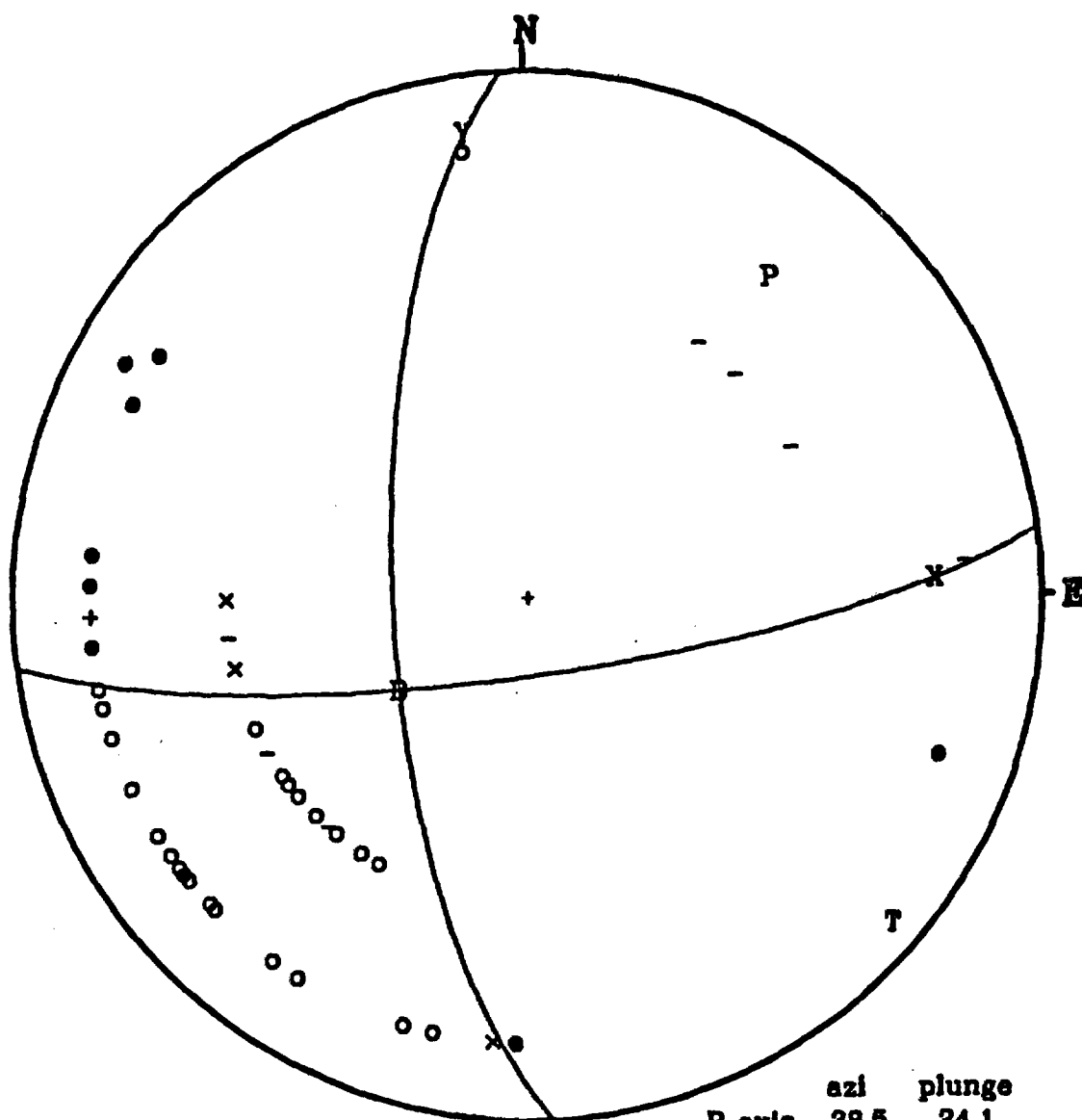
COMPOSITE WITH 831120 10 54 33.13

831127 23 39 32.56 831211 8 14 47.67

	azi	plunge
P axis	237.45	10.14
T axis	330.59	17.05
B axis	118.01	70.00
X axis	283.14	19.38
Y axis	14.81	4.75
	strike	dip
F.P. 1	104.81	85.25

Log10(SV/P)z			
Observed	Theoretical	Difference	Station
0.8293	0.7594	0.0699	LOP
0.2487	0.5333	-0.2846	NOP
-0.3010	0.4718	-0.7728	CPX
0.7852	0.6274	0.1578	LOP
0.6520	0.1183	0.5337	SDH
0.8004	0.6431	0.1573	LOP
0.8086	-0.0030	0.8116	LSM
1.3034	1.2954	0.0080	YHT6
0.6878	0.7129	-0.0251	GMR
0.3685	0.6837	-0.3152	NOP
The average (rms) ratio error = .185			

Figure E18. This composite mechanism is fairly well constrained without the amplitude data.



HIKO NE  
 DATE/TIME: 820708 2 10 43.09  
 LAT: 37.698 LONG: 115.037  
 DEPTH, km: 2.56 +/- 0.5 ML: 3.1

	azi	plunge
P axis	38.5	24.1
T axis	131.3	6.3
B axis	235.0	65.0
X axis	87.5	21.5
Y axis	352.6	12.2

Figure E19. This mechanism is constrained by first-motion polarities alone.



## APPENDIX F

### Stereoplots of southern Great Basin earthquake hypocenters at selected locations

For all stereographic plots in appendix F: (1) The two views are separated by a stereo angle of 1.75 degrees from positions 50 km above sea-level; (2) All hypocenters, regardless of depth error estimate, for the time period August 1, 1978, through December 31, 1983, are plotted as "x"s (*feathered* if a focal mechanism for that earthquake exists); (3) Edges of a hypocenter-containing box whose surface is at sea-level and whose base is at 10 km are dotted or dashed to help the reader establish a depth perspective; and (4) The page is at sea-level; shallower-focus earthquakes "float" above the page. Some figures contain faults and/or cultural features, plotted in all cases at a perspective 1 km above sea-level. Seismograph stations are designated as inverted triangles, towns as darkened squares, and roads and highways as double lines. Faults are plotted regardless of age. They are dashed where inferred or uncertain, dotted where concealed. For some figures, noted in the captions, we have not attempted to include all known faults.

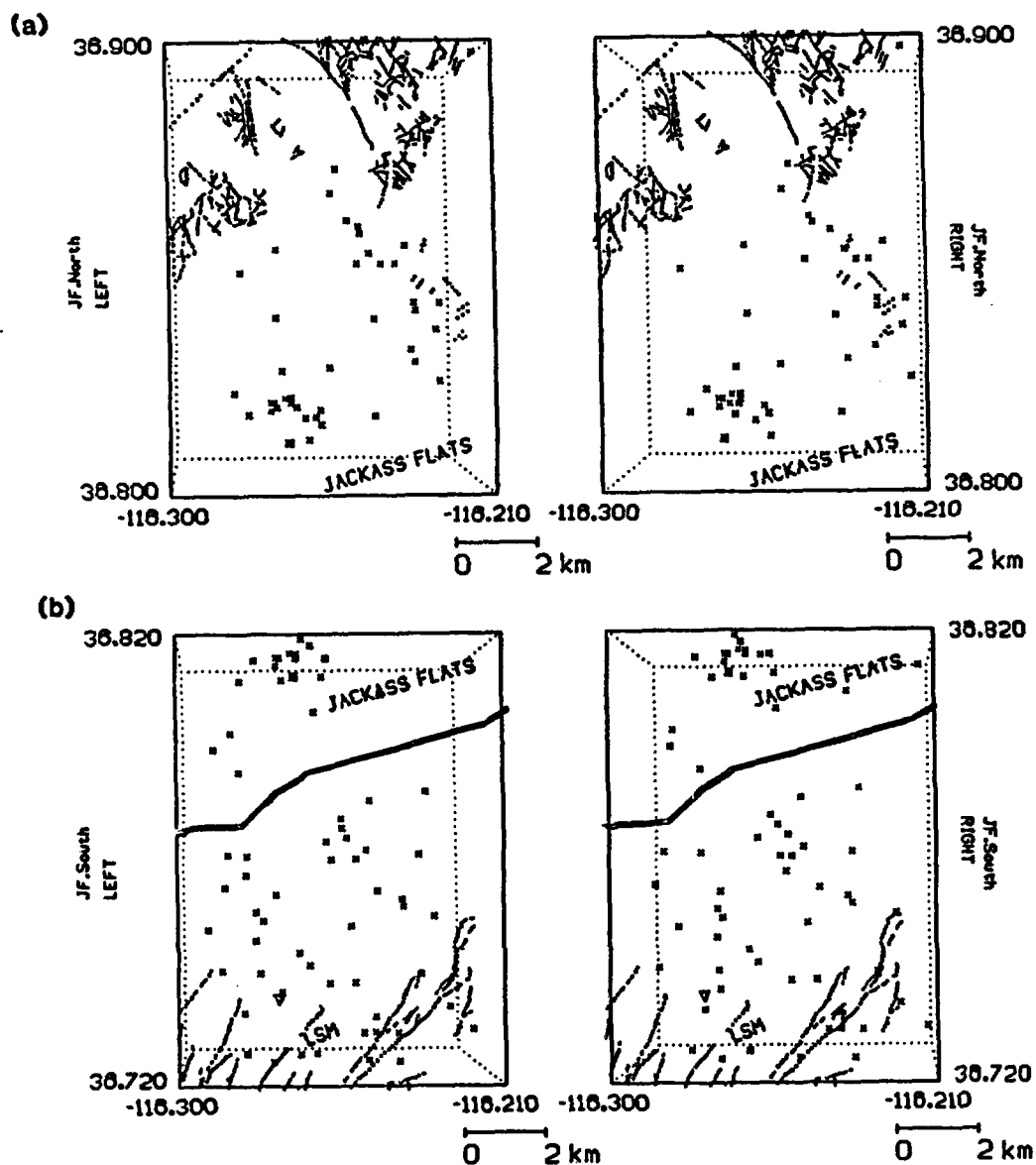


Figure F1. (a) Stereo projections of hypocenters in northern Jackass Flats and adjacent regions. This region is the same as in main text, Figure 18 (a). (b) Stereo pair for southern Jackass Flats and Little Skull Mountain (LSM). Same region as in main text, Figure 18 (b). Faults from Michael J. Carr (written comm., 1987).

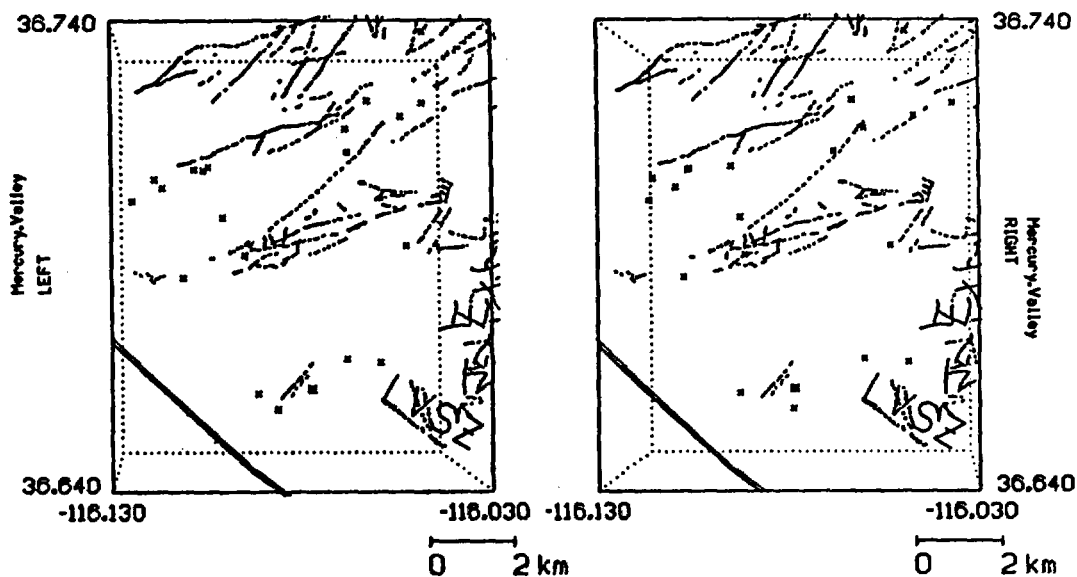


Figure F2. Stereo pair for Mercury Valley hypocenters. Same region as in Figure 19. Faults from Michael J. Carr (written comm., 1987). LVSZ - Las Vegas Shear and Flexure Zone.

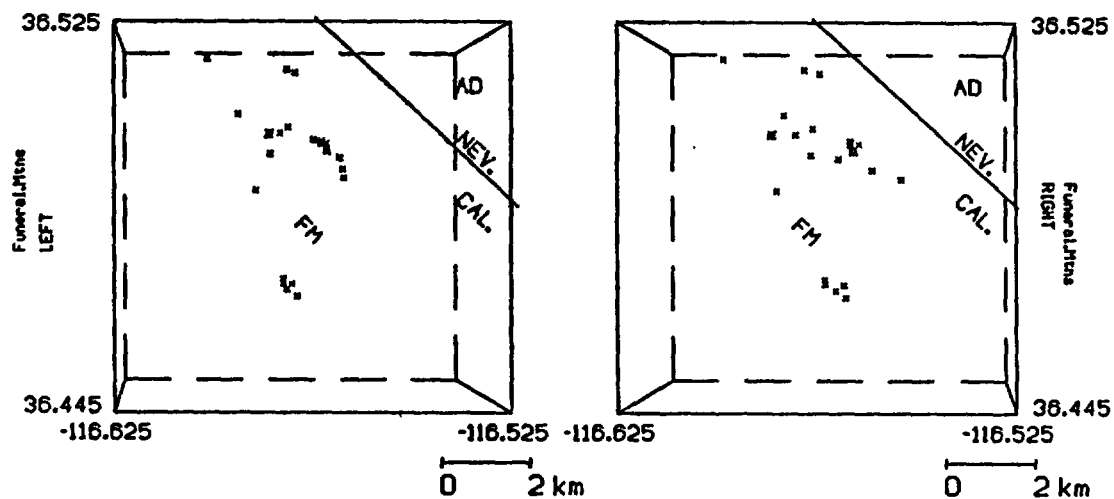


Figure F3. Stereo pair for Funeral Mountains hypocenters. Same region as in Figure 20. FM - Funeral Mountains. AD - Amargosa Desert.

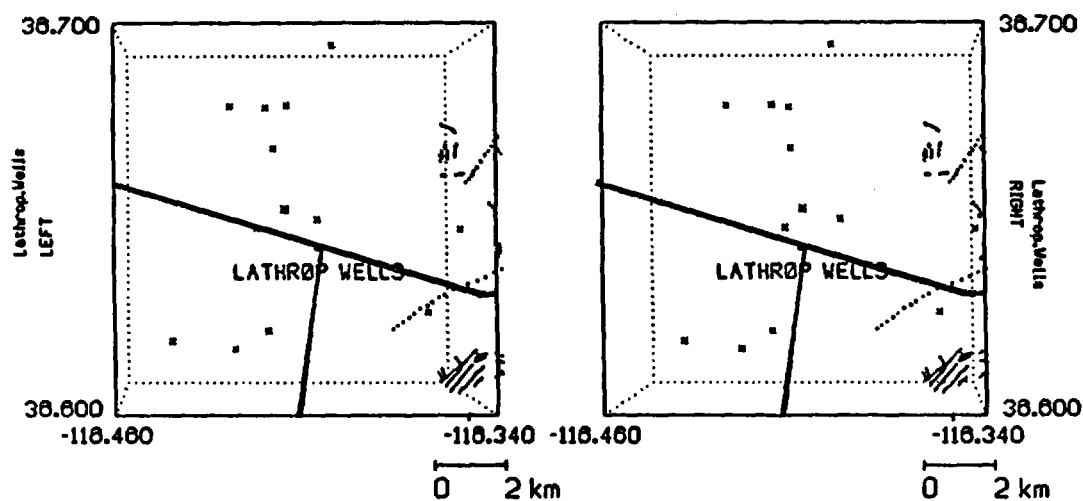


Figure F4. Stereo pair for Lathrop Wells hypocenters. Same region as in Figure 21. Faults from Michael J. Carr (written comm., 1987).

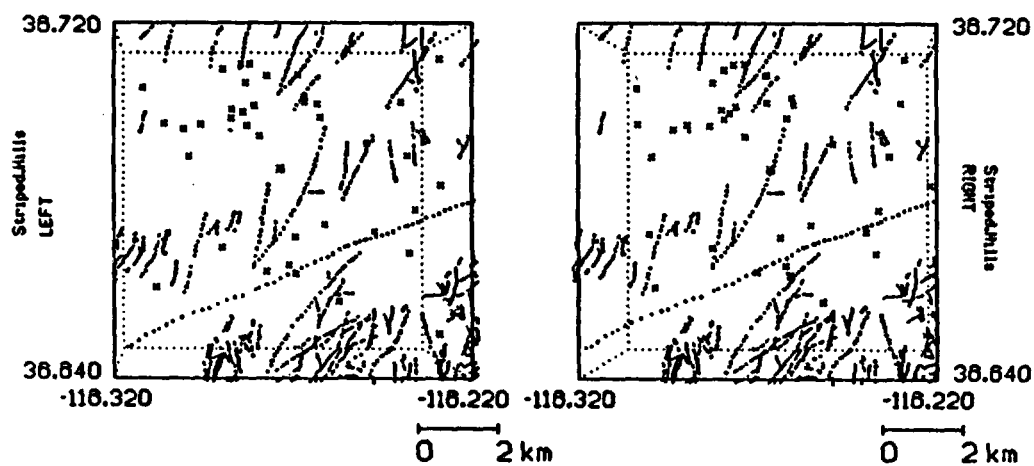


Figure F5. Stereo pair for Striped Hills hypocenters. Same region as in Figure 22. Faults from Michael J. Carr (written comm., 1987).

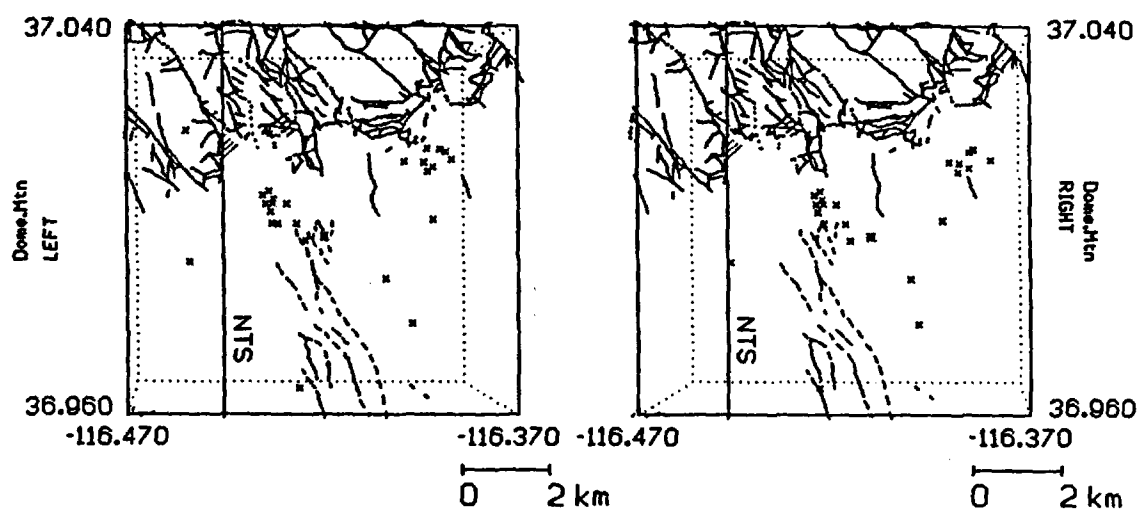


Figure F6. Stereo pair for the Dome Mountain hypocenters. Same region as in Figure 23. Faults from Vergil Frizzell (written comm., 1987). NTS - Nevada Test Site west boundary.

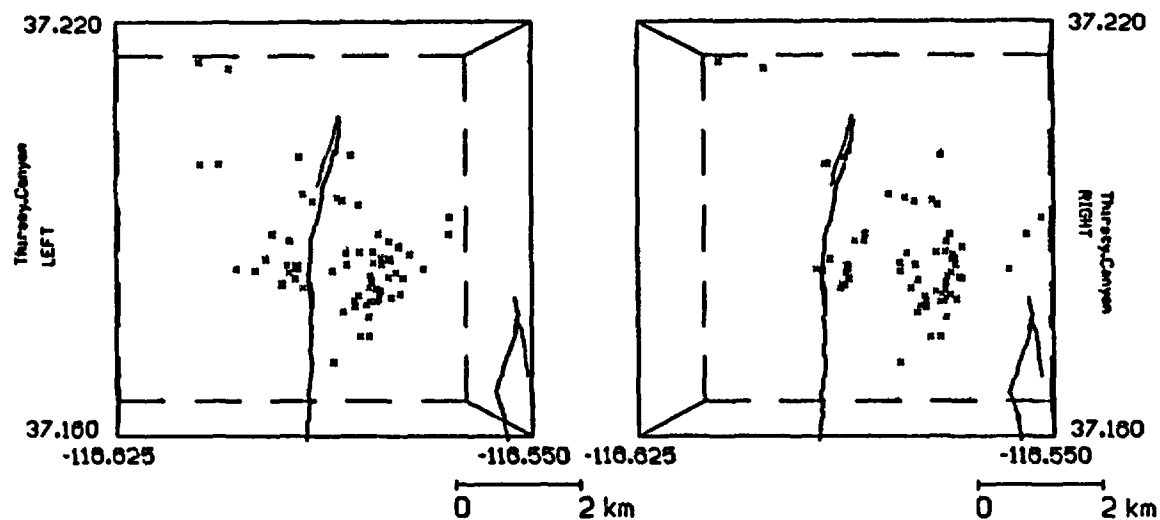


Figure F7. Stereo pair for the Thirsty Canyon - Black Mountain hypocenters. Same region as in Figure 24. Faults from O'Conner and others (1968).

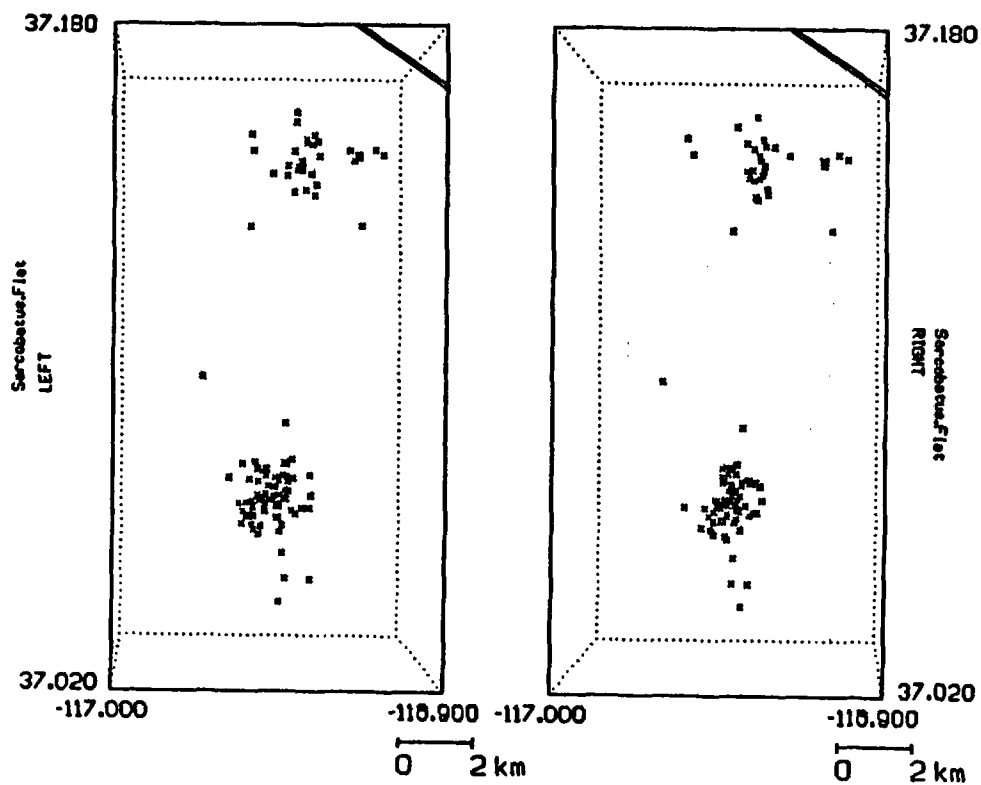


Figure F8. Stereo pair for the Sarcobatus Flat hypocenters, series b and c. Same region as in Figures 25 and 26.

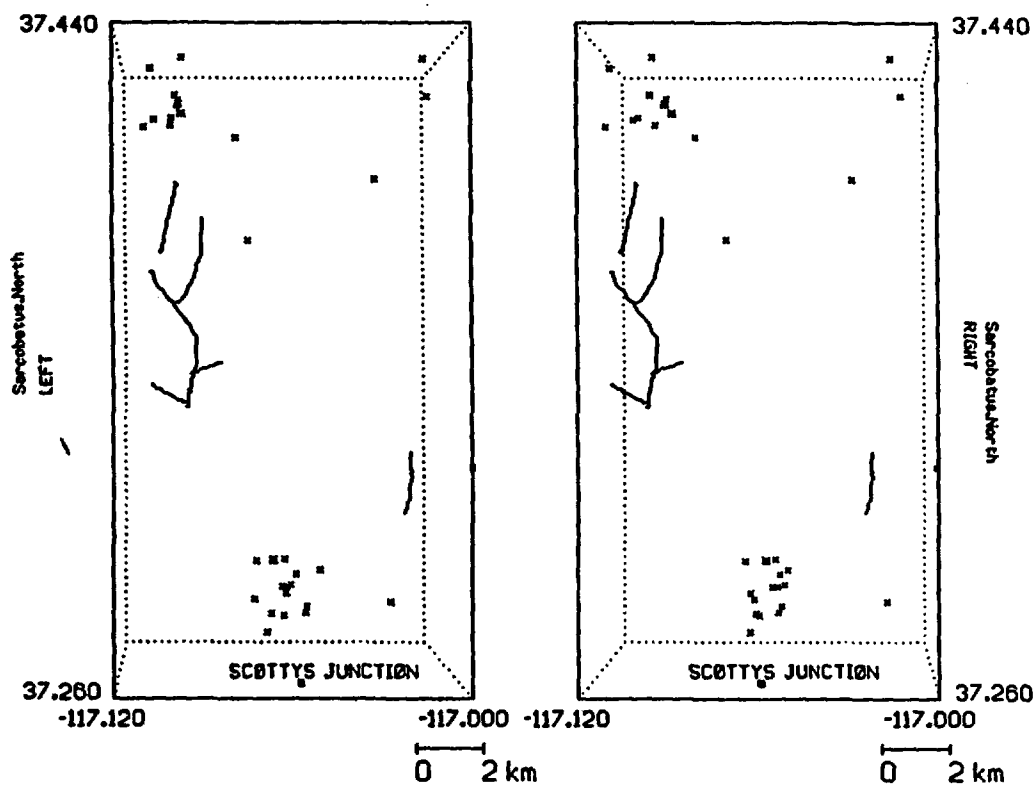


Figure F9. Stereo pair for the Sarcobatus Flats hypocenters, series a and d. Same region as in Figure 27. Faults from Stewart and Carlson (1978).

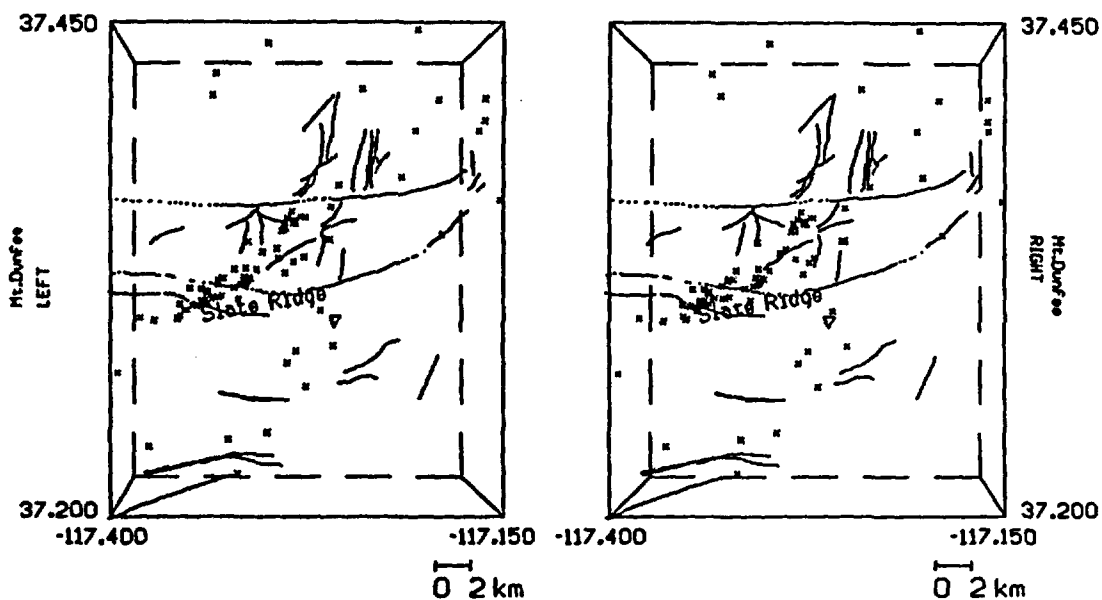


Figure F10. Stereo pair for the Slate Ridge - Mt. Dunfee hypocenters. Same region as in Figure 28. Faults from Albers and Stewart (1965). Faults shown are *incomplete* outside the immediate area of Slate Ridge - Mt. Dunfee.

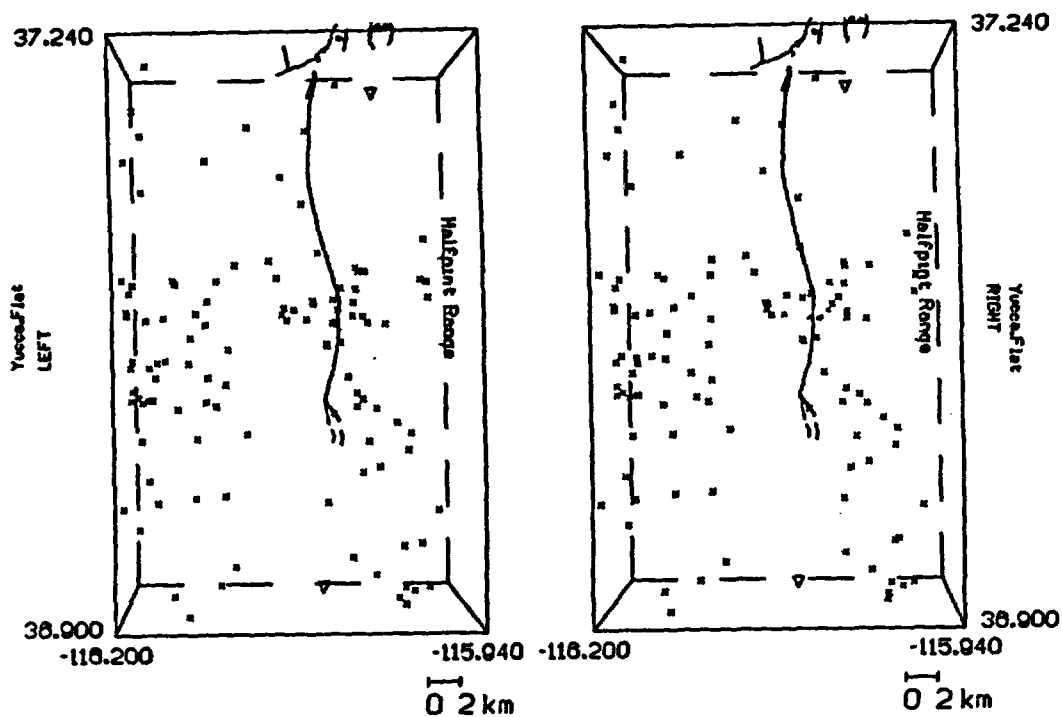


Figure F11. Stereo pair for the Yucca Flat hypocenters. Same region as in Figure 29. Yucca Fault from Stewart and Carlson (1978).

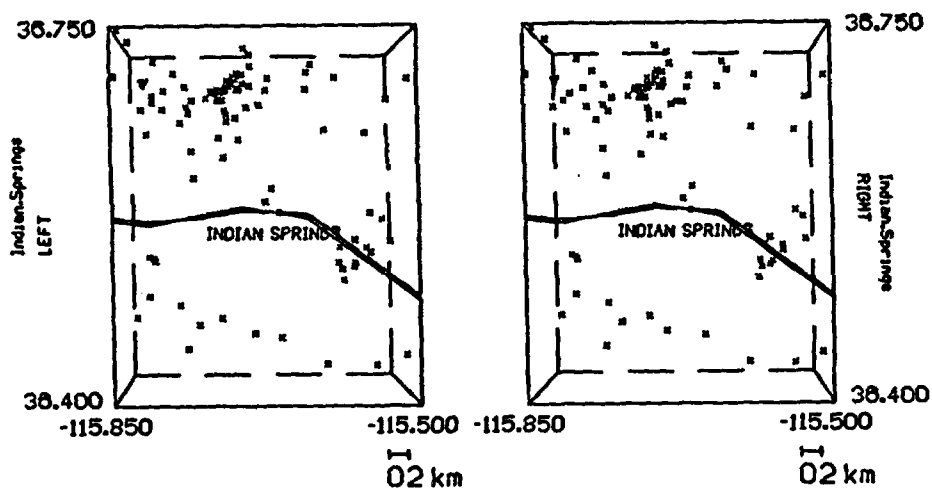


Figure F12. Stereo pair for the Indian Spring Valley hypocenters. Highway 95 is shown. Same region as in Figure 30.



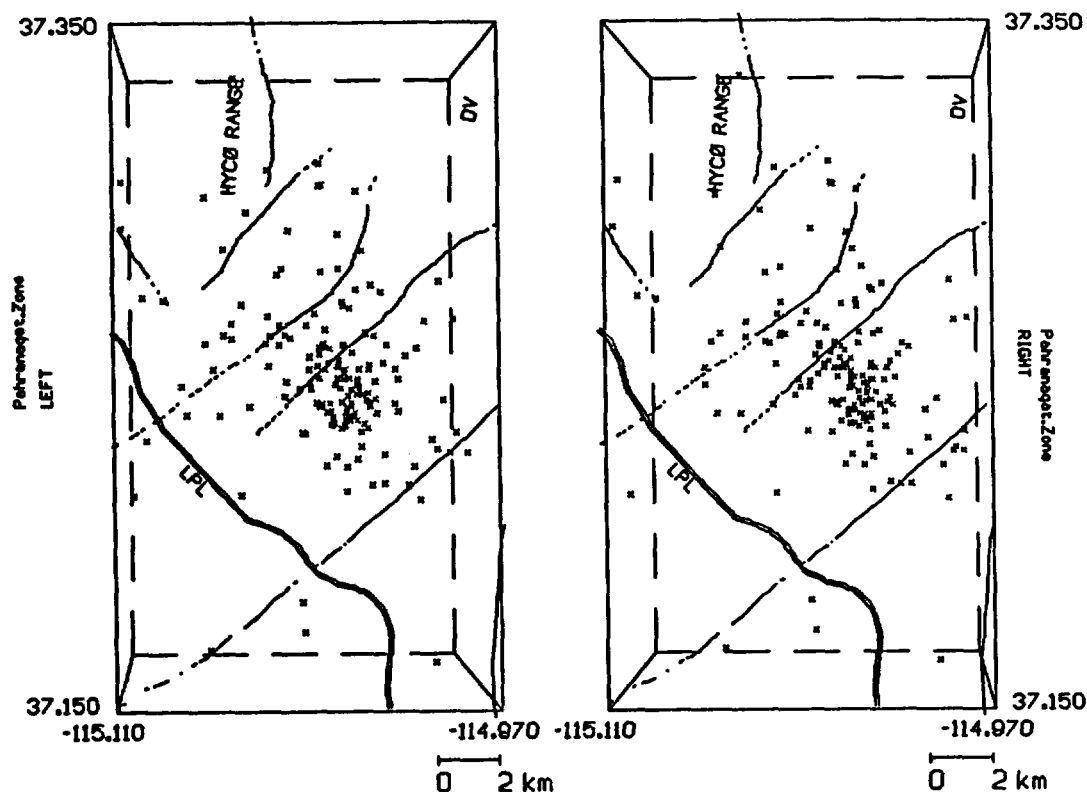


Figure F13. Stereo pair for the Pahranaagat Range hypocenters. Same region as in Figure 31. Northeast trending faults from Ekren and others (1977). North trending faults, though numerous in this region, are not shown (see Ekren and others, 1977, or Figure 15, this report). LPL - Lower Pahranaagat Lake. DV - Delamar Valley. Highway 93 is shown.

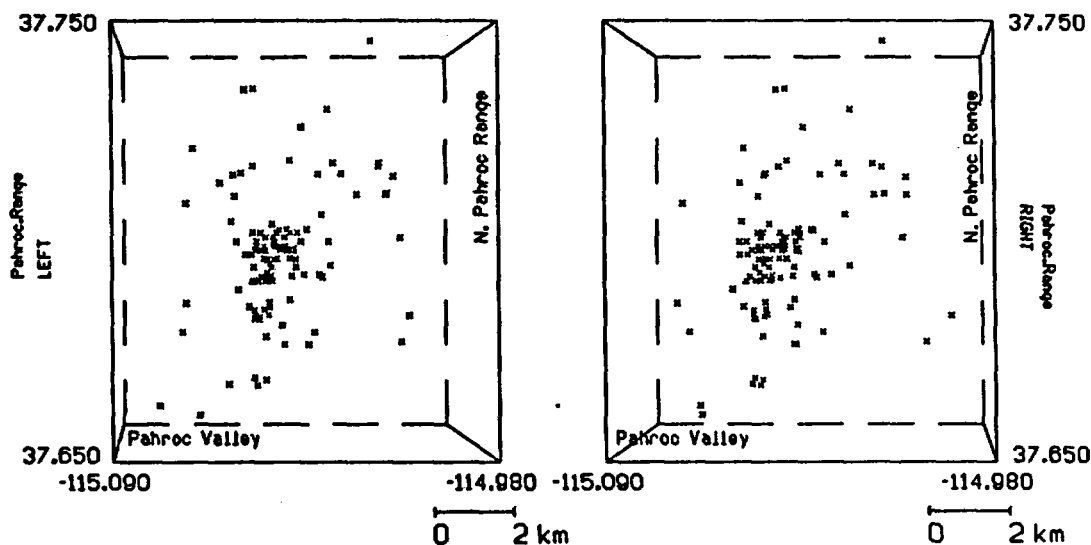


Figure F14. Stereo pair for the North Pahroc Range hypocenters. Same region as in Figure 32.

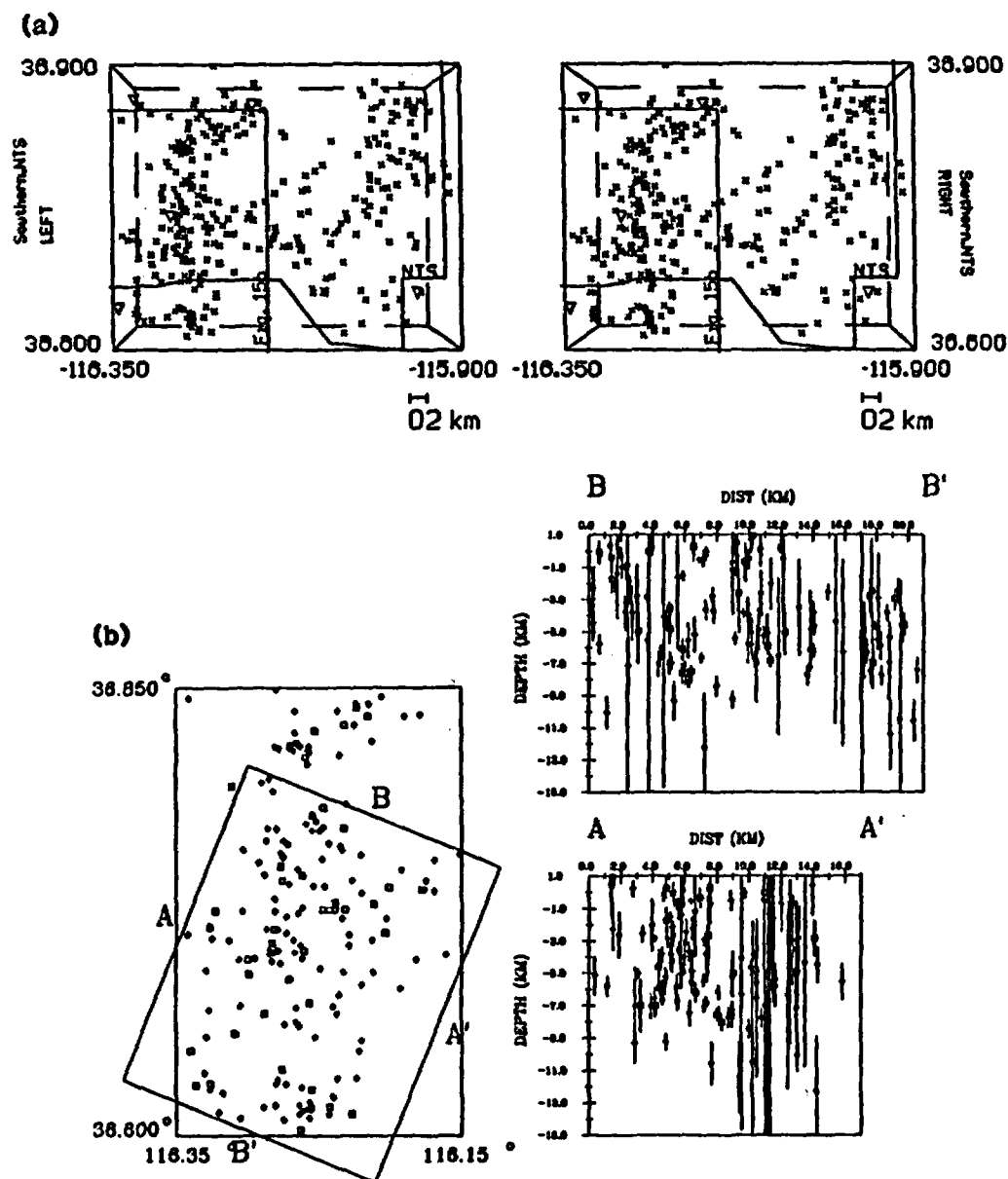


Figure F15. (a) Stereo pair for the southern Nevada Test Site (NTS, boundary shown) hypocenters for the 1978 - 1983 monitoring period. (b) Depth sections for hypocenters in the western part of Figure F15(a).

### **Errata for USGS-OFR-87-596**

page 1. Because the event of Mar 9, 1984, 17:18:29 was repeated with different origin times (see below), the count of earthquakes for 1984 should be 645 rather than 646.

page 26. Delete hypocenter entry of Mar 9, 17:19:13 (Dead Horse Flat quadrangle).

page 26. For the hypocenter entry of Mar 17, 17:18:29, change the date to Mar 9, 17:18:29 (Dead Horse Flat quadrangle).

page 79. Figure captions E1 and E2. The 30°-dipping nodal plane has left-lateral slip (not right-lateral as indicated in the figure captions).

**THIS PAGE IS AN  
OVERSIZED  
DRAWING OR  
FIGURE,**

**THAT CAN BE VIEWED AT  
THE RECORD TITLED:**

**"Seismicity of the Southern  
Great Basin August 1, 1978  
through December 31, 1983"**

**WITHIN THIS PACKAGE..**

**D-01**